

# 4D printing magnetically activated shape morphing objects

Master Thesis – Integrated product design

Kevin van der Lans

July 2022



## **Master Thesis**

Integrated Product Design  
July 2022  
Faculty of Industrial Design Engineering  
Delft University of Technology

## **Author**

Kevin R. van der Lans

## **Delft University of Technology**

Faculty of Industrial Design Engineering  
Landbergstraat 15  
2628 CE Delft  
The Netherlands  
Phone: +31 15 278 4750  
Email: [info@tudelft.nl](mailto:info@tudelft.nl)  
Website: [www.io.tudelft.nl](http://www.io.tudelft.nl)

## **Chair**

Dr. Sepideh Ghodrat  
Sustainable Design Engineering  
Emerging Materials  
[s.ghodrat@tudelft.nl](mailto:s.ghodrat@tudelft.nl)

## **Mentor**

Dr. Ir. Zjenja Doubrovski  
Sustainable Design Engineering  
Mechatronic Design  
[e.l.doubrovski@tudelft.nl](mailto:e.l.doubrovski@tudelft.nl)

## **2<sup>nd</sup> Mentor**

Dr. Ir. Andres Hunt  
Faculty of 3ME  
Precision and Microsystems Engineering  
[a.hunt@tudelft.nl](mailto:a.hunt@tudelft.nl)

# Executive Summary

Magnetic Soft (shape memory) Materials (MSM for short) are a form of shape memory hybrid in which the shape change is initiated by magnetic particles embedded in an elastomer matrix. When an external magnetic field is applied, these magnetized particles will align themselves to this magnetic field, straining the elastomer in a specific shape. Once the magnetic field is removed, the elastic properties of the elastomer pull the object back to its original shape.

This report describes the work done on the development of a 4D printer, in which the shape change of the MSM objects is programmed during manufacturing by controlling the orientation of the pre-magnetized particles in the still uncured silicone. An external dual extrusion system is used to mix a two component silicone during 4D printing, so that the material cures upon hitting the build plate, while staying liquid during printing. The goal of developing a reliable system capable of extruding and printing the highly viscose magnetic material was however not achieved, as the extrusion motors lacked the needed force and the system was not rigid enough to deal with the high pressures involved. Adoption of a new printer design in which the path from extruder to build plate is severely limited is recommended.

In addition, a literature review has been conducted into applications of generic shape memory materials (SMM), metamaterials and magnetic soft materials with the purpose to draw inspiration from proposed applications of these materials for a novel MSM application design. It was found that MSM applications showed many overlaps with SMM and metamaterials, but that there were also some gaps in the reported application proposals of MSM where SMM and metamaterials are currently used for. MSM could be a valuable material used for (haptic) communication and

texture change. More (indirect) relations with MSM, SMM and metamaterials have been identified which could serve as inspiration for future projects.

Lastly, a novel demonstrator concept design has been developed that shows the unique fast and multi-directional characteristics of MSM, using the findings of the literature review and the use of the Material Driven Design method. With additional input from peer students in a workshop, the idea of a 3-way changing texture is proposed. This texture utilizes specific magnetization patterns in an array of MSM actuators to generate two texture variations depending on the direction of the applied magnetic field, in addition to a neutral state when the field is removed. Its feasibility is proven by small scale prototypes.

This project has been the second time this material has been researched at the Faculty of Industrial Design Engineering at the Delft University of Technology, building upon previously delivered work and paves a path for further iterations on manufacturing and design of applications of the magnetic soft material.

# Acknowledgement

I would like to express my gratitude to a number of people that have assisted and supported me throughout this graduation project.

In the first place I would like to thank my supervisors Zjenja Doubrovski and Sepideh Ghodrat for meeting with me almost every week and in general guiding me through the project with valuable feedback. I would like to thank Zjenja especially for getting my attention to what my work meant for the project as a whole and not wasting time on too many side tracks and exploration. And for struggling together, trying to understand the fluid dynamics mathematics. In addition, I would like to thank Sepideh for her inexhaustible enthusiasm for the project, her support during working in the lab and providing me lots of opportunities to take the project to a higher level.

Thanks for Andres Hunt from the faculty of 3ME for his input and ideas in development of the 4D printer set-up and his many offers (which I did not always make enough use off to my regret).

I also want to thank Anton Lefering from the Reactor Institute for magnetizing the ink and for receiving us so quickly every time.

Many thanks also for the people from the Applied Labs, Adrie, Martin and Joris for their help with lab or supply related questions. If I needed something, they would always be happy to provide it. Special thanks goes out to Israel Carrete, supervisor of the Material Lab with whom I spend much time with during my experiments. He would always be there for support, both practically with ordering materials or helping to use equipment as mentally throughout the entire project. Or just to have a relaxing talk and a laugh.

In addition, many thanks goes out to my graduation community group, Adriaan, Asli, Jack, Natalie, Parastou and Tessa for our weekly meetings and supporting each other with each others graduation projects. As well as a general thank you to my family and friends who were always willing to provide a listening ear or distraction in good and bad times in this project and my studies as a whole.

# Table of content

Executive summary	4	4.6.1 Travel resistance and length	71
Acknowledgement	5	4.6.2 Newly designed pistons	72
1. Introduction	7	4.6.3 Magnetic shield material and shape	72
2. Methodology	8	4.6.4 Static mixing nozzle redesign	73
2.1 manufacturing process	8	4.6.5 clamps and cooling	74
2.2 Demonstrator product design	9	4.7 Modification results	75
3. Literature review	11	4.7.1 Unmagnetized ink extrusion	75
3.1 Shape morphing materials	12	4.7.2 Magnetized ink extrusion	75
3.1.1 Shape memory materials	12	4.8 viscosity, resistance, flow rate and radius	78
3.2 Magnetic soft materials	14	4.9 4D printing conclusions	80
3.2.1 MSM fabrication and demonstration	15	4.10 Recommendations	80
3.2.2 magnetic shape memory polymers	18	5. Demonstrator product design	82
3.3 Metamaterials	20	5.1 Manually made shape morphing demonstrators	82
3.4 Applications	22	5.1.1 Squares, wires and grippers	82
3.4.1 Shape memory material applications	22	5.1.2 Active metamaterials	83
3.4.2 Metamaterial applications	26	5.1.3 Shape recovery	83
3.4.3 MSM applications	30	5.2 Material Driven Design	84
3.5 Relationships between metamaterials, SMM and MSM	35	5.2.1. Sensory characterization	84
3.5.1 VENN diagram	35	5.2.2 Technical characterization	87
3.5.2 Indirect relations	38	5.2.3 Materials Experience Vision	88
3.5.3 MSM application gaps	40	5.2.4 Material experience patterns	90
3.6 Literature conclusions	42	5.3 Design conceptualisation	91
4. 4D printing	43	5.3.1 Requirements & wishes	91
4.1 4D printing and Direct ink Writing	43	5.3.2 Ideation	91
4.4.1 Direct ink writing	44	5.4 Final design and prototype	94
4.2 4D printing of MSM	46	5.4.1. Double actuator design	94
4.2.1 DIW and programming of MSM	46	5.4.2 Single actuator design	95
4.2.2 Different manufacturing approaches	48	5.4.3 Workings and further capabilities	96
4.3 Magnetic ink	50	5.4.4 prototypes	98
4.3.1. Ink preparation	50	5.4.5 MSM texture change use cases proposals	99
4.3.2. Rheological properties	50	5.5 Demonstrator design conclusion	101
4.4 3D printer set-up	57	6. Conclusion	102
4.4.1 Extrusion system	57	6.1 Discussion	102
4.5 Extrusion and other difficulties	68	6.2 Recommendations	103
4.5.1 Travel tubes	68	6.3 Reflection	104
4.5.2 Pressure	69	7. References	105
4.5.3 Magnetic shield	70	Appendices	112
4.6 4D printer design interventions	71		

# 1. Introduction

Magnetic Soft (shape memory) Materials are soft elastomer materials with hard magnetic particles embedded inside. They have the ability to transform to a programmed shape when exposed to an external magnetic field.

More well known shape memory materials, such as nitinol, can revert back to a trained shape under the influence of heat. It is often quite slow and needs to be deformed manually before a new shape memory cycle can be started. In contrast to these materials, the shape change of magnetic soft materials is very fast, within one second. The material will revert back to the original shape once the trigger, the magnetic field, is removed. The shape change is also bi-directional. By flipping the magnetic field direction, the material will revert to a third shape.

Shape memory alloys and polymers are a well researched material with proposed applications in a large variety of fields, both at a global level as at the faculty of Industrial Design Engineering (IDE) at the Delft University of Technology. Research on Magnetic Soft (shape memory) Materials however has only really taken off in the last decade or so. This project is only the second project this material has been researched at the faculty of IDE.

In this previous project by Sanne van Vilsteren (2021), parameters have been researched on the composition of the material itself. A recipe had been designed to fabricate this material at the IDE faculty. In addition, a start had been made on the development of manufacturing the magnetic soft material objects by means of 4D printing.

In order to continue the research on the magnetically activated shape morphing material, it is important the material and objects made from the material can be manufactured. As the raw material can be manufactured at the TU Delft as proven in the previous project, the manufacturing of objects made out of this material remains.

In addition, because the Magnetic Soft Material is a relatively new material, its application domain is limited. Reported applications mostly originate in biomedical and soft robotic fields, but very limited applications have been proposed in other fields like (haptic) communication. Nor have magnetic soft materials been compared to other shape memory materials (alloys and polymers) in terms of application potentials. In order to inspire and empower (new) designers and engineers, both in our faculty and beyond, to work with this material, demonstrator designs need to be made that show the potential of the material beyond the established application domains.

In this project, development of the 4D printing set-up is continued. Parameters are investigated that effect the performance of 4D printing with the highly viscose, two component silicone with embedded magnetic particles. Solutions to problems arising from thick dual paste extrusion are designed and implemented in an attempt to make a low-viscosity silicone 3D printing set-up capable of 4D printing magnetically activated shape morphing objects (Chapter 4).

In addition, a concept design of a demonstrator object showing the characteristics and potential of the material is designed (Chapter 5). In order to do this, the established applications of magnetic soft (shape memory) materials are reviewed and compared to applications of two other types of smart materials: metamaterials and shape memory alloys/polymers. (Chapter 3). It is investigated where applications of these materials overlap, but more importantly which currently proposed applications of shape memory alloys and polymers and metamaterials are suited for use of magnetic soft materials or where magnetic soft materials could potentially outperform the aforementioned smart materials.

Chapter 2 explains more on the taken approach of the project and followed methodologies.

# 2. Methodology

In this section, the methodology with which this project was tackled will be discussed. In short, this project consisted of two main parts: Development of the manufacturing process and the design of a demonstrator product. The manufacturing process was developed in relation to the proposed (metamaterial) demonstrator application. Both these parts had a slightly different approach.

## 2.1 Manufacturing process

In this project, a modified Ultimaker 3 was used with the intention to use this machine to manufacture complex metamaterial geometries with the magnetic silicone material. This 3D printer was also used in the previous project on the same topic, where a start was made with making the 3D printer suitable to print the magnetic particles embedded silicone (Van Vilsteren, 2021). At the start of this project, however, the system did not operate as desired, being unable to reliably extrude the silicone due to the material's viscosity.

In this project, development of a 4D printer set-up is picked up. The development process was iterative, but generally consisted of three stages: Analysis, Design and Evaluation (Figure 2.1).

### 2.1.1 Analysis

In the analysis phase, the 3D printer was tested on its capabilities in an experimental way. Issues that were identified in these experiments were then further investigated in an attempt to find the cause of the found limitations. Findings and measurements of these experiments were documented and formed the basis of a design idea that was believed to improve the systems capabilities and reliability. In addition, literature was consulted to get more insight into the process and criteria of 3D printing with silicone materials. Later on, fluid mechanics theory and accompanying mathematics was consulted to

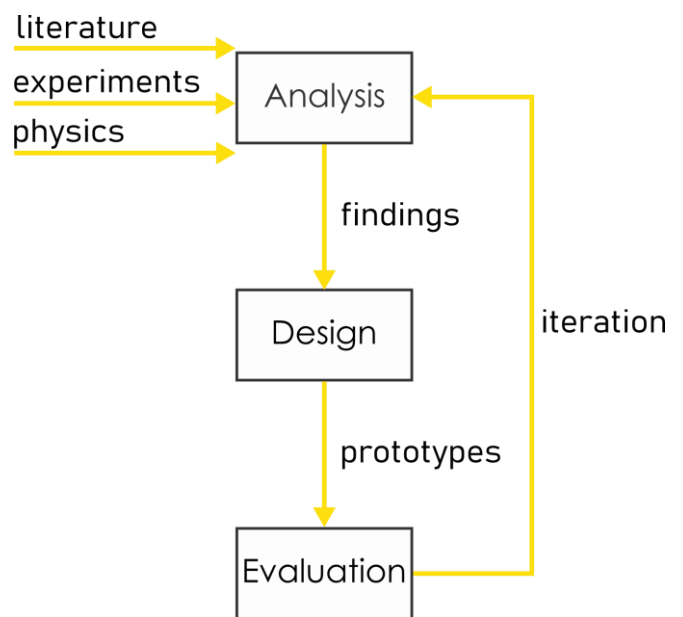


Figure 2.1: Design process of improving the 4D printer set-up consisting of three main stages.

find where in the system improvements could be made to make extruding the highly viscous material easier.

### 2.1.2 Design

Solutions that would mitigate the identified problem causes were ideated and prototyped. These prototypes were then used in new experiments to evaluate the solutions.

### 2.1.3 Evaluation

The designs were evaluated by a new experiment or redoing the previous experiment to see if the designed improvement was successful. Findings of the evaluation then formed the input of a new iteration of the cycle. This process was always aimed at minimal effort for maximum results, meaning implementing possible solutions always went from the quickest, easiest solution towards more time consuming and elaborate solutions until an acceptable result was achieved. In the



beginning, the process was very practical and hands-on. Later on, fluid mechanics were used to get a better theoretical basis before a new design was implemented.

## 2.2 Demonstrator product design

The design for the demonstrator product partly followed the Material Driven Design method by Karana, Barati, Rognoli and Zeeuw van der Laan (2015). This methodology is specifically aimed at finding suitable applications of novel materials, taking into account technical and experiential properties. In addition to this method, a literature review was conducted in which present applications of the material were examined, along with applications of other, more established shape morphing materials (alloys and polymers) and metamaterial structures.

In the beginning of the project, special attention was paid to the use of shape memory materials for active disassembly, with the intention to use the MSM material for this

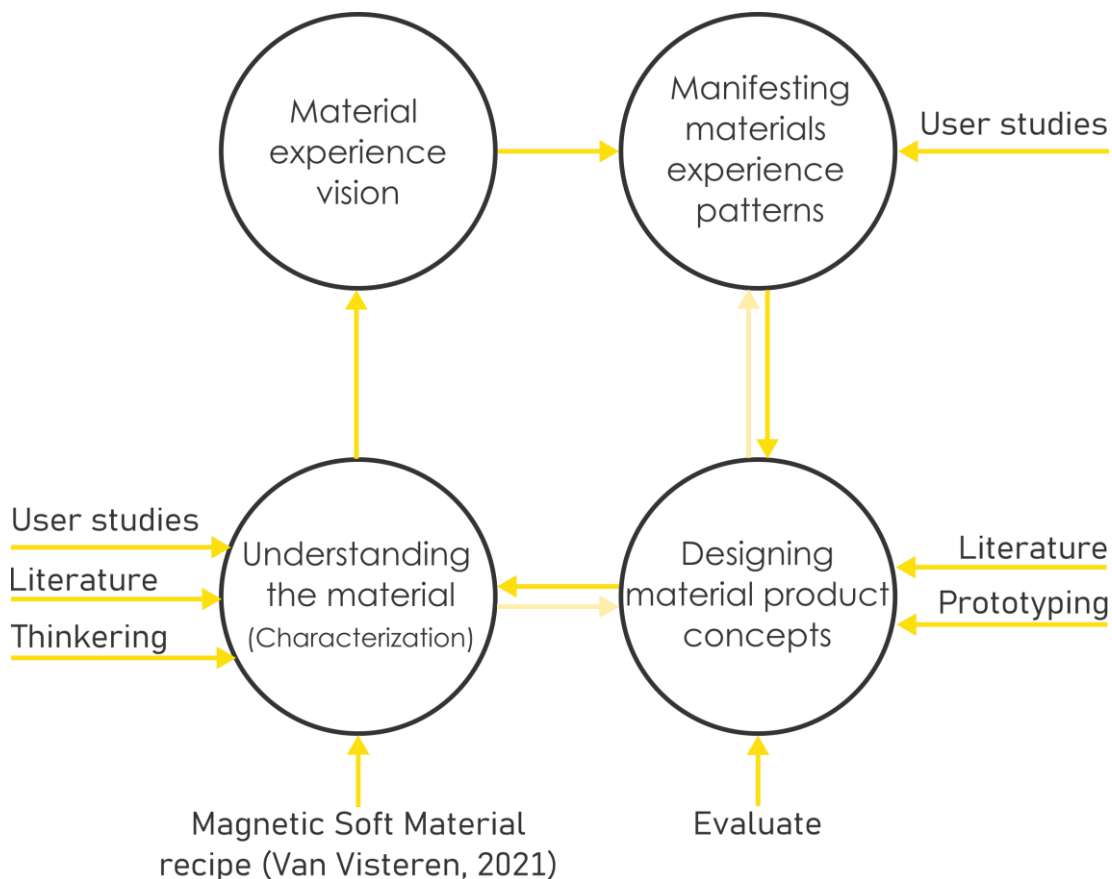
purpose. However, because time constrains and a lack of confidence in the usability of MSM for this application, it was cut short.

### 2.2.1 Material Driven Design

The Material Driven Design method (MDD) consists of 4 stages: *Understanding the material*; *Material experience*; *Manifesting experience patterns* and *Designing concepts* (Figure 2.2).

#### *Understanding the Material*

In the first stage, the material characteristics are identified. These include technical characteristics (stiffness, tensile strength, etc.), experiential properties (look, feel, meaning, etc.) as well as magnetic properties. Input for this stage is tinkering with the material (e.g. during 4D printer testing) and literature on experiments with the material by other researchers, as well as the recipe, findings and recommendations from the previous graduation project with this material (Van Vilsteren, 2021).



**Figure 2.2:** Material Driven Design approach followed in this project, adapted from Karana et al. (2015)

### *Material Experience Vision*

In the second stage, the place of the material in a design is envisioned after reflecting on the materials characteristics. E.g. what characteristics, unique to the material, can be emphasized in a product and in what context would the material be applied to the most effect. But also how its envisioned user would interact with the material and how they would experience the material.

### *Manifesting materials experience patterns*

This stage is all about understanding the user and how they interact with the material in the way you envisioned it. From the experience vision, meanings can be identified. These meanings need to be evoked to the user in a certain way. Relationships between the meanings and the material properties need to be identified. Input from the user (group) can be of great help. Because of time constrains in the project, however, this step of the MDD method was cut short.

### *Designing product concepts*

For designing product concepts, several inputs are used. Literature review on existing applications is used to identify application gaps and potentials, e.g., existing applications of Shape Memory Materials where Magnetic Soft Materials might provide a superior function.

### 2.2.2 Conceptualization

With the outcomes of the MDD method (with help of peer students), the material characteristics are linked to the most promising gap from the literature review to make a simple demonstrator object that would show these characteristics in an inspiring way for future designers in a product design concept. The key principle behind this design was prototyped.

# 3. Literature review

To gain a better understanding of shape morphing materials in general, a literature review was performed on the current types of shape memory and shape shifting materials. These materials include shape memory materials (SMM) such as shape memory alloys (SMA), shape memory polymers (SMP), shape memory hybrids (SMH) and magnetic soft materials (MSM), which is what this project is about. MSM differ from better known shape morphing materials in that they are soft elastomer materials which shape change is caused by magnetic particles embedded. The shape morphing properties are thus caused by a mixture of two (or more) materials. SMMs have these properties from their molecular structure or composition. While SMMs are rigid materials, MSM are soft materials. The force required to deform them manually is thus very low. However, their automatic shape change is fast compared to that of thermally activated SMMs (e.g. alloys and polymers) and is triggered remotely with a magnetic field instead of the most common trigger for SMMs: heat.

The review focusses primarily on the applications of these materials, shape memory materials and magnetic soft materials. Because MSM are a rather new kind of smart material, their application domain is quite limited. SMMs have been used and researched more intensively and thus have wider application domains, such as human-machine interaction, soft-robotics and aerospace systems. Applications for SMMs are thus reviewed to gain knowledge about these domains to see where MSM could be applied to the same or maybe better effect than conventional SMMs.

A well-documented application domain for MSM is that of active, untethered metamaterial structures. These objects are impressive to look at, but have little value in the field of product design as of now. Metamaterials consists of a number of cells that interact with each other to perform complex actuations. To gain more knowledge about the workings and applications of metamaterial structures, this topic is also incorporated into this review. This overview serves as an inspiration of how magnetic metamaterial structures can be applied in valuable product design.

## 3.1 Shape morphing materials

Shape morphing materials (SMMs) are materials that can alter their shape without the use of motors. SMMs fall under the stimulus-responsive materials (SRMs; Sun et al., 2021). These materials alter their physical or chemical properties in response to external influences, such as heat, pressure, light, magnetic fields and chemicals.

### 3.1.1 Shape Memory Materials

Shape memory materials are a kind of SRM that revert back to a previous (remembered or trained) shape under an external influence. This is known as the shape memory effect (SME; Huang et al., 2010). The most common stimulus is heat (temperature).

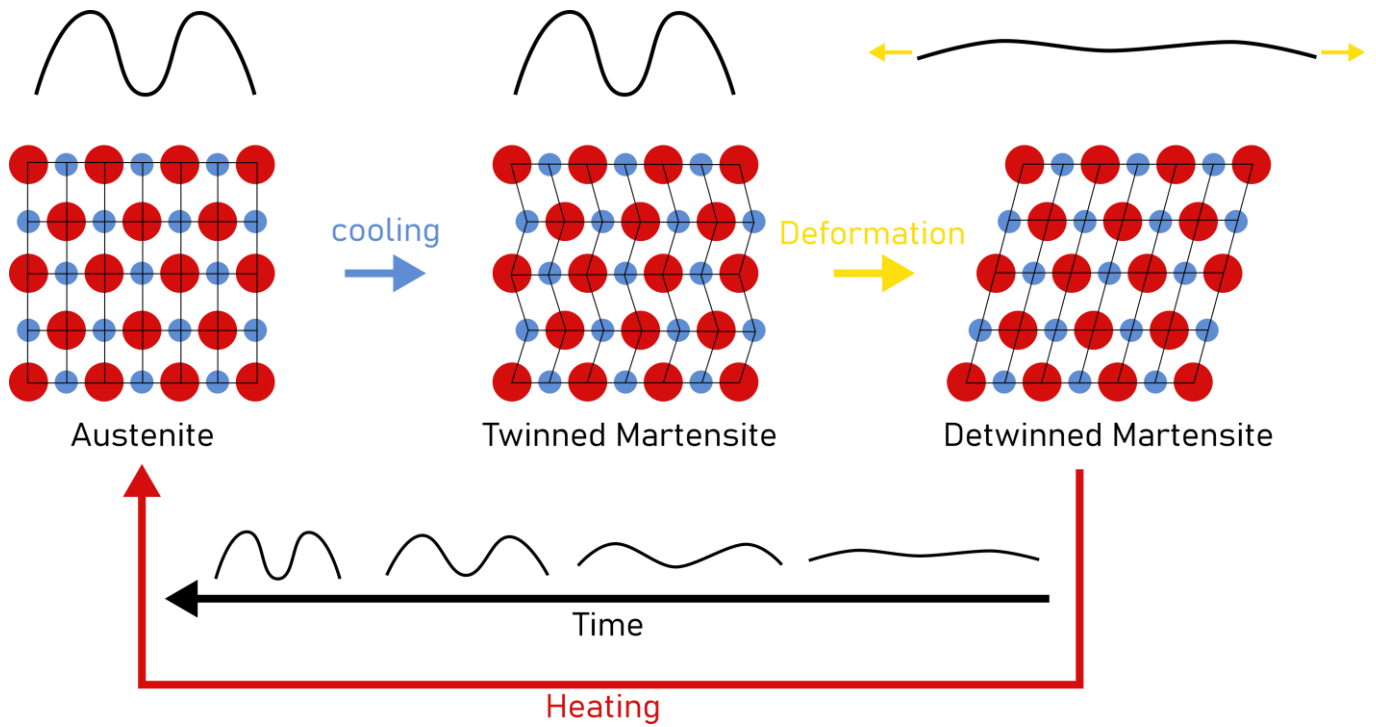
#### *Shape memory alloys*

Shape memory alloys are metals. Nitinol (NiTi), a nickel-titanium alloy, is a well known shape memory alloy (SMA). It mostly comes in wires, but it is also possible to produce NiTi thin films (Kruevitch et al., 1996; He et al., 2004). The SME comes from the crystal structures in the metal. When heated to 500°C, the atoms configure themselves in a cubic arrangement (austenite phase). In this temperature, the material can be trained or programmed into the ground shape. After cooling (twinned martensite phase), the material can be deformed (detwinned martensite phase). When heat is applied again (but less than the 500°C used to train it), the atoms return to the cubic arrangement and the remembered shape returns (Figure 3.1).

#### *Shape memory polymers*

Compared to SMAs, shape memory polymers (SMPs) are cheaper, lighter and easier to tailor the properties (Huang et al., 2010). Examples of SMPs are polyurethanes (SMPU; Fu et al, 2015) and polyesters (Zhang, Tan & Li, 2018). PLA (polylactic acid), used extensively in FDM 3D printing, is such a polyester with shape memory properties. The polymer is manufactured in Shape B, the permanent shape. When the polymer is deformed above its glass transition temperature (often above 60°C), it requires Shape A. When the applicable external stimulus is applied, it reverts back to the permanent Shape B (Behl & Lendlein, 2007). The shape change is based on two segments or domains within the material; an elastic segment and a

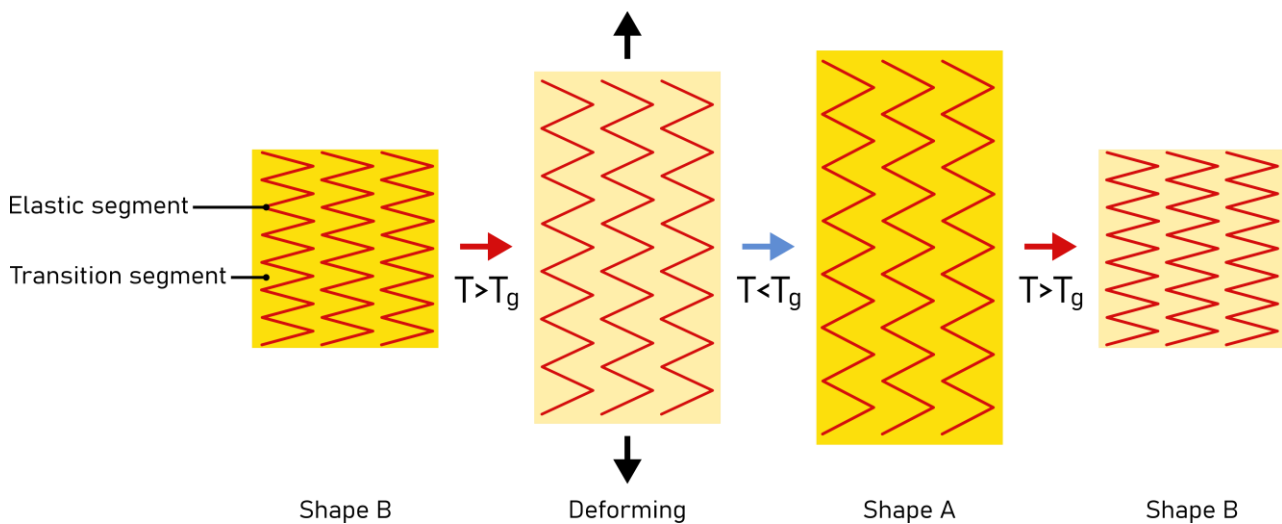
transition segment (Sun et al., 2012; Figure 3.2). The elastic segment remains elastic during the SME cycle, while the transition segment becomes soft during heating, allowing for plastic deformation. If the material is cooled, the transition segment becomes hard again in order for the material to remain in the deformed shape. When heated, the transition segment softens, and the material is pulled back into its original shape by the elastic segment.



**Figure 3.1:** Formation of atoms from austenite to martensite phase in a SMA cause the shape memory effect. Adapted from Stachiv, Alarcon & Lamac (2021)..

### Shape memory hybrids

Shape memory hybrids (SMH) are a type of SMM that consists of a minimum of two components. Individually, these components do not show shape memory properties individually. The SME relies on the interaction between an elastic domain and a transition domain, just like conventional thermal responsive SMPs (Sun et al., 2012; Huang et al., 2010). Only in hybrid materials, the elastic and transition domain are separate materials mixed together, rather than part of one material. For example, Moreno-Marcelino et al. (2020) fabricated a SMH with polyvinyl alcohol for the elastic segment and silver nanoparticles as transition segment.

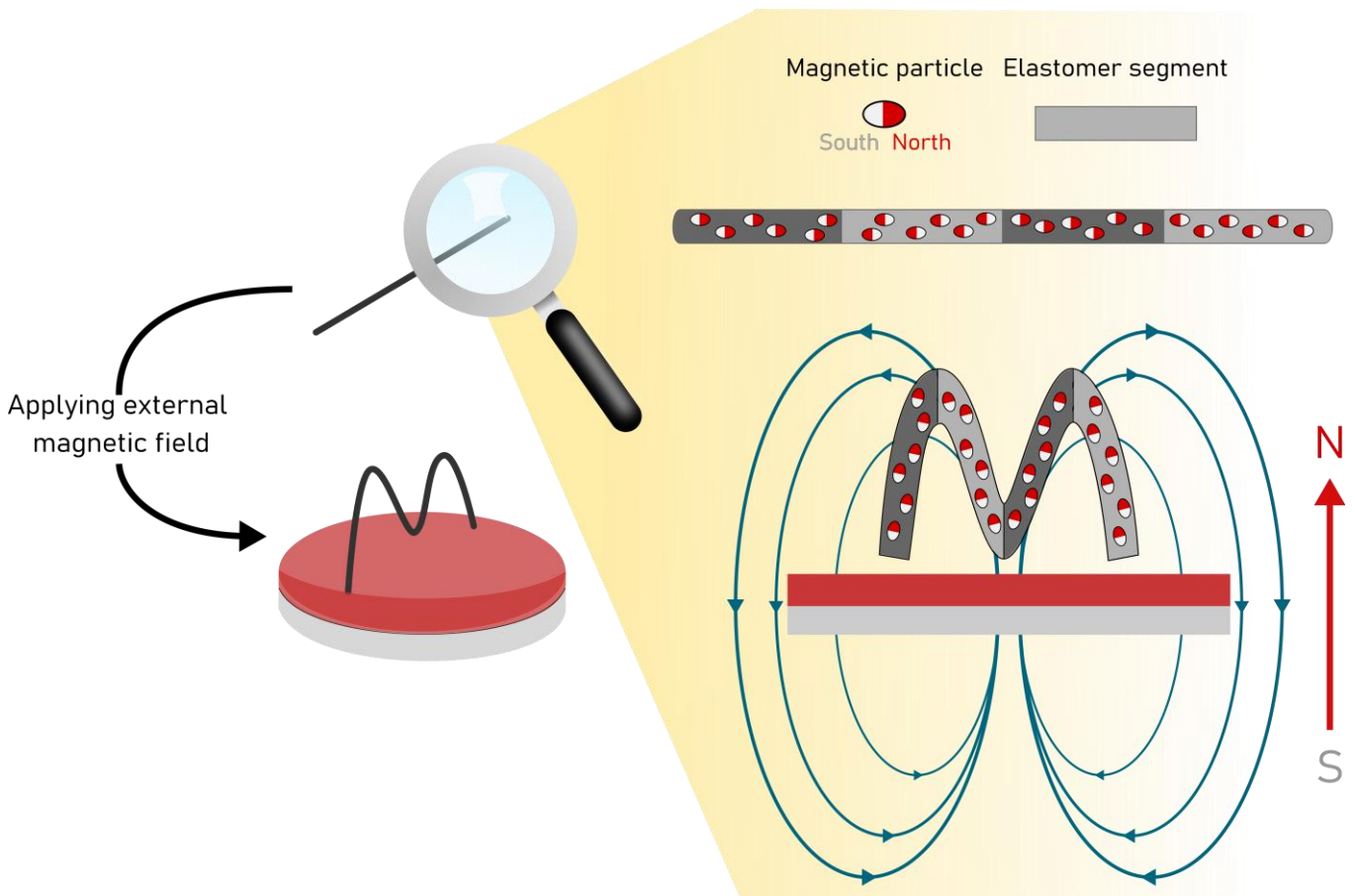


**Figure 3.2:** Schematic representation of shape memory effect in shape memory polymers caused by heating the transition segment above its glass temperature. After cooling, the transition segment becomes rigid again. The elastic segments pulls the material back into the remembered shape upon re-heating. Adapted from Sun et al., 2012.

### 3.2 Magnetic Soft Materials

Magnetic soft materials, also known as Magnetic-responsive soft materials (Wu et al., 2019), shape-morphing magnetoactive soft materials (Bastola & Hossain, 2021) or Magpol (Nguyen, Ahmed & Ramanujan, 2012), is a soft material matrix, such as silicone or hydrogels (Roh et al., 2019; Kim et al., 2018; Ilg, 2013; Fuhrer et al., 2009), with magnetic particles embedded. When introducing an external magnetic field, the magnetic poles of these particles align with the magnetic field whereby these particles rotate, straining the elastomer into a different shape. When the magnetic field is removed, the elastomer material will return to the initial shape, pulling the magnetic particles along with it (Figure 3.3). A big advantage of this material, is that it does not have to be attached

to anything to activate the shape change. The material is thus remotely activated or untethered (Kim et al., 2018; Li et al., 2018). While, in shape memory alloys, the material is often heated by passing electricity through it. Compared to heat (e.g. hot water or an otherwise warm environment), the stimulus for MSMs, a magnetic field between 2 and 200 mT (Bastola & Hossain, 2021), is harmless for (human) tissue. For reference, magnetic fields in MRI machines used in hospitals can reach over 10 Tesla (Ladd et al., 2018). The shape change can also be mirrored or otherwise changed in direction by applying the magnetic field in the opposite direction (Wu et al., 2019; Lum et al., 2016; Kim et al., 2018). The shape change is also fast, nearly instantaneous (0.5 seconds; Kim et al., 2018), while conventional SMMs take seconds to minutes to deform.

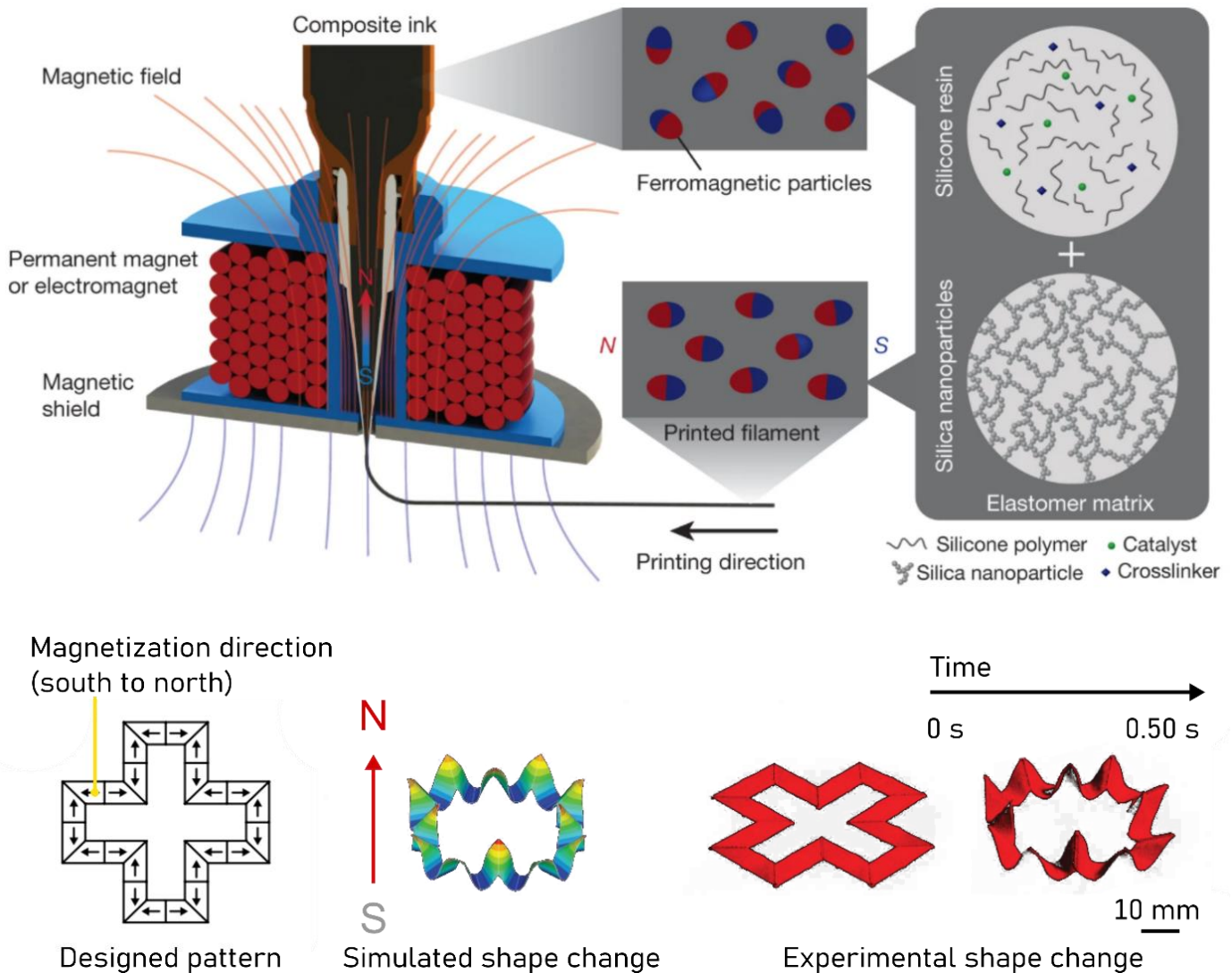


**Figure 3.3** A wire of MSM material, consisting of four segments, morphs into an M-shape when exposed to an external magnetic field induced by a disk-magnet, as the magnetic particles align with the poles of the magnetic field. Adapted from Kim et al., 2018.

### 3.2.1 MSM fabrication and demonstration

MSMs are soft materials, often elastomers or hydrogels, with magnetic fillers embedded. However, there are many reported ways of fabricating such materials. The most common hard magnetic fillers are NdFeB (Neodymium-Ferrite-Boron) microparticles. Iron Oxide is mostly used as a soft magnetic filler. Hard magnetic fillers are preferred however in most shape morphing objects as these particles keep their magnetization whereas soft magnetic particles lose their magnetization when the external field is removed due to their low coercivity (Zhao et al., 2019). The downside is

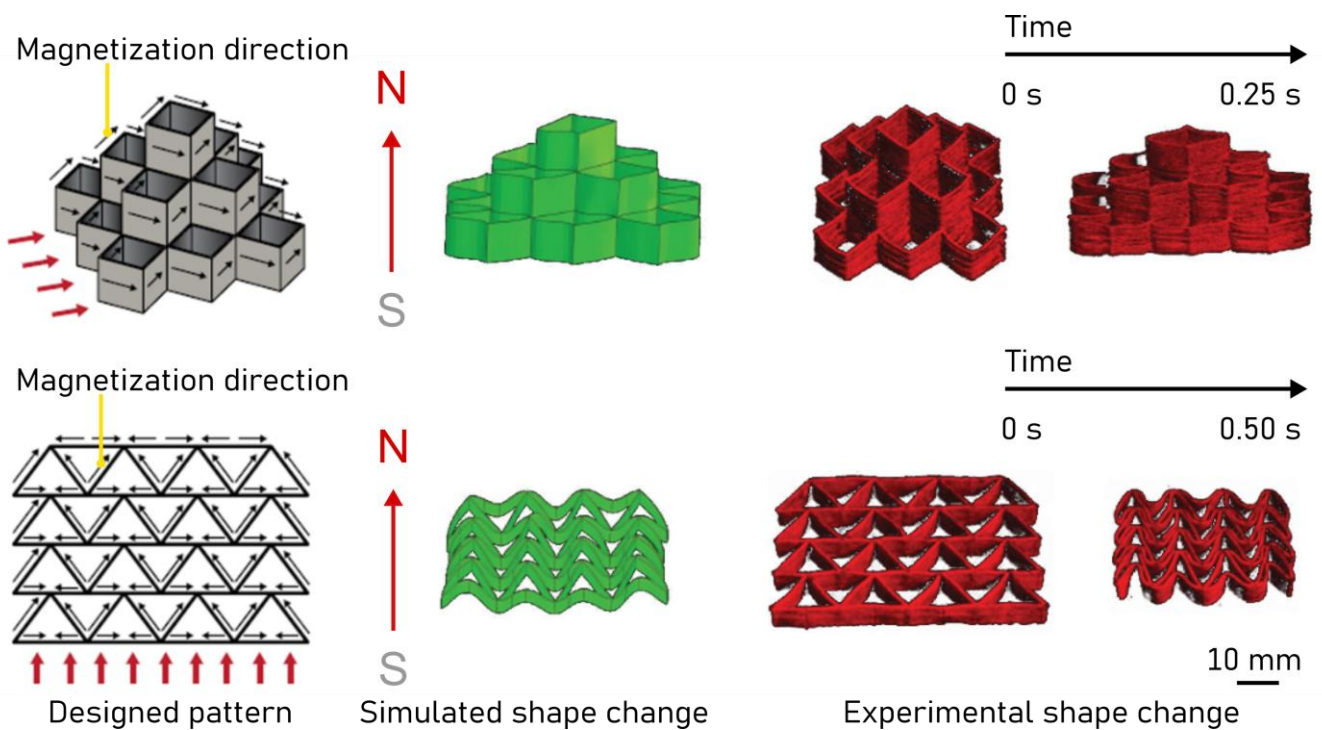
that the NdFeB hard magnetic particles used are toxic, rare earth metals (Lenntech, n.d.). Magnetization of the filler particles require large magnetic strengths, typically between 1.5 and 3 Tesla. Kim et al (2018) made their MSM out of a mix of SE 1700 and Ecoflex 00-30 Part B silicone with added fumed silica nanoparticles and 5 $\mu$ m NdFeB magnetic particles. The fumed silica was added to achieve desired rheological (i.e. shear-thinning) properties of their manufacturing technique: Direct Ink Writing using a custom 3D printer. The mixed ingredients (the 'ink' used in direct ink writing) was magnetized with an impulse magnetizer of 2.7T. During printing, the magnetic NdFeB particles are aligned to the magnetic field of



**Figure 3.4:** While printing, Kim et al. (2018) use a magnet at the end of the nozzle to control the alignment of the magnetic particles in the print direction. Fumed silica was added to make the printed filament more rigid, while the silicone mixture stays low in viscosity when pressure is applied while printing. With this technique, they designed patterns that could change shape as desired.

50mT of a permanent or electromagnet at the end of the nozzle of the print head. By changing print direction or changing the direction of the magnetic field, the particles are printed with the desired alignment of magnetic moment such that the geometry morphs into the desired shape when an external magnetic field is applied (Figure 3.4).

Kim et al. (2018) made active 3D metamaterial structures with this principle, with the help of a supporting, dissolvable elastomer material for extra stabilization of the objects during direct ink writing (Figure 3.5).



**Figure 3.5:** Active metamaterial structures that collapse or fold under a magnetic field due to the 3D printed magnetization direction of the particles in the elastomer material (Kim et al., 2018).



Wu et al. (2019) made their MSM from PDMS resin mixed with NdFeB particles. They made use of the reversible shape change by making asymmetric joints out of Ecoflex 00-30 resin. This made the MSM object able to articulate in asymmetrical ways under a one-directional magnetic field (Figure 3.6). Rather than 3D print the objects, they casted the sections with unmagnetized particles and magnetized these strips afterwards in a set direction.

In addition to one-dimensional objects, they were able to apply this principle in two-dimensional metamaterial structures and by doing so, achieve different actuations out of metamaterial structures with the same overall composition (squares) in the same surface area (Figure 3.7).

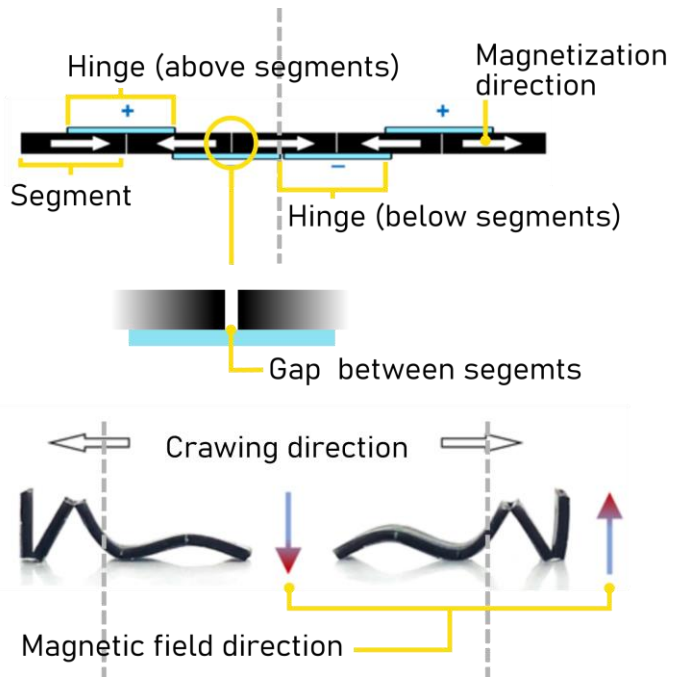


Figure 3.6: Wu et al (2019) were able to produce an asymmetrical crawling motion by making use of asymmetrical joints.

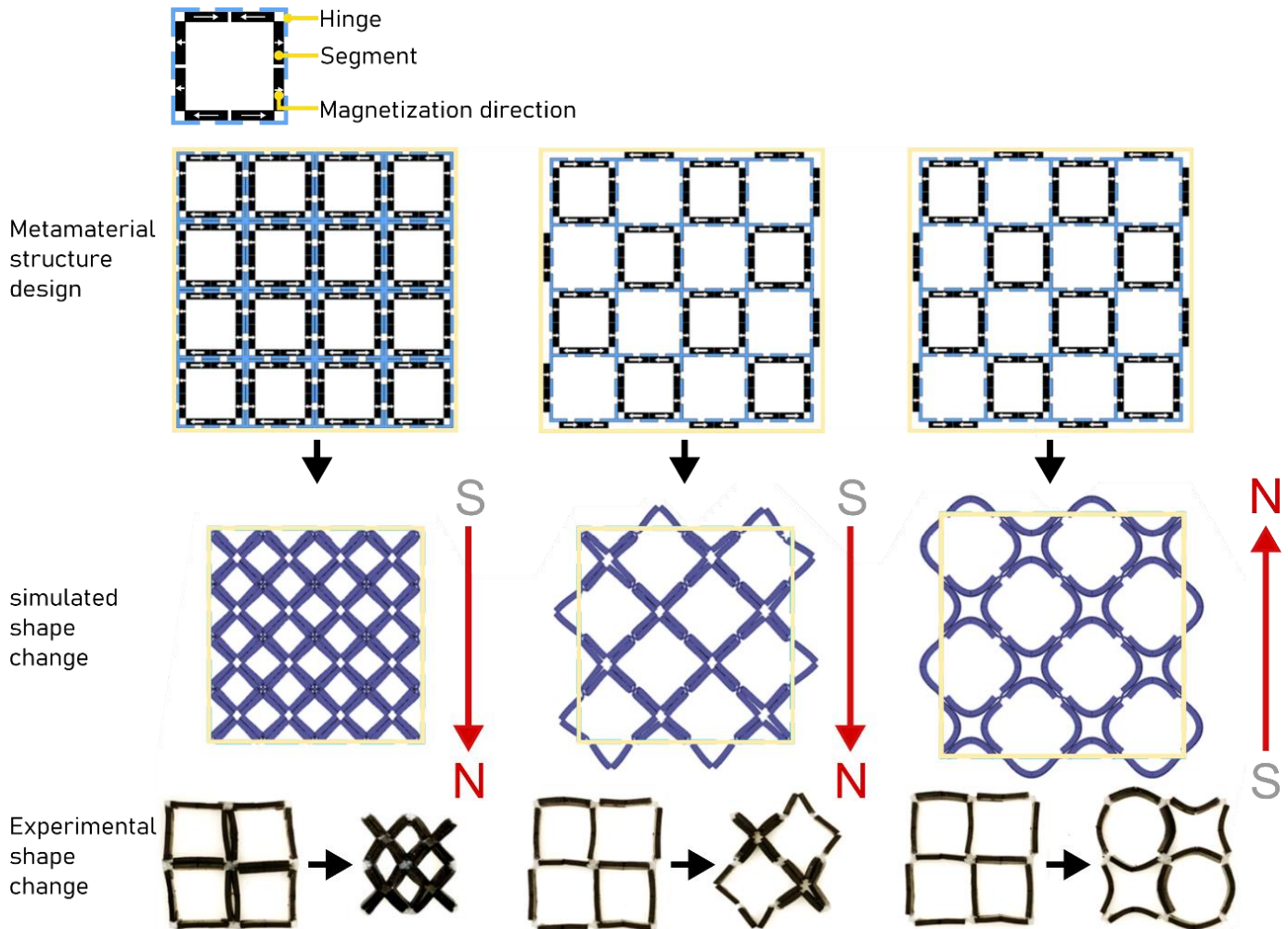


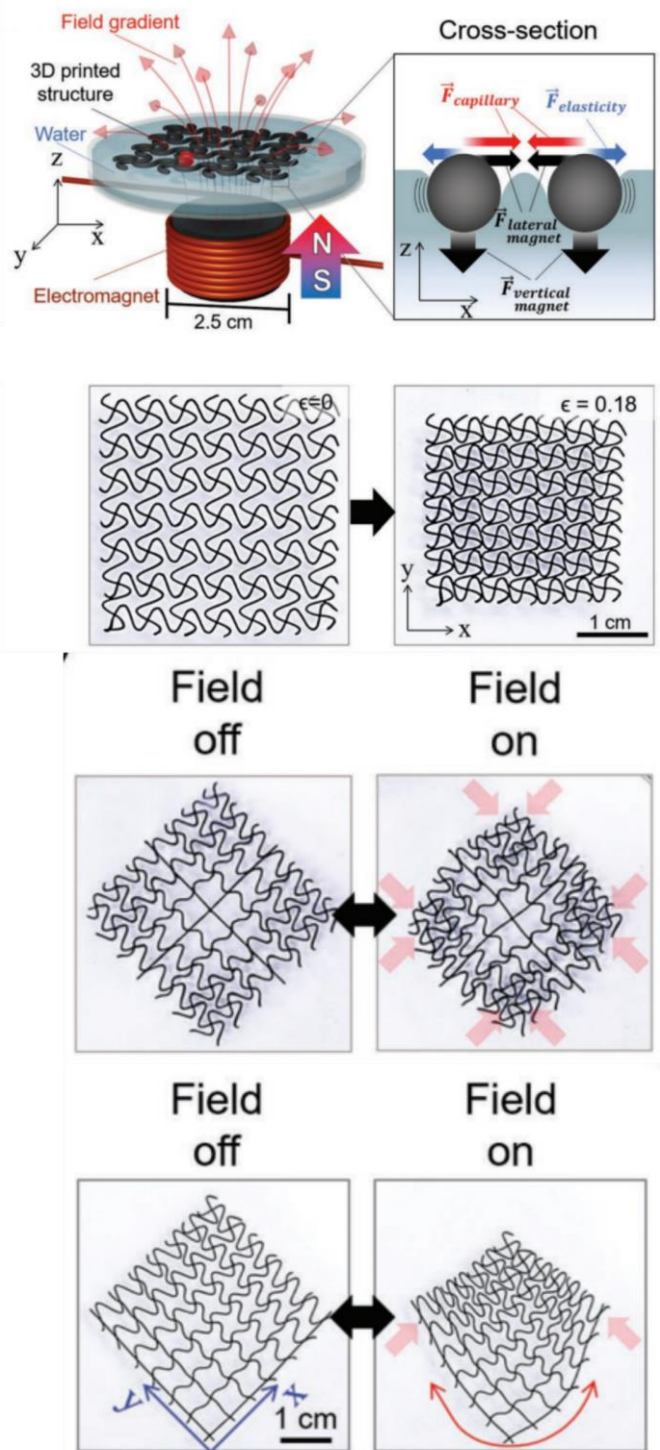
Figure 3.7 2D active metamaterial structures by Wu et al (2019). By strategically placing hinges and segments in three different 4 by 4 square grids of the same dimensions, different actuations can be achieved under a magnetic field.

More active metamaterial structures were made by Roh et al., 2019. They 3D printed a silicone material with iron nanoparticles in specific patterns of 3.6 cm width. Rather than relying on orientation direction of the particles, they actuated their structures by using the designed elasticity of line segments, achieved by printing them in specific (curved) shapes. The magnetic particles were pulled to the center of an electromagnetic field while the metamaterial structure was floating on water, causing it to collapse. By varying elasticity of the segments, different ways of collapsing could be realized (Figure 3.8).

### 3.2.2 Magnetic Shape Memory Polymers

Another form of magnetically activated smart materials is a rigid polymer with embedded magnetic particles that becomes soft when heated above its glass transition temperature ( $T_g$ ). This material is referred to as Magnetic Shape Memory Polymer (M-SMP; Ma et al., 2020; Ze et al., 2019). When soft, the material can be actuated just like a MSM by means of aligning the magnetic particles to an external magnetic field. When cooled, the now again rigid M-SMP material stays in its deformed shape. Ze and colleagues (2019) embedded two different types of magnetic particles in their M-SMP: Iron Oxide ( $Fe_3O_4$ ) and Neodymium-Iron-Boron (NdFeB). They heated up the M-SMP by means of inductive heating of embedded  $Fe_3O_4$  particles in order to deform the material by means of the NdFeB particles under a magnetic field (Figure 3.9).

Ma and colleagues (2020) created a M-SMP/MSM hybrid by making segments of M-SMP and MSM materials in the same product (Figure MSM-3). This allows for individual control of only the MSM or both the M-SMP and MSM simultaneously. Both the M-SMP and MSM contained NdFeB particles and heating/softening of the M-SMP materials was done by increasing environmental temperatures (Figure 3.10).



**Figure 3.8:** Active metamaterial structures by Roh et al. (2019), which collapses in different ways towards a magnetic field in the middle induced by an electromagnet. The way the structures collapse is controlled by varying stiffness of line segments.

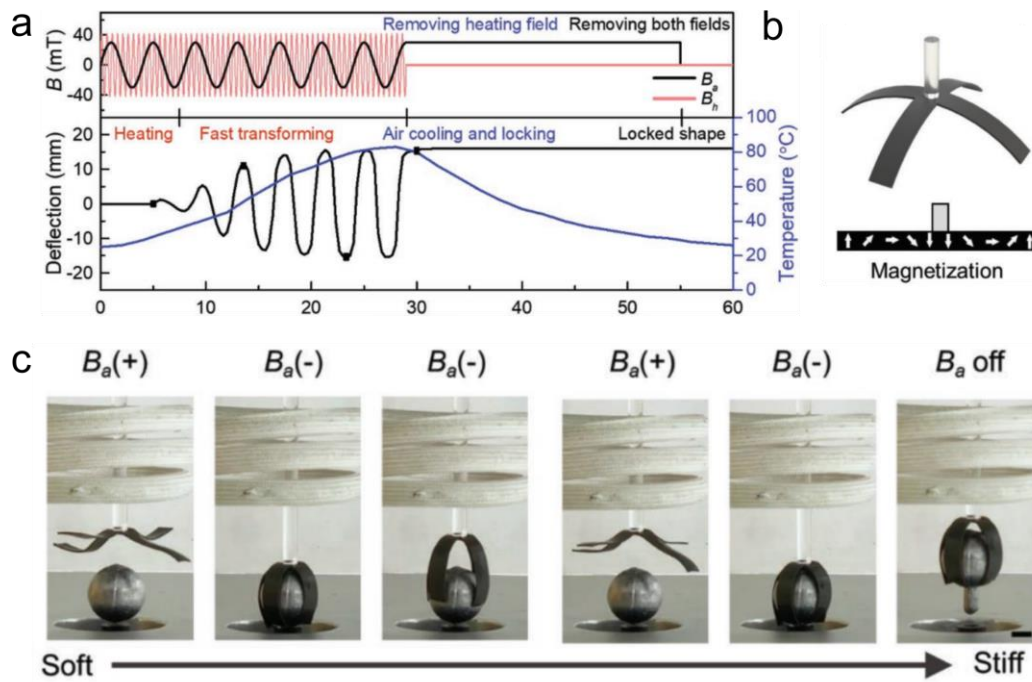


Figure 3.9: Ze et al (2019) made a M-SMP material that softens by induction heating of  $Fe_3O_4$  particles (magnetic field  $B_h$  - the red line) and is actuated by magnetic field  $B_a$  (a). NdFeB particles are magnetized according to a specific pattern (b) that allows a gripping movement (c).

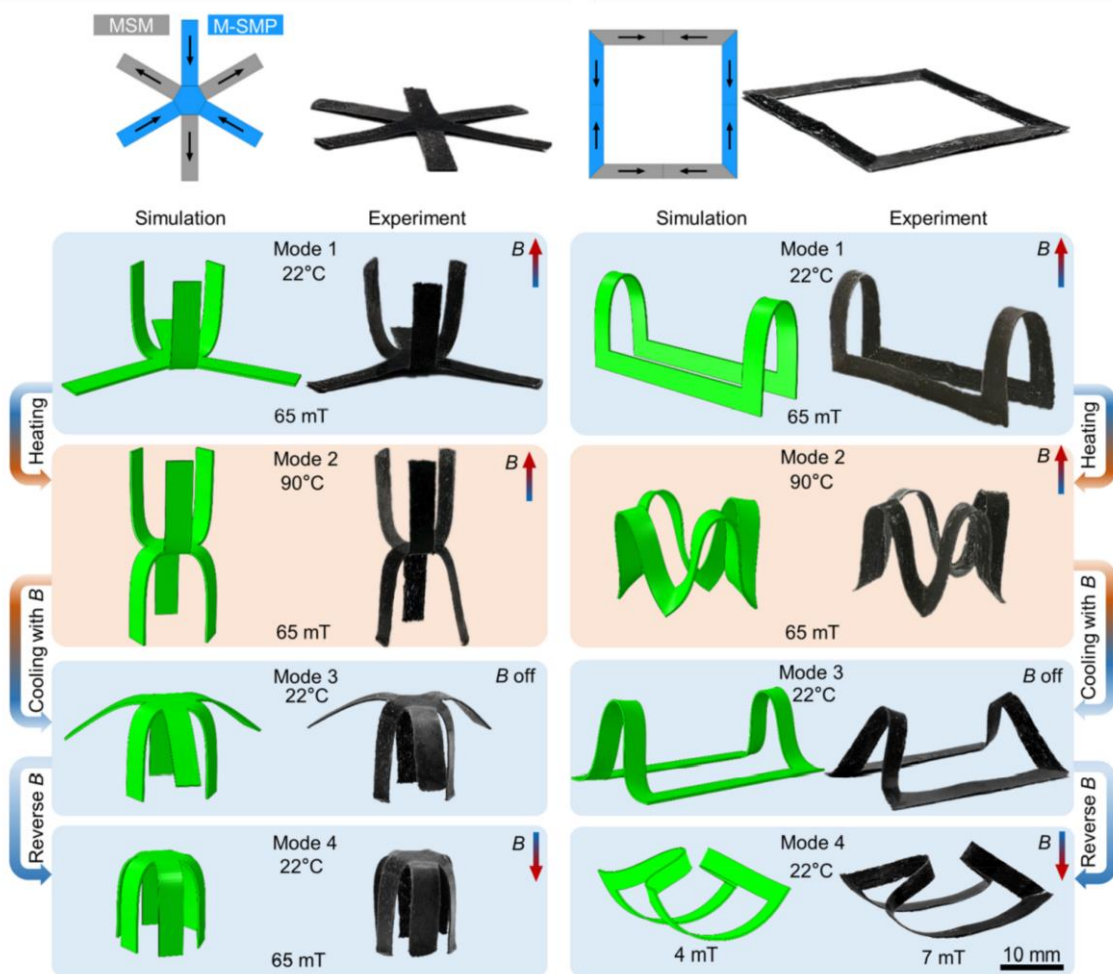
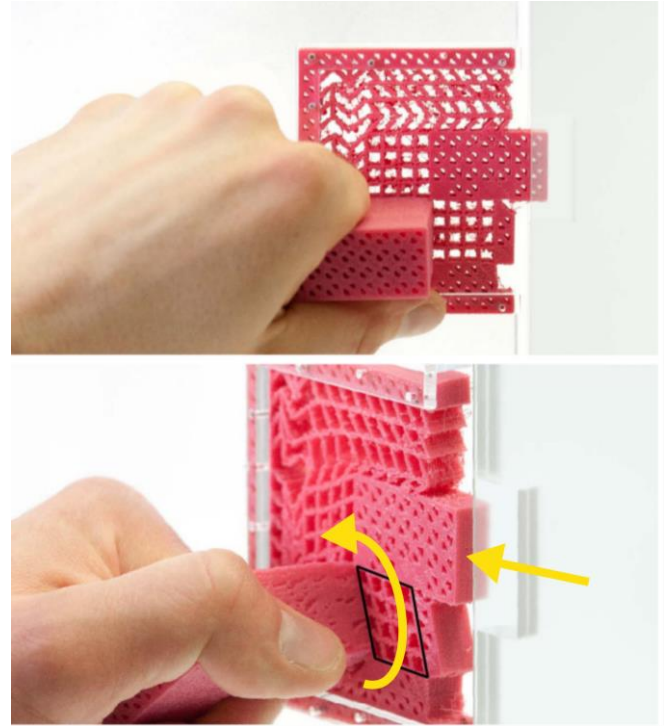


Figure 3.10: In the same objects, different segments of MSM and M-SMP are used. By heating and cooling the M-SMP material at certain moments, the designs can be morphed into a variety of shapes (Ma et al., 2020).

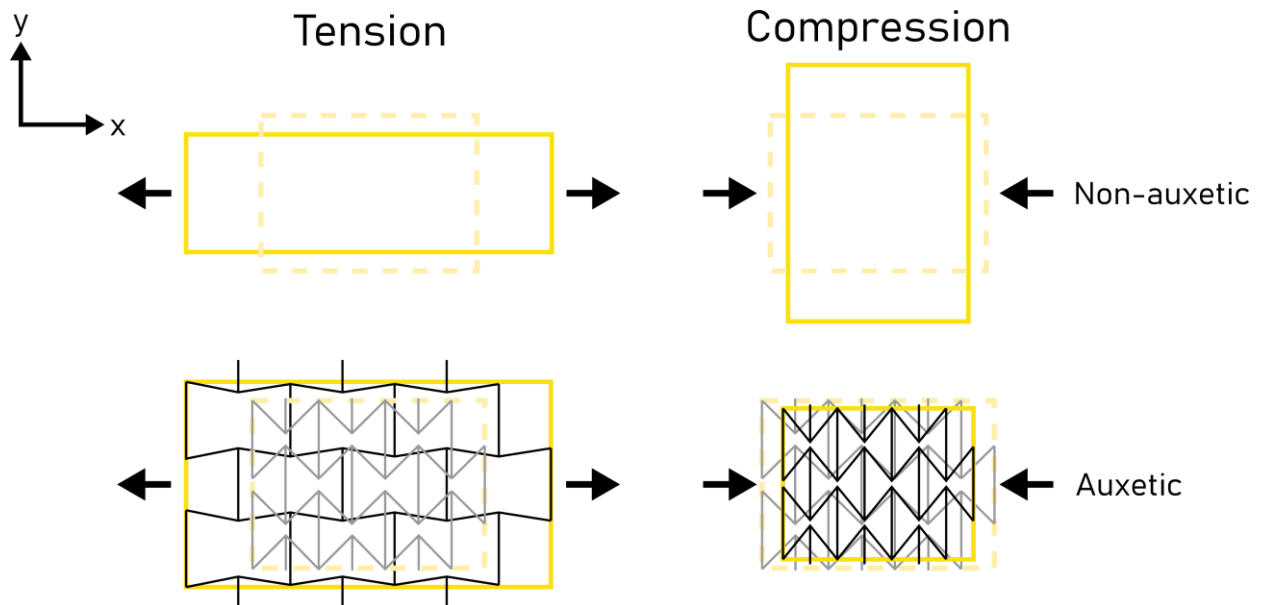
### 3.3 Metamaterials

Metamaterials are mechanisms composed of cell structures (Ion et al., 2016, 2017, 2019). The architecture of these cell structures allows for tuning of material properties that go beyond modification of the material composition (Surjadi et al., 2019). Auxetic structures for example have a negative Poisson's ratio, meaning they get wider when stretched (Ren et al., 2018; Novak, Vesenjajk & Ren, 2016; Liu & Hu, 2010b; Figure 3.11). Designing such a structure is challenging, because all the different cells are connected and constrain and influence each other (Ion et al., 2019). An example of such a mechanical cell structure where cells influence each other is the door hinge by Ion et al. (2016), where a rotating motion of a doorhandle is transformed into a linear motion of the latch (Figure 3.12). A transformation that would normally require a set of gears.

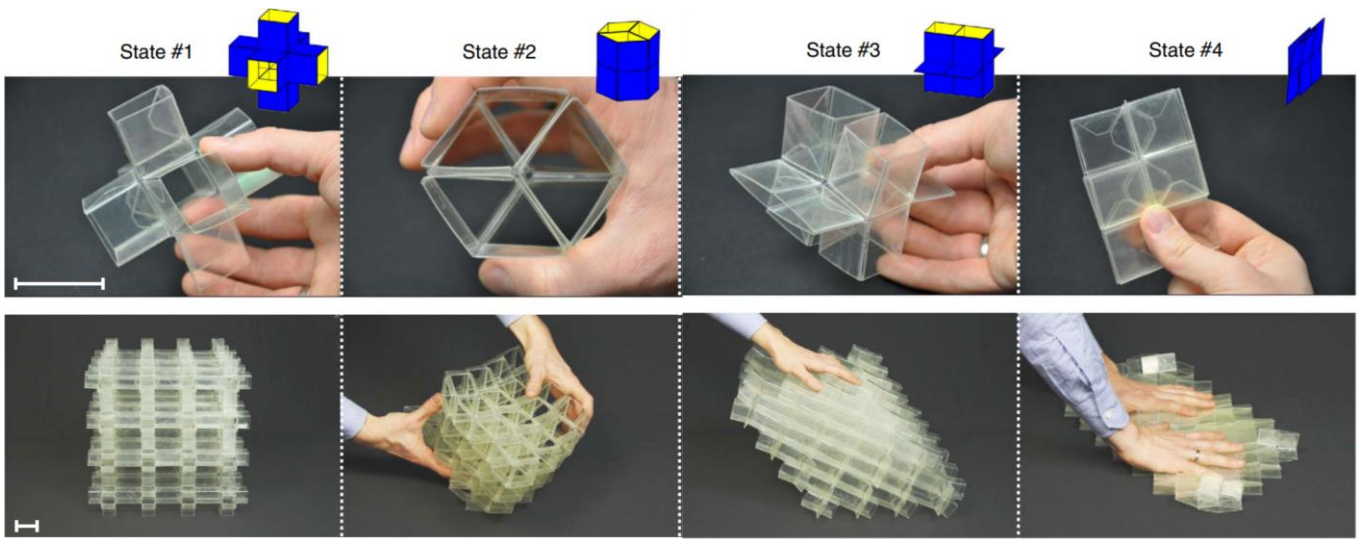
Besides cell structures, there are other mechanical systems that can be categorized under metamaterials. Origami and Kirigami (origami involving cutting) enable a material to make complex actuations, for example fast unfolding or locomotion (Rafsanjani, Bertoldi & Studart, 2019). Overvelde and colleagues (2016) developed a deployable 3D structure based on origami. The structure is stiff when deployed and can be folded into a flat sheet (Figure 3.12).



**Figure 3.12:** Metamaterial mechanism consisting of individual cells that transform a rotating motion into a linear motion (Ion et al., 2016).



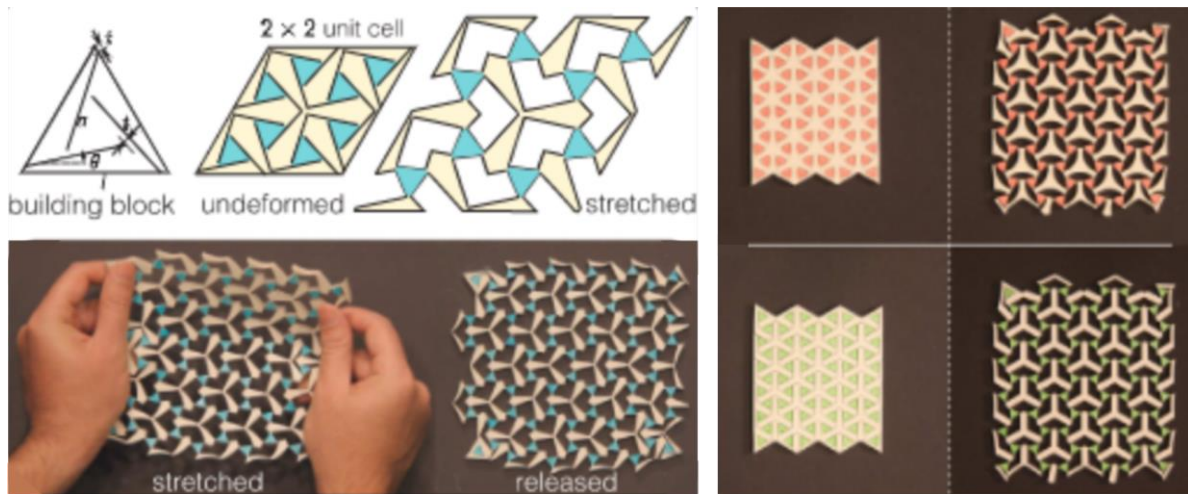
**Figure 3.11:** Auxetic metamaterial cell structures show a negative Poisson's ratio and thus show the same behaviour in X and Y direction. Non-auxetic materials with positive Poisson's ratio show the opposite behaviour in X and Y direction. Adapted from Novak, Vesenjajk & Ren, 2016 and Liu & Hu, 2010b.



**Figure 3.12:** Deployable metamaterial structure using folding principles of origami. A single cell (above) and a 3D structure of multiple cells (below; Overvelde et al., 2016).

Bistable mechanisms are mechanisms that have two stable states, somewhat like a switch. These mechanisms can also be categorized as metamaterial (Rafsanjani, Bertoldi & Studart, 2019) or incorporated into a cell structure as Rafsanjani & Pasini (2016) showed in their auxetic bistable metamaterial (Figure 3.13). Ion et al. (2017) incorporated bistable switches to make a digital lock mechanism for their door handle.

Many more applications of metamaterials and shape morphing materials can be found in literature besides the ones presented in this paragraph. Paragraph 3.4 aims to give an overview on these applications found in the researched literature in this project.



**Figure 3.13:** Bistable mechanism incorporated into an auxetic metamaterial structure. The bistable elements make the auxetic sheet remain in the stretched position (Rafsanjani & Pasini, 2016).

### 3.4 Applications

Magnetic soft materials are *Emerging materials*, meaning they are not well known to designers (yet) and thus rarely applied in product designs. To inspire and motivate engineers and designers, novel applications of these and other emerging materials need to be found and presented. In order to find appropriate and valuable application domains for MSM, a benchmark study has been conducted on applications of shape memory materials, metamaterials and MSM in literature. By also reviewing SMM and Metamaterials, it is attempted to find overlap in application domains and find areas where (metamaterials made from) MSM can be applied to the same or better effect.

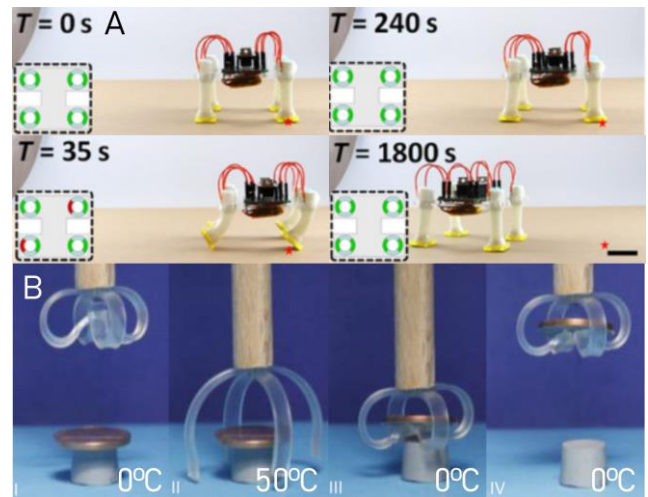
#### 3.4.1 Shape memory materials applications

Proposed applications of Shape memory materials can be found in a variety of fields, such as biomedical applications, aerospace engineering, soft robotics and human-machine interaction. This chapter aims to give an overview of these applications to find potential gaps in the application domain where new designs can be made for.

Table 3.1 holds a benchmark study of found application domains of SMM including some example designs found in literature. As stated in the project brief (Appendix A), special attention was given to the application of SMM in Active Disassembly; the automatic disassembly of products. An extended literature review of this can be found in Appendix B.

**Table 3.1:** Benchmark study of some examples of applications of shape morphing materials

#### Soft Robotics



**Source:** He et al., 2019 (A) and Behl et al., 2013 (B)

**Actuation:** Liquid crystal elastomer (LCE) based tubular actuator (A) and reversible, bidirectional shape memory polymer (rbSMP)

**Info:** By heating tiny wires inside the front and back of soft tubes, the legs of the robot can be moved to make it walk (A). With two-way (bi-directional) SMP, a gripping device is able to pick up a coin (A) the lifting is done manually.

#### Communication

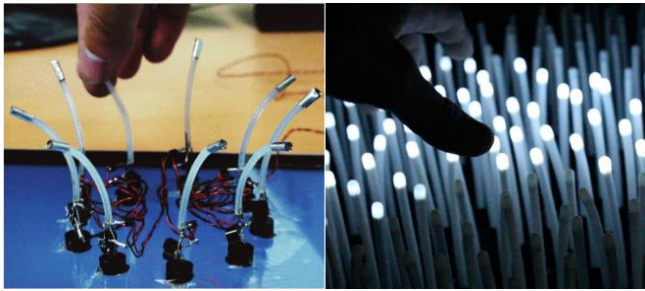


**Source:** Coelho & Maes, 2009

**Actuation:** Electronic heating of SMA

**Info:** These shutters consist of squares which can open by means of embedded SMA wires. They are meant to communicate messages in architectural context, for example by displaying abstract letters, as well as ventilation and daylight control.

## Interactive surface displays



Source: Nakayasu, 2016 and Nojima et al., 2013

Actuation: Electronic heating of SMA

Info: Surface comprised of a number of SMA wires with LED light at the top to form a display. SMA wires can move reacting to touch by conducting electricity.

## Human-machine interaction

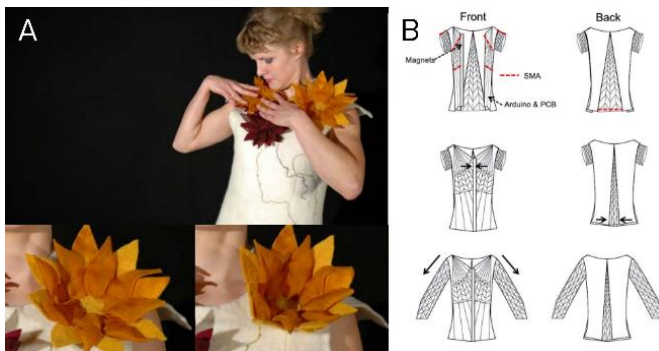


Source: Park, Park & Nam, 2015 and Nakagawa, Kamimura & Kawaguchi, 2012

Actuation: Electronic heating of SMA

Info: Additions to how people interact to mobile phones. SMA wires provide haptic feedback by moving soft structures on the devices.

## Clothing

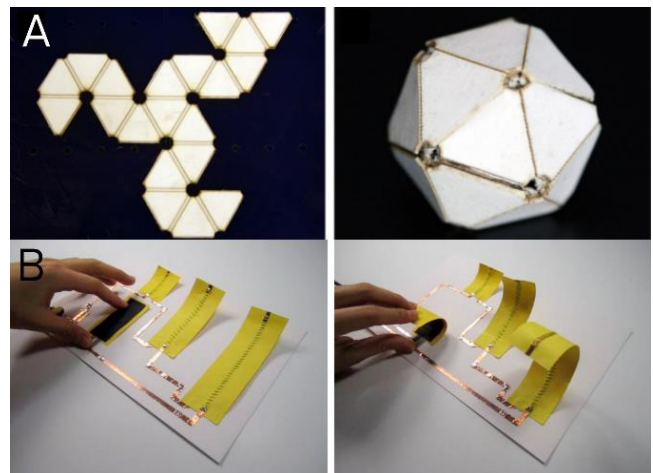


Source: Perovich, Mothersill & Farah, 2013 (A) and Lin et al., 2015 (B)

Actuation: Electronic heating of SMA

Info: Clothing with SMA wires embedded that make the fabric move for hedonic purposes (A) or functional purposes like making the process of putting on clothes easier for disabled people (B).

## Self-folding origami

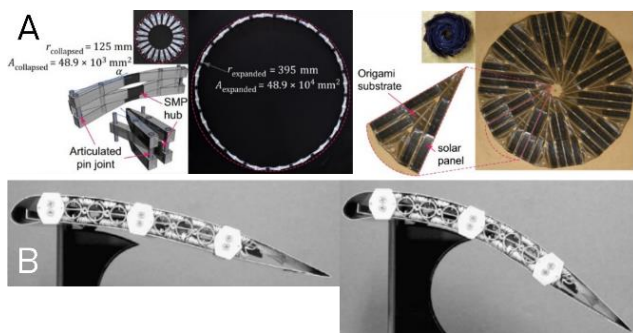


Source: Tolly et al., 2014 and Qi et al., 2012

Actuation: Ambient heating of SMP (A) and Electronic heating of SMA (B)

Info: By uniformly heating a folding pattern consisting of multiple layers, including a SMP layer), the pattern folds itself to a ball in 62 seconds (A). Similarly, SMA wires can be used to bend and fold paper (B).

## Aerospace systems

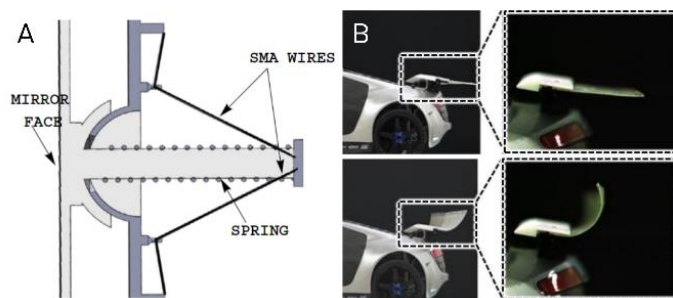


**Source:** Chen et al, 2019 (A) and Sofla et al., 2010 (B).

**Actuation:** SMP (A) and electronic heating of SMA (B)

**Info:** Because SMMs are light weight compared to motors, they are interesting to use in aerospace industry where saving weight is important. They can be used in opening a solar panel for satellites, where they move hinges in an origami structure (A) or to morph aircraft wings to achieve different aerodynamic properties, e.g. to generate more lift when landing (B).

## Automotive industry

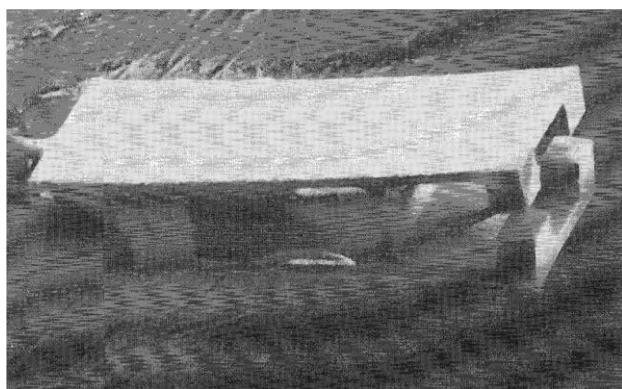


**Source:** Williams, Shaw & Elahinia (A) and Han et al., 2015 (B).

**Actuation:** Electronic heating of SMA

**Info:** Also in automotive industry, saving weight is beneficial. In the mentioned examples, a rear-view mirror is changed in angle by SMA wires rather than conventional motors (A). The spoiler, consisting of SMA and glass fiber wires embedded in a soft polymeric matrix, is able to morph its shape in order to achieve different aerodynamic properties (B).

## (Micro)actuators

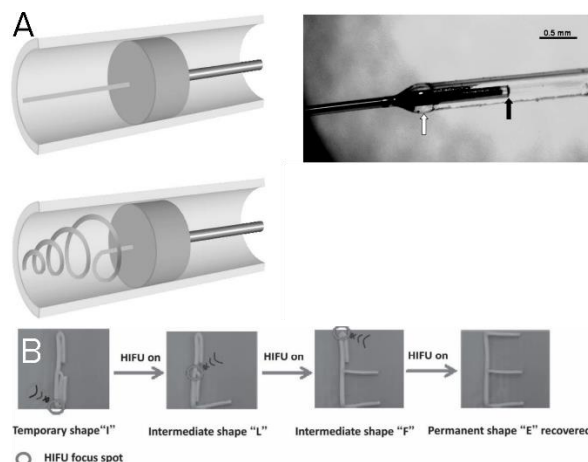


**Source:** Krulevitch et al., 1996

**Actuation:** thin film SMA

**Info:** Krulevitch et al managed to produce an actuator of just 0.9 mm long and 0.38 mm wide by using a thin film of 5  $\mu\text{m}$  Ni-Ti-Cu on top and bottom of the actuator.

## Biomedical



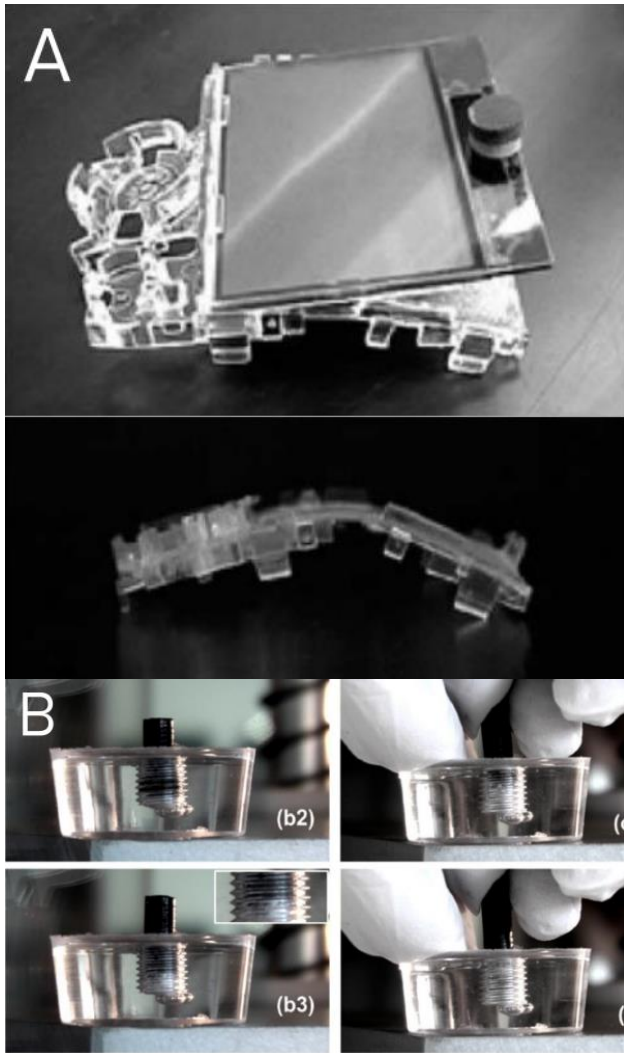
**Source:** Small et al., 2005 (A) and Han et al., 2013 (B).

**Actuation:** Heat induced by a laser directed at the SMP through an attached optic wire (A) and high intensity focused ultrasound (HIFU) irradiation (B).

**Info:** These biomedical devices can be used for removal of cloths in blood vessels by capturing them with the spiral end (A) or multi-stage drug delivery by opening and closing (individual) compartments with focused HIFU irradiation (B).



## Active disassembly



**Source:** Chiodo et al, 2000 (A) and Purnawali et al., 2012

**Actuation:** SMP

**Info:** The display bracket by Chiodo et al. (2000), folds open when heated, releasing the display which it holds (A). The PMMA SMP screw by Purnawali et al. (2012), loses its threads when heated, thus losing grip on the part it was screwed into and releasing it (B).

## Active disassembly review extension

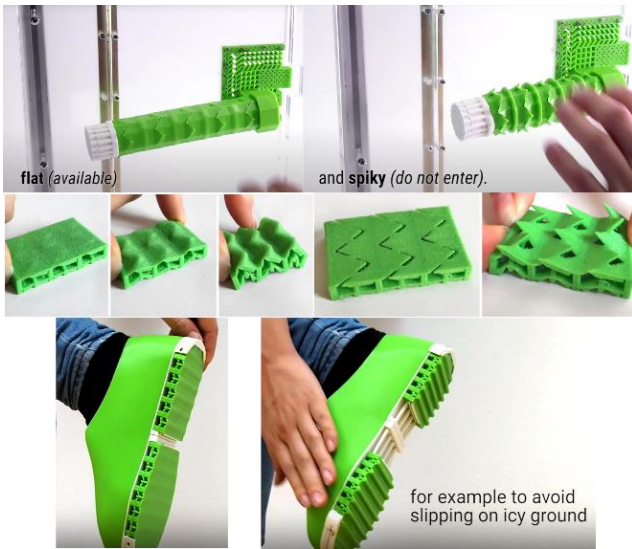
The use of MSM for active disassembly was a personal interest, defined in the original project brief. However, due to time constraints and increasing lack of faith this material could be valuably applied in this field, the idea was no longer pursued. Nonetheless, a more elaborate review has been done on the topic which was cut from this literature review to not interrupt the flow of the overall story. It can now be found in Appendix B for those who are interested

### 3.4.3 Metamaterial applications

Metamaterials are not commonly found in consumer products, but literature suggests various interesting mechanics and structures based on (auxetic) cell structures, origami and kirigami. Table 3.2 aims to give an overview of some of these proposed metamaterials and some possible applications, for example in soft robotics.

**Table 3.2:** Benchmark study of some proposed metamaterials and applications found in literature.

#### Changing textures

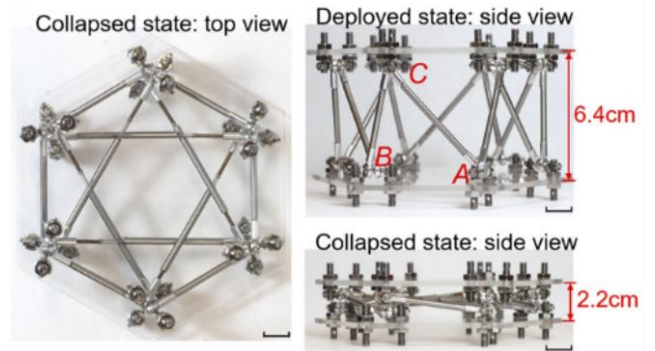
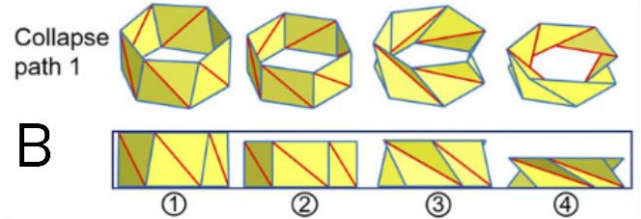
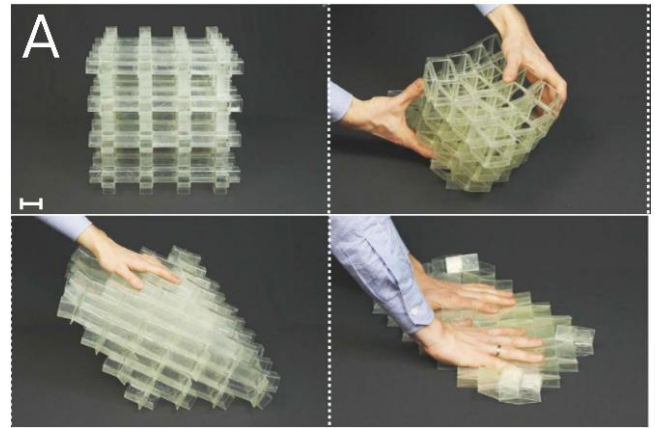


**Source:** Ion et al., 2018

**Actuation:** Folding of cells when external load is applied.

**Info:** These textures consists of metamaterial cells inspired by origami/kirigami that fold when compressed, causing the outer surface to wrinkle and thus change the smooth texture into a rough one. Including cuts make some spikes come out. It can be used for grip (shoe sole) or tactile communication (door handle).

#### Deployable structures

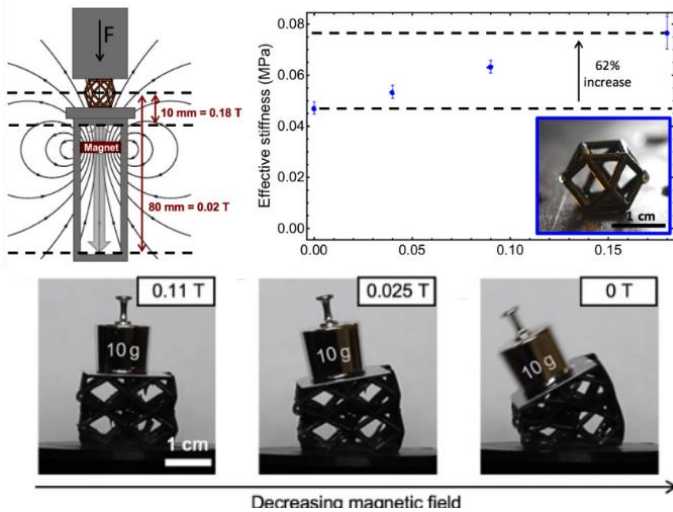


**Source:** Overvelde et al., 2016 (A) and Zhai, Wang & Jiang, 2018 (B).

**Actuation:** Kirigami (A) and Origami (B) inspired folding structures that collapse and/or expand under an external force.

**Info:** (A) consists of multiple cells that can be easily folded flat but are rigid when unfolded. (B) is a cylindrical tube (paper design and metal design consisting of rods in the same folding

## Variable stiffness

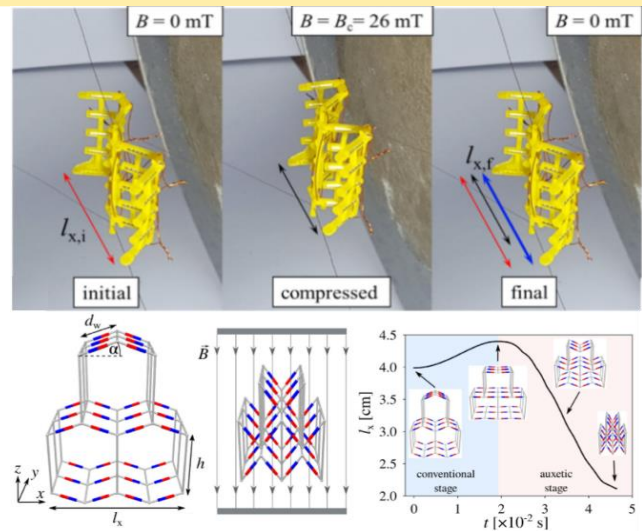


Source: Jackson et al., 2018.

**Actuation:** 3D lattice structure filled with magnetorheological (MR) fluid suspensions. The particles order themselves under the influence of the magnetic field.

**Info:** The 3D lattice structure was made by 3D printing and filled with the MR fluid afterwards. By applying a magnetic field, the structure showed a 62% increase in effective stiffness.

## Magnetically activated actuation

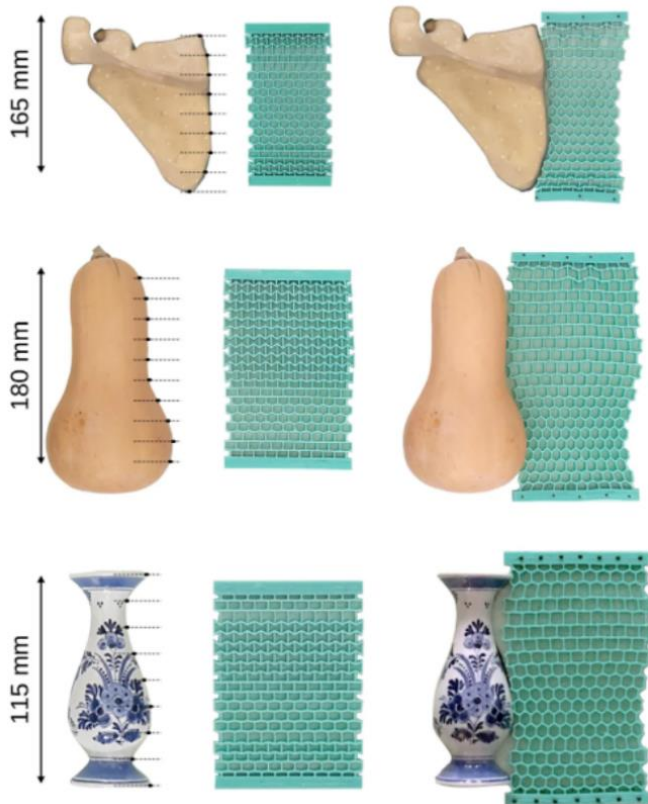


Source: Galea et al., 2022.

**Actuation:** An external magnetic field causes the embedded magnets to pull the (auxetic) segments, reconfiguring the metamaterial structure.

**Info:** Galea et al. use embedded magnets rather than nano powders used in MSM. They propose some applications of their design such as smart filters that open and close their apertures and deployment of medical devices.

## Shape matching soft metamaterials

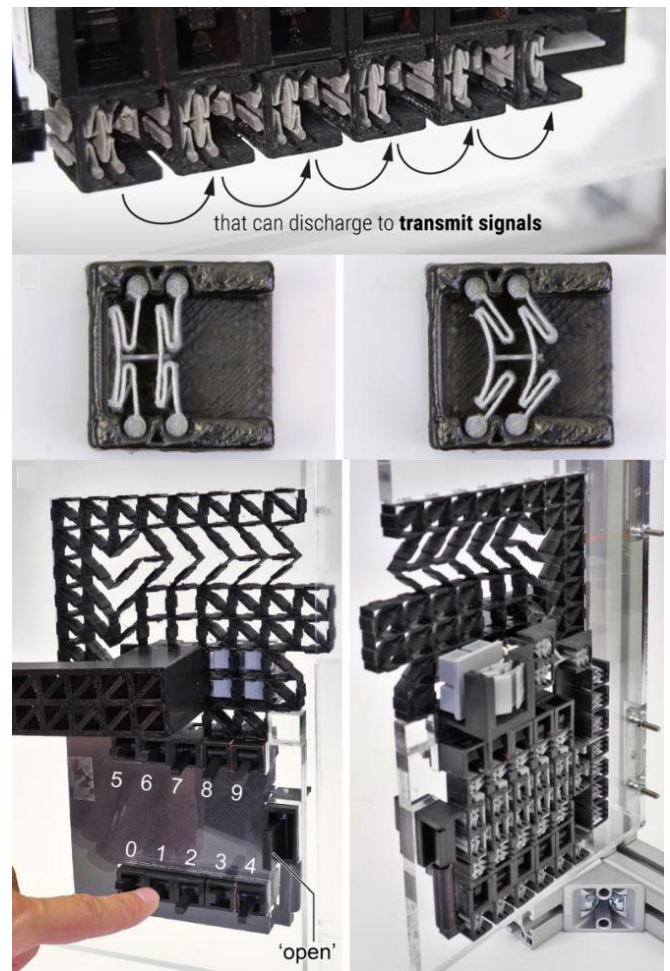


Source: Mirzaali et al., 2018

**Actuation:** Combination of auxetic and normal unit cells cause a deformation when the material is stretched under external load.

**Info:** The combination of auxetic and normal unit cells cause the material to widen in certain areas and so shaping the outer edge in the same curve as the object.

## Digital mechanical systems

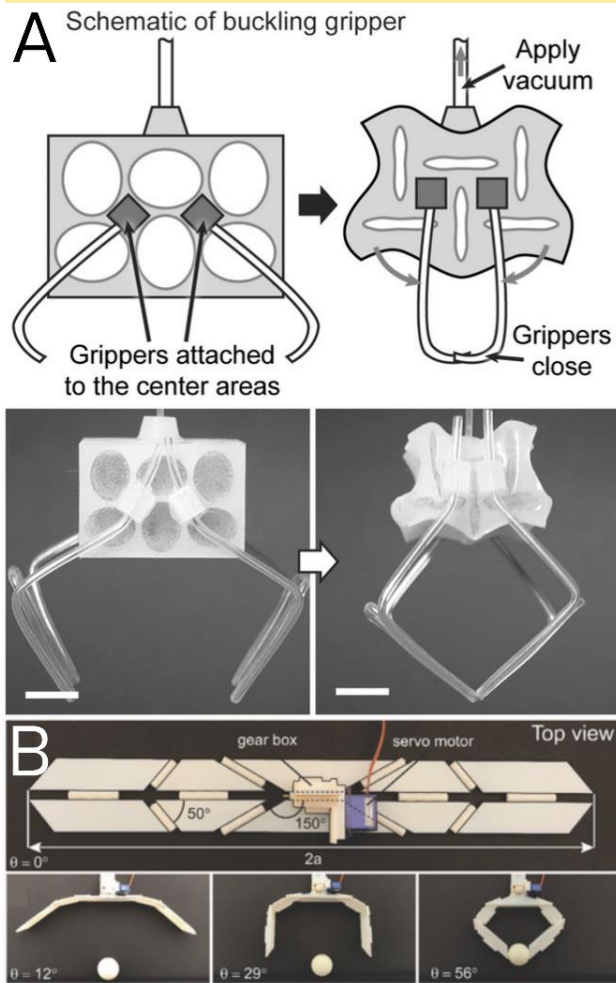


Source: Ion et al., 2017

**Actuation:** Bistable mechanisms in some cells transfer a digital mechanical system and movement of the latch is done with interacting cells actuated by an external force.

**Info:** Bistable systems have two states and can therefore be used to transfer a digital signal (on or off) mechanically. Using a chain of these cells results in a movement at the end of the chain, in this case unlocking the lock. The signal can be jammed with the use of blockers

## Soft robotic grippers

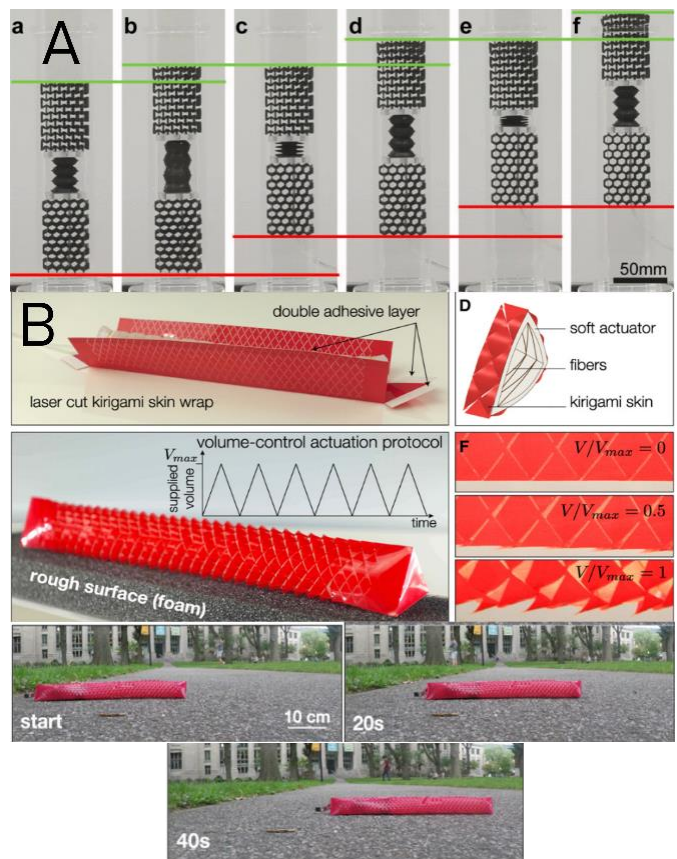


**Source:** Yang et al., 2015 (A) & Kamrava et al., 2018 (B).

**Actuation:** Pneumatic contraction of chambers (A) and origami folding by means of servo motor (B).

**Info:** (A) uses a structure with collapsible chambers by vacuuming in a predefined orientation so that the grippers attached to this structure close. (B) Uses an origami folded sheet with hinges or folding lines attached to a servomotor. When the motor spins, the middle hinge is folded causing the gripper to close.

## Crawling soft robotics



**Source:** Mark et al., 2016 (A) & Rafsanjani et al., 2018 (B).

**Actuation:** Pneumatic linear actuator (A; middle part and soft elastomeric actuator (B).

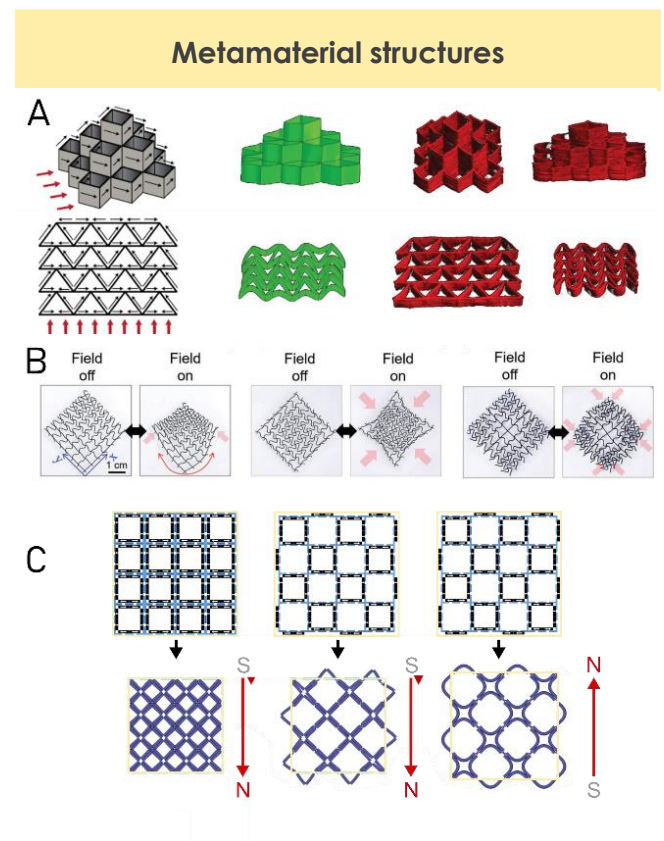
**Info:** (A) by the interaction between auxetic structure that expands under tension (top) and normal structure that compresses under tension (bottom), the crawler is able to press itself against the tube, preventing it to fall down. In the snake-like kirigami skin of (B), the scales move in and out depending on inflation of the inner tube, making the scales act like tiny feet.

### 3.4.4 Magnetic Soft Material applications

Magnetic Soft Material has been used in a small selection of applications, mainly in the biomedical field (drug delivery and endoscopy) and (very) small scale soft robotics.

Table 3.3 aims to give a (far from complete) overview of current applications of MSM that show the unique characteristics of this material.

**Table 3.3:** Benchmark study of found applications of MSM in literature.

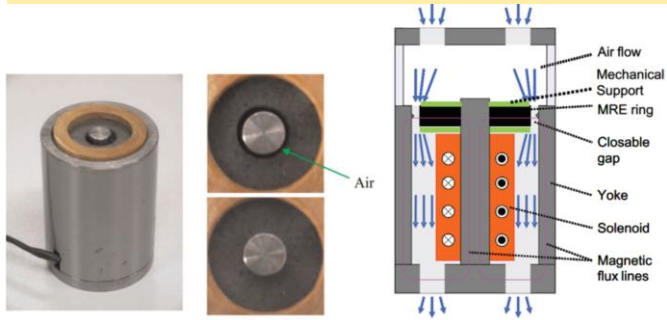


**Source:** Kim et al., 2018 (A), Roh et al., 2019 (B) and Wu et al., 2019 (C)

**Actuation:** Alignment of magnetized NdFeB particles in elastomer matrix (A, C) and attraction of Iron particles towards an electromagnet in the center (B).

**Info:** Metamaterials consisting of cell structures that contract based on the magnetization pattern of embedded NdFeB particles in the segments (A, C) or stiffness of segments when Fe particles get attracted towards a magnet in the center. In (C), the segments are attached with asymmetric joints.

## Mechanical components

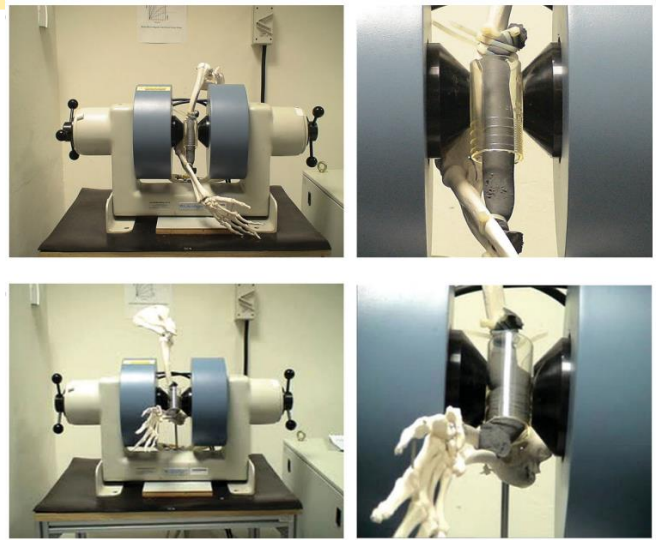


Source: Böse, Rabindranath and Ehrlich, 2012.

**Actuation:** Air valve made from MSM film. A ring opens and closes a little when magnetic field is applied.

**Info:** Iron particles embedded in silicone elastomer, cured under the presence of an magnetic field to arranged the particles in radially oriented chains.

## Artificial muscles

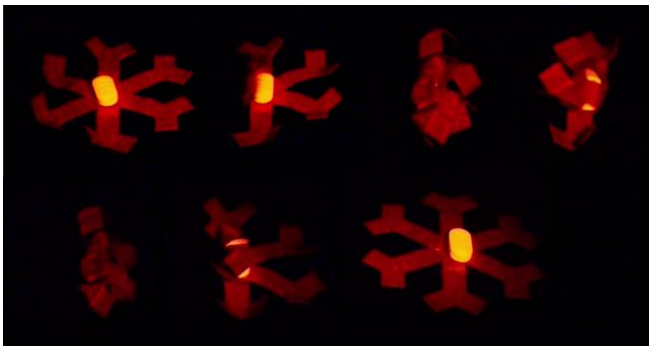


Source: Nguyen, Ahmed & Ramanujan, 2012.

**Actuation:** A elastomer “muscle” in between two electromagnets contracts, pulling the arm up.

**Info:** Large magnetic field (1T) is used to contract the “muscle” with Fe particles embedded in elastomer material.

## Biomedical (drug delivery)

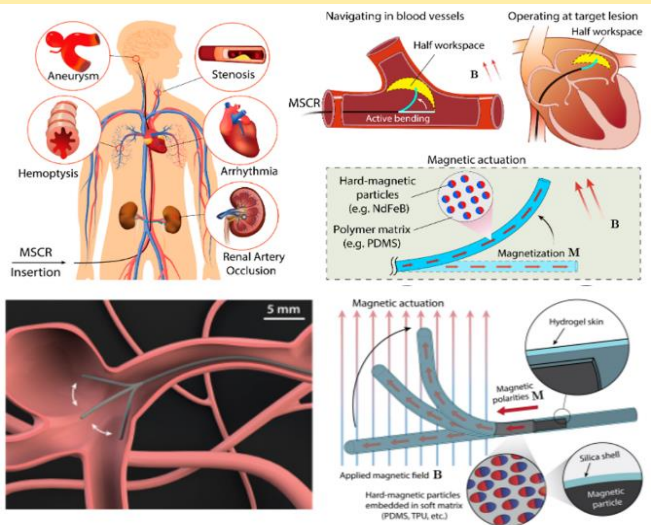


Source: Kim et al., 2018.

**Actuation:** Star like device that raps itself around a pill when magnetic field is applied, rolls and unfolds to deliver the drug while moving the magnetic field.

**Info:** Magnetic pattern achieved by 3D printing a silicone with 20 vol% NdFeB particles, aligning the magnetized NdFeB particles by using an (electro)magnet attached to the nozzle.

## Biomedical (Vascular) endoscopy

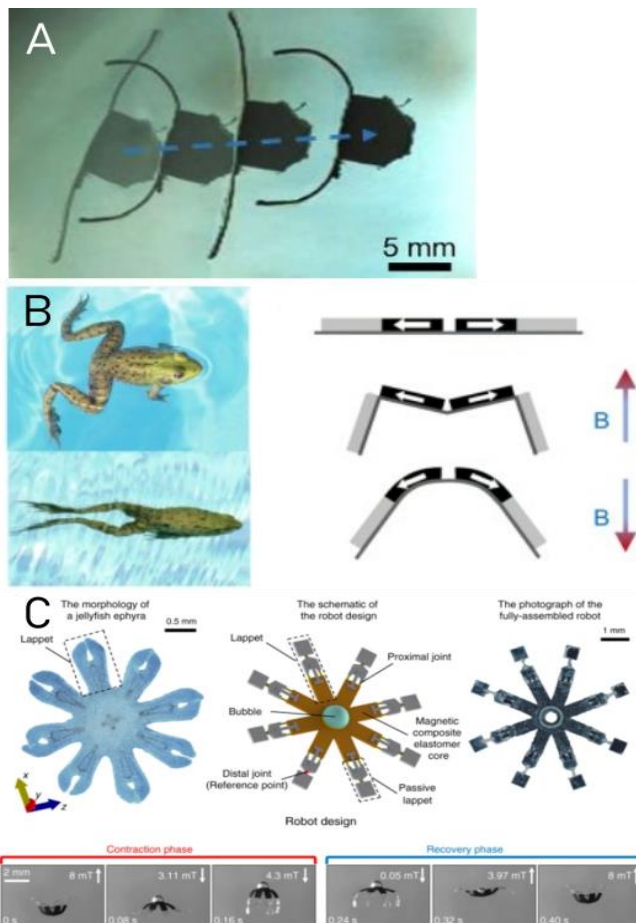


Source: Wang et al., 2021 and Kim et al., 2019

**Actuation:** End of a guiding wire made out of elastomer material with embedded magnetic particles that allows for steering in narrow spaces by (electro)magnets outside the body.

**Info:** The MSM tip can be made by casting the material and magnetizing in one direction or 3D printing a line with pre-magnetized particles aligned in one direction by a magnet attached to the nozzle.

## Soft robotic swimming objects

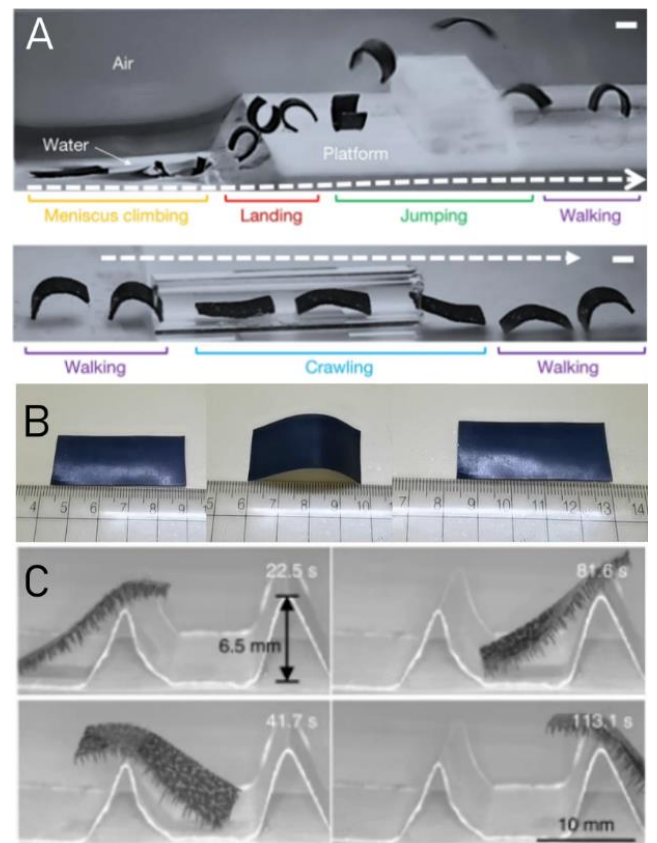


**Source:** Lum et al., 2019 (A) Wu et al., 2019 (B) and Ren et al., 2019 (C)

**Actuation:** Changing direction of external magnetic field morphs a magnetic particles embedded elastomer.

**Info:** Same kind of motion is achieved in different ways. (A) and (C) use multi-directional magnetic patterns by magnetizing the elastomer while folded into a specific shape, while (B) uses one-directional patterns with asymmetric joints.

## Soft robotics crawling objects



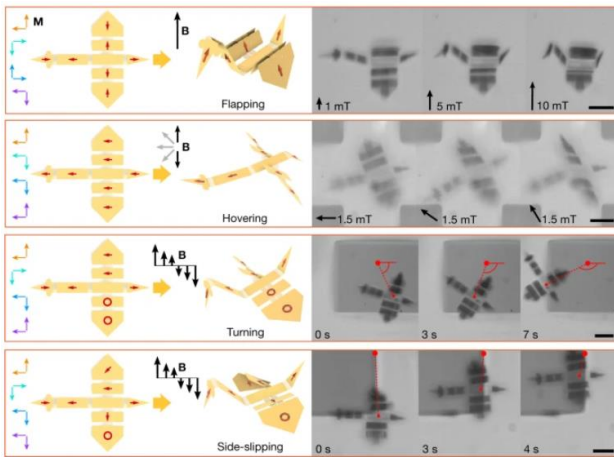
**Source:** Hu et al., 2018 (A), Wang et al, 2022 (B) Lu et al., 2018 (C)

**Actuation:** Changing direction of external magnetic field morphs an magnetic particles embedded elastomer.

**Info:** (A) is made by magnetizing a strip of NdFeB particles embedded elastomer after curing rolled around a tube. (B) is made by 4D printing PDMS elastomer with magnetized Fe<sub>304</sub> particles. (C) is made by curing a sheet of PDMS silicone with iron particles while a magnetic field is applied, resulting in the spikes or "legs".



## Self-folding sheets

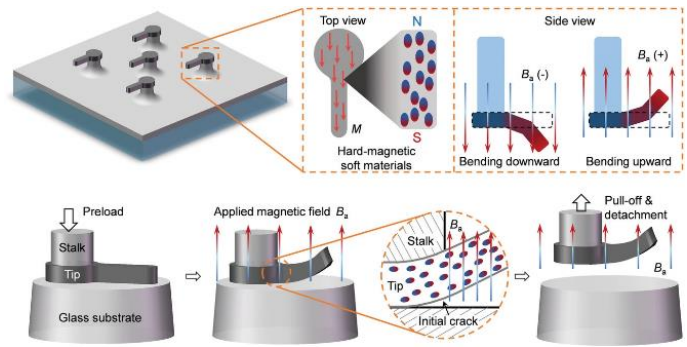


Source: Cui et al., 2019

**Actuation:** Microscopic sheets with nanomagnets in different directions connected through a soft fabric that allows for twisting and bending movements of the sheets.

**Info:** The panels containing nanomagnets are rigid and can only move because of the soft spring hinges between them, Nanomagnets are magnetized after incorporating them into the sheets and are actuated by external magnetic fields.

## Smart adhesive

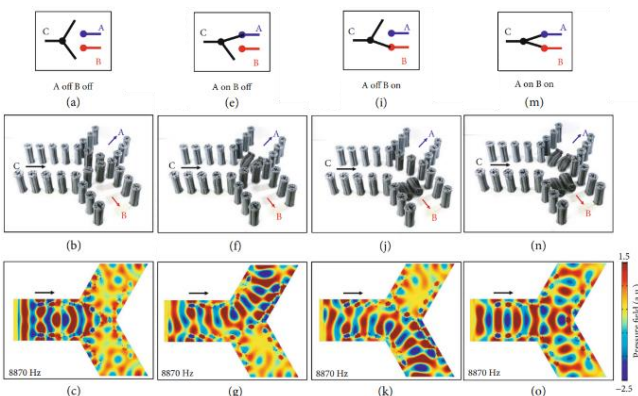


Source: Zhao et al., 2022

**Actuation:** Up or down movement of magnetized NdFeB particles in elastomer MSM by applying magnetic field in up or down direction.

**Info:** This smart adhesive is made out of a large number of MSM tips with a tail. By applying a magnetic force in the upward direction, making the tail bend upward, a crack is initialized between the tip and the object (glass substrate) causing the clamping force to degrees from 5 to 1 mN.

## Acoustic control

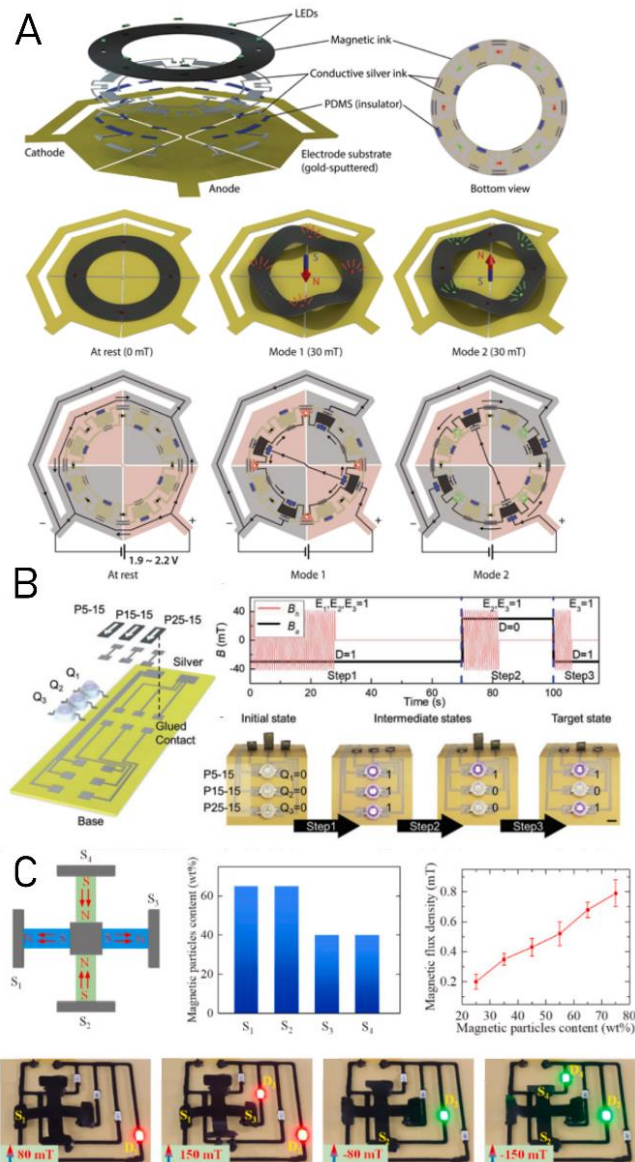


Source: Lee et al., 2020.

**Actuation:** Iron nanoparticles filled elastomer compound is collapsed by a magnetic field as the iron particles attract to the magnet, pulling the elastomer pillar with it.

**Info:** The standing pillars block or dampen the acoustic waves. By opening and closing the paths by collapsing the corresponding pillars with a magnet, the waves can travel more freely and the direction they travel in can be controlled. The design was inspired by shark skin.

## Electrical circuits

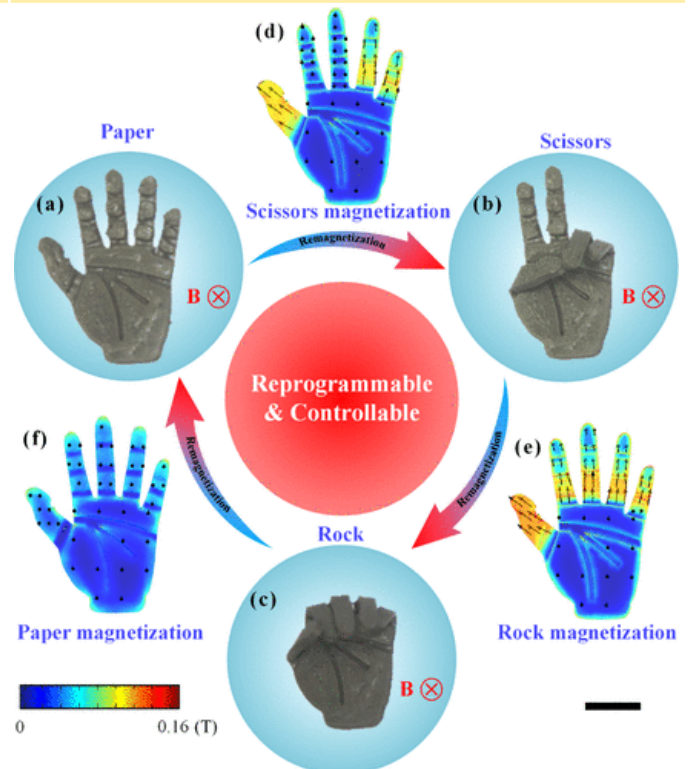


Source: Kim et al., 2018 (A), Ze et al., 2019 (B) and Wang et al., 2022 (C)

**Actuation:** Elastomer embedded with magnetized NdFeB particles (A) and Fe<sub>3</sub>O<sub>4</sub> particles (B) and M-SMP material with Fe particles for inductive heating and NdFeB particles for actuation of strips (B).

**Info:** Different electronic circuits are opened or closed by actuating the MSM/M-SMP materials. The MSM/M-SMP material act like switches, activated by external magnetic fields.

## Rock-paper-scissors game



Source: Zhang et al., 2021.

**Actuation:** Applying external magnetic field to magnetized NdFeB filled silicone.

**Info:** Zhang et al. used direct ink writing to 4D print various objects including this hand using PDMS elastomer filled with NdFeB particles which was magnetized after the printing process. One hand can only make Rock and Paper or Scissors and paper..

### 3.5 Relationships between metamaterials, SMA and MSM

The previous paragraph provided an overview of applications of shape memory materials, metamaterials and magnetic soft materials. In these applications, some overlap can be found. In this paragraph, the aforementioned material categories are compared to each other by means of a VENN diagram. This way, overlaps in application domains are identified. These overlaps and possible gaps are later used as inspiration for an MSM demonstrator product design where the characteristics of the material could be put to valuable and effective use.

#### 3.5.1. VENN Diagram

Figure 3.14 shows a VENN diagram containing all applications mentioned in the benchmark study. Overlap can be observed in the fields of soft robotics, biomedical and (active) metamaterials. Also, some less obvious relations can be found when observing the found applications. Lastly, there are also some gaps in the application domain of MSM that are found in the applications of the other material types.

##### *Biomedical - Figure 3.15*

In both SMM and MSM, biomedical applications are popular, both in drug delivery (Han et al., 2013; Kim et al., 2018) as endoscopic devices (Small et al., 2005; Kim et al., 2019). SMM are activated with attached wires inside the body, as they often need heat or another trigger that cannot pass through tissue effectively. MSM offer an advantage as magnetic fields can pass through tissue without harm. However, SMM seem more suitable for grabbing obstacles such as cloths inside the body, as MSM actuators cannot output much force. A combination device of a SMM gripper and MSM steering mechanism could be an interesting direction to follow.

##### *Self folding objects – Figure 3.16*

There is also overlap between the use of SMM and MSM for self-folding objects. However, the objects made with SMM will likely stay in their folded position once the stimuli has been removed, while the magnetically actuated object will unfold again when the magnetic field has been removed,

##### *(Active) metamaterial structures – Figure 3.17*

Metamaterial objects in a popular demonstrator for MSM Kim et al., 2018; Roh et al., 2019; Wu et al., 2019). It is therefore not a surprise that there is an overlap between metamaterials and MSM. Compressed auxetic structures that decrease in both length and width are reported, e.g., Kim et al., 2018 and Wu et al., 2019. A 3D auxetic structure is proposed and conceptualized by Galea et al., 2022, however not realized physically as of now.

##### *Acoustic control – Figure 3.18*

Lee et al. (2020) proposed the control of acoustic waves with a MSM structure which they classify as a metamaterial. While other acoustic metamaterials are not presented in this benchmark, there are more examples

##### *Crawling soft robotics – Figure 3.19*

Soft robotics are explored to great extend in all three materials described. Documented MSM soft robots are generally very small and controlled remotely, while metamaterial or SMM crawling robots often need some wire attached to heat up the SMA wired or otherwise actuate the material.

##### *Grippers – Figure 3.20*

Grippers made out of SMM and metamaterials are reported. However, a MSM gripper without the use of M-SMP material is not found. MSM probably does not have the load bearing capacity to grip, hold and lift an object beyond a few milligrams.

# Shape Memory Materials

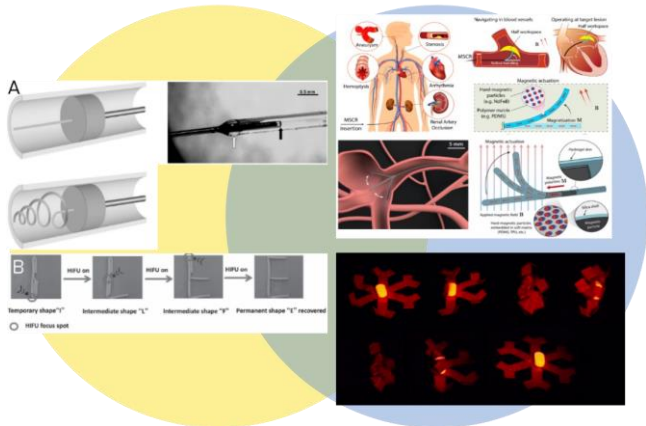


Metamaterials

Magnetic Soft Materials

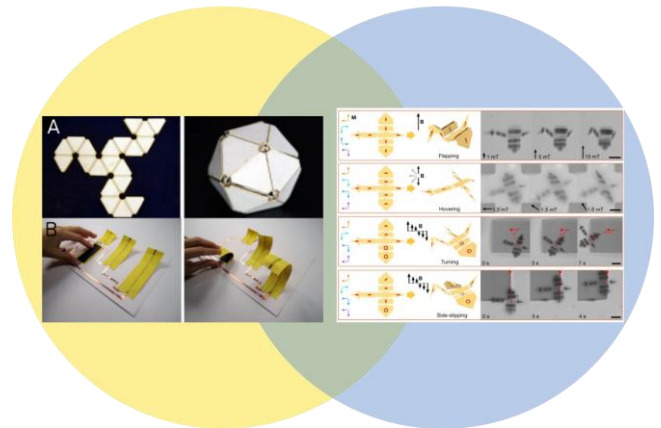
Figure 3.14: VENN diagram of applications found in literature benchmark study for shape memory materials, magnetic soft materials and metamaterials. Overlap can be seen between all three material types.

## Biomedical



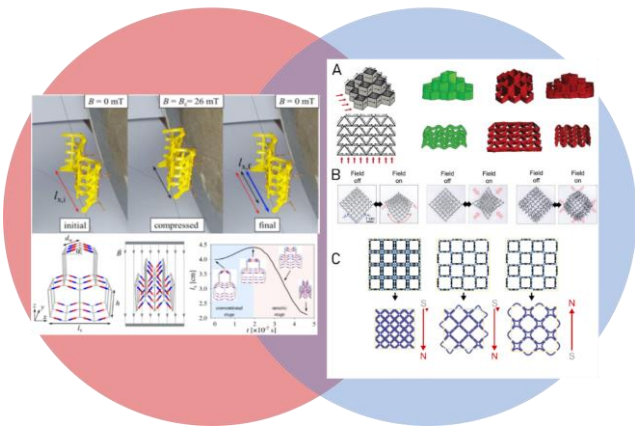
**Figure 3.15:** Overlap between SMM and MSM in biomedical applications (Small et al., 2005; Han et al., 2013; Kim et al., 2018, 2019 and Wang et al., 2021).

## Self folding objects



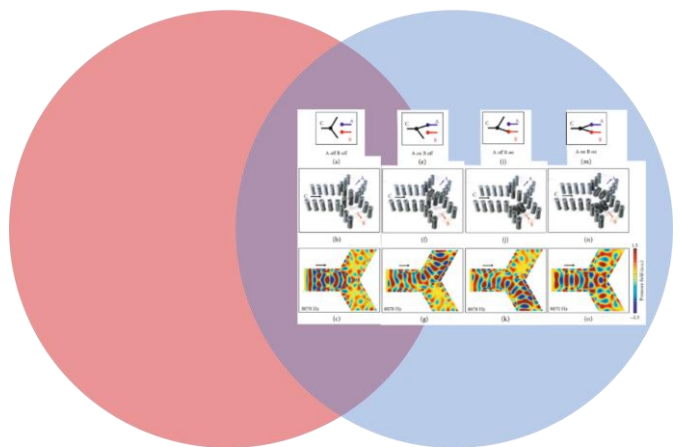
**Figure 3.16:** Overlap between SMM and MSM for self folding objects (Tolly et al., 2014; Qi et al., 2012 and Cui et al., 2019).

## (Active) metamaterial structures



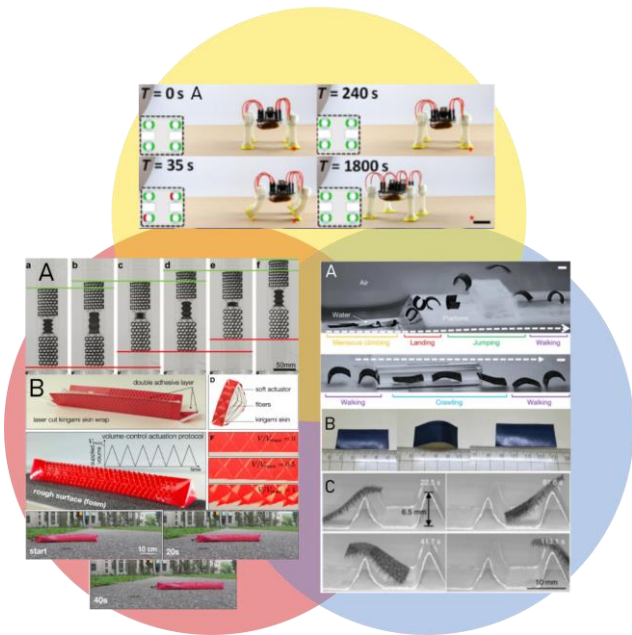
**Figure 3.17:** Found overlap in active (magnetic) metamaterials and MSM metamaterial structures (Galea et al., 2022 and Kim et al., 2018).

## Acoustic control



**Figure 3.18:** The acoustic wave control system by Lee et al. (2020) can also be categorized as a metamaterial (Lee et al., 2020).

## Crawling soft robots



**Figure 3.19:** Crawling soft robots are popular in all three material fields (He et al., 2019; Mark et al., 2016; Rafsanjani et al., 2018; Hu et al., 2018; Wang et al., 2022 and Lu et al., 2018).

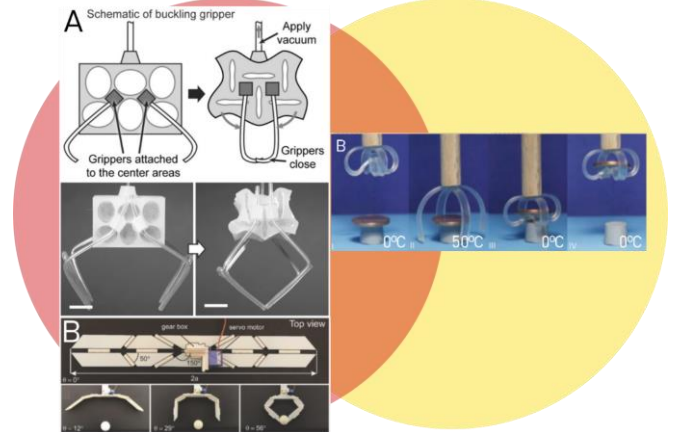
### 3.5.2 Indirect relationships

Besides obvious overlaps in applications between the three materials, there are indirect relations that can be identified between the found use of the materials. These indirect relations can lead to less obvious, more novel application ideas of MSM.

#### Digital systems - Figure 3.21

Ion et al. proposed a digital metamaterial mechanism composed of bistable systems. The term digital here refers to having two digits or states, 0 (on) and 1 (of), which is achieved by the bistable mechanism that can be in one state (0) or the other (1). MSM are used in digital systems but in another way; by incorporating them in a digital electronic circuit, where they turn on or off LED lights. It would be interesting to think of MSM as bistable switch that could activate for example an electronic circuit and stay activated once the magnetic field is removed and can be de-activated once the magnetic field is reversed.

## Grippers



**Figure 3.20:** Grippers are a popular object made with SMM and metamaterials, but when wanting to make a gripper out of MSM, a M-SMP material is needed (Yang et al., 2015; Kamrava et al., 2018 and Behl et al., 2013).

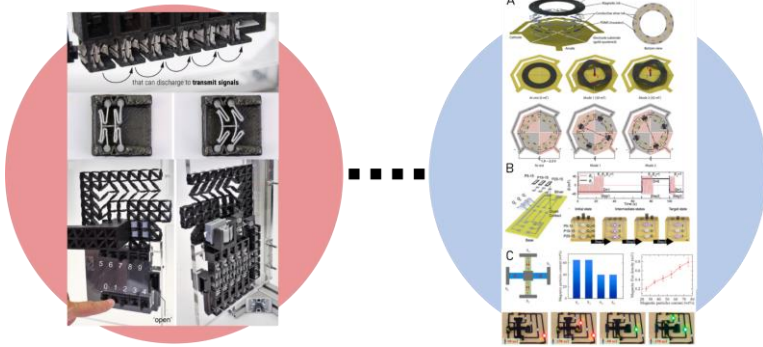
#### Deployable structures – Figure 3.22

Metamaterial deployable structures are rigid once deployed but can be folded flat. Kim et al. (2018) proposed a structure that can be folded flat when a magnetic field is applied. It therefore shows a resemblance to deployable metamaterials, however it was not proposed for this purpose.

#### Active Disassembly – Figure 3.23

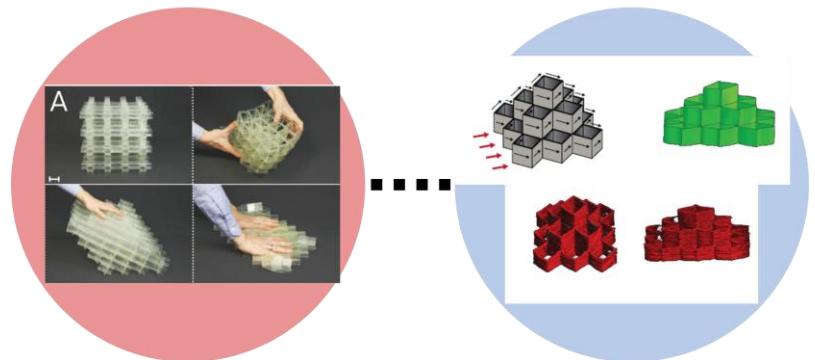
Although no direct use of metamaterials or MSM has been reported for active disassembly, some proposed application might be suitable. For example, the shape matching metamaterial structure proposed by Mirzaali et al. (2018) might be suitable to fill wholes and so clamp two components together. The smart adhesive by Zhao et al. (2022) cannot hold much force (5nN), but maybe a larger surface area or more contact points can make it suitable for an adhesive that can be used for “gluing” components together and actively releasing them.

## Digital systems



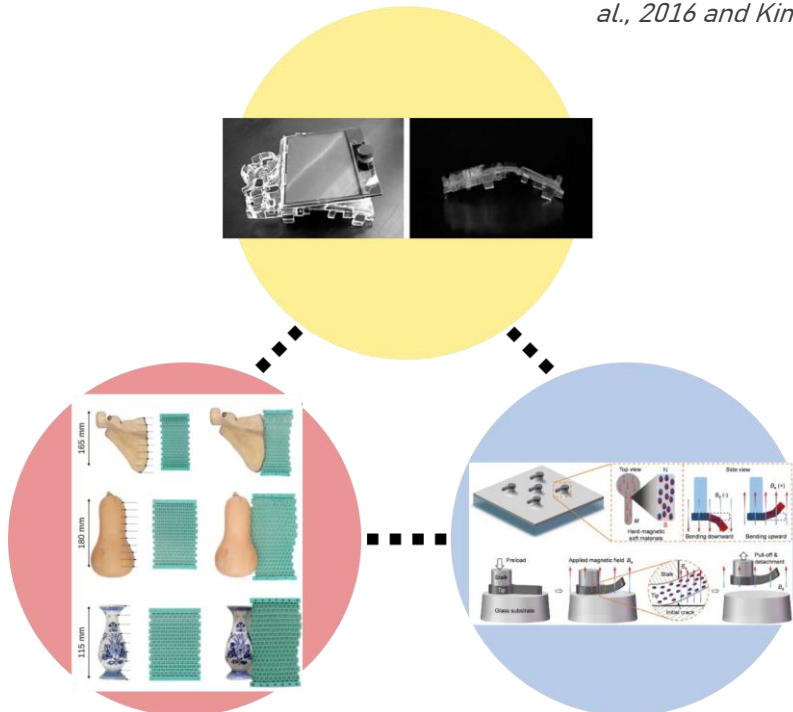
**Figure 3.21:** Bistable metamaterial structures can be seen as digital systems as they have two states. A parallel can be drawn towards digital electrical systems seen in MSM literature (Ion et al., 2017; Kim et al., 2018; Ze et al., 2019 and Wang et al., 2022).

## Deployable structures



**Figure 3.22:** Kim et al. (2018) demonstrated a foldable 3D structure. Could such a structure be used as a magnetically deployable structure that is rigid once deployed (Overvelde et al., 2016 and Kim et al., 2018).

## Active disassembly



**Figure 3.23:** Some proposed MSM and metamaterials applications might be able to be used in the field of Active Disassembly (Chiodo et al., 2000; Mirzaali et al., 2018 and Zhao et al., 2022).

### 3.5.3 MSM application gaps

SMM and metamaterials have applications listed in this study that are lacking for MSM. These gaps can be an opportunity to broaden the scope of applications of MSM and so come up with novel ideas for the use of this material. It might be even that MSM is better suited for this missing applications that the other aforementioned materials are used for.

#### *(Haptic) communication – Figure 3.24*

SMM has some application in haptic communication because the thin wires or sheets can be easily embedded into small object without the use of motors. However, the actuation is often slow and might take a few seconds. In addition, Rasmussen et al. (2012) expressed their concerns about the low resolution of the SMM actuators (for example the 4x4 grid of the shutters by Coelho & Maes, (2009) and whether this would be suitable for conveying certain information. MSM shape change is very fast, so there is an opportunity for MSM to be used in applications where fast haptic communication is required. The MSM objects can also be made very small, so a higher resolution can be achieved. However, the stimuli to actuate an MSM object (magnetic fields) need to be produced somehow. Embedding electromagnets into a haptic device might take up even more space and energy than a generic motor does.

#### *Changing textures – Figure 3.25*

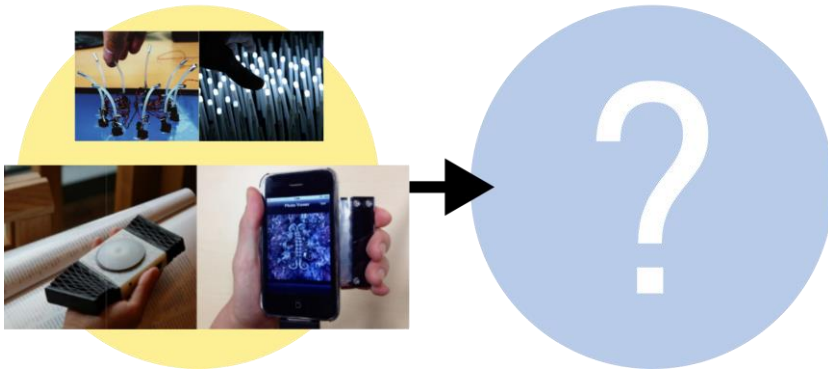
MSM are very flexible and can morph into a variety of shapes. Therefore, it might be very well suited for changing texture applications, including texture changes that need to be very quick. Where in the example of Ion et al. (2018), the texture change is initialized by pulling a rope, the MSM texture change can be triggered remotely, possibly with the inclusion of a bistable mechanism so that the magnet does not have to be permanently on or present. A condition would be, that the MSM texture must not be loaded (for example something standing on it) for it to change, as it is unlikely the material would be able to overcome the friction caused by the load. A changing texture can also be used for communication purposes.

#### *Grippers – Figure 3.26*

Grippers are not seen made by pure MSM materials, other than soft medical robots that roll themselves around a drug to be delivered (Kim et al., 2018; Hu et al., 2018) or a gripper made out of M-SMP material (Ze et al., 2019). They simply lack the strength to lift objects because they are not rigid enough. However, would it be possible to make an MSM gripper that is rigid enough by using a metamaterial mechanical structure, for example the origami structure by Kamrava et al. (2018)? Could MSM be otherwise incorporated into a gripper design, for example by only morphing the tips of the gripper to fit certain shapes better?

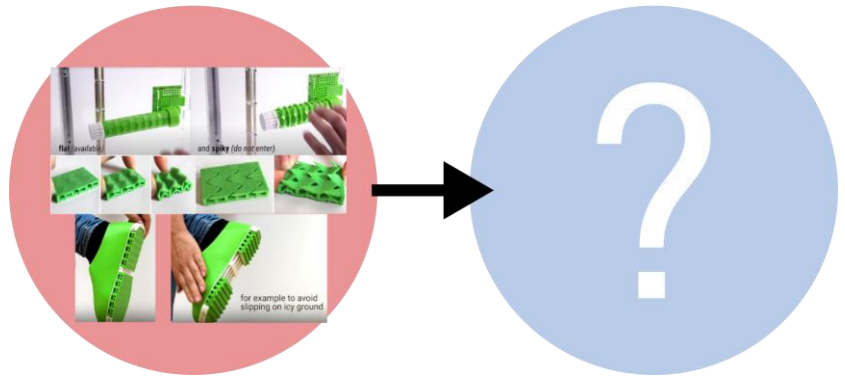


### (Haptic) communication



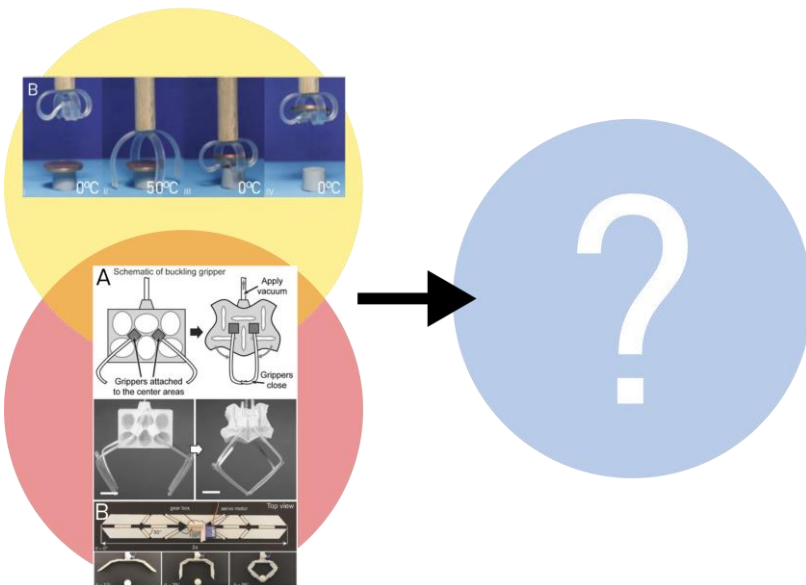
**Figure 3.24:** Haptic communication with SMM is slow, compared to MSM. A potential valuable application? (Nakayasu, 2016; Noijmma et al., 2013; Park, Park & Nam, 2015 and Nakagawa, Kamimura & Kawaguchi, 2012).

### Changing textures



**Figure 3.25** Due to its flexibility and fast response, MSM might be excellent to use for changing textures (ion et al, 2018).

### Grippers



**Figure 3.26** Grippers made from MSM are weak. Can they be made stronger with help of metamaterial mechanisms? (Behl et al., 2013; Yang et al., 2015 and Kamrava et al., 2018)

### 3.6 Literature conclusions

Shape memory materials are materials that deform to a remembered shape under an external influence, of which heat is the most common. The shape change needs programming or training to take shape. Magnetic soft materials are elastic materials with magnetic particles embedded. The combination of the elastic silicone and the magnetic particles introduce a sort of shape memory effect, so this material could be seen as a shape memory hybrid. The shape change can be programmed during manufacturing under a magnetic field.

This review showed various applications of shape memory materials, metamaterials and magnetic soft materials. The most interesting to take out of this review is the gaps in applications of MSM for which shape memory materials of metamaterials are used. Two potential application gaps are identified for which MSM could be beneficial, that is the haptic communication and texture change. For grippers, MSM does seem to lack load bearing capabilities. However, very small objects might be able to be grabbed by MSM grippers. MSM objects are able to lift higher loads if the applied magnetic field is high enough (for example, a field of 1T was used in the muscle design by Nguyen, Ahmed & Ramanujan, 2012), In most use cases, however, it is unlikely the use of such a large field is feasible, considering the large and heavy necessary equipment.

The application gaps (Chapter 3.5.4) and indirect links (Chapter 3.5.3) will be used later on in the project in the design of an application demonstrator, where the technical characteristics of the magnetic soft material will be combined with the Material Driven Design method in an attempt to design a meaningful new application for MSM. Any interesting indirect links or gaps that do not end up in the design, could hopefully serve as inspiration for future designers.

# 4. 4D Printing

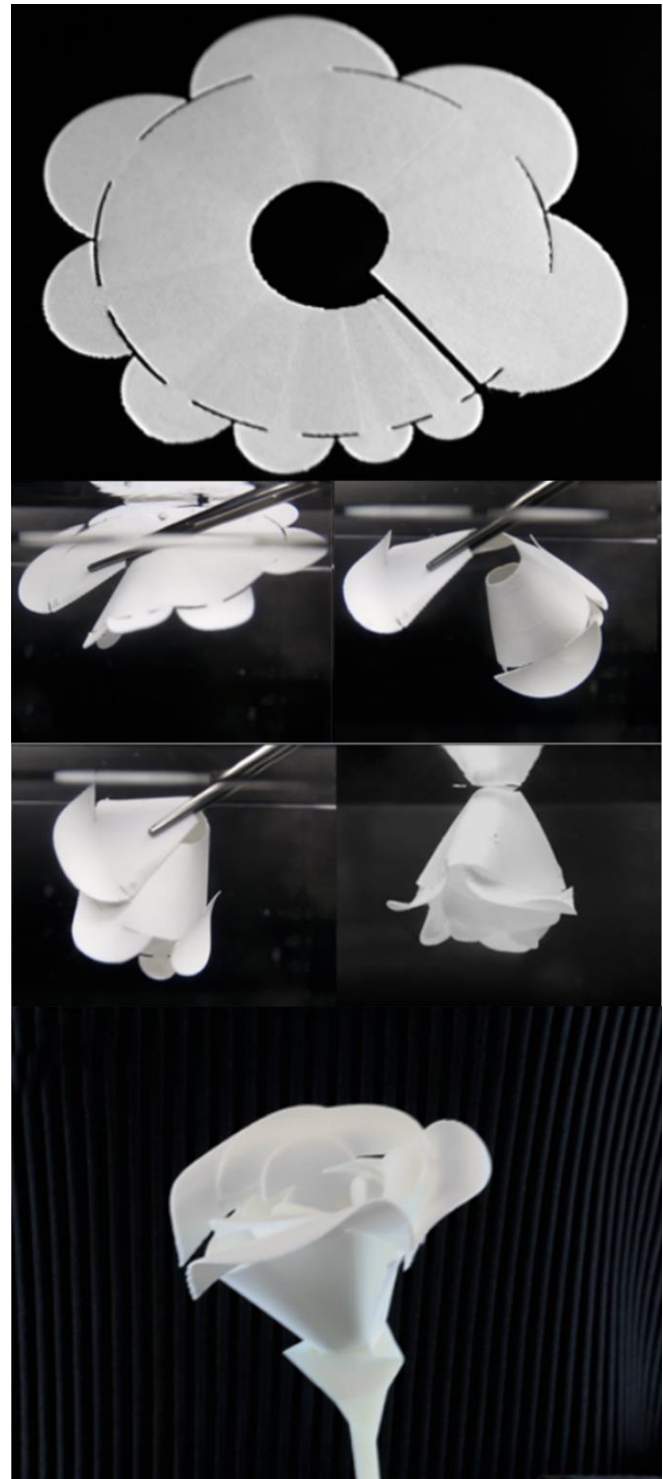
4D printing is an additive manufacturing technique whereby 3D geometries (that are 3-dimensionally printed) are given properties that change over time (the 4th dimension; Wan et al., 2020). This changing properties include shape change under external stimuli such as heat or (in this case) magnetic fields. In essence, the shape change is programmed while the geometry is printed, rather than the shape morphing material is trained to a specific remembered shape after fabrication.

In this project, a modified Ultimaker 3 FDM 3D printer was used and converted for Direct Ink Writing. This set-up was based upon the research by Yoonho Kim and colleagues (2018), where they used Direct Ink Writing with a silicone containing NdFeB particles to print various shape morphing objects.

The starting point of the development of a 4D printing set-up was the work done on the same set-up by Sanne van Vilsteren (2021). Parameters that influence the performance of the system were investigated experimentally and theoretically. Solutions to improve the performance were proposed, prototyped and tested.

## 4.1 4D printing and direct ink writing

4D printing is 3D printing (width, length and height) with the added dimension of time. It has been widely used in the manufacturing of shape memory materials (Khoo et al., 2015). These 3D shape memory structures change their shape over time when exposed to external stimuli. One example of this is the self-folding rose by An et al. (2018; Figure 4.1). By FDM 3D printing a flat rose of PLA (a shape memory polymer) in a specific order and direction, the flat geometry transforms into a 3D rose when heat is applied (Figure 4.2).



*Figure 4.1: A flat 3D printed geometry folds itself into a rose in warm water (An et al., 2018).*

#### 4.1.1 Direct Ink Writing

Direct Ink Writing (DIW) is a 3D printing technique where a paste like material is used. This material is fluid and thus no heat is needed to melt the material in order to deposit it, like in FDM 3D printers. The material is deposited out of a nozzle and is typically held in a syringe, different from SLA/DLP printing, where a liquid resin in a reservoir is cured with light (Figure 4.3).

DIW is suitable for a large variety of materials. A common material is silicone (Kim, Y. et al., 2018 & 2019; Ching et al., 2019; Ortiz-Acosta et al., 2018). Materials can be filled with a variety of fillers, for example metallic or ceramic (Biasetto et al., 2021). But also liquid metals can be used in DIW, for example to produce soft sensors (Kim, S. et al., 2018; Figure 4.4). Because the material used can be soft and flexible (e.g. silicones or hydrogels) and easily tailored compared to a flexible FDM filament such as Ninjaflex, it is a popular technique in the field of soft robotics (Yap, Sing & Yeong, 2020). For example, Cheng et al. (2019) used DIW to 3D print a flexible soft starfish and soft robotic actuators such as tentacles and photo-responsive grippers (Figure 4.5).

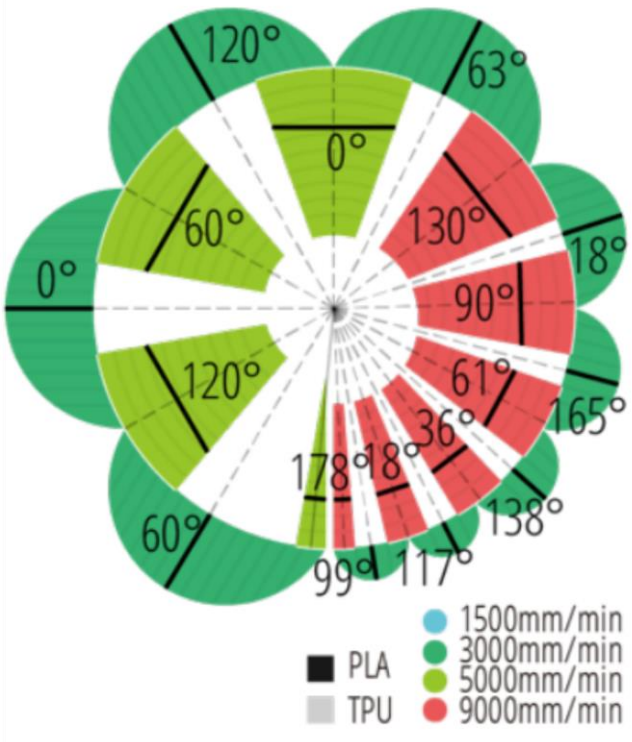
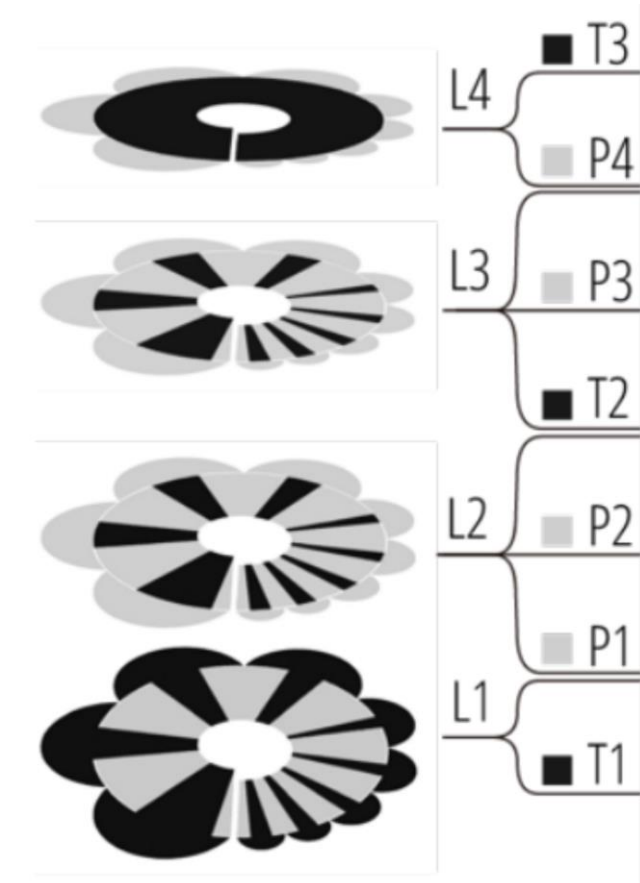


Figure 4.2: 3D printing the flat geometry with a combination of PLA and TPU, using specific directions and speeds results in the self-folding behaviour.

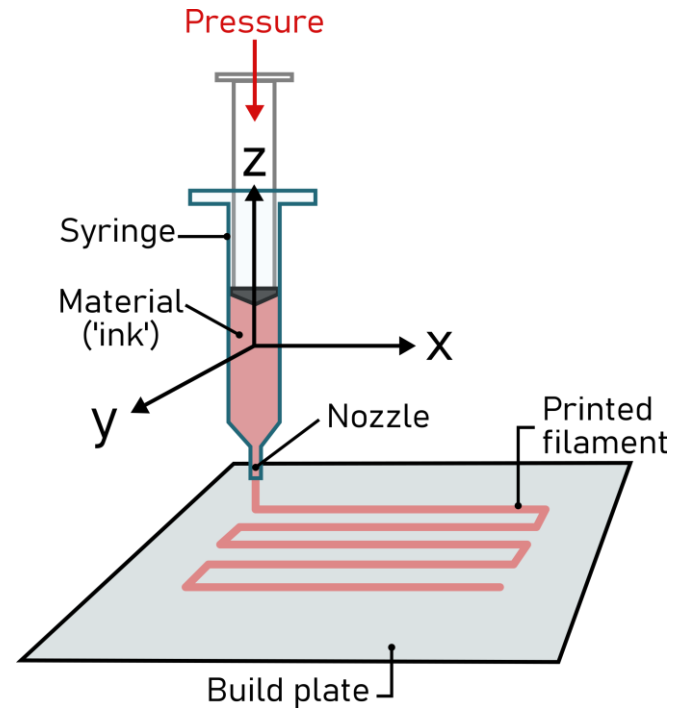
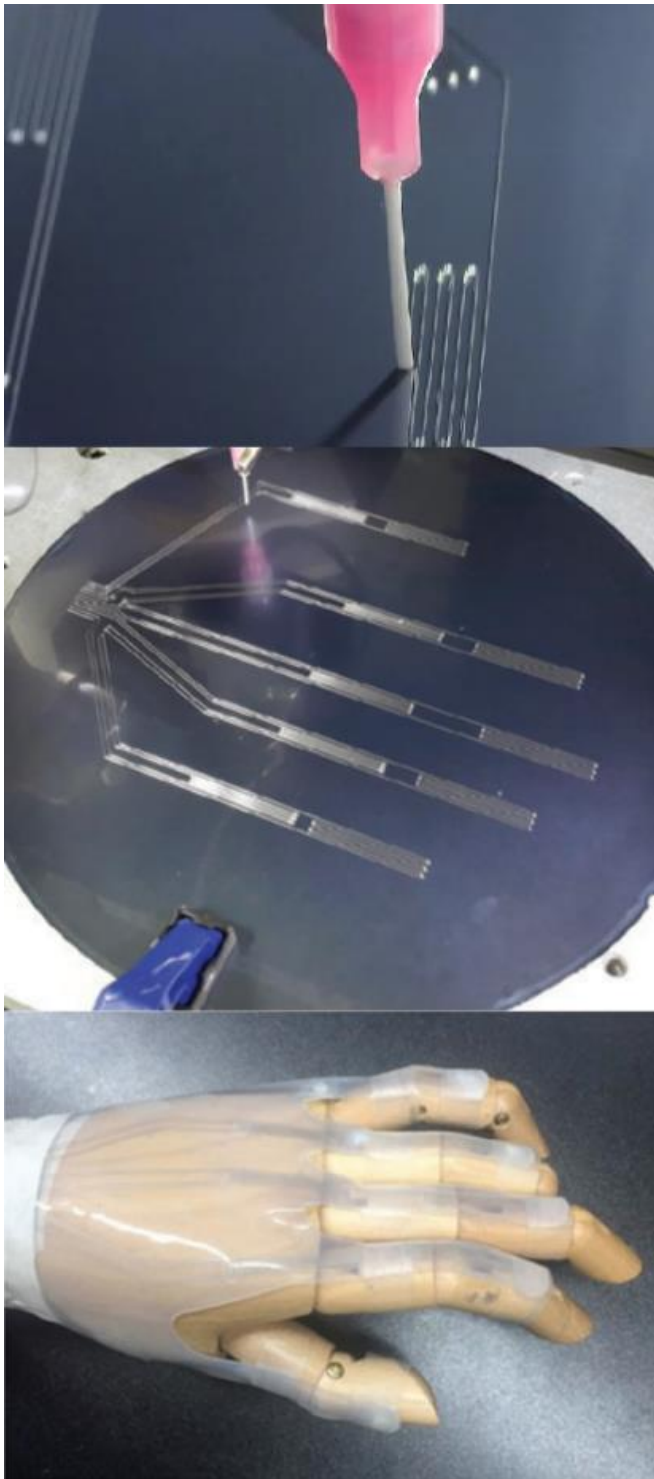
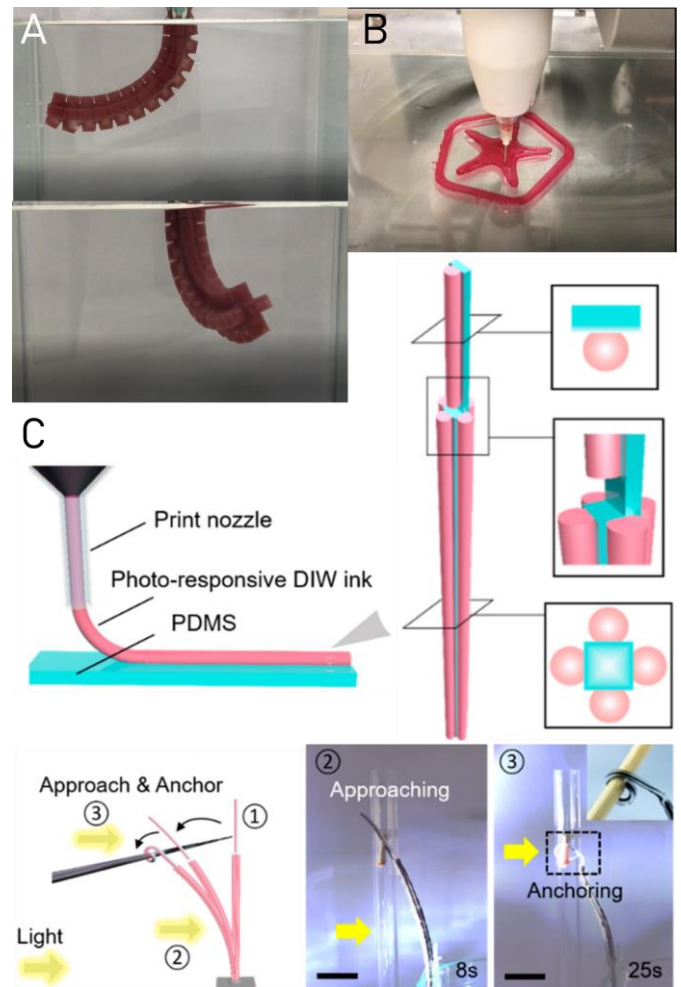


Figure 4.3: Schematic of typical DIW 3D printer set-up and working.



**Figure 4.4:** DIW with Eutectic Gallium-Indium conductive metal to make soft sensors (Kim, S. et al., 2018).



**Figure 4.5:** Soft robotic tentacle actuator made with DIW of soft hydrogel (A), DIW of a flexible starfish (B) and gripper design made with DIW of photo-responsive shape morphing material (C; Cheng et al., 2019).

## 4.2. 4D printing of MSM

In this project, MSM is printed using the DIW technique. This and the previous project (Van Vilsteren, 2021) is mostly based on the research by Kim et al. (2018) where the material was 3D printed by means of DIW with an (electro)magnet attached to the nozzle to control the orientation of the magnetic particles. (Figure 4.6; see also Chapter 3.2.1 and Figure 3.3). In this chapter the DIW process specific to MSM is further explained. Besides this process, other means of fabrication are discussed as possible inspirational material for a future project.

### 4.2.1. DIW and programming of MSM

As mentioned, the process used in this project was inspired by the research of Kim et al. (2018), who used a NdFeB/silicone-mixture which was magnetized prior to printing, extruded out of a nozzle with a magnet attached

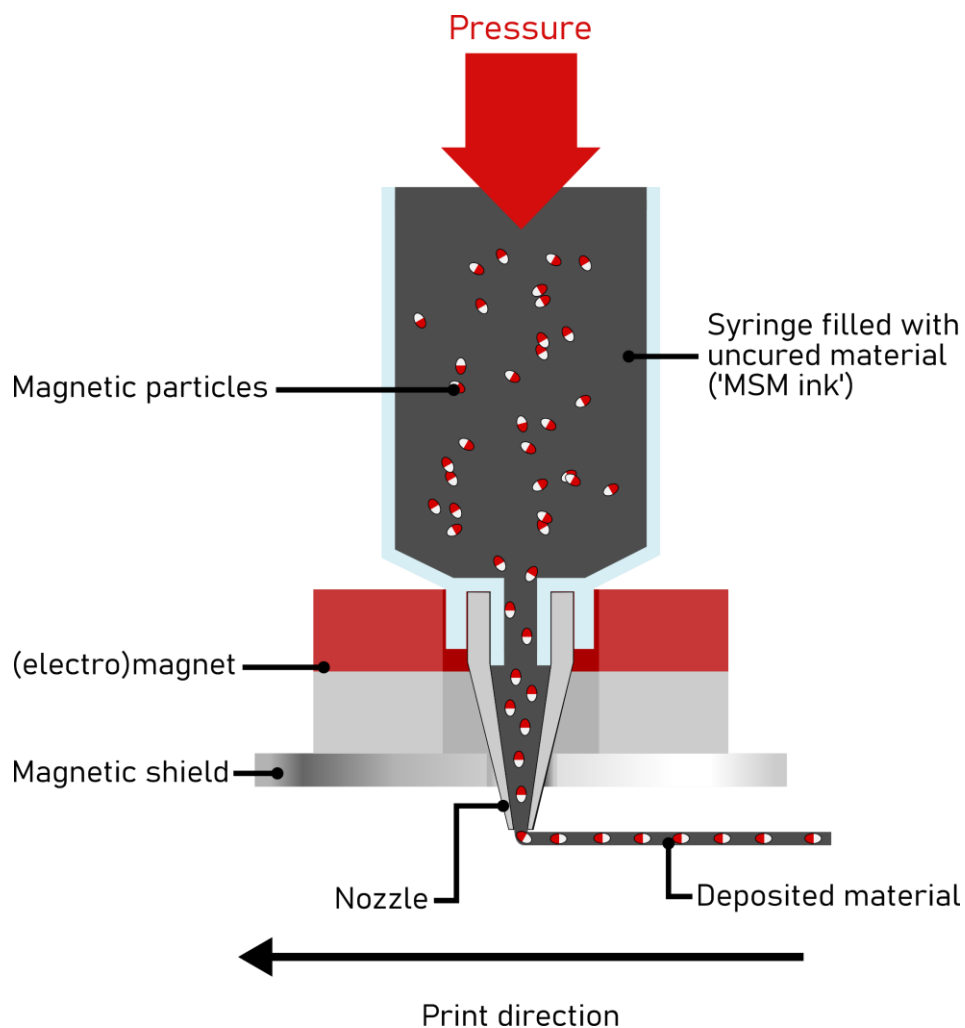
to control the orientation of magnetic particles in the material. The control of the orientation of magnetic particles can be done in two ways: by altering the print direction using a permanent magnet or changing the magnetic polarity during printing using an electromagnet.

#### *Permanent magnet (A)*

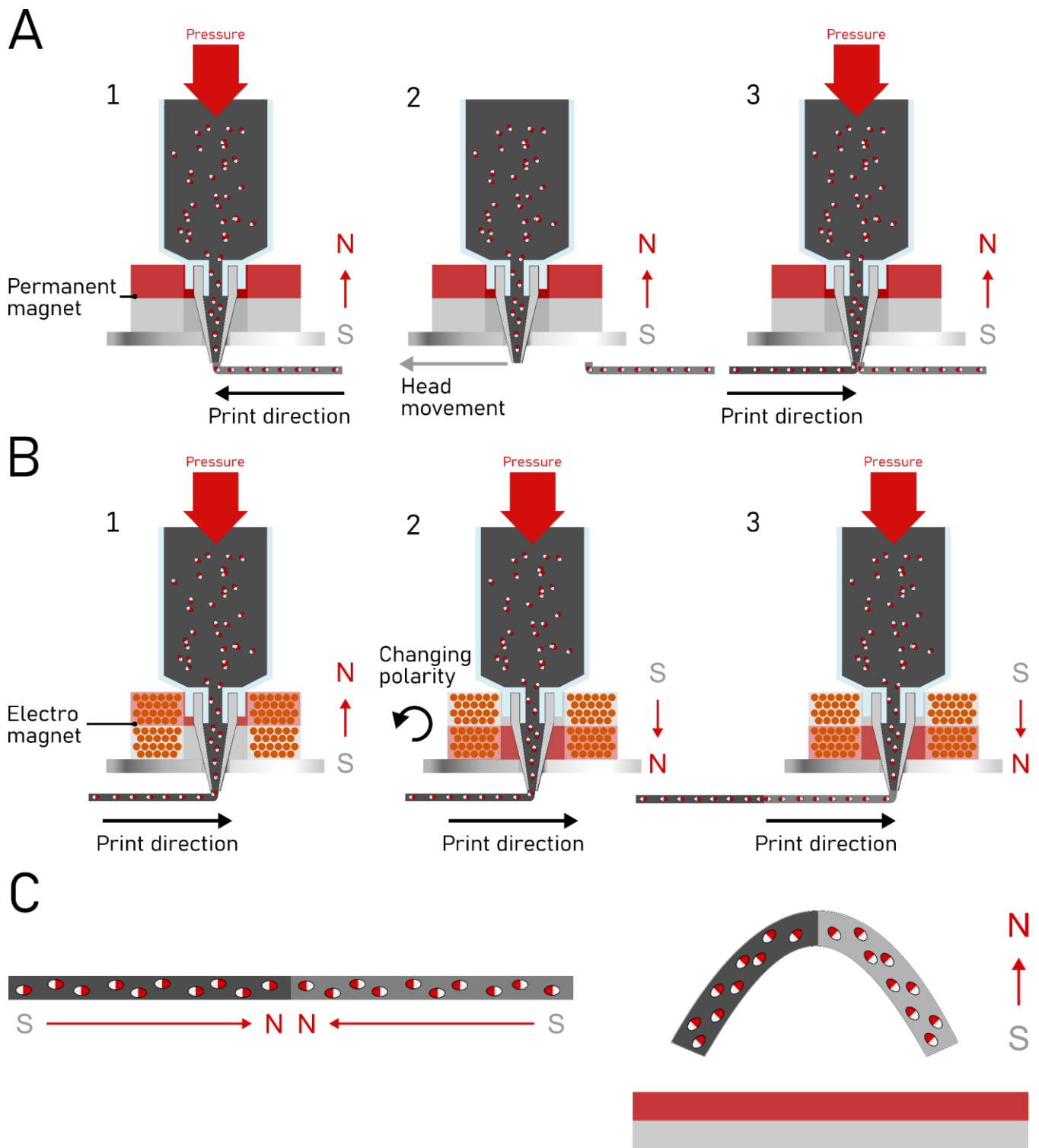
A permanent magnet causes the particles to be aligned in one specific direction relative to the print direction. By altering the print direction, the absolute orientation of the particles can thus be changed as desired (Figure 4.7A).

#### *Electromagnet (B)*

Another approach is the use of an electromagnet. An electromagnet enables the switch of magnetic polarity during printing by alternating the direction of the current running



*Figure 4.6: Schematic representation of DIW 4D printing of MSM. Adapted from Kim et al. (2018).*



**Figure 4.7:** The same programmed shape change of an MSM object during 4D printing achieved in two ways: (A1) a permanent magnet aligns magnetic particles in one specific direction relative to the print direction. (A2) The print head is moved to a new location during which no pressure is applied so no ink is extruded. (A3) A new section is printed in the opposite direction, resulting in a line of ink with a two-direction magnetization profile (C). (B1) An electromagnet aligns the orientation of magnetic particles in one of two directions. (B2) The polarity of the electromagnet is changed during printing in the same direction, causing magnetic particles to re-align with the new polarity. (B3) The next segment is printed directly attached to the first segment, as there is no movement of the printhead needed in between, resulting in the same two-direction magnetization profile (C).

through it. This means that the alignment of particles relative to the print direction can be changed. Because of this, there is no need to alter print direction to control the orientation of the particles and thus the programmed shape change (Figure 4.7B).

The upside of approach A is that there is no additional electronics needed, resulting in a less complex machine. The downside is that connecting two segments can leave blobs of material or the segments don't connect at all. In approach B, segments can be printed continuously resulting in a smoother print.

### Magnetic shield

A magnetic shield protects the already printed material from the magnetic field of the magnet so that the alignment of the particles inside the deposited material is not influenced and to keep the material from curling up from the build plate towards the magnet as it is attracted by it. The best material to use as magnetic shield is so called MuMetal, a specific alloy of nickel, iron and cobalt (K&J Magnetics, n.d). However, every ferromagnetic metal should work. For example, Ma et al. (2020) reported using a steel magnetic shield. More about magnetic shielding can be found in Chapter 4.5.3

### 4.2.2 Different manufacturing approaches

In this project and the aforementioned research by Kim et al (2018), a silicone is used in which the NdFeB particles are magnetized before printing. This makes the ink more viscose than without magnetizing the ink (see Chapter 4.3). The more viscose the ink is, the harder it is to print (see Chapter 4.5). It is also possible to 3D print a non-magnetized object and magnetizing this after printing when it is in a specific shape (Zhu et al., 2022; Figure 4.8).

The silicone used in this project consists of two parts. Mixing these parts together causes it to cure. There are also ink types that cure when exposed to UV light. Ma et al. (2020) used such an ink in their research (Figure 4.9). To make silicone cure by UV light, a photoinitiator must be added (Foerster et al., 2021).

A variation on DIW was done by Wang et al. (2022). By electrohydrodynamic printing, the ink

is pulled out of the nozzle by a current between the nozzle and the print bed. The magnetized iron oxide ( $\text{Fe}_3\text{O}_4$ ) particles were again aligned with a permanent magnet surrounded by a magnetic shield while printing (Figure 4.10).

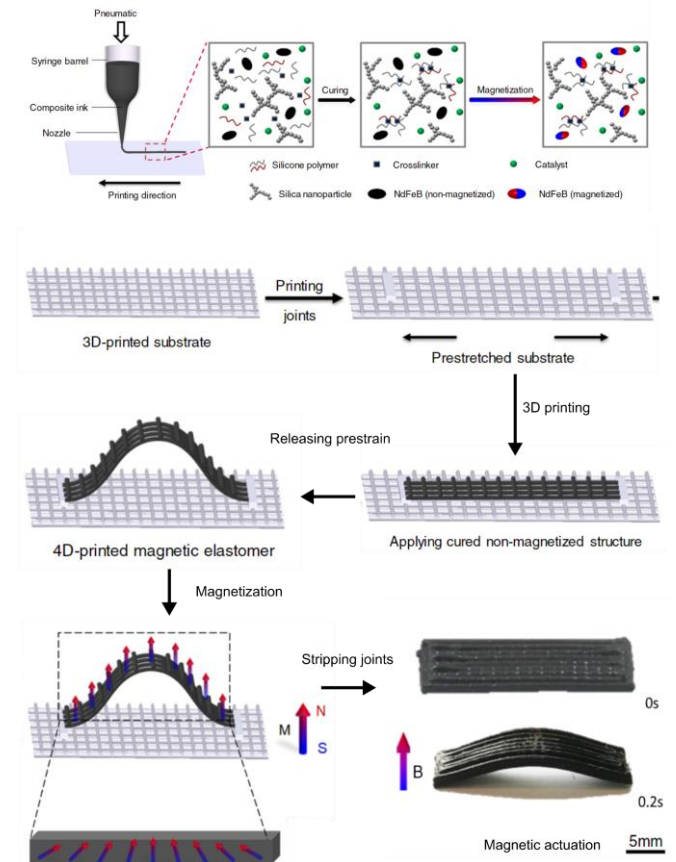


Figure 4.8: Magnetizing a 3D printed strip after printing when it is in a specific shape to achieve the desired magnetization profile (Zhu et al., 2022).

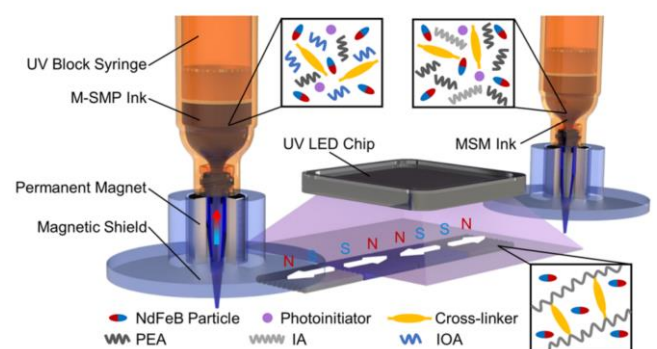


Figure 4.9: MSM and M-SMP material is loaded into two separate syringes to make a MSM/M-SMP hybrid material. The material is cured by UV light by the addition of a photoinitiator, which enables the cross-linker to link the monomers together. The uncured ink is stored in UV light blocking syringes to prevent curing.



Shinoda et al. (2019) based their production of MSM on the 3D printing technique SLA. A build plate in a bath of UV curable resin moves down layer by later. The resin is cured selectively by a UV laser. The magnetic orientation of embedded particles was controlled with a rotating permanent magnet (Figure 4.11).

Lastly, Cao et al. (2021) made a more traditional FDM filament out of thermoplastic rubber (TPR) and carbonyl iron particles. Their MSM objects were not magnetized and instead relied on the attraction or repulsion of the particles by an external magnet (Figure 4.12).

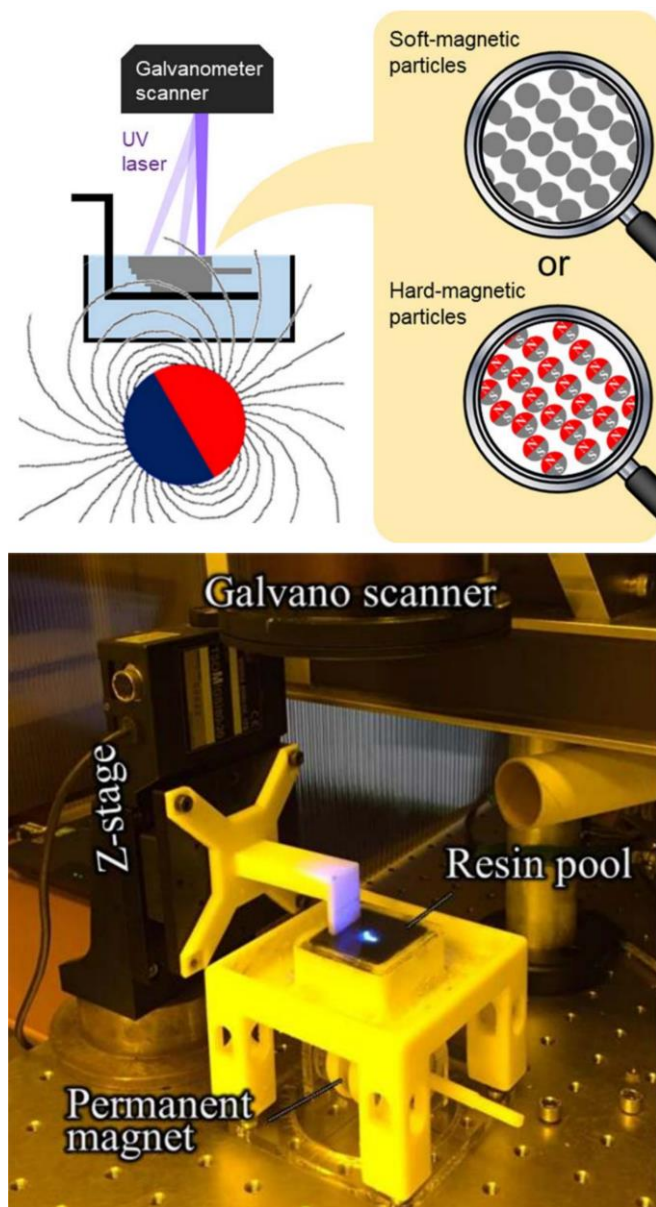


Figure 4.11: SLA technique approach of 4D printing MSM by Shinoda at al. (2019). A rotating permanent magnet is used to align magnetic particles while selectively curing a bath of resin by a UV laser.

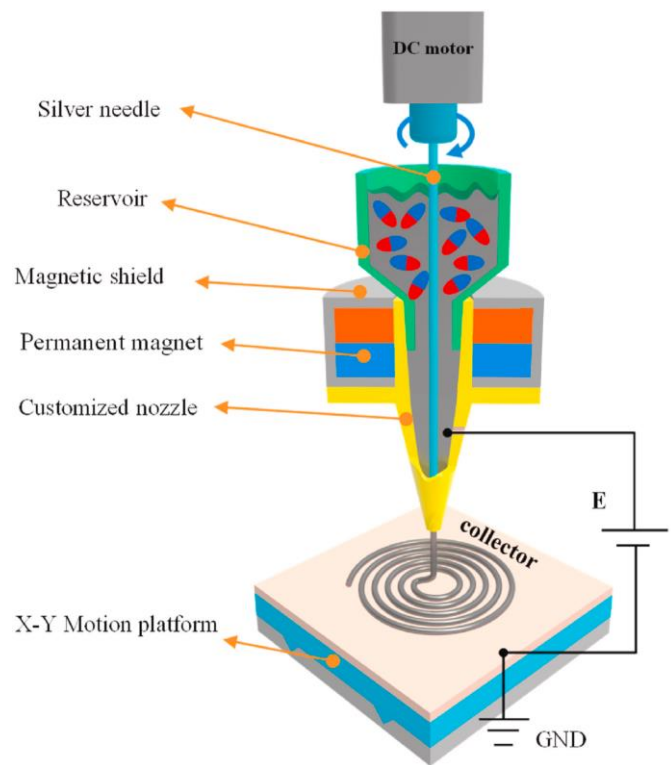


Figure 4.10: A current between the nozzle and the print bed helps overcoming flow resistance of magnetic ink, ensuring a steady and even flow of material.

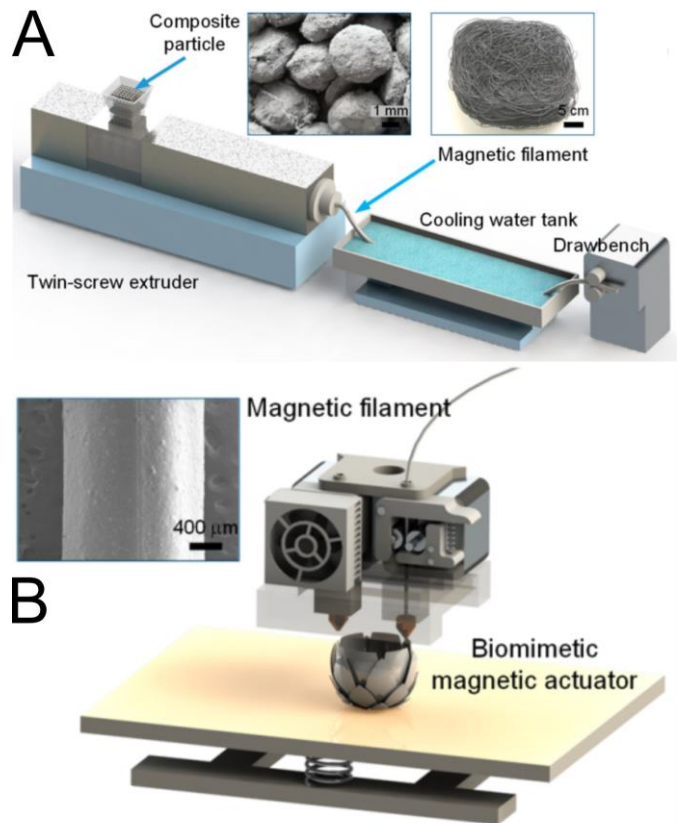


Figure 4.12: Making of a TPR filament with carbonyl iron microparticles embedded (A) and FDM 3D printing a magnetic object (A; Cao et al., 2021).

### 4.3. Magnetic ink

The material used in this project is a two component silicone with 63 weight percent (wt%) Neodymium-Iron-boron nanoparticles (NdFeB; 5  $\mu\text{m}$ ) and 0.85 wt% fumed silica ( $\text{SiO}_2$ ). The silicone used is Ecoflex 00-10 by Smooth-On (n.d.). The silicone consists of two components (A and B) that need to be mixed to a 1:1 weight or volume ratio in order for the silicone to cure. The curing process takes 4 hours at room temperature, but can be sped up by elevated temperatures, for example an oven. Attention is to be given to the temperature of the oven, because the magnetic particles will lose their magnetization when exposed to temperatures higher than the *Curie temperature*. For NdFeB particles, Ze et al. (2019) reported this temperature to be 150°C.

#### 4.3.1. Ink preparation

The recipe of magnetized ink used in this project was the result of the previous project on this topic by Sanne van Vilsteren (2021). More specifically, ink with the designation 'T8E1'. This recipe was in turn based on the paper by Kim et al (2018). NdFeB particles and fumed silica were added to the two separate Ecoflex components, resulting in two samples of uncured ink. The two samples were then magnetized in a Versa Lab magnetizer at field strength of 3 Tesla at the Reactor Institute at the TU Delft. Figure 4.14 shows the procedure of preparing the ink samples. In the beginning of the project, a different recipe was made replacing the NdFeB particles with 64wt% Iron particles (spherical, <10  $\mu\text{m}$ ). This ink was meant to be used in testing of the 3D printer setup, because the Iron particles are much cheaper than NdFeB particles in addition to not being a rare earth metal. See Appendix C.1 for more detailed reports of preparing the ink.

#### 4.3.2. Rheological properties

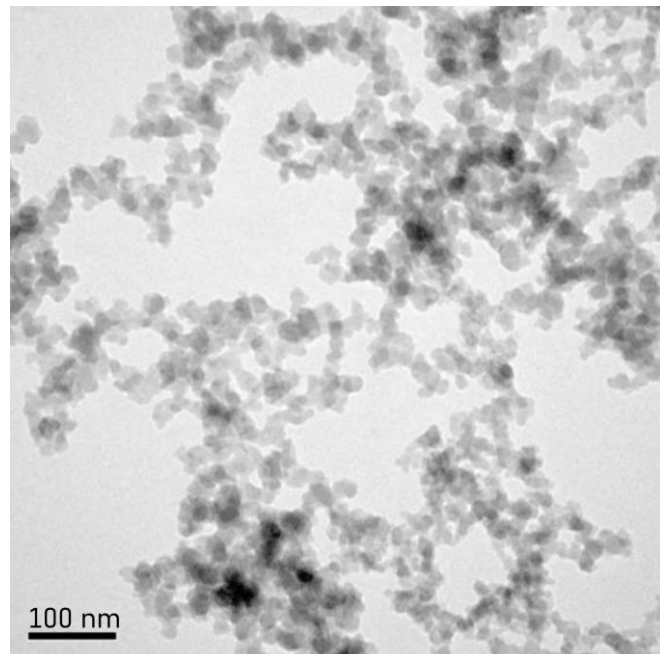
For 3D printing liquid material, it is important that the material is not so low in viscosity that the printed object is not able to hold its shape when it is printed. As an extreme example, water is not suitable for 3D printing, as it will simply flow away once extruded. It is also not desired that the material has a very high

viscosity, as it will be very hard to push through a small nozzle. Another extreme example: clay holds its shape very well, however is so thick that it is as good as impossible to push through a small diameter nozzle. Therefore, ink is desired that shows pseudoplastic (a.k.a. thixotropic) or shear-thinning properties (Kim et al., 2019).

Shear-thinning fluids are non-Newtonian fluids, meaning their viscosity is not constant. The viscosity decreases when a shear stress is applied, meaning that while the ink is extruded (by means of a pressure), the viscosity drops because of the shear stress it undergoes. Once the ink exits the nozzle, the shear stress is relieved, causing the viscosity to increase again and allowing the ink to maintain its shape once on the print bed.

#### *Fumed silica*

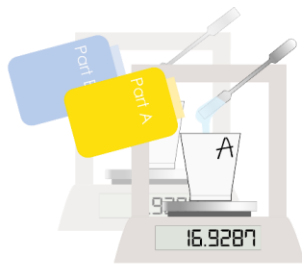
The ingredient that provides the shear-thinning properties in the magnetic ink is fumed silica. The silica particles form chains inside the silicone, creating a network that increases the inks viscosity. These chains are easily broken, however, by a shear force, making the silicone less viscose again. Once the shear force is removed (i.e. the silicone exits the nozzle), the bridges are quickly reformed, making the ink more viscose again and thus printed shape more stable (Zhang et al., 2014; Figure 4.13).



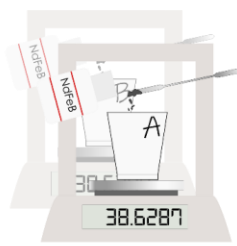
**Figure 4.13:** Chains of silica nanoparticles bridges seen through a microscope (Zhang et al., 2014).



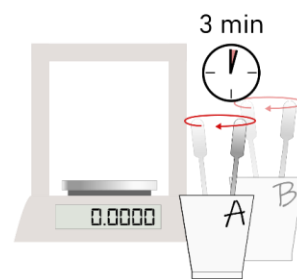
1. Place a cup on the scale and measure its weight.



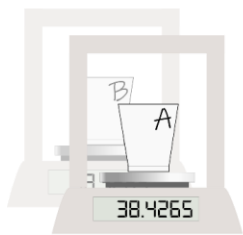
2. Pour the prescribed amount of silicone (part A or B) in the cup, adding to the weight of the cup.



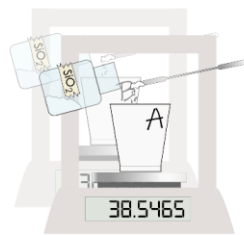
3. Add the prescribed amount of NdFeB microparticles to the silicone in the cup.



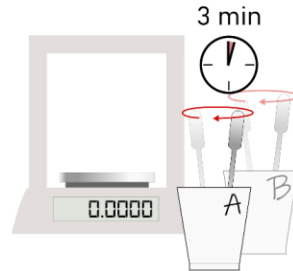
4. Stir the silicone-NdFeB mixture by hand for 3 minutes



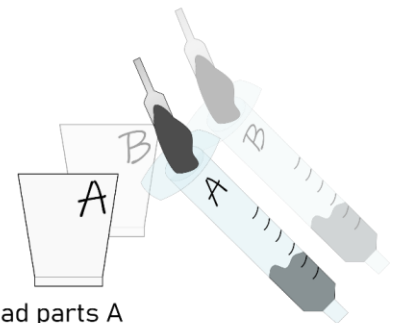
5. Measure again the weight of the mixture after mixing, as some of the material will be left on the spatula.



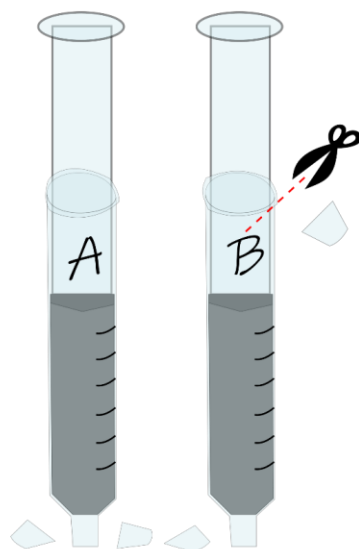
6. Add the prescribed amount of fumed silica to the silicone mixture.



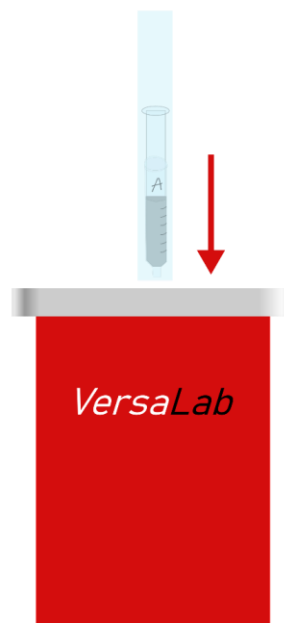
7. Stir the silicone-NdFeB-SiO<sub>2</sub> mixture again by hand for 3 minutes



8. Load parts A and B in separate, labelled syringes.



9. Tabs of the syringes must be cut off all around in order to fit into the magnetizer.

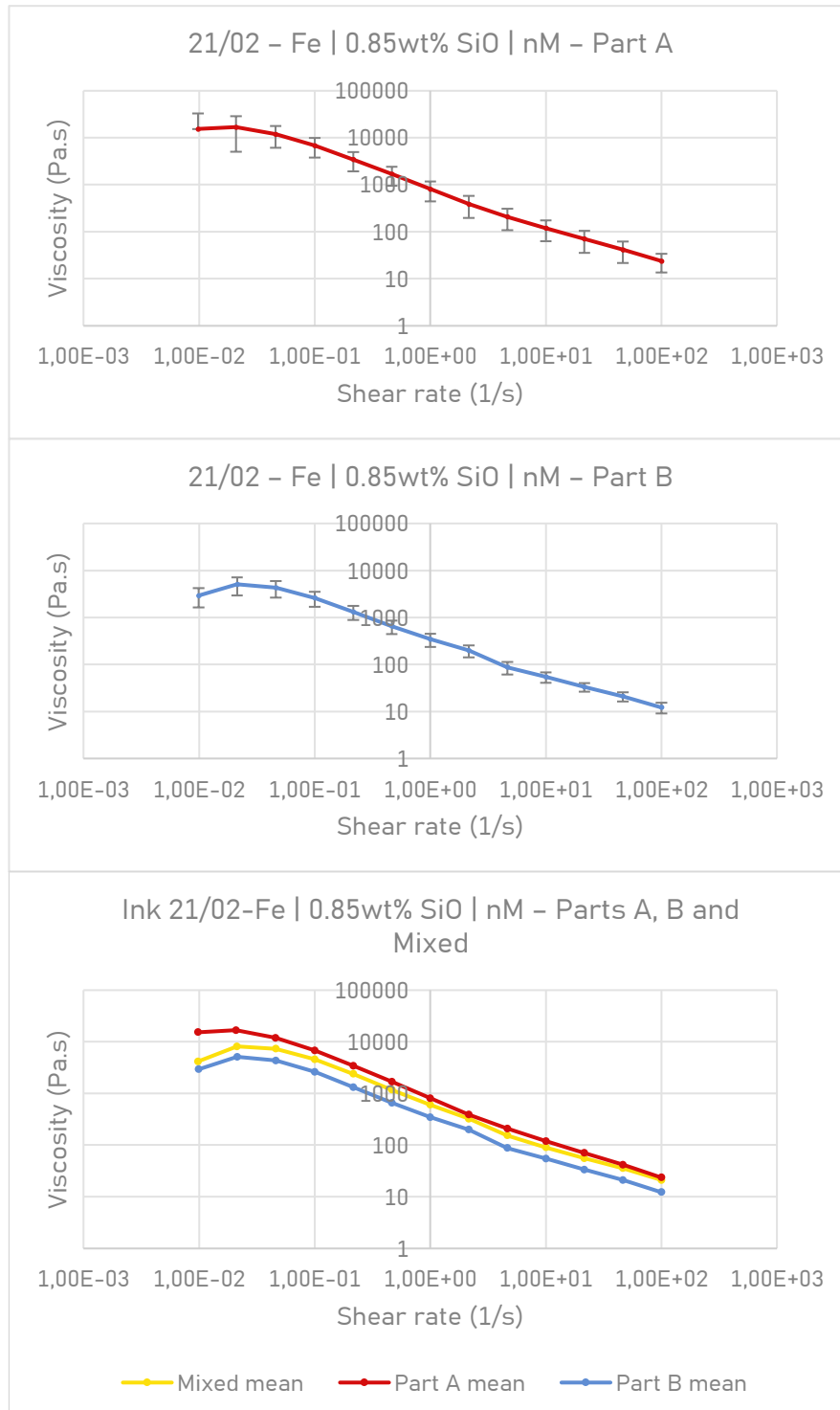


10. The samples are magnetized with the Versa Lab magnetizer at a field strength of 3 Tesla.

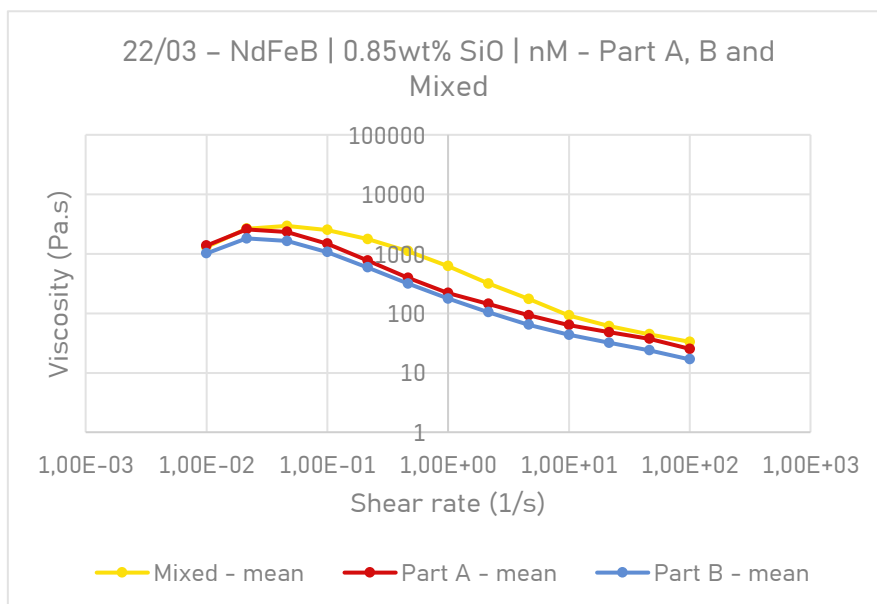
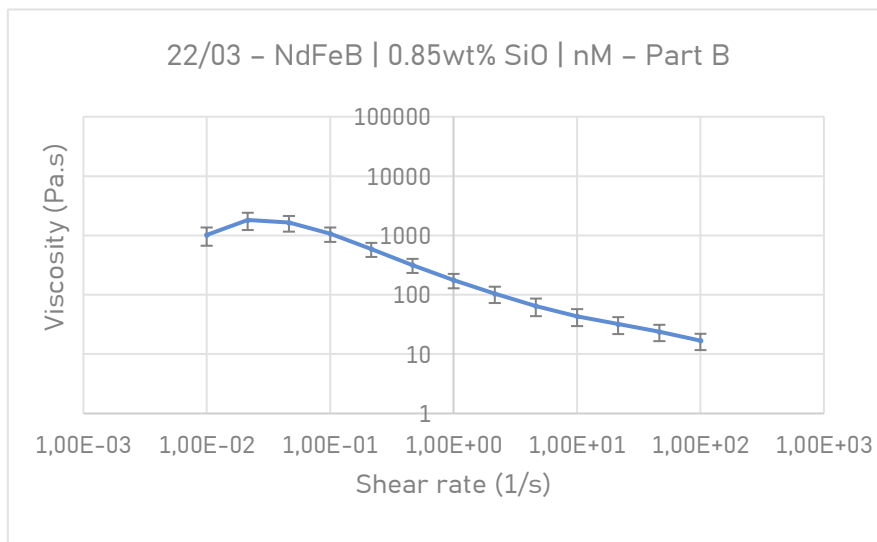
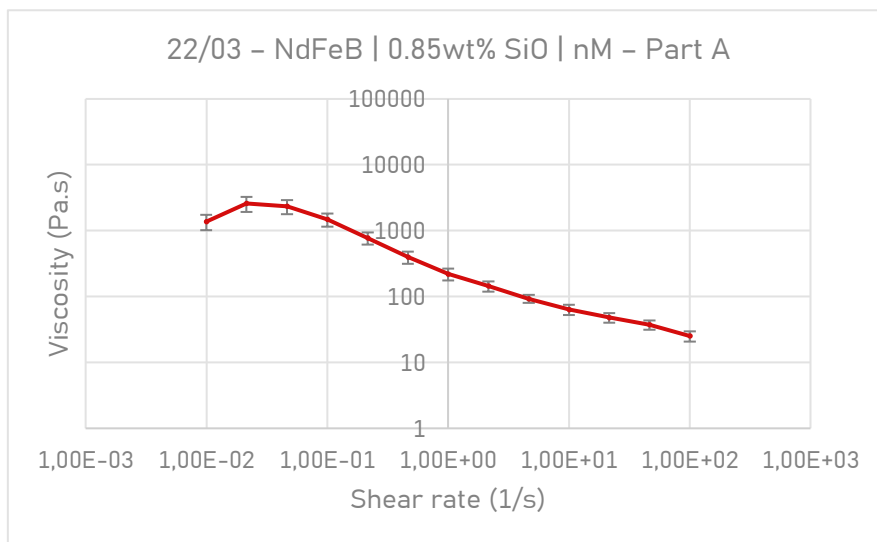
**Figure 4.14:** Procedure of preparing magnetic ink A and B samples to be magnetized at the reactor institute. The procedure for component A and B are identical, with the same amounts of ingredients.

## Rheological data on prepared ink

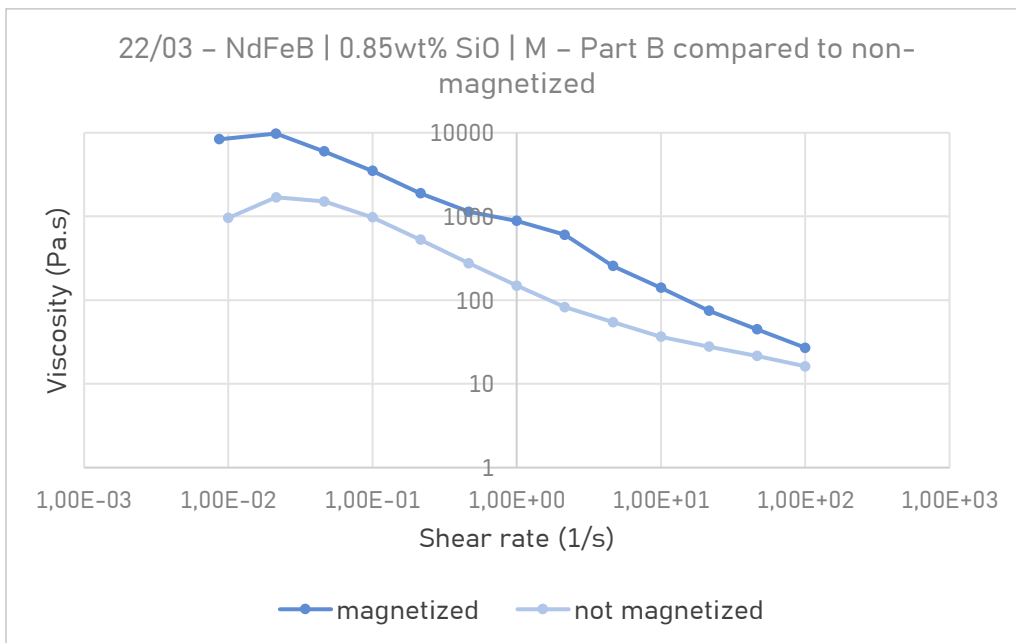
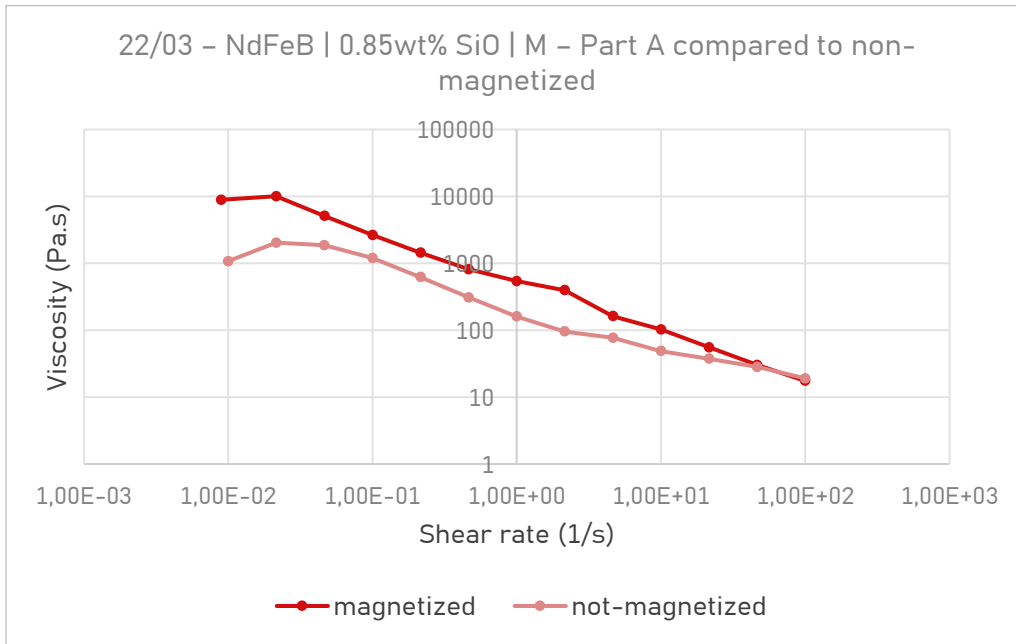
To test the ink samples prepared during this project, a TA Instruments AR-G2 Magnetic Bearing Rheometer equipped with a 40 mm steel plate geometry at a measuring gap of 0,5 mm was used. Out of the data, the pseudoplastic properties of the ink can clearly be seen, as the viscosity drops when the shear rate increases. Figure 4.15 shows the data of the early 3D printer test ink with Iron particles replacing the NdFeB particles. Figure 4.16 shows the data of the non-magnetized ink containing NdFeB particles and in Figure 4.17, the same ink but magnetized is shown.



**Figure 4.15:** Rheological data of test ink containing non-magnetized iron particles. Average value taken of three measurements.



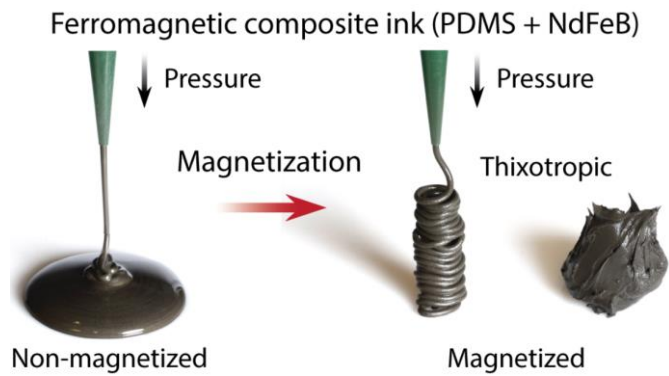
**Figure 4.16:** Rheological data of ink containing non-magnetized NdFeB particles. Average value taken of three measurements.



**Figure 4.17:** Rheological data of ink containing magnetized NdFeB particles compared to the same samples not magnetized. Values of magnetized samples taken of a single measurement.

#### Influence of magnetization on ink properties

As can be seen from Figure 4.17, magnetizing the ink increases the ink viscosity by a factor of 10, while retaining the pseudoplastic properties. The magnetization has another influence on the rheological properties, namely that it too provides shear-thinning properties. Similar to fumed silica, the magnetic particles create bonds between them, as like all magnets, opposite poles are attracted to each other. Because the magnetic particles are very small ( $5\mu\text{m}$ ), the magnetic force keeping the particles together is very weak and thus easily broken. Fumed silica is therefore not needed in the recipe to introduce this properties. Kim et al. (2019) demonstrated this in their research on the use of MSM for a steerable vascular endoscope (Figure 4.18).

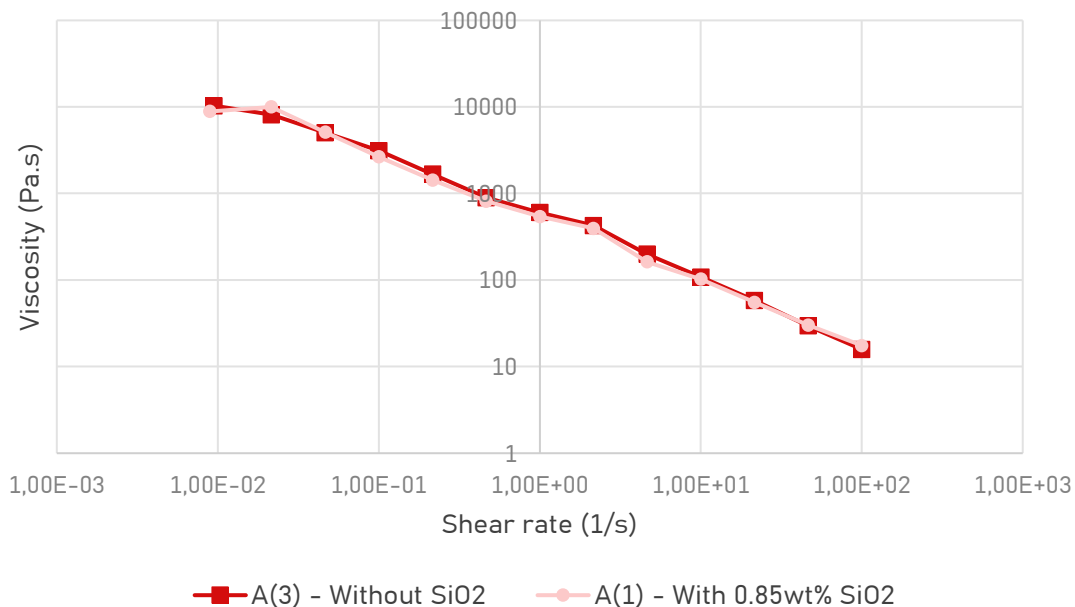


**Figure 4.18:** Once the PDMS silicone with embedded NdFeB particles used by Kim et al. (2019) is magnetized, the ink shows shear-thinning or thixotropic properties. NdFeB particles were coated with a silica shell to prevent oxidation.

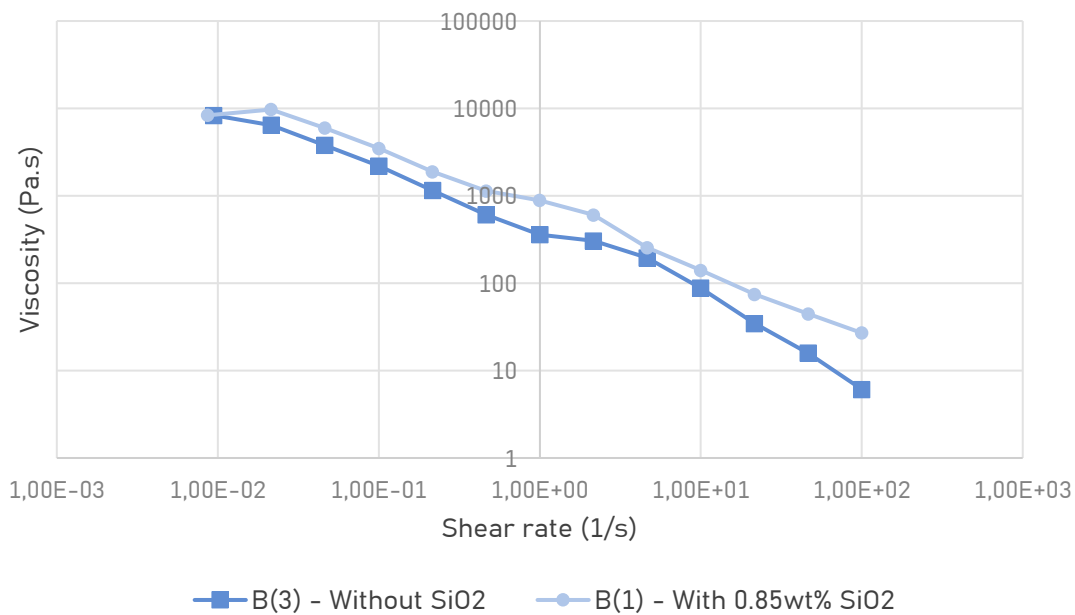
This principle was also validated ourselves during this project. Figure 4.19 shows a comparison between a sample of magnetized ink containing fumed silica and the exact same recipe without fumed silica. It can be seen that the measurements taken are almost the same, proving that fumed silica is not needed to give the ink the desired shear-thinning properties.

In the research by Kim et al. (2019), silica (not 'fumed') was used to create a coating around the NdFeB particles to protect them from oxidation. That is not done during this project. It is unknown if adding the fumed silica to the silicone in the original recipe by Sanne van Vilsteren (2021) used throughout this project also generates a protective layer and thus shields the NdFeB particles from the elements. It might be possible that the fumed silica prevents the MSM from degradation because of this shielding effect. Therefore, for the continuation of the project, fumed silica was continued to be added to the prepared ink to be on the safe side.

### Part A - with and without SiO<sub>2</sub> (magnetized)



### Part B - with and without SiO<sub>2</sub> (magnetized)



**Figure 4.19:** Comparison of magnetized ink samples with added fumed silica and without added fumed silica. Samples made on March 22nd.



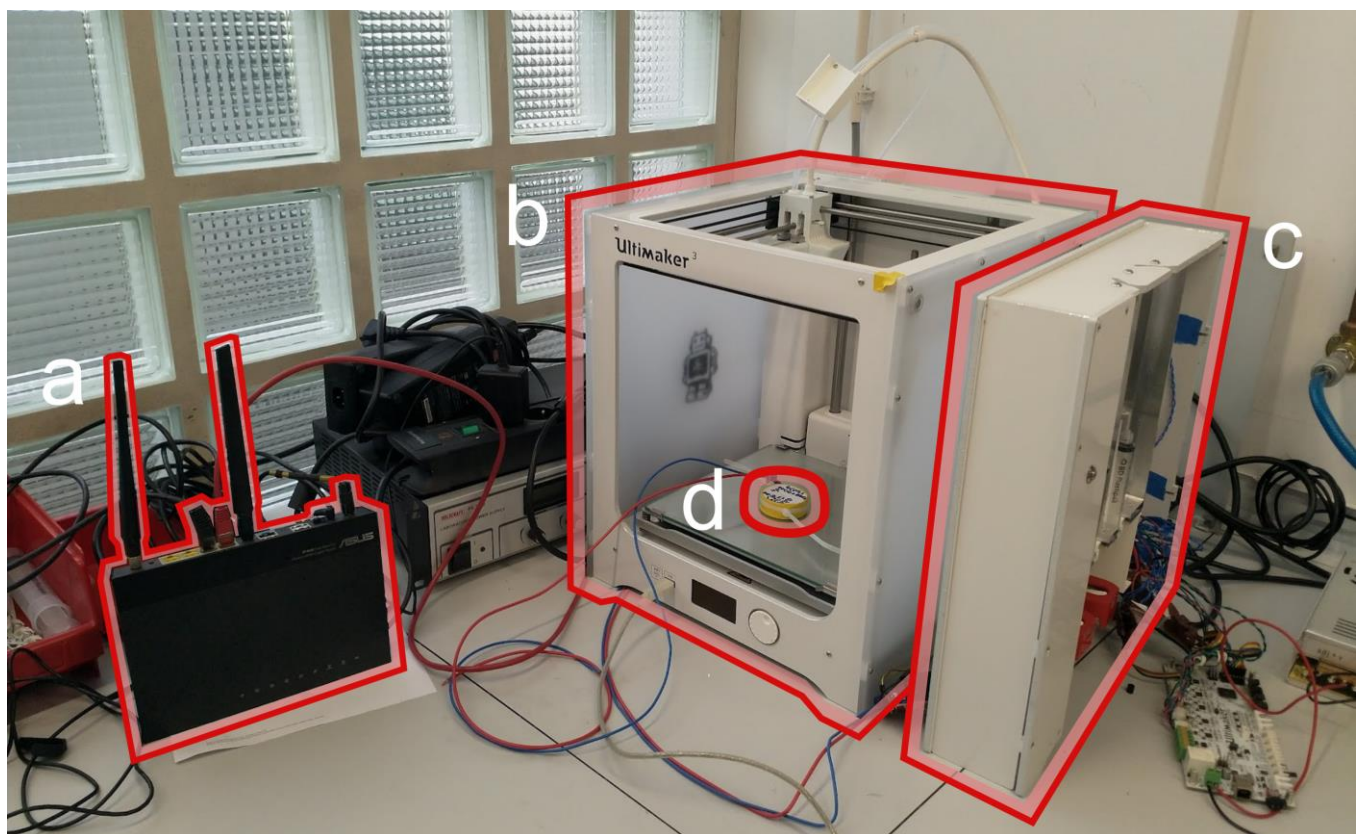
## 4.4 3D printer set-up

The 3D printer used in this project was an Ultimaker 3 with modified firmware to make it suitable for DIW (Figure 4.20). Ink was contained in the external extrusion system in two syringes; one for silicone Part A the other for silicone Part B. The extrusion system is controlled by USB via the 3D printer. It is therefore not possible to print g-code from a USB drive, because this port is occupied by the extrusion system. Instead, a router is used to establish a network with the printer and a PC, to send g-code over this network. The ink is transported from the extrusion system via flexible tubes into a static mixing nozzle, where the two silicone parts are mixed together during printing, so that the material cures. It was the intention to use an electromagnet to control the orientation of the magnetic particles. However, this was not accomplished (for more information, see Chapter 4.4.2: Electromagnet and Appendix C.3). Figure 4.21 shows a

schematic overview of the used 3D printing set-up with attached electromagnet. Figure 4.22 shows the same set-up, but with the use of a permanent ring magnet.

### 4.4.1 Extrusion system

The ink is extruded out of two separate syringes by an external extrusion system provided by Ultimaker. In this system, made to hold two 60ml syringes, the syringe pistons are pushed on by plates attached to rods that are moved up and down by a stepper motor. Figure 4.23 shows a schematic of the workings of this system. The two component ink is extruded by a pressure generated by the system via tubes into a *static mixing nozzle*. This 3D printed nozzle contains a spiral which mixes the two components while travelling through it (Figure 4.24 and 4.25).



**Figure 4.20:** Used Ultimaker 3 3D printer consisting off (a) router to establish a network connection with the 3D printer to send g-code instructions to the printer; (b) 3D printer itself containing the print head and bed where the geometry is printed on; (c) Dual extrusion system prototype by Ultimaker. This part contains the pistons which are extruded by means of two individual motors; (d) The electromagnet made during the last project (Van Vilsteren, 2021) intended to change magnetic particle orientation during printing (not attached).

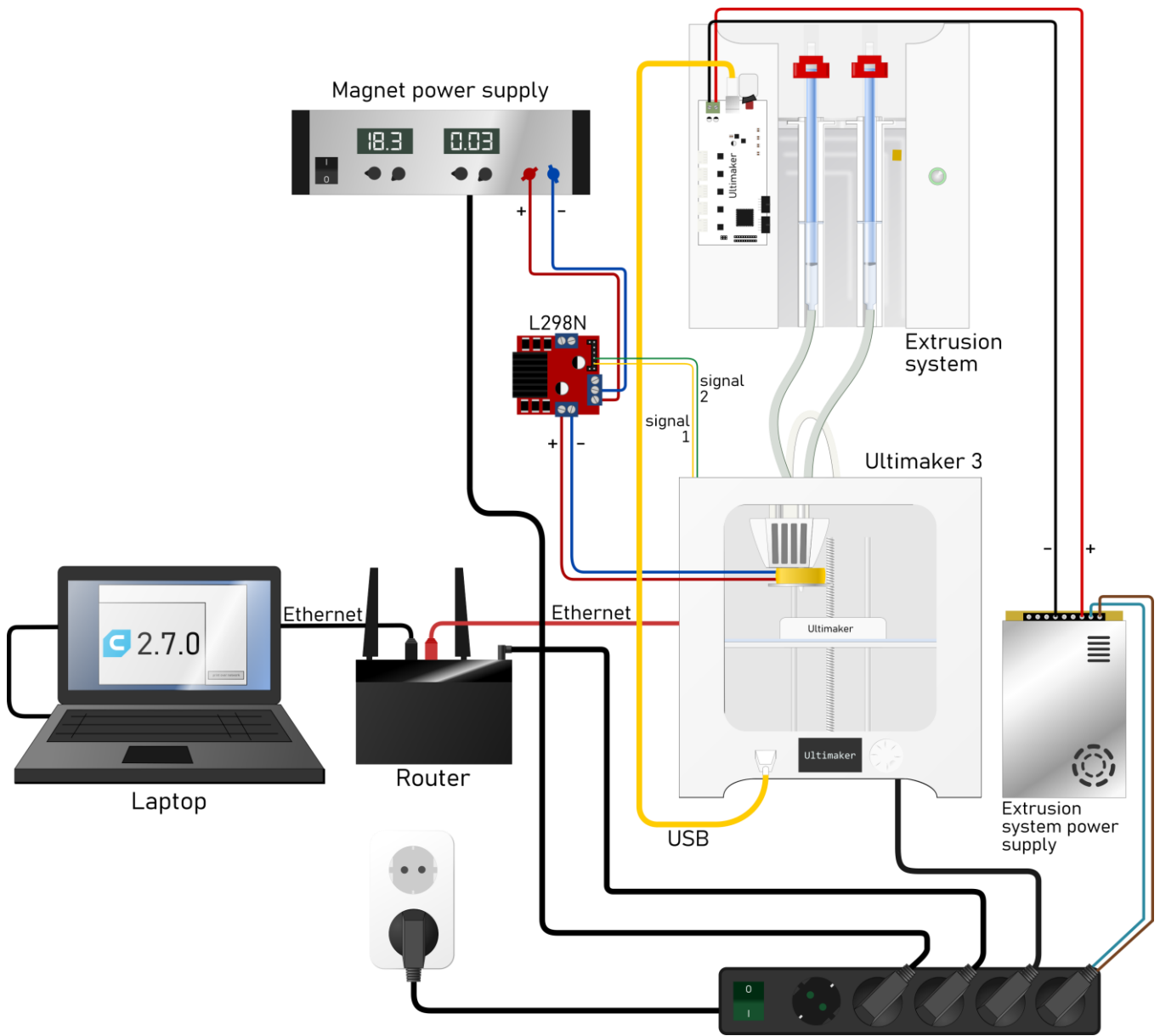
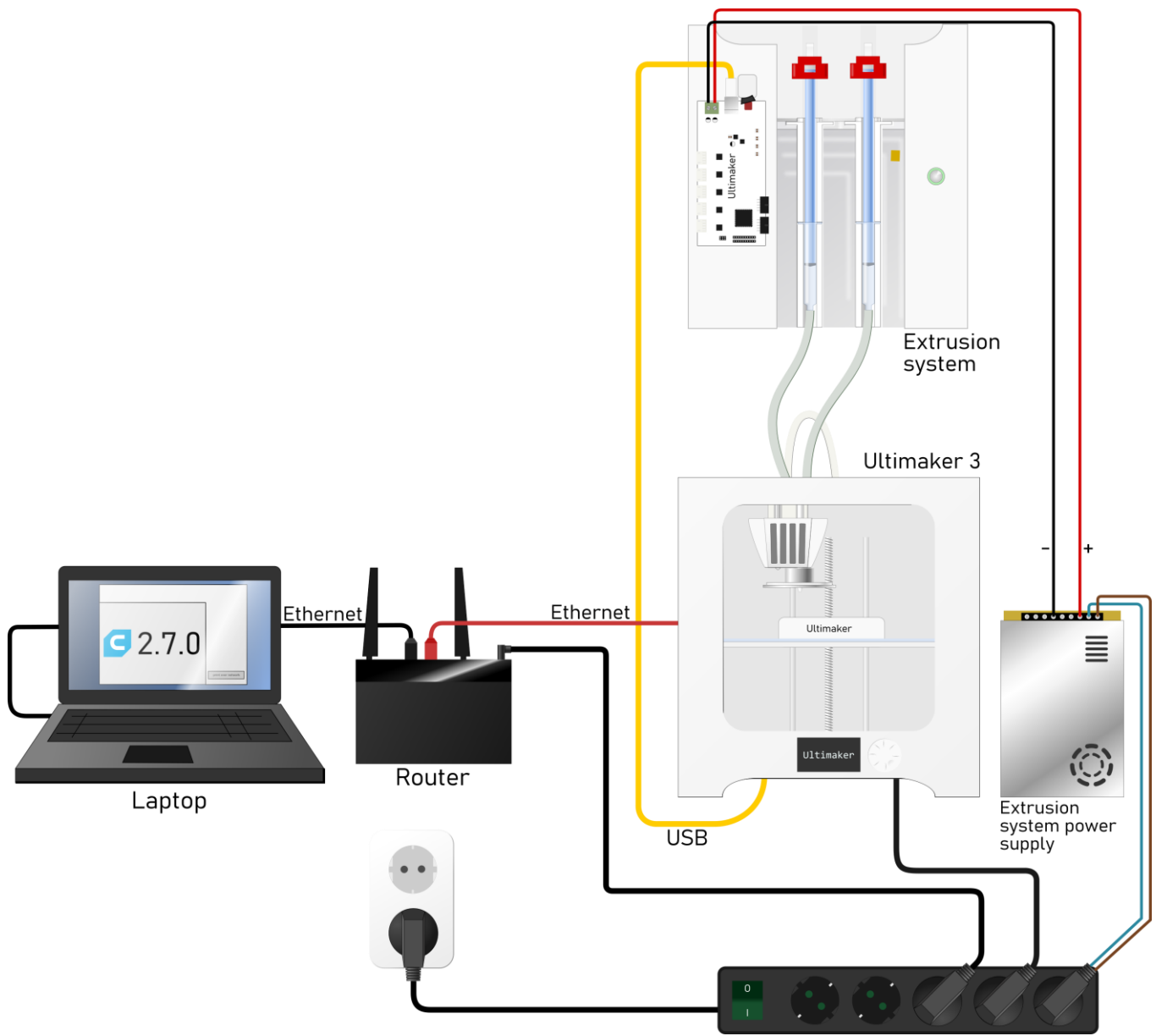
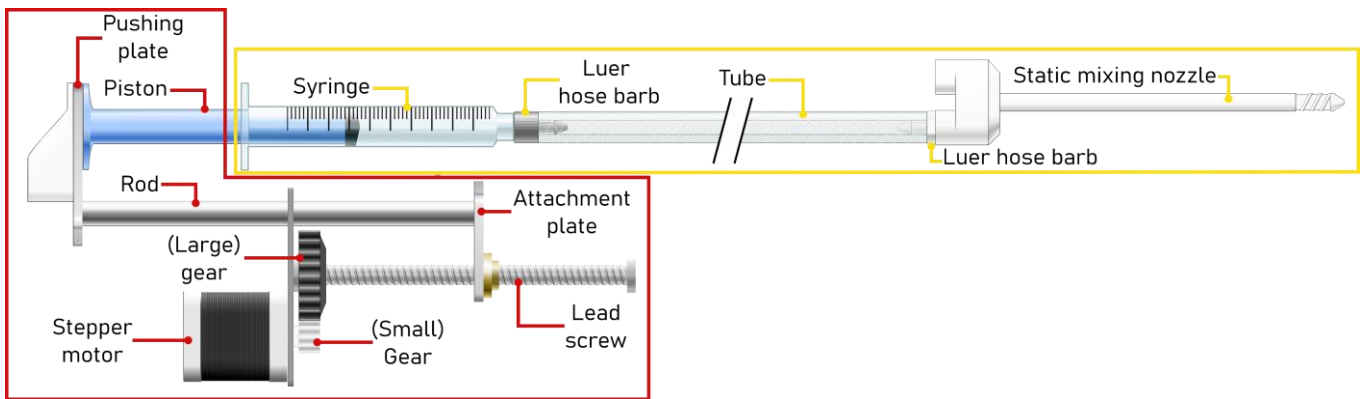
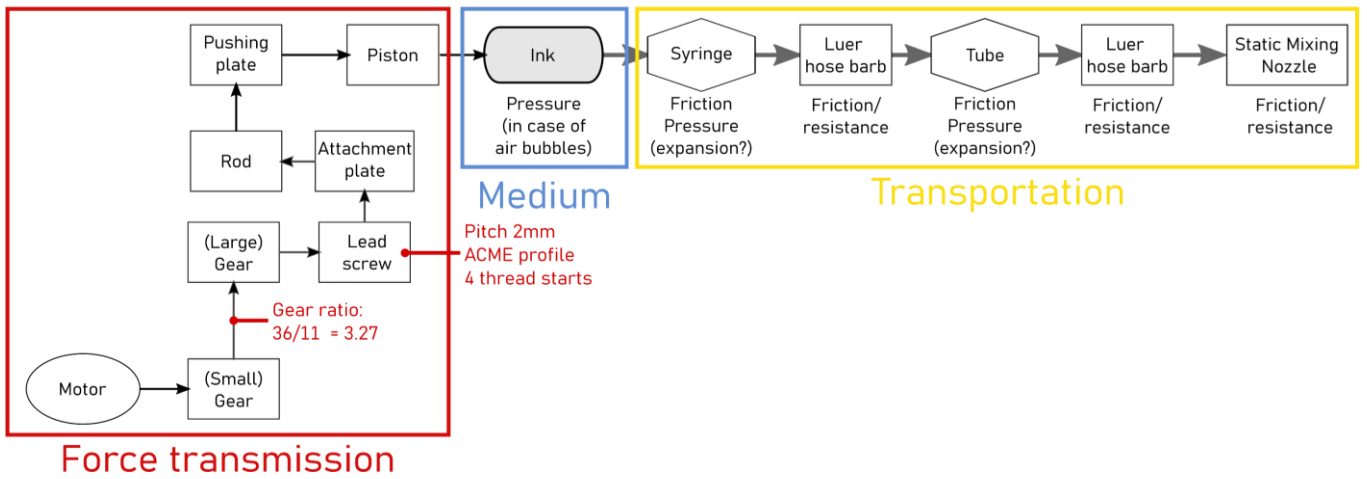


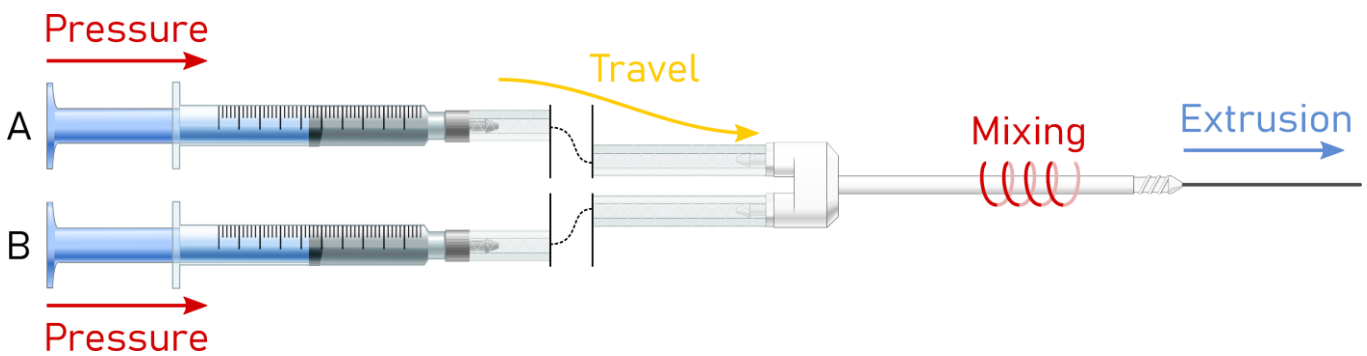
Figure 4.21: Schematic overview of used 3D printer set-up with intended electromagnet control.



*Figure 4.22 :Schematic overview of used 3D printer set-up with the use of a permanent ring magnet to control the orientation of magnetic particles.*



**Figure 4.23:** Schematic representation of external extrusion system. Within the system, two identical mechanisms as depicted are present.



**Figure 4.24:** The two component silicone is being extruded through tubes into a 3D printed static mixing nozzle where it is mixed together and comes out as one homogeneous material. While the two components are separated in their own syringes, the silicone does not solidify.

The system can be divided into two main components: the force transmission from the 17HD6482-01N stepper motor to the piston and the transportation of the ink from the piston out of the nozzle. This ink path causes a *laminar flow resistance* (equation 1). The higher this resistance, the lower the *volumetric flow rate* ( $Q$ ; equation 2), and the more torque the motors need to produce to overcome this. By pushing the pistons down, the motors create a pressure difference between the start of the transport section (i.e. the syringe) and the end, the outside environmental air pressure ( $\Delta P$ ; equations 2 and 3). This pressure is dependant on the force the motor is able to generate (via the gears and the lead screw) and the area of the piston that pushes against the ink (equation 4).

$$R = \frac{8 \mu L}{\pi r^4} \quad (1)$$

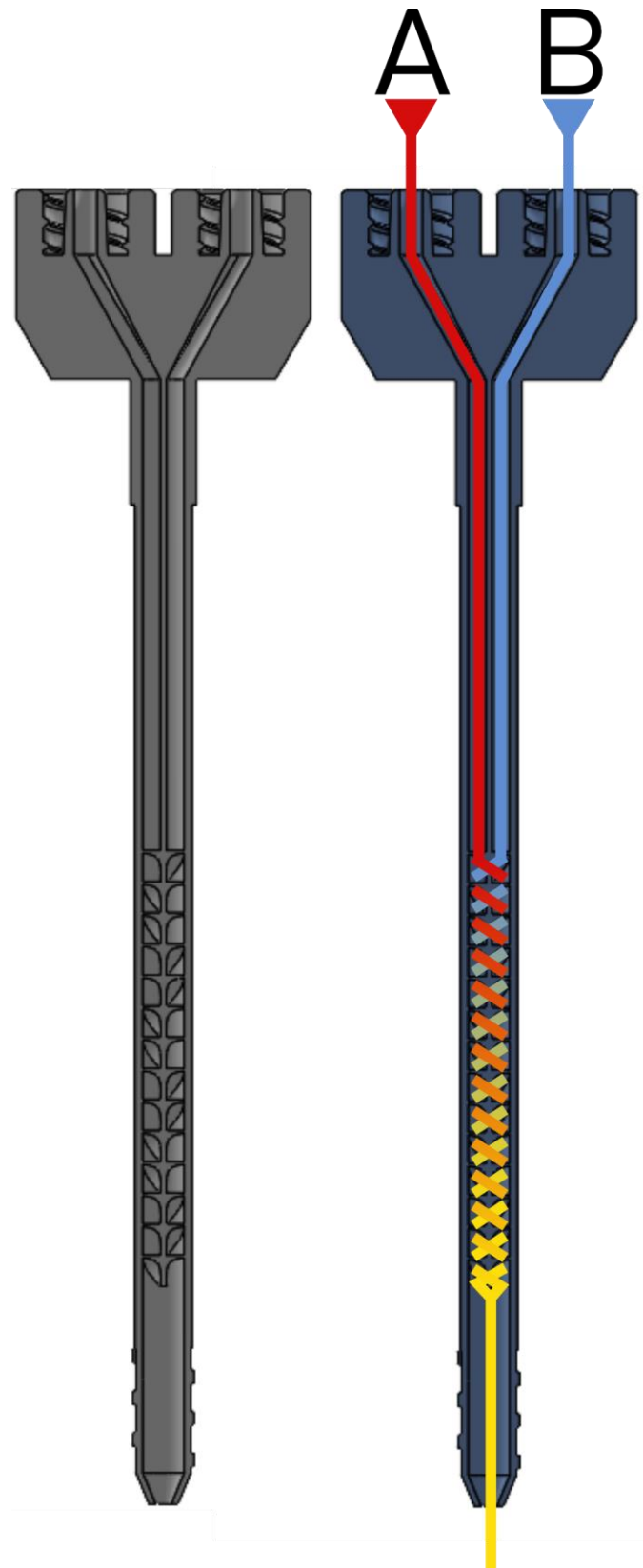
$$Q = \frac{\Delta P}{R} \quad (2)$$

$$\Delta P = P_{piston} - P_{air} \quad (3)$$

$$P_{piston} = \frac{F_{motor}}{A_{piston}} \quad (4)$$

Equations 1-4 can be rewritten into equation 5. Table 4.1 shows al (measured) values of the mentioned parameters.

$$Q = \frac{\left( \frac{F_{motor}}{A_{piston}} - P_{air} \right) \pi r^4}{8 \mu L} \quad (5)$$



**Figure 4.25:** The static mixing nozzle contains a spiral structure inside, which mixes the silicone while it is pushed through.

## Viscosity

As mentioned in Chapter 4.3.2, the viscosity ( $\mu$ ) of the magnetic ink is not constant. It is dependant on the shear rate. Determining the viscosity can be done via equation 6. The values for  $m$  and  $n$  (the so called power law coefficient and index respectively; Bastola, Paudel & Li, 2018) can be found via curve fitting, where a straight line can be drawn through the viscosity measurement data (Figure 4.26). The equation of this trendline corresponds to equation 6.

The shear rate itself is dependant on the radius ( $r$ ) of the whole the material has to go through, the linear flow speed ( $V$ ) at which this happens and the rheological properties of the material, namely the power law index ( $n$ ; equation 7; Bastola, Paudel & Li, 2018). The speed  $V$  is dependant on the flow rate (equation 8).

## Force transmission

The force transmission itself is dependant on the gear ratio (equation 9) and the type of lead screw. The gear ratio transfers the torque generated by the motor to the lead screw (equation 10), which turns the rotation into a linear movement. The resulting total force the motors perform on the syringe pistons can be calculated with equation 11 (Less Boring Lectures, 2020) and is dependent on the type of lead screw that is used. For example using a single threaded screw versus a screw with 4 threads. See Figure 4.27 for explanations of used terms in relation to the screw thread profile. However, equation 11, although it is a common equation used in a variety of sources (e.g. Engineers Edge, n.d.), shows very odd behaviour. In Figure 4.28, outputted force is plotted against the pitch and shows a weirdly shaped graph not in line with what one would expect by intuition. Why this is, is unknown at this point and for time reasons it was not further investigated.

## Interdependence

Overall, the individual components in the system are highly dependant on each other. The flow rate ( $Q$ ) is dependant on the viscosity of the ink ( $\mu$ ), which in turn is dependent on the linear speed ( $V$ ), which is dependent on the flow rate

( $Q$ ). This makes it difficult to calculate the expected flow for the whole system. Usually, interdependent systems give rise to a differential equation. However due to the limited time left in the project to work in this model, further elaboration of this was not pursued. Instead, the aforementioned equations were used to predict the behaviour of individual components and to determine which intervention would be most effective.

$$\mu = m \dot{\gamma}^{(n-1)} \quad (6)$$

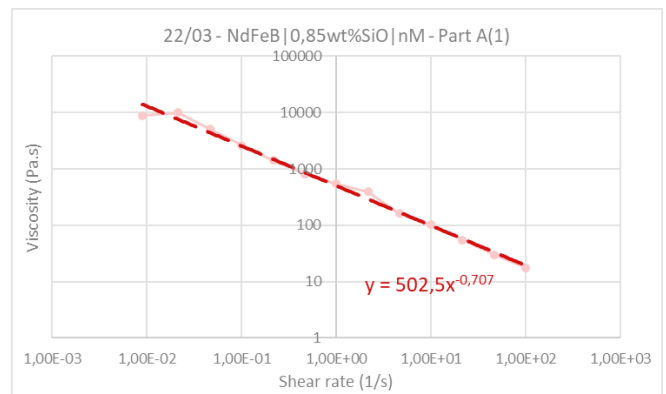
$$\dot{\gamma} = \frac{V r^{(2+n)}}{\left(\frac{n}{3n+1}\right) r^{\left(\frac{3n+1}{n}\right)}} \quad (7)$$

$$V = \frac{Q}{A_{tube}} \quad (8)$$

$$GR = \frac{G_{out}}{G_{in}} \quad (9)$$

$$T_{out} = T_{in} GR \quad (10)$$

$$F_{motor} = \frac{2 T_{out}}{d_p} \left( \frac{\pi d_p - f l \sec(\alpha)}{l + \pi f d_p \sec(\alpha)} \right) \quad (11)$$



**Figure 4.26:** The values for the power lay coefficient and index can be found by the equation of the trendline through the rheometer measurement data in Excel. In this case,  $m = 502.5$  and  $(n - 1) = -0.707$ , meaning  $n = 0.293$ .

**Table 4.1:** Extrusion system parameters

	Parameter	Symbol	Value	Unit
<b>Transportation</b>	Tube length	L	0.3	Meter (m)
	Tube radius	r	0.002	Meter (m)
	Motor Force	$F_{\text{motor}}$	210	Newton (N)
	Piston area	$A_{\text{piston}}$	0.00016	Square meter (m <sup>2</sup> )
	Air pressure	$P_{\text{air}}$	$1.013 \times 10^5$	Pascal (Pa)
	Volumetric flow rate	Q		Cubic meter per second (m <sup>3</sup> /s)
	Flow resistance	R		(N.s/m <sup>5</sup> )
<b>Viscosity</b>	Shear stress	$\tau$		Pascal (Pa)
	Shear rate	$\dot{\gamma}$		(1/s)
	Power law coefficient	m	502.5	n/a
	Power law index	n	0.293	n/a
	Viscosity	$\mu$		Pascal second (Pa.s)
	Linear flow speed	V		Meter per second (m/s)
<b>Force transmission</b>	Input torque	$T_{\text{in}}$		Newton meter (Nm)
	Output torque	$T_{\text{out}}$		Newton meter (Nm)
	# of teeth in driving gear	$G_{\text{in}}$	11	n/a
	# of teeth in driven gear	$G_{\text{out}}$	36	n/a
	Gear ratio	GR	3.27	n/a
	Pitch diameter	$d_p$	0.007	Meter (m)
	Pitch	P	0.002	Meter (m)
	Lead (= pitch * # of threads)	l	0.008	Meter (m)
	Flanck angle	$\alpha$	$0.081\pi$	Radians
	Friction coefficient	f	0.15	n/a

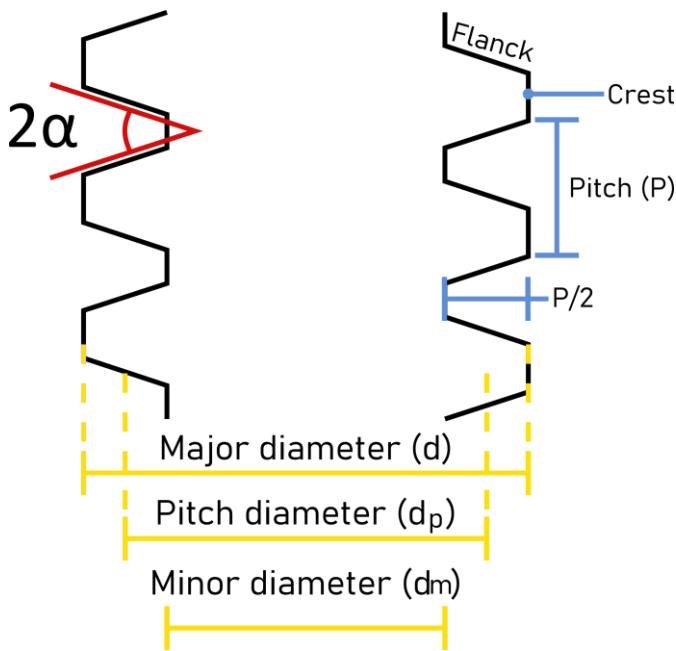


Figure 4.27: Meaning of screw profile terms for an ACME thread profile.

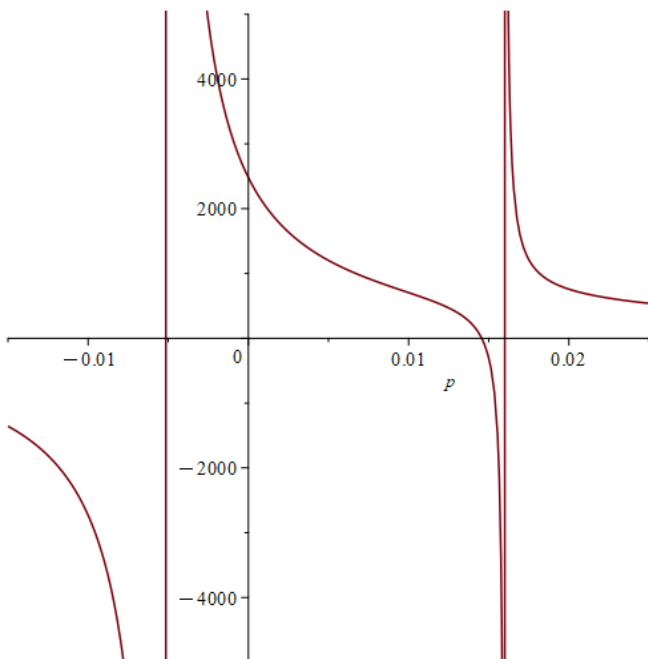


Figure 4.28: Equation 11 gives a curiously shaped graph when the outputted force ( $x$ -axis) is plotted against the thread pitch ( $y$ -axis).

A Simulink model was constructed in an attempt to predict the impact of performed modifications on the extrusion system as a whole. However, this too proved harder than anticipated and was not continued in the project due to time constraints. The model in its current state of progress can be seen in Appendix E.

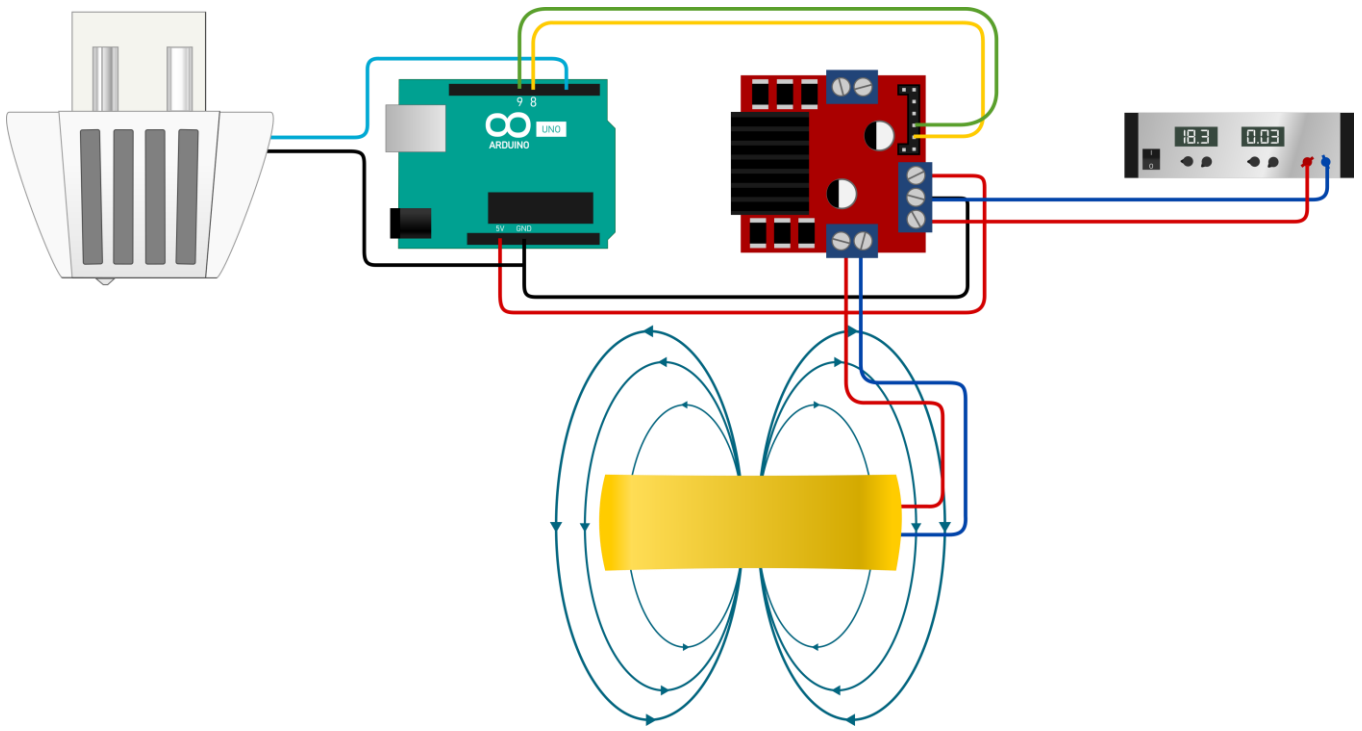
#### 4.4.2 Electromagnet

The electromagnet used in this project originated from the previous project by Sanne van Vilsteren (2021) and was designed by Andres Hunt. It has a supposed field strength of 64.9 mT at the core and 50mT at the edge, operated with a current of 3mA and 24V.

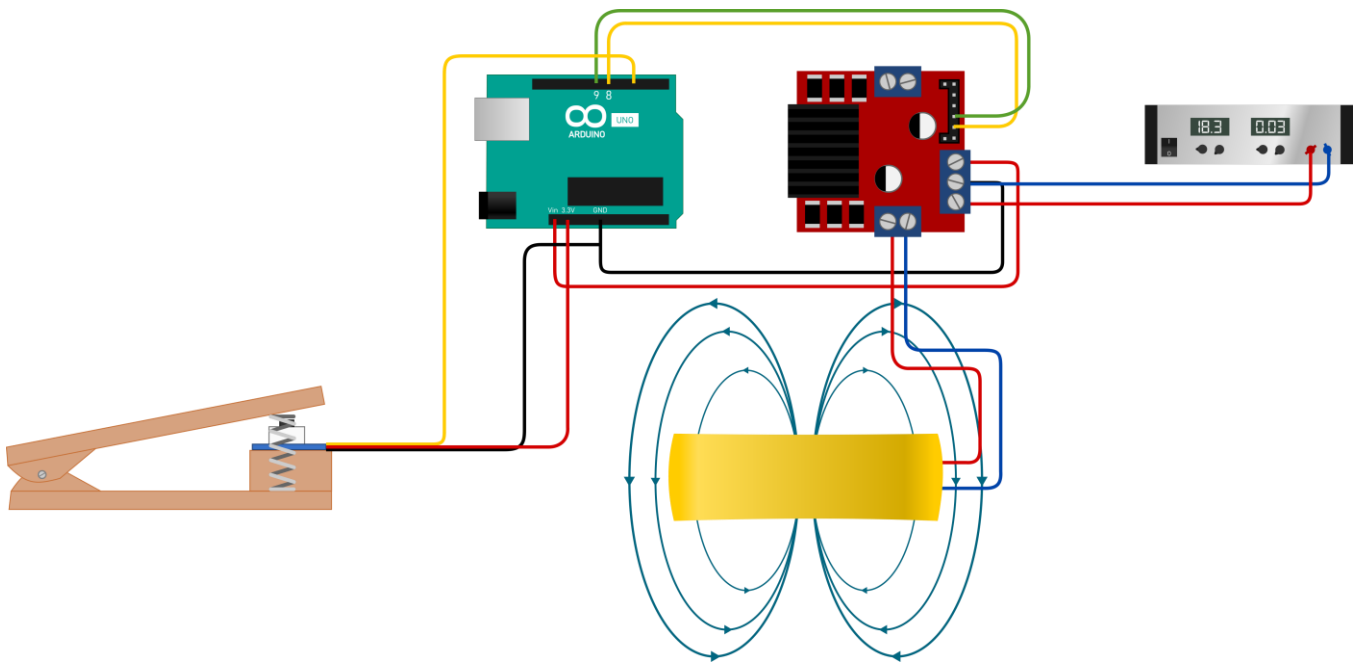
The electromagnet which should have been attached to the end of the static mixing nozzle would change the orientation of magnetic particles and so program the shape change, as explained in Chapter 4.2.1 and Figure 4.7B. However, it was found that the 3D printer did not allow for the control of the electromagnet through G-code in the conventional way by addressing the general pins on the PCB by G-code command `M42 P[pin number]` (RepRap, n.d.; Van Vilsteren, 2021). To allow for electromagnet control easily without having to alter 3D printer firmware, it was tried to use the fan control to control the electromagnet. Part cooling fans on the side of the print head are controlled via G-Code `M106 S[PWM value]` to turn on the fans at a certain speed and `M107` to turn them off (RepRap, n.d.). It was believed that by reading the value send to the fans by the 3D printer with a separate Arduino microcontroller would allow the control of the magnet (Figure 4.29). However, while it was possible to read a control PWM signal generated by the Arduino itself, it was not possible to read these values from the fan headers on the print head (see Appendix C.3a).

In order to check whether the electromagnet would work to reorientate the magnetic particles to begin with, the control of the magnet was hooked up to a button embedded into a foot pedal to allow changing the magnetic polarity of the electromagnet by foot, leaving the hands free for manual ink extrusion (Figure 4.30). To attach the electromagnet to a syringe directly, a special nozzle was designed and 3D printed (Figure 4.31; Appendix D.4).

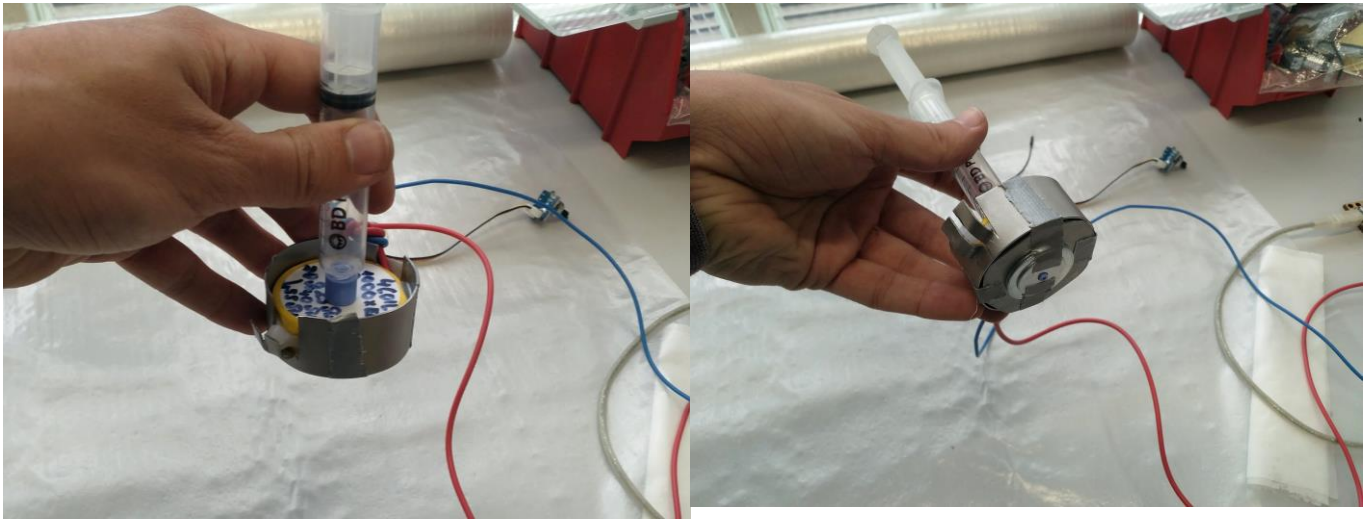




*Figure 4.29: Electromagnet control via reading the PWM values from the fan headers on the print head via an Arduino microcontroller. This approach did not work however.*



*Figure 4.30: Electromagnet control by a foot pedal with button inside. When the button was pressed by pressing down on the pedal, the magnet would flip orientation.*



**Figure 4.31:** The electromagnet mounted to a syringe by means of a 3D printed mounting nozzle screwing into the luer connection on the syringe (seen in blue). The tip has the same thread as the electromagnet and this the magnet screws onto the blue mounting nozzle.

### Validating magnetic programming with electromagnet

To validate the workings of the electromagnet and the principle of using the polarity change to program the orientation of magnetic particles in the silicone (Figure 4.7B), several simple demonstrator shapes were made with manual extrusion (Figure 4.32).

However, testing the electromagnet brought to light some problems. For starters, the magnet gets warm when active. The heat generated by the magnet is enough to warm up PLA above its glass transition temperature, meaning the material will get soft and will warp (Figure 4.33). This poses a problem when working with 3D printed PLA nozzles as has been done during this and the previous project (Van Vilsteren, 2021), implying there is a risk that the magnet or the whole nozzle might fall off during printing. To avoid this, either another material should be used to 3D print the nozzles (like ABS or ASA), the magnet needs to be cooled during printing, or another nozzle needs to be designed or used all together.

Next, the demonstrator samples produced showed curious behaviour. Upon removing the cured silicone from the plate, the samples immediately curled up on themselves (Figure 4.34). Also, the shapes did not shape-change as expected, suggesting the segments do not have the magnetization profile that should have been programmed theoretically when switching magnetic polarity (Figure 4.35).



**Figure 4.32:** demonstrator shapes made with electromagnet.

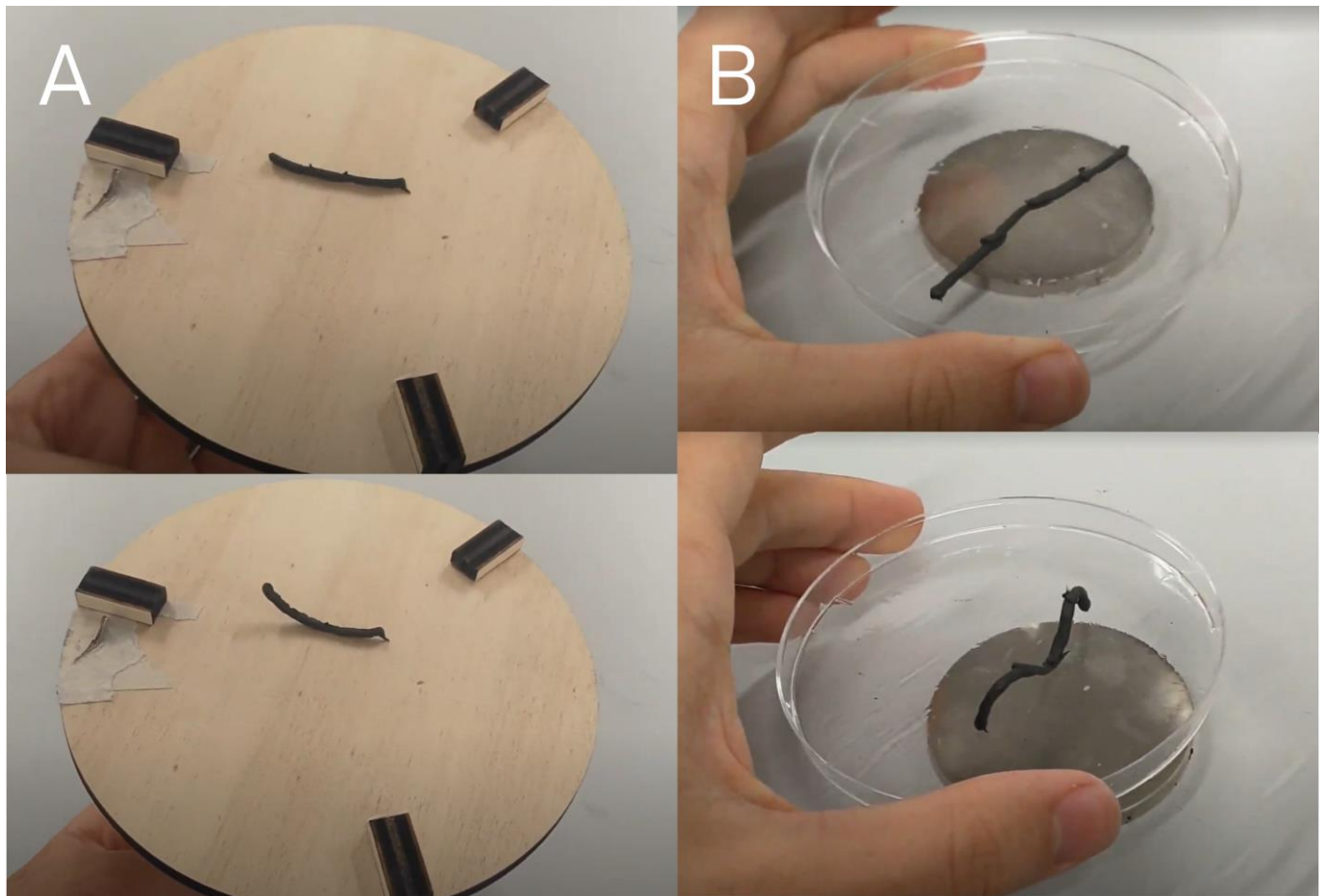


**Figure 4.33:** The heat generated by the electromagnet was enough to make the PLA nozzle piece soft, which caused it to elongate, get thinner and crooked (right). Left, an unused piece can be seen.



It could be that the electromagnet was not strong enough, for example because not enough current was flowing through the coil. Another possibility is that the shield was not sufficient, as it did not extend beyond the edges of the electromagnet because of dimensional restrictions when using the 3D printer. The extra metal material around the edge of the magnet (which was found laying around the lab) was no satisfactory shielding material. More about magnetic shielding can be found in Chapter 4.5.3 and 4.6.3.

**Figure 4.34:** Shapes created with the use of the electromagnet curled up upon themselves immediately after taking off the cured silicone from the glass (build) plate.



**Figure 4.35:** Magnetic actuation of an M-shape wire made with programming using the electromagnet (A) versus an M-shape wire with programming done by a permanent magnet with alternating print direction (B).

## 4.5 Extrusion and other difficulties

In the previous project by Sanne van Vilsteren (2021), the 3D printer set up had trouble extruding the non-magnetized ink (containing Carbonyl Iron particles instead of NdFeB to save costs). Symptoms the system was showing were swelling of tubes, skipping of the stepper motors and tubes disconnecting from the syringes. Ink would drip out of the nozzle after several minutes of trying to get it extruded. In the first half of the project, most time was spend on finding out causes of these limitations and to resolve these by trial and error.

### 4.5.1 Travel tubes

In work done on the 3D printer in the previous project (Van Vilsteren, 2021), Clear PVC tubes with an inner diameter of 3mm and outer diameter of 6mm were used to transport the ink from the extrusion system (standing next to the printer) towards the static mixing nozzle. Because of the thin walls of these tubes and the high viscosity of the material, it was suspected that swelling of these tubes contributed to the delay of several minutes of extrusion of the non-magnetic ink.

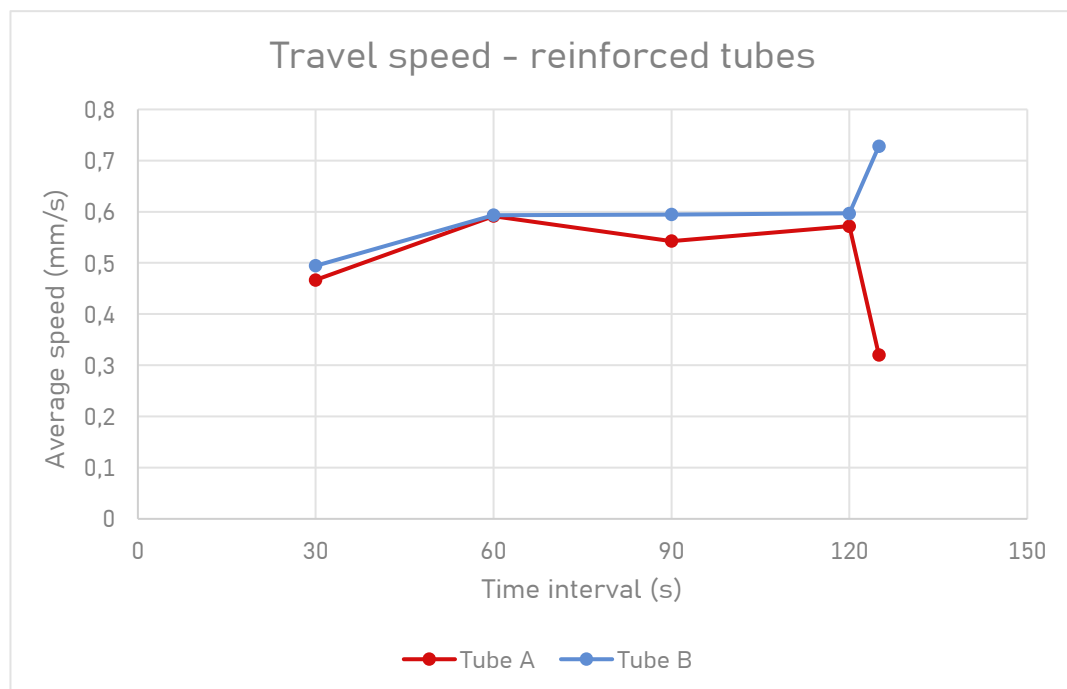


**Figure 4.36:** Refitexx Cristallo PN30 4x10mm tubes with reinforced, 3mm thick walls used for the majority of this project (Arestho, n.d.).

To minimize tube swelling, tubes were used with larger wall thickness (3mm) and larger inner diameter (4mm) in the majority of this project. Walls of these tubes were reinforced with wiring inside (Figure 4.36).

#### Ghost extrusion

To find out the cause of the delay in extrusion, experiments were done whereby ink was pushed into the tubes towards the static mixing nozzle.



**Figure 4.37:** Average travel speed in the first 30 seconds of extrusion was noticeably lower than the remaining 95 seconds of active extrusion.

by the extrusion system, by feeding it the G-code:

```
G1 F1 A89 B89
```

This code corresponds with moving the pushing plates 6mm, which should extrude 1 ml of ink out of each syringe in 125 seconds (Van Vilsteren, 2021; Figure 4.39).

While the ink travelled inside the tubes, the distance it travelled was marked at intervals of 30 seconds. It was found that the average speed at which the ink travelled was lower in the first 30 seconds compared to remaining 95 seconds (Figure 4.37 and 4.38). After active extrusion had stopped, the ink would continue traveling through the tubes. This uncontrolled extrusion was called ghost extrusion, as the ink seemed to be pushed by an otherworldly entity when the extrusion motors had stopped (Figure 4.38).

The ghost extrusion and the acceleration of ink travel speed in the first 30 seconds of active extrusion, suggested a build up of pressure inside the extrusion system that was released after active extrusion.

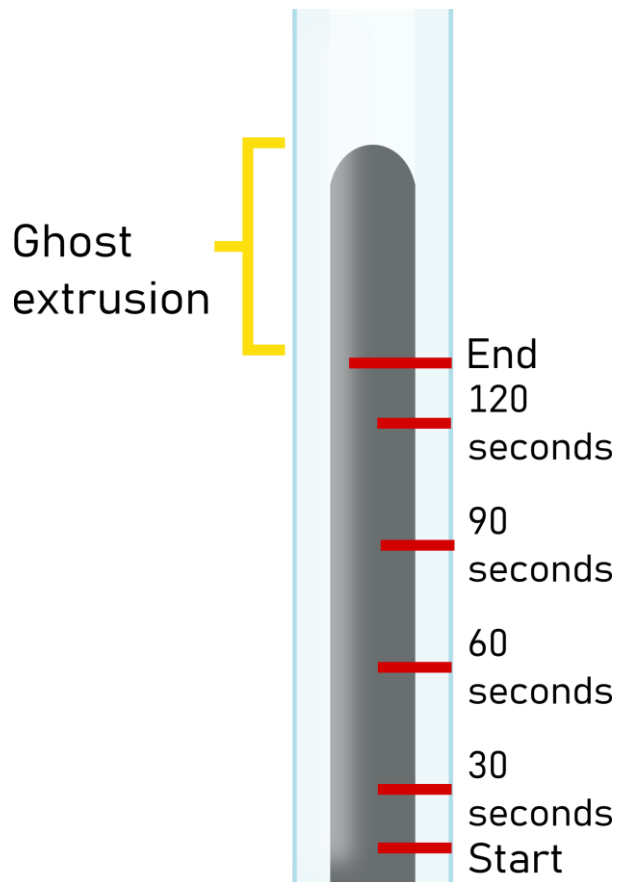
#### 4.5.2 Pressure

To find the origin of the pressure build up in the system, several hypothesis have been considered. Besides swelling of the travel tubes (paragraph 4.5.1), other possibilities include compression of air bubbles inside the ink caused when the ink was transferred to the syringes after fabrication (paragraph 4.3.1) and minor flexibility of the extrusion system itself.

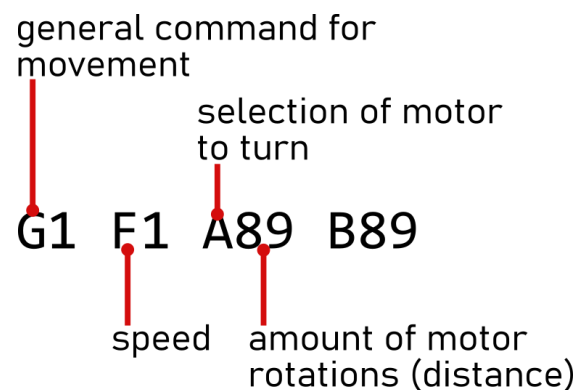
##### *Motor skipping and pressure*

A characteristic of stepper motors, such as the ones used in the extrusion system, is that they skip steps when they do not have enough strength to turn. When this happens, they make a loud ticking noise. This characteristic was used in experiments to find indications of where the pressure build up was originating from.

Syringes with an incompressible content were loaded into the extrusion system. G-codes with increasing distance values were fed to the system. If the system would be infinitely stiff, motors would be skipping immediately. However, it was found that this happened



*Figure 4.38: Marking while ink travelled through the tube revealed an acceleration in the beginning of extrusion and a release of build up pressure in the form of ghost extrusion.*



*Figure 4.39: Explanation of G-code meaning per section*

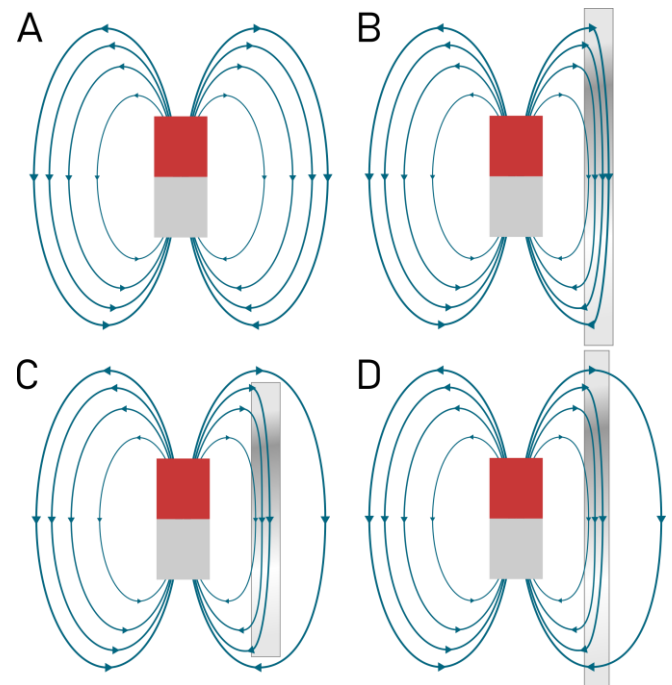
at a distance value of 90 (about 6mm of travel), indicating flexibility in the mechanical components of the extrusion system (Appendix C.2f) These components would thus elastically deform during extrusion and would have internal stresses. These stresses could then be translated into a pressure that was gradually released after active extrusion, resulting in ghost extrusion. Observations showed the default pistons of the syringes where buckling under the pressure.

To test the hypothesis of air bubbles present in the ink, the same motor skipping experiment was conducted with blocked off syringes filled with unmagnetized ink containing Iron particles. It was found that the motors would skip at a distance value of 200, indicating air bubbles present in the ink that would be compressed during extrusion, creating a pressure inside the ink that would be released after active extrusion and thus caused ghost extrusion. After applying a degassing sequence, the skipping distance was decreased to 90, the same value as with the incompressible syringe contents (Appendix C.2h).

#### 4.5.3 Magnetic shield

A magnetic shield redirects the magnetic flux travelling from one pole to the other. The shield provides an easier path for the flux to travel through than air. This results in there being no magnetic field present beyond the shield (K&J Magnetics, n.d.; MuShield, n.d.; Figure 4.40).

The material used for the shielding was initially Grain Oriented Electrical Steel from Nippon Steel. This material reports a high magnetic permeability (Nippon Steel, n.d.), meaning magnetic flux can travel through it very easily, making it a good shielding material because magnetic flux chooses the path with the least resistance. A problem with such high permeability material is the saturation. The material is saturated at very low field strengths, meaning that any magnetic field higher than this saturation threshold, will simply pass through the shield. Saturation also has to do with the thickness of the shield. The thicker the shield, the higher the saturation because there is more material to be satisfied.



**Figure 4.40:** magnetic flux travels from the north to south pole of a magnet (A). A magnetic shield 'absorbs' the magnetix flux, as it likes to take this route rather than plain air (B). If the shield is too short, magnetic flux can pass in at the sides (C). If the shielding material is saturated or the shield is too thin, magnetic flux will pass through it (D). Adapted from K&J Magnetics, n.d.

#### Magnetic shield redesign recommendation

To shield off a powerful magnet, a double material design can be made, in which a low/medium permeability material with high saturation point is used in the layer closest to the magnet. This will absorb most of the large magnetic flux. A second layer of high permeability, low saturation material will absorb the remaining, small magnetic flux (MuShield, n.d.). This design approach was not implemented in this project because of insufficient time.

## 4.6 4D printer design interventions

With the outcomes of the experiments done in the first half of the project and the consultation of fluid mechanics and associated mathematics, improvements were done to the 4D printing set-up to make extrusion of the highly viscose magnetic ink easier.

### 4.6.1 Travel resistance and length

The tubes used in this project with inner diameter of 4 mm and wall thickness of 3 mm where chosen because it was believed they were less prone to swell up under the ink pressure. These tubes do however bring another advantage. Because of the larger inner diameter, the resistance in the tubes is decreased, according to equation 1. Length also contributes to resistance. The lower the resistance, the higher the flow rate or the lower the pressure difference needs to be to achieve the same flowrate  $Q$  (equation 2). As can be seen from equation 5, flow rate is directly dependant on the motor force, as this is creating the pressure difference. Equation 5 can be written as equation 12, from which becomes clear that a lower  $R$  and constant  $Q$ , the motor force becomes smaller.

In order to make the tubes as short as possible to lower the resistance, an overhead support structure was designed in which the extrusion system could be placed. This way, the extrusion system is placed 20 cm above the print head (Figure 4.41; Appendix D.7).

The extrusion system is build for 60ml syringes, to further lower the force needed to generate a higher pressure, the 60 ml syringes were replaced with 10ml syringes, which had a smaller piston area (van Vilsteren, 2021). For this, conversion pieces were designed by Van Vilsteren (2021). To enable the syringes to be placed lower down the extrusion system to further reduce the length (and thus flow resistance) of the tubes, new conversion pieces were designed (Figure 4.42: Appendix D.6).

The total tube length was brought down to 30 cm, compared to the 70 cm needed with the extrusion system placed on the side of the 3D printer.

$$R = \frac{8 \mu L}{\pi r^4} \quad (1)$$

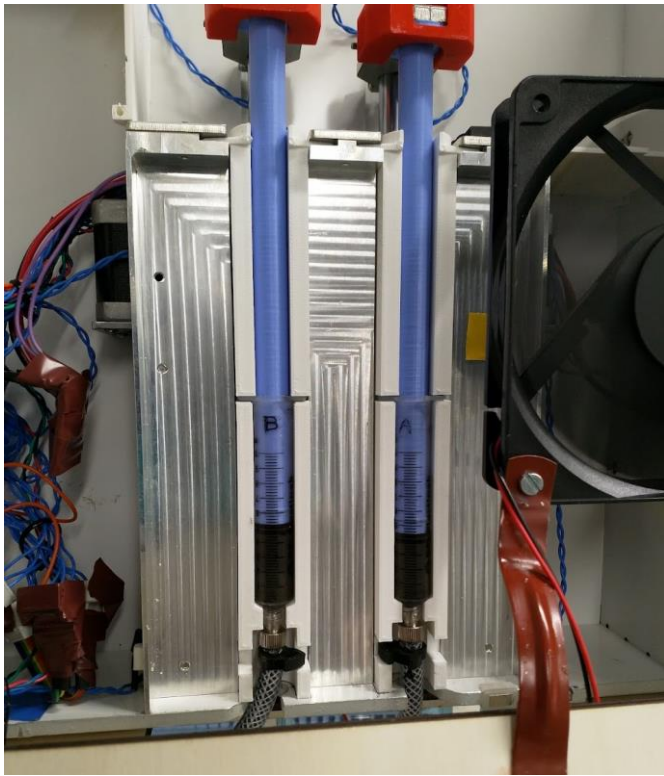
$$Q = \frac{\Delta P}{R} \quad (2)$$

$$Q = \frac{\left(\frac{F_{motor}}{A_{piston}} - P_{air}\right) \pi r^4}{8 \mu L} \quad (5)$$

$$F_{motor} = (Q R + P_{air}) A_{piston} \quad (12)$$



*Figure 4.41: The designed overhead support structure allowed the extrusion system to be placed 20 cm above the printhead.*



**Figure 4.42:** New conversion pieces allowed the syringes to be seated 10 cm closer to the print head, thus saving tube length and reducing resistance. Longer pistons needed to be made because of this.

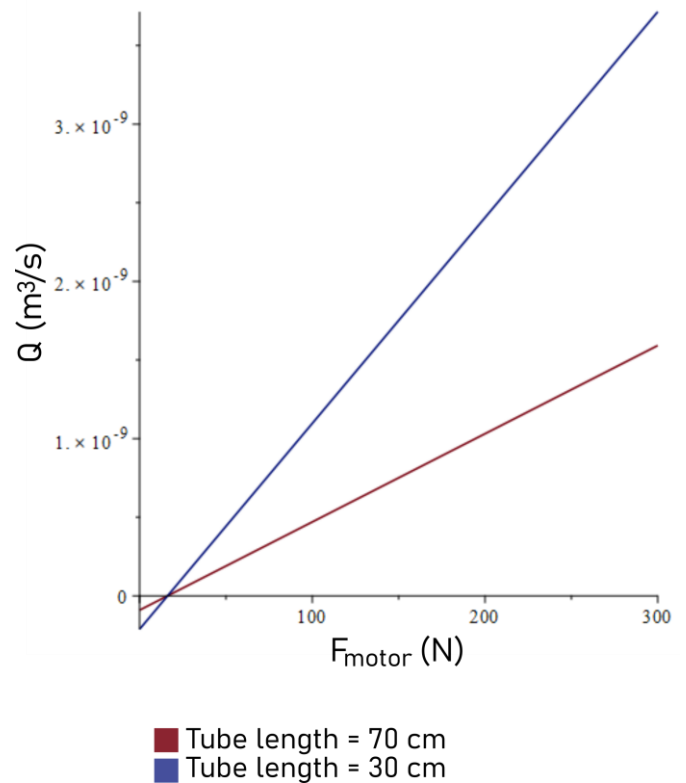
In the plot of equation 5 in Figure 4.43, it can be seen that the reduction of tube length results in a much lower force required for the same flow rate, assuming a constant viscosity of 10000 Pa.S.

#### 4.6.2 Newly designed pistons

The default syringe pistons would buckle under the pressure generated by the extrusion system. Stiffer, 3D printed pistons were made, which resulted in a decrease in distance value until motor skipping occurred from 90 to 70 (Appendix C.2j). To account for the larger distance between syringe and pushing plate now that the syringes were placed further down the system, pistons were also made longer (Figure 4.42; Appendix D.5; the parts in blue).

#### 4.6.3 Magnetic shield material and shape

The very thin grain oriented steel did not properly work as magnetic shield, probably because of the low saturation point. The ink would still be attracted by the magnet during



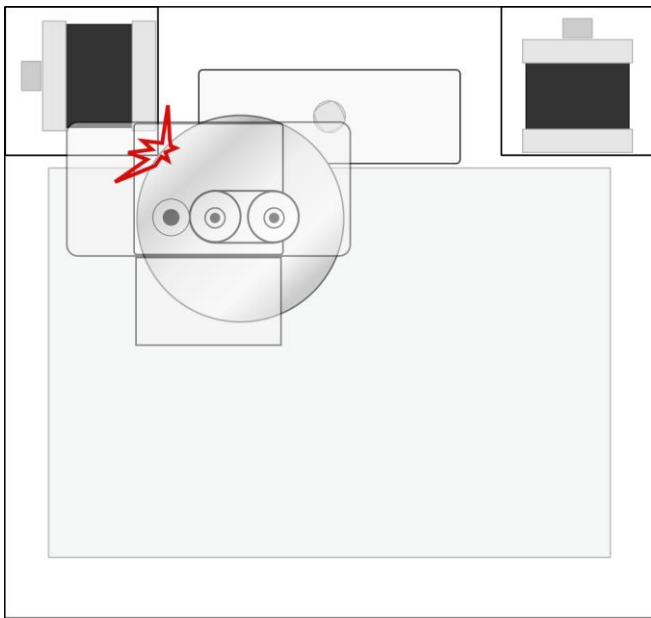
**Figure 4.43:** Reduction of tube length from 70 to 30 cm means the motors need to generate less force ( $F$ ) to achieve the same flow rate ( $Q$ ).

printing or manual extrusion. By adding more layers to the shield, the shielding got better, but not satisfactory. Normal steel was also tried. This material has a higher saturation, which is preferred when using the very strong NdFeB ring magnets. This material seemed to work better, giving a slightly better shielding at a lower thickness.

#### Dimensional constraints

Because the magnetic shield was supposed to work with the 4D printer, the shield had to meet certain dimensional restrictions. Otherwise, the magnet would jam into the motor shrouds in the corners of the Ultimaker 3 3D printer (Figure 4.44). Therefore, the magnetic field probably passed the shield, like depicted in Figure 4.40C. From experience, the edges of the shield showed a larger magnetic attraction than the center (Figure 4.45). By adding one or two layers of steel around the sides of the (permanent) magnet, it was attempted to minimize this.





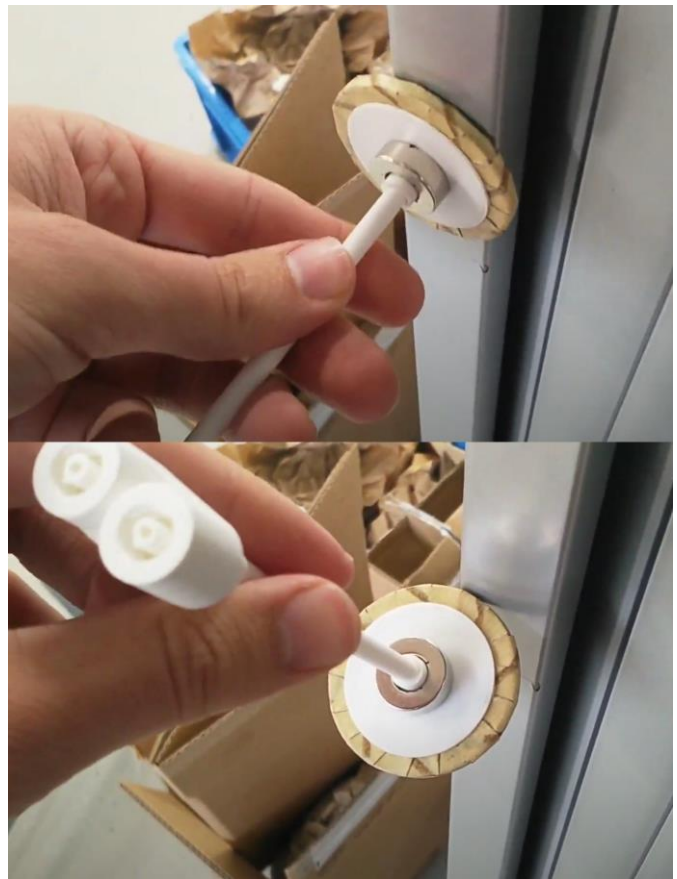
**Figure 4.44:** When too large, the magnetic shield would jam into the motor shrouds in the corners of the 3D printer, potentially breaking the static mixing nozzle to which it is attached.

#### 4.6.3 Static mixing nozzle redesign

The original static mixing nozzle design was narrow and long, because it had to fit through the original print head. However, evident from equation 1, narrow long tubes lead to a high resistance. Added to this, the mixing spiral was very long, adding even more resistance.

##### *Mixing spiral length*

The two component silicone is mixed together in the mixing spiral. It is important this happens sufficiently for the silicone to cure. However, the longer the spiral is, the more flow resistance it causes. Therefore, the mixing spiral was brought down to just four turns

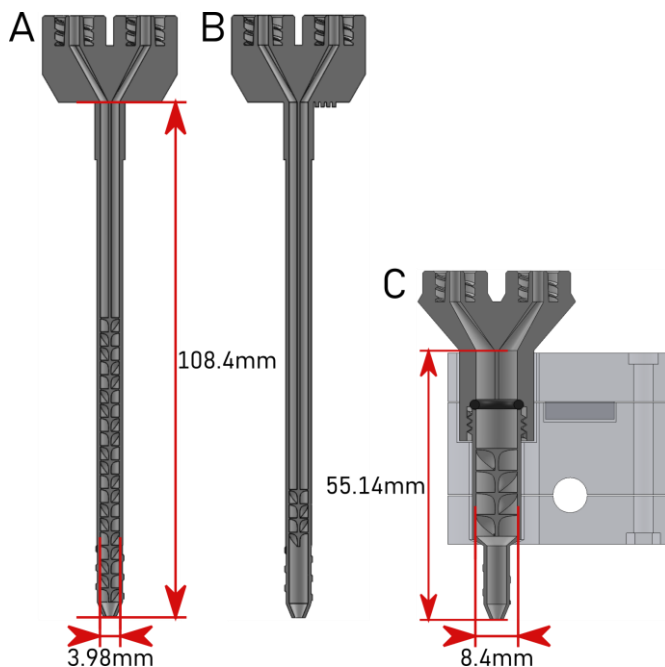


**Figure 4.45:** The centre of the magnetic shield showed a lesser attraction to metal surfaces than the edges of the shield.

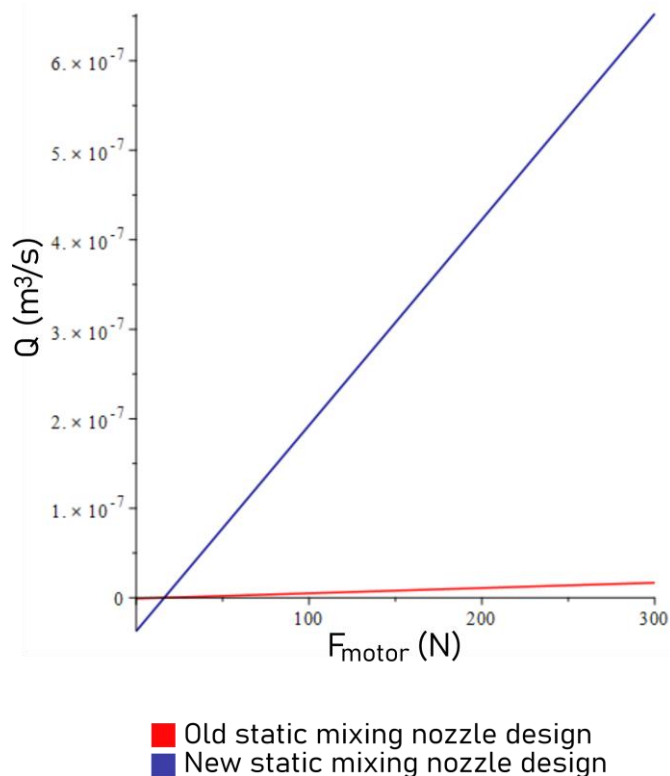
(Figure 4.46B). This proved sufficient to mix plain silicone (so without metallic particles added) to make it cure.

##### *Overall length and width*

Eliminating 80% of the mixing spiral was not enough to ensure a smooth extrusion. Therefore, a new design was made for both the mixing nozzle and the print head. By replacing the head, it was possible to make the mixing nozzle wider and overall shorter (Figure 4.46C), theoretically lowering the force needed to achieve a certain flow rate with 89.5% (Figure 4.47).



**Figure 4.46:** Three iterations of the static mixing nozzle designs: the original length and width with original mixing spiral (A); the original length/width with shorter mixing section (B) and new shorter and wider design (C).



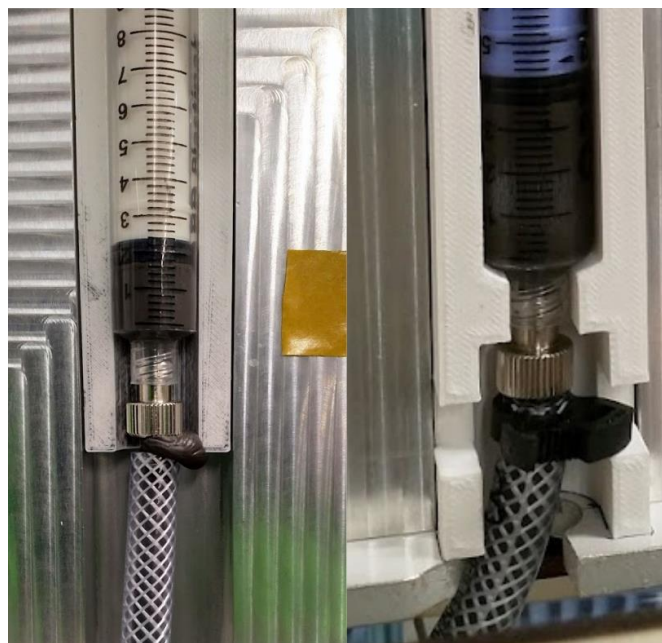
**Figure 4.47:** The new mixing nozzle design (Figure 4.46C) would theoretically result in a reduction of motor force needed of 89.5%, not taking into account the preceding tube length.

#### 4.6.4 clamps and cooling

Some other minor additions were done as well: tube clamps to stop leaking and a cooling fan to cool the motors after receiving more current. By feeding more current to the motors, they become a bit more powerful, being able to generate more torque, thus apply more pressure to the ink. It was measured that the force the motors could apply to the pistons was 210 newton, which translates to a pressure of 1.3 MPa (equation 4).

Because of the high pressure involved, leaking occurred between the tubes and luer hose barb connections. To mitigate this problem, plastic tube clamps were used to tighten the tubes around the hose barbs. This prevents them from sliding off and closes off any gaps (Figure 4.48).

A cooling fan was added to cool down the motors actively which quickly heated up due to the increased current. Directed at motor A, the airflow would travel behind the extrusion system past motor B and exit at the other side.



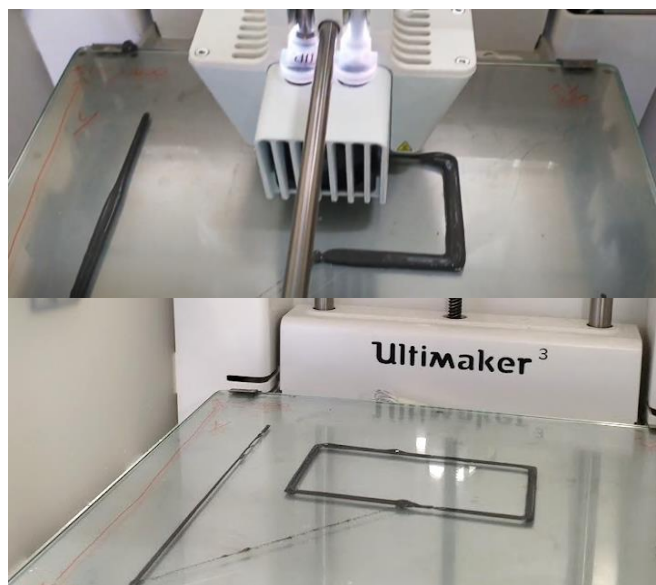
**Figure 4.48:** Leaking occurred because of the high pressures involved when using powerful motors. Plastic tube clamps solved this problem when tightened far enough.

## 4.7 Modification results

All listed modifications in Chapter 4.6 had the objective to make the Ultimaker 3 3D printer with separate dual syringe extrusion system be able to reliably extrude the viscose magnetic ink. This was successful up to a certain degree, but still some issues remain that prevents the system to be used to 4D print shape morphing objects.

### 4.7.1 Unmagnetized ink extrusion

Around half way of the project, it was established that unmagnetized ink containing Iron particles was able to be reliably extruded by the 3D printer when equipped with the extrusion overhead support structure and stiffer syringes. No motor skipping occurred and printed samples did cure well at room temperature (4 hours time). An important finding was that prior to printing objects, the system needed to be 'primed', during which pressure was built up until there would not be any flex left in the system. This was done using a priming line at the edge of the print bed (Figure 4.49; Appendix C.2k).



**Figure 4.49:** It was possible to 3D print unmagnetized ink with the 3D printer after modifying the pistons and using shorter tubes without issues like motor skipping. The priming line on the left made sure sufficient pressure was present at the start of the print. Even too much ink was extruded initially.

### 4.7.2 Magnetized ink extrusion

Unmagnetized ink is about 10 times less viscose than magnetized ink while showing the same shear-thinning properties (Chapter 4.3.2; Figure 4.17). It is therefore easier to extrude than magnetized ink. However, without magnetized particles, it is not possible to program the magnetization profile and thus it cannot be called 4D printing.

In order to be able to print magnetized ink, more modifications needed to be implemented. That is the new conversion pieces (Figure 4.42); and static mixing nozzle alterations (Figure 4.46 B and C). The result of these modifications can be seen in Figure 4.50. While the results may look promising, it is not without a fair share of issues. It also showed inconsistent behaviour, working well one day and not at all the next without changing any parameters (Appendix C.2q and C.2r).

#### Motor force

Despite squeezing 210 N out of the extrusion motors, this force is not good enough. Motor skipping still occurred with all design interventions. To try and extrude magnetized ink anyway, the motors were assisted by pushing the plates down by hand.



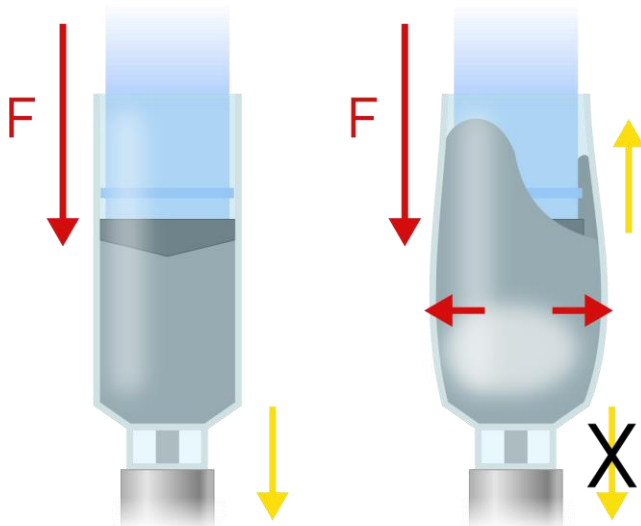
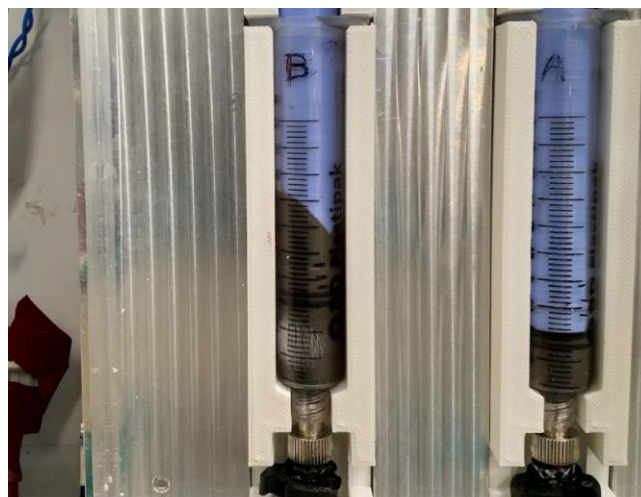
**Figure 4.50:** With all implemented modifications, magnetic ink was able to be extruded. However, this was no smooth experience, of which the attraction of ink by the magnet despite the shielding is just one example.

### Syringe swelling

Helping the extrusion motors generated more pressure, which presented more problems. The most prominent being the swelling of the syringes. The pressure was not directed downward to push the ink through the nozzle, but instead outward, plastically deforming the syringes (Figure 4.51). Not only did the ink not extrude because of this, but as the syringes expand, the diameter increases, leaving a gap between syringe and piston. Ink is therefore pushed up past the piston (Figure 4.52).

### Ink curing

In all attempts to 4D print with the magnetized ink, the printed samples did not cure (Figure 4.53). It was found that this was because of under extrusion of component B. The Ecoflex 00-10 silicone is meant to be mixed at a 1:1 ratio (Smooth-On, n.d.). Under extrusion of one component leads to an imbalance in this ratio, thus not curing the silicone. This also corresponds with observations showing component A being more extruded than component B (Figure 4.54).

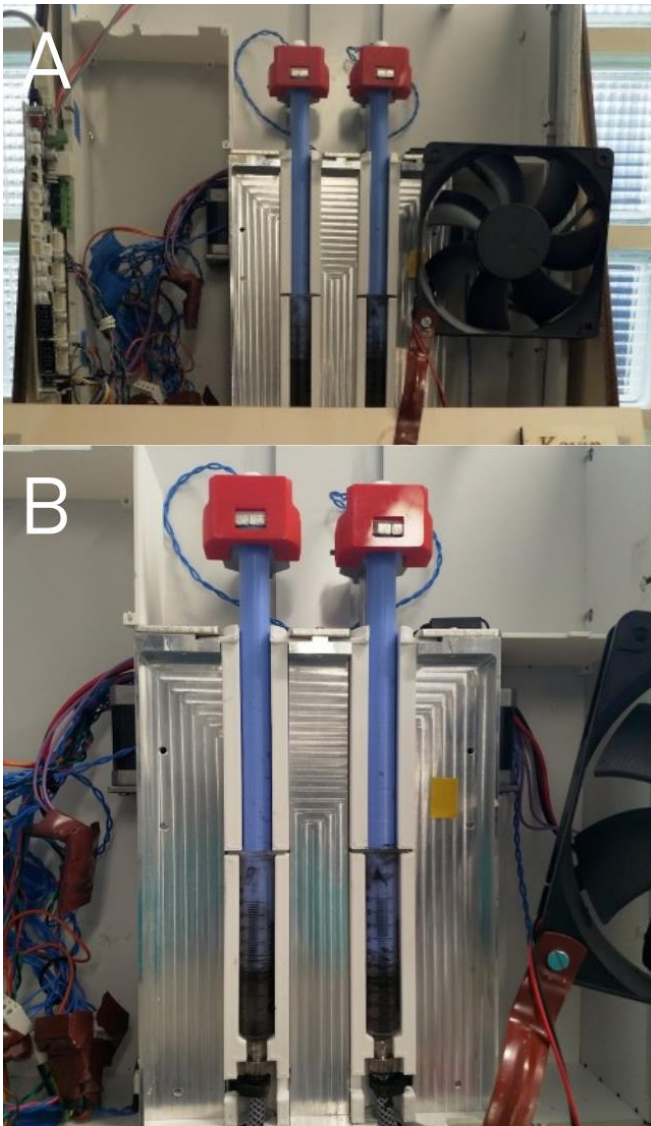


**Figure 4.51:** Because of the high pressure, syringes started swelling, leading to under extrusion of ink.

**Figure 4.52:** Pressure from the extrusion system is exerted on the walls of the syringe, as the pressure needed to push ink down the nozzle is higher than the yield strength of the plastic walls. Instead of travelling down, ink is travelling up.



**Figure 4.53:** At every attempt, the printed samples did not cure because of a wrong A/B ratio.



**Figure 4.54:** At the start of a printing session, component A is filled more than component B, evident from the higher position of the piston. However, some time in the session, this height has dropped below component B, showing component B is extruding less than component A.

#### Insufficient shielding

As could already be seen in Figure 4.50, the magnetic shield does not work properly. While the remaining field strength is very weak, it is large enough for the magnetic ink to curl up and attach to the magnet (Figure 4.55). This makes it difficult to print objects, as the ink does not properly stick to the build plate.

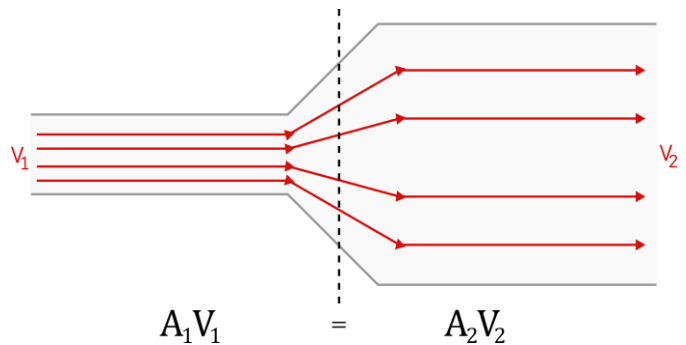
#### New mixing nozzle design

The wider and shorter mixing nozzle should have made it more easy to extrude ink (Figure 4.47). However, it seemed extrusion was more



**Figure 4.55:** Once extruded, ink is still attracted towards the magnet because of the low magnetic field still present.

$$A_1 V_1 = A_2 V_2 \quad (13)$$



**Figure 4.56:** The principle of continuity states that the flow speed decreases as area increases (adapted from Khan academy, n.d.).

Difficult. No ink came out of the nozzle. This could have been because of the shear rate.

The viscosity of the magnetized ink is dependent on shear rate. The higher the shear rate, the lower the ink viscosity (Chapter 4.3.2). By increasing the diameter of the mixing nozzle, the speed at which the ink travels was decreased, according to the principle of continuity (Khan Academy, n.d.; equation 13; Figure 4.56). From equations 6 and 7 (Chapter 4.4.1), we can see that a decrease in linear flow speed ( $V$ ) leads to a lower shear rate, which leads to an increase in viscosity. Flow resistance is dependant on viscosity: higher viscosity means higher flow resistance (equation 1).

### Successful print using short tubes

In an experiment to test whether the magnetic ink would cure as good as plain silicone when using the short mixing spiral in the long, thin static mixing nozzle (Figure 4.46B), this nozzle was hung down from the syringes using 10 cm long tubes (Figure 4.57). Initially, this was done to save material as there was not much left at the time. This experiment proved that it was possible to reliably print magnetized ink using this set-up, without skipping motors or other high-pressure problems. By moving a small glass dish under the static nozzle, a small scribble was made, which showed very well magnetic response (Figure 4.58).

Downside to this set-up was that the ink did not cure at room temperature. It did however cure well in the oven at 120 C for one hour.



**Figure 4.57:** 10 cm long tubes were used to test a new static mixing nozzle design, which ended up proving magnetic material could be extruded when making use of very short transport tubes.

### 4.8 viscosity, resistance, flow rate and radius

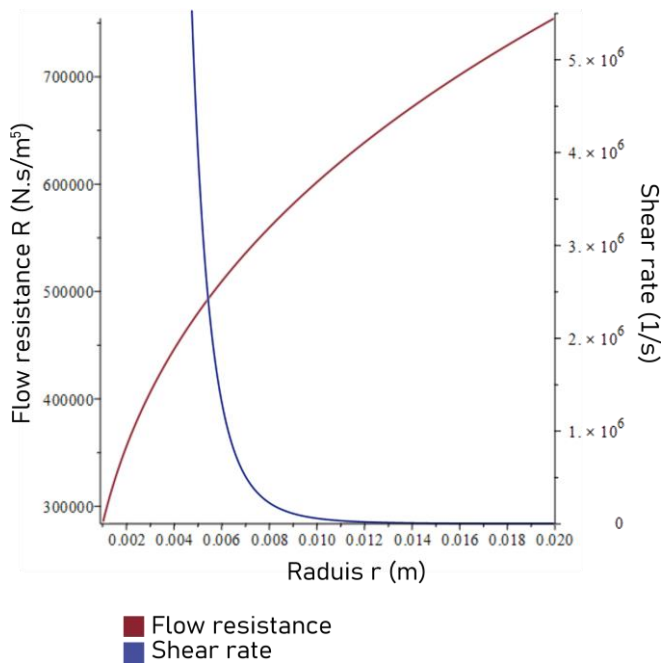
Equations 1 (flow resistance), 6 (viscosity), 7 (shear rate) and 8 (linear flow velocity) can all be combined into equation 14. Plotting the radius against the resulting resistance using a constant flow rate (0.016ml/s) and length (0.0108m) reveals behaviour contradicting to that what men would expect when dealing with Newtonian fluids; the resistance increases when the tube radius increases (Figure 4.59).

The resistance can be lowered by increasing the flow rate, giving the ink more speed and thus more experienced shear rate (Figure 4.60).

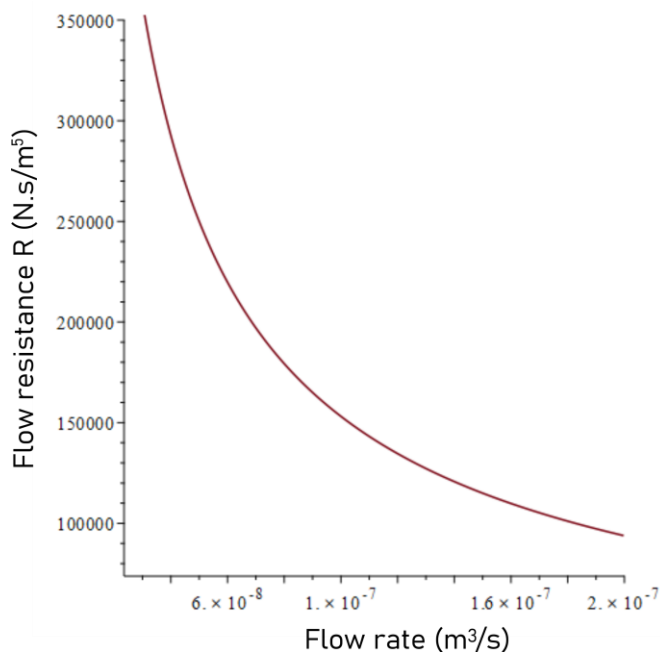
Using the new, thicker nozzle, the extrusion speed was increased simply by increasing the F-value in the g-code from F1 to F10 (Figure 4.39). This resulted in fast extrusion of magnetic ink for about one second, after which both motors started to skip rapidly. They seemed to lack the force needed to maintain this flowrate. In addition, the extruded ink again did not cure this time (Figure 4.61).



**Figure 4.58:** A scribble could be 4D printed when using 10 cm tubes and showed good magnetic response.



**Figure 4.59:** Flow resistance increases when the radius of the tube where the non-Newtonian liquid passes through increases, because the shear rate decreases as the flow speed decreases. Depicted shear rate is however extremely high. Viscosity measurements only went up to  $100 \text{ s}^{-1}$ . Likely, the flow rate of  $0.016 \text{ ml/s}$  is much too high or the equation for shear rate by Bastola & Paudel (2018) is not correct (ly used).



**Figure 4.60:** Increasing the flow rate, thus giving the ink more speed, increases shear rate and lowers flow resistance.

While it seems the resistance was increased because of the larger diameter, the length of the mixing nozzle was also decreased. This resulted in a lower resistance in the section leading up to the mixing spiral, but a higher resistance in the spiral itself, because this had roughly the same length.

In Appendix F, resistance values have been calculated for all components of the transportation section with fixed viscosity and dynamic viscosity using equation 14.

$$R = \frac{8 m \left( \frac{Q r^{2+n} (3n+1)}{\pi r^2 n r^{\frac{3n+1}{n}}} \right)^{n-1} L}{\pi r^4} \quad (14)$$



**Figure 4.61:** With increased extrusion speed, ink got extruded briefly. Again, the extruded sample did not cure.

## 4.9 4D printing conclusions

Despite the efforts done on the 4D printing set-up done throughout this project, the current system is still not able to reliably extrude the highly viscose magnetized ink. The done improvements did make a difference compared to the state of the printing set-up at the start of this project. For example, it is possible to reliably print non-magnetized ink, which has a overall lower viscosity compared to magnetized ink. Also, this ink cured well at room temperature (because a longer static mixing nozzle can be used).

The system is able to extrude magnetized ink to some degree., but the performance is very inconsistent. The printed samples also did not cure because of a wrong A/B ratio of the silicone. These problems are also not easily solved by using bigger, stronger motors. Even if the pressure generated by the motors would be large enough, there is still the problem of swelling of the plastic syringes and leaking of ink out of the hose barb connections because the pressure becomes so high it pushes the tubes off from these connectors. To address these issues, metal or glass syringes could be used and strong hose clips, but this would be combatting symptoms rather than fighting the source of the problems.

The best bet would be to limit the resistance in the system. This can be done by shortening the travel tubes from the syringes to the static mixing nozzle. It was possible to reliably extrude magnetized ink out of the thin and long static mixing nozzle when using tubes of 10 cm (Chapter 4.7). The motors were not skipping steps, and the ink extruded cured well in the oven, meaning the A/B ratio was good. However, to make this possible with the current system, it would have to be redesigned in such a way that the build plate is moving in X, Y and Z direction, as the separate extrusion system is quite large and heavy and would be difficult to mount on the Ultimaker print head.

While resistance can be lowered by increasing the tube/outlet diameter for Newtonian fluids, for shear-thinning fluids, this would actually increase material viscosity and with that increase the flow resistance. The only easy-to-predict way to decrease the flow resistance, is again by lowering travel length. Increasing flow rate is another option, as this would increase linear speed and thus shear rate, in turn

lowering viscosity and thus resistance. However in order to increase flow rate, a larger pressure difference is needed and thus more motor force is needed. With that, we are back in the vicious circle of variables depending on each other, which makes it so hard to fully predict system behaviour on a theoretical level.

The approach of mixing two silicone components during printing seems to be unique in 4D printing magnetic materials. All reviewed literature on this topic describes single syringe extrusion (or a different 3D-print/manufacturing technique all together). Inspiration could be taken from these approaches, for example single syringe extrusion using UV curable ink. This way, the ink does not cure inside the syringe and the set-up can be made less complex.

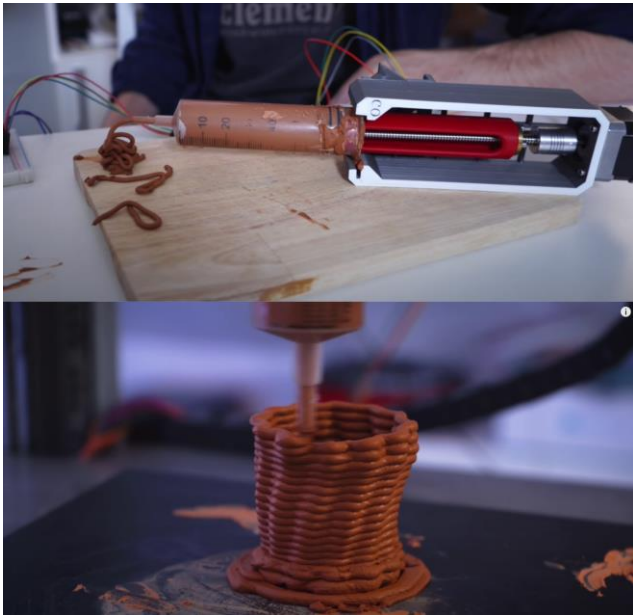
## 4.10 Recommendations

For further development of the 4D printing system, it is recommended to adopt a different platform than the one in use now. It was proven the magnetized ink could be printed with when using 10 cm tubes. However, placing the existing extrusion system on the print head of the Ultimaker 3 is difficult, because it is quite heavy (about 5 kg). The rails might not be able to support this and the small motors used to move the head would probably not be strong enough.

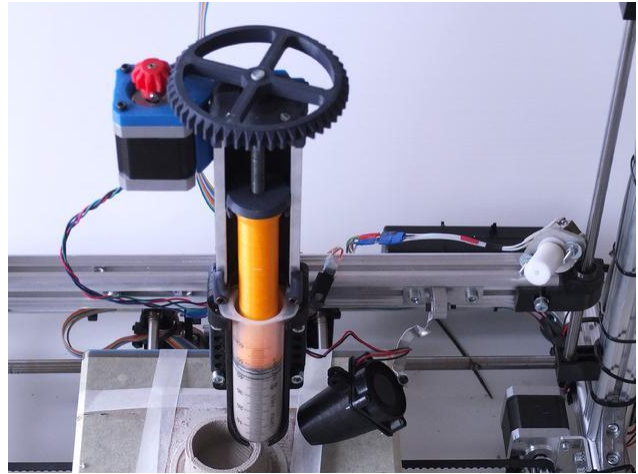
That being said, other people have demonstrated the possibilities of 3D printing with viscose materials. For example, the YouTuber Constantijn (2019) successfully 3D printed with clay using an DIW printhead with a stepper motor directly driving a syringe piston (Figure 4.62). Similar designs have been proposed by other people, like the one depicted in Figure 4.63. The same approach could be taken to print magnetic ink, adapting the aforementioned designs to make dual extrusion possible without the need to tubing, making the travelling distance from syringe to print bed very short (Figure 4.64).

Because two motors are used, the design idea in Figure 4.64 might be too heavy to mount on a moving print head. Therefore, it is beneficial to use a 3D printer platform that uses a stationary head and a build plate moving in X and Y direction, like the *3D PotterBot Micro 10* by 3D Potter (3D Potter, n.d.; Figure 4.65), which is designed to 3D print very viscose materials.

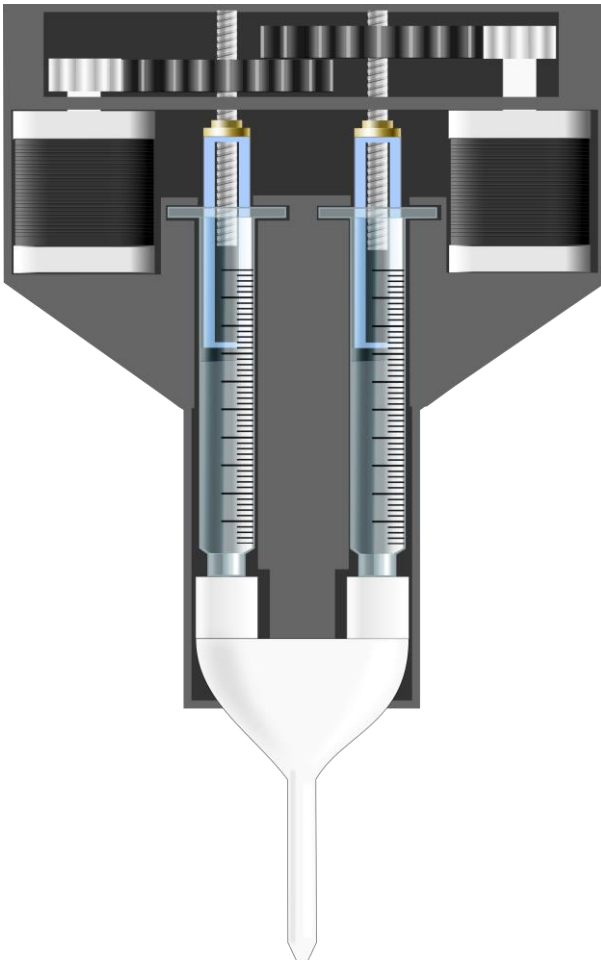




**Figure 4.63:** Thick paste material can be printed with using a DIW solution. However, the viscosity of the used material in this YouTube video was not specified (Constantijn, 2019).



**Figure 4.63:** Another paste printing solution by +Lab, which uses a large gear ratio to generate enough pressure to extrude thick paste materials. The 3D printer used here has a stationary head (Milkert, 2014).



**Figure 4.64:** A design idea that takes the principle of a DIW paste extrusion system (Constantijn, 2019; Milkert, 2014) converted for dual syringe extrusion.



**Figure 4.65:** The 3D PotterBot Micro 10 by 3D Potter is a clay extrusion 3D printer used for 3D printing ceramic objects. It used a bed moving in X and Y direction with the head moving on the Z axis. It might be used in the default state using UV curable silicone or be converted to dual syringe extrusion using the idea in Figure 4.64.

# 5. Demonstrator product design

Magnetic Soft Materials are a relatively new type of material and thus not largely utilized. Applications for this material are currently mostly found in fields like soft robotics and biomedical applications (see Chapter 3: Literature review). Because the material is not implemented in current product designs, few designers know its potential and possibilities, and thus do not use it in their own designs. To break this vicious circle, a demonstrator with MSM is designed and prototyped, to inspire and empower future (design) engineers.

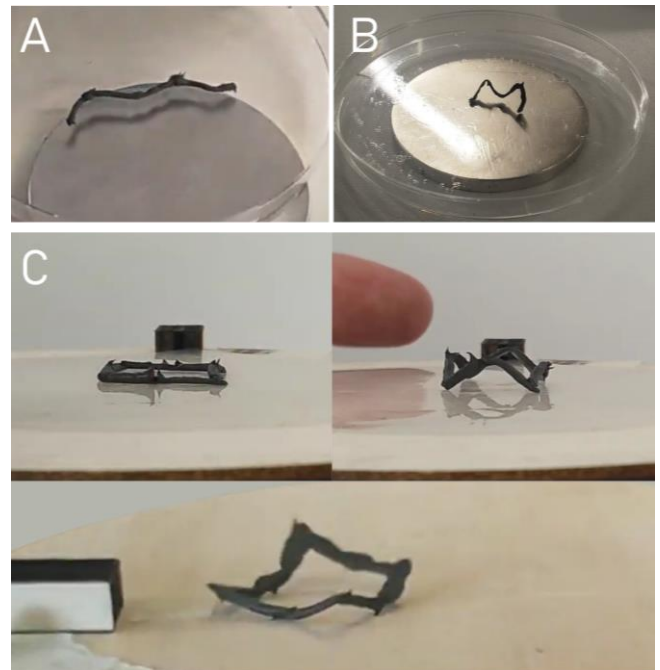
## 5.1 Manually made shape morphing demonstrators

Throughout the project, several small shape morphing objects were made manually with the purpose of testing the made material and tinkering with the possibilities and limitations.

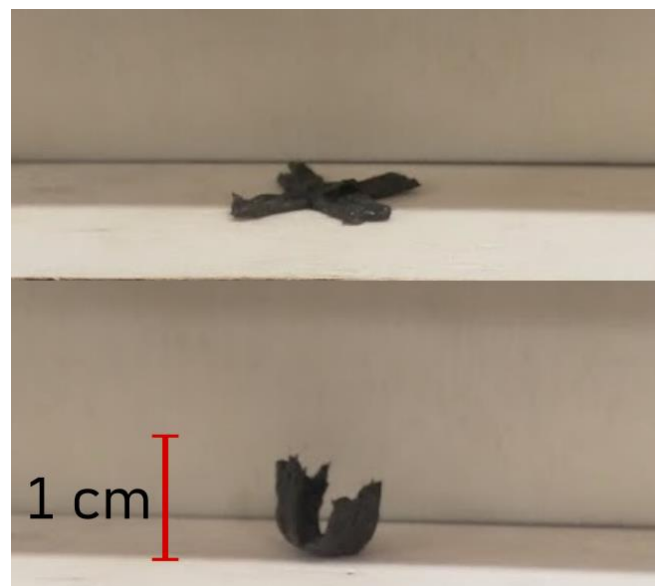
### 5.1.1 Squares, wires and grippers

Inspired by the objects made by Kim et al. (2018) and Ma et al. (2019), simple M-shape wires and morphing squares were made (Figure 5.1). A simple cross shape was also made that could act like a gripper for small lightweight objects (Figure 5.2).

It was found that a thinner nozzle (so smaller line width) resulted in better actuation/response of the shapes, but made them lighter and more eager to be attracted by the edges of the magnets, as the field strength is higher there. Smaller diameter nozzles fitted on the syringes made it also harder to manually extrude ink out of the syringe. This in contrast to what the mathematics shows, namely that a smaller diameter nozzle results in more shear rate and thus a lower resistance (Figure 4.59; Chapter 4.8)



*Figure 5.1: M and square shape-morphing demonstrator objects. The objects with thicker lines (A) show less response than thinner extruded objects (B). The sides of a MSM square arch up when placed on a permanent magnet. The tips move up when the field is reversed (C).*



*Figure 5.2: A small simple cross shape can be a gripper for small, light weight objects as its arm curl up in a magnetic field.*

### 5.1.2 Active metamaterials

Inspired by Kim et al. (2018), active auxetic metamaterial structures were made (Figure 5.3). However, these did not work as demonstrated by Kim et al. (2018; Chapter 3.4.4). It seemed only a few cells responded to the magnetic field. Why this is, is unknown. It might be just human error.

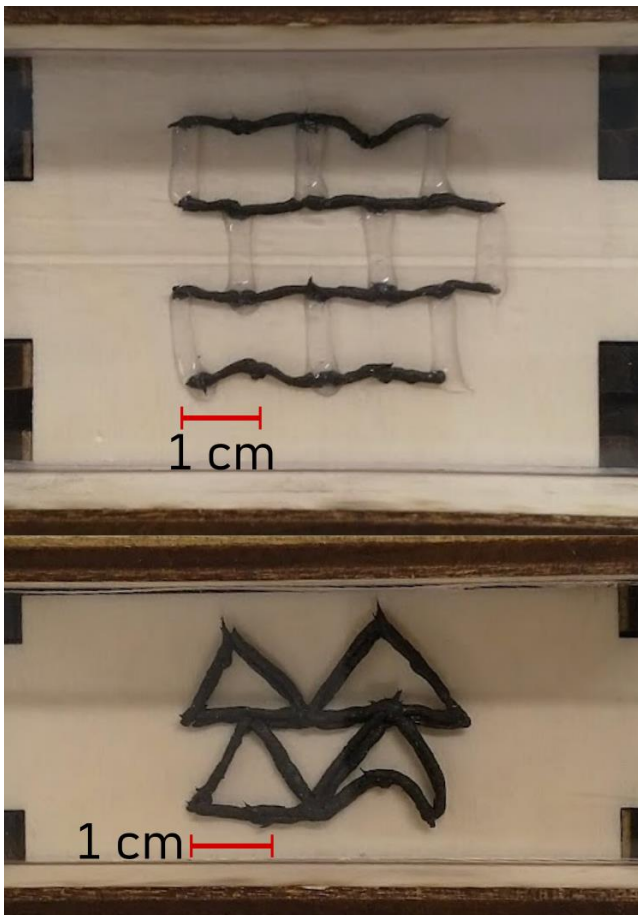


Figure 5.3: Maximum height and residual height after shape recovery of the analysed W-shape.

### 5.1.1 Shape recovery

Something that always returns in shape memory materials literature, but is not often mentioned in MSM literature is shape recovery ratio. This is the amount the material is able to recovered to the trained shape after it has been deformed. Shape recovery ratio is calculated with equation 15 (Liu et al., 2010a; Gall et al., 2005).

$$R_r = \frac{\theta_m - \theta_p(N)}{\theta_m - \theta_p(N-1)} * 100\% \quad (15)$$

In this equation,  $R_r$  is the recovery ratio in percent,  $\theta_m$  is the maximum strain or angle the object is deformed by and  $\theta_p$  is the residual angle present after shape recovery.  $N$  is the

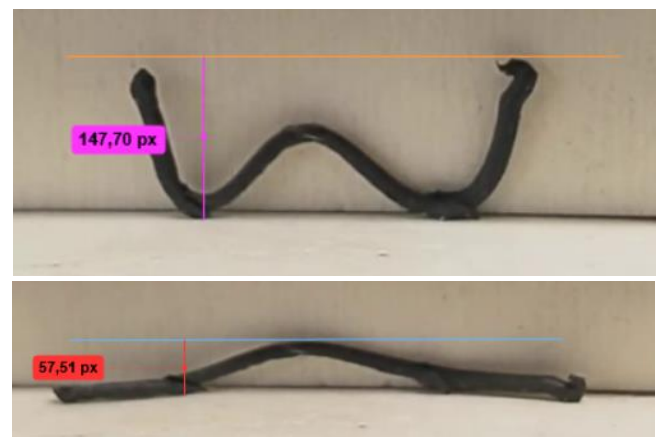
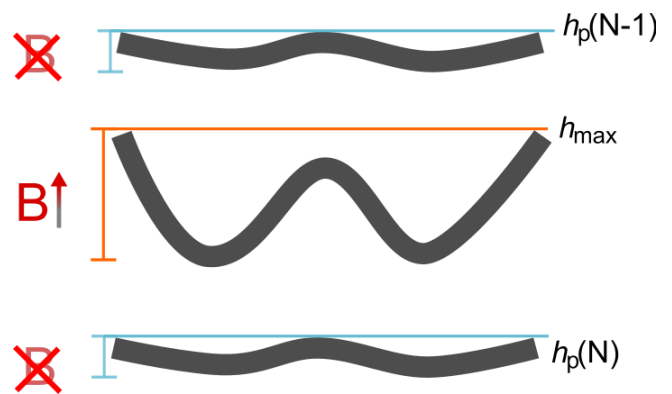
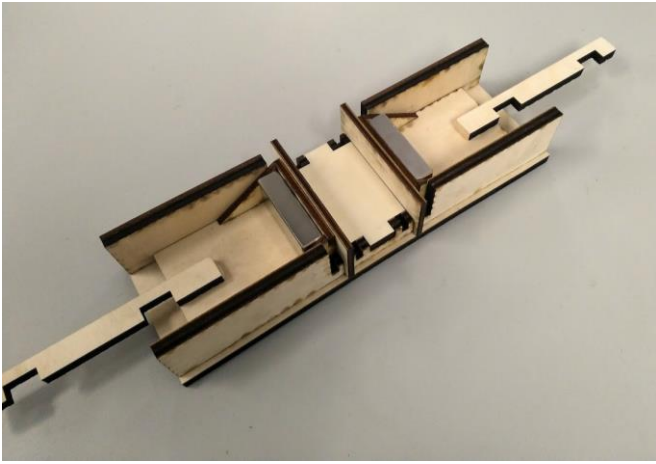
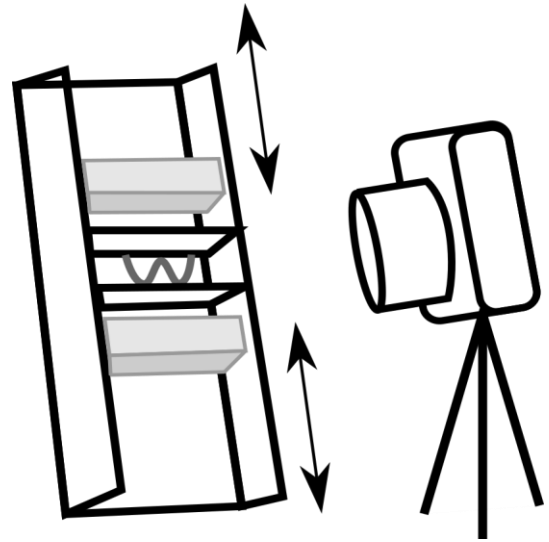


Figure 5.4: Maximum height and residual height after shape recovery of the analysed W-shape.



**Figure 5.5:** The manufactured box with space for a magnetic shape morphing object in the middle and two magnets on the side, creating a magnetic field in between. The two neodymium block magnets can be slid towards the centre without the risk of the two magnets jamming into each other.



**Figure 5.6 :** Sketch of the test set-up used to analyse shape recovery. The box was set up at an angle to that the object would rest against the back to limit tilting. A camera was pointed perpendicular to the object.

shape recovery cycle. In stead of the bending angles, the height of the analysed shapes was used in this project to calculate the shape recovery (Figure 5.4), as angle was found to be too subjective (it depends on where the analyser draws the lines to be measured).

To analysed the shape recovery, a set-up was made in which two magnets could be moved towards the magnetic shape morphing object (Figure 5.5 and 5.6).

It was found that the M-shape (or W-shape, depending on the direction of the magnetic field), had an average shape recovery of 90.5% in between cycles and 79.3% compared to the starting shape (Appendix C.3f).

## 5.2 Material Driven Design

As explained in Chapter 2: Methodology, the Material Driven Design method (MDD), developed by Karana et al. (2015) was used to develop new application ideas beyond the domains found in literature. In this method, the strengths and weaknesses of the material are analysed, both technical and perceptual (sensory and emotionally), to be able to put these qualities to good use.

This method was partially executed with the help of some peer students in a one-hour workshop (Figure 5.7) on the first step of the MDD method and ideas derived from that. In this session, participants were able to touch, smell and play with the MSM shape morphing demonstrator objects made with manual extrusion (Chapter 5.1).

### 5.2.1. Sensory characterization

The characterization of the material is divided in sensory qualities, associations with other materials, meaning and emotions it evokes and envisioned interaction.

### Sensory qualities

Figure 5.8 shows the outcome of the sensory characterization of the material done together with peer students. Main insights derived from it is that the *quick response* of the material is a highly valued feature. Also, interacting with the material is seen as a rich experience, as it *evokes curiosity, care*, and it responds quickly. When pulled towards a magnet, users reported feeling a very subtle spring-like *force feedback* because of the elasticity of the material.

However, there are also some unpleasant qualities reported. The most obvious being the *colour* of the material being seen as *unappealing* and associated with feces. In addition, because of the small size of the demonstrator objects, participants reported associations with *bugs* or *spiders* and feel hesitant to interact with the material because they feel the material is weak and delicate. Another interesting aspect is that the material is recognized as being *high-tech*, although the warm appearance of MSM does not match with the participants perception of high-tech products being cold, harsh and metal-like.



Figure 5.7: Snapshot of organized workshop with peer students on the characterization of the magnetic shape morphing material.

### Associations with other materials

The material was mostly associated with other elastomers like *rubber*, like O-rings or gaskets or *silicone* found on toothbrush grips. Interesting associations were made with *bugs* (consistent with the sensory qualities) and squishy, unsatisfying silicone buttons found on old *TV remotes*. Movement of some demonstrators reminded participants of *plants moving in the wind*.

### Meanings the material evokes

The question what meanings the material evoked was a difficult one, as meaning is a vague concept. Answers given include associations with *clucky*, *wonderous technology* from the 90's and science fiction horror movies from the 80's. Because of the alive looking quick moments, the bug associations came back and more movie associations with the *Monster Book of Monsters* from Harry Potter and the 1997 movie *Flubber* starring Robbin Williams (Figure 5.9).

### Emotions the material evokes

Participants felt a combination of *curiosity* and *uneasiness*. Uneasiness because of the quick, some times alarming movement of the material and the associations with *bugs*, which make the material look 'too alive'. Curiosity because of the unfamiliarity with the material and *cute and fun vibes* participants got when the different demonstrators were "dancing" together in a group. Making the materials move with the magnet was enjoyed by the participants, who came up with all kinds of ways to make the materials move by changing the position of the magnet. Feelings of *care* and *responsibility* were briefly mentioned because of the delicate and small appearance of some objects and cute movements.

### How do people interact with the material?

To the question how participants envision interacting with this material, they reported wanting to *approach the material with care* and would *not want to touch it* in first instance.

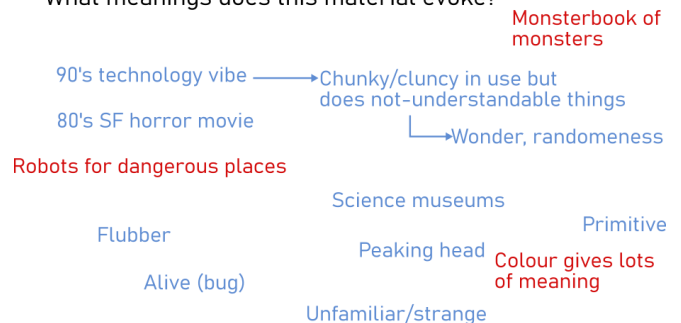
However, when the objects were moving in a group, participants reported feeling much less hesitant to interact with the material.

What are the sensory qualities of the material?



Figure 5.8: outcomes session on sensory qualities and associations with other materials.

What meanings does this material evoke?



Does the material evoke certain emotions?



How do people interact with the material?



Figure 5.9: outcomes session on meaning, emotion and interaction.

## 5.2.2 Technical characterization

In addition to the sensory characterization, some (more or less) technical qualities of the material were identified prior to the workshop. These were written down as key words on pieces of A3 paper. Participants were asked to write down their associations with these keywords, positive or negative. Full sheets of these associations can be found in Appendix G.

### Shape change

The shape changing ability of the material made participants think of *customizability*, *living*, *surprising*, *shifting identity* and shape shifting fictional characters like *Barbapapa* and *Optimus Prime* (Figure 5.10). But also *weak and unsteady* was a (negative) thing that was mentioned.

### Magnetic field

The trigger of the shape change, a magnetic field, triggered answers like *high-tech*, *compass* and *wireless charging*.

### Flexible

Because the elastomer material is flexible, words like *adaptable*, *snails and worms*, *no fixed-size/volume* and *fitting into unconventional spaces* are some that were written down by participants.

### Soft

The term *Soft* made the participants think of *safe*, *cosy*, *friendly* but it can also be something negative, for example *slimy*.

### Remote control (small distance)

MSMs are controlled with a magnetic field, which is generated outside of the material and can pass through certain barriers. The material is thus controlled remotely, however the distance the magnetic field can travel is short, as it quickly weakens when getting further from the source. Participants suggested terms like *inviting* because you need to get close to the material to make it move. Therefore it would be



**Figure 5.10:** Optimus Prime, leader of the Autobots from the Transformers franchise, can shape change from a truck into his robot form (Bay et al., 2007).

necessary that the material is *not intimidating*. Another plus is that the material would be very useful for *magic tricks*. One participant suggested to extend the distance of remote control by control the magnetic field close to the MSM object via remote control.

### Small size

The fact that the shape morphing objects can be very small, made participants think it was *dangerous for small children*. It has *surgical benefits* can could be used in *small hand held devices*. Also one participant associated the small size with *cuteness of babies* and made her feel she needed to *care for it more*.

### Multi-directional

The shape morphing objects can change in different directions depending on the direction of the magnetic field. According to participants, this brings *many opportunities*, *different modes* and makes the material more *versatile*. However, it makes it also more *unpredictable*. An association was made with *breathing* or a *heartbeat (expanding and contracting)*.

## Fast

The fact that the shape change is fast makes participants think it is *smart* but also *unpredictable*. It makes the materials more *enjoyable* and *usable in scenarios with limited available time*.

## Low forces

A big downside to the material is that the forces it can generate or the load it can hold is very limited because of the low stiffness of the elastomer and the small size of the particles.. This leads to *reduces usefulness*. Participants also ask whether the forces can be increased with the use of *very powerful magnets*, which should be possible, but would bring other issues, like size, costs and safety.

Figure 5.11 gives a visual overview of the key words mentioned organized per category.

## 5.2.3 Materials Experience Vision

The second step in the MDD method is to take the insights from the first step and envision what these characteristics mean for the product and the experience people have with the product (Karana et al., 2015). For example, which (unique) characteristic should be emphasised in the product design? These experiences can give a certain expression to the product or a certain interaction. For example, does the material make people curious or is the material so delicate that it requires people to operate the product with great care?

This step was not meant to be executed with participants involved and it was also not possible to do so because of time constraints of the workshop organized.

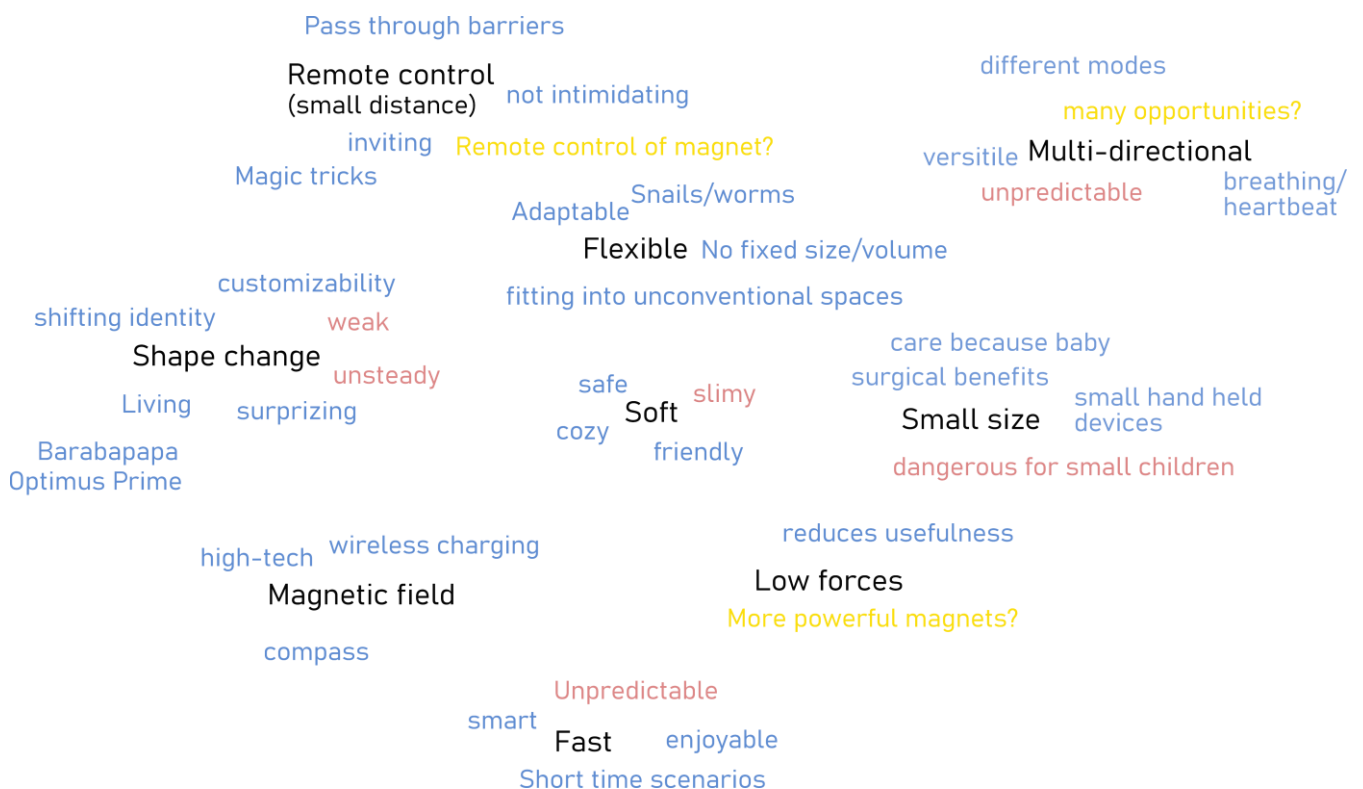


Figure 5.11: Overview of associations with technical qualities key words by participants during the workshop.



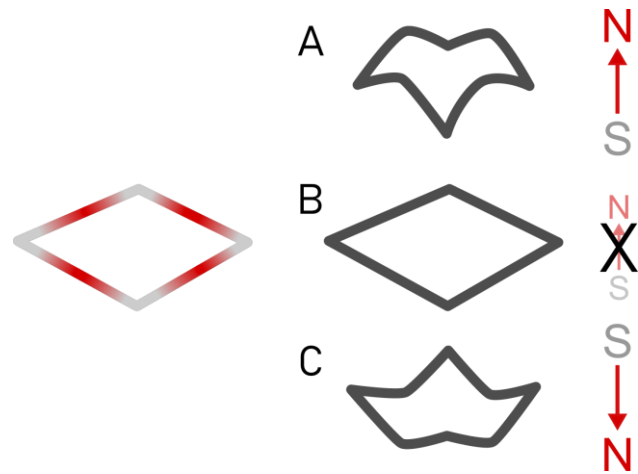
### Unique characteristics

Compared to more conventional shape memory materials, MSM have a few unique characteristics that would be valuable to show in the demonstrator product design. The main advantages of the material is that the shape change is very fast, allowing for quick conveying of information or quick adaptation to the environment. Another aspect is the reversibility of the shape change, so that the material has basically three possible states (Figure 5.12). The material is soft and flexible, while most other shape memory materials are rigid. This brings the disadvantage that the magnetic soft material cannot hold much load. On the other hand, it is an advantage in that it can be more pleasing to touch and because it is flexible, can be more easily stretched over curved areas and easily folded.

In terms of sensory qualities, the fact that the material changes shape quickly evokes curiosity and makes the material feel alive. The softness and scale of the material also brings feelings of carefulness. These are all positive sensory qualities that would be nice to emphasize in the design. However, the material also does not look very appealing, which makes it less approachable (which is contradicting to the curiosity). It is unknown at this point whether the appearance of the material can be tweaked. It could be that the material can be made less revolting by adding a color for example. Because this is not known (yet), the appearance of the material was left out of the to-be-shown characteristics.

### Sensation and interaction

Another important thing to consider is how the material is sensed and how people would interact with the (product made with the) material. It was already established that the material is gentle to the touch, but that people are hesitant to approach the material because of the association with bugs. Because it is a tangible object, rather than visualizing information quickly in a purely visual way, like with LED lights, the information can also be conveyed haptically, by physically touching the material and feeling, for example, the shape of the object. Important to consider is, however that the to-be-touched object is not associated.



**Figure 5.12:** The MSM object with magnetization pattern shown left has three possible shape states, depending on the direction of the magnetic field; A, north facing up; B, no magnetic field applied; C, north facing down.

with bugs, to lower the hesitation to interact with the material.

### Material Experience Vision

From all collected and preferred material qualities, an *Experience Vision* can be formulated, that expresses how it is envisioned how users should experience the (product made from the) material. The experience vision for the magnetic soft material is formulated as:

*The material application will allow users to experience communication of information in a visual and haptic way. It will do so by evoking curiosity and care by looking alive. It will show 3 different states of information and must do its best to not scare off users but invite users to interact despite its appearance.*

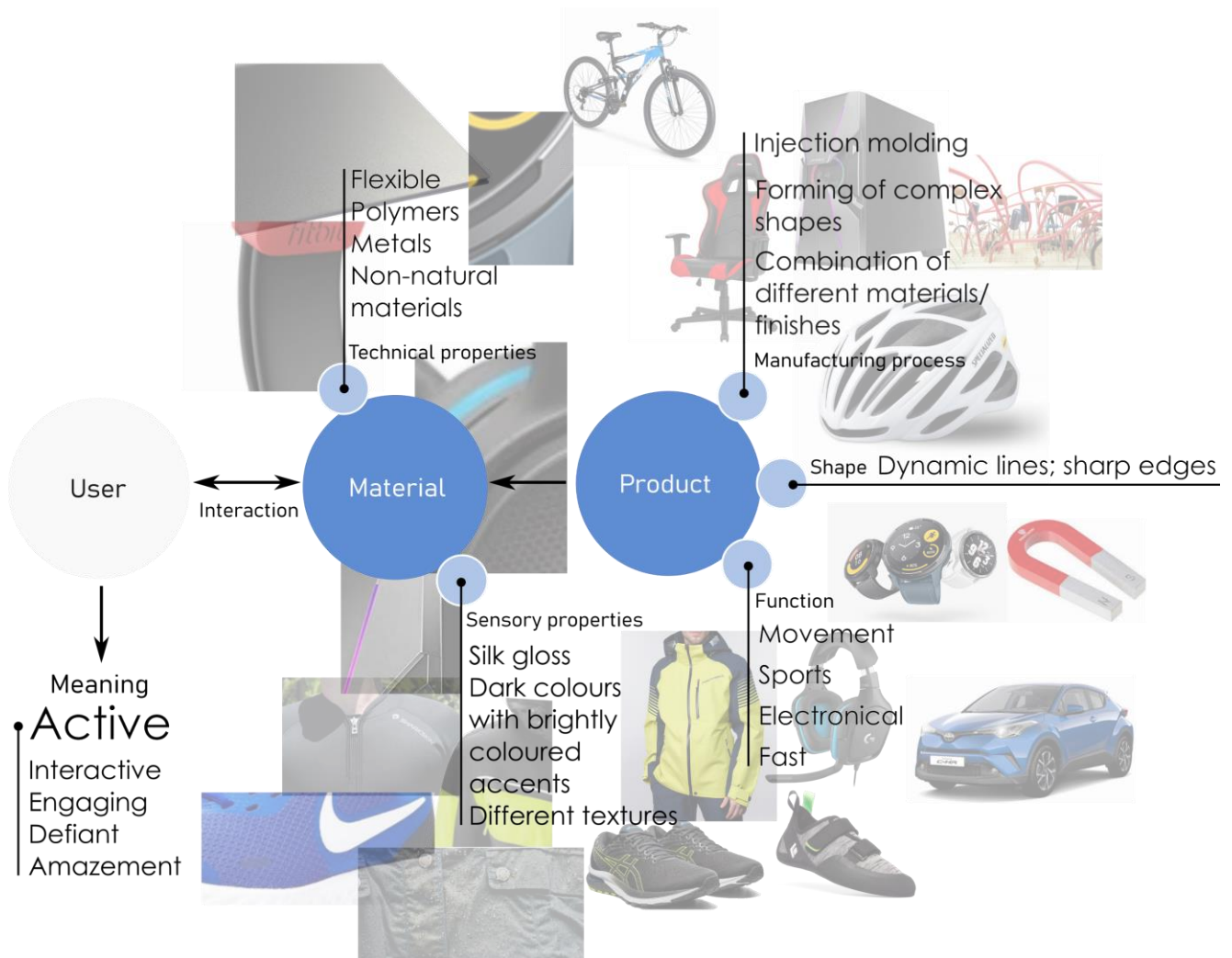
## 5.2.4 Material experience patterns

Meanings can now be distilled out of the experience vision. For this, the material experience pattern can be used (Karana et al., 2015). According to the MDD method, this step needs to be done with the help of data gathered from quantitative and qualitative user studies. However, in this project there is a very limited time for this step and therefore only one meaning is elaborated upon with some input from peer students but no quantitative study.

Figure 5.13 shows the resulting filled in template with the meaning *Active*. This meaning

was chosen because it entails an engaging interaction and is defiant in that it dares people to interact. Certain activities can also provoke amazement, which is something the material should evoke.

Many products associated with the term *Active* are activity or sports related. Dynamic, sharp lines suggest (fast) movement. Materials associated are mostly synthetic, like polymers or composites. They can be rigid, like plastic or metal casings, or flexible like fabrics or silicone wristbands. What stands out are the dark colours with brightly coloured accents.



**Figure 5.13** : Material experience pattern filled in for the meaning *Active*. Materials included are mostly synthetic materials in dark colours with bright accents and can be found in sportswear or other (fast) movement related items and products with dynamic, sharp lines.

## 5.3 Design conceptualisation

During the literature review (Chapter 3) and the first 3 steps of the Material Driven Design method, many insights into possibilities, characteristics and limitations of the material have been gathered. In this chapter, these insights are collected to form requirements of which novel applications can be ideated that utilize the characteristics of the material.

### 5.3.1 Requirements & wishes

The following *requirements* were drawn up originating from the assignment, literature review, found material characteristics and experience vision and model. It was allowed that the design does not fully fulfil the *Experience Vision* because of the limited time left in the project to ideate possible applications.

1. The application must be something else than already applied domains (Chapter 3.4.4);
2. The design should show at least 4 technical properties including a limitation (unique characteristics);
3. The material should be valuable to the application in ways conventional shape memory materials can't or lack;
4. The design conveys information in a visual **or** haptic way;
5. The object should be able to convey at least two distinct states by means of shape change;
6. The object should show movement in sharp, dynamic lines in at least one of its states;
7. The object (or critical part or small section of the design) should be able to be made with manual extrusion with permanent magnet;
8. The design should limit the hesitation people experience to interact with the design.
9. The design creates an overlap from the indirect relations **or** fills a application gap of MSM.

Next to hard requirements, there are also a few *wishes* that would be nice to have, in order of importance. Fulfilling these wishes would bring the design closer to the *Experience Vision*:

1. The design shows three distinct states by means of shape change;

2. The design conveys information in a visual **and** haptic way;
3. The design invites users to interact with it;
4. The object shows an 'active' colour pallet (dark surface with bright accents);
5. The design fills a gap found in current applications of MSM.

### 5.3.2 Ideation

The next step is to come up with application ideas, which are then selected by means of the aforementioned requirements.

#### *Ideas generated during organized workshop*

Despite not being able to complete all four steps of the MDD method with the participants during the workshop described in Chapter 5.4, step 4, creating application ideas, was executed in small. Figure 5.14 shows the ideas originating from the workshop.

#### *Additional ideation*

The ideas generated during the workshop are from before step 2 and 3 of the MDD method was done. Therefore, an additional ideation was done. An overview of this ideation can be seen in Figure 5.15.

#### *Idea selection*

For the initial filtering of ideas, the PMI-method (Plus, Minus, Interesting) was used. The ideas considered most valuable were then evaluated using the *wishes* by means of a Harris Profile. The idea contributing the most to the wishes was chosen to be further developed (Appendix H).

The selected idea was that of the changing texture, because it showed the most unique technical characteristics of the material in a valuable context and showed the most potential in fulfilling the wishes.

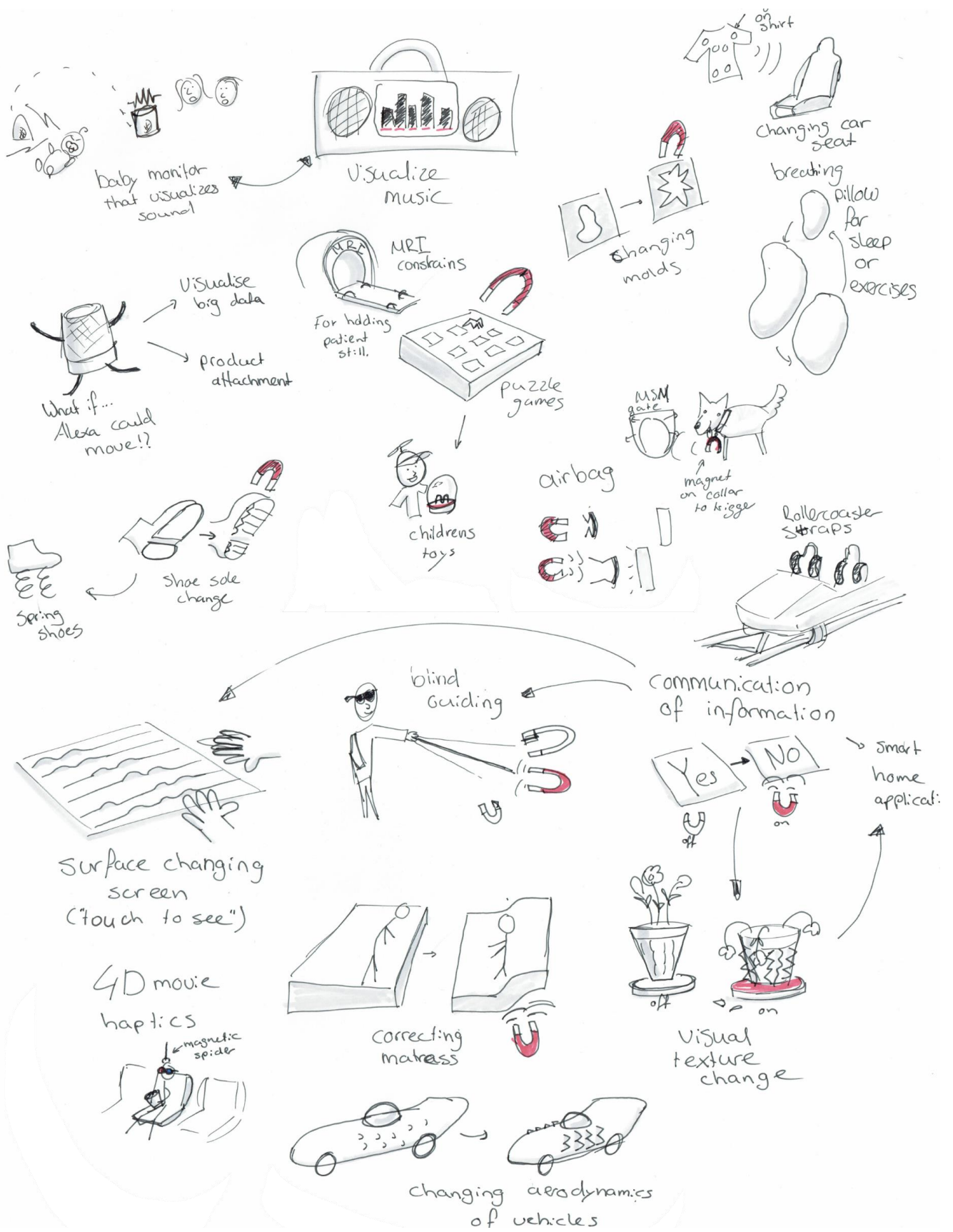


Figure 5.14: Generated ideas by participants during workshop. Redrawn for presentation purposes.

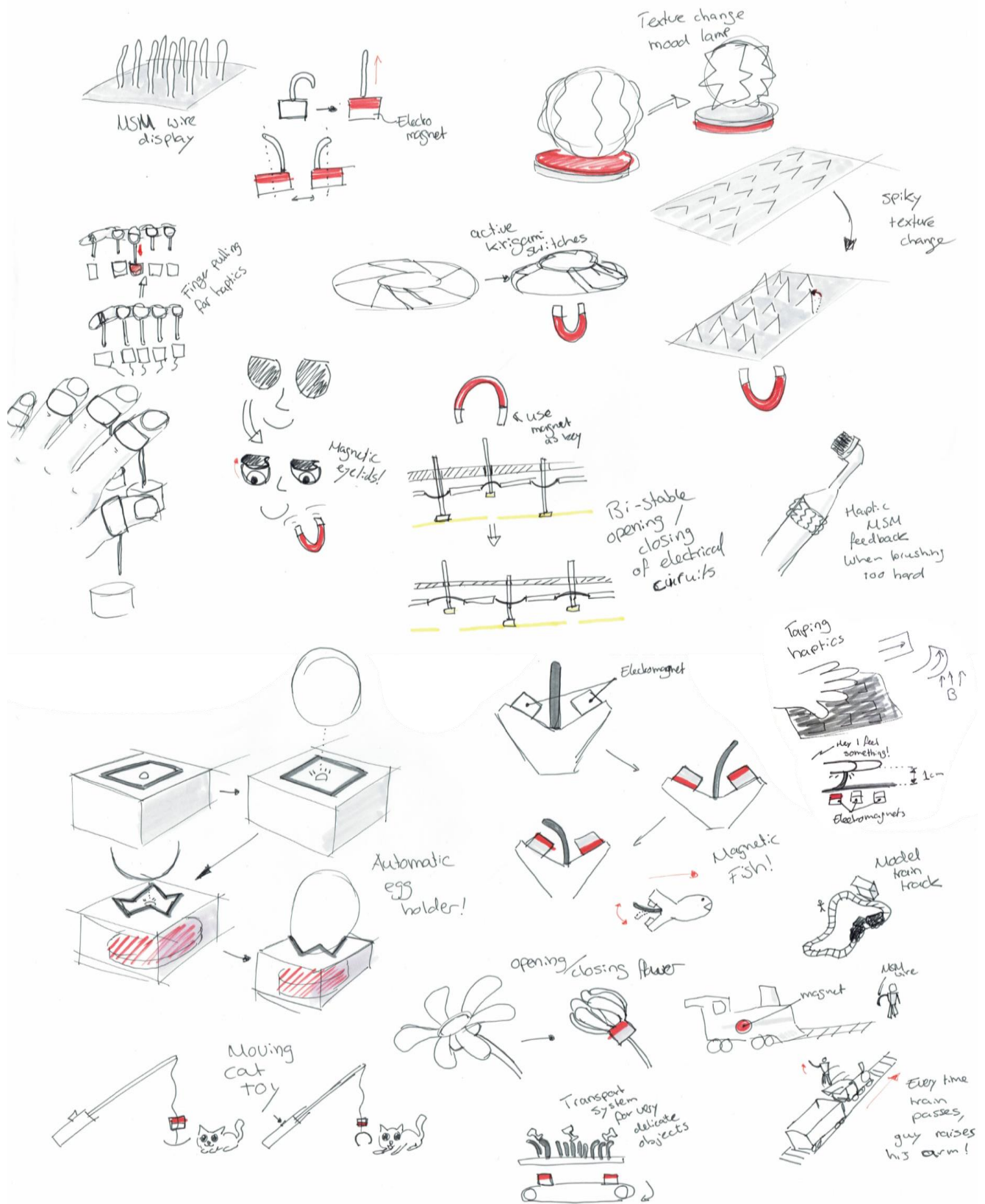


Figure 5.15: Result from additional ideation after completion of MDD method steps 2 and 3.

## 5.4 Final design and prototype

In this demonstrator design proposal (Figure 5.16), a surface can change its texture in three states. As proposed by Ion et al. (2018), texture change can be used for communication, both visually and haptically. Communication is one of the application gaps of MSM as described in Chapter 3.5.3 for which MSM could be used effectively because of its fast response.

This chapter presents two variations of a changing texture which show not only two different types of actuation but also two purposes of communication.

The MSM shape change has three states, as each magnetic pole of the embedded particles can either be attracted or repelled or not actuated at all (Figure 5.12). This characteristic is represented in the way the different texture variations are generated.

### 5.6.1. Double actuator design

In the first design, two different shapes with alternating magnetization direction are pushed out by an external magnetic field. Depending on the direction of the magnetic field, the texture

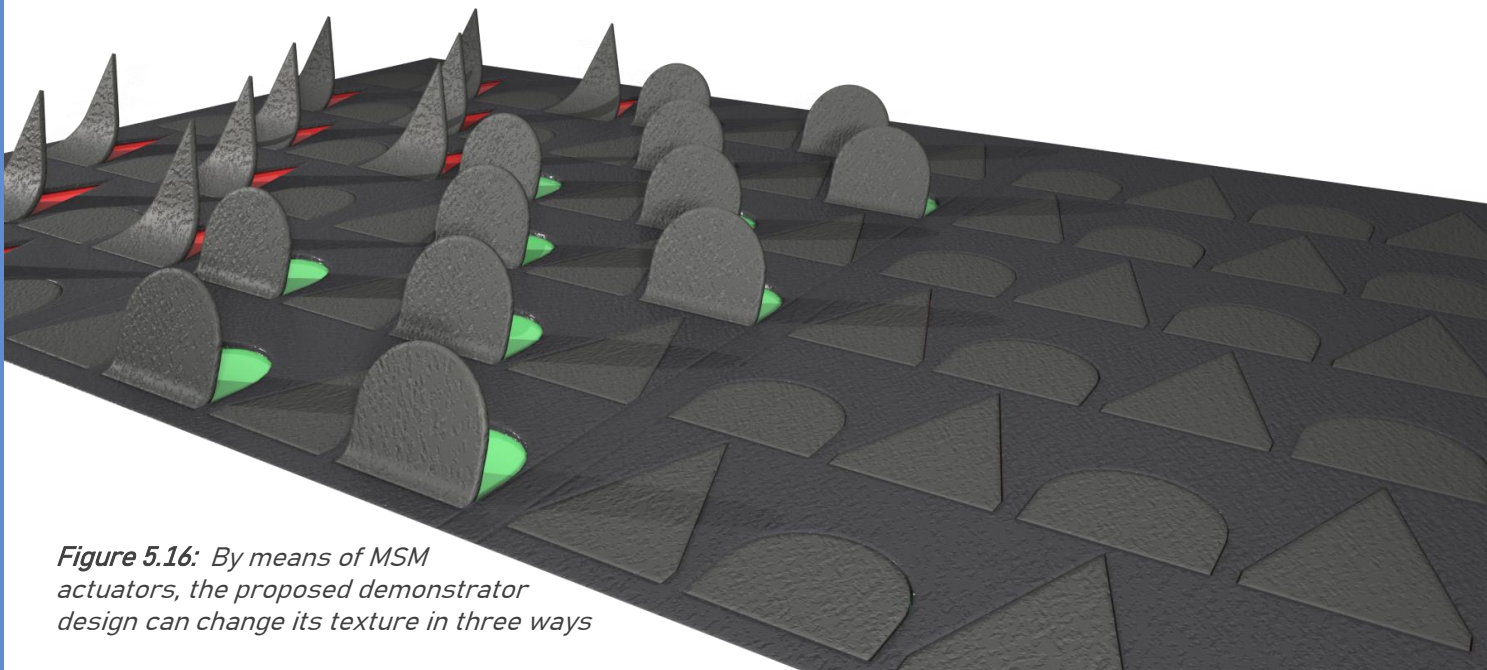
changes from spikey to more round, as different shapes are being pushed up (Figure 5.17). The individual actuators expose a colour underneath, corresponding and enhancing the textures state visually.

#### *Aggressive state*

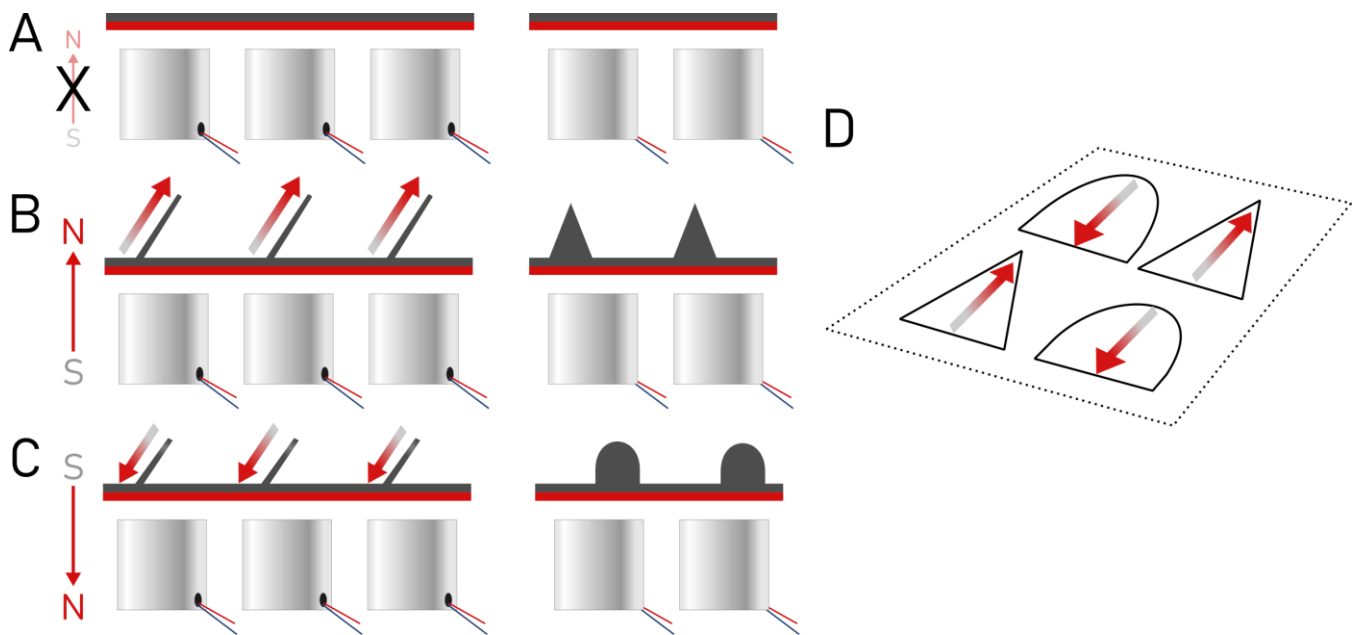
The first state has an angry or aggressive expression, evident from the spiky texture and the red colour being exposed (Figure 5.18a). This texture is inspired by the way some animals, for example porcupines, put up their quills when they feel threatened (National Geographic, n.d.). This state could thus communicate 'stay away' or something else that requires immediate attention, similarly how the door handle metamaterial texture by Ion et al. (2018) communicates 'please, do not enter'.

#### *Friendly state*

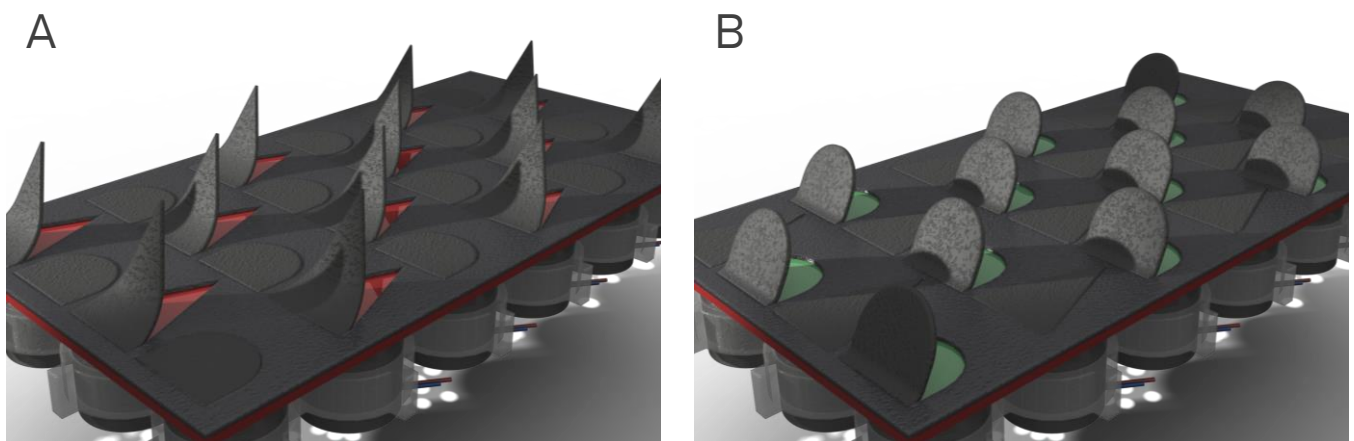
The friendly state shows more friendly, rounded shapes popping up from the surface. They expose a green colour (Figure 5.18b). This texture is meant to be more inviting and approachable. It communicates: 'please feel free to approach me' or some other positive state.



**Figure 5.16:** By means of MSM actuators, the proposed demonstrator design can change its texture in three ways



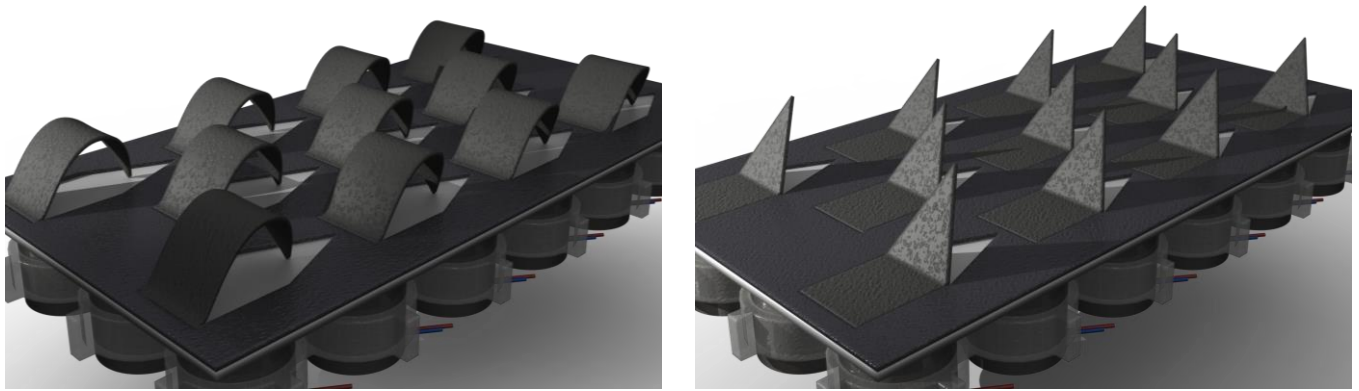
**Figure 5.17:** By alternating the magnetic field direction, different shapes pop up from the surface resulting in three possible states: neutral, no magnetic field (A), angry, spikey texture (B) and a round, friendly texture (C). The two different active elements have opposite magnetization profiles (D).



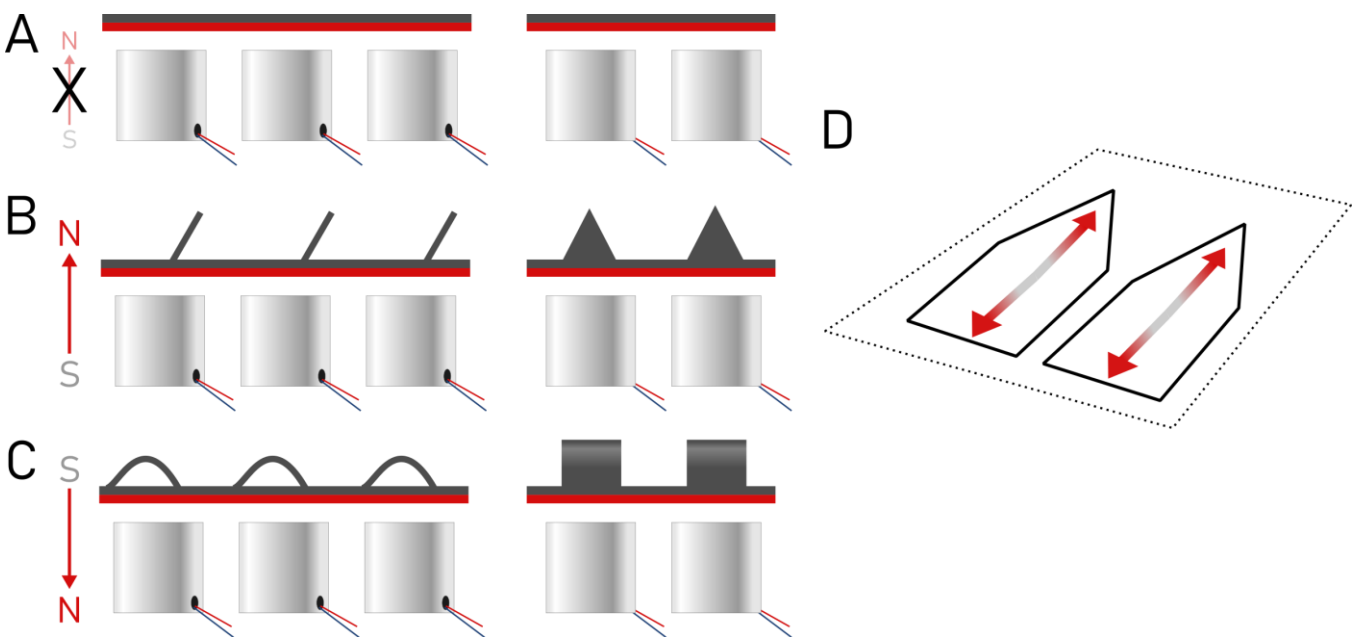
**Figure 5.18:** The spikey texture state exposes red colour underneath, emphasizing its state of danger (A). The more friendly texture state of rounded actuators show a green colour signalling all is good (B).

#### 5.4.2 Single actuator design

The double actuator design is a simple technique, but does not show that MSM is capable of more complex movements. It also has the limitation of not feeling very different to the touch, because of the soft nature of the silicone material. In the following design, the texture change is embedded into a single actuator type (Figure 5.19). It is achieved by two segments with opposing magnetization profiles (Figure 5.20).



**Figure 5.19:** A single type of MSM actuator is responsible for the texture change in this design: A bobbly texture (A) and a spiky texture (B).



**Figure 5.20:** A single actuator with facing magnetization pattern allows for two different textures depending on the direction of the magnetic field; neutral state (A); spiky texture (B); wobbly texture (C). The facing magnetization profile is embedded into a single shape (D).

#### 5.4.3 Workings and further capabilities

The proposed design makes use of an array of electromagnets (Figure 5.21). By individual 25 mm diameter electromagnets, the magnetic field can be (de)activated without moving the magnet(s). By individually controlling the electromagnets, animations are possible, thanks to the fast shape change of the magnetic material (Figure 5.21). In addition, actuators can be activated in specific areas, for example to draw attention to something (Figure 5.22).



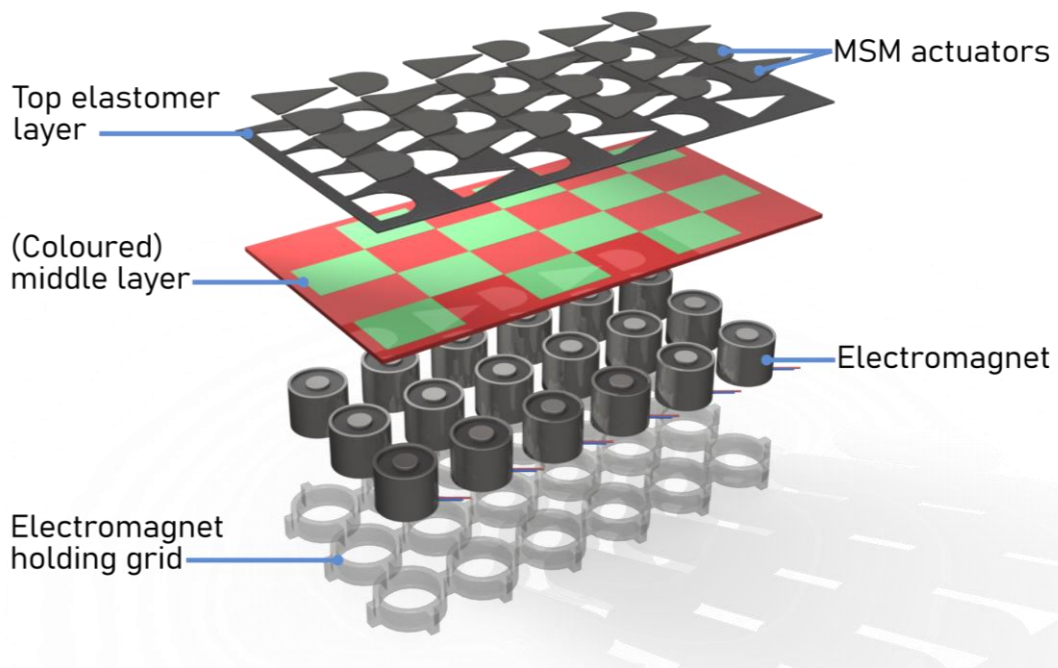


Figure 5.21 Exploded view of the changing texture design and its components.

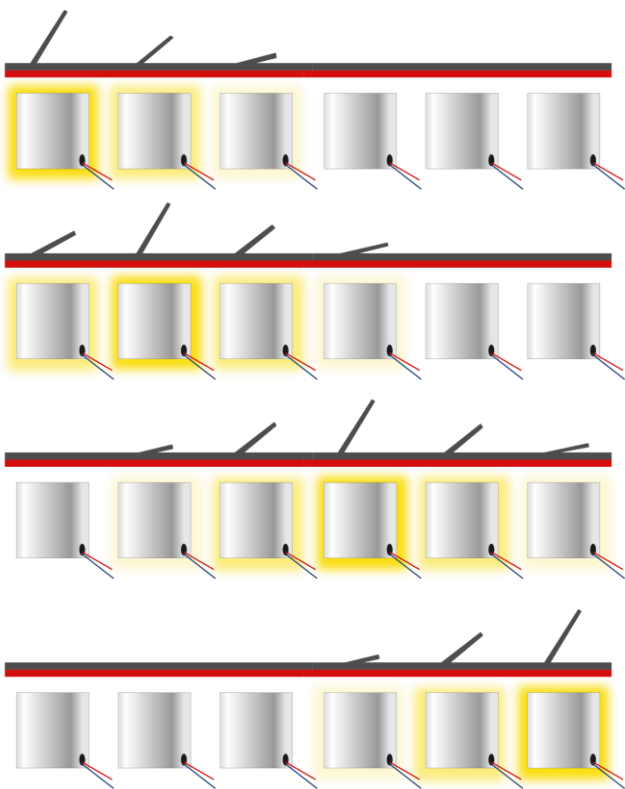


Figure 5.21: Activating electromagnets in a sequence allows for making animations by means of rapid texture change.

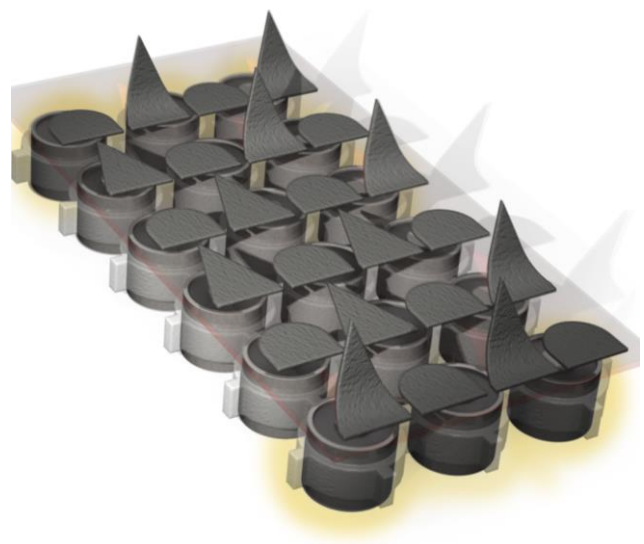


Figure 5.22: By selectively activating certain electromagnets (highlighted in yellow), part of the texture can be changed in specific areas.

#### 5.4.4 prototypes

To show the core working principle of both designs, small scale prototypes were made manually.

##### *Alternating actuator design*

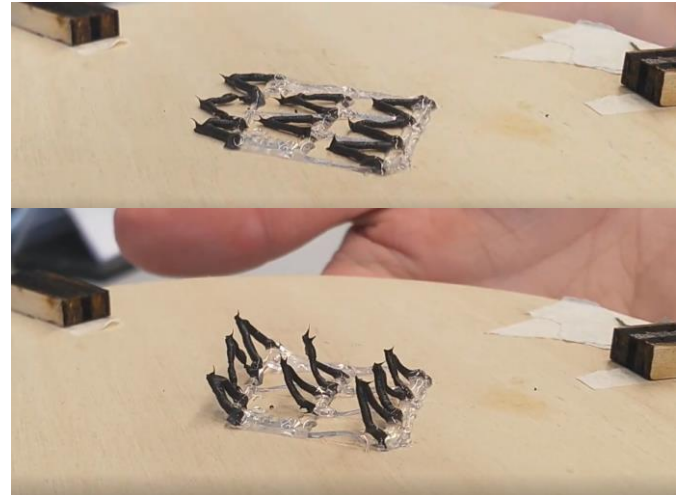
The concept of two separate actuators with opposite magnetization profile has been prototyped by making one of each actuator, attached to each other with plain (passive) silicone (Figure 5.23). The prototyped showed the principle worked well and fast. Also an array of one shape and profile was prototyped, showing a fast texture change (Figure 5.24).

##### *Single actuator design*

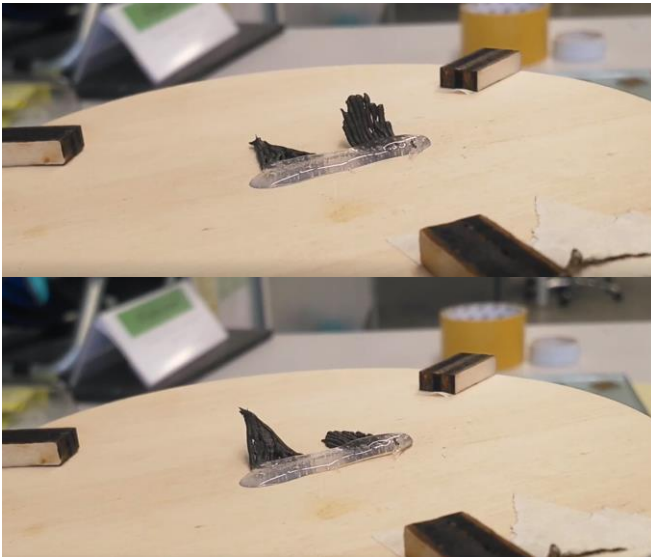
To test the single actuator with two states, one full-size actuator was prototyped that curl up and moved the tip upward, just as designed (Figure 5.25). To test the principle with multiple actuators, a row of wires with the same magnetization profile as the design was made. The wires morphed well into the bumpy texture, but in order to achieve the spiky texture, one end needed to be taped down to avoid both ends bending upward (Figure 5.26).

#### *Paper prototypes*

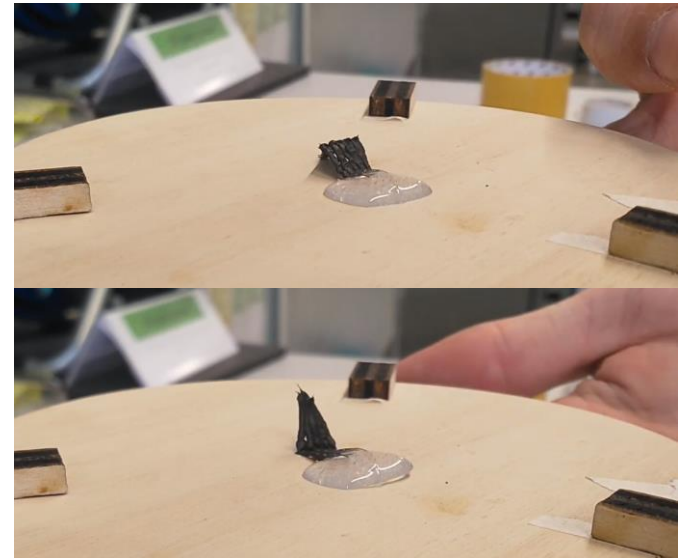
To show the envisioned texture change on a larger scale, paper prototypes were made of both variations. Figure 5.27 shows these prototypes for the dual actuator design, including the colour reveal. Figure 5.28 shows the same for the single actuator design.



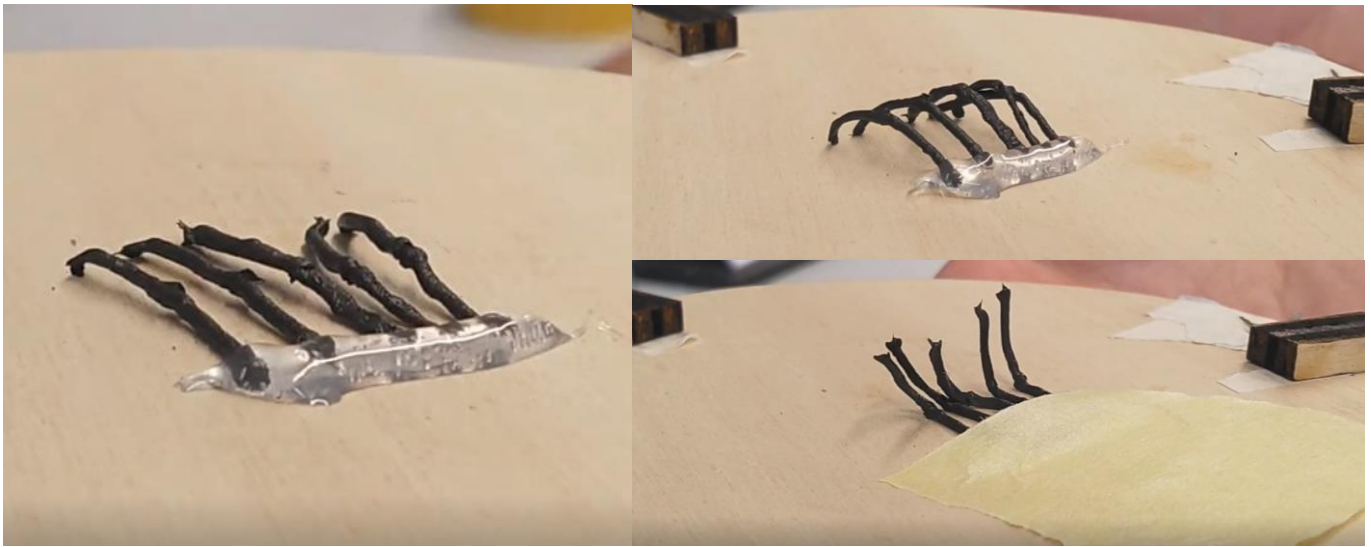
*Figure 5.24: An array of spike MSM shapes connected via plain silicone pops upward when a magnet is placed underneath, changing the texture*



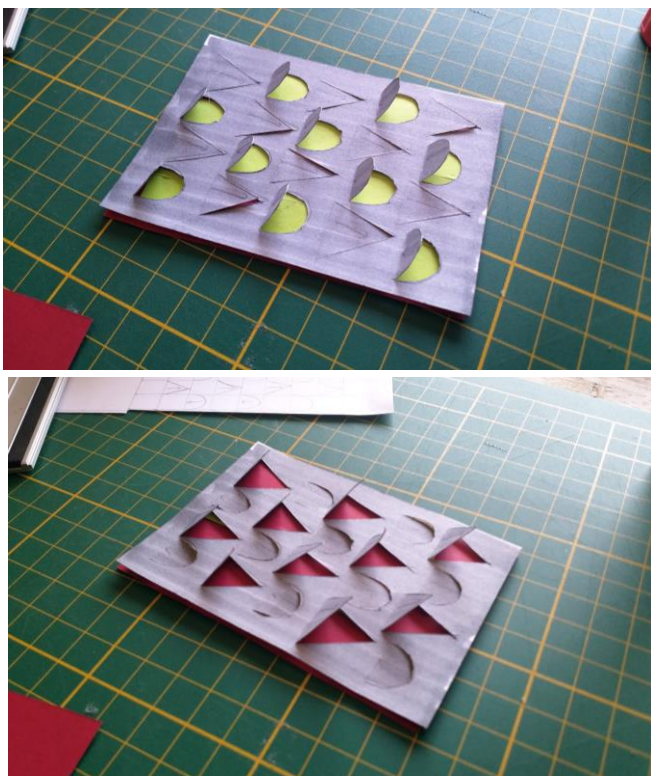
*Figure 5.23: Two differently shaped actuators prototyped with opposite magnetization. Flipping the magnet causes another shape to flip upward.*



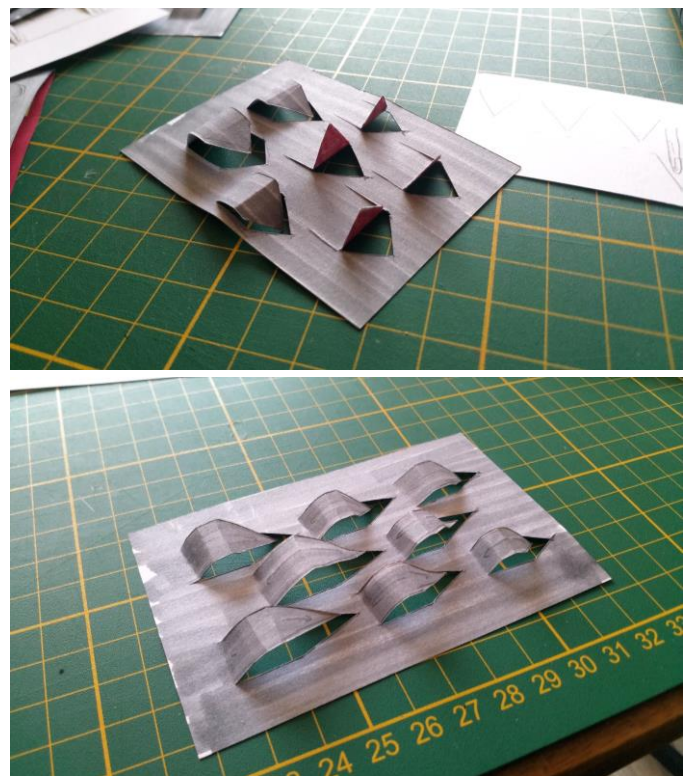
*Figure 5.25: Prototype of the single actuator design showing a bumpy shape and a spiky shape.*



*Figure 5.26: Row of wires that show texture change as designed in the single actuator variation*



*Figure 5.27: Paper prototype of the dual actuator texture change design.*



*Figure 5.28: Paper prototype of the single actuator texture change design.*

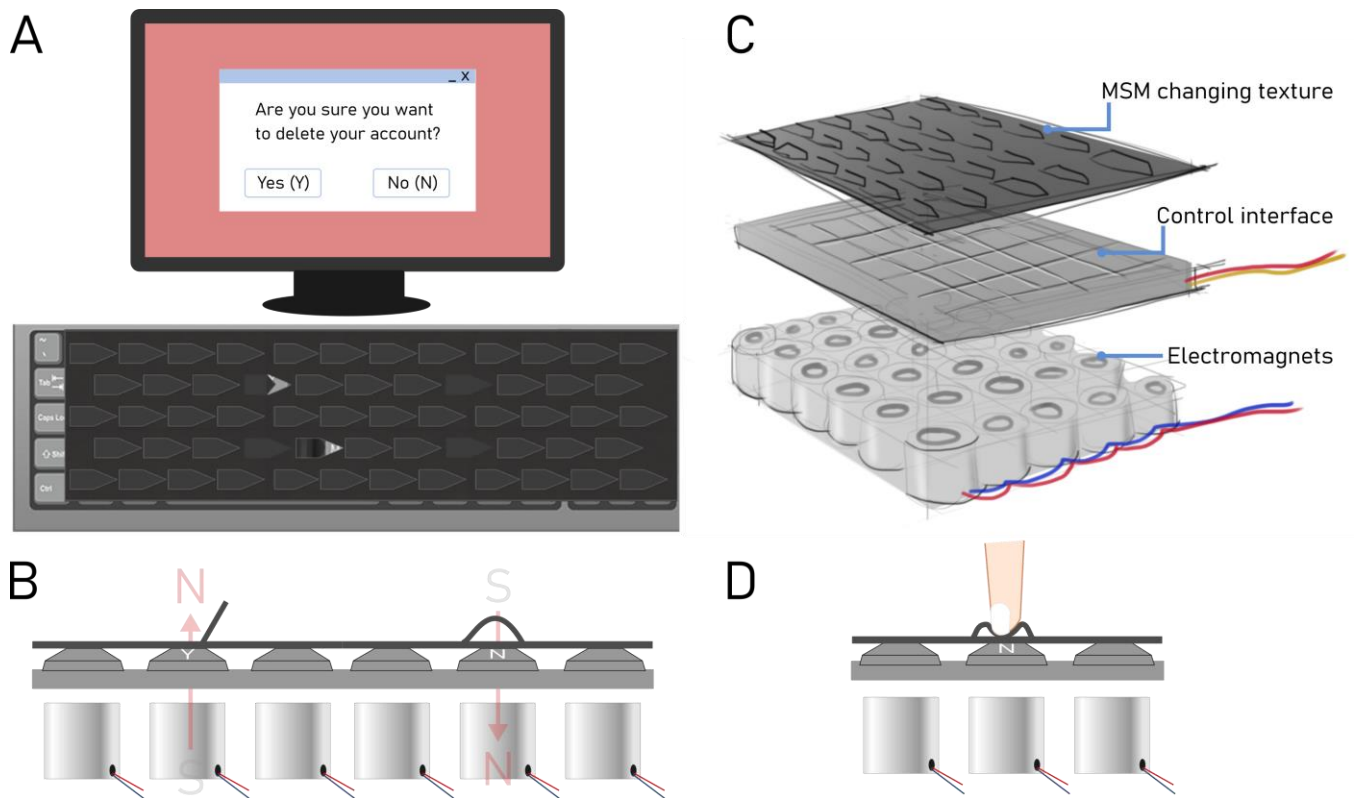
#### 5.4.5 MSM texture change use cases proposals

In this paragraph, some ideas are proposed how the changing texture concept can be applied in a product design. These are just some application proposals to show the potential, so that others might pick up the idea for future work or get inspired.

##### *Haptic feedback for control interfaces for visually impaired*

The first application proposal makes use of the soft nature of the MSM actuators. A control interface with (physical) buttons is positioned underneath the changing texture (Figure 5.29A and C)), above an array of electromagnets. The user gets feedback on which buttons can be pressed

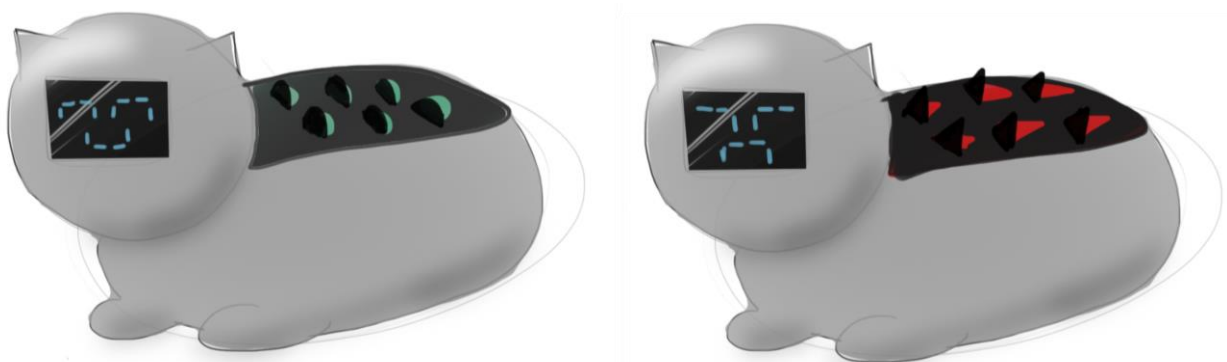
And what potential outcomes are, positive or negative, by means of different actuators popping up over the corresponding buttons (Figure 5.29B). Because the MSM actuators are soft, they can be pushed through, thus allowing the user to press the desired button underneath (Figure 5.29D).



**Figure 5.29:** The MSM changing texture is laid over a control interface (e.g. a keyboard) with an array of electromagnets underneath (C) and gives haptic feedback on available buttons. In this case, the user is asked if he/she wants to delete their account for which the options are Yes (the Y button) or No (the N button). The safest option would be to not delete the account, so this button gets a bumpy texture. The Y button gets the spiky texture (A, B). The user can press either buttons through the MSM texture because it is a soft material (D).

### Human robot interaction

The next idea uses the changing texture to convey a 'mood' a robot is in, similar to the principle found in the animal kingdom (e.g. porcupines; National Geographic, n.d.). Different textures pop up, revealing a corresponding colour (Figure 5.30).



**Figure 5.30:** The depicted cat robot uses the MSM changing texture to communicate its 'mood'. Left shows a happy, content state, while right shows an agitated state. Perhaps the owner forgot to charge him?

## 5.5 Demonstrator design conclusion

In this chapter, several objects made with Magnetic Soft (shape memory) Material are shown. The small demonstrator shapes made throughout the project showed the material developed at TU Delft can be used to make a variety of objects with two-way shape morphing capabilities. Not all of these shapes are however immediately useful, such as the M-shape. The cross shape could however be a gripper for small, lightweight objects. The M-shape analysed for shape recovery showed about 80% shape recovery. Likely, the shape recovery is limited because of the friction the MSM object has with the surface it is standing/lying on. The elastic forces of the silicone are not sufficient to overcome the friction and pull the shape back to its original shape.

To show the characteristics of the magnetic elastomer material, a demonstrator concept design was developed using the Material Driven Design method. With input from a workshop with several peer students, insights and ideas were collected which led to an experience vision and design requirements. The proposed concept is that of a changing texture which has three possible states. The design shows the following unique characteristics of the material:

- **Fast shape change:** The texture has the ability to change shape fast. Therefore, fast moving texture animations can be made by control of electromagnets. This would be difficult with shape memory materials, as the speed of the animation would be severely limited by the slow shape morphing of these materials.
- **Multi-directional:** The texture is able to morph into three different states by changing direction of the magnetic field.
- **Remote control:** The magnets initiating the shape change is separated from the MSM actuators by a middle layer. The magnetic field passes through this (non-ferromagnetic) layer. The middle layer can be used to reveal different colours underneath the MSM actuators.
- **Low forces:** It was hard to feel the texture change of the dual actuator design because of the soft nature of the material, so an alternate design was made. However, this had limitations in revealing colour used to an advantage. The soft nature can also be, for example, in the control feedback design idea in Figure 5.29.

The design of the texture change aligns with the experience vision as it is a grid of actuators that can move together or in small groups. During the workshop, participants reported to be more drawn to the material as the objects were moving in groups. The design gives visual feedback by means of the visual shape change, which is emphasized with the reveal of bright colours underneath. The dark colour of the magnetic material itself provides an 'active' colour pallet as identified in the Experience Pattern template (Figure 5.13). The single-actuator design lacks in the visual feedback, but shows more potential for haptic communication as the texture change is felt better.

The design was partly inspired by the metamaterial textures by Ion et al. (2018), as well as kirigami metamaterials such as the crawling robot by Rafsanjani et al. (2018). It fills a gap in current MSM applications found in literature, as a texture changing MSM design was not previously reported (to my knowledge). It therefore broadened the application scope of the material a little more. Hopefully, this will inspire future designers to develop the (applications of the) Magnetic Soft (shape memory) Material.

The prototypes made showed the core principles working, but a larger scale prototype would have been nice to have. What is also lacking, it a more thought-out and validated application of the texture change. The proposed applications serve mostly an inspirational purpose on which can be build on in future work.

# 6. Conclusion

In this report, the development of Magnetic Soft (shape memory) Material has been taken a little further. A literature review has been conducted into shape memory materials, metamaterials and magnetic soft materials. Magnetic soft materials distinguish themselves by their fast response and multi-directional shape change, which can be played with to form complex shape changes. Many applications of MSM have been proposed, however not as much as more conventional shape memory materials, because of its more recent 'discovery'. The literature review had the purpose of leaning more about applications from the three different materials and to draw inspiration from this for a novel application concept.

This novel concept ended up being a changing texture, which shows the fast and multi-directional characteristics of the magnetic soft (shape memory) material. Small scale prototypes showed the core principles of both design variations being feasible. However, while the concept complies with the assignment of designing a demonstrator that shows possibilities and limitations of the material, it does not fully succeed on finding a new value for the magnetic soft material (See Paragraph 6.1: Discussion). Nonetheless, the presented research on material applications opens up more directions on which future designers and researchers can elaborate on, together with the idea directions proposed by Sanne van Vilsteren (2021) in the previous project on this topic.

The 4D printer system has been further developed taking the aforementioned previous project as a starting point. This resulted into a system that is capable of printing non-magnetized ink. However, the goal of developing a system that is capable of 4D printing MSM objects has not been met, unfortunately. The system is limited by the needed travel distance and lack of rigidity in its components (e.g. swelling syringes. The non-Newtonian nature of the material makes it hard to theoretically predict the behaviour of the system. For

example, applied mathematics point to a much lower resistance with decreasing nozzle diameters, while experience demonstrates a larger diameter loaded on a syringe for manual extrusion resulted in less force required compared to a smaller diameter nozzle. Likely, the mathematics is applied incorrectly.

The method of controlling the magnetization pattern of the printed objects with an electromagnet (Figure 4.7B) also presented some issues. The heat generated by the magnet limits the use of a 3D printed PLA nozzle, so another material of manufacturing approach needs to be developed for this. Also, the objects did not seem to have the desired magnetization programming. Why this is, is unknown at this point, but might have to do with the magnetic field strength or shielding.

## 6.1 Discussion

Throughout the project, rheometric measurements have been conducted on the prepared NdFeB-embedded silicone. However, these measurements do not align with the measurements done by Sanne van Vilsteren (2021). Data of measured samples were mostly off by sometimes a factor of 10. However, because ink preparation was not in the scope of the project, not much attention has been given to the cause of this. Suspected is that the fumed silica used was degraded, as samples with and without fumed silica showed almost the same values (Appendix C.1f).

While the texture change demonstrator concept complies with the assignment of developing a demonstrator application of MSM that shows potential and limitations, the proposed applications of the changing texture are not fully thought out or validated, so the real value of the idea is not fully known. The material also has some limitations that prevent it from being the holy grail of shape morphing materials. For example, the magnetic field which activates the

shape change needs to be generated somehow. In the proposed concept, this is done by electromagnets. These magnets take up quite a bit of space, maybe even more than what common servomotors do. The same texture change concept could thus be achieved with an array of servomotors moving the shapes. This could potentially be a more efficient solution as well, as generating a large enough magnetic field takes more energy than driving a servomotor. Not to mention the neodymium magnetic particles used, which is a toxic, rare-earth metal (Lenntech, n.d.). This kind of defeats the purpose of using a shape memory material in the first place. Something that could justify the choice of MSM over motor actuation could be to miniaturize the design; many very small scale active MSM elements, actuated in small groups using electromagnets.

The consultation of fluid dynamics and accommodating mathematics was done pretty late in the project. Therefore, there was no sufficient time left to find out why the mathematics does not (fully) align with experience, for example nozzle diameter and needed pressure. The graph of Figure 4.59 shows shear rates of  $5 \times 10^6 \text{ s}^{-1}$  and up, while in measurement data, shear rate only reached 100 (because experiments were programmed this way) and in the paper by Bastola Paudel & Li, (2018), maximum shear rates of  $534.5 \text{ s}^{-1}$  were reported. It might have to do with the minimum viscosity of the silicone material.

## 6.2 Recommendations

As all projects, there is limited time. There are a few large topics that are not addressed, but are relevant to think about when picking up projects surrounding magnetic soft materials.

### *Sustainability*

This topic raises some concerns, as the magnetic particles used are toxic rare earth metal and very expensive. The silicone/NdFeb mixture is currently also not recyclable. As Van Vilsteren (2021) already pointed out, these are concerns that prevent MSM to be a valuable material to use in (consumer) products.

### *Further technical characterization*

More research needs to be done in understanding technical properties of the material, for example accurately measuring yield stress or load bearing capabilities of MSM structures and how material composition, magnetic field strength, manufacturing and shape relate to this.

### *Manufacturing technique*

Manual extrusion was to some extent successfully used during this project to make MSM objects, but is highly dependant on human error. Development of a 4D printer was also in this project not fully successful. Before a new project on meaningful applications of the material can be initiated, it is recommended to invest in a functioning manufacturing procedure. This can be by means of a fully functioning 4D printer set-up or by considering other manufacturing techniques like casting and magnetizing afterwards.

### *Material Appearance*

The appearance of a material has a large influence on the perception of it. During the workshop (Chapter 5.2), participants reported being uncomfortable with the feces resembling appearance of the material. Perhaps it could be enhanced by adding colourant to the recipe.

### 6.3 Reflection

In the original project brief, some personal learning goals were formulated on which are reflected here.

#### *Gain hands on experience in scientific research*

From my time spend in the lab I have gained much experience in working in a scientific context. How scientifically valuable my work has been I would like to keep in the middle for my supervisors and other more skilled researchers to judge.

#### *Learn scientific discussion and presentation skills*

In the many meetings I have had with my supervisors in which I explained my procedures and results, I often received many feedback on small things that would slip by my attention, like showing graphs with the same scale and always with labelled axis. These seemed small obvious things for them, but are easily missed by an untrained eye like me. At some points, I felt I was biased at my results and my supervisors would often point out if the result actually told what I thought (or wanted) it to tell. Also, sometimes I was biased towards quantity rather than quality, putting out lots of material which was actually not that meaningful for the larger scope of the project.

#### *Improve my prototyping skills*

In the project, I have prototypes several things, like parts for the 3D printer. For this, I have mainly used tools I was already familiar with, like 3D printing, Solidworks and laser cutting. I therefore have gained some more experience with these tools, however have not learned new prototyping tools or methods. For this learning goal, it might have been better to also pick up unfamiliar tools and step a bit more out of my comfort zone. However, by gaining more experience, I think (and hope) I also got even better in these tools.

*Learn more about the technology (hardware and software) of 3D printing.*

I have learned primarily about direct ink writing and required ink (rheological) properties. I also dug a bit into the structure and workings of G-code. However, I have not spent much time in leaning about 3D printing firmware and how the machines are actually controlled. Converting a new 3D printer system from the start to use in this project (which was on the table depending on the performance of the existing set-up) would have been more in line with this learning goal and maybe ultimately be more beneficial for the project as a whole.

#### *Experience in using new materials using the Material Driven Design methodology*

The demonstrator concept idea was made rather late in the project, the last week before the green light. Therefore, there was very little time left to fully dive into this design method. I however did my best to capture its essence in a shorter version. I liked how this method takes a specific material as a starting point in designing a suitable application which evokes certain meaning in line with the materials characteristics. I did however spend little time in the meaning of the material for the larger context, for example its meaning in relation to the environment. I feel like thinking about this should maybe be a first step in designing with new materials in the first place, because what would be the point in finding applications for a material of which you know is destructive for the planet and (most of) its inhabitants? Unless this material has a purpose or application which is beneficial to the greater good and is handled with care and responsibility.



# 7. References

- 3D Potter. (n.d.). *3D PotterBot Micro 10*. Retrieved on June 29, 2022, from: <https://3dpotter.com/printers/potterbot-micro-10>
- An, B., Tao, Y., Gu, J., Cheng, T., Chen, X., Zhang, X., Zhao, W., Do, Y., Takahashi, S., W, H.Y., Zhang, T. & Yao, L. (2018). Thermorph: Democratizing 4D Printing of Self-Folding Materials and Interfaces. In *Proceedings of the 2018 CHI Conference on Human Factors in Computing Systems - CHI '18*. <http://doi.org/10.1145/3173574.3173834>
- Arestho. (n.d.). *Luchtslang in transparant PVC*. Retrieved on June 9, 2022, from: <https://www.arestho.nl/refitexx-cristallo-transparant.html>
- Bastola, A.K., Paudel, M. & Li, L. (2018). Development of hybrid magnetorheological elastomers by 3D printing. *Polymer*, 149, 213-228. <https://doi.org/10.1016/j.polymer.2018.06.076>
- Bastola, A.K. & Hossain, M. (2021). The shape-morphing performance of magnetoactive soft materials. *Materials & Design*, 211. <https://doi.org/10.1016/j.matdes.2021.110172>
- Bay, M. (director), Spielberg, S. (executive producer), DeSanto, T. (producer), Murphy, D. (producer), Orci, R. (writer) & Kurzman, A. (writer). (2007). *Transformers* [Motion Picture]. Glendale, California: DreamWorks.
- Behl, M. & Lendlein, A. (2007). Shape-memory polymers. *Materials today*, 10(4), 20-28. [https://doi.org/10.1016/S1369-7021\(07\)70047-0](https://doi.org/10.1016/S1369-7021(07)70047-0)
- Behl, M., Kratz, K., Zotzmann, J., Nöchel, U., & Lendlein, A. (2013). Reversible Bidirectional Shape-Memory Polymers. *Advanced Materials*, 25(32), 4466-4469. <https://doi.org/10.1002/adma.201300880>
- Biasetto, L., Franchin, G., Elsayed, H., Boschetti, G., Huang, K. & Colombo, P. (2021). Direct Ink Writing of cylindrical lattice structures: A proof of concept. *Open Ceramics*, 7. <https://doi.org/10.1016/j.oceram.2021.100139>
- Chen, T., Bilal, O.R., Lang, R., Daraio, C., & Shea, K. (2019). Autonomous Deployment of a Solar Panel Using Elastic Origami and Distributed Shape-Memory-Polymer Actuators. *Physics Review Applied*, 11(6). <https://doi.org/10.1103/PhysRevApplied.11.064069>
- Cheng, Y., Chan, K. H., Wang, X.-Q., Ding, T., Li, T., Lu, X., & Ho, G. W. (2019). Direct-Ink-Write 3D Printing of Hydrogels into Biomimetic Soft Robots. *ACS Nano*, 13, 13176-13184. <https://doi.org/10.1021/acsnano.9b06144>
- Ching, T., Yingying, L., Karyappa, R., Ohno, A., Toh, Y.-C., & Hashimoto, M. (2019). Fabrication of Integrated Microfluidic Devices by Direct Ink Write (DIW) 3D Printing. *Sensors and Actuators B: Chemical*, 297. <https://doi.org/10.1016/j.snb.2019.05.086>
- Chiodo, J., McLaren, J., Billett, E.H. & Harrison, D. (2000). Isolating LCD's at end-of-life using active disassembly technology: A feasibility study. In *Proceedings of the IEEE International Symposium on Electronics and the Environment*, page 318 - 323. <http://doi.org/10.1109/ISEE.2000.857668>
- Coelho, M & Maes, P. (2009). Shutters: A Permeable Surface for Environmental Control and Communication. In *Proceedings of the Third International Conference on Tangible and Embedded Interaction (TEI'09)*, Cambridge, UK. <https://doi.org/10.1145/1517664.1517671>
- Constantijn. (March 14, 2019). *Easiest Way to Print With Clay* [YouTube video]. Retrieved on June 29, 2022, from: <https://www.youtube.com/watch?v=Q3A4NqTPOYY>

- Cui, J., Huang, T.-Y., Luo, Z., Testa, P., Gu, H., Chen, X.-Z., Nelson, B.J. & Heyderman, L. J. (2019). Nanomagnetic encoding of shape-morphing micromachines. *Nature*, 575(7781), 164–168. <https://doi.org/10.1038/s41586-019-1713-2>
- Engineers Edge. (n.d.). *Power screws design equation and calculator*. Retrieved on June 22, 2021, from: [https://www.engineersedge.com/mechanics\\_machines/power\\_screws\\_design\\_13982.htm](https://www.engineersedge.com/mechanics_machines/power_screws_design_13982.htm)
- Foerster, A., Annarasa, V., Terry, A., Wildman, R., Hague, R., Irvine, D., De Focatiis, D.S.A. & Tuck, C. (2021). UV-curable silicone materials with tuneable mechanical properties for 3D printing. *Materials & Design*, 205. <https://doi.org/10.1016/j.matdes.2021.109681>
- Fu, Y.Q., Huang, W.M., Luo, J.K. & Lu, H. (2015). Polyurethane shape-memory polymers for biomedical applications. In L. Yahia (Ed.), *Biomaterials, Shape Memory Polymers for Biomedical Applications* (167–195). Cambridge, United Kingdom: Woodhead Publishing. <https://doi.org/10.1016/B978-0-85709-698-2.00009-X>
- Fuhrer, R., Athanassiou, E. K., Luechinger, N. A., & Stark, W. J. (2009). Crosslinking Metal Nanoparticles into the Polymer Backbone of Hydrogels Enables Preparation of Soft, Magnetic Field-Driven Actuators with Muscle-Like Flexibility. *Small*, 5(3), 383–388. <http://doi.org/10.1002/sml.200801091>
- Galea, R., Dudek, K.K., Farrugia, P.S., Mangion, L.Z., Grima, J.N. & Gatt, R. (2022). Reconfigurable magneto-mechanical metamaterials guided by magnetic fields. *Composite Structures*, 280. <https://doi.org/10.1016/j.compstruct.2021.114921>
- Gall, K., Yakacki, C.M., Liu, Y., Shandas, R., Willett, N. and Anseth, K.S. (2005), Thermomechanics of the shape memory effect in polymers for biomedical applications. *Journal of Biomedical Materials Research*, 73A(3), 339–348. <https://doi-org.tudelft.idm.oclc.org/10.1002/jbm.a.30296>
- Han, J., Fei, G., Li, G., & Xia, H. (2013). High Intensity Focused Ultrasound Triggered Shape Memory and Drug Release from Biodegradable Polyurethane. *Macromolecular Chemistry and Physics*, 214(11), 1195–1203. <https://doi.org/10.1002/macp.201200576>
- Han, M.-W., Rodrigue, H., Cho, S., Song, S.-H., Chu, W.-S., Choi, H., & Ahn, S.-H. (2015). Design and Performance Evaluation of Soft Morphing Car-Spoiler. In *Proceedings of the ASME 2014 International Design Engineering Technical Conferences & Computers and Information in Engineering Conference*, Buffalo, New York. <https://doi.org/10.1115/detc2014-34915>
- He, Q., Hong, M.H., Huang, W.M., Chong, C.T., Fu, Y.Q. & Du, H.J. (2004). CO2 laser annealing of sputtering deposited NiTi shape memory thin films. *Journal of Micromechanics and Microengineering*, 14(7). <https://doi.org/10.1088/0960-1317/14/7/016>
- He, Q., Wang, Z., Wang, Y., Minori, A., Tolley, M. T., & Cai, S. (2019). Electrically controlled liquid crystal elastomer-based soft tubular actuator with multimodal actuation. *Science Advances*, 5(10). <https://doi.org/10.1126/sciadv.aax5746>
- Hu, W., Lum, G. Z., Mastrangeli, M., & Sitti, M. (2018). Small-scale soft-bodied robot with multimodal locomotion. *Nature*, 554(7690), 81–85. <https://doi.org/10.1038/nature25443>
- Huang, W.M., Ding, Z., Wang, C.C., Wei, J., Zhao, Y. & Purnawali, H. (2010). Shape memory materials. *Materials today*, 13(7-8), 54–61. [https://doi.org/10.1016/S1369-7021\(10\)70128-0](https://doi.org/10.1016/S1369-7021(10)70128-0)
- Ion, A., Frohnhofen, J., Wall, L., Kovakcs, R., Alistar, M., Lindsay, J., Lopes, P., Chen, H.-T. & Baudisch, P. (2016). Metamaterial Mechanisms. In *Proceedings of the 29th Annual Symposium on User Interface Software and Technology*, 529–539. <https://doi.org/10.1145/2984511.2984540>
- Ion, A., Wall, L., Kovacs, R., & Baudisch, P. (2017). Digital Mechanical Metamaterials. In *Proceedings of the 2017 CHI Conference on Human Factors in Computing Systems - CHI '17*. <https://doi.org/10.1145/3025453.3025624>

- Ion, A., Kovacs, R., Schneider, O. S., Lopes, P., & Baudisch, P. (2018). Metamaterial Textures. Proceedings of the 2018 CHI Conference on Human Factors in Computing Systems - CHI '18. <https://doi.org/10.1145/3173574.3173910>
- Ion, A., Lindlbauer, D., Herholz, P., Alexa, M., & Baudisch, P. (2019). Understanding Metamaterial Mechanisms. Proceedings of the 2019 CHI Conference on Human Factors in Computing Systems - CHI '19. <https://doi.org/10.1145/3290605.3300877>
- Jackson, J. A., Messner, M. C., Dudukovic, N. A., Smith, W. L., Bekker, L., Moran, B., Gogobic, A.M., Pascall, A.W., Duoss, E.B. & Spadaccini, C. M. (2018). Field responsive mechanical metamaterials. *Science Advances*, 4(12). <https://doi.org/10.1126/sciadv.aau6419>
- Kamrava, S., Mousanezhad, D., Felton, S. M., & Vaziri, A. (2018). Programmable Origami Strings. *Advanced Materials Technologies*, 3(3). <https://doi.org/10.1002/admt.201700276>
- Karana, E., Barati, B., Rognoli, V., & Zeeuw van der Laan, A. (2015). Material driven design (MDD): A method to design for material experiences. *International Journal of Design*, 9(2), 35-54. <http://hdl.handle.net/11311/979536>
- Khan Academy. (n.d.). *Volume flow rate and equation of continuity*. Retrieved on June 29, 2022, from: <https://www.khanacademy.org/science/physics/fluids/fluid-dynamics/v/fluids-part-7>
- Kim, S., Oh, J., Jeong, D., Park, W. & Bae, J. (2018). Consistent and Reproducible Direct Ink Writing of Eutectic Gallium-Indium for High-Quality Soft Sensors. *Soft Robotics*, 5(5), 601-612. <https://doi.org/10.1089/soro.2017.0103>
- Kim, Y., Yuk, H., Zhao, R., Chester, S.A. & Zhao, X. (2018). Printing ferromagnetic domains for untethered fast-transforming soft materials. *Nature*, 558, p. 274 - 279. <https://doi.org/10.1038/s41586-018-0185-0>
- Kim, Y., Parada, G. A., Liu, S., & Zhao, X. (2019). Ferromagnetic soft continuum robots. *Science Robotics*, 4(33). <https://doi.org/10.1126/scirobotics.aax7329>
- Khoo, Z. X., Teoh, J. E. M., Liu, Y., Chua, C. K., Yang, S., An, J., Leong, K.F. & Yeong, W. Y. (2015). 3D printing of smart materials: A review on recent progresses in 4D printing. *Virtual and Physical Prototyping*, 10(3), 103-122. <https://doi.org/10.1080/17452759.2015.1097054>
- Krulevitch, P., Lee, A.P., Ramsey, P.B., Trevino, J.C., Hamilton, J. & Northrup, M.A. (1996). Thin film shape memory alloy microactuators. *Journal of Microelectromechanical Systems*, 5(4), 270-282. <http://doi.org/10.1109/84.546407>
- K&J Magnetics, inc. (n.d.). *Shielding materials*. Retrieved on June 23, 2022, from: <https://www.kjmagnetics.com/blog.asp?p=shielding-materials>
- Ladd, M.E., Bachert, P., Meyerspeer, M., Moser, E., Nagel, A.M., orris, D.G., Schmitter, S., Speck, O., Straub, S. & Zaiss, M. (2018). Pros and cons of ultra-high-field MRI/MRS for human application. *Progress in Nuclear Magnetic Resonance Spectroscopy*, 109, 1-50. <https://doi.org/10.1016/j.pnmrs.2018.06.001>
- Lee, K.H., Yu, K., Ba'ba'a, H.A., Xin, A., Feng, Z. & Wang, Q. (2020). Sharkskin-Inspired Magnetoactive Reconfigurable *Acoustic Metamaterials*. *Research*. <https://doi.org/10.34133/2020/4825185>
- Lenntech. (n.d.). *Neodymium*. Retrieved on July 1, 2022, from: <https://www.lenntech.nl/periodiek/elementen/nd.htm>
- Li, M., Wang, Y., Chen, A., Naidu, A., Napier, B. S., Li, W., Rodriguez, C.L., Crooker, S.A. & Omenetto, F. G. (2018). Flexible magnetic composites for light-controlled actuation and interfaces. In *Proceedings of the National Academy of Sciences*, 115(32), 8119-8124. <http://doi.org/10.1073/pnas.1805832115>
- Lin, J., Zhou, J. & Koo, H. (2015). Enfold: Clothing for People with Cerebral Palsy. In *Adjunct Proceedings of the 2015 ACM International Joint Conference on Pervasive and Ubiquitous Computing and Proceedings of the 2015 ACM International Symposium on Wearable Computers*, 563-566. <https://doi.org/10.1145/2800835.2801671>

- Liu, Y., Han, C., Tan, H. & Du, X. (2010a). Thermal, mechanical and shape memory properties of shape memory epoxy resin, *Materials Science and Engineering: A*, 527(10–11), 2510–2514. <https://doi.org/10.1016/j.msea.2009.12.014>
- Liu, Y. & Hu, H. (2010b). A review on auxetic structures and polymeric materials. *Scientific Research and Essays*, 5(10), 1052–1063. <https://doi.org/10.5897/SRE.9000104>
- Lu, H., Zhang, M., Yang, Y., Huang, Q., Fukuda, T., Wang, Z., & Shen, Y. (2018). A bioinspired multilegged soft millirobot that functions in both dry and wet conditions. *Nature Communications*, 9(1). <http://doi.org/10.1038/s41467-018-06491-9>
- Lum, G. Z., Ye, Z., Dong, X., Marvi, H., Erin, O., Hu, W., & Sitti, M. (2016). Shape-programmable magnetic soft matter. In *Proceedings of the National Academy of Sciences*, 113(41). <https://doi.org/10.1073/pnas.1608193113>
- Ma, C., Wu, S., Ze, Q., Kuang, X., Zhang, R., Qi, H. J., & Zhao, R. (2020). Magnetic Multimaterial Printing for Multimodal Shape Transformation with Tunable Properties and Shiftable Mechanical Behaviors. *ACS Applied Materials & Interfaces*, 13(11). <https://doi.org/10.1021/acsami.0c13863>
- Mark, A.G., Palagi, S., Qiu T. & Fischer, P. (2016). Auxetic metamaterial simplifies soft robot design. In *Proceedings of the IEEE International Conference on Robotics and Automation (ICRA)*, 4951–4956. <https://doi.org/10.1109/ICRA.2016.7487701>
- Milkert, H. (2014). *Turn Almost any 3D Printer Into a Paste Extrusion Printer With +Lab's 3D Printed Attachment*. Retrieved on June 29, 2022, from 3D Print.com: <https://3dprint.com/17882/lab-paste-extruder/>
- Mirzaali, M.J., Janbaz, S., Strano, M., Vergani, L. & Zadpoor, A.A. (2018). Shape-matching soft mechanical metamaterials. *Scientific Reports* 8. <https://doi.org/10.1038/s41598-018-19381-3>
- Moreno-Marcelino, J.E., Gutierrez-Segura, E., Vilchis-Nestor, A.R., Castro-Longoria, E. & López-Téllez, G. (2020). Shape memory hybrid based on polyvinyl alcohol and 0D silver nanoparticles. *Polymer Testing*, 90. <https://doi.org/10.1016/j.polymertesting.2020.106668>
- Mushield. (n.d.). How magnetic shielding works. Retrieved on June 23, 2022, from: <https://www.mushield.com/magnetic-shielding/magnetic-shields-how-magnetic-shielding-works/>
- Nakagawa, Y., Kamimura, A., & Kawaguchi, Y. (2012). MimicTile. In *Proceedings of the 2012 ACM Annual Conference on Human Factors in Computing Systems - CHI '12*. <https://doi.org/10.1145/2207676.2207782>
- Nakayasu, A. (2016). Luminescent Tentacles: A Scalable SMA Motion Display. In *Proceedings of the 29th Annual Symposium on User Interface Software and Technology*, 33–34. <https://doi.org/10.1145/2984751.2985695>
- National Geographic. (n.d.). *Porcupines*. Retrieved on June 27, 2022, from: <https://www.nationalgeographic.com/animals/mammals/facts/porcupines>
- Nguyen, V. Q., Ahmed, A. S., & Ramanujan, R. V. (2012). Morphing Soft Magnetic Composites. *Advanced Materials*, 24(30), 4041–4054. <https://doi.org/10.1002/adma.201104994>
- Nippon Steel. (n.d.). *Grain-Oriented Electrical Steel Sheets* [Technical Data Sheet]. Retrieved on May 13, 2022, from: [https://www.nipponsteel.com/product/catalog\\_download/pdf/D004je.pdf](https://www.nipponsteel.com/product/catalog_download/pdf/D004je.pdf)
- Nojima, T., Ooide, Y., & Kawaguchi, H. (2013). Hairlytop interface: An interactive surface display comprised of hair-like soft actuators. *IEEE World Haptics Conference (WHC)*. <http://doi.org/10.1109/whc.2013.6548447>
- Ortiz-Acosta, D. Moore, T., Safarik, D.J., Hubbard, K.M. & Janicke, M. (2018). 3D-Printed Silicone Materials with Hydrogen Getter Capability. *Advanced Functional Materials*, 28(17). <https://doi.org/10.1002/adfm.201707285>

- Overvelde, J. T. B., de Jong, T. A., Shevchenko, Y., Becerra, S. A., Whitesides, G. M., Weaver, J. C., Hoberman, C. & Bertoldi, K. (2016). A three-dimensional actuated origami-inspired transformable metamaterial with multiple degrees of freedom. *Nature Communications*, 7. <https://doi.org/10.1038/ncomms10929>
- Park, Y.-W., Park, J., & Nam, T.-J. (2015). The Trial of Bendi in a Coffeehouse. In *Proceedings of the 33rd Annual ACM Conference on Human Factors in Computing Systems - CHI '15*. <https://doi.org/10.1145/2702123.2702326>
- Perovich, L., Mothersill, P., & Farah, J. B. (2013). Awakened apparel. In *Proceedings of the 8th International Conference on Tangible, Embedded and Embodied Interaction - TEI '14*. <https://doi.org/10.1145/2540930.2540958>
- Purnawali, H., Xu, W.W., Zhao, Y., Ding, Z., Wang, C.C., Huang, W.M. & Fan, H. (2012). Poly(methyl methacrylate) for active disassembly, *Smart Materials and Structures*, 21(7). <http://doi.org/10.1088/0964-1726/21/7/075006> (also see these movies: <https://iopscience.iop.org/article/10.1088/0964-1726/21/7/075006/data>)
- Qi, J., & Buechley, L. (2012). Animating paper using shape memory alloys. In *Proceedings of the 2012 ACM Annual Conference on Human Factors in Computing Systems - CHI '12*. <https://doi.org/10.1145/2207676.2207783>
- Rafsanjani, A. & Pasini, D. (2016). Bistable auxetic mechanical metamaterials inspired by ancient geometric motifs. *Extreme Mechanics Letters*, 9(2), 291-296. <https://doi.org/10.1016/j.eml.2016.09.001>
- Rafsanjani, A., Bertoldi, K., & Studart, A. R. (2019). Programming soft robots with flexible mechanical metamaterials. *Science Robotics*, 4(29). <https://doi.org/10.1126/scirobotics.aav7874>
- Rasmussen, M. K., Pedersen, E. W., Petersen, M. G., & Hornbæk, K. (2012). Shape-changing interfaces. In *Proceedings of the 2012 ACM Annual Conference on Human Factors in Computing Systems - CHI '12*, 735-744. <http://doi.org/10.1145/2207676.2207781>
- Ren, X., Das, R., Tran, P., Ngo, T. D., & Xie, Y. M. (2018). Auxetic metamaterials and structures: a review. *Smart Materials and Structures*, 27(2). <https://doi.org/10.1088/1361-665x/aaa61c>
- Ren, Z., Hu, W., Dong, X. & Sitti, M. (2019). Multi-functional soft-bodied jellyfish-like swimming. *Nature Communications*, 10. <https://doi.org/10.1038/s41467-019-10549-7>
- RepRap. (n.d.). *G-Code*. Retrieved on March 24, 2022, from: <https://reprap.org/wiki/G-code>
- Roh, S., Okello, L. B., Golbasi, N., Hankwitz, J. P., Liu, J. A.-C., Tracy, J. B., & Velev, O. D. (2019). 3D-Printed Silicone Soft Architectures with Programmed Magneto-Capillary Reconfiguration. *Advanced Materials Technologies*, 4(4). <https://doi.org/10.1002/admt.201800528>
- Shinoda, H., Azukizawa, S., Maeda, K., & Tsumori, K. (2019). Bio-Mimic Motion of 3D-Printed Gel Structures Dispersed with Magnetic Particles. *Journal of The Electrochemical Society*, 166(9), B3235-B3239. <https://doi.org/10.1149/2.0361909jes>
- Small, W., Metzger, M. F., Wilson, T. S., & Maitland, D. J. (2005). Laser-activated shape memory polymer microactuator for thrombus removal following ischemic stroke: preliminary in vitro analysis. *IEEE Journal of Selected Topics in Quantum Electronics*, 11(4), 892-901. <https://doi.org/10.1109/jstqe.2005.857748>
- Smooth-On. (n.d.). *Ecoflex 00-10*. Retrieved on May 19, 2022, from: <https://www.smooth-on.com/products/ecoflex-00-10/>
- Sofla, A.Y.N., Meguid, S.A., Tan, K.T. & Yeo, W.K. (2010). Shape morphing of aircraft wing: Status and challenges. *Materials & Design*, 31(3), 1284-1292. <https://doi.org/10.1016/j.matdes.2009.09.011>

- Stachiv, I., Alarcon, E. & Lamac, M. (2021). Shape Memory Alloys and Polymers for MEMS/NEMS Applications: Review on Recent Findings and Challenges in Design, Preparation, and Characterization. *Metals*, 11(3), 415. <https://doi.org/10.3390/met11030415>
- Sun, L., Huang, W.M., Ding, Z., Zhao, Y., Wang, C.C., Purnawali, H. & Tang, C. (2012). Stimulus-responsive shape memory materials: A review. *Materials & Design*, 33, 577-640. <https://doi.org/10.1016/j.matdes.2011.04.065>
- Surjadi, J. U., Gao, L., Du, H., Li, X., Xiong, X., Fang, N. X., & Lu, Y. (2019). Mechanical Metamaterials and Their Engineering Applications. *Advanced Engineering Materials*, 21(3). <https://doi.org/10.1002/adem.201800864>
- Tolley, M. T., Felton, S. M., Miyashita, S., Aukes, D., Rus, D., & Wood, R. J. (2014). Self-folding origami: shape memory composites activated by uniform heating. *Smart Materials and Structures*, 23(9). <https://doi.org/10.1088/0964-1726/23/9/094006>
- Van Vilsteren, S. (2021). Designing Magnetic Soft Materials for 4D Printing [Master Thesis, Delft University of Technology]. Tu Delft Educational Repository. <http://resolver.tudelft.nl/uuid:7e05bd4c-4720-4e1f-b13b-7b048602ce42>
- Wan, X., Luo, L. Liu, Y. & Leng, J. (2020). Direct Ink Writing Based 4D Printing of Materials and Their Applications. *Advanced Science*, 7(16). <https://doi.org/10.1002/advs.202001000>
- Wang, L., Zheng, D., Harker, P., Patel, A.B., Guo, C.F. & Zhao, X. (2021). Evolutionary design of magnetic soft continuum robots. In *Proceedings of the National Academy of Sciences of the United States of America*, 118(21). <https://doi.org/10.1073/pnas.2021922118>
- Wang, Z., Wu, Y., Wu, D., Sun, D. & Lin, L. (2022). Soft magnetic composites for highly deformable actuators by four-dimensional electrohydrodynamic printing. *Composites Part B: Engineering*, 231. <https://doi.org/10.1016/j.compositesb.2021.109596>
- Williams, E.A., Shaw, G & Elahinia, M. (2010). Control of an automotive shape memory alloy mirror actuator. *Mechatronics*, 20(5), 527-534. <https://doi.org/10.1016/j.mechatronics.2010.04.002>
- Wu, S., Ze, Q., Zhang, R., Hu, N., Cheng, Y., Yang, F., & Zhao, R. (2019). Symmetry-breaking Actuation Mechanism for Soft Robotics and Active Metamaterials. *ACS Applied Materials & interfaces*, 11, 41649-41658. <https://doi.org/10.1021/acsami.9b13840>
- Zhang, G.-D., Wu, J.-R., Tang, L.-C., Li, J.-Y., Lai, G.-Q., & Zhong, M.-Q. (2014). Rheological behaviors of fumed silica/low molecular weight hydroxyl silicone oil. *Journal of Applied Polymer Science*, 131(17). <https://doi.org/10.1002/app.40722>
- Zhang, X., Tan, B.H., Li, Z. (2018). Biodegradable polyester shape memory polymers: Recent advances in design, material properties and applications. *Material Science and Engineering: C*, 92, 1061-1074. <https://doi.org/10.1016/j.msec.2017.11.008>
- Zhang, Y., Wang, Q., Yi, S., Lin, Z., Wang, C., Chen, Z., Jiang, L. (2021). 4D Printing of Magnetoactive Soft Materials for On-Demand Magnetic Actuation Transformation. *ACS Applied Materials and interfaces*, 13(3). <https://doi.org/10.1021/acsami.0c19280>
- Zhai, Z., Wang, Y. & Jiang, H. (2018). Origami-inspired, on-demand deployable and collapsible mechanical metamaterials with tunable stiffness. *PNAS*, 115(9), 2032-2037. <https://doi.org/10.1073/pnas.1720171115>
- Zhao, R. Kim, Y., Chester, S.A., Sharma, P. & Zhao, X. (2019). Mechanics of hard-magnetic soft materials. *Journal of the Mechanics and Physics of Solids*, 124, 244-263. <https://doi.org/10.1016/j.jmps.2018.10.008>
- Zhao, J., Li, X., Tan, Y., Liu, X., Lu, T. & Shi, M. (2022). Smart Adhesives via Magnetic Actuation. *Advanced Materials*, 34(8). <https://doi.org/10.1002/adma.202107748>

Ze, Q., Kuang, X., Wu, S., Wong, J., Montgomery, S. M., Zhang, R., Kovitz, J.M., Yang, F., Qi, J. & Zhao, R. (2019). Magnetic Shape Memory Polymers with Integrated Multifunctional Shape Manipulation. *Advanced Materials*, 32(4). <https://doi.org/10.1002/adma.201906657>

Zhu, H., He, Y., Wang, Y., Zhao, Y. and Jiang, C. (2022), Mechanically-Guided 4D Printing of Magnetoresponse Soft Materials across Different Length Scale. *Advanced Intelligent Systems*, 4(3). <https://doi.org/10.1002/aisy.202100137>

# Appendices

- A: Original project brief
- B: Active disassembly literature review extension
- C: Experiment documentation
- D: 3D printer parts (re)designs
- E: Extrusion system Simulink model (unfinished)
- F: Flow resistance per section of transport system
- G: Material Driven Design workshop raw data
- H: Demonstrator concept idea selection



# Appendix A: Original project brief



## Designing and 4D printing magnetically activated smart materials \_\_\_\_\_ project title

Please state the title of your graduation project (above) and the start date and end date (below). Keep the title compact and simple. Do not use abbreviations. The remainder of this document allows you to define and clarify your graduation project.

start date 04 - 02 - 2022 \_\_\_\_\_ 15 - 07 - 2022 \_\_\_\_\_ end date

### INTRODUCTION \*\*

Please describe, the context of your project, and address the main stakeholders (interests) within this context in a concise yet complete manner. Who are involved, what do they value and how do they currently operate within the given context? What are the main opportunities and limitations you are currently aware of (cultural- and social norms, resources (time, money,...), technology, ...).

Metamaterials are synthetic materials that show unique (electromagnetic or mechanical) properties that do not exist naturally due to their structure. Shape Morphing Materials (SMM) are materials that change their shape automatically by an external influence (heat, light, pH, magnetic fields) without the need for motors. There are different types of shape shifting materials, of which Shape Memory Alloys (like nitinol) and Shape Memory Polymers (like PLA) that deform under the influence of heat are the most known.

Magnetically Activated Smart Materials are a relatively new form of SMMs that can alter their shape by influence of an external magnetic field. They therefore allow for remote control without the need for heat and can change shape very quickly. In Magnetic Soft Material (MSM), the shape change is realised by embedded magnetic particles inside an elastomer. The position of the north and south poles of these particles is controlled via a (electro) magnet in the manufacturing process (Figure 1). When the magnetic field is introduced, the magnetic field of the particles align with the external magnetic field, pulling and pushing the elastomer in a specific shape. By changing the north and south pole position of the particles during the 3D printing process, the material is given its shape morphing properties, i.e. its programmed shape. By including these properties during 3D printing, the process becomes 4D printing.

Some current applications for SMM and MSM lie in the field of haptics (e.g. shape-shifting interfaces; Quamar et al., 2018) soft robotics and biomimicry (e.g. grippers) biomedical devices (e.g. bone support structures; Zhang et al., 2019), hedonic (non-instrumental: aesthetic, fashion) and active disassembly of products (Chiodo et al., 2002).

When speaking of emerging materials, like SMMs or MSMs, few designers know the potentials, possibilities and limitations of these materials. Let alone apply them in their designs. To make these materials more known among designers and fill the knowledge gap about SMM characteristics, demonstrators need to be made to show potential use cases of these materials and how they can elevate a design.

This project builds on the work done in the Master Thesis of Sanne van Vilsteren, in which a 4D printer set-up was initialized and designs for a proof of concept were made (Figure 2). The initial objective of this project was to create a demonstrator to show potential usecases of MSMs. Due to the dynamic nature of objectives in research, they change along the process depending on results and encountered obstacles. Therefore, this initial objective was moved to this new assignment, where work on the 4D printer setup is continued and a demonstrator of a tangible application is realised.

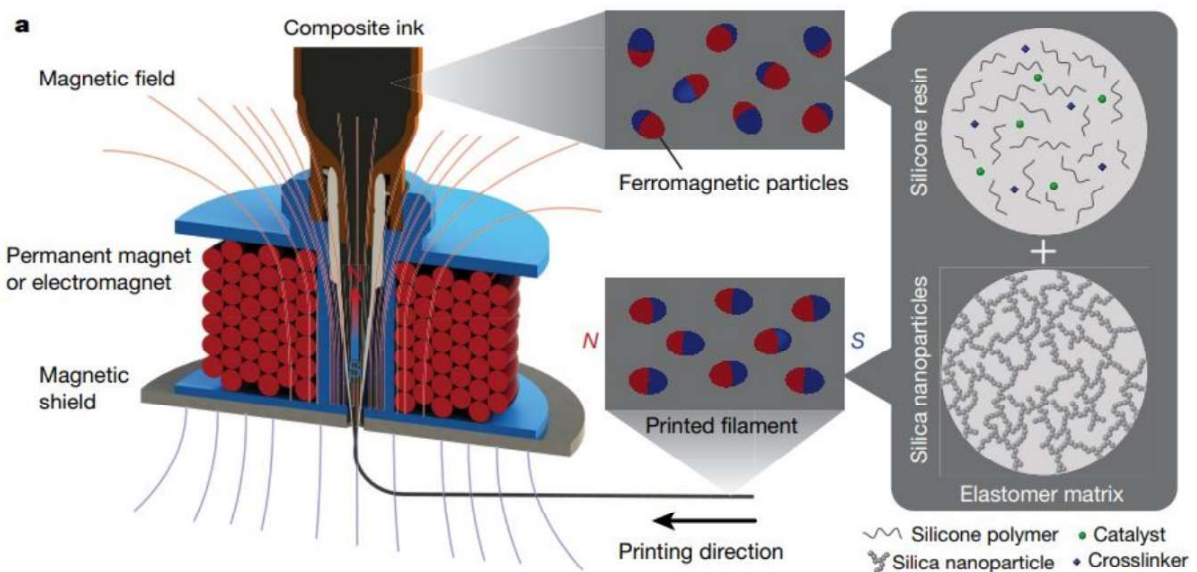
Chiodo, J.D., Jones, N., Billett, E.H. & Harrison, D.J. (2002) Shape memory alloy actuators for active disassembly using 'smart' materials of consumer electronic products, *Materials & Design*, 23(5), 471-478.  
[https://doi.org/10.1016/S0261-3069\(02\)00018-3](https://doi.org/10.1016/S0261-3069(02)00018-3)

Quamar, I.P.S., Groh, R., Holman, D & Roudaut, A. (2018). HCI meets Material Science: A Literature Review of Morphing Materials for the Design of Shape-Changing. *Proceedings of the 2018 CHI Conference on Human Factors in Computing Systems*, Montréal, QC, Canada, pp 1-23.

Zhang, F.; Wang, L.; Zheng, Z.; Liu, Y. & Leng, J. (2019). Magnetic programming of 4D printed shape memory composite structures. *Composites Part A: Applied Science and Manufacturing*, 125.

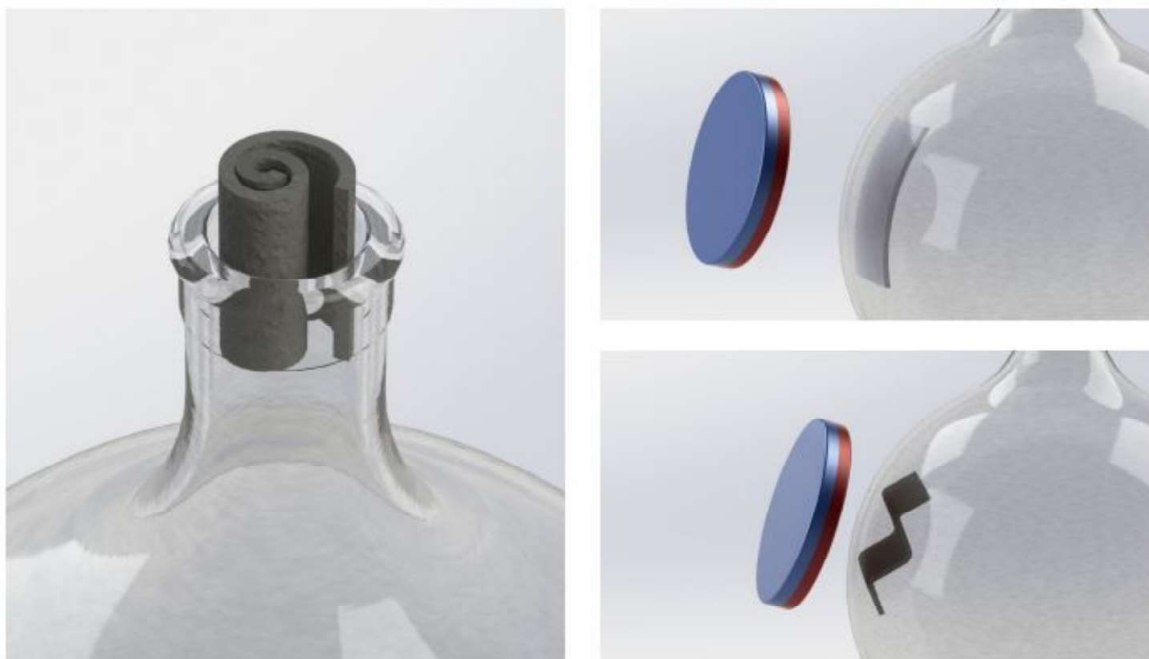
space available for images / figures on next page

introduction (continued): space for images



Kim, Y., Yuk, H., Zhao, R., Chester, S. A., & Zhao, X. (2018). Printing ferromagnetic domains for untethered fast-transforming soft materials. *Nature*, 558(7709), 274–279. doi:10.1038/s41586-018-0185-0

image / figure 1: 4D printing of magnetically activated soft materials by Kim et al, 2018.



Van Vilsteren, S. (2021). Designing Magnetic Soft Materials for 4D Printing [Master Thesis, Delft University of Technology]. TU Delft educational repository. <http://resolver.tudelft.nl/uuid:7e05bd4c-4720-4e1f-b13b-7b048602ce42>

image / figure 2: Proof of concept designed in the Master Thesis by Sanne Van Vilsteren (2021).

**PROBLEM DEFINITION \*\***

Limit and define the scope and solution space of your project to one that is manageable within one Master Graduation Project of 30 EC (= 20 full time weeks or 100 working days) and clearly indicate what issue(s) should be addressed in this project.

Magnetic soft materials (MSM) are a relatively new and unknown kind of material. Thus, little research is available on manufacturing and applications of magnetically activated meta materials (e.g. Van Vilsteren et al, 2021) and few designers know about its functionalities and possibilities. In the master Thesis by Sanne van Vilsteren, a lot of parameters on the properties of the material, ink production and manufacturing using 4D printing were investigated and idea directions for applications of these materials were made. However, a real functional demonstrator was not realised during the 20 week project. Therefore, there is still a need for a proof of concept that shows the potential of the MSM material.

Furthermore, some material and manufacturing parameters still need to be researched, i.e. the amount of deflection the material shows and the properties that influence this (amount of particles, strength magnetic field...), and the influence of 3D printing parameters on the behaviour, such as speed and thickness.

In addition, due to technical difficulties, the intended 4D printing set-up was not fully realised. This continuation on the previous project thus aims to resolve the issues with the 4D printing set-up to be used in the design and manufacturing of a demonstrator for an inspiring use case of this new material. In the end, we want to demonstrate the potential, characteristics, limitations and possibilities of MSMs to inspire and empower designers and engineers to make use of these materials in their future designs in an effective way.

Van Vilsteren, S.J.M., Yarmand, H. & Ghodrat, S. (2021). Review of Magnetic Shape Memory Polymers and Magnetic Soft Materials. *Magnetochemistry*, 7, 123. <https://doi.org/10.3390/magnetochemistry7090123>

**ASSIGNMENT \*\***

State in 2 or 3 sentences what you are going to research, design, create and / or generate, that will solve (part of) the issue(s) pointed out in "problem definition". Then illustrate this assignment by indicating what kind of solution you expect and / or aim to deliver, for instance: a product, a product-service combination, a strategy illustrated through product or product-service combination ideas, ... . In case of a Specialisation and/or Annotation, make sure the assignment reflects this/these.

The goal of this project is to design and prototype a proof of concept that inspires future designers about the possibilities of magnetic smart materials. In order to do this, the 4D printing setup which resulted from the previous Master Thesis will be re-evaluated and improved through systemic testing of parameters that influence the performance of the printer set-up and the printed material.

The ultimate end result of this project is the design and prototype of a demonstrator for the use of magnetically activated metamaterials in product design to showcase its potential and limitations and to inspire (future) designers. The minimal aim is to make a 1D mechanism with the 4D printer and the ultimate goal is a 3D metamaterial structure.

To produce the prototype, the current 4D printing set-up needs to be evaluated and improved. The starting point would again be the result of the previous Master Thesis on this subject and the unsolved issues that still remain. That is the high viscosity of the material ink that limits the extrusion of the ink by the printer; firmware issues that do not allow the control of the electromagnet properly and the magnetic shield that does not function as desired. The printer set-up must thus be adapted and improved to resolve these issues. The ink used will be made by recipe, magnetized at the reactor institute and possibly improved to make it work with the printer. During the 4D printer redesign, metamaterial structures will be made and experimented with, from 1D to 2D and eventually 3D structures.

In parallel, domains of application of this new material will be researched. By experimenting with the material, the characteristics of the material are listed and form the basis for ideation of a demonstrator product design, which will also be prototyped. Special attention is given to the use of magnetic metamaterials in active disassembly of products. By tinkering with the material (e.g. possible movements and required forces) and researching existing metamaterial structures and applications, it is investigated whether or not the application in this use case is realistic or not.

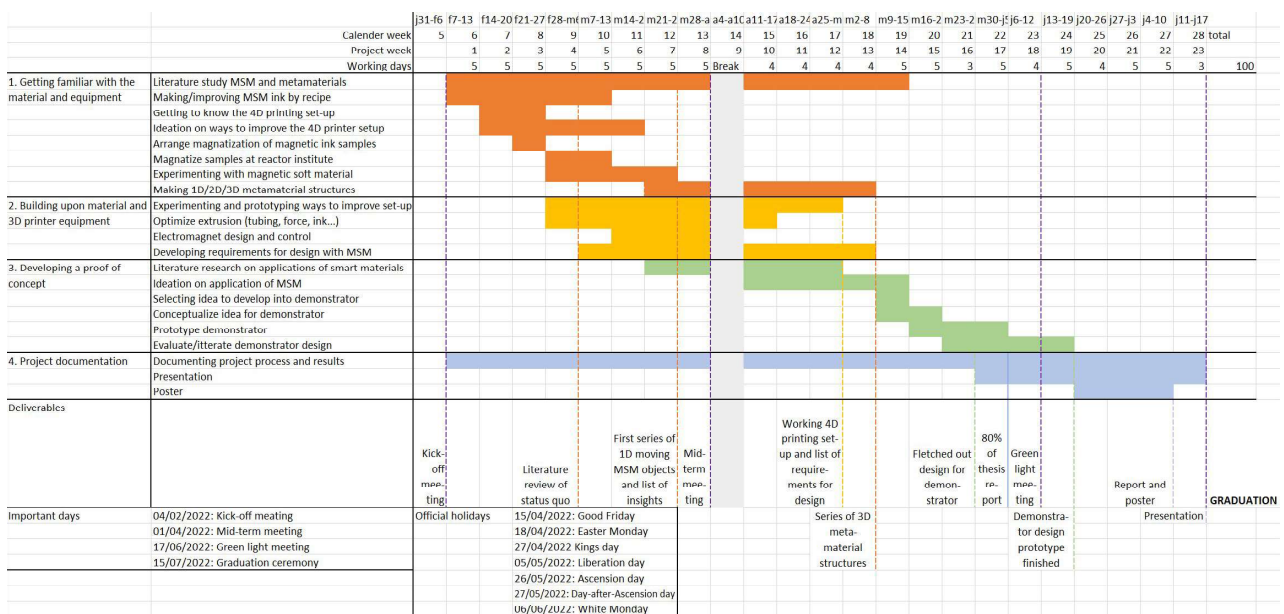
**PLANNING AND APPROACH \*\***

Include a Gantt Chart (replace the example below - more examples can be found in Manual 2) that shows the different phases of your project, deliverables you have in mind, meetings, and how you plan to spend your time. Please note that all activities should fit within the given net time of 30 EC = 20 full time weeks or 100 working days, and your planning should include a kick-off meeting, mid-term meeting, green light meeting and graduation ceremony. Illustrate your Gantt Chart by, for instance, explaining your approach, and please indicate periods of part-time activities and/or periods of not spending time on your graduation project, if any, for instance because of holidays or parallel activities.

start date 4 - 2 - 2022

15 - 7 - 2022

end date



The project is divided in an exploration phase (1) in which I get to know the material and the current printer set-up. By tinkering with the material, I get a better feel of its possibilities and limitations. The last few experiments from the previous project by Sanne are redone to make sure I get the ink and 3D printer at the same point as where the previous project left off. Deliverable for this phase would be a literature review of the status quo in the field of MSM and its applications and existing possible mechanisms. In addition, a collection of small objects is made to test and demonstrate possible mechanisms. It is started simple, with a 1D mechanism and built up towards a single cell 3D structure and ultimately a 3D structure consisting of multiple cells to make it a metamaterial. Next, the 4D printing set-up needs to be examined (2). With the findings of the previous master thesis, the printer is further modified, improved and tested in order to make 4D printing possible. This is already started during the exploration of the material as this is an iterative procedure. The printer needs to be used in the making of the metamaterial structures. In phase (3), ideas for applications are generated (although ideas will undoubtedly pop up during tinkering with and researching the material). One application that will be examined is the use of a magnetic metamaterial structure for use in active/self disassembly. When a concept direction is chosen, it will be evaluated if this usecase is realistic or that it is better to continue with another product idea. The chosen concept direction will be further developed into an inspiring demonstrator prototype, which is evaluated and iterated upon. Documenting (4) is done throughout the project and presentation and poster are made after the green light meeting.

Planned break of one week:  
28/03/2022 - 03/04/2022 and one extra day off at 24/06/2022

## MOTIVATION AND PERSONAL AMBITIONS

Explain why you set up this project, what competences you want to prove and learn. For example: acquired competences from your MSc programme, the elective semester, extra-curricular activities (etc.) and point out the competences you have yet developed. Optionally, describe which personal learning ambitions you explicitly want to address in this project, on top of the learning objectives of the Graduation Project, such as: in depth knowledge a on specific subject, broadening your competences or experimenting with a specific tool and/or methodology, ... . Stick to no more than five ambitions.

I have always had an intrest in tinkering with simple materials to investigate and evaluate designs. By reading through older master thesises I found that projects related to Shape Morphing Materials always included prototyping movements with simple materials such as paper or cardboard. The tinkering and experimenting with new materials is an important step in the Material Driven Design methods, introduced to me by Sepideh Ghodrat, which I find very interesting because it resonated with my own interest in learning by playing around with the tools.

By looking at emerging materials, I always find it difficult to picture realistic use cases for these materials. however, in previous master thesises, I was inspired by the way they managed to incorporate emerging materials in their desings in a subtle yet effective way. In this project, I wish I can inspire my fellow designers just as my predecesors inspired me.

For my minor, I wanted to follow the Advanced Prototyping minor because it entailed making great designs by exploring and tinkering with different (emerging) materials and production methods. Unfortunately, I was not selected. In this project, I want to experience what I have missed out and get to know more about the possibilities of emerging materials in a hands on way.

Around Christmas 2020, I got a 3D printer for myself. Playing around with the machine, printing presents for my family, I developed an interest in the working behind the printing process. In this assignment, I get to hands on learn more about the technology of 3D printing while trying to adapt the technology to suit the needs for printing the magnetically activated metamaterials, including adding and controlling additional components such as the electro magnet by means of software.

Furthermore, during my studies at IDE I developed an intrest in circular product design and came across the use of Shape Memory Materials for active disassembly of products, to increase retrieval of components for recycling/remanufacturing. However, this application is currently not very present at the IDE faculty. In this graduation project, I want to investigate if magnetic soft materials could be utilized for this purpose and how.

Personal learning goals:

- Hands on experience in scientific research
- Learn scientific discussion and presentation skills
- Improve my prototyping skills
- Learn more about the technology (hardware and software) of 3D (extrusion) printing
- Experience in using new materials using the Material Driven Design methodology

## FINAL COMMENTS

In case your project brief needs final comments, please add any information you think is relevant.

# Appendix B: Literature review extension on active disassembly

The following section is a literature review done on the use of shape memory alloys and polymers for active disassembly: the disassembly of fasteners in (consumer) products by means of a single trigger. In the original project brief, it was established that the use of Magnetic Soft Material would be researched in this specific application field. However, during the project, it was found that the magnetic material had such low load bearing capabilities, it was unlikely the material would be successful in this use case.

In addition, more and more time went into the development of the 4D printer. Ultimately, the idea was abandoned and the section on active disassembly was cut from the literature review because it added little to the overall story, which is already long without this section. Nonetheless, time went into it and I learned a lot about this specific application of shape memory materials. To not let it go to waste, it is included here in the appendix for anyone who is interested in the topic.

B1: Active disassembly

B2: Use of MSM for Active Disassembly

B3: B3. Active Disassembly references

## B1. Active disassembly

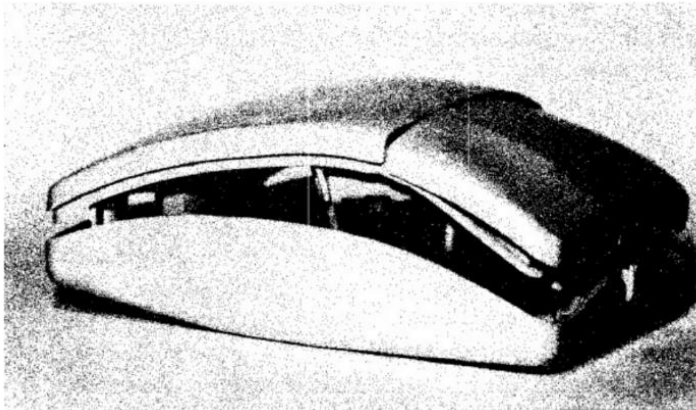
Design for disassembly (DfD) is a term often used in the context of circular economy business models (Bocken et al., 2016). It allows for easy retrieval of product components for repair, remanufacturing or recycling purposes, and thus reducing environmental impact and increase product value at end-of-life (Mule, 2012). In short, DfD means simplifying the de-manufacturing process; reducing disassembly time and making recovery of components and materials possible (Abuzied et al., 2020). One-to-one disassembly, one action to undo one connection, is more time intensive compared to more innovative one-to-many connection techniques, where a single action disassembles a higher number of components (Willems, Dewulf & Duflou, 2004 & 2005; Soh, Ong & Nee, 2014). Generally, designing a one-to-many fastening structure, where multiple fasteners are linked to a single trigger, is time and resource intensive and the number of linked fasteners is limited, depending on the product (Willems, Dewulf & Duflou, 2005). Disassembly embedded design (DED) relies on such one-to-many disassembly methods. Triggers to releasing these fastener structures can include mechanical (Braunschweig, 2004; Figure B.2a), pneumatic (Braunschweig, 2004; Figure B.2b), electrical (Braunschweig, 2004; Figure B.2c; Masui et al., 1999; Figure B.2e), magnetic (Braunschweig, 2004; Figure B.2d) or thermal

(Li et al., 2001; Figure B.2f) triggers (Duflou et al., 2008).

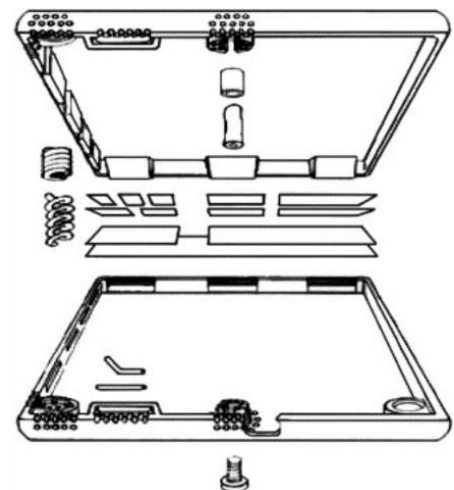
Active disassembly, self-disassembly or automatic product disassembly is the use of shape memory materials for fasteners inside products (Hussein & Harrison, 2004). When activating the shape memory effect, the fasteners open and the product components disconnect. It therefore falls under the one-to-many disassembly method, as one action (e.g. a temperature change) can open multiple shape memory connections and thus disconnect multiple components (Soh, Ong & Nee, 2014).

Chiodo et al. (1998) where one of the first to propose the use of SMMs for the use of disassembling products (Active Disassembly using Smart Materials; ADSM). In their paper, they inserted SMA actuators (NiTi and CuZnAl helical cores and NiTi rods and discs) in a variety of consumer products, like PC keyboard and mouse, cell phones and calculators. The products containing SMA actuators were placed inside a chamber heated to 75 and 115°C. By snap-fit and compression fit expansion using the SMA actuators, they were able to successfully disassemble 17 out of 21 tested products (Figure B.1a). In a follow-up study, they found product design changes would be necessary to successfully incorporate SMA actuators to avoid damage done to the product itself and ensure the actuators can be heated efficiently (Figure B.1b).

a

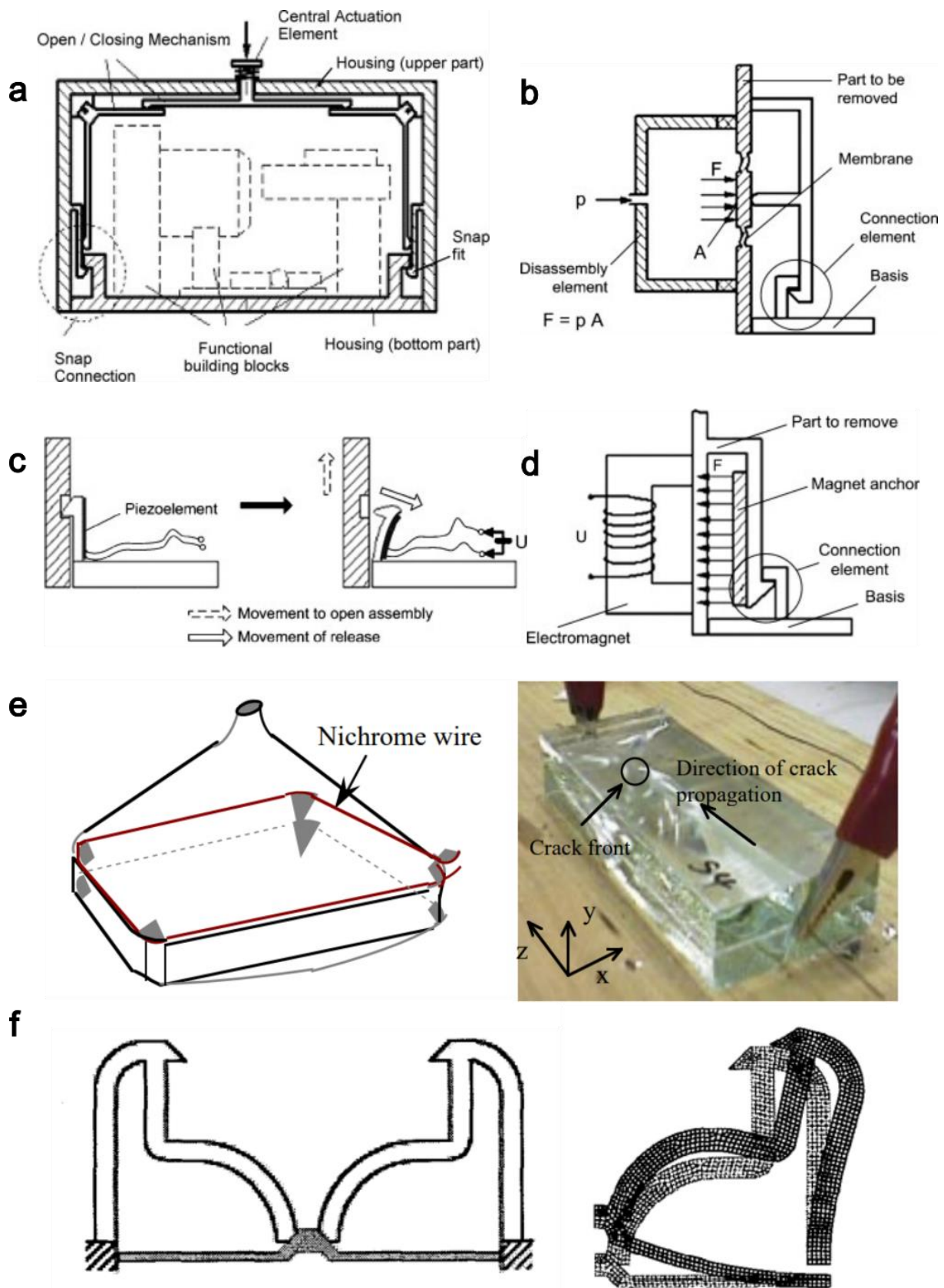


b



*Figure B.1 (a) Chiodo et al. (1998) successfully disassembled this PC mouse using NiTi and CuZnAl SMA actuators. (b) Some product design changes should be made to make ADSM more efficient, such as moving actuators to the edge of the products to more efficiently heat up the SMA actuators (Chiodo et al., 2002).*



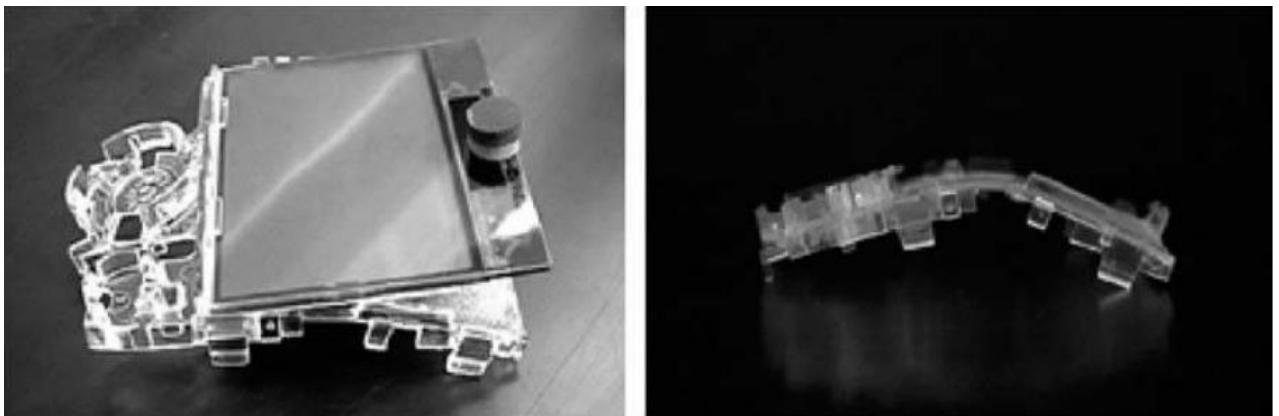


**Figure B.2:** Examples of DED connections. (a) One central trigger opens all snap-fits mechanically connected to it (Braunschweig, 2004). (b) By pressurizing the void inside the disassembly element, the snap-fit is pushed open (Braunschweig, 2004). (c) The piezo element deforms when applying an electrical current and pulls open the snap-fit (Braunschweig, 2004). (d) An electromagnet attracts a magnet attached to the snap-fit in turn opening the snap-fit (Braunschweig, 2004). (e) By heating a Nichrome wire embedded in a CRT television set by means of an electrical current, the glass between the two components is cracked and separates (Masui et al., 1999). (f) Heating a specifically shaped element in a snap-fit design causes it to deform and open due to thermal stresses (Li et al., 2001).

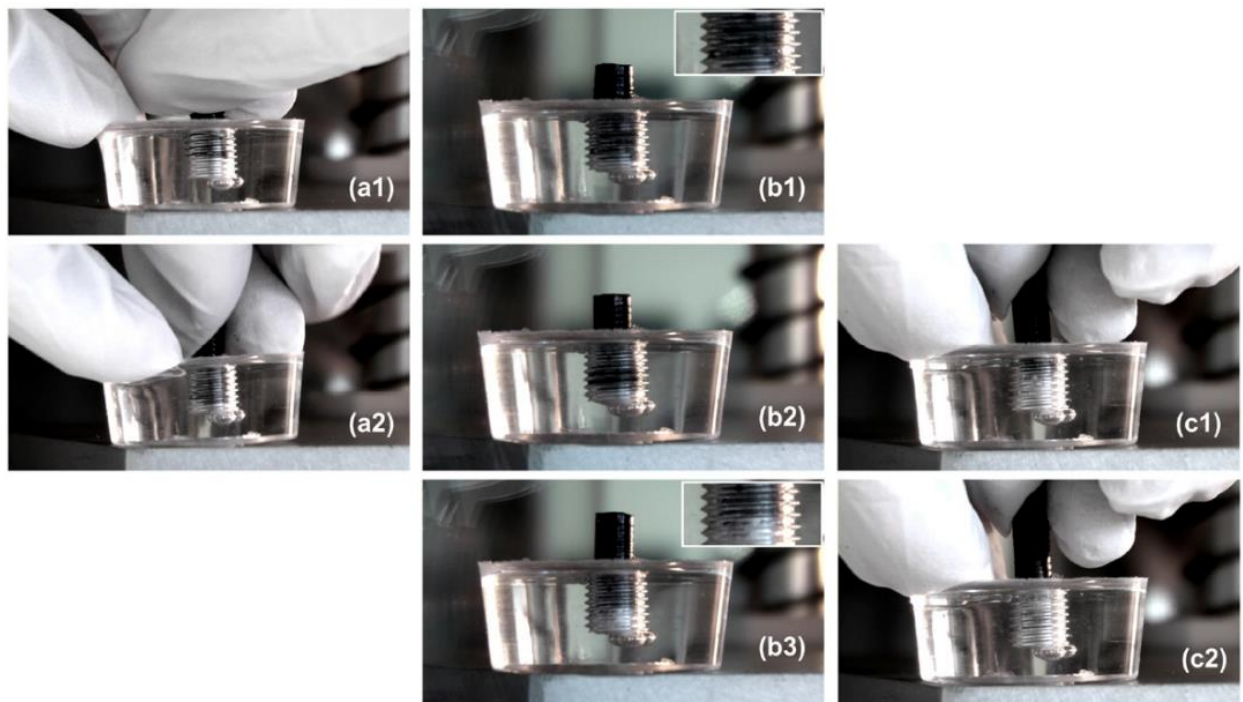
Next to shape memory alloys, Chiodo et al. (2000) explored the use of shape memory polymers in the design active disassembly fasteners. One example is a SMP display bracket that folds open upon heating, releasing the display attached to the bracket with snap fits (Chiodo et al, 2000; Figure B.3). In 1999, they presented thread losing screws for active disassembly of cell phones. The cell phones were assembled with the original screws replaced by SMP screws that loose hold of the threads. Springs were placed inside the products that push the housings open when the screws had lost grip on the threads. Use of these SME-SMP screws resulted in self-dismantling of the phones without damage to the product and with no additional costs, as the

SMPs used had the same costs as generic polymers. The same thread losing screw idea was achieved by Purnawali et al. (2012) by using Poly(methyl methacrylate) (PMMA; Figure B.4).

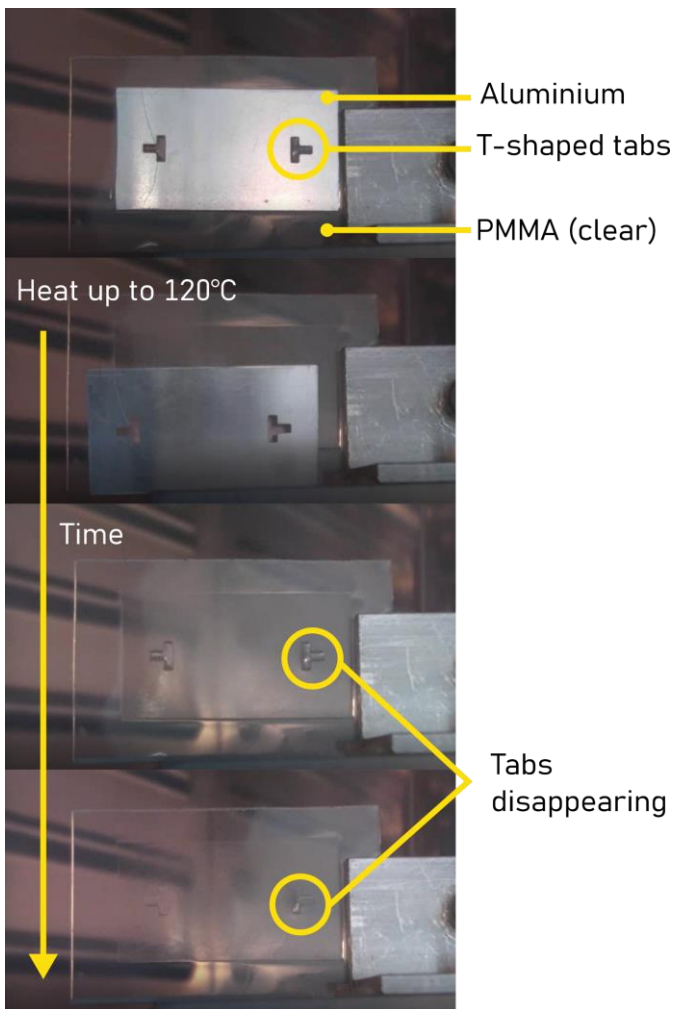
Next to the thread-losing screws, Purnawali et al. (2012) were able to create several other AD actuators out of the PMMA material, such as T and X shapes tabs on which another part can be clamped. Upon heating, the tabs disappear, releasing the attached part (Figure B.5). Several techniques were put together in the design of a box that unfolds when shape recovery is triggered. First, the top components falls off when heating to 110°C. Secondly, after heating to 130°C, the box folds open (Figure B.6).



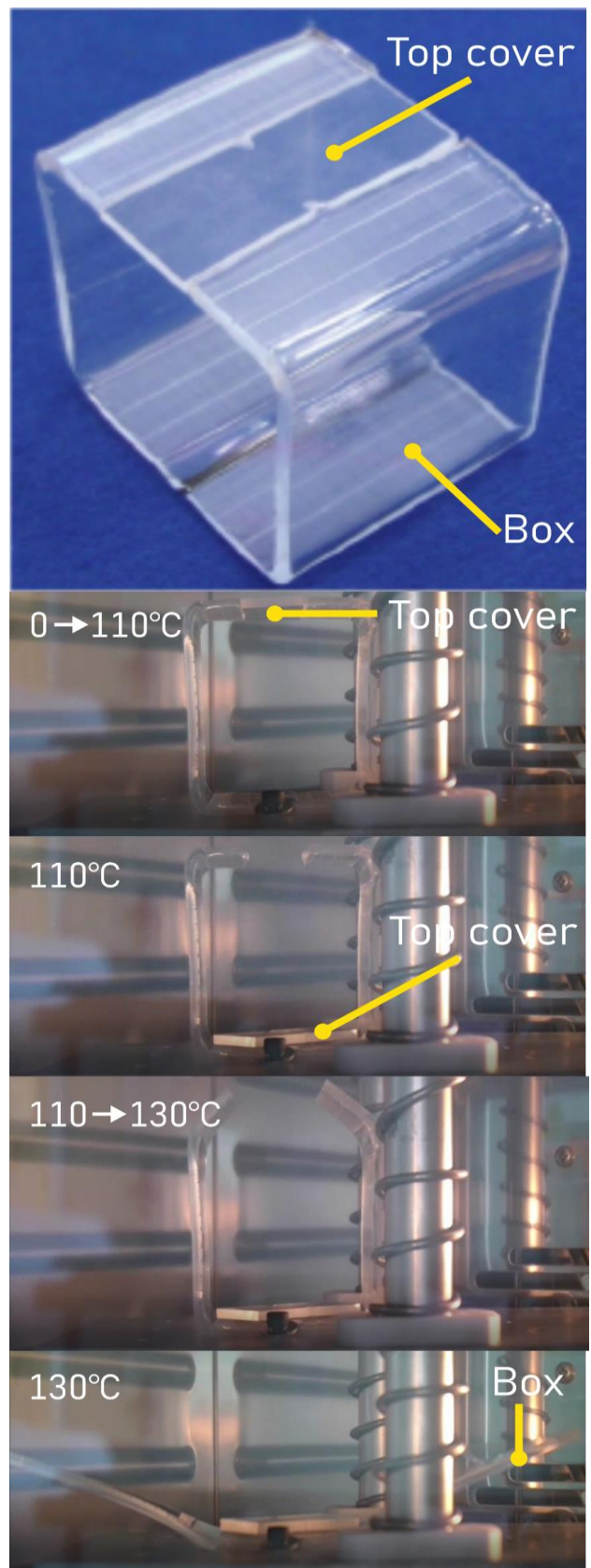
*Figure B.3: SMP display bracket opens when heated, releasing the display (Chiodo et al., 2000).*



*Figure B.4: Demonstration of a PMMA SMP screw that loses its thread after heating. (a) Screw is threaded into a transparent resin. (b) The SMA screw is heated at 130°C for 30 minutes. (c) The screw is pulled out the resin as the threads have disappeared (Purnawali et al., 2012).*



**Figure B.4:** T-shaped tabs holding onto an aluminum plate disappear when heating the PMMA material to trigger shape recovery (Purnawali et al., 2012).



**Figure B.5:** A multi-stage PMMA box unfolds automatically when heated, first releasing the top cover at 110°C and unfolding at 130°C (Purnawali et al, 2012).

Additionally, to the more generic snap fit fasteners made from SMM (Figure B.6; Chiodo & Jones, 2012), more alternative fasteners have been explored, such as the hook-and-loop fastener (commonly known as Velcro) made from SMP by Jones et al. (2003; Figure B.7). The hooks that would tie in with the loops open when heated above the glass temperature ( $T_g$ ), releasing the hoops and opening the fastener automatically.

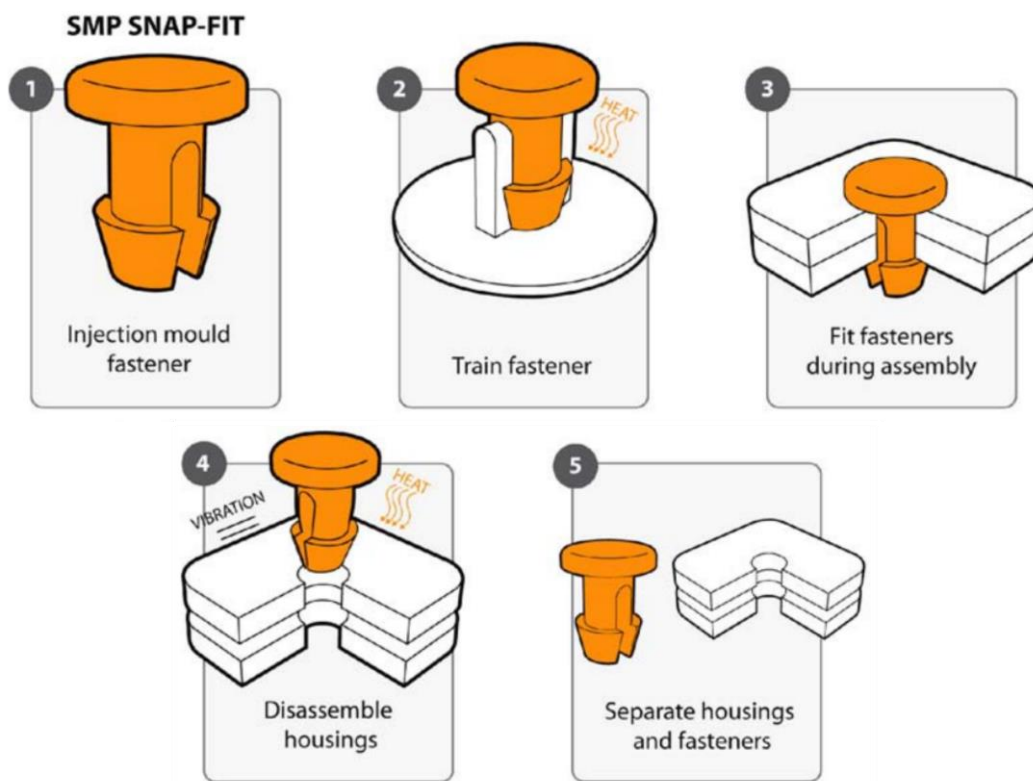


Figure B.6: Design and working of a SMP snap-fit fastener (Chiodo et al., 2012).

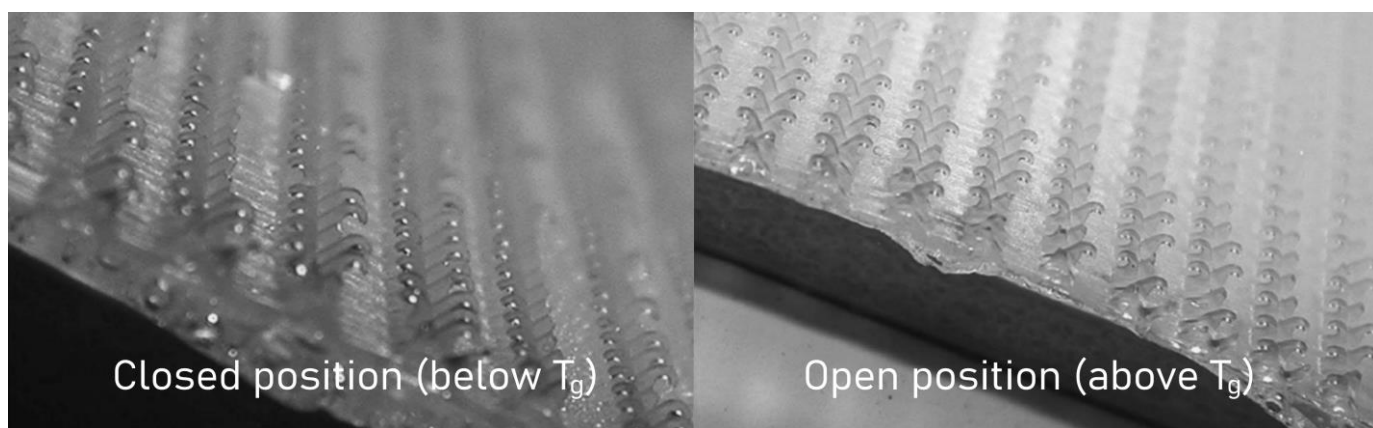
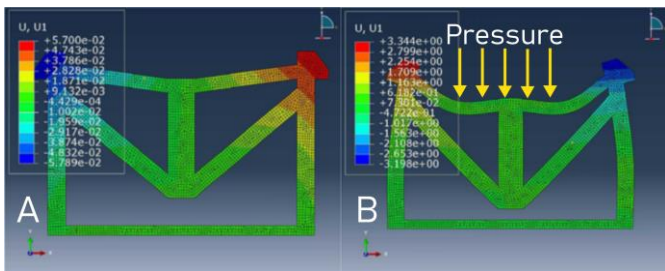


Figure B.7: Hooks made out of a SMP for a hook-and-loop fastener in closed (left) and open (right) position (Jones et al., 2003).

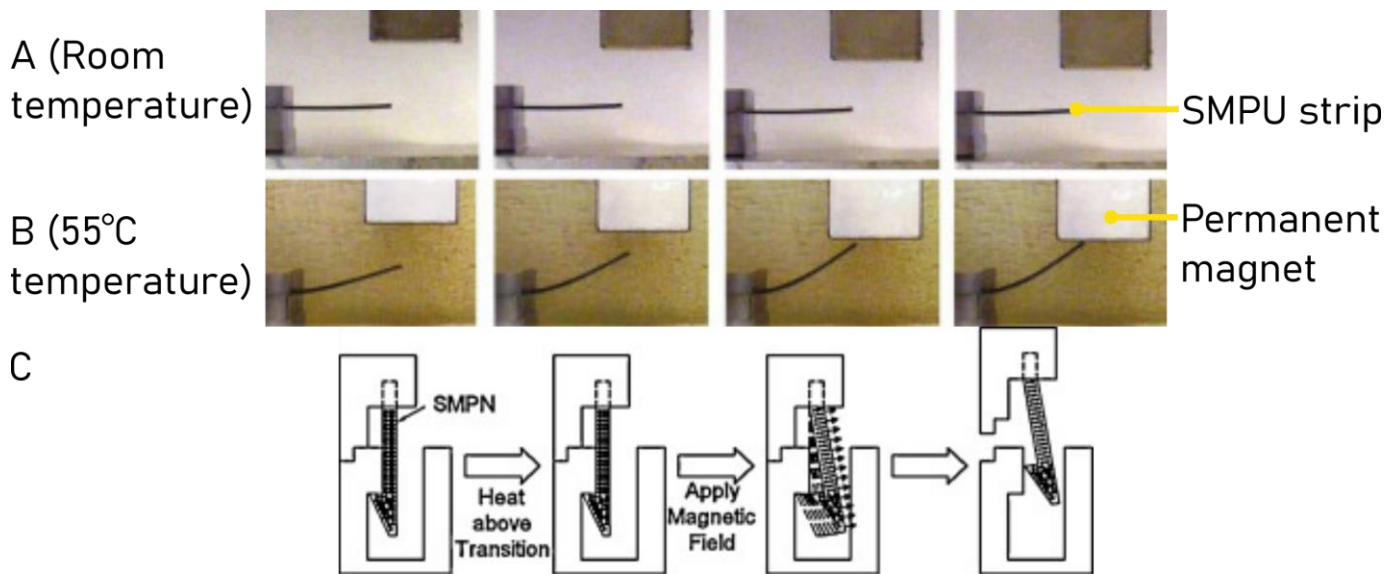
## Unintended triggering

Despite most SMM need a temperature of above 100°C to trigger the shape change, there is a risk of triggering the shape memory effect unintended, which would inconveniently disassemble the product. To combat this issue, several solutions have been proposed where opening SMM fasteners needs multiple stimuli. Liu et al (2013) proposed a solution that involved pressure. A PVC snap fit is heated to 90°C, which causes a slight deformation, but not enough to be able to disassemble the product. Adding a pressure of 0.2 MPa deforms the fastener enough to enable disassembly (Figure B.8).



**Figure B.8:** A PVC snap fit is only able to be opened enough to unfasten the attached component when a pressure is applied during heating (Lui et al., 2013).

Another design to combat accidental triggering of an AD fastener comes from Zhang et al. (2012). They discuss a snap fit fastener out of a shape memory polyurethane with 15 wt% Iron (III) oxide particles embedded. The shape change does not originate from the shape memory effect of the polyurethane, but the use of a magnet to attract the Iron particles inside the polymer. The polymer is heated above  $T_g$  making the material soft and easily bendable. Applying a magnetic field makes the strip move up or down, depending of the direction of the field (Figure B.9). In contrast to the M-SMP made by Ze et al. (2019; Chapter 3.2.2), the material is not heated by induction heating of the iron oxide particles but by elevation ambient temperature. The particles are also not magnetized, meaning they do not have distinct north and south poles, as is the case in the M-SMP presented by Ma et al. (2020; Chapter 3.2.2).



**Figure B.9:** A strip of polyurethane with 15 wt% Iron (III) oxide particles embedded does not morph at room temperature when exposed to a magnetic field (A), but does alter shape when under a magnetic field when temperature is elevated to  $T_g$  because of the attraction of iron particles towards the magnet when stiffness of the material is reduced (B). Below, a schematic design of a AD snap fit application (C).

## Viability of Active Disassembly

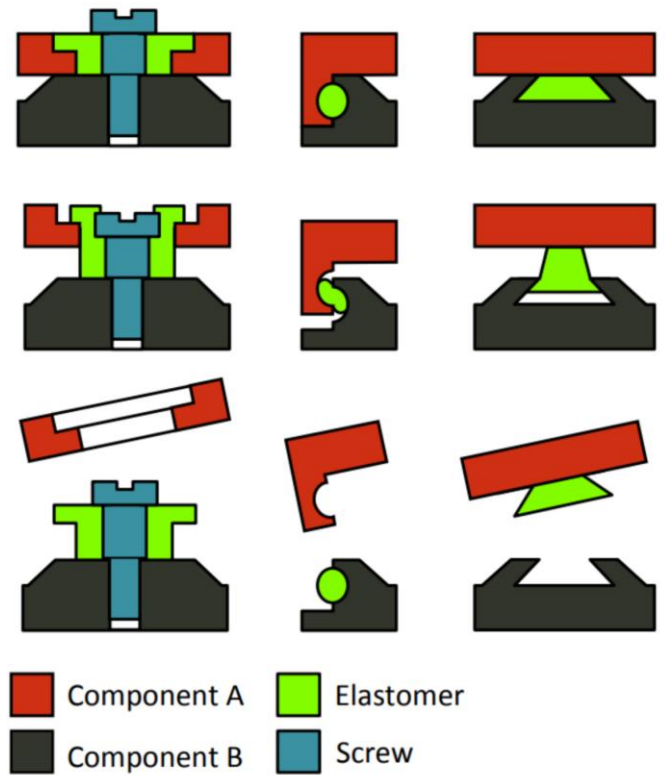
Research done by Ijomah & Chiodo (2010) revealed that disassembling (small) electronic products using AD is economically viable when done in large batches at once, whereas disassembly by hand would require so much time and labor that it makes remanufactured products too expensive to interest consumers.

ADSM seems more beneficial to an over-engineered disassembly system such as in Figure AD1a, as it takes less time, no interference of human handling, less product space and allows using a single technique in various situations (Abduzied et al., 2020). In theory, a single trigger (e.g. heat) can unfasten all connections in the product, no matter how (in)accessible they are. However, SMM actuators can generate only a small disassembly force and large displacement. Abduzied and colleagues are critical about ADSM for larger assemblies that require large disassembly forces.

### Soft material fasteners

Because holding product components together requires some clamping force, soft, elastic materials such as silicones are generally not suitable for making fasteners, as they can be deformed (thus opened) with very small forces, leading to very high risks of the product falling apart during normal use. Literature research into elastomer fasteners thus did not lead to valuable insights. One found example of the use of elastomer fasteners in active disassembly is a proposition by Peeters et al. (2015), in which they presented an elastomer washer in between the bolt and the two product components (Figure B.10). Because the elastomer is deformable, with enough force, the components can be separated without unscrewing the bolt.

In experiments using this principle in TV's, they were able to bring down disassembly times by 70% (Peeters et al., 2015).



**Figure B.10:** Elastomer washer design in between the two product components and the bolt or screw along with two other propositions that were not further elaborated on. Disassembly of the backpanel of a LED TV now takes 70% less time (Peeters et al., 2015).

## B2. Use of MSM for Active Disassembly

The low (clamping) forces MSM are able to apply, pose difficulties when applying this material in Active Disassembly. Materials of which ADSM fasteners are made, need to be able to keep the product together when they are not activated or otherwise need to exceed the (clamping) force non-smart material fasteners are applying to the product in order to loosen these connections to disassemble the product.

What could be a valuable alternative to SMM are M-SMP. These materials are rigid, but heated above their glass temperature they become soft and are able to be actuated, magnetically or non-magnetically by the use of the shape memory effect. These materials can be heated by induction heating of embedded ferromagnetic (e.g., Iron particles), rather than heating up the environment (Ze et al., 2019; Chapter 3.2.2). The use of these kinds of material could be value for use in Active Disassembly, because fasteners made from these materials could be targeted more precisely by applying the induction magnetic field more selectively. Not having to heat up the entire disassembly environment could also save energy, although it needs to be calculated how much energy it takes to heat up a certain space versus how much it would take to generate a strong enough induction magnetic field to heat up the M-SMP material sufficiently. What also needs to be taken into account, is the damage such a field would do to any electrical components in the product.

### B3. Active Disassembly references

- Abuzied, H., Senbel, H., Awad, M. & Abbas, A. (2020). A review of advances in design for disassembly with active disassembly applications. *Engineering Science and Technology, an International Journal*, 23, 618-624. <https://doi.org/10.1016/j.jestch.2019.07.003>
- Bocken, N.M.P., De Pauw, I., Bakker, C. & Van der Grinten, B. (2016) Product design and business model strategies for a circular economy. *Journal of Industrial and Production Engineering*, 33(5), 308-320, <https://doi.org/10.1080/21681015.2016.1172124>
- Braunschweig, A. (2004). Automatic Disassembly of Snap-in Joints in Electromechanical Devices. In *Proceedings of the 4th International Congress Mechanical Engineering Technologies*, page 48-56.
- Chiodo, J.D., Billett, E.H., Harrison D.J. & Harry, P. (1998) Investigations of generic self disassembly using shape memory alloys. In *Proceedings of the 1998 IEEE International Symposium on Electronics and the Environment*, page 82-87 <https://doi.org/10.1109/ISEE.1998.675036>
- Chiodo, J., McLaren, J., Billett, E.H. & Harrison, D. (2000). Isolating LCD's at end-of-life using active disassembly technology: A feasibility study. In *Proceedings of the IEEE International Symposium on Electronics and the Environment*, page 318 - 323. <http://doi.org/10.1109/ISEE.2000.857668>
- Chiodo, J. D., Jones, N., Billett, E. H., & Harrison, D. J. (2002). Shape memory alloy actuators for active disassembly using "smart" materials of consumer electronic products. *Materials & Design*, 23(5), 471-478. [https://doi.org/10.1016/S0261-3069\(02\)00018-3](https://doi.org/10.1016/S0261-3069(02)00018-3)
- Chiodo, J. & Jones, N. (2012). Smart materials use in active disassembly. *Assembly Automation*, 32(1), 8-24. <https://doi.org/10.1108/01445151211198683>
- Duflou, J.R., Seliger, G., Kara, S., Umeda, Y., Ometto, A & Willems, B. (2008). Efficiency and feasibility of product disassembly: A case-based study. *CIRP Annals*, 57(2), 583-600. <https://doi.org/10.1016/j.cirp.2008.09.009>
- Hussein, H. & Harrison, D. (2004). Investigation into the use of engineering polymers as actuators to produce 'automatic disassembly' of electronic products. In T. Bhamra (Ed.) & B. Hon (Ed.), *Design and Manufacture for Sustainable Development* (35-49). Hoboken, United States: John Wiley & Sons.
- Ijomah, W.L. & Chiodo, J.D. (2010). Application of active disassembly to extend profitable remanufacturing in small electrical and electronic products. *International Journal of Sustainable Engineering*, 3(4), 246-257. <https://doi.org/10.1080/19397038.2010.511298>
- Jones, N., Harrison, P.D., Hussein, H., Billet, E. & Chiodo, J. (2003). Towards self-disassembling vehicles. *The Journal of Sustainable Product Design*, 3, 59-74. <https://doi.org/10.1023/B:JSPD.0000035559.65334.d7>
- Li, Y., Saitou, K., Kikuchi, N., Skerlos S.J. & Papalambros, P.Y. (2001). Design of heat-activated reversible integral attachments for product-embedded disassembly. In *Proceedings Second International Symposium on Environmentally Conscious Design and Inverse Manufacturing*, 360-365, <https://doi.org/10.1109/ECODIM.2001.992381>
- Liu, Z., Zhan, Y., Cheng, H., Li, X. & Pan, S. (2013). Design Method of Active Disassembly Structure Triggered by Temperature-Pressure Coupling. *International Journal of Precision Engineering and Manufacturing*, 14(7), 1223-1228. <https://doi.org/10.1007/s12541-013-0166-z>
- Ma, C., Wu, S., Ze, Q., Kuang, X., Zhang, R., Qi, H. J., & Zhao, R. (2020). Magnetic Multimaterial Printing for Multimodal Shape Transformation with Tunable Properties and Shiftable Mechanical Behaviors. *ACS Applied Materials & Interfaces*, 13(11). <https://doi.org/10.1021/acsami.0c13863>



- Masui, K., Mizuhara, K., Ishii, K., & Rose, C. M. (1999). Development of products embedded disassembly process based on end-of-life strategies. In *Proceedings First International Symposium on Environmentally Conscious Design and Inverse Manufacturing*. <https://doi.org/10.1109/ecodim.1999.747676>
- Mule, J.Y. (2012). Design for Disassembly Approaches on Product Development. *International Journal of Scientific & Engineering Research*, 3(6). <https://www.ijser.org/researchpaper/design-for-disassembly-approaches-on-product-development.pdf>
- Peeters, J.F., Vanegas, P., Van den Bossche, W., Devoldere, T., Dewulf, W. & Duflou, J.R. (2015). Elastomer-based fastener development to facilitate rapid disassembly for consumer products. *Journal of Cleaner Production*, 94, 177 – 186. <https://doi.org/10.1016/j.jclepro.2015.01.081>
- Purnawali, H., Xu, W.W., Zhao, Y., Ding, Z., Wang, C.C., Huang, W.M. & Fan, H. (2012). Poly(methyl methacrylate) for active disassembly, *Smart Materials and Structures*, 21(7). <http://doi.org/10.1088/0964-1726/21/7/075006> (also see these movies: <https://iopscience.iop.org/article/10.1088/0964-1726/21/7/075006/data>)
- Soh, S.L., Ong, S.K. & Nee, A.Y.C. (2014). Design for Disassembly for Remanufacturing: Methodology and Technology. In *Proceedings of the 21st CIRP conference on Life Cycle Engineering*, 15, 407-412. <https://doi.org/10.1016/j.procir.2014.06.053>
- Willems B., Dewulf W. & Duflou J. (2004). End-Of-Life Strategy Selection: A Linear Programming Approach to Manage Innovations in Product Design. In *Proceedings of the 11th CIRP LCE International Seminar*, Belgrade, Servië, June 20-22, 35-43.
- Willems, B., Dewulf W. & Duflou, J. (2005). Design for active disassembly (DfAD): an outline for future research. In *Proceedings of the 2005 IEEE International Symposium on Electronics and the Environment*, 129-134. <https://doi.org/10.1109/ISEE.2005.1437007>
- Ze, Q., Kuang, X., Wu, S., Wong, J., Montgomery, S. M., Zhang, R., Kovitz, J.M., Yang, F., Qi, J. & Zhao, R. (2019). Magnetic Shape Memory Polymers with Integrated Multifunctional Shape Manipulation. *Advanced Materials*, 32(4). <https://doi.org/10.1002/adma.201906657>
- Zhang, H.-C., Carrell, J., Wang, S., Tate, T. & Imam, S. (2012). Investigation of a multiple trigger active disassembly element. *CIRP Annals*, 61(1), 27-30. <https://doi.org/10.1016/j.cirp.2012.03.109>

# Appendix C: Experiment documentation



C.1: Magnetic Soft Material Ink Preparation

C.2: 3D printer trials

C.3: Miscellaneous experiments

# C.1: Magnetic Soft Material Ink Preparation

This part holds all attempts in making the magnetic ink, sorted by date

---

## C.1a Ink preparation trial 1

Januari 25 and Februari 4, 2022 - Kevin van der Lans, Israel Carret

### Introduction

This attempt in making the two component magnetic ink for use in direct ink writing in the dual syringe 3D printer prototype was made for the occasion of showing the lab assistant from the materials and chemical lab in the IDE building of TU Delft the procedure in order for him to tailor (safety) instruction for this use case. In addition, the prepared samples were used for instructions in using the rheometer present in the same lab.

The ink is made according to the Experiment 1.2 recipe made by Sanne van Vilsteren (2021), taken from "Magnetizer experiments: try 1" (page 169). In this experiment, she tried the magnetic response of different metal particles embedded in an elastomer (Ecoflex 00-10; Smooth-on, n.d.). This experiment was chosen to pick a recipe from, because it was uncertain how much of which metal particles was left in stock. This experiment held recipes with four different particles, so it was easy to pick one recipe based on the particles that were the most of left in stock on the spot. This turned out to be Iron(II,III) oxide ( $\text{Fe}_3\text{O}_4$ ) particles.

### Materials

2-component ink ingredients:

- 4.2 grams Ecoflex 00-10 Part A
- 4.2 grams Ecoflex 00-10 Part B
- 9.6 grams Iron(II,III) oxide ( $\text{Fe}_3\text{O}_4$ ) powder (<5 micron, 95% purity)
- 0.24 grams fumed silica ( $\text{SiO}_2$ )

Utensils:

- Two paper cups
- Two 10 mm syringes
- Mixing Spatulas
- Analytical scale with precision up to 3 decimals
- Masking tape
- Pen
- Paper towels

For measurements:

- Glass cup
- Mixing spatula
- TA Instruments AR-G2 Rheometer
- ARG2 control program
- Isotropic alcohol
- Paper towels

### Method

The Ecoflex elastomer used consists of two components (A and B) that remain fluid on themselves, but start to cure once they are mixed together. The ink was made separately to make sure it does not cure while it is stored so it can be analyzed and used for direct ink writing later. The rheometer measurements were done to measure the viscosity of the ink and top measure the shear-thinning properties of the ink caused by the fumed silica.

### *Ink preparation*

The procedure to make the ink is as follows:

## Part A

- Turn on the scale and tare it without anything on it.
- Place one of the cups on the scale. Read its mass from the scale.
- Poor 4.2 grams of Ecoflex Part A in the cup on the scale with a spatula. This mass needs to be added to the mass of the cup on the scale. E.g., when the cup measures 4 grams, the cup needs to be filled with Ecoflex Part A until the scale reads 8.2 grams. Alternatively, the scale can be tared between each step.
- Poor half the amount of Iron(II,III) oxide powder ( $9.6/2=4.8$  grams) in the cup with the Ecoflex Part A using a spatula. Again, add this mass to the mass that is already on the scale or tare the scale in between steps.
- Take the cup from the scale and mix the Iron(II,III) oxide and Ecoflex Part A together manually using a spatula.
- Place the cup back on the scale and add half the amount of fumed silica ( $0.24/2=0.12$  grams) to the Ecoflex Part A/ Iron(II,III) oxide mixture.
- Mix again my hand.

## Part B

- Take everything off the scale and tare if necessary without anything on it.
- Place the other cup on the scale. Read its mass from the scale.
- Poor 4.2 grams of Ecoflex Part B in the cup on the scale with a spatula. This mass needs to be added to the mass of the cup on the scale. Alternatively, the scale can be tared between each step.
- Poor half the amount of Iron(II,III) oxide powder ( $9.6/2=4.8$  grams) in the cup with the Ecoflex Part B using a spatula. Again, add this mass to the mass that is already on the scale or tare the scale in between steps.
- Take the cup from the scale and mix the Iron(II,III) oxide and Ecoflex Part B together manually using a spatula.
- Place the cup back on the scale and add half the amount of fumed silica ( $0.24/2=0.12$  grams) to the Ecoflex Part B/Iron(II,III) oxide mixture.
- Mix again my hand.

Part A and B is put each in a separate 10mm syringe using a spatula. Each syringe is labeled with the part it contains using masking tape and a pen. Residue is cleaned off with paper towels.

### *Rheometer measurements*

For measuring the rheometric properties of the magnetic ink, a TA Instruments AR-G2 Magnetic Bearing Rheometer was used. The following geometry was used:

- 40-mm-diameter steel plate geometry.
- Gap of 500 micron (0,5 mm)
- Material: Stainless steal
- Environmental system: Peltier plate
- Surface finish: Standard

The procedure was a steady-state flow sweep using the following settings:

- Environmental control:  
Temperature of 25°C, Soak time of 60 seconds
- Test parameters:  
Logarithmic sweep  
Shear rate between 0.01 1/s to 100 1/s  
Points per decade: 3  
Equilibration time 5.0 s  
Averaging time 30.0 s

The samples were put in the middle of the peltier plate by extruding them from the syringes in which they were stored. The peltier plate and the 40mm diameter steel plate were cleaned after each test using isotropic alcohol and paper towels. Part B was measured first, then Part A and lastly a mixture of parts A and B. To measure the mixture of Part A and B, these were first mixed in a glass cup using a spatula after a small amount of part A and B was extruded into the cup out of the syringes. The mixture was then placed on the peltier plate with a spatula directly after mixing to minimize the effects of curing of the elastomer, which should take 4 hours. Results were copy-pasted into an excel file.

## Results

Figure 1 shows the results from measuring the rheometric properties of the prepared ink.

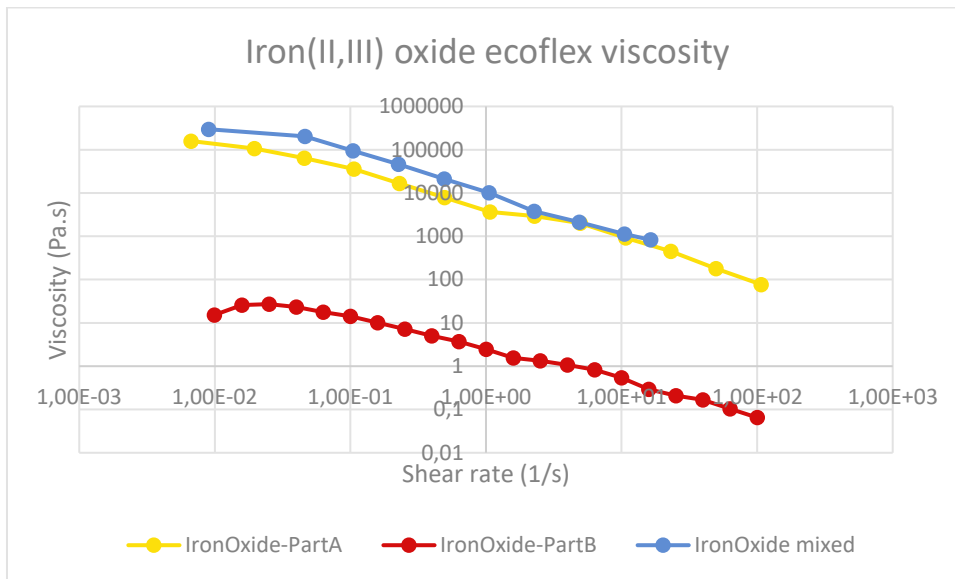


Figure 1: Measured rheometric properties of the prepared Iron(II,III) oxide magnetic ink, part A and B separately and mixed.

## Conclusion

Out of the measurements can be concluded that Part A is much more viscose than Part B and that both Part A and B show shear thinning properties. The mixed ink is the highest in viscosity of the three variants but also the most difficult to measure.

## Discussion

Part B was tested first, using the described parameters without any issues. Part A however was much more viscose than part B, therefor the steel plate could not be brought further down than 532 microns. In addition, the machine started to make strange hissing noises.

In the middle testing the part A and B mixture, the machine again started making hissing noises. The control program gave the error "Magnetic Bearing unstable". Retrieving the sample was difficult as the 40mm steel plate seemed stuck on the peltier plate. In an attempt to make the ink less viscose, the temperature of the machine was increased to 40°C, to no effect. The peltier plate was removed together with the 40mm steel plate. Eventually, the steel plate could be removed, which revealed the elastomer had cured and a disk had formed, making further measurements impossible, see Figure 2).



Figure 2: cured elastomer disk.

To find the elastomer cured was very odd, given the fact that it should take the Ecoflex mixture 4 hours to cure and the sample has not been mixed for longer than 30 minutes after retrieving it. probably, we speed up the curing process by increasing the temperature in an attempt to lower the viscosity in order to raise the 40mm plate. Other contributions to the faster curing could be that the samples were stored for about 10 days after preparation. Maybe this started some degradation in the separate parts that speed up curing after mixing. Also, the Ecoflex used was about one year old, while it has limited shelf life (although no expiration date was given). The results, however could not be compared to earlier measurements done by Sanne, as this specific sample was not examined on rheometric properties and only used for magnetization tests.

#### Further research

In a follow up ink preparation trial, a recipe will be picked that is measured on rheometric properties to be able to compare the results and see if I am able to reproduce the results from Sanne's thesis. For this, ink T7E1 will be used containing:

- 12,6 g Ecoflex 00-10 part B
- 2 x 22,5 g Iron powder (carbonyl iron: 12)
- 12,6 g Ecoflex 00-10 part A
- 2x 0,30 g fumed silica

This is because it is measured extensively (part A, B and Mixed) and is the ink that was successfully extruded with the 3D printer set-up, so this sample can be used in an attempt to recreate this experiment.

## References

Smooth-on. (n.d.). *Ecoflex 00-10*. Retrieved on Januari 7, 2021, from: <https://www.smooth-on.com/products/ecoflex-00-10/>

Van Vilsteren, S. (2021). Designing Magnetic Soft Materials for 4D Printing [Master Thesis, Delft University of Technology]. Tu Delft Educational Repository. <http://resolver.tudelft.nl/uuid:7e05bd4c-4720-4e1f-b13b-7b048602ce42>



## C.1b Ink preparation trial 2

Februari 9, 2022 - Kevin van der Lans, Israel Carret

### Introduction

The last ink that was used by Sanne in the 3D printer was the ink with the code Fe31,25%SiO-nM, which means ink with Iron particles, 31,25% fumed silica of the MiT recipe (Kim et al., 2018), not magnetized (Van Vilsteren, 2021). This ink was used to test the extrusion of the 3D printer. The ink did extrude, but there was quite a delay. To troubleshoot the printer, this ink has to be remade to see if the printer behaves the same and to find out where the problem is with. In this experiment, it is attempted to remake this recipe and test its properties so see if the results are the same as this "T7E1" ink by Sanne.

### Materials

2-component ink ingredients:

- 12.6 grams Ecoflex 00-10 Part A
- 12.6 grams Ecoflex 00-10 Part B
- 2x 22.5 grams Iron powder (<10 microns, 99,5% purity)  
<https://www.fishersci.nl/shop/products/iron-powder-spherical-10-micron-99-9-metals-basis-99-5-thermo-scientific/11360689>
- 2x 0.30 grams fumed silica (SiO<sub>2</sub>)

Utensils:

- Two paper cups
- Two 10 ml syringes
- Mixing Spatulas
- Analytical scale with precision up to 3 decimals
- Masking tape
- Pen
- Paper towels

For measurements:

- Glass cup
- Mixing spatula
- TA Instruments AR-G2 Rheometer
- ARG2 control program
- Isotropic alcohol
- Paper towels

For force extrusion test:

- static mixing nozzle for force measurements
- Two 10ml syringes
- Scale up to 24kg

### Method

The Ecoflex elastomer used consists of two components (A and B) that remain fluid on themselves, but start to cure once they are mixed together. The ink was made separately to make sure it does not cure while it is stored so it can be analyzed and used for direct ink writing later. The rheometer measurements were done to measure the viscosity of the ink and to measure the shear-thinning properties of the ink caused by the fumed silica. Also, the amount of force it takes to extrude through a static mixing nozzle was tested.

### *Ink preparation*

The procedure to make the ink is as follows:

#### Part A

- Turn on the scale and tare it without anything on it.
- Place one of the cups on the scale. The measured mass was 4.318 g.
- Poor 12.6 grams of Ecoflex Part A in the cup on the scale with a spatula. The total mass was at this point 16.923 g.
- Poor half the amount of Iron powder (22.5 g) in the cup with the Ecoflex Part A using a spatula. The total mass at this point was 39,440 g
- Take the cup from the scale and mix the Iron and Ecoflex Part A together manually using a spatula.
- Place the cup back on the scale. The measured mass was now 39,238 g.
- Add half the amount of fumed silica (0.30 g) to the Ecoflex Part A/ Iron powder mixture. The total mass now was 39,538 g.
- Mix again my hand.

#### Part B

- Take everything off the scale and tare if necessary without anything on it.
- Place one of the cups on the scale. The measured mass was 4.348 g.
- Poor 12.6 grams of Ecoflex Part B in the cup on the scale with a spatula. The total mass was at this point 16.957 g.
- Poor half the amount of Iron powder (22.5 g) in the cup with the Ecoflex Part B using a spatula. The total mass at this point was 39,469 g
- Take the cup from the scale and mix the Iron and Ecoflex Part B together manually using a spatula.
- Place the cup back on the scale. The measured mass was now 39,162 g.
- Add half the amount of fumed silica (0.30 g) to the Ecoflex Part B/ Iron powder mixture. The total mass now was 39,363 g
- Mix again my hand.

Part A and B is put each in a separate 10mm syringe using a spatula. Each syringe is labeled with the part it contains using masking tape and a pen. Residue is cleaned off with paper towels. Some part A and B mixture was left in the cups for rheometer measurements.

### *Rheometer measurements*

For measuring the rheometric properties of the magnetic ink, a TA Instruments AR-G2 Magnetic Bearing Rheometer was used. The following geometry was used:

- 40-mm-diameter steel plate geometry.
- Gap of 500 micron (0,5 mm)
- Material: Stainless steel
- Environmental system: Peltier plate
- Surface finish: Standard

The procedure was a steady-state flow sweep using the following settings:

- Environmental control:  
Temperature of 25°C, Soak time of 60 seconds
- Test parameters:  
Logarithmic sweep  
Shear rate between 0.01 1/s to 100 1/s  
Points per decade: 3  
Equilibration time 5.0 s  
Averaging time 30.0 s

The left over samples from the cups were put in the middle of the peltier plate by means of two steel spatulas. The peltier plate and the 40mm diameter steel plate were cleaned after each test using isopropanol and paper towels. Part A was measured first, then Part B and lastly a mixture of parts A and B. To measure the mixture of Part A and B, these were extruded through a static mixing nozzle directly onto the peltier plate, to minimize the effects of curing of the elastomer, which should take 4 hours. Results were copy-pasted into an excel file from the AR-G2 control software.

*Extrusion force*

To measure the amount of force it would take to extrude the two-component ink through the static mixing nozzle was measured by putting the two syringes, attached to the “static mixing nozzle for force measurements” on a scale with the nozzle facing upwards. The syringes were then pushed down while a second person films the display to see the measured weight when ink comes out of the nozzle (Figure 1).

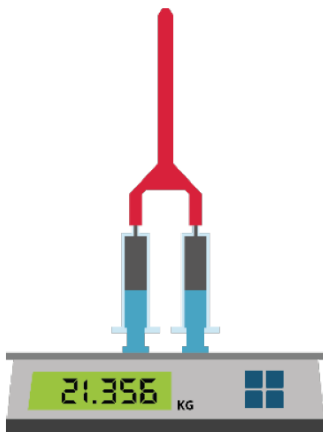
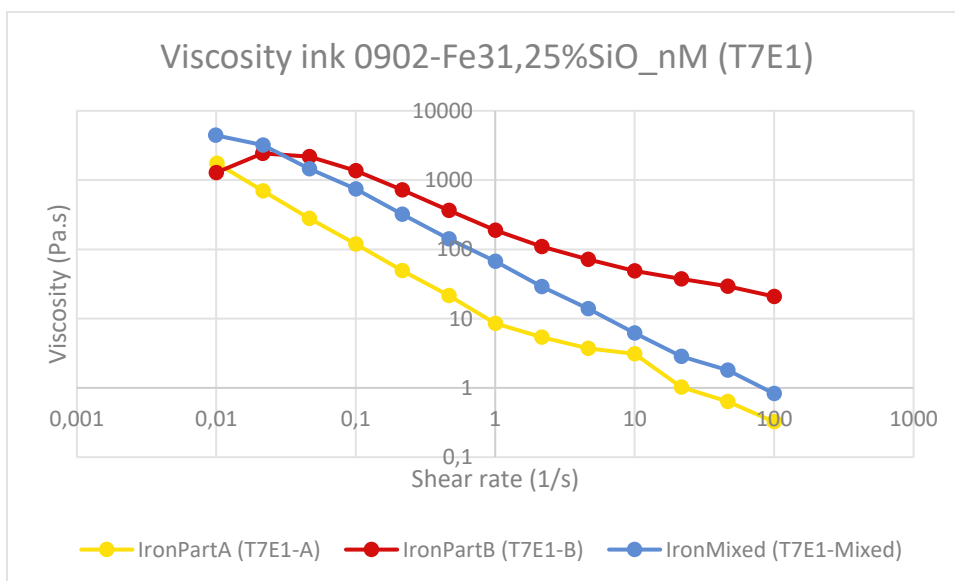


Figure 1: Force measurement set-up (Van Vilsteren, 2021)

Results

Out of the force extrusion force measurements came a maximum force of 18,550 kg, which translates to  $(18,550 \cdot 10) / 2 = 92,75$  N per syringe. This is lower than the 116,96 N measured by Sanne.

The Rheometer measurements gave the following results (Figure 2):



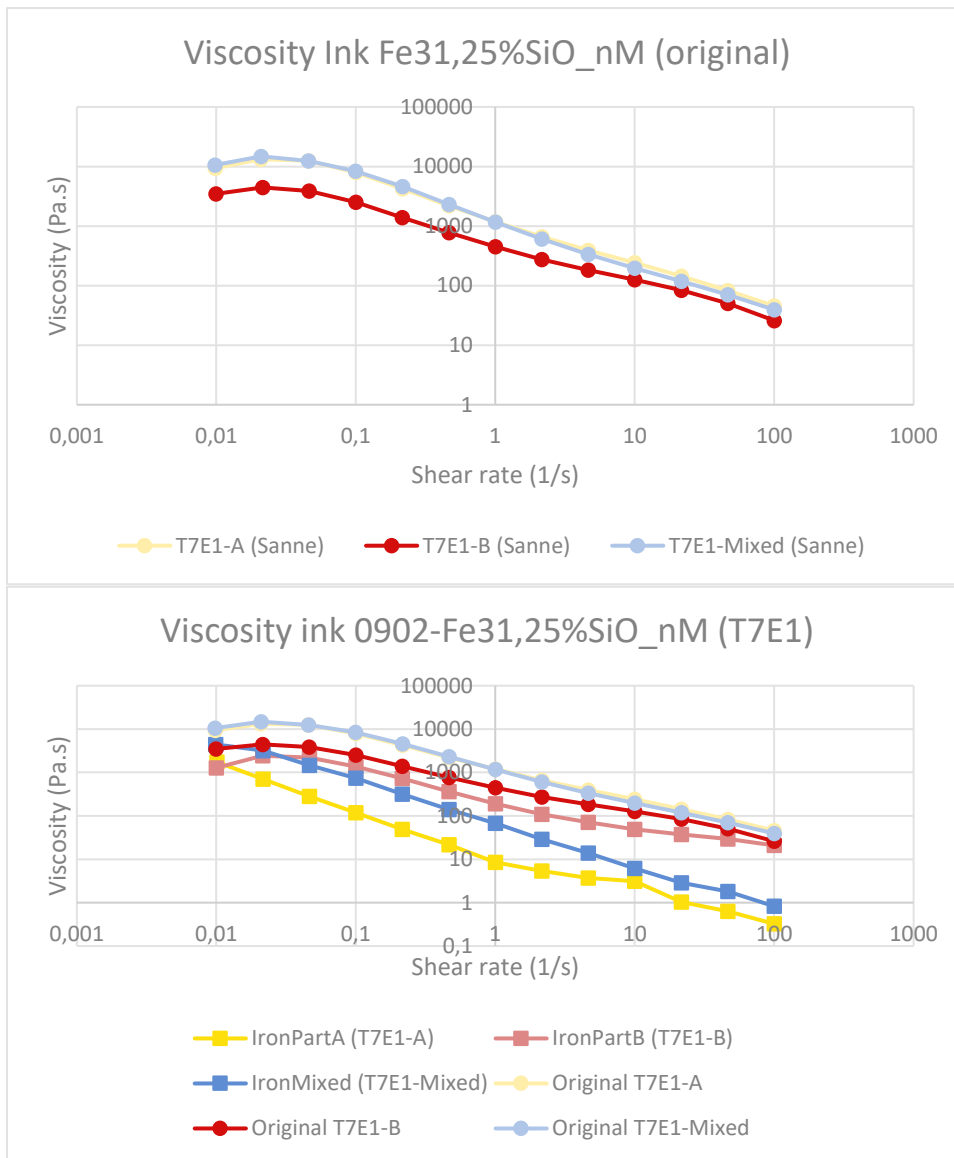


Figure 2: Rheometer results of the prepared ink (above), rheometer results from original ink by Sanne (middle) and both results compared (bottom).

The graphs show that both Part A and Part B poses shear-thinning properties. However, Part A shows a lower viscosity overall, which should not be the case as Ecoflex part A should be the most viscos one and also felt like it was more viscose. The starting point (shear rate = 0.01) does show a slightly higher viscosity than part B (1741.05 Pa.s for Part A vs 1276.13 Pa.s for Part B). Part B is close to the original result by Sanne, but a bit lower.

### Conclusion

The ink made in this experiment did not show the same properties as ink T7E1 from Sanne's thesis (Van Vilsteren, 2021). Part A had a lower overall viscosity than Part B wich should not be the case. The shape of the graphs for Part A and Mixed did also not resample the shape from Sanne's experiment. In this experiment, it dived almost linearly under a viscosity of 1 Pa.s, while it should go up a bit before starting a slow decent. Part B, however, did show the expected behaviour and was close to Sanne's results. It can be concluded that there is something gone wrong in this experiment and that the prepared ink is not similar enough to Sanne's results.

## Discussion

The ink prepared in this experiment did not show the expected properties. Possible causes of this could be:

### *Age of Eco-flex silicone*

The silicone used was about one year old at this point, The packaging states a limited shelf life, although no expiration date was given.

### *Error in rheometer measurements*

It is possible an error was made during the rheometric measurements of the ink. Part B at least shows the expected behaviour, although not the expected values. However, Part A was measured first, then Part B and lastly a mixture. This would mean that the first measurement went wrong, the second measurement went well, and the third one went wrong again. In all three measurements, the exact same settings were used, so it is unclear what would have to gone wrong.

### *Difference in particles*

The particles used in this experiment were slightly different than the ones used in the original recipe. In the original recipe, Carbonyl Iron was used with a particle size of 5-9 micron (<https://www.sigmaaldrich.com/NL/en/product/aldrich/44890>). In this experiment, Iron particles were used with a particle size of <10 micron (<https://www.fishersci.nl/shop/products/iron-powder-spherical-10-micron-99-9-metals-basis-99-5-thermo-scientific/11360689>). This can mean many sizes, from 1 to 9.9 micron, but is close to the original value.

The specified density of both powders is slightly different, but very similar. The original powder had a density of 7.86g/cm<sup>3</sup> at 25°C. The particles used in this experiment had a density of 7.87g/cm<sup>3</sup> at a temperature of 20°C. It is uncertain if this is a large enough difference to account for the strange measurements.

It is uncertain what the difference is between Carbonyl Iron and Iron particles, as the molecular formula specified is the same (Fe) as well as the CAS-number (7439-89-6) and molecular density (55.85 g/mol).

### *Error in making recipe*

It was attempted to recreate all the steps specified in Sanne's recipe as close as possible. However, it cannot be dismissed that there is a change that still an error was made in preparing the ink.

## Further research

Despite the errors in the ink measurements, I still continue testing this ink in the 3D printer. It is expected that this ink will extrude easier because the viscosity seems lower than the original recipe. In addition, the rheometer experiments need to be redone with the same samples to see if I get the same results or that indeed something went wrong with the measurements. Another possible next step is to remake the ink under the supervision of an experienced person to see if something goes wrong in preparation of the ink. Lastly, more (desk)research can be done to find out more about the difference between Carbonyl Iron and regular Iron.

## References

Van Vilsteren, S. (2021). Designing Magnetic Soft Materials for 4D Printing [Master Thesis, Delft University of Technology]. Tu Delft Educational Repository.  
<http://resolver.tudelft.nl/uuid:7e05bd4c-4720-4e1f-b13b-7b048602ce42>

## C.1c Ink preparation trial 3

February 15, 2022 – Kevin van der Lans

### Introduction

In the last ink preparation test, the rheometer results did not match the expected results measured by Sanne (Van Vilsteren, 2021). Therefore, this test has two purposes:

- 1) Redo rheometer measurements to see if the measurements done last time were faulty
- 2) Remake the T7E1 ink made February 9 with the new silicone to see if degradation of silicone is the cause of the weird measurements

### Materials

2-component ink ingredients:

- 12.6 grams Ecoflex 00-10 Part A
- 12.6 grams Ecoflex 00-10 Part B
- 2x 22.5 grams Iron powder (<10 microns, 99,5% purity)  
<https://www.fishersci.nl/shop/products/iron-powder-spherical-10-micron-99-9-metals-basis-99-5-thermo-scientific/11360689>
- 2x 0.30 grams fumed silica (SiO<sub>2</sub>)

Utensils:

- Two paper cups
- Two 10 ml syringes
- Mixing Spatulas
- Analytical scale with precision up to 3 decimals
- Masking tape
- Pen
- Paper towels

For measurements:

- Mixing spatulas
- TA Instruments AR-G2 Rheometer
- ARG2 control program
- Isotropic alcohol
- Paper towels

For force extrusion test:

- static mixing nozzle for force measurements
- Two 10ml syringes
- Scale up to 24kg

### Method

The ink was made separately (Part A and B) to make sure it does not cure while it is stored so it can be analyzed and used for direct ink writing later. The rheometer measurements were done to measure the viscosity of the ink and to measure the shear-thinning properties of the ink caused by the fumed silica. Also, the amount of force it takes to extrude through a static mixing nozzle was tested.

### *Ink preparation*

For the re-measuring of the ink made on February 9, left-overs were used from that date that were still in the syringes. In addition, new ink was made with newly arrived silicone, for which the procedure was as follows:

## Part A

- Turn on the scale and tare it without anything on it.
- Place one of the cups on the scale. The measured mass was 4.4068 g.
- Poor 12.6 grams of Ecoflex Part A in the cup on the scale with a spatula. The total mass was at this point 17.0034 g.
- Poor half the amount of Iron powder (22.5 g) in the cup with the Ecoflex Part A using a spatula. The total mass at this point was 39,5946 g
- Take the cup from the scale and mix the Iron and Ecoflex Part A together manually using a spatula.
- Place the cup back on the scale. The measured mass was now 39,4747 g.
- Add half the amount of fumed silica (0.30 g) to the Ecoflex Part A/ Iron powder mixture. The total mass now was 39,7720 g.
- Mix again my hand.

## Part B

- Take everything off the scale and tare if necessary without anything on it.
- Place one of the cups on the scale. The measured mass was 4.3589 g.
- Poor 12.6 grams of Ecoflex Part B in the cup on the scale with a spatula. The total mass was at this point 16.9551 g.
- Poor half the amount of Iron powder (22.5 g) in the cup with the Ecoflex Part B using a spatula. The total mass at this point was 39.4614 g
- Take the cup from the scale and mix the Iron and Ecoflex Part B together manually using a spatula.
- Place the cup back on the scale. The measured mass was now 39.3082 g.
- Add half the amount of fumed silica (0.30 g) to the Ecoflex Part B/ Iron powder mixture. The total mass now was 39.6076g
- Mix again my hand.

Part A and B is put each in a separate 10mm syringe using a spatula. Each syringe is labeled with the part it contains using masking tape and a pen. Residue is cleaned off with paper towels. Some part A and B mixture was left in the cups for rheometer measurements.

### *Rheometer measurements*

For measuring the rheometric properties of the magnetic ink, a TA Instruments AR-G2 Magnetic Bearing Rheometer was used. The following geometry was used:

- 40-mm-diameter steel plate geometry.
- Gap of 500 micron (0,5 mm)
- Material: Stainless steal
- Environmental system: Peltier plate
- Surface finish: Standard

The procedure was a steady-state flow sweep using the following settings:

- Environmental control:  
Temperature of 25°C, Soak time of 30 seconds  
Not wait for temperature
- Test parameters:  
Logarithmic sweep  
Shear rate between 0.01 1/s to 100 1/s  
Points per decade: 3  
Equilibration time 5.0 s  
Averaging time 30.0 s

The left over samples from the cups were put in the middle of the peltier plate by means of two steel spatulas. The peltier plate and the 40mm diameter steel plate were cleaned after each test using isopropanol and paper towels. Part A was measured first, then Part B and lastly a mixture of parts A and B.

The mixture of Part A and B, these were extruded through a static mixing nozzle directly onto the peltier plate, to minimize the effects of curing of the elastomer, which should take 4 hours.

The Part A and B measurements were done 3 times, from which the mean and standard deviation can be calculated. The Mixed ink was measured 2 times, because I was afraid the curing inside the static mixing nozzle would influence the results too much and because I wanted to make sure I had enough ink to test with the stiffer tubes.

Results were copy-pasted into an excel file from the AR-G2 control software.

#### *Extrusion force*

To measure the amount of force it would take to extrude the two-component ink through the static mixing nozzle was measured by putting the two syringes, attached to the “static mixing nozzle for force measurements” on a scale with the nozzle facing upwards. The syringes were then pushed down while a second person films the display to see the measured weight when ink comes out of the nozzle (Figure 1).

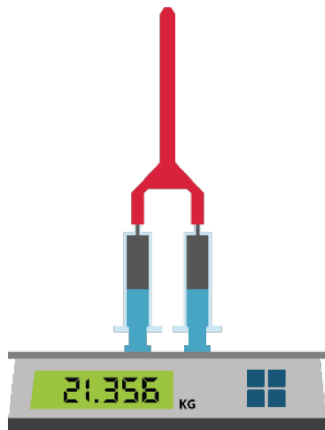


Figure 1: Force measurement set-up (Van Vilsteren, 2021)

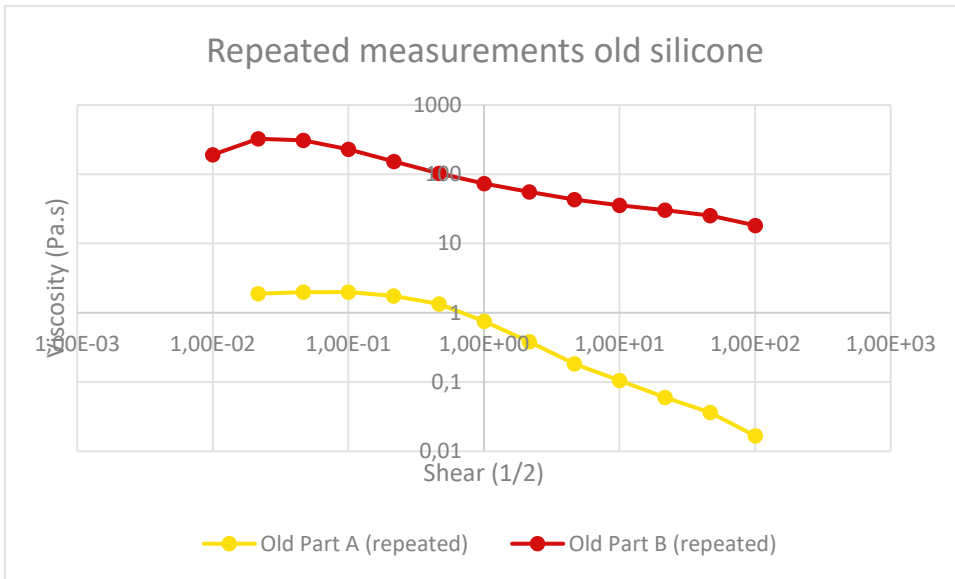
#### Results

The following section holds the results from the rheometric measurements of the old silicone and the new silicone. The measurements are compared, also to the original values of the T7E1 ink by Sanne (Van Vilsteren, 2021).

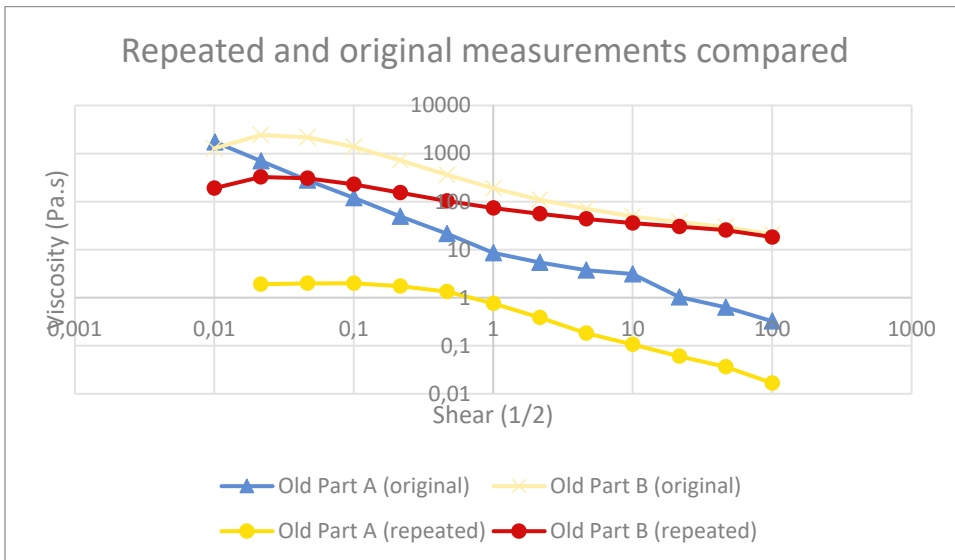
#### *Repeated rheometric measurements old silicone*

The next graph shows the results of the repeated measurements from the left over samples of the old silicone. These measurements were only done once, because there was not enough ink left for multiple measurements.





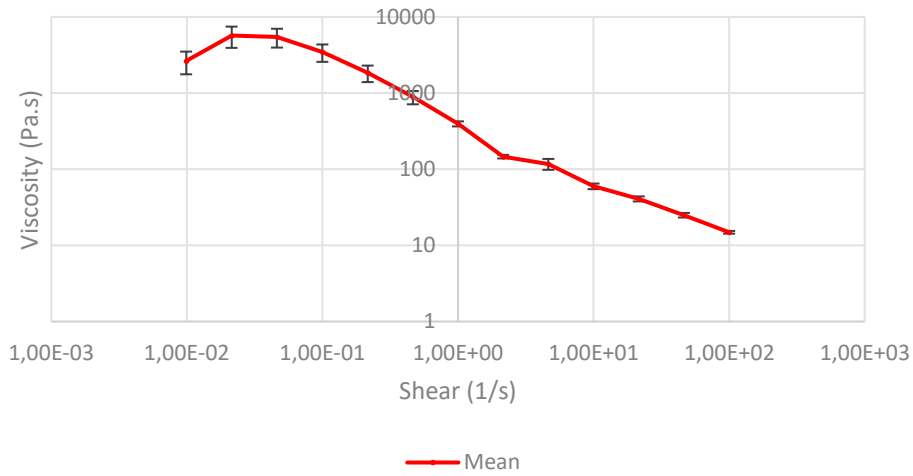
Compared to the original measurements, the inks show the same, weird unexpected behaviour, but the overall viscosity has decreased even more.



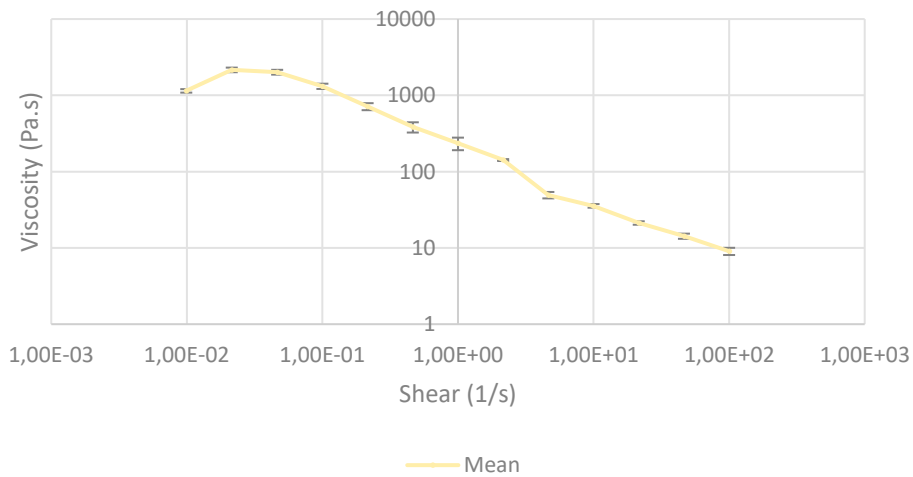
*Rheometric measurements new silicone*

The rheometric measurements of the new ink made with the new silicone gave the following results:

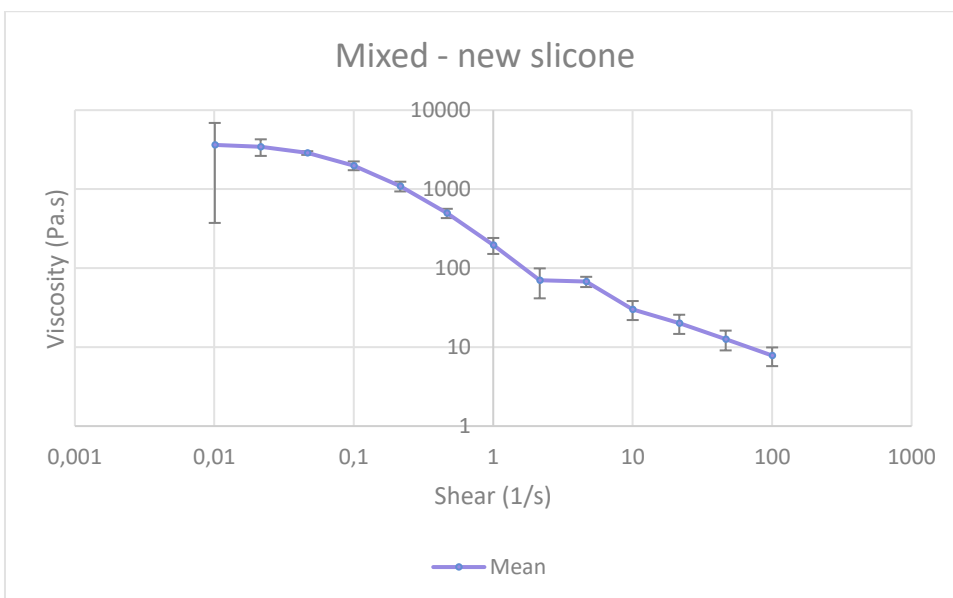
### Part A- new silicone

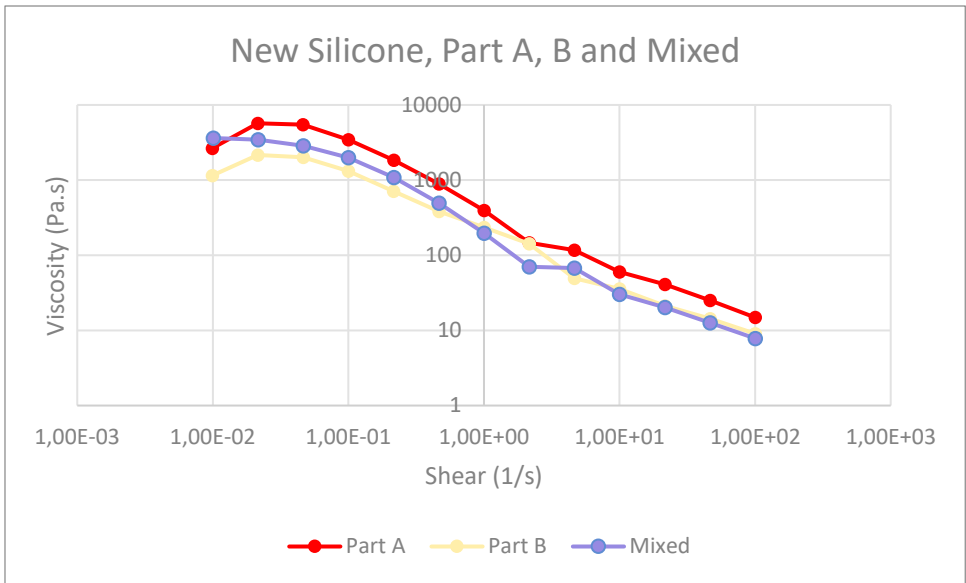


### Part B - new silicone

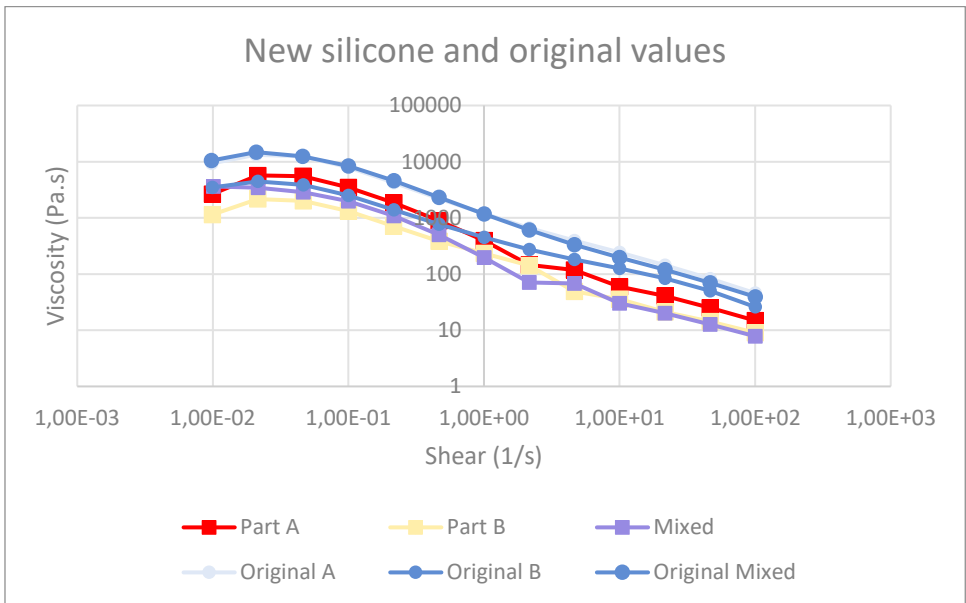


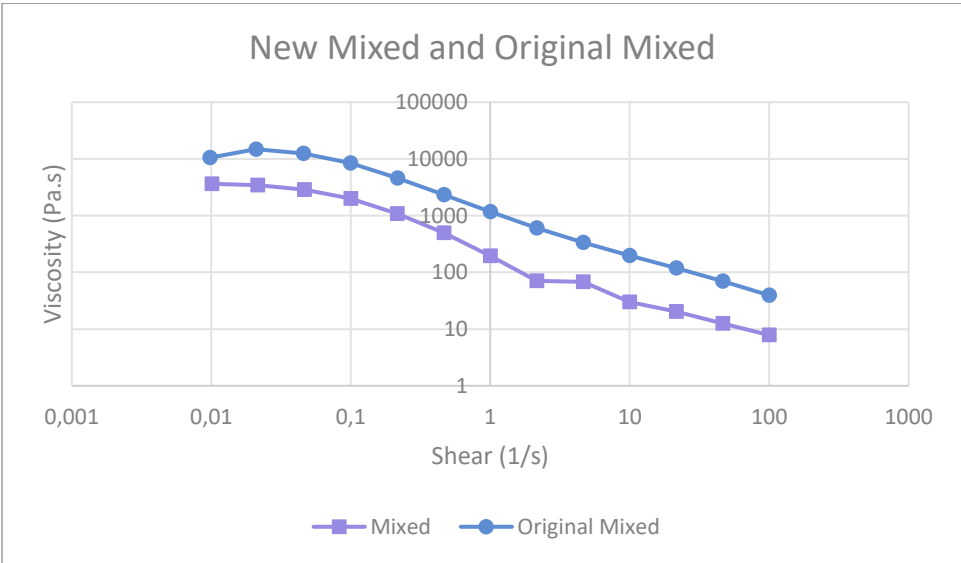
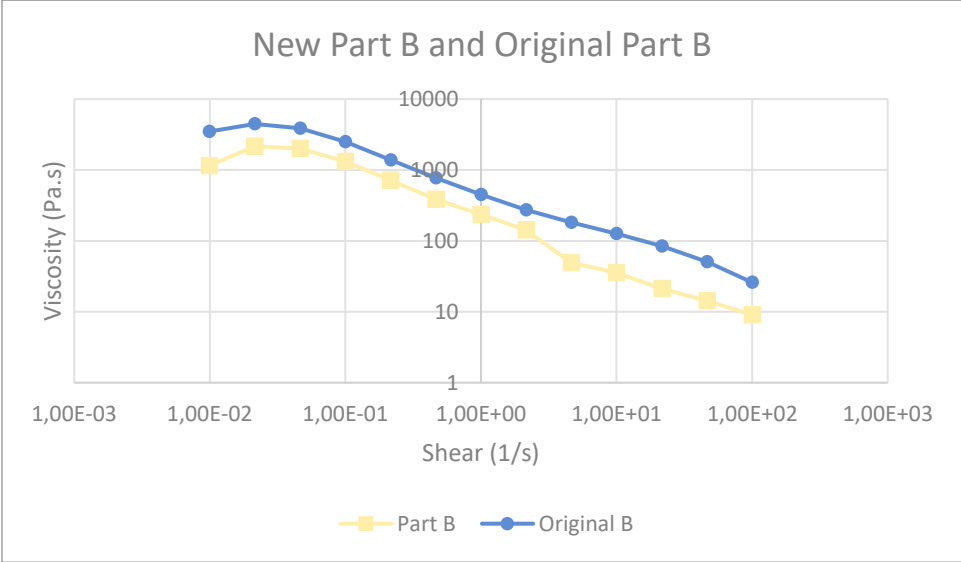
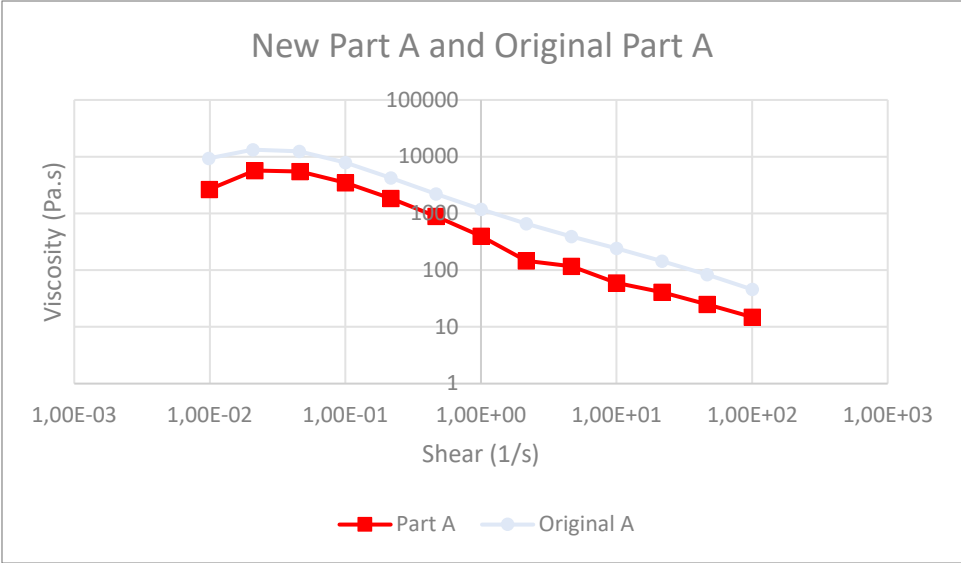
### Mixed - new silicone



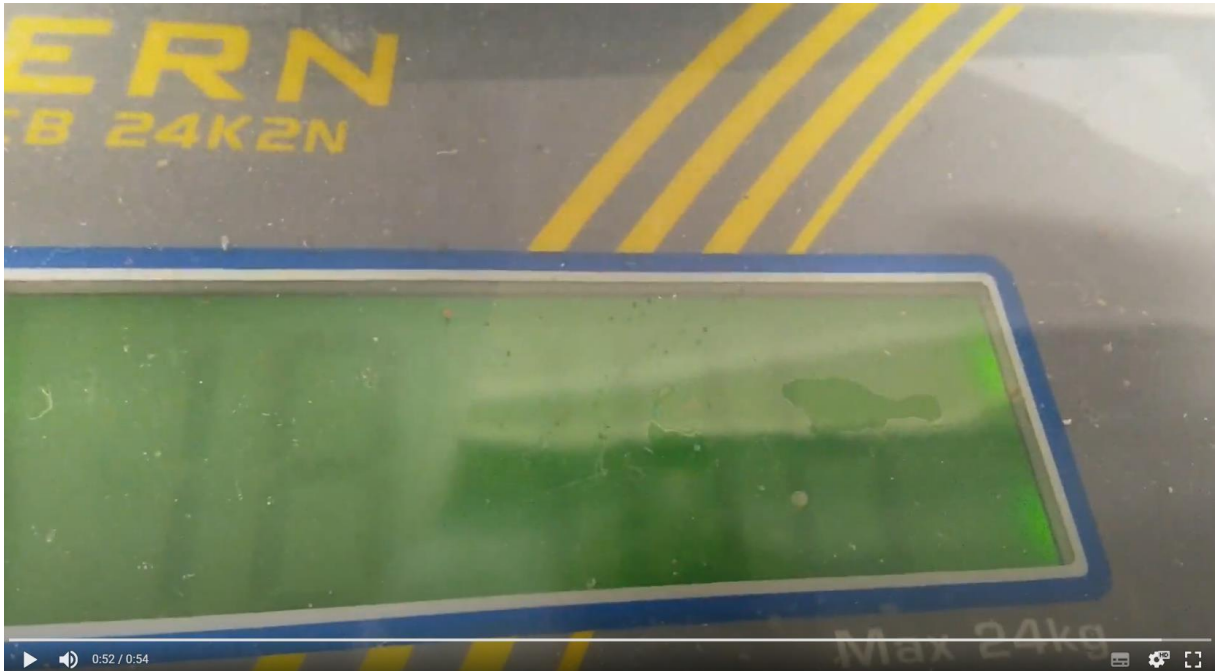


The shape of the graph looks already better than the shapes of the old silicone. Compared to the original ink measurements done by Sanne (Van Vilsteren, 2021), the new ink is still less viscose:





Force extrusion result



Out of the force extrusion force measurements came a maximum force about of 18kg, which translates to  $(18 \cdot 10) / 2 = 90\text{N}$  per syringe. This is lower than the 116,96 N measured by Sanne.

The silicone extruded through the static mixing nozzle that was saved to see if it would cure did not cure



It is therefore possible that the ink was not mixed properly also when it was extruded onto the peltier plate during rheometer measurements.

## Conclusion

The new measurements of the ink made on February 6 also show weird behaviour. It is therefore likely that the measurements were not faulty, but that this unexpected behaviour is part of the old silicone. However, the samples used in the repeated measurements show even more unexpected behaviour compared to the first measurements. Possibly, this is due to further degeneration of the silicone while stored in the syringes.

The newly made ink with the new silicone shows an improvement in the rheometric properties compared to the one made with the old silicone. The behaviour (the shape of the graph) is more in line of what is expected from Sanne's values. However, the overall viscosity of the ink is still lower than Sanne's values. Also, all components show a small pit at a shear of 2.15 1/s for Part A and Mixed and 4,64 1/s for part B. This pit is consistent for all three measurements.

It can be concluded that the old silicone was in part responsible for the deviation from the original T7E1 ink values from Sanne. However, there is still an unknown factor that causes the slight decrease in viscosity. In the recipe by Sanne, Carbonyl Iron was used. In this recipe, plain Iron was used. Carbonyl iron is used as a supplement to combat iron deficiency. According to Feosol (n.d.), producer of such supplements, Carbonyl Iron is 100% elemental Iron. They compare it to Iron gained from salt (Ferrous sulfate). The Iron particles used in this recipe do not state their origin, but the description (e.g. 99.5% purity and the keyword "elemental") does suggest it is elemental iron.

## Discussion

The rheometric values of the ink still do not show the expected results. The new silicone does however show improvement. The further deviation could be explained by the difference in particles (Iron vs Carbonyl Iron), however this seems unlikely. Another possibility is that the fumed silica used has degraded and has a negative influence on the viscosity.

What also stands out, is that Part A is higher in viscosity than the mixed silicone. In one of Sanne's experiments, this was also the case in the first preparation of the T7E1 ink and it was concluded that this had to do with a wrong amount of added Carbonyl Iron particles to Part A. However, in this experiment, it was found that in high shear rates, Part B is even higher in viscosity than Mixed.

Part A and B show a low standard deviation. Mixed shows a higher standard deviation. This might have to do with the slight curing of the ink, but faulty measurements is also still possible. Especially because the low shear viscosity of the first measurement shows unexpected behaviour.

The mixed ink extruded to see the curing behaviour did not cure. It is very well possible that this is caused by under extrusion of Part A, as this is the part that is the hardest to extrude. If this is the case, only Part B came out of the nozzle (with maybe a littlebit of part A). This could explain why the rheometer measurements of the mixed ink is below that of Part A, while we would expect that it is equal or above.

## Limitations

In the repetition measurements of the old silicone based ink, ink was used that had been stored in the syringes for about six days. Because of degradation of the ink, it cannot be concluded that the original measurements of the old silicone were faulty or not, because the conditions are not the same.

The display on the scale used in force extrusion measurement test was not very readable on the movie made. In addition, it is unlikely that the force needed to extrude the ink is the same for each syringe. Part A has a generally higher viscosity, so it is logical that this syringe needs a greater force to extrude ink through the static mixing nozzle.

#### Further research

In a new attempt to make the ink, two things can be tried to match Sanne's results more:

- Try with new fumed silica to eliminate the possibility that the degradation of the silica used resulted in a negative influence on the viscosity.
- Try with NdFeB particles which we know are the same as in Sanne's recipe. New Carbonyl Iron particles cannot be acquired until April. But NdFeB particles can be acquired in short notice, so we can try these particles in a NdFeB recipe by Sanne to see if this recipe does behave the same to eliminate the possibility that the Iron particles used are responsible for the unexpected behaviour compared to the Carbonyl Iron particles.

#### References

Feosol. (n.d.). *What's the difference between carbonyl iron and ferrous sulfate?* Retrieved on February 17, 2022, from: <https://www.feosol.com/about-iron/feosol-natural-release-faq/>

Van Vilsteren, S. (2021). *Designing Magnetic Soft Materials for 4D Printing* [Master Thesis, Delft University of Technology]. Tu Delft Educational Repository. <http://resolver.tudelft.nl/uuid:7e05bd4c-4720-4e1f-b13b-7b048602ce42>

## C.1d Ink preparation trial 4

Kevin van der Lans, Houman Yarman, Sepideh Ghodrat – February 21, 2022

### Introduction

Today we make ink together because it allows us to share thoughts and see where ink preparation might go wrong.

### Materials

2-component ink ingredients:

- 12.6 grams Ecoflex 00-10 Part A
- 12.6 grams Ecoflex 00-10 Part B
- 2x 22.5 grams Iron powder (<10 microns, 99,5% purity)  
<https://www.fishersci.nl/shop/products/iron-powder-spherical-10-micron-99-9-metals-basis-99-5-thermo-scientific/11360689>
- 2x 0.30 grams fumed silica (SiO<sub>2</sub>)

Utensils:

- Two paper cups
- Two 10 ml syringes
- Mixing Spatulas
- Analytical scale with precision up to 3 decimals
- Masking tape
- Pen
- Paper towels

For measurements:

- Mixing spatulas
- TA Instruments AR-G2 Rheometer
- ARG2 control program
- Isotropic alcohol
- Paper towels

Extrusion and curing test

- static mixing nozzle for force measurements
- Two 10ml syringes filled with magnetic ink
- Oven at 120 degrees C for 60 minutes

### Method

The ink was made separately (Part A and B) to make sure it does not cure while it is stored so it can be analyzed and used for direct ink writing later. The rheometer measurements were done to measure the viscosity of the ink and to measure the shear-thinning properties of the ink caused by the fumed silica. To see if the ink would cure, lines were extruded through the “static mixing nozzle for force measurements” manually on a glass plate and put into the oven at 120 degrees C for 60 minutes.

#### *Ink preparation*

Ink was made in two parts, for which the procedure was as follows:

Part A



- Turn on the scale and tare it without anything on it.
- Place one of the cups on the scale. The measured mass was 4.4763 g.
- Poor 12.6 grams of Ecoflex Part A in the cup on the scale with a spatula. The total mass was at this point 17.0776 g.
- Poor half the amount of Iron powder (22.5 g) in the cup with the Ecoflex Part A using a spatula. The total mass at this point was 39,6776 g
- Take the cup from the scale and mix the Iron and Ecoflex Part A together manually using a spatula.
- Place the cup back on the scale. The measured mass was now 39,4178 g.
- Add half the amount of fumed silica (0.30 g) to the Ecoflex Part A/ Iron powder mixture. The total mass now was 39,7166 g.
- Mix again my hand.

#### Part B

- Take everything off the scale and tare if necessary without anything on it.
- Place one of the cups on the scale. The measured mass was 4.3900 g.
- Poor 12.6 grams of Ecoflex Part B in the cup on the scale with a spatula. The total mass was at this point 16.9985 g.
- Poor half the amount of Iron powder (22.5 g) in the cup with the Ecoflex Part B using a spatula. The total mass at this point was 39.5366 g
- Take the cup from the scale and mix the Iron and Ecoflex Part B together manually using a spatula.
- Place the cup back on the scale. The measured mass was now 39.0825 g.
- Add half the amount of fumed silica (0.30 g) to the Ecoflex Part B/ Iron powder mixture. The total mass now was 39.3852g
- Mix again my hand.

Part A and B is put each in a separate 10mm syringe using a spatula. Each syringe is labeled with the part it contains using masking tape and a pen. Residue is cleaned off with paper towels. Some part A and B mixture was left in the cups for rheometer measurements.

#### *Rheometer measurements*

For measuring the rheometric properties of the magnetic ink, a TA Instruments AR-G2 Magnetic Bearing Rheometer was used. The following geometry was used:

- 40-mm-diameter steel plate geometry.
- Gap of 500 micron (0,5 mm)
- Material: Stainless steal
- Environmental system: Peltier plate
- Surface finish: Standard

The procedure was a steady-state flow sweep using the following settings:

- Environmental control:  
Temperature of 25°C, Soak time of 30 seconds  
Not wait for temperature
- Test parameters:  
Logarithmic sweep  
Shear rate between 0.01 1/s to 100 1/s  
Points per decade: 3  
Equilibration time 5.0 s  
Averaging time 30.0 s

The left over samples from the cups were put in the middle of the peltier plate by means of two steel spatulas. The peltier plate and the 40mm diameter steel plate were cleaned after each test

using isopropanol and paper towels. Part A was measured first, then Part B and lastly a mixture of parts A and B.

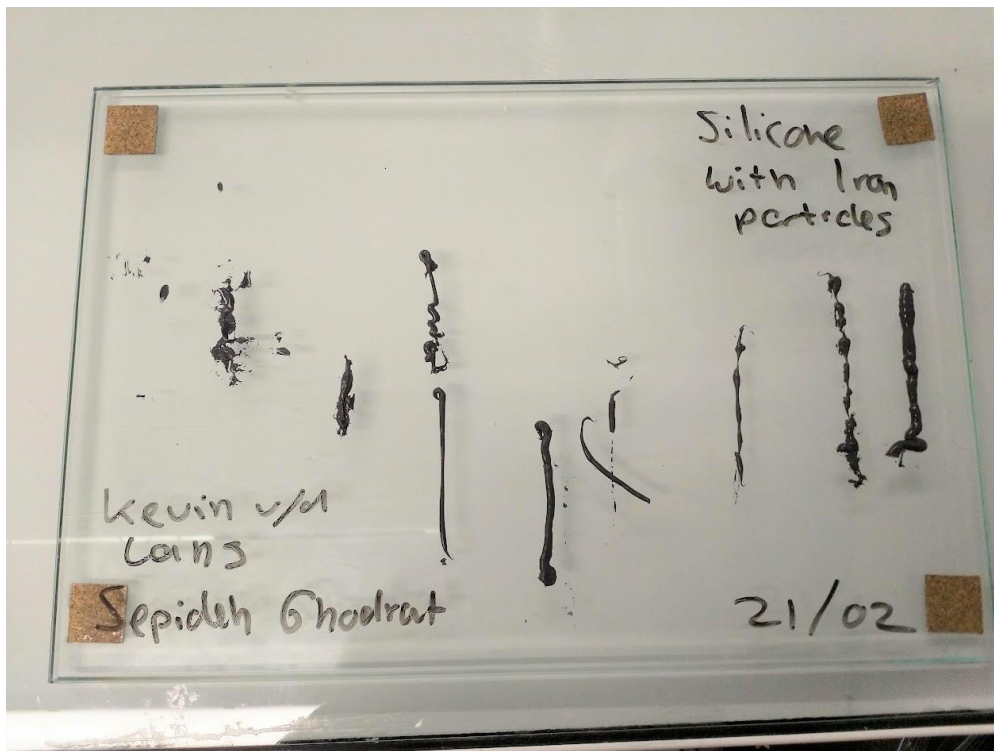
Part A and B were mixed manually for the rheometer tests by putting the same weight of part A and B together in a cup and stir with a spatula.

The Part A and B measurements were done 3 times, from which the mean and standard deviation can be calculated. The Mixed ink was measured 3 times, each time making a new mixture.

Results were copy-pasted into an excel file from the AR-G2 control software.

## Results

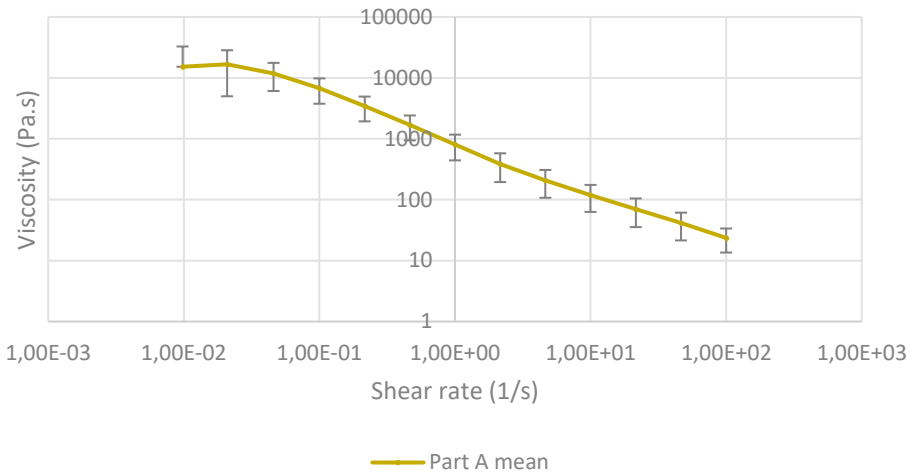
The ink extruded manually on the glass plate cured after 60 minutes in the oven.



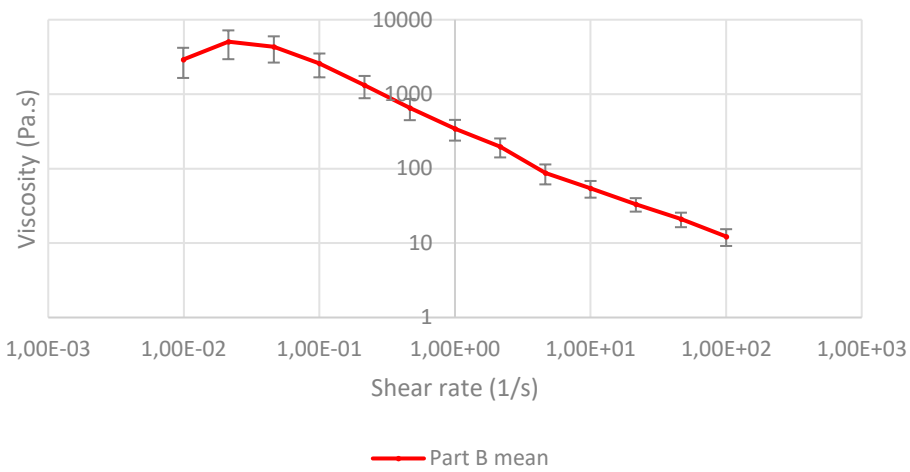
### *Rheological measurements*

The measurements done on the ink with the rheometer gave the following results.

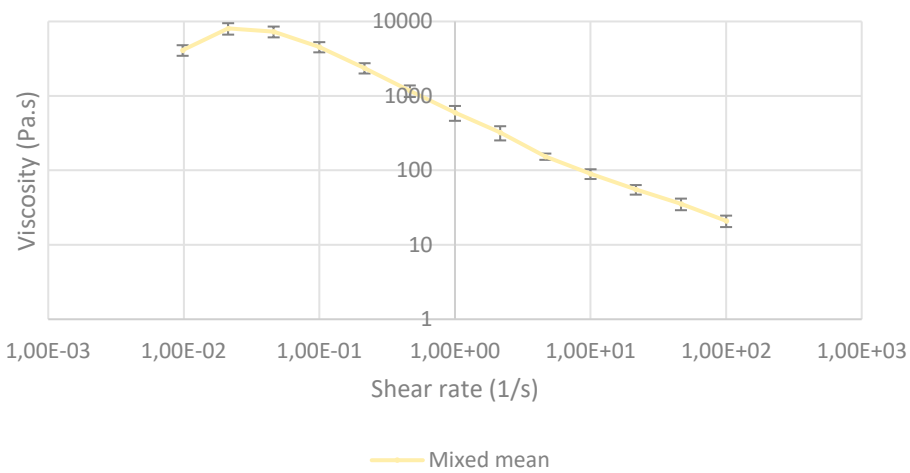
### Rheological measurements - Part A

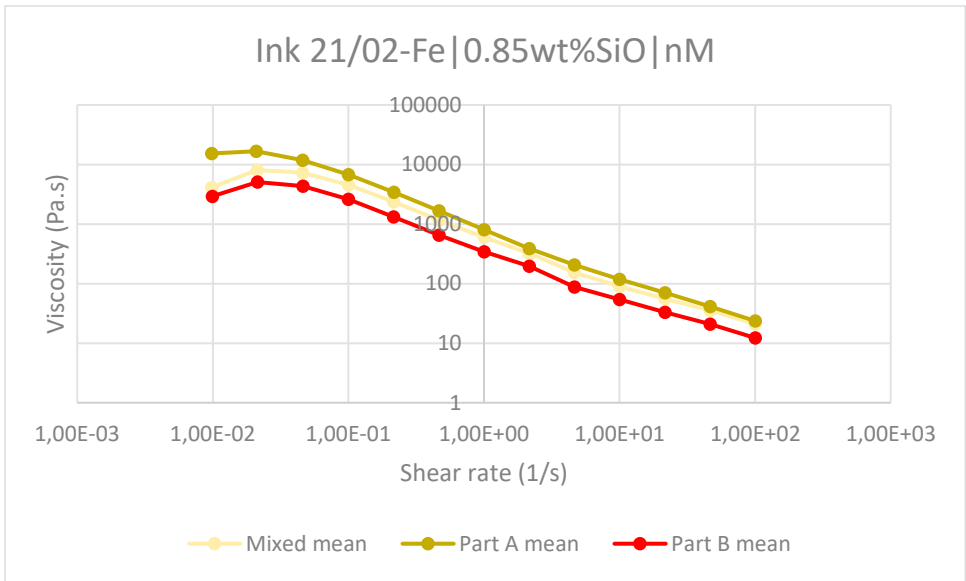


### Rheological measurements - Part B

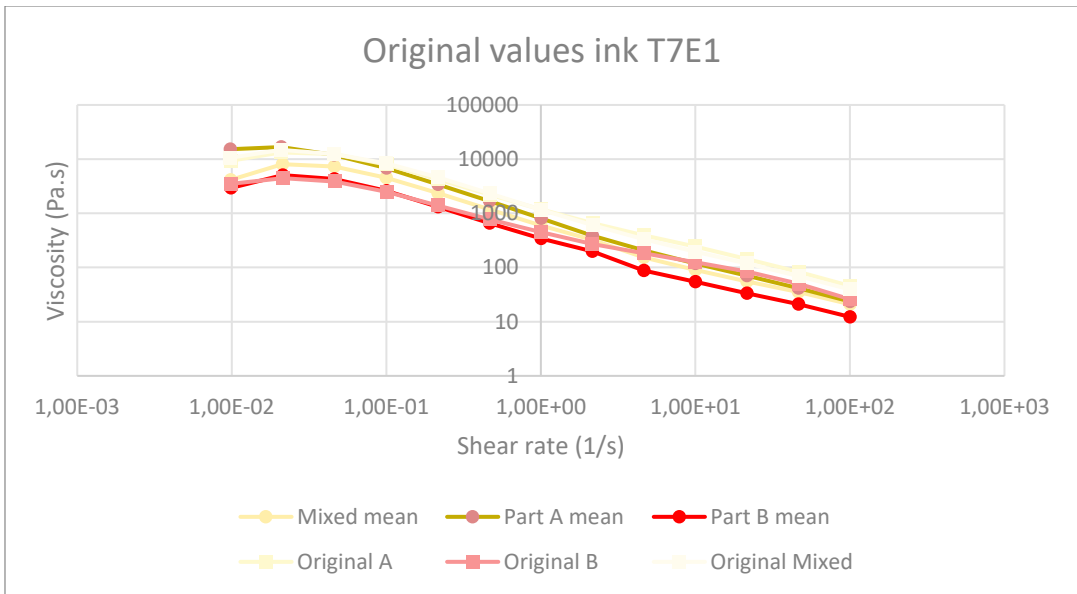


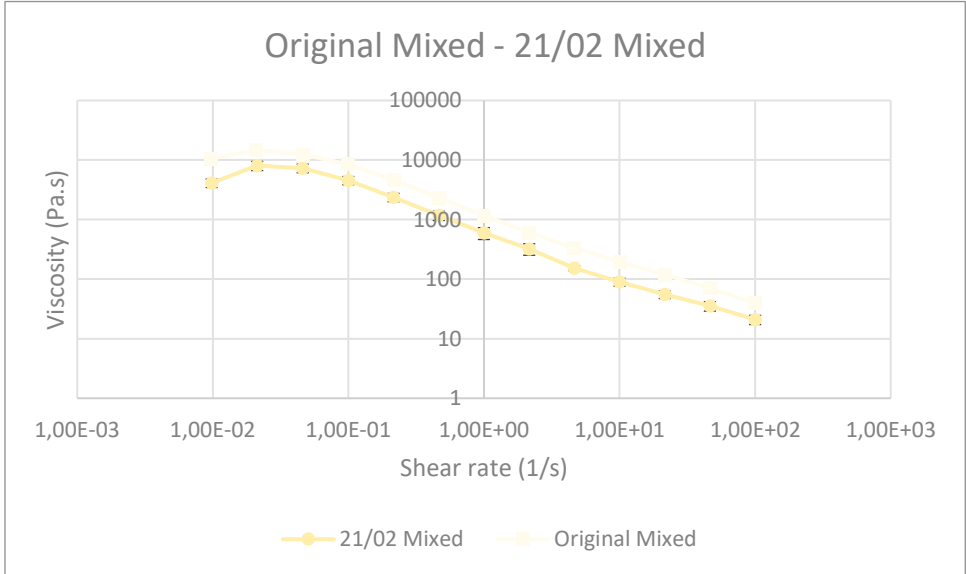
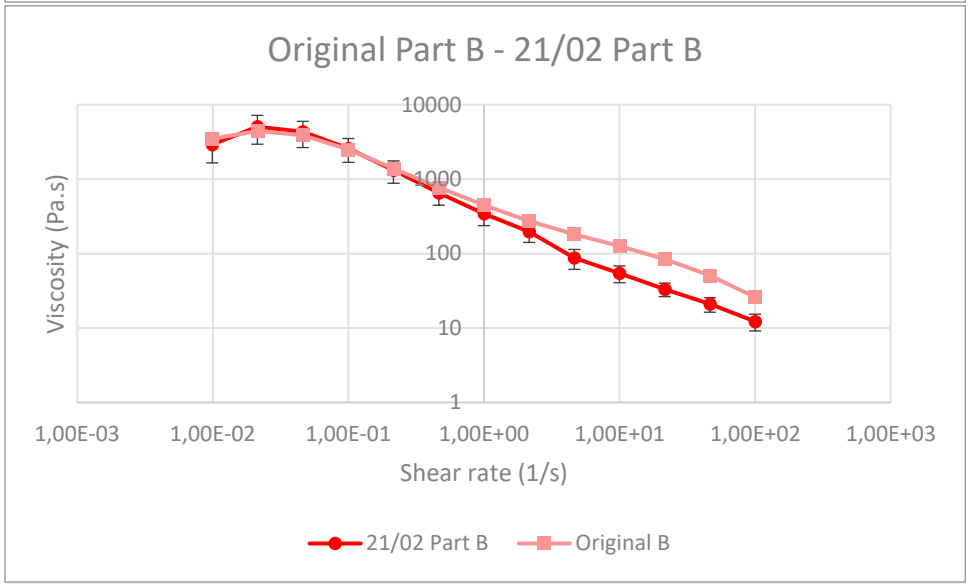
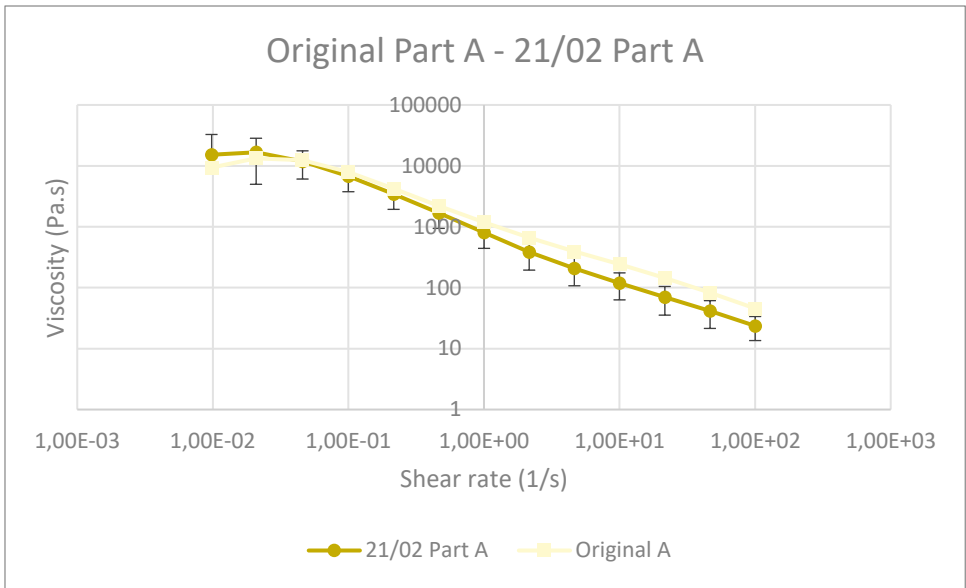
### Rheological measurements - Mixed



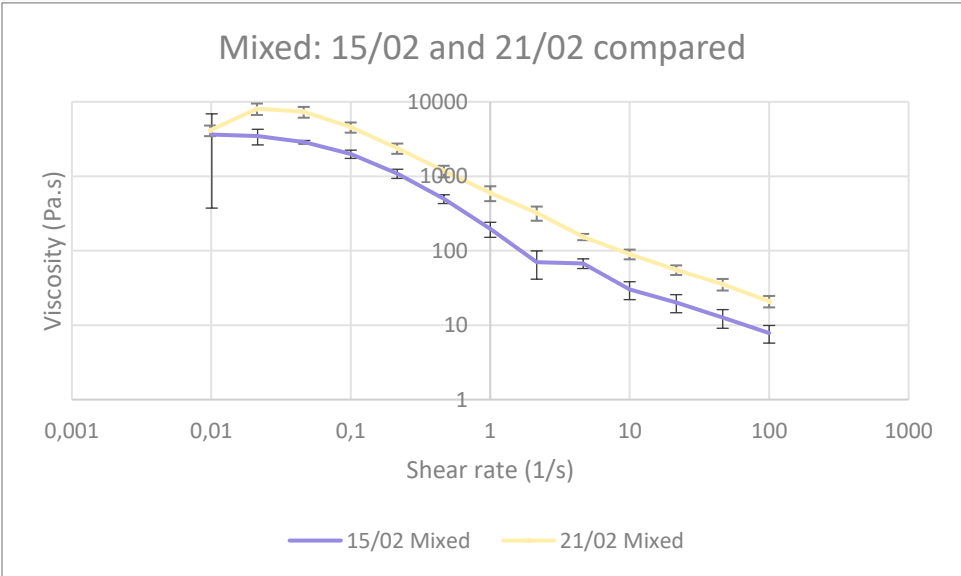
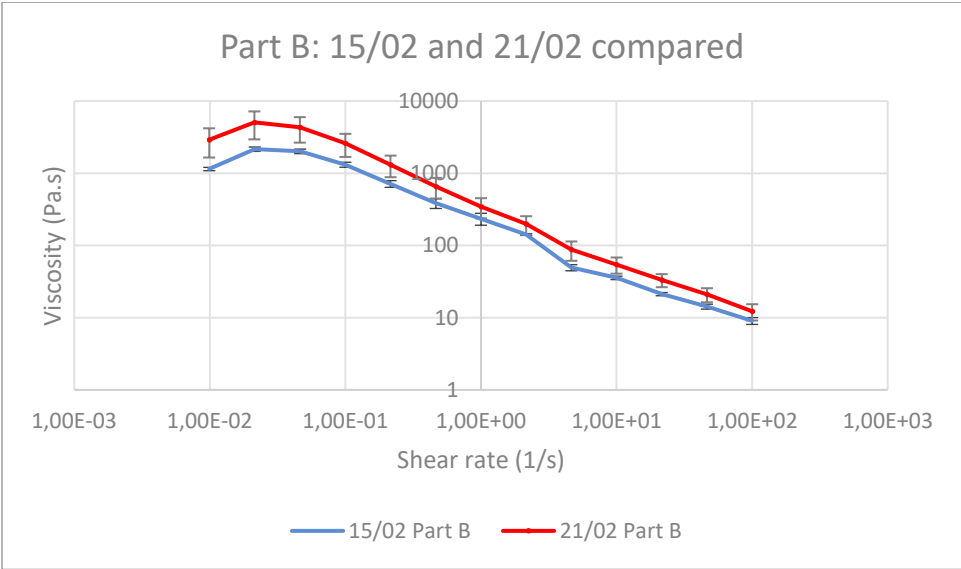
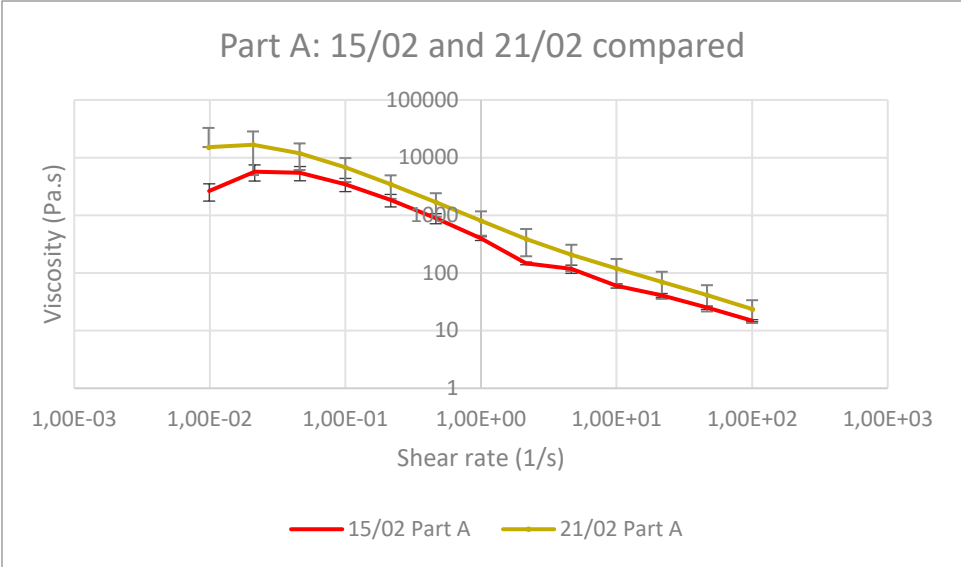


Compared to the original values from Sanne (Van Visteren, 2021), it looks like this:





The results are also compared to the ink prepared on 15/02, following the same recipe with the same ingredients.



## Conclusion

This time, the rheological values for the ink made today (21/02 – Fe|0,85wt%SiO|nM) came closer to the original values from Sanne. However, they are not yet the same. They are still slightly lower, especially at the end of the graph (shear rates of 1 to 100 1/s). The mixed ink especially shows a consistent lower value than the original. The pit the previous samples (version 15/02) showed at shear rate around 2.15 1/s for Part A and Mixed and 4,64 1/s for part B now seems gone.

Compared to the values of the ink made on February 15 following the same recipe using the same ingredients, the viscosity of today's ink is higher.

## Discussion

It is uncertain what caused the difference in measurements this time. The ingredients and recipe for ink version 15/02 and 21/02 are exactly the same. The timeframe between preparing and measuring were also very similar. The measurements were done within hours after preparation.

The difference in values between the Mixed ink between 15/02 and 21/02 can be explained by the means in which they were mixed, as it is possible the mixing through the static mixing nozzle went wrong the last time (at February 15) and this time the inks were mixed manually.

Another possible explanation for the improvements (i.e. closer to Sannes original value) could be that the preparation went better with supervision of Houman and Sepideh. However, I did everything exactly the same as previous times so this is an unlikely cause.

A possible explanation for the difference between the original values and the 21/02 values could be the particles: It is possible the Iron used is oxidizing and the carbonyl iron used by Sanne is oxidizing less or not at all.

## Further research

It is still possible the possible degradation of the fumed silica is responsible for the difference in measurements, as this was not researched in this test. To rule out the role of the (oxidation of the) particles, a recipe can be made with NdFeB particles as we know these are the same as the ones Sanne used.

Another possibility that can be looked into is the calibration of the rheometer. This can be tested with test samples of which the rheological properties are known.

## References

Van Vilsteren, S. (2021). Designing Magnetic Soft Materials for 4D Printing [Master Thesis, Delft University of Technology]. Tu Delft Educational Repository.  
<http://resolver.tudelft.nl/uuid:7e05bd4c-4720-4e1f-b13b-7b048602ce42>

## C.1e Ink preparation trial 5

Kevin van der Lans – March 8, 2022

### Introduction

Goal: make ink with NdFeB particles to check influence of Iron particles and see if the ink can be magnetized with just a ring magnet.

## Materials

The recipe T8E1 (NdFeB125%SiO-nM) by Sanne (Van Visteren, 2021) was used for this experiment. 50% of the ingredients were used to not waste NdFeB particles as they are super expensive.

- 6.3 grams Ecoflex 00-10 Part A
- 6.3 grams Ecoflex 00-10 Part B
- 2x 10.85 grams NdFeB powder (5 microns, 99,9% purity)  
<https://www.nanochemazone.com/product/neodymium-iron-boron-magnetic-powders/>
- 2x 0.06 grams fumed silica (SiO<sub>2</sub>)

## Utensils:

- Tree paper cups
- One 10 ml syringe
- Mixing Spatulas
- Spoon
- Analytical scale with precision up to 4 decimals
- Pen
- Glass marker
- Two glass plates
- Paper towels

## For measurements:

- Mixing spatulas
- TA Instruments AR-G2 Rheometer
- ARG2 control program
- Isotropic alcohol
- Paper towels

## Extrusion and curing test

- NdFeB ring magnet
- Ferrite ring magnet
- Oven at 60 degrees C for 120 minutes

## Method

The ink was made in two components (A and B). After preparation, they were mixed in a third cup. The mixture was put into the syringe with the permanent magnet attached. Lines were drawn on the first glass plate. The syringe with the mixed ink and the magnet attached was left to magnetize for a while during cleaning of the work space, after which more lines were drawn on the plate until the ink had cured too much to be extruded through the syringe.

### *Ink preparation*

Ink was made in two parts, for which the procedure was as follows:

#### Part A

- Turn on the scale and tare it without anything on it.
- Stir the ecoflex silicone thoroughly with a spoon.
- Place one of the cups on the scale. The measured mass was 3.4419 g.
- Pour 6.3 grams of Ecoflex Part A in the cup on the scale with a spatula. The total mass was at this point 9.7421 g.



- Poor half the amount of NdFeB powder (10,85 g) in the cup with the Ecoflex Part A using a spatula. The total mass at this point was 20,5954 g
- Take the cup from the scale and mix the Iron and Ecoflex Part A together manually using a spatula.
- Place the cup back on the scale. The measured mass was now 20,3792 g.
- Add half the amount of fumed silica (0.06 g) to the Ecoflex Part A/ NdFeB powder mixture. The total mass now was 20,4391 g.
- Mix again my hand.

#### Part B

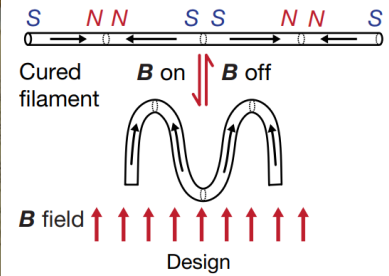
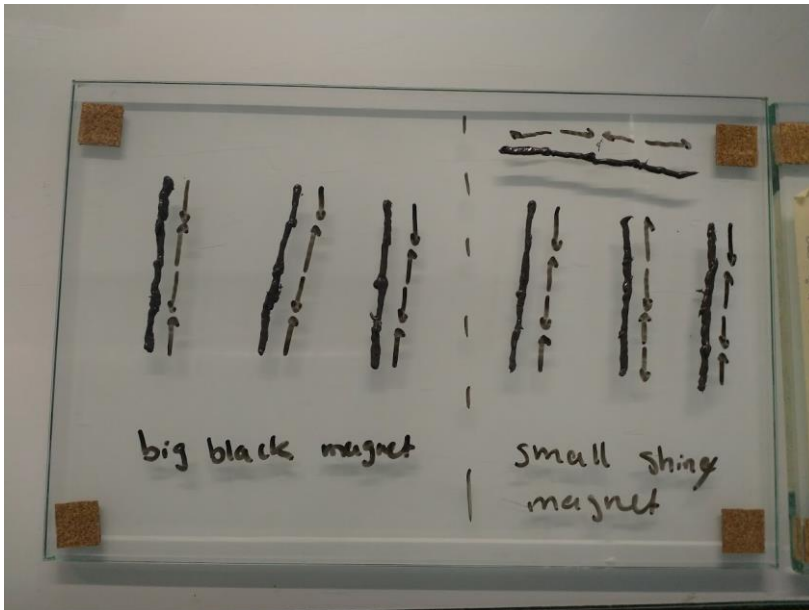
- Take everything off the scale and tare if necessary without anything on it.
- Place one of the cups on the scale. The measured mass was 3,4580 g.
- Poor 6.3 grams of Ecoflex Part B in the cup on the scale with a spatula. The total mass was at this point 9.7671 g.
- Poor half the amount of NdFeB powder (10.85 g) in the cup with the Ecoflex Part B using a spatula. The total mass at this point was 20.6562 g
- Take the cup from the scale and mix the Iron and Ecoflex Part B together manually using a spatula.
- Place the cup back on the scale. The measured mass was now 20.4470 g.
- Add half the amount of fumed silica (0.06 g) to the Ecoflex Part B/ NdFeB powder mixture. The total mass now was 20.5090g
- Mix again my hand.

#### Mixing

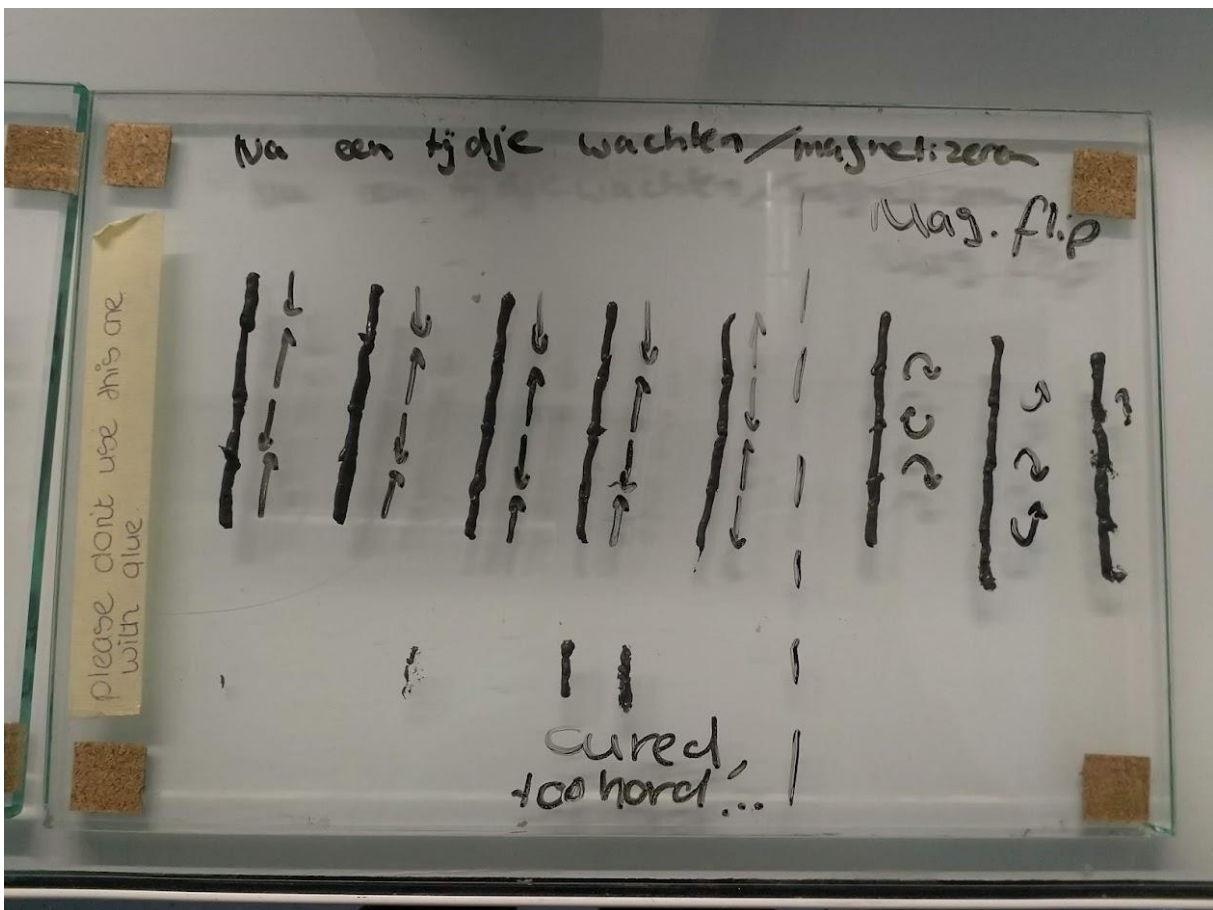
- An empty cup was placed on the scale. The measured weight was 3.4347.
- 8 grams of the Part A ink mixture was put inside the cup with a spatula. The cup measured 11.5121 grams.
- 8 grams of the Part B ink mixture was put in the cup with a spatula. The total weight measured 19.6467 grams.
- Both ink components were mixed by hand using a mixing spatula and put into the 10ml syringe on which a NdFeB permanent magnet (which was small and shiny) was attached to the nozzle or a ferrite permanent magnet (which was big and black) placed slightly higher.



With the two variations of magnets, lines were drawn on a glass plate. In the pattern, the simple N-shape was tired to be recreated from the MIT paper by Kim et al. (2018).



After leaving the mixed ink magnetize by the NdFeB magnet for a few minutes, more lines were drawn. Some of which made by extruding in one direction and flipping the magnet in between sections rather than changing drawing direction of segments.



Both class plates were placed inside an oven for 2 hours at 60°C to cure.

#### Rheometer measurements

For measuring the rheometric properties of the magnetic ink, a TA Instruments AR-G2 Magnetic Bearing Rheometer was used. The following geometry was used:

- 40-mm-diameter steel plate geometry.
- Gap of 500 micron (0,5 mm)
- Material: Stainless steel
- Environmental system: Peltier plate
- Surface finish: Standard

The procedure was a steady-state flow sweep using the following settings:

- Environmental control:  
Temperature of 25°C, Soak time of 30 seconds  
Not wait for temperature
- Test parameters:  
Logarithmic sweep  
Shear rate between 0.01 1/s to 100 1/s  
Points per decade: 3  
Equilibration time 5.0 s  
Averaging time 30.0 s

The left over samples from component A and B in the cups were put in the middle of the peltier plate by means of two steel spatulas. The peltier plate and the 40mm diameter steel plate were cleaned after each test using isopropanol and paper towels. Part A was measured first, then Part B and lastly a mixture of parts A and B.

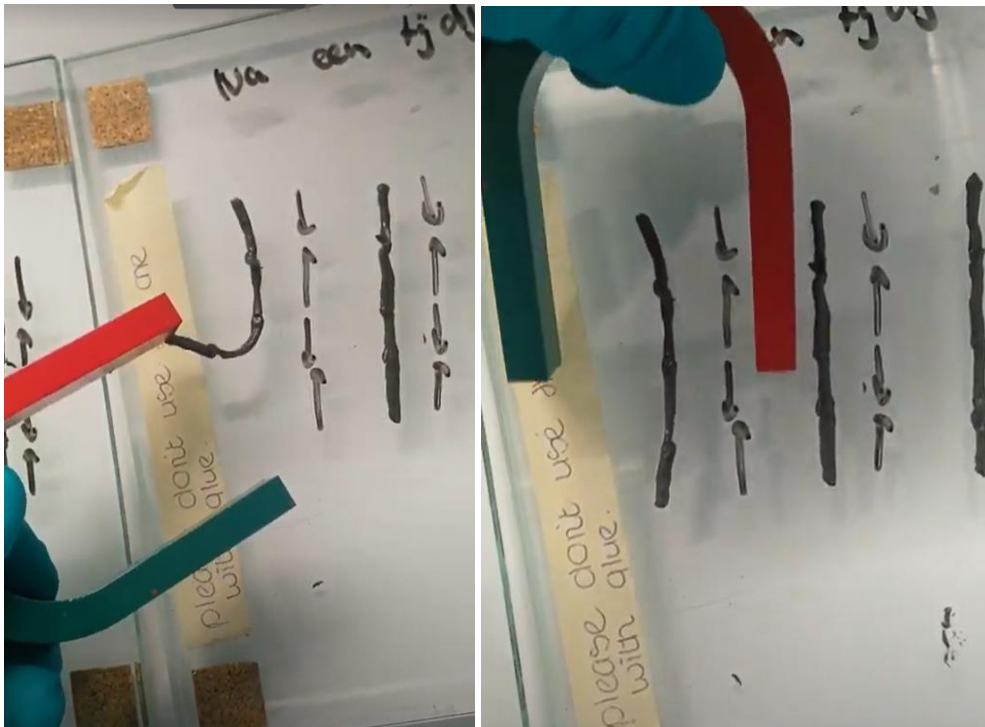
Part A and B were mixed manually for the rheometer tests by putting the same weight of part A and B together in a cup and stir with a spatula.

The Part A and B measurements were done 3 times, from which the mean and standard deviation can be calculated. The Mixed ink was measured 2 times, each time making a new mixture.

Results were copy-pasted into an excel file from the AR-G2 control software.

## Results

The particles inside the silicone where the line segments were drawn with were not magnetized enough to be able to morph the lines into the M-shapes. The lines of silicone did cure and were attracted to the horse-shoe magnet (they stuck to the magnet), but did not show shape morphing properties.

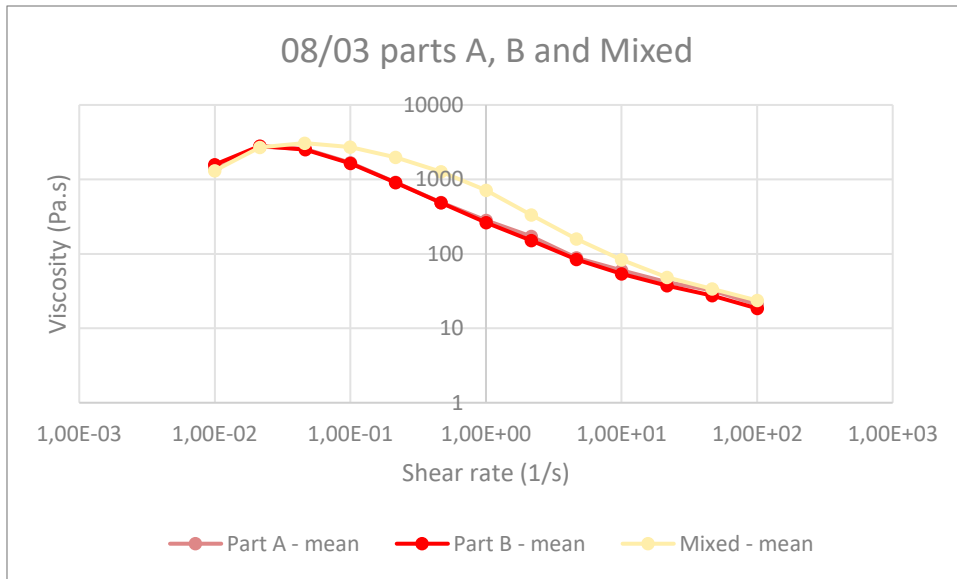


The sampled did stick better to the red part of the magnet (north) than the green part (south).



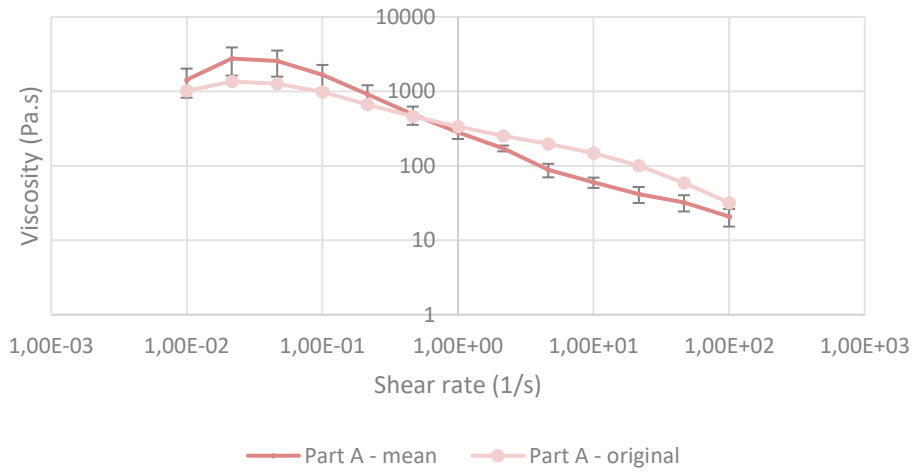
*Rheological measurements*

Out of the rheological measurements, it seems that Part A and B have the same viscosity. The parts mixed seems to have a higher viscosity than the two separate parts.

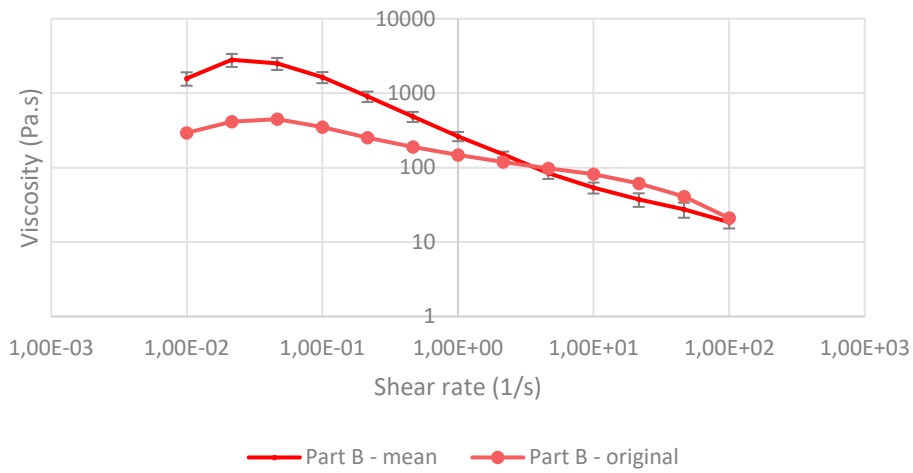


Compared to the original values by Sanne (Van Vilsteren, 2021), the viscosity of the separate and mixed parts, do again not match.

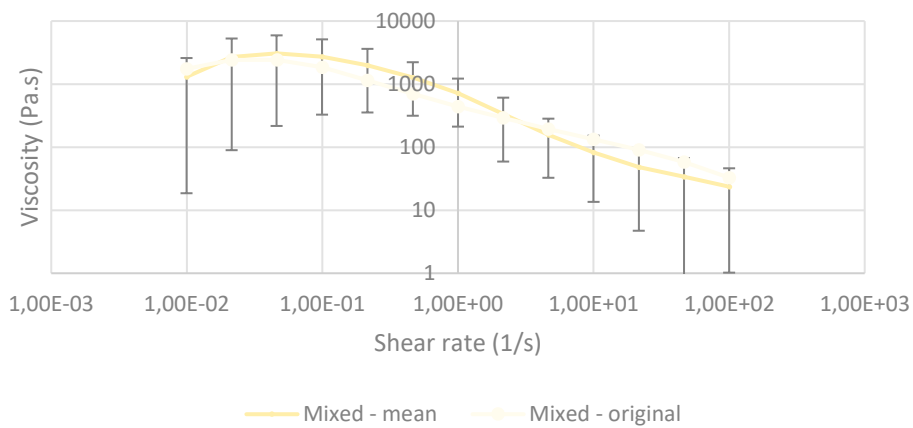
08/02 Part A and original Part A values compared



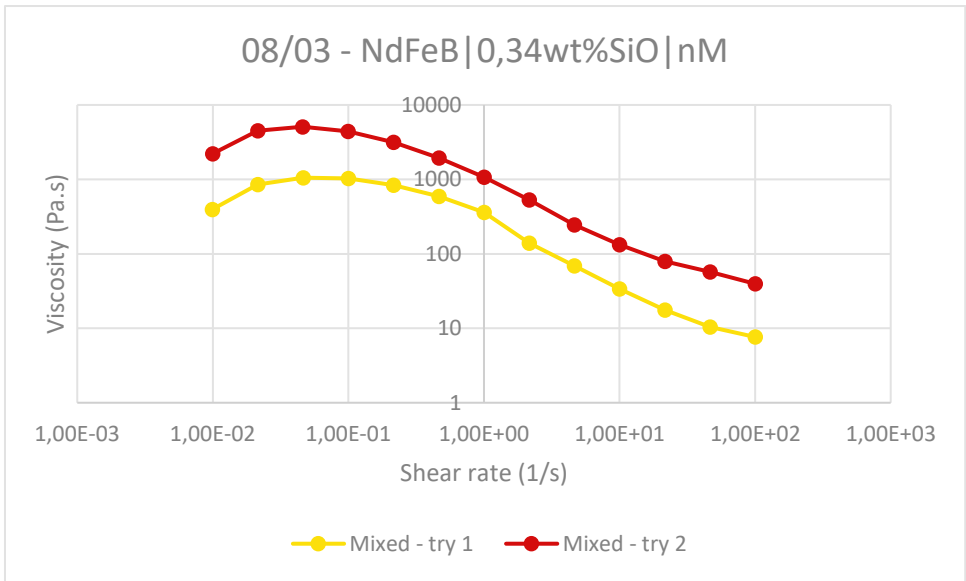
08/02 Part B and original Part B values compared



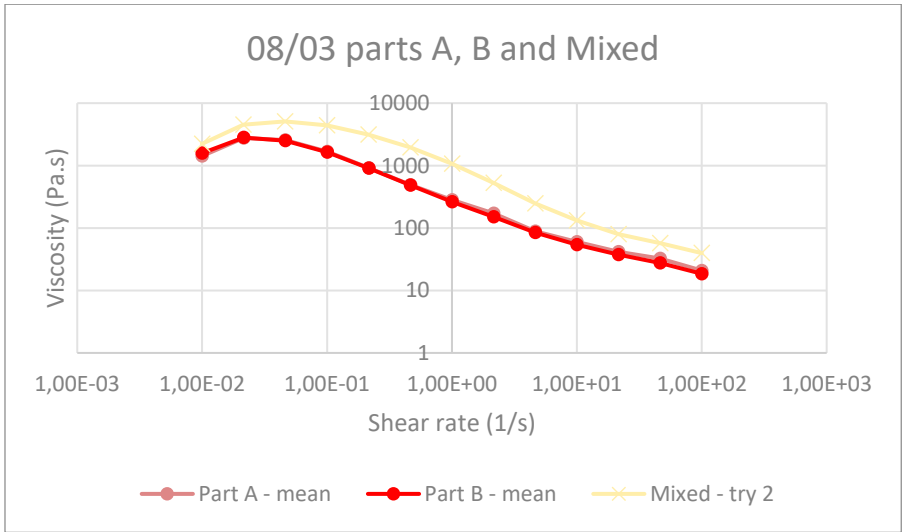
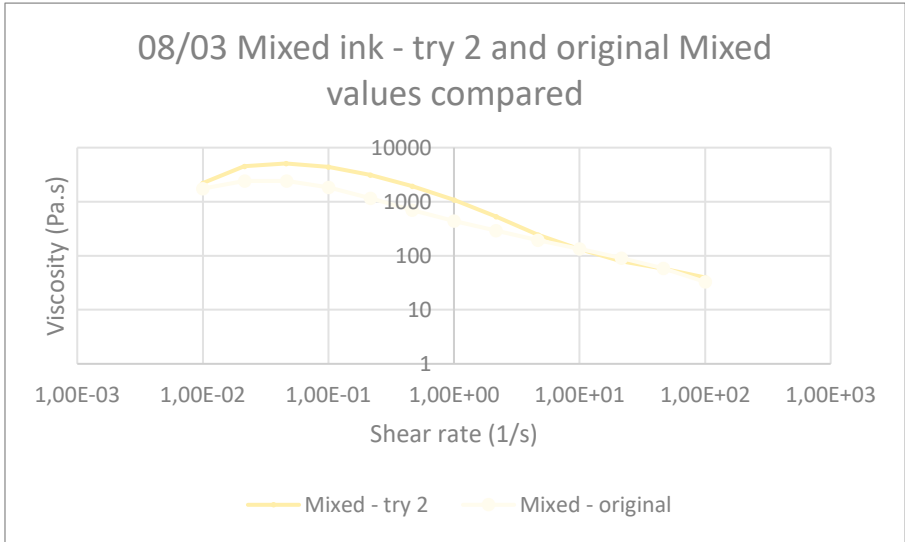
Mixed ink (08/03) and original Mixed values compared



The two measurements of the mixed component were also very far apart. It is likely that one of the measurements had gone wrong.



As the second try is the most likely to be accurate (it seems to give a more logical value, as the sum of A and B is very unlikely to have lower viscosity of A and B separately), the first try was taken out. The result:



## Conclusion

It was likely not the iron particles that caused the deviation in measurements from those from Sanne. As in this new measurements with NdFeB particles, the ink properties still don't line up with the expected result. Although, this time, the ink is not lower in viscosity than Sanne's measurements, but overall higher. This can also have been caused by the thorough stirring of the silicone at the start of preparation, which was also done for the first time in this research.

The particles cannot be magnetized with a simple (ring) magnet. The line segments did not show a distinct north and south pole, as they stuck to the north and south poles of the horse shoe magnet and the lines did not alter their shape in the presence of the magnetic field created by the horse shoe magnet.

## Discussion

Weird stuff happening.

Difference between mixed try one and two is maybe because samples were not mixed properly.

It seems that A and B have the same viscosity. This should not be the case. Also unlikely that I measured A twice because I had run out of A and B simultaneously. Also not made A twice because ink mixed and extruded did cure.

Rheometer calibration done, seemed fine.

## Future research

Get new fumed silica? But its not that big of a deal maybe that the measurements are off...

## References

Kim, Y., Yuk, H., Zhao, R., Chester, S.A. & Zhao, X. (2018). Printing ferromagnetic domains for untethered fast-transforming soft materials. *Nature*, 558, p. 274 – 279.

<https://doi.org/10.1038/s41586-018-0185-0>

Van Vilsteren, S. (2021). Designing Magnetic Soft Materials for 4D Printing [Master Thesis, Delft University of Technology]. Tu Delft Educational Repository.

<http://resolver.tudelft.nl/uuid:7e05bd4c-4720-4e1f-b13b-7b048602ce42>



## C.1f Ink Preparation test 6

Kevin van der Lans, Sepideh Ghodrat – March 22, 2021

### Introduction

In this test, ink is made and magnetized in the reactor institute for three purposes:

- Be able to test magnetized ink with the 3D printer
- Make M-shape demonstrator
- See if magnetized particles give the desired rheological properties to the ink or that fumed silica is necessary.

Kim et al. (2019) have made a magnetic ink without the inclusion of fumed silica using PDMS silicone and it showed shear-thinning properties by itself. Maybe it is possible also for us to do this, as this eliminates a parameter and presumably lowers the overall viscosity of the ink so that it becomes more suitable for direct ink writing.

### Materials

The recipe T8E1 (NdFeB1,25%SiO-nM) by Sanne (Van Visteren, 2021) was used for this experiment. 50% of the ingredients were used for Sample 1:

- 6.3 grams Ecoflex 00-10 Part A
- 6.3 grams Ecoflex 00-10 Part B
- 2x 10.85 grams NdFeB powder (5 microns, 99,9% purity)  
<https://www.nanochemazone.com/product/neodymium-iron-boron-magnetic-powders/>
- 2x 0.06 grams fumed silica (SiO<sub>2</sub>)

100% of the recipe was used for Sample 2:

- 12.6 grams Ecoflex 00-10 Part A
- 12.6 grams Ecoflex 00-10 Part B
- 2x 21.7 grams NdFeB powder (5 microns, 99,9% purity)
- 2x 0.12 grams fumed silica (SiO<sub>2</sub>)

25% of the recipe was used for Sample 3 and fumed silica was left out:

- 3.15 grams Ecoflex 00-10 Part A
- 3.15 grams Ecoflex 00-10 Part B
- 2x 5.425 grams NdFeB powder (5 microns, 99,9% purity)

### Utensils:

- Six paper cups
- Six 10 ml syringes
- Mixing Spatulas
- Spoon
- Analytical scale with precision up to 4 decimals
- Pen
- Glass marker
- Paper towels

For measurements:

- Mixing spatulas
- TA Instruments AR-G2 Rheometer

- ARG2 control program
- Isotropic alcohol
- Paper towels

#### Demonstrator making

- NdFeB ring magnet
- Steel magnetic shield
- Go Electrical steel magnetic shield
- Oven at 60 degrees C for 120 minutes
- Two glass plates

#### Method

Three samples were made in this test for three purposes:

- 1) 50% T8E1 to make demonstrator shapes with
- 2) 100% T8E1 for trying with the 3D printer
- 3) 25% T8E1 without SiO<sub>2</sub> to compare properties to recipe with SiO<sub>2</sub>

Sample 2 was degassed prior to putting it in the syringes by putting the cups in the vacuum oven for about 10 minutes at 950 mbar at room temperature.

Tabs of the syringes were cut off (all around!) to be able to fit in magnetizer tube. The samples were magnetized with the Versa Lab Magnetizer at the reactor institute at a field strength of 3 Tesla.

For Sample 1 and 2, a bit of ink was left prior to magnetizing to be able to measure and compare rheological properties.

#### *Ink preparation*

The ink was made in two components (A and B). The mixture was put into the corresponding syringes after which the tabs were cut off.

Procedure for making **Sample 1** was as follows:

#### Part A

- Turn on the scale and tare it without anything on it.
- Stir the ecoflex silicone thoroughly with a spoon.
- Place one of the cups on the scale. The measured mass was 4.3326 g.
- Poor 6.3 grams of Ecoflex Part A in the cup on the scale with a spatula. The total mass was at this point 10.6480 g.
- Poor half the amount of NdFeB powder (10,85 g) in the cup with the Ecoflex Part A using a spatula. The total mass at this point was 21.4953 g
- Take the cup from the scale and mix the Iron and Ecoflex Part A together manually using a spatula.
- Place the cup back on the scale. The measured mass was now 21.3028 g.
- Add half the amount of fumed silica (0.06 g) to the Ecoflex Part A/ NdFeB powder mixture. The total mass now was 21.3693 g.
- Mix again my hand.

#### Part B

- Take everything off the scale and tare if necessary without anything on it.
- Place one of the cups on the scale. The measured mass was 4,3669 g.
- Poor 6.3 grams of Ecoflex Part B in the cup on the scale with a spatula. The total mass was at this point 10.6726 g.

- Poor half the amount of NdFeB powder (10.85 g) in the cup with the Ecoflex Part B using a spatula. The total mass at this point was 21.5213 g
- Take the cup from the scale and mix the Iron and Ecoflex Part B together manually using a spatula.
- Place the cup back on the scale. The measured mass was now 21.3672 g.
- Add half the amount of fumed silica (0.06 g) to the Ecoflex Part B/ NdFeB powder mixture. The total mass now was 21.4279 g
- Mix again my hand.

Procedure for making **Sample 2** was as follows:

#### Part A

- Turn on the scale and tare it without anything on it.
- Stir the ecoflex silicone thoroughly with a spoon.
- Place one of the cups on the scale. The measured mass was 4.3287 g.
- Poor 12.6grams of Ecoflex Part A in the cup on the scale with a spatula. The total mass was at this point 16.9475 g.
- Poor half the amount of NdFeB powder (21.7 g) in the cup with the Ecoflex Part A using a spatula. The total mass at this point was 38.6556 g
- Take the cup from the scale and mix the Iron and Ecoflex Part A together manually using a spatula.
- Place the cup back on the scale. The measured mass was now 38.4596 g.
- Add half the amount of fumed silica (0.12 g) to the Ecoflex Part A/ NdFeB powder mixture. The total mass now was 38.5797 g.
- Mix again my hand.

#### Part B

- Take everything off the scale and tare if necessary without anything on it.
- Place one of the cups on the scale. The measured mass was 4.3540 g.
- Poor 12.6 grams of Ecoflex Part B in the cup on the scale with a spatula. The total mass was at this point 16.9568 g.
- Poor half the amount of NdFeB powder (21.7 g) in the cup with the Ecoflex Part B using a spatula. The total mass at this point was 38.6578 g
- Take the cup from the scale and mix the Iron and Ecoflex Part B together manually using a spatula.
- Place the cup back on the scale. The measured mass was now 38.5433 g.
- Add half the amount of fumed silica (0.12 g) to the Ecoflex Part B/ NdFeB powder mixture. The total mass now was 38.6637 g
- Mix again my hand.

Procedure for making **Sample 3** was as follows:

#### Part A

- Turn on the scale and tare it without anything on it.
- Stir the ecoflex silicone thoroughly with a spoon.
- Place one of the cups on the scale. The measured mass was 4.2845 g.
- Poor 3.15 grams of Ecoflex Part A in the cup on the scale with a spatula. The total mass was at this point 7.4378 g.
- Poor half the amount of NdFeB powder (5.425 g) in the cup with the Ecoflex Part A using a spatula. The total mass at this point was 12.8686 g

- Take the cup from the scale and mix the Iron and Ecoflex Part A together manually using a spatula.

#### Part B

- Take everything off the scale and tare if necessary without anything on it.
- Place one of the cups on the scale. The measured mass was 4.3124 g.
- Poor 3.15 grams of Ecoflex Part B in the cup on the scale with a spatula. The total mass was at this point 7.442 g.
- Poor half the amount of NdFeB powder (5.425 g) in the cup with the Ecoflex Part B using a spatula. The total mass at this point was 12.8947 g
- Take the cup from the scale and mix the Iron and Ecoflex Part B together manually using a spatula.

#### *Rheometer measurements*

For measuring the rheometric properties of the magnetic ink, a TA Instruments AR-G2 Magnetic Bearing Rheometer was used. The following geometry was used:

- 40-mm-diameter steel plate geometry.
- Gap of 500 micron (0,5 mm)
- Material: Stainless steel
- Environmental system: Peltier plate
- Surface finish: Standard

The procedure was a steady-state flow sweep using the following settings:

- Environmental control:  
Temperature of 25°C, Soak time of 30 seconds  
Not wait for temperature
- Test parameters:  
Logarithmic sweep  
Shear rate between 0.01 1/s to 100 1/s  
Points per decade: 3  
Equilibration time 5.0 s  
Averaging time 30.0 s

The left over samples from Sample 2. component A and B in the cups were put in the middle of the peltier plate by means of two steel spatulas. The peltier plate and the 40mm diameter steel plate were cleaned after each test using isopropanol and paper towels. Part A was measured first, then Part B and lastly a mixture of parts A and B.

Part A and B were mixed manually for the rheometer tests by putting the same weight of part A and B together in a cup and stir with a spatula.

The Part A, B and Mixed measurements were done 3 times, from which the mean and standard deviation can be calculated. Each time, a new mixture of ink was prepared.

Sample 1 was measured once per part (A and B) unmagnetized and magnetized. Sample 3 was only measured once per part when magnetized.

Results were copy-pasted into an excel file from the AR-G2 control software.

#### *Demonstrator making*

For making the demonstrator actuating shapes, ink from Sample 1 were mixed together in a cup and put into a new syringe. The syringe was fitted with a permanent NdFeB magnet and magnetic shield. To create the needed distance between the shield and the extruded ink, a luer lock hose

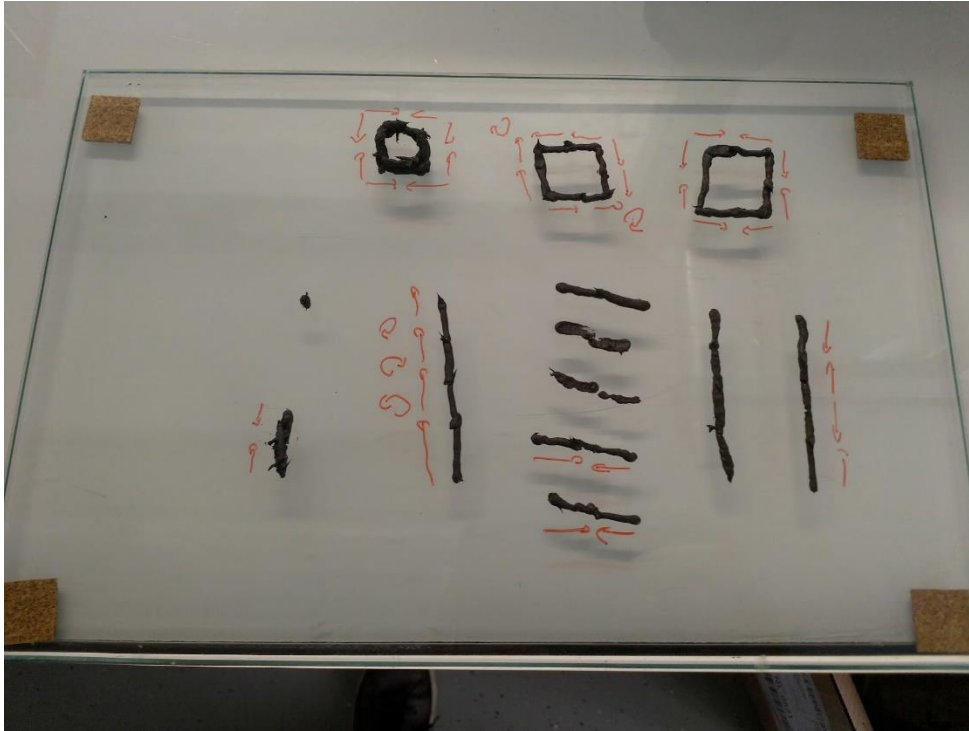
barb connector was used. Otherwise, the extruded ink would still be attracted by the magnet despite the shield.



Lines were drawn onto a glass plate. The magnetization pattern was influenced by changing the extrusion direction. Also flipping the magnet was tried once.



While the first plate was put in the oven at 120°C for one hour to cure, a second mixture was made and a new glass plate was filled with objects, this time using the Go Electrical Steel magnetic shield. Also a thinner luer hose barb connector was used to be able to make thinner lines.

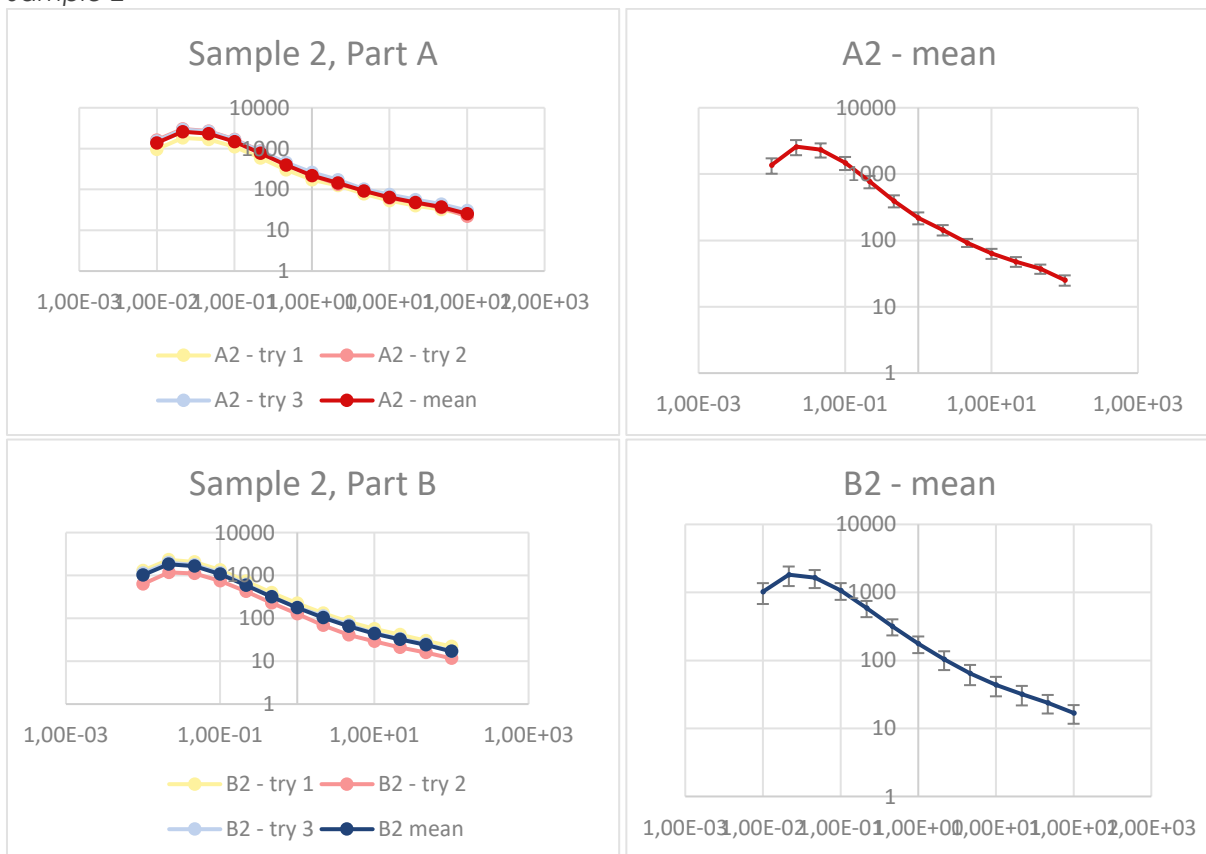


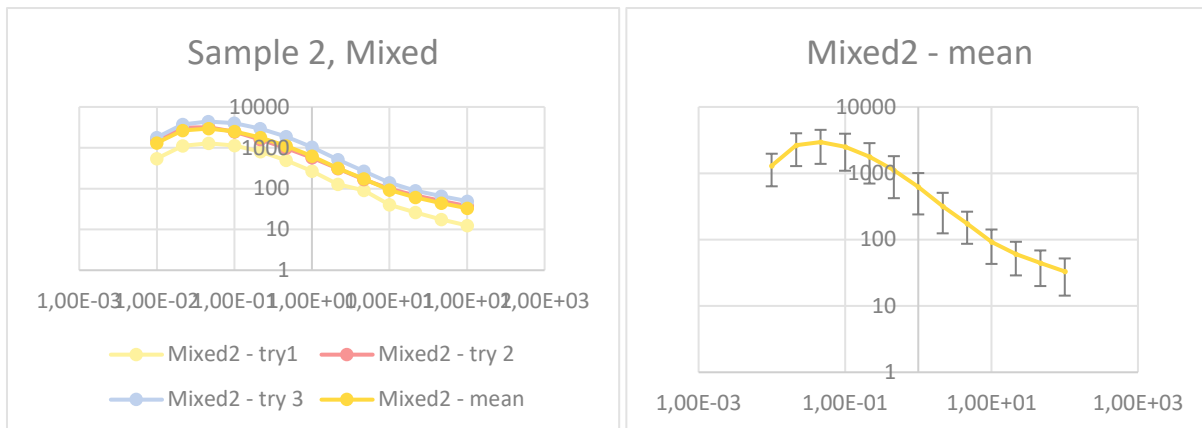
This plate was also left to cure in the oven at 120°C for one hour.

### Results

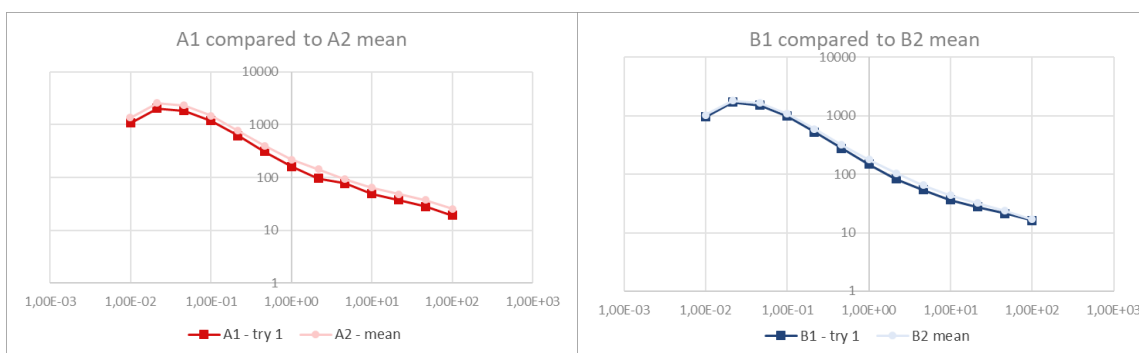
The rheological measurements of the inks made showed the following:

#### Sample 2

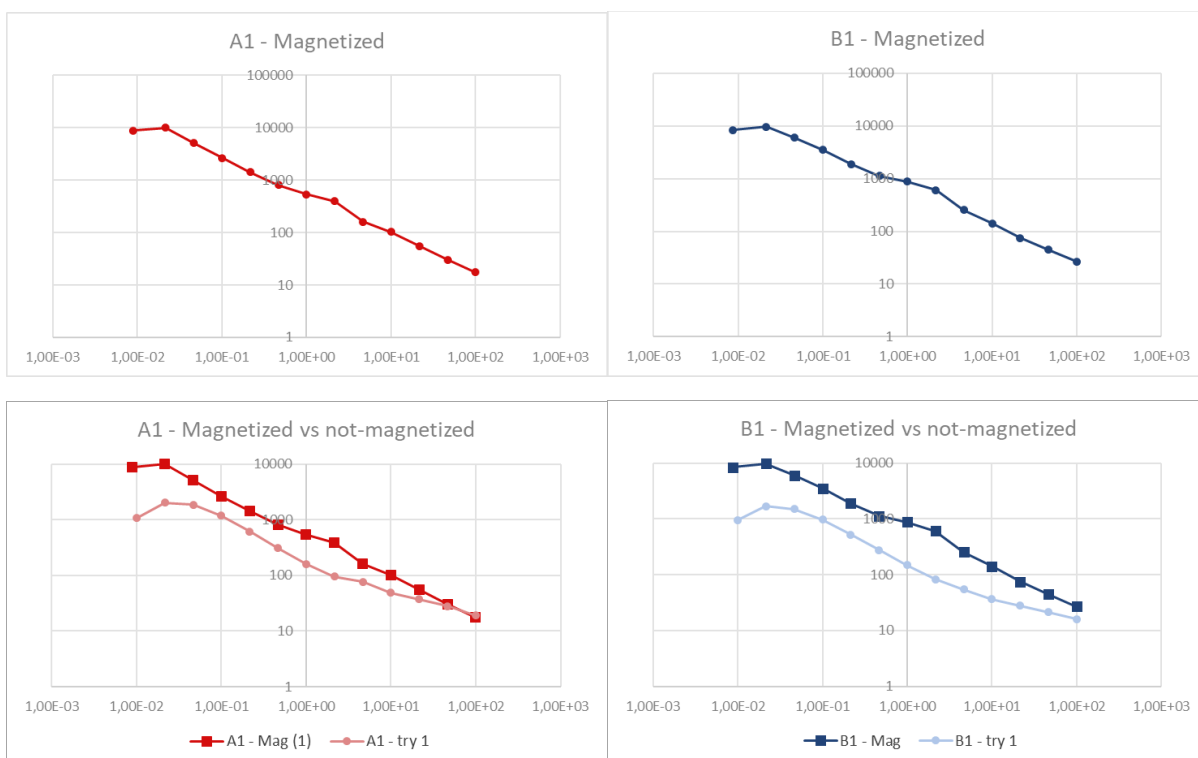




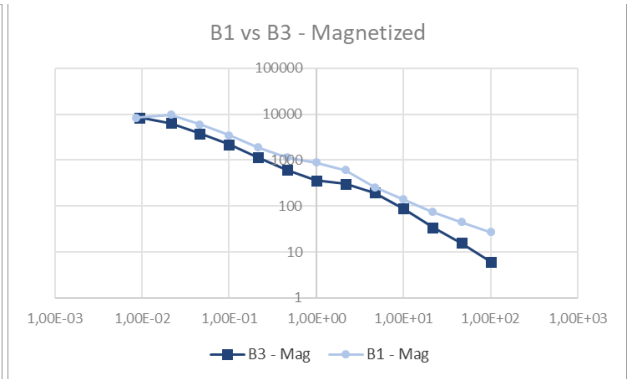
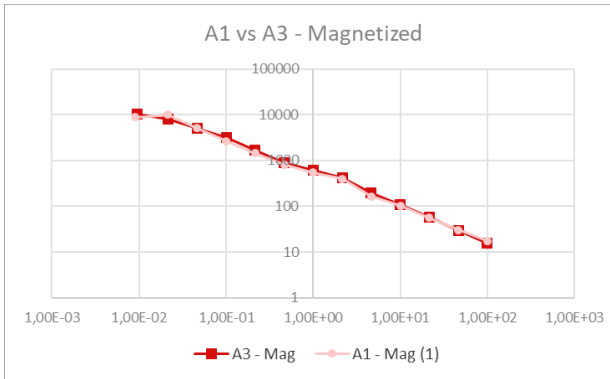
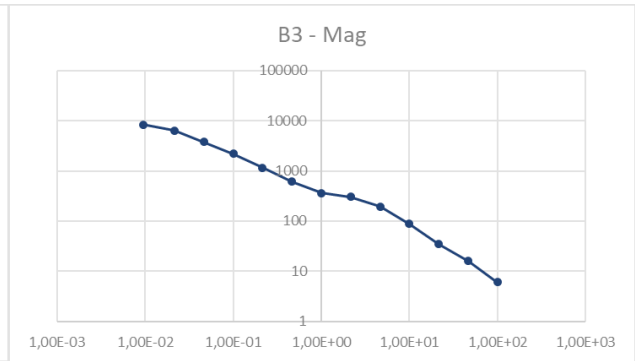
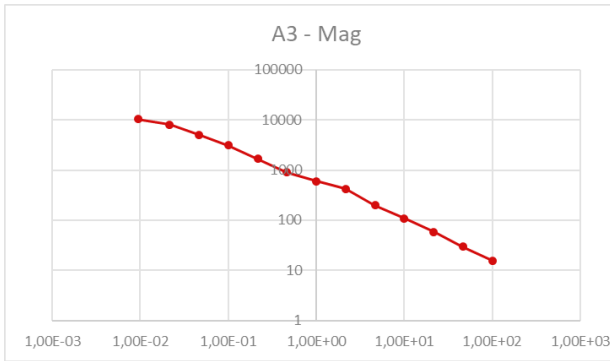
Sample 1 showed similar behavior in the one measurement. So it was believed this measurement was accurate and Sample 1 would show representative values to which magnetized ink could be compared.



Magnetized, Sample 1 showed the following behavior:



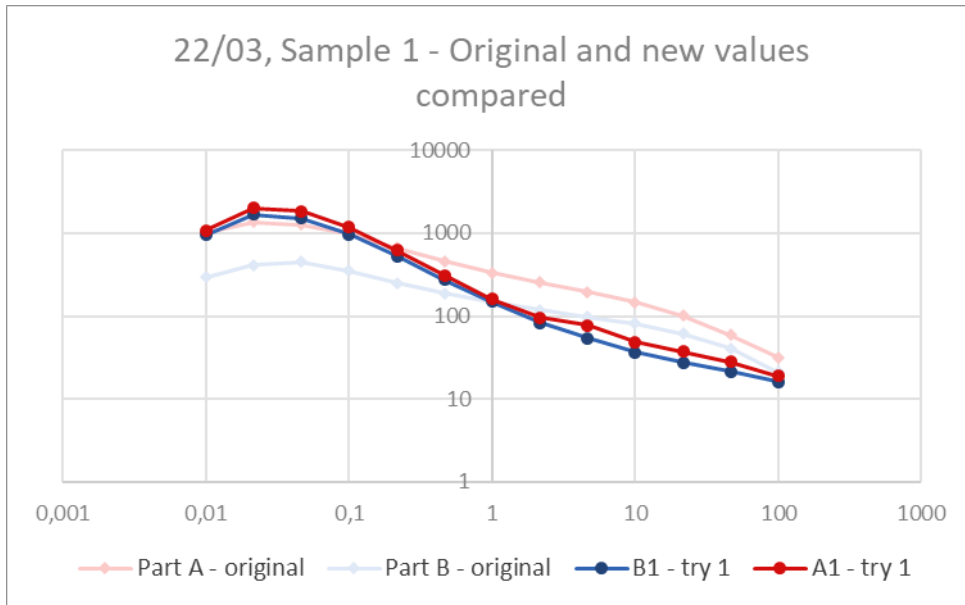
Sample 3, without fumed silica was also measured when magnetized. This showed almost the same values as the magnetized ink with fumed silica.



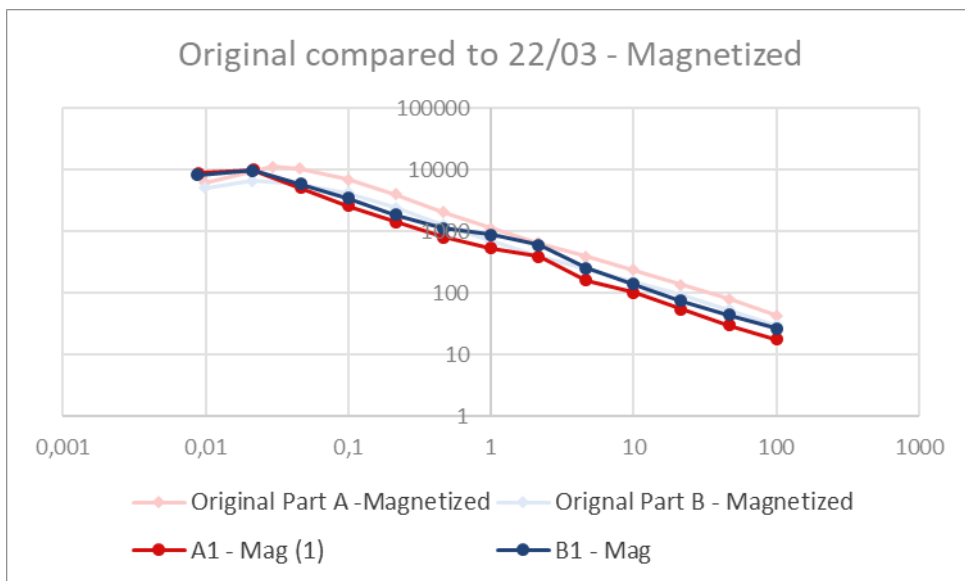


*Measured values vs original values*

Compared to the original values measured by Sanne (Van Vilsteren, 2021), viscosity of the non-magnetized inks are not the same, following the same deviation as Ink Preparation 5 (March 8).

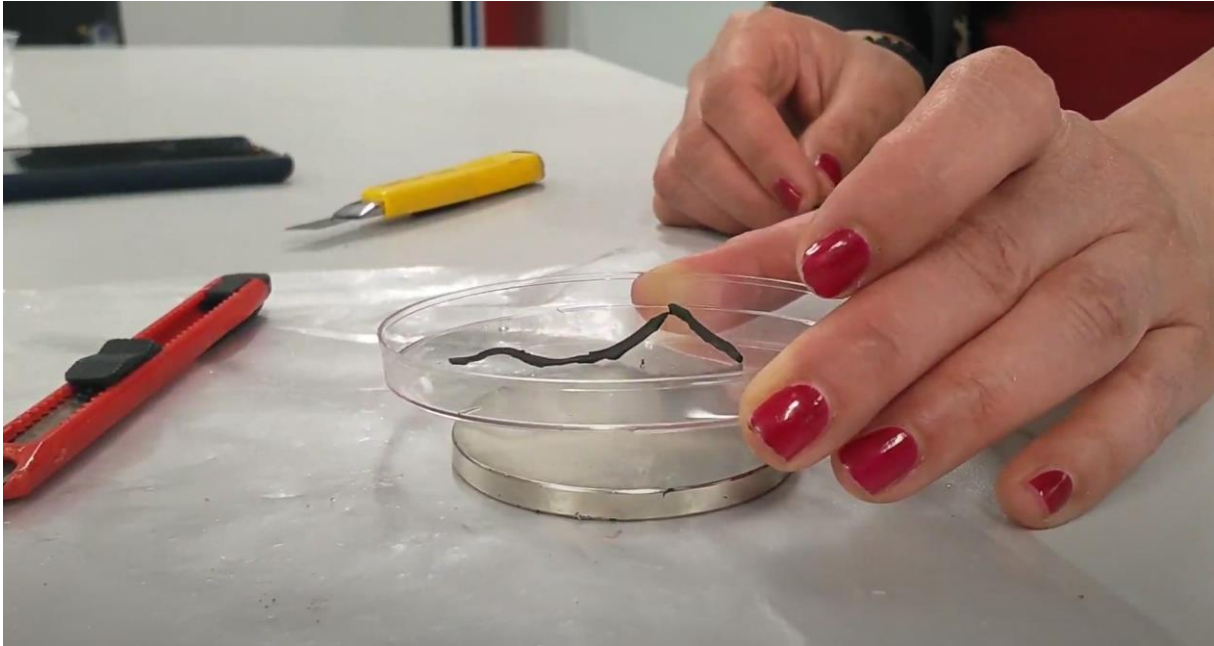


When magnetized, the measurements are more in line with each other.

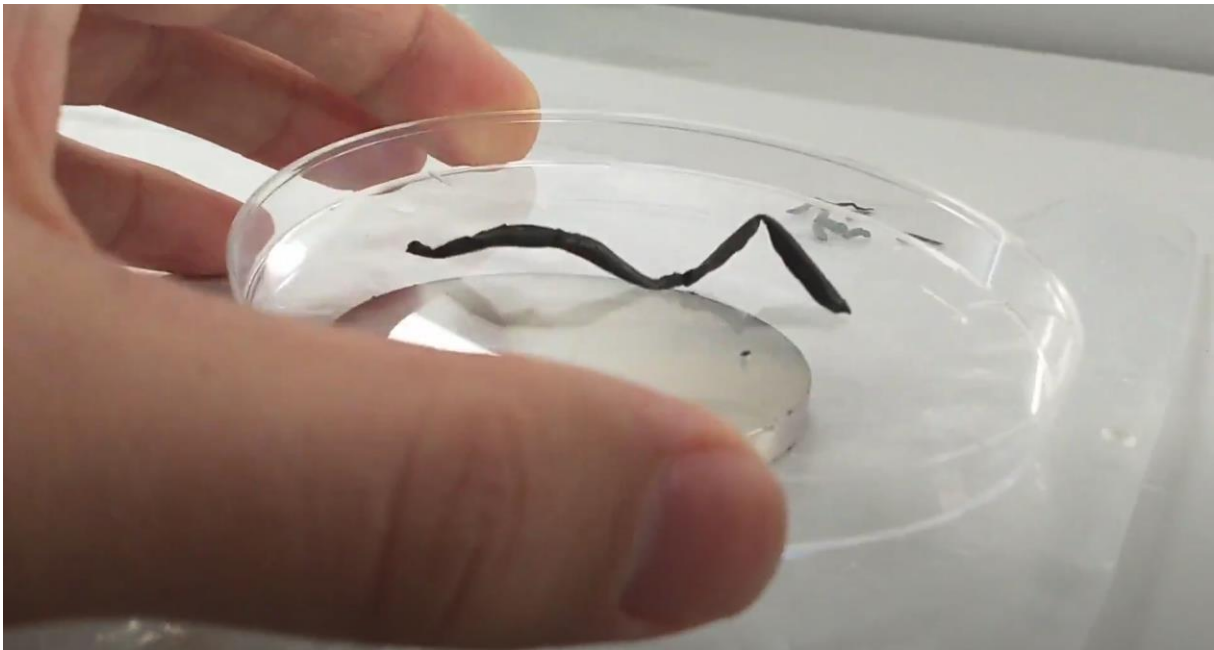


*Demonstrators*

Out of made demonstrators, the first batch showed the least amount of actuation. Some samples could only move one "leg".



The thinnest wires showed the most actuation, especially where the “hinges” are thinnest.



The second batch showed more actuation. Here, the plate was made slippery by using multi-purpose oil. Especially the square showed very stable shape change. Probably because the shape has four points to stand stable on.



### Conclusions

Fumed silica is not needed to give the ink shear thinning properties once it is magnetized. The interaction between the magnetized particles is causing this behavior. It seems the fumed silica is overruled by the magnetization effect, as the graphs of Sample 1 (with  $\text{SiO}_2$ ) and 3 (without  $\text{SiO}_2$ ) are almost identical. This confirms the findings of Kim et al. (2019) in their recipe with PDMS resin.

The soft materials demonstrators show once again that actuating soft magnetic material can be made in the faculty of IDE. Important for good actuation is that the samples must not be too thick, so the smaller the nozzle, the better. Both changing magnet orientation and alternating extrusion direction seems to work to make the magnetization pattern.

The friction the material has with the surface of the plate hinders actuation. When friction is reduced (e.g. with oil), actuation is much more smoothly. This might prove difficult when making products with the material, as the necessity of a slippery surface might prove a difficult criteria to meet.

### Discussion

Measurements were only done once on sample 1 and 3, so it cannot be sure that these measurements are really accurate. It could also be said carefully that the fumed silica was the cause of the measurement difference with the original values throughout the project, as the magnetized values are very similar and the samples with and without fumed silica are very much alike also.

### Further research

The magnetized ink needs to be tried in the 3D printer. Further influence of fumed silica on shape demonstrators (e.g. bonding silicone with particles that would hinder the amount of shape transformation) needs to be examined.

### References

Kim, Y., Parada, G. A., Liu, S., & Zhao, X. (2019). Ferromagnetic soft continuum robots. *Science Robotics*, 4(33). <https://doi.org/10.1126/scirobotics.aax7329>

Van Vilsteren, S. (2021). Designing Magnetic Soft Materials for 4D Printing [Master Thesis, Delft University of Technology]. Tu Delft Educational Repository. <http://resolver.tudelft.nl/uuid:7e05bd4c-4720-4e1f-b13b-7b048602ce42>

## C.1g Ink preparation test 7

Kevin van der Lans – April 5, 2022

### Introduction

Compare shape demos made from sample 1 and 3 of previous test. Influence of fumed silica on shape morphing/bonding silicone with magnetic particles. Also see if thinner nozzles make nicer actuating shapes

### Method

The ink used in this test were the magnetized samples 1 (with fumed silica) and 3 (without fumed silica) from Ink Preparation test 6, March 22.

Shapes were made manually using syringe with a ring magnet attached at the end and a plain steel magnetic shield. Different nozzle bits were used to make smaller/thinner lines. These were:

Nozzle bit color	Inner diameter (mm)	Used for samples
Orange	1.37	1, 3
Green	0.84	1, 3
Pink	0.60	1

The shapes were extruded on two glass plates, for each sample a different plate. Each plate was put in an oven at 120°C for about one hour to cure.

The cured shapes were put on a plastic tray which was made slippery with multi-purpose oil or dishwashing soap mixed with a little bit of water. A NdFeB disk magnet was used to initiate the shape change. Shape articulation was observed and notes were taken to describe how well the shapes morphed.

Testing the shapes was also filmed with a mobile phone. On 4 of these videos, shape recovery analysis was performed with Kinovea software. For the square shapes, the outlines were taken and measurements (in pixels) were compared. By means of the formula  $(\text{NEW}-\text{OLD})/\text{OLD} * 100\%$ , the percentual difference was calculated and the average %-difference was taken.

For the M-shapes, the length of the segments was looked at as well as the angles between segments.

### Results

The notes taken during observation of the shape morphing test of batch 1, made with ink sample 1 (with fumed silica) are as follows:

Test Object	Shape	Nozzle	Observations
1	M	Green	Very good articulation. Unstable because of thinness. Sticks to tray very much (oil used).
2	Square	Orange	Very good articulation. Stable because of shape. Less sticky than previous, but more oil was put on the plate.
3	M, 4 lines thick	Orange	Very bad articulation. Sticks to tray very much (oil used). Does weird flipping movement.
4	M	Pink	Mild articulation, wants to jump to edge of magnet (because it is so thin and light?)

5	O, 4 lines thick	Orange	Mild articulation, sticks to tray very much (with oil) and tries to flip around towards edge of magnet when less sticky (with soap)
6	M	Green	Quite good articulation, remarkably stable despite being a thin single line.
7	Square	Pink	Very good articulation. Very jumpy because small.
8	Square, 3 lines thick	Orange	Good articulation, just wanky movement.
9	2x2 Grid	Green	OK articulation. Very stable.
<b>Very good actuation</b>		3 (33%)	
<b>(Quite) good actuation</b>		2 (22%)	
<b>OK/Mild actuation</b>		3 (33%)	
<b>Bad actuation</b>		1 (11%)	

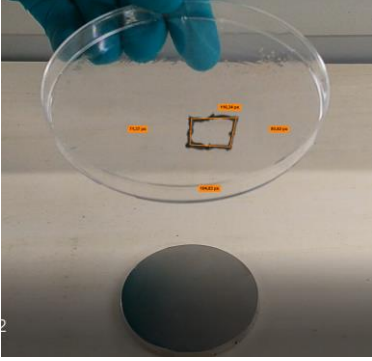
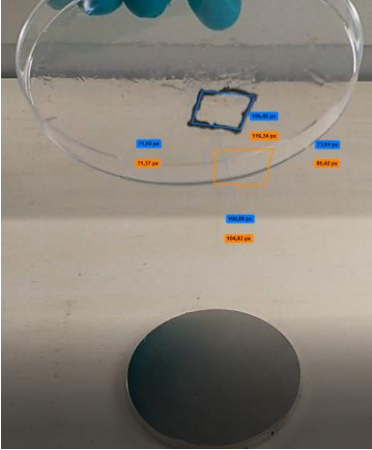
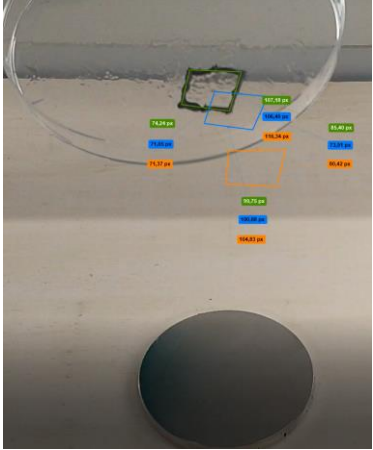
For Batch 2 (without fumed silica) the observations were as follows:

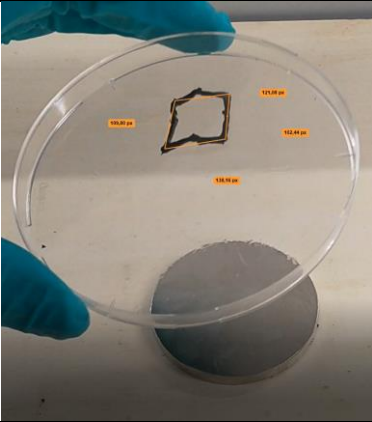
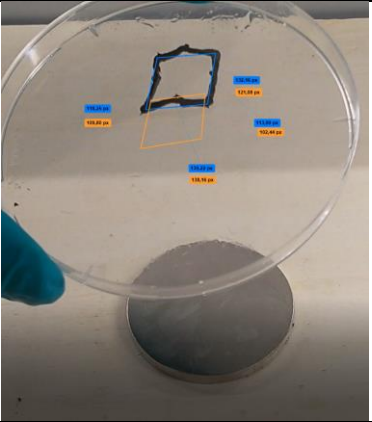
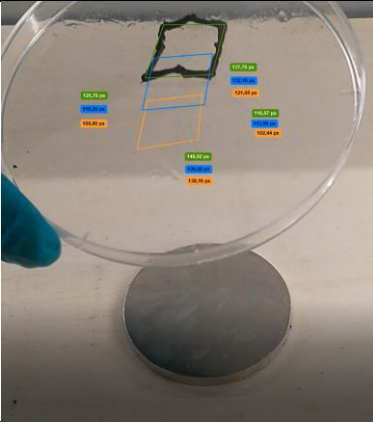
Test Object	Shape	Nozzle	Observations
1	M	Orange	Very good articulation when on soap, but shape is not M but more N.
2	M	Orange	Very unstable. Quite sticky to tray OK articulation when loose, but vertical
3	Square	Orange	Very sticky, quite good articulation once loose
4	Square	Orange	Again sticky, even with soap. Articulation OK (also cut loose from the plate unevenly).
5	Square	Green	Weird articulation, probably not "printed" well.
6	M, 2 lines thick	Green	Very good articulation and excellent stability. Good shape recovery as well
7	X-2 lines thick	Green	Very stable and very good articulation
8	Square, 2 lines thick	Green	Jumpy, articulation is very good but not the correct shape.
9	M, 4 lines thick	Orange	Better articulation than Batch 1. Weak articulation but very stable
10	Square	Green	Very good articulation, not super stable because of thinness.
11	2x2 grid	Green	Good articulation, just weird shape
12	M	Green	Good articulation, OK stability.
<b>Very good actuation</b>		5 (42%)	
<b>(Quite) good actuation</b>		3 (25%)	
<b>OK/Mild actuation</b>		2 (17%)	
<b>Bad actuation</b>		2 (17%)	

#### Shape recovery analysis

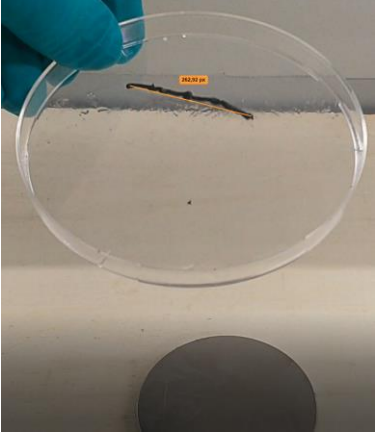
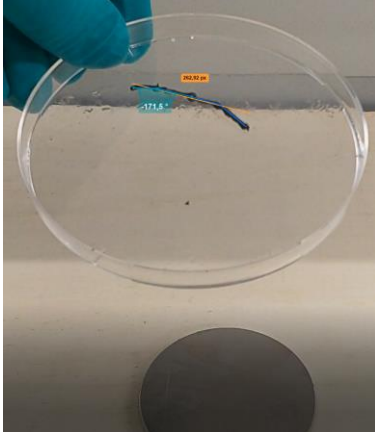
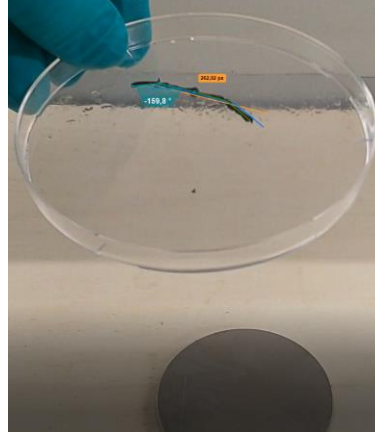
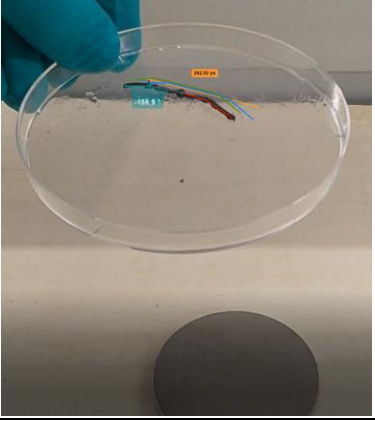
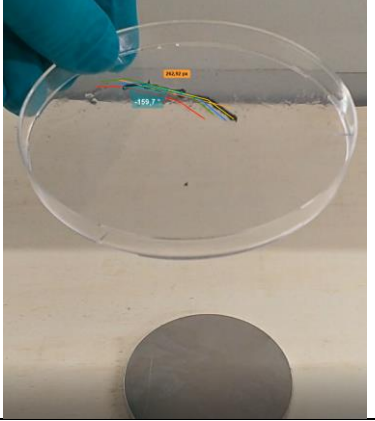
The shapes were outlined before actuation and after 2-3 more times of actuating the object with the magnet.

Test Object 2, Batch 1 (Square)		
Before	1 <sup>st</sup> actuation	2 <sup>nd</sup> actuation

		
116,34 80,42 104,83 71,37	106,45 73,91 100,88 71,05	107,18 85,4 99,75 74,24
	-5,2%	-0,63%


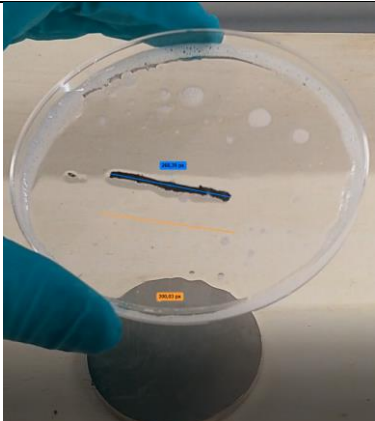
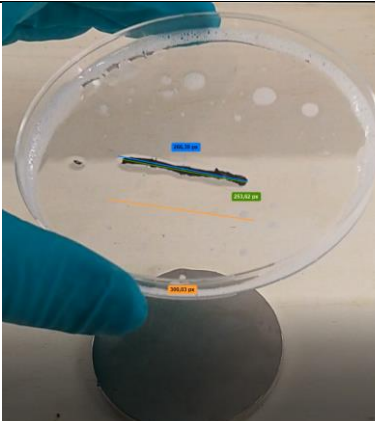
Test Object 3, Batch 2 (Square)		
Before	1 <sup>st</sup> actuation	2 <sup>nd</sup> actuation
		
121,08 102,44 138,16 109,8	132,16 113,99 139,22 118,25	137,76 116,97 148,92 125,76
	+7,22%	+12,57%

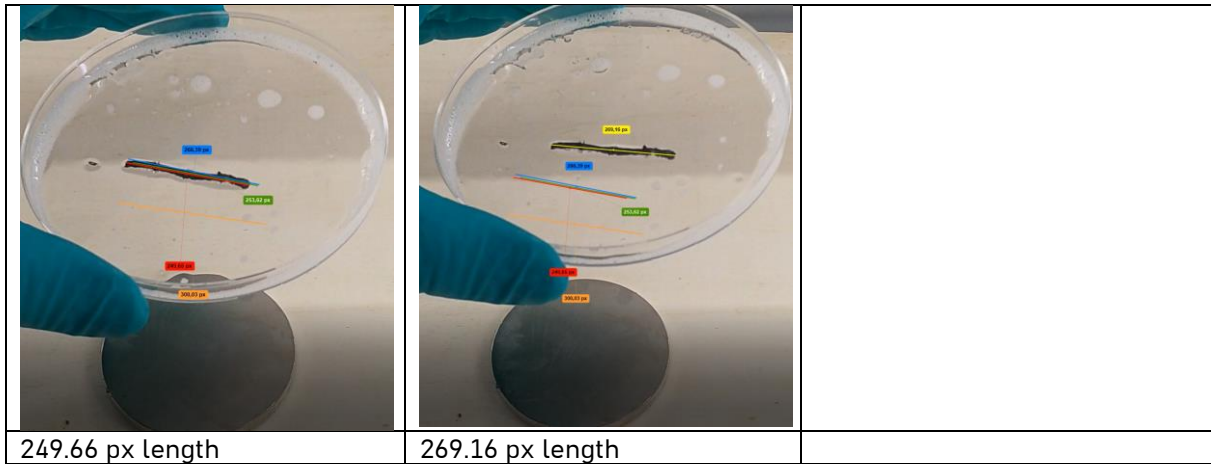
Test Object 6, Batch 1 (M)		
Before	1 <sup>st</sup> actuation	2 <sup>nd</sup> actuation

		
262,92 px length	-171.5 deg angle	-159.8 deg angle
3 <sup>rd</sup> actuation	4 <sup>th</sup> actuation	
		
-166.9 deg angle	-159.7 deg angle	

The angle between the two left sections indicates that the shape does not fully recover to the flat line. The average deviation angle is 15,5 degrees (-164,5).

For the M-shape from the second batch, no angle was measured because there was no measurable angle present in the object, so the length was measured to see how much compressed the shape was as result of having been the M-shape.

Test Object 6, Batch 2 (M)		
Before	1 <sup>st</sup> actuation	2 <sup>nd</sup> actuation
		
300.03 px length	266.39 px length	253.62 px length
3 <sup>rd</sup> actuation	4 <sup>th</sup> actuation	



The length is not entirely consistent, indicating that the object does not recover fully. De average length deviation is 40 px (259,7 px; 13,4%)

### Conclusion

Thinner objects seem to actuate better but are also less stable. Friction between object and tray is a very limiting factor for shape morphing.

No difference in articulation was observed for fumed silica and non-fumed silica samples. Both sample batches shape-morphed good but the shape they morphed into was not always as expected/printed. This could just be human error in making the shapes.

The stability of the shape seems to influence the shape recovery, friction between plate and object might also play a role



## C.1h Ink preparation test 8

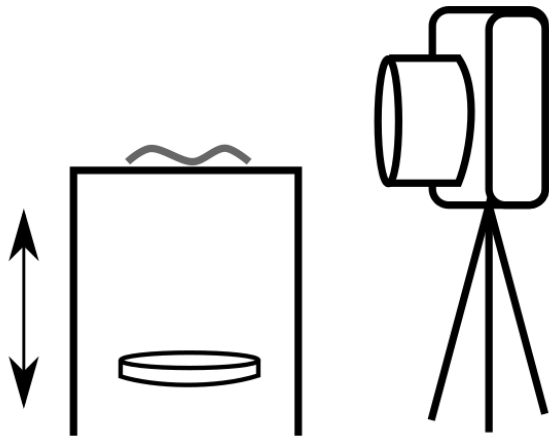
Kevin van der Lans – April 22, 2022

### Introduction

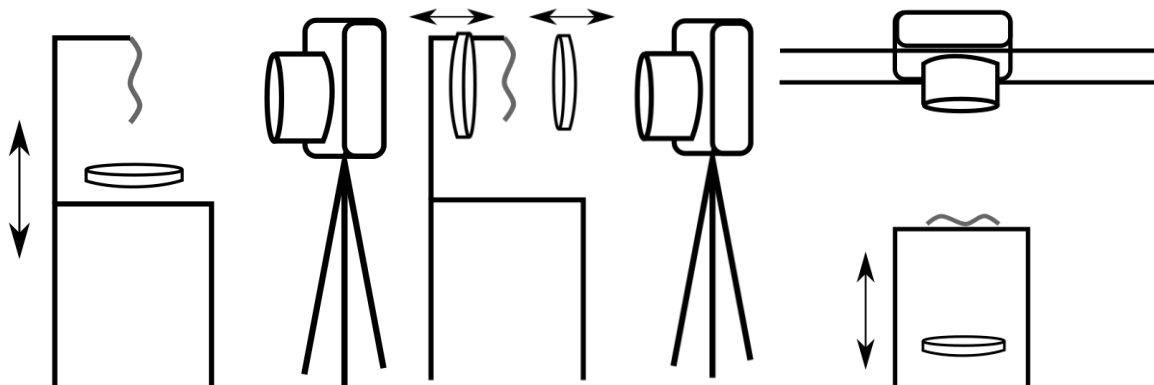
In this experiment, shape recovery is retried with a new test set-up to hopefully get a more consistent result.

### Method

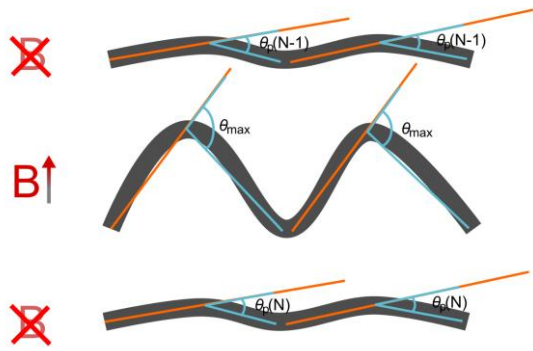
The MSM object was placed on a platform, underneath which a permanent magnet was moved up and down to activate the shape change. A (phone) camera was placed besides the platform on a stand looking at the MSM object almost perpendicular.



It was also tried to hang the MSM object from a boom arm and filming its elongation and contraction in two magnetization ways and filming the MSM object straight from above.



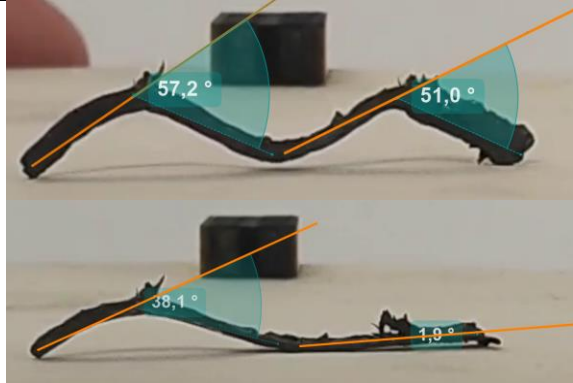
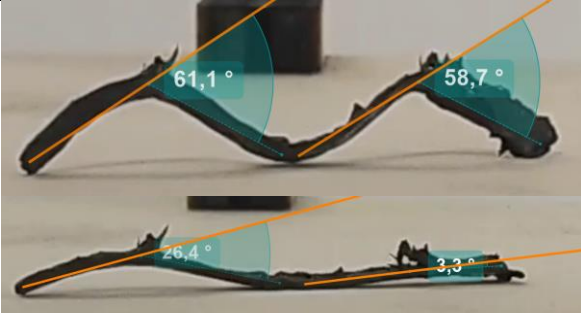
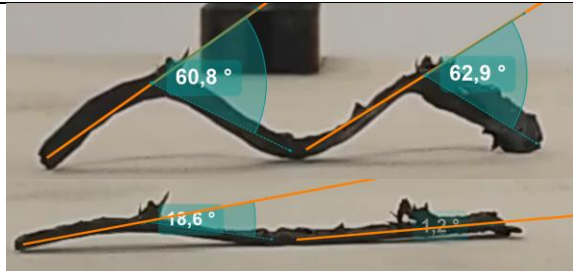
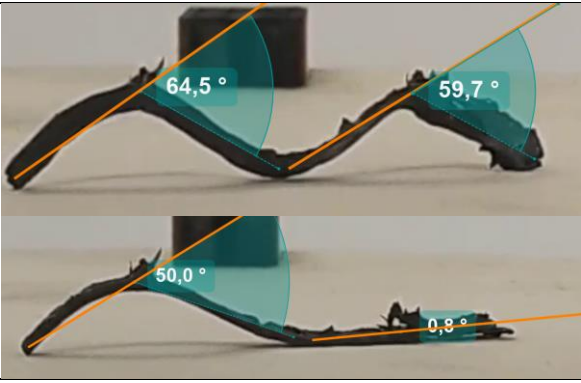
The shape recover ratio is calculated by the formula  $R_r = \frac{\theta_{max} - \theta_p(N)}{\theta_{max} - \theta_p(N-1)} * 100\%$  where  $\theta_{max}$  is the maximum angle in the deformed state and  $\theta_p$  is the difference between the (previous) default, non actuated angle and the recovered angle, also known as the permanent angle after recovery  $\theta_p = \theta_{default} - \theta_{recovered}$  (Zhu et al., 2012; Lui et al., 2010; Gall et al., 2005).



Because the tested M-shape has two angles (actually three),  $R_r$  of both angles was calculated and the average was taken. It is possible that the shape achieved a shape recovery of more than 100%, because sometimes the remaining angle ( $\theta_p$ ) was less than the previous actuation cycle. Therefore, the  $R_r$  related to the original (default) shape is put behind each value in brackets.

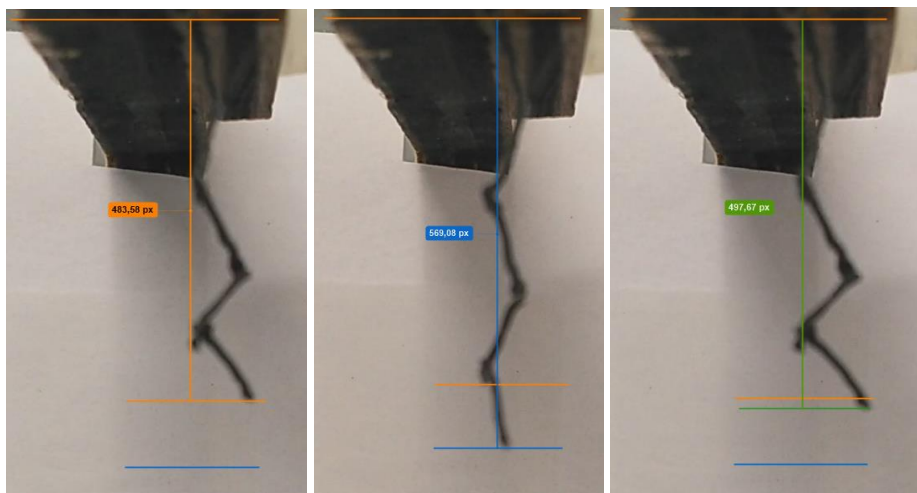
### Results

Default shape	1 <sup>st</sup> actuation
	$R_r = (81,1\% + 95,9\%)/2 = 88,5\%$ (88,5%)
2 <sup>nd</sup> actuation	3 <sup>rd</sup> actuation
$R_r = 103,147\%$ (90,2%)	$R_r = 100,8\%$ (90,6%)
4 <sup>th</sup> actuation	5 <sup>th</sup> actuation

	
Rr = 69,4% (64,8%)	Rr = 124,2 (75,6%)
6 <sup>th</sup> actuation	7 <sup>th</sup> actuation
	
Rr = 113,1% (83,8%)	Rr = 66,13% (60,6%)

### Strain

In a different experiment, the elongation of a zigzag wire was measured.



Out of this one (pilot) measurement, using the same formula, the  $\square_p$  is  $497,67 - 483,58 = 14,09$  px.  $\square_{\max}$  is  $569,08$  px. Rr is thus  $(569,08 - 14,09)/569,08 * 100\% = 97,6\%$

### Conclusion

If the left leg does not get stuck on the wood, the shape recovery ratio is around 90% which is Ok I guess...

Moving the magnet instead of the tray with the shape makes it much easier to analyze the shape recovery.

## References

- Gall, K., Yakacki, C.M., Liu, Y., Shandas, R., Willett, N. and Anseth, K.S. (2005), Thermomechanics of the shape memory effect in polymers for biomedical applications. *Journal of Biomedical Materials Research*, 73A(3), 339-348. <https://doi-org.tudelft.idm.oclc.org/10.1002/jbm.a.30296>
- Liu, Y., Han, C., Tan, H. & Du, X. (2010). Thermal, mechanical and shape memory properties of shape memory epoxy resin, *Materials Science and Engineering: A*, 527(10-11), 2510-2514. <https://doi.org/10.1016/j.msea.2009.12.014>
- Zhu, Y., Hu, J., Luo, H., Young, R.J., Deng, L., Zhang, S., Fanc Y. & Yec, G. (2012). Rapidly switchable water-sensitive shape-memory cellulose/elastomer nano-composites. *Soft Matter*, 8, 2509-2517. <https://doi.org/10.1039/C2SM07035A>

## C.2 3D printer trials

This section holds all experiments and trials with the Ultimaker 3D printer, sorted by date.

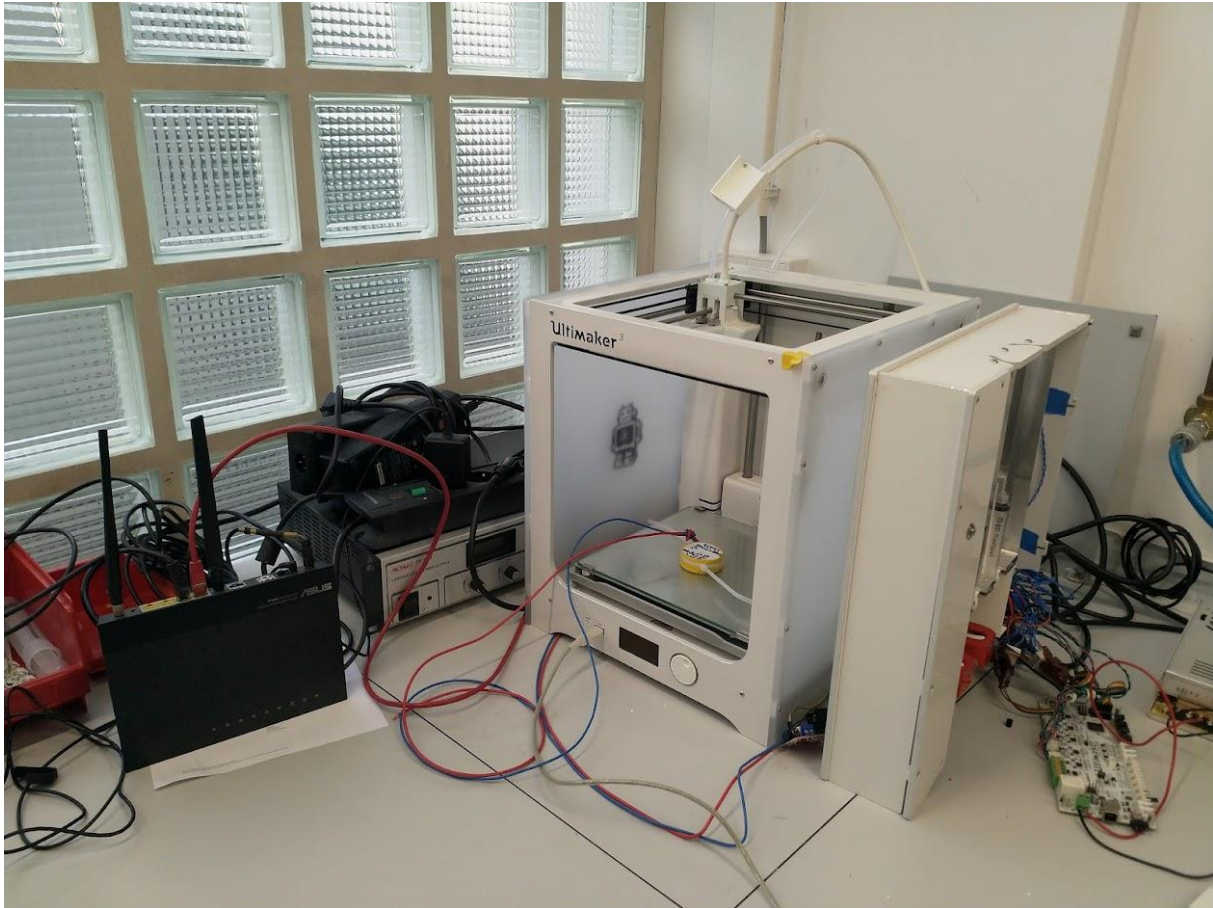
---

## C.2a 3D printer trial 1

Februari 8, 2022 - Kevin van der Lans

### Introduction

For the manufacturing of magnetic shape objects, a modified 3D printer is used. The 3D printer used in the Thesis of Sanne is an Ultimaker 3 with a special extrusion system prototype with two syringes (Van Vilsteren, 2021; Figure 1).



*Figure 1: Dual syringe printer with experimental extrusion system (right) and router (left).*

Because this printer has not been used for about five months and I have never used this machine before, the goal of this experiment is to get the printer moving to see if it has survived its hibernation and to see if all necessary components are still around. In addition, a first attempt was made to write some G-Code and sent to the printer.

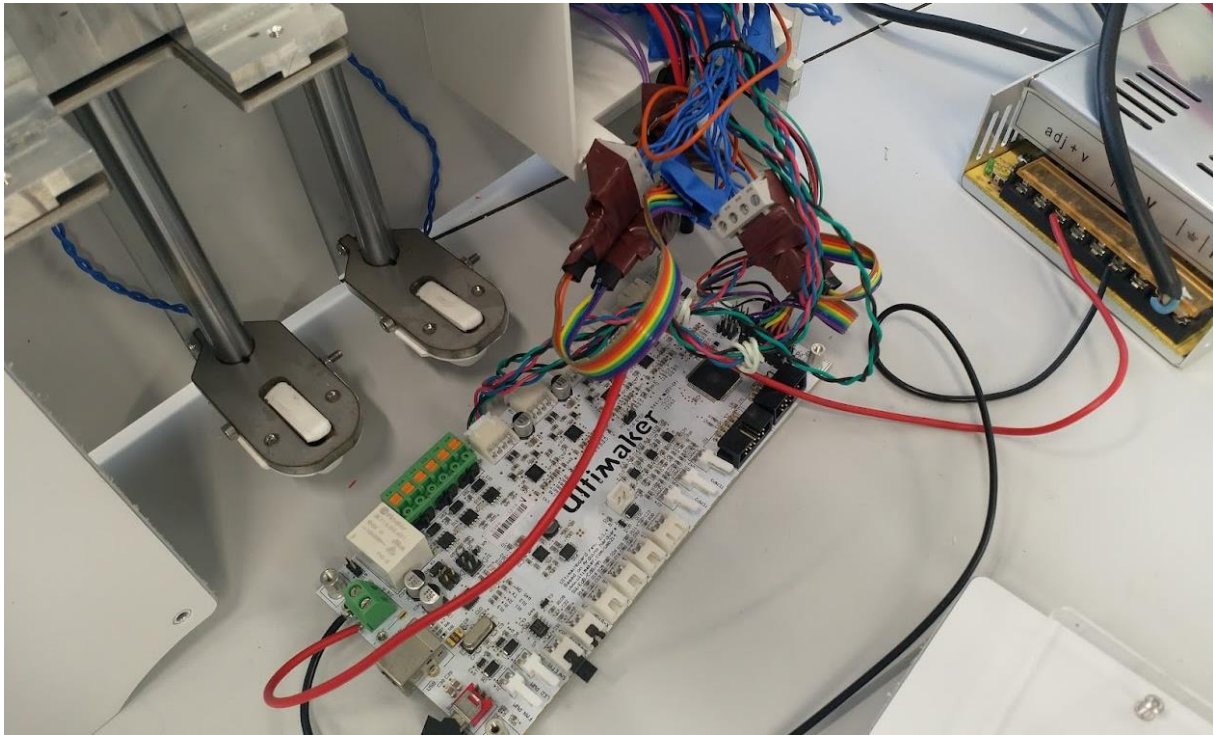
### Materials

- Modified Ultimaker 3
- Dual syringe extrusion system (prototype by Ultimaker)
- USB type A to USB type B cable
- Ethernet router
- 2x ethernet cable
- Laptop
- Cura 2.7 (downloaded from: <https://github.com/Ultimaker/Cura/releases/tag/2.7.0>)
- Power supply
- Power strip
- 60ml to 10ml syringe conversion piece

- Piston grip enlargers
- Red holding caps
- Extended static mixing nozzle with thread

## Method

The printer was found in one piece, however some components were missing and/or disorganized. For example, the PCB of the extrusion system was laying loose on the desk (Figure 2). The printer was first put together and afterwards it was attempted to send G-code to the printer.



*Figure 2: the extrusion PCB hanging out of the casing under a nest of wires.*

### *Assembling the printer*

To make the 3D printer move again, the instructions by Sanne van Vilsteren were used (2021; page 264 – 267). First, all components mentioned were gathered, that are the 60ml to 10ml syringe conversion piece, grip enlargers, holding caps and mixing nozzles.

Next the printer was plugged into the power strip and turned on. The printer turned on without a problem. The printer was turned off, after which the extrusion system was connected via the USB cable. The extrusion system has a separate power supply that plugs into the power strip. First the printer was turned on again, after which the extrusion system was turned on via the on/off switch on the extrusion PCB.

Next, the round button was pressed for a few seconds. If the two plates that push the syringe pistons up and down are not completely down already, they move down completely at this step. The button is blinking green.

The 60 to 10 ml syringe conversion pieces with the 10 ml syringes in them are now placed in the syringe slots. The syringe pistons should be brought down (open) completely for this test and were not filled.

The button was again pressed for a few seconds and the plates started moving up until the triggers on the plates were pressed down by the syringe pistons. The button stopped blinking and gave a solid green light.

The piston grip enlargers were placed on the ends where the piston touches the plate. The red cap was placed over the plates and pistons to make sure the piston remains stuck on the moving plate so that the pistons can be moved down (open) by the plates by a negative G-code value for retraction of the ink to stop extrusion and limit spilling.

#### Connecting to a laptop

To send G-code to the Ultimaker 3D printer, it should be connected to a laptop via a router. This is because the USB slot of the printer is occupied by the dual syringe extrusion system and thus cannot be used to load G-code in the printer.

To connect the 3D printer to a laptop, an ethernet cable is connected in the back of the 3D printer to a router. The laptop is connected to the same router. This makes it possible to find the 3D printer via the now established network. The router does not have to be connected to the internet.

To find the printer and send G-code over the ethernet connection, Cura 2.7.0 was used. The printer must first be found manually via settings > printers > manage printers. To find the printer on the network, the printer's IP address is needed, which can be read off the 3D printer display. When filled in the IP address, the button on the 3D printer needs to be pressed to give permission to connect, after which the printer is connected.

#### Sending G-code

The Cura 2.7.0 program is only used to send G-code to the printer. It cannot be used to slice a model, presumably because of the heavily modified firmware on the printer. When loading the G-code into Cura, it also cannot be modified (Figure 3).

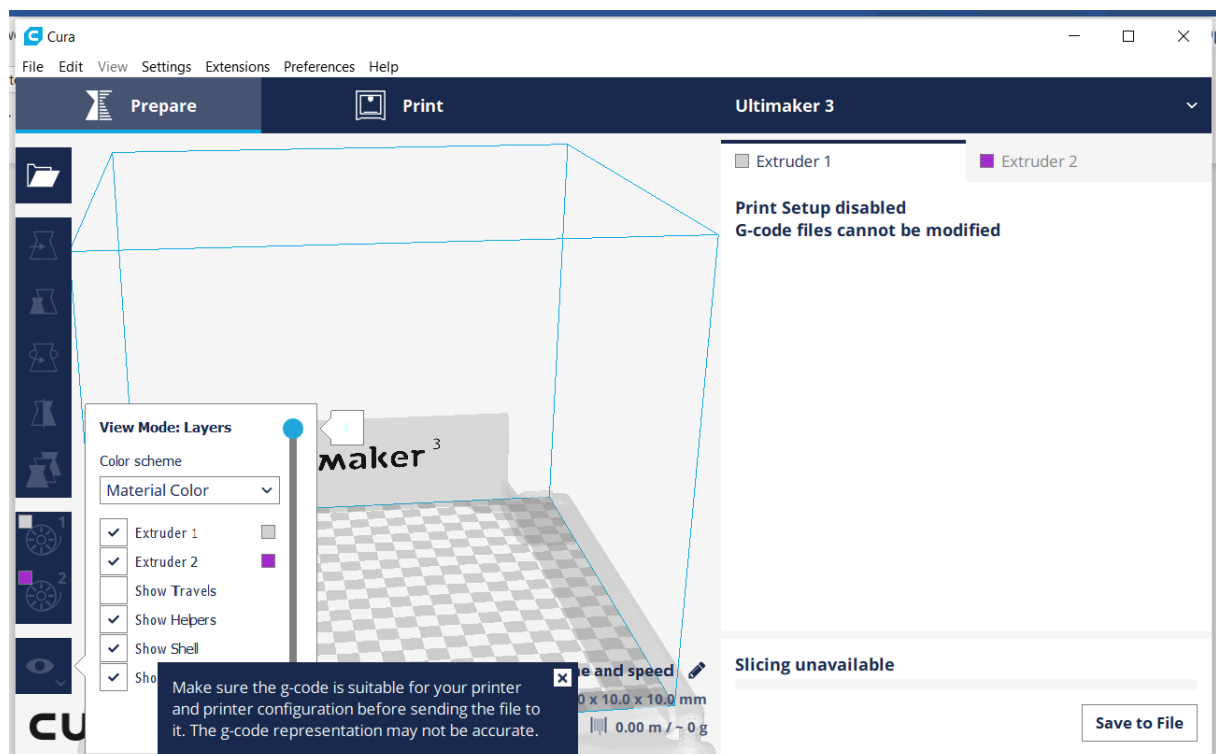


Figure 3: Cura is in this case only used to send G-code to the printer. No g-code can be generated and loaded g-code cannot be edited.

The G-code send was the file "Measuring volume and speed" by Sanne. This G-code does the following:

#### Some initialization commands

```
;START_OF_HEADER  
;HEADER_VERSION:0.1
```



```

;FLAVOR:Griffin
;GENERATOR.NAME:Cura_SteamEngine
;GENERATOR.VERSION:2.3.1
;GENERATOR.BUILD_DATE:2016-11-04
;TARGET_MACHINE.NAME:Ultimaker 3
Setting initial nozzle and bed temperatures
;EXTRUDER_TRAIN.0.INITIAL_TEMPERATURE:60
;EXTRUDER_TRAIN.0.MATERIAL.VOLUME_USED:5429
;EXTRUDER_TRAIN.0.MATERIAL.GUID:506c9f0d-e3aa-4bd4-b2d2-23e2425b1aa9
;EXTRUDER_TRAIN.0.NOZZLE.DIAMETER:0.4
;BUILD_PLATE.INITIAL_TEMPERATURE:32
Specifying print bed size
;PRINT.TIME:2718
;PRINT.SIZE.MIN.X:0
;PRINT.SIZE.MIN.Y:0
;PRINT.SIZE.MIN.Z:0
;PRINT.SIZE.MAX.X:215
;PRINT.SIZE.MAX.Y:215
;PRINT.SIZE.MAX.Z:200
;END_OF_HEADER
;Generated with Cura_SteamEngine 2.3.1

G0 F10000 X178 Y6 Z190 Move print head to coordinates X=178 and Y=6 and the build plate to Z=190 at
feedrate (speed) 10000 mm/min
M107 Turn off the cooling fan
G0 F10000 X100 Y100 Z190 Move print head to coordinates X=100 and Y=100 and the build plate to Z=190 at
feedrate 10000 mm/min
M84 Disable all motors
M400 Wait until all previous commands are finished
G1 F1 A89 B89 Move extrusion A and B (= both of the dual syringe extrusion units on the separate system) a
value of 89 at feedrate of 1 mm/min
M400 Wait until all previous commands are finished
G4 P1000 Do nothing for 1000 milliseconds
M400 Wait until all previous commands are finished
M106 Turn on cooling fan

M104 S0 Set extruder temperature to 0
M104 T1 S0 Set the other extruder temperature to 0

;End of Gcode
;SETTING_3 {"global_quality": "[general]\\nversion = 2\\nname = empty\\ndefinit
;SETTING_3 on = ultimaker3\\n\\n[metadata]\\ntype = quality_changes\\nquality_ty
;SETTING_3 pe = draft\\n\\n[values]\\n\\n", "extruder_quality": "[[general]\\nve
;SETTING_3 rsion = 2\\nname = empty\\ndefinition = ultimaker3\\n\\n[metadata]\\n
;SETTING_3 type = quality_changes\\nextruder = ultimaker3_extruder_left\\nqualit
;SETTING_3 y_type = draft\\n\\n[values]\\nbrim_width = 0\\n\\n", "[general]\\nve
;SETTING_3 rsion = 2\\nname = empty\\ndefinition = ultimaker3\\n\\n[metadata]\\n
;SETTING_3 type = quality_changes\\nextruder = ultimaker3_extruder_right\\nquali
;SETTING_3 ty_type = draft\\n\\n[values]\\n\\n"}

```

It was used because it moved both the print head and the extrusion system so it could be checked if all components were (still) working. Also it saved time opposed to writing a new G-code myself.

## Results

The printer could be turned on and made moving successfully. Also the uploading of the G-code had no troubles. However, when executing the “Measuring volume and speed” G-code file, the

motors made a weird noise, but did turn slowly. The F-value (speed) to control the extrusion motors was adjusted in the G-code to a higher value and the noise was less reduced.

### Conclusion

The modified Ultimaker 3 3D printer and the separate extrusion system works after 5 months of hibernation. All necessary components are present to make the printer move and try to extrude the magnetic ink.

### Discussion

The H-Bridge to control the electromagnet was not found, however it was not relevant for this test. Trying to control the electromagnet intended to change the magnetic particles in the elastomer during printing was not done in this test. However, the goal was for me to be able to control the machine for further testing of the extrusion system.

### Further research

In further tests, the extrusion of the two-component magnetic ink should be tested, using the latest 3D print experiment from Sanne (Van Vilsteren, 2021, page 229 – 239) as a reference. In order to do this, the magnetic ink recipe that was used in this experiment must be remade and tested on its rheometric properties to see if they are the same as the ink made by Sanne. The ink will be loaded into the syringes and attempted to be extruded using the PVC tubes used in the latest experiment to troubleshoot the problems present. In a later stage, stiffer tubes will be used to see if this improves the extrusion of the ink.

### References

Van Vilsteren, S. (2021). Designing Magnetic Soft Materials for 4D Printing [Master Thesis, Delft University of Technology]. Tu Delft Educational Repository.  
<http://resolver.tudelft.nl/uuid:7e05bd4c-4720-4e1f-b13b-7b048602ce42>

## C.2b 3D printer trial 2

Februari 8, 2022 - Kevin van der Lans

### Introduction

In the former 3D printer trial, it was attempted to get the printer out of hibernation and see if it was still operative. In this previous test, no ink was used (a “dry” test). In this test, the goal is to try and extrude (non-magnetized) ink to recreate the latest progress Sanne made on the printer (Van Vilsteren, 2021, page 229-239) and start to troubleshoot the issues she faced.

### Materials

For this test, both the 3D printer from Ultimaker with external dual syringe extrusion system and non-magnetized ink made on February 9 was used.

#### 3D printer set-up

- Modified Ultimaker 3
- Dual syringe extrusion system (prototype by Ultimaker)
- USB type A to USB type B cable
- Ethernet router
- 2x ethernet cable
- Laptop
- Cura 2.7 (downloaded from: <https://github.com/Ultimaker/Cura/releases/tag/2.7.0>)
- Power supply
- Power strip
- 60ml to 10ml syringe conversion piece
- Piston grip enlargers
- Red holding caps
- Extended static mixing nozzle with thread
- 2x65 cm of PVC tubing 3x6mm diameter (<https://www.arestho.nl/transparante-pvc-slang.html>)
- 2x female Luer lock (4.8mm)

#### Measurements

- Digital caliper
- ruler

*Non-magnetized ink (from “ink preparation trial 2”, February 9)*

2-component ink ingredients:

- 12.6 grams Ecoflex 00-10 Part A
- 12.6 grams Ecoflex 00-10 Part B
- 2x 22.5 grams Iron powder (<10 microns, 99,5% purity)  
<https://www.fishersci.nl/shop/products/iron-powder-spherical-10-micron-99-9-metals-basis-99-5-thermo-scientific/11360689>
- 2x 0.30 grams fumed silica (SiO<sub>2</sub>)

Utensils:

- Two paper cups
- Two 10 ml syringes
- Mixing Spatulas
- Analytical scale with precision up to 3 decimals
- Masking tape
- Pen
- Paper towels

## Method

The ink used was the ink made on February 9 (see “ink preparation trial 2”). In summary, the procedure was as follows:

- Poor 12.6 grams of Ecoflex Part A in the cup on the scale with a spatula.
- Poor half the amount of Iron powder (22.5 g) in the cup with the Ecoflex Part A using a spatula.
- Take the cup from the scale and mix the Iron and Ecoflex Part A together manually using a spatula.
- Place the cup back on the scale.
- Add half the amount of fumed silica (0.30 g) to the Ecoflex Part A/ Iron powder mixture.
- Mix again my hand.
- Repeat for Ecoflex part B
- Put two-component ink in two separate 10ml syringes and label them.

### *3D printer initialization*

The instructions by Sanne van Vilsteren were used (2021; page 264 – 267) to assemble the 3D printer for extrusion. First, all components mentioned were gathered, that are the 60ml to 10ml syringe conversion piece, grip enlargers, holding caps and mixing nozzles.

Next the printer was plugged into the power strip and turned on, after which the extrusion system was turned on via the on/off switch on the extrusion PCB.

Next, the round button was pressed for a few seconds. If the two plates that push the syringe pistons up and down are not completely down already, they move down completely at this step. The button is blinking green.

The 60 to 10 ml syringe conversion pieces with **empty** 10 ml syringes in them are now placed in the syringe slots. The syringes were not filled to first see if the extrusion system still worked. Empty tubes were attached to see if the length was good.

The button was again pressed for a few seconds and the plates started moving up until the triggers on the plates were pressed down by the syringe pistons. The button stopped blinking and gave a solid green light.

The piston grip enlargers were placed on the ends where the piston touches the plate. The red cap was placed over the plates and pistons to make sure the piston remains stuck on the moving plate so that the pistons can be moved down (open, retracted) by the plates by a negative G-code value for retraction of the ink to stop extrusion and limit spilling.

After it was established the printer was operative, the syringes filled with ink made on February 9 were placed in the holders. In order to fit the tubes, female Luer locks (4.8mm) were placed on the syringes where the tubes were pressure-fitted on. The other end of the tubes were pressure-fitted on the ends of the static mixing nozzle.

The static mixing nozzle was not placed in the printhead, because it was found that it increased the changes of the mixing nozzle to break and it was not necessary because only extrusion was tested and there was not need to print any geometry yet.

### *Connecting to a laptop*

To send G-code to the Ultimaker 3D printer, it should be connected to a laptop via a router. This is because the USB slot of the printer is occupied by the dual syringe extrusion system and thus cannot be used to load G-code in the printer.

To connect the 3D printer to a laptop, an ethernet cable is connected in the back of the 3D printer to a router. The laptop is connected to the same router. This makes it possible to find the 3D printer via the now established network. The router does not have to be connected to the internet.

To find the printer and send G-code over the ethernet connection, Cura 2.7.0 was used. The printer must first be found manually via settings > printers > manage printers. To find the printer on the network, the printer's IP address is needed, which can be read off the 3D printer display. When filled in the IP address, the button on the 3D printer needs to be pressed to give permission to connect, after which the printer is connected.

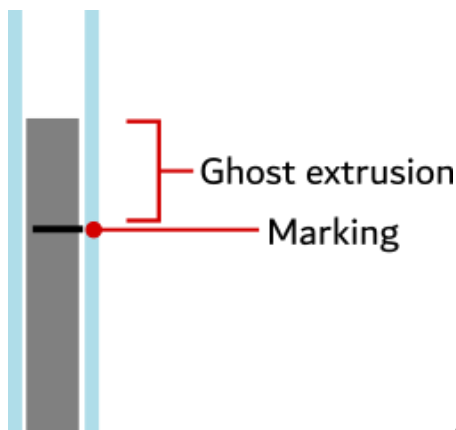
The Cura 2.7.0 program is only used to send G-code to the printer.

#### *Tubes*

As the length of the tubes used by Sanne were not specified, a length of 65 cm was chosen because it had good reach from the printhead to the syringes. Every 10 centimeters, a marking was put on both tubes (A1-A6 and B1-B6) to measure the outer diameter of the tubes at the same points during the test to see if the tubes were expanding. Measuring was done with a digital caliper.

#### *Ghost extrusion*

During extrusion, it was noticed that ink would keep rising in the tube when the extrusion motors had stopped. To measure this "ghost extrusion". Lines to where the ink had come were marked on the tubes. After 2, 5 and 10 minutes after the motors had stopped, the ghost extrusion was measured with a caliper (Figure 1).



*Figure 1: measuring ghost extrusion.*

#### *Extrusion calibration*

In an attempt to calibrate the amount of extrusion for the A and B parts of the ink, A value of 100 was sent to the printer for one part at the time:

"G1 F2 A100 B5" to extrude part A or "G1 F2 A5 B100" to extrude part B

The height the corresponding ink had travelled in the tube was measured with a ruler.

The ink was first extruded up until the static mixing nozzle by means of feeding pieces of G-code one after the other to the printer. When the ink reached the nozzle, attempt were made to extrude ink through the nozzle. First by extruding both inks with the same distance value, secondly by giving A a higher distance value (ratio of A to B = 4:1), thirdly with a 1.36:1 A to B extrusion ratio.

#### *Results*

It was found that the ink used in this experiment did extrude through the mixing nozzle. However, it was not easy. Due to the large amount of ghost extrusion, it was difficult to control the flow. It

also seemed that to extrude the two components, different values in the G-code were needed. Component A needed larger values to travel the same distance. In addition, one motor made a clipping sound and thus had trouble extruding the ink.

After the ink reached the static mixing nozzle through the tubes, it was found that Part B had less trouble travelling through the nozzle. Holding a light behind the nozzle revealed the following view (Figure 2):

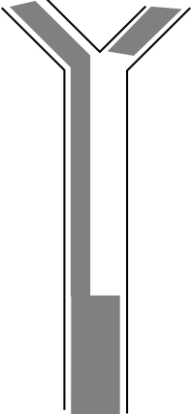


Figure 2: The distribution in the static mixing nozzle after trying to extrude both components after they reached the nozzle through the tubes. Component B is on the left and has reached the mixing mechanism while component A (right) has trouble entering the nozzle.

The ink that came out of the nozzle the first time also showed no print stability. This ink also did not cure.

The second extrusion attempt with a 4:1 extrusion ratio showed much better print stability and did cure.

The third extrusion attempt with a 1.36:1 ratio also did cure, but looked a little bit shinier (more wet). It did however not leave marks when touching after curing. It also showed a slightly lower print stability than the second extrusion.

*Tube expanding*

Table 1 shows the measured outer diameters of both tubes in mm. Figure 3 and 4 show the expansion figures in a visual way.

Table 1: Tube expanding figures (mm)						
Tube A	A1	A2	A3	A4	A5	A6
Before	6.08	6.0	6.1	5.86	5.91	5.96
During	6.18	6.24	6.37	6.38	6.34	6.0
After	6.2	6.08	6.08	6.4	6.3	6.18
Tube B	B1	B2	B3	B4	B5	B6
Before	5.7	5.76	6.2	5.9	5.96	6.01
During	6.2	6.29	6.0	6.3	6.34	6.37
After	6.36	6.18	6.13	6.36	6.0	6.16

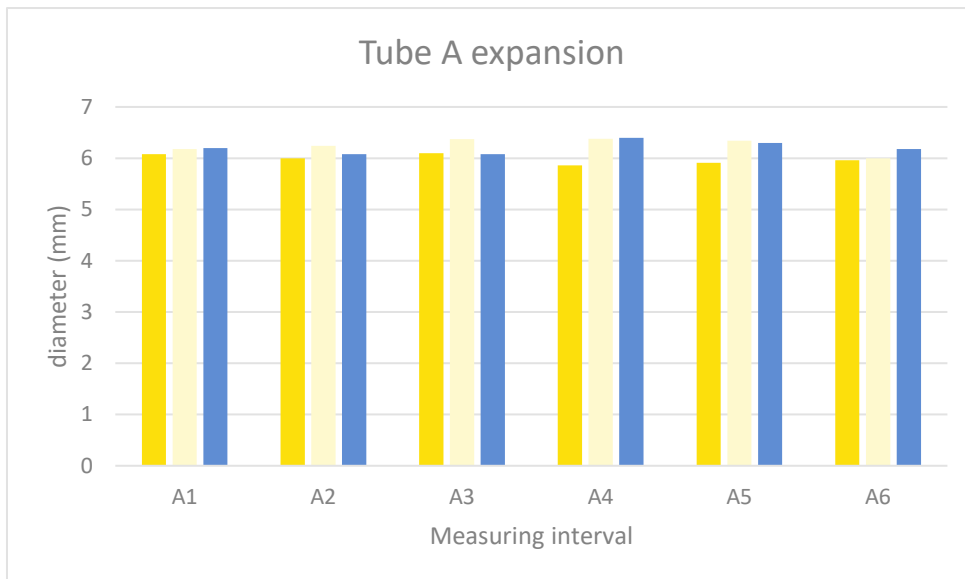


Figure 3: Tube expansion of tube A

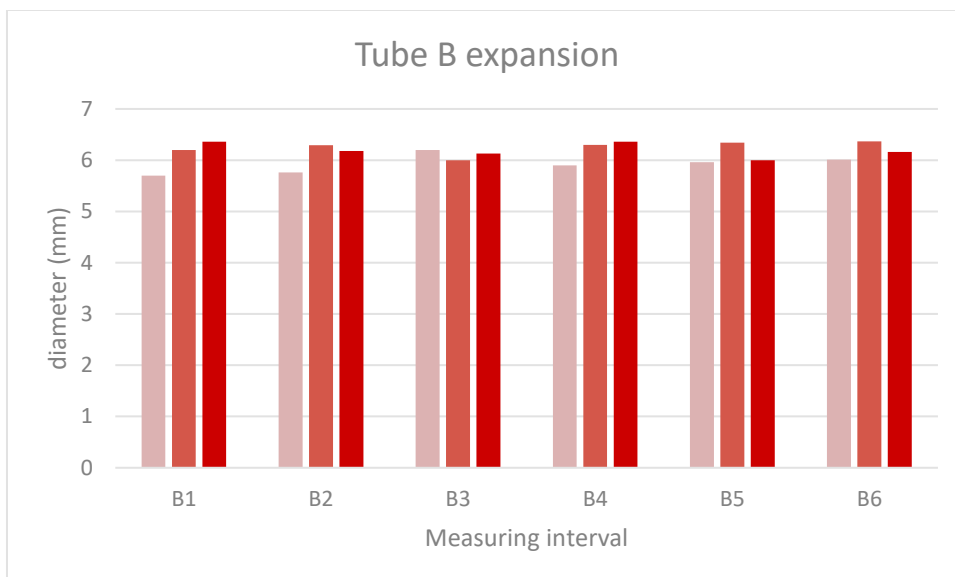


Figure 4: Tube expansion of tube B

#### Ghost extrusion results

During extrusion of the ink, the following ghost extrusion values were measured (Table 2). Figure 5 gives a visual representation.

Time	Ghost extrusion (mm)			
	Tube A	Difference to last measurement	Tube B	Difference to last measurement
2 minutes	4.4	4.4	10.3	10.3
5 minutes	6.1	1.7	14	3.7
10 minutes	9	2.9	15.1	1.1

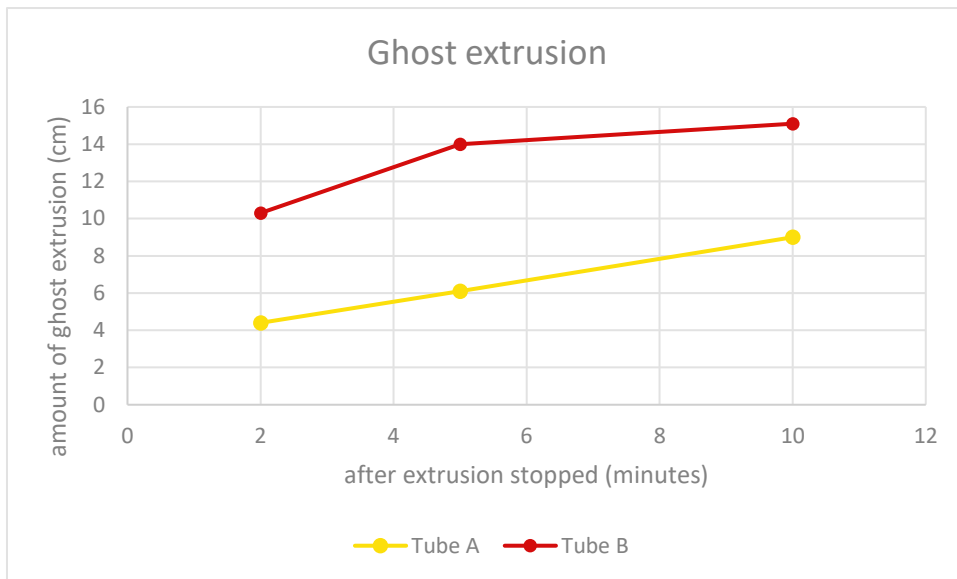


Figure 5: ghost extrusion in tube A and B

#### *Extrusion calibration results*

Taking into account ghost extrusion, it was measured that for a G-code distance value of 100, Part A travelled 11.4cm and Part B travelled 15cm. This corresponds to a distance value of 8.77/cm extrusion for Part A and a distance value of 6.67/cm extrusion for Part B.

Ignoring ghost extrusion, these values were 7.6 cm per 100 distance value for Part A and 10.3cm per 100 distance value for Part B. This corresponds to an extrusion ratio of A:B = 1.36:1

#### *Observations*

During the extrusion trial, it was observed that the G-code command M400 (wait until finished) did not seem to work (properly) with the external extrusion system. The printhead would start to move to home and/or state "print finished" on the display before the extrusion was finished. Also a clipping sound was heard when the ink had reached the static mixing nozzle, indicating at least one motor had trouble extruding the ink through this nozzle.

It was also observed that if no value or a 0 value for the distance of extrusion A or B was send in the g-code, the extrusion system would be skipped al together and thus did not extrude any ink. To be able to extrude only one of the two syringes, the other syringe had to be given a value (e.g. 1). This means that this ink would still be extruded a little bit.

#### *Conclusion*

The ink made on February 9 was able to be extruded by the 3D printer set-up. However, it went difficult. It seemed to go more difficult than Sanne's attempts, even though my version of the ink showed a lower viscosity (see Ink preparation trial 2). The tubes showed expansion, although the numbers are very close to each other. Sanne mentioned a maximum measured tube thickness of 6.1, or an expanding of 0.1 mm. In this experiment, expanding up to 0.54 mm was measured. There was a significant amount of ghost extrusion present. Part A travelled double the amount through the tubes 10 minutes after extrusion had stopped.

In Sanne's experiment, it was mentioned that the two inks were brought to the static mixing nozzle with the following values (Van Vilsteren, 2021, page 231):

F2 A5 B356 and F2 A178 B10



This would imply that part B is more difficult to extrude than part A, as B is given the larger value. However, in this experiment, it was found that Part A needed the larger distance value.

## Discussion

The length of the tubes were not specified in Sanne's experiment. It is possible that a different length of tubes was used, which could explain some differences in this experiment.

When measuring the ghost extrusion, the distance value given in the G-code was not remembered or written down. This makes it more difficult to give hard conclusions on the presented values.

To extrude the ink up to the static mixing nozzle, no structure in feeding values was present. It went with trial and error, trying a guessed value and see how far it got. This is not very helpful in trying to find the correct values for extrusion.

The tube expanding figures are very near each other. It is unclear whether this means the tube expanding is very small or that these values are in the margin of error. It is very possible that the tubes are not 100% cylindrical. This means that the angle from which the tube is measured has a significant influence on the result. However, a careful assumption can be made that the tubes do show expanding. This could also be (one of) the causes for the ghost extrusion.

During extrusion through the static mixing nozzle, a motor clipping sound was heard. However, it was not determined which motor it was (Because I had my hands full). Presumably, it was motor A, because this was the case in Sanne's experiment.

The extrusion distance values to reach the static mixing nozzles were B356 and A178 in Sanne's experiment. In my experiment, A would have needed the larger number. This difference, however, could have been caused by the amount the syringes were manually extruded into the tubes, leaving an uneven distribution of ink in the tubes. This was not specified in Sanne's documenting of her experiment.

## Further research

In further experiments, a better way to determine the expansion of tubes must be found. A possibility is to measure the speed at which the ink travels in the tubes with a constant speed of the extrusion system. A lower speed of the ink should correspond with a larger tube expansion. This way, the expansion between the PVC tubes used in this experiment and the stiffer reinforced tubes used in a later experiment can be compared.

The M400 command did not work for the extrusion system because of the way it is controlled (via USB). The amount of extrusion flow that corresponds to the distance travelled by the printhead should therefore be found. Printer tuning attempts made by Sanne can be used as a starting point.

The amount of retraction by the extrusion system should be optimized so that there is no ghost extrusion. Possibly, it works best to start with this after the stiffer tubes are tested.

It is still a possibility that the ink made for this experiment was not correct and thus influenced the results. Therefore, a better prepared ink with the correct rheometric properties should be tested in the system to see if these give better results.

## References

Van Vilsteren, S. (2021). Designing Magnetic Soft Materials for 4D Printing [Master Thesis, Delft University of Technology]. Tu Delft Educational Repository.  
<http://resolver.tudelft.nl/uuid:7e05bd4c-4720-4e1f-b13b-7b048602ce42>

## C.2c 3D printer trial 3

February 14, 2022 – Kevin van der Lans

### Introduction

The goal is to measure the expanding of tubes in a different way: by measuring and comparing the flow speed inside the tubes.

Flow speed is here defined as the amount of mm the fluid travels per second

The thin tubes are compared to the thicker reinforced tubes to see if there is a difference in ghost extrusion and/or expansion of tubes. It is expected that the speed of part A is less constant than the speed of part B and that the speed in the reinforced tubes is more constant than the speed in the thinner tubes.

First Sanne's results on distance values that correspond with the mm travelled by the extrusion system is verified.

### Method

First try to see if distance value of 89 results in 6mm movement and F1 in 125 seconds of movement duration

Then measure speed with thin PVC tubes with water (as pilot and comparison);

- Move syringe a littlebit up to ensure it is tight to the plate (g-code A/B30)
- Mark starting point
- Start print (G1 F1 A89 B89) and start stopwatch when extrusion starts (audio cue)
- Mark every 30 seconds the height of water in the tube
- Mark height of water when extrusion stopped (at 125 seconds)
- Measure distance between marks
- Divide measured distanced by 30 seconds = speed in mm/s
- Should be constant (horizontal line)

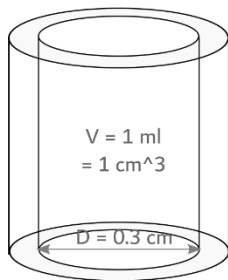
Then repeat above steps for ink with thin and thick tubes. For the experiment with water, only one tube was used with extrusion piston A. In the experiment with ink, both tube A and B were filled and measured simultaneously.

The thick tubes have larger diameter. Therefore, the mm/s speed data was corrected by volume according to:

$$V = A * h \rightarrow V = \pi * r^2 * h$$

R is the inner diameter of the tube (0.3 cm and 0.4 cm) divided by 2.

### Thin



$$V = A * h$$

$$V = r^2 * \text{Pi} * h$$

$$1 = 0.15^2 * \text{Pi} * h$$

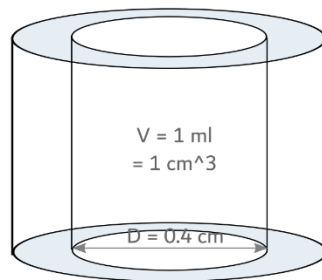
$$1 = 0.0225 * \text{Pi} * h$$

$$1 = 0.070686 * h$$

$$h = 1/0.070686$$

$$h = 14.147 \text{ cm} = 141.47 \text{ mm}$$

### Reinforced



$$V = A * h$$

$$V = r^2 * \text{Pi} * h$$

$$1 = 0.2^2 * \text{Pi} * h$$

$$1 = 0.04 * \text{Pi} * h$$

$$1 = 0.125664 * h$$

$$h = 1/0.125664$$

$$h = 7.957747 \text{ cm} = 79.57747 \text{ mm}$$

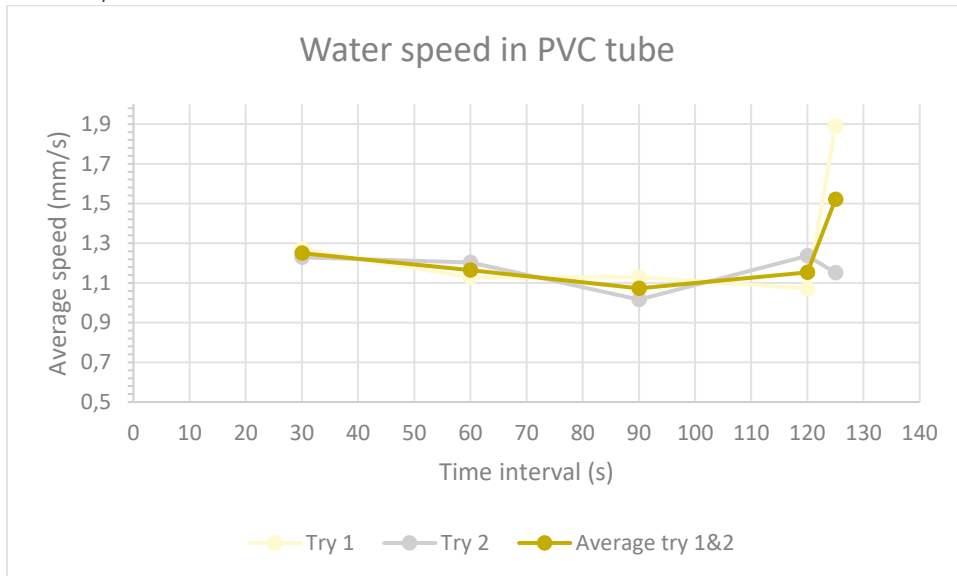
### Results

*G-code related to 6mm of travel.*

Syringe Piston Movement	F	A	B	time (s)	A distance (mm)	B distance (mm)
	1	89	89	125,09	6,18	6,12
	1	89	89	125,02	6,13	6,1
	1	89	89	125,01	6,15	6,03
	1	89	89	124,97	6,1	6,19
Average	1	89	89	125,0225	6,14	6,11

The results verify Sanne's results that the G-code of A/B89 results in approximately 6mm of travel by the pistons, which corresponds to 1 ml according to the markings on the syringe. There is no difference between piston A and B.

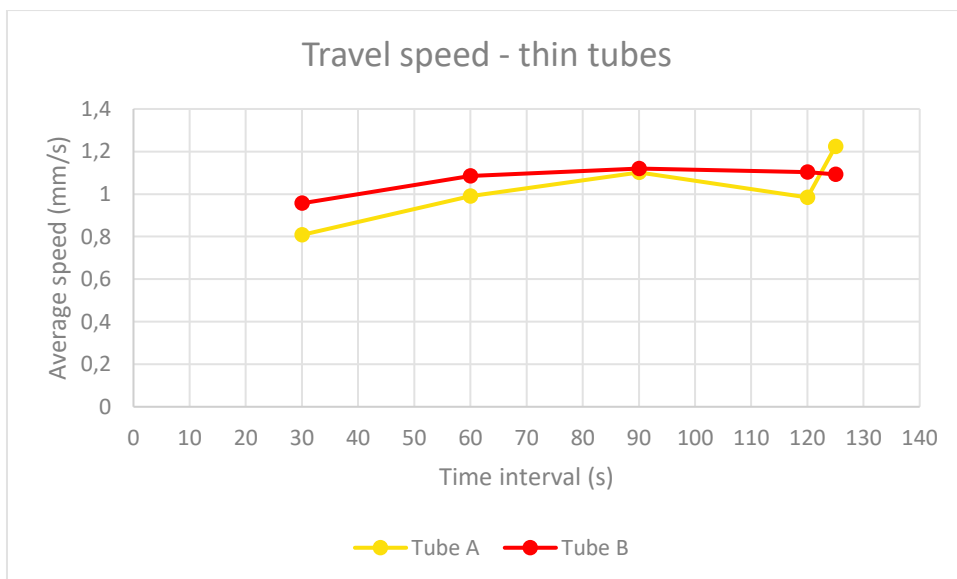
### Water speed test

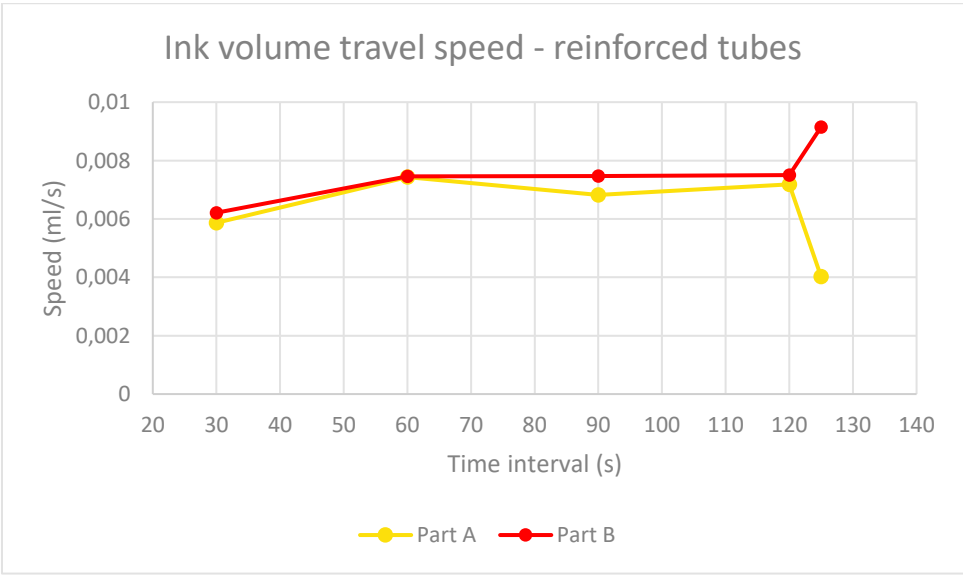
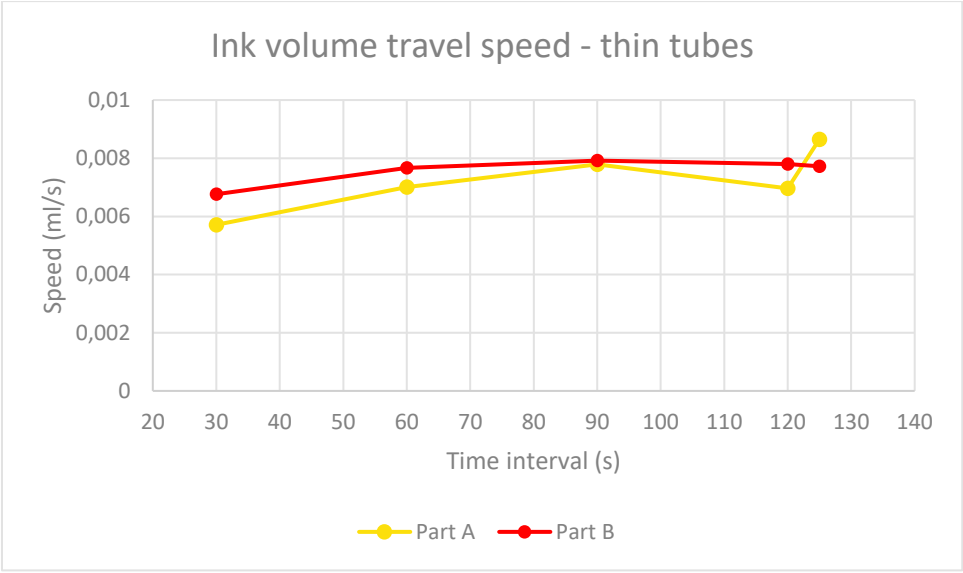
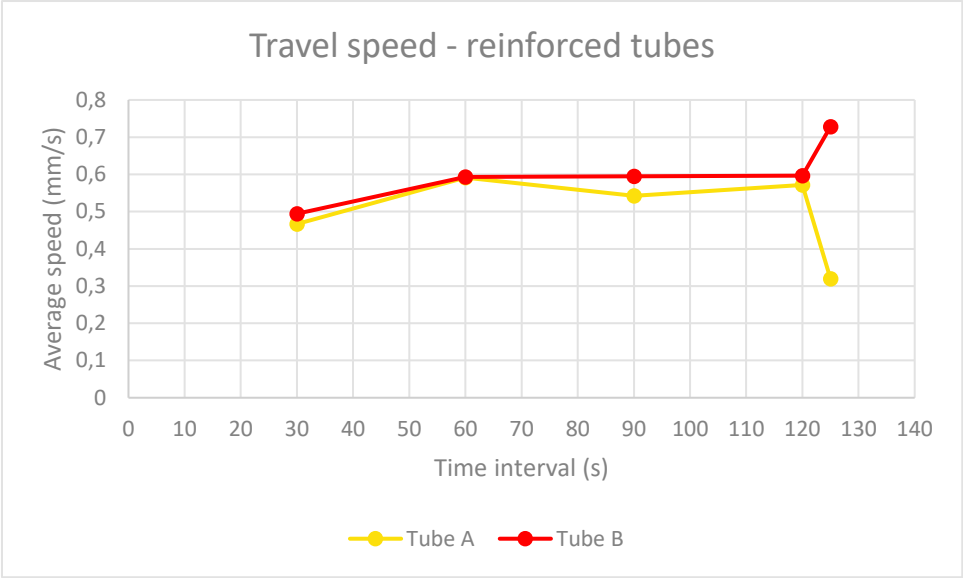


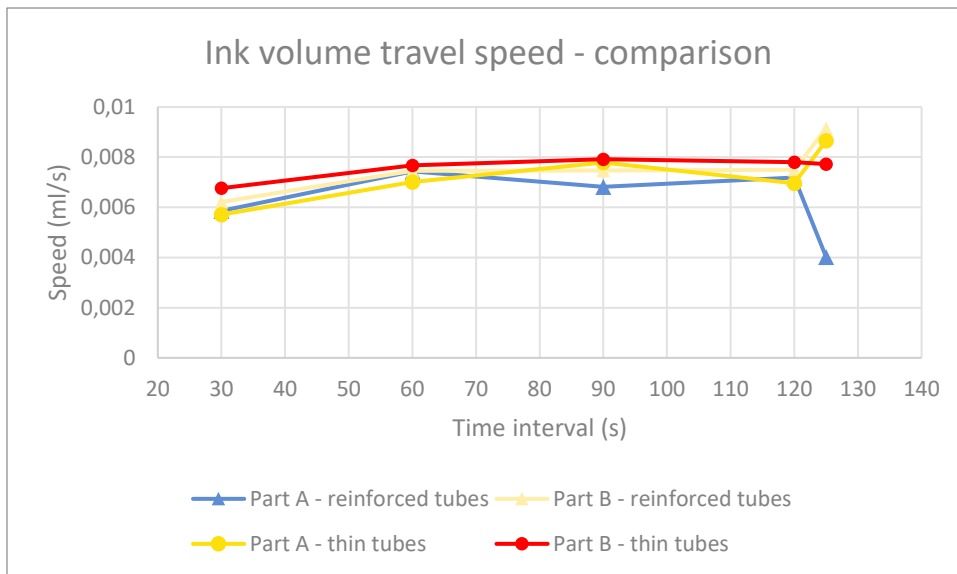
The trial test with the water shows that the speed is not entirely constant. But the values are so close to each other it is hard to draw hard conclusions on this.

### Speed experiment with ink

The following graphs show the results of the measured speeds







It can be seen that all parts in all tubes show some acceleration in the beginning and ended quite constant near the end. The reinforced tubes are more constant than the thin tubes overall.

#### Distance travelled

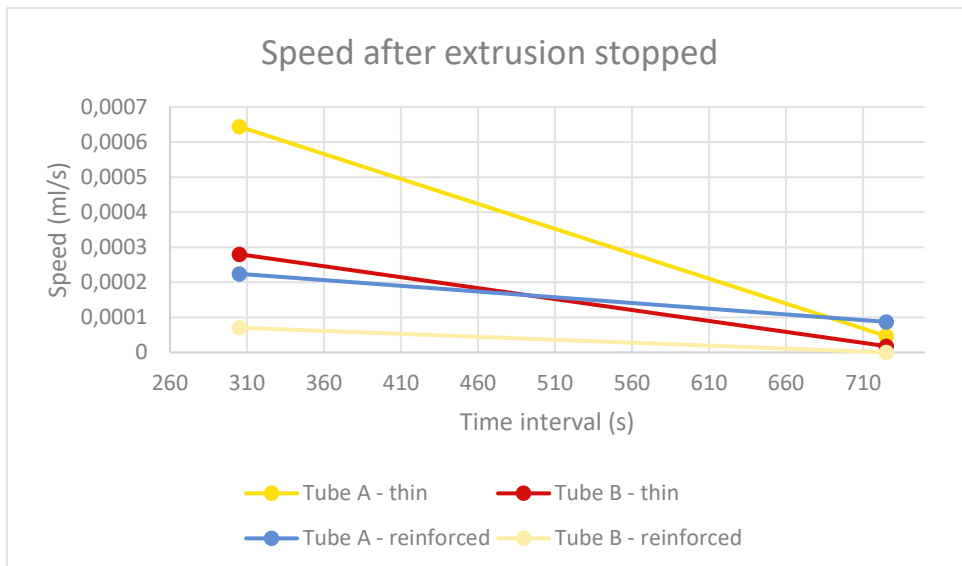
Distance travelled (mm)	Water	A- thin	B-thin	A-thick	B-thick
calculated	141,471	141,471	141,471	79,5775	79,5775
active extrusion	146,657	122,68	133,42	66,77	72,01
after 10 min	146,657	141,86	141,61	72,89	73,02

Volume extruded (ml)	Water	A- thin	B-thin	A-thick	B-thick
calculated	1	1	1	1	1
active extrusion	1,036657	0,867174	0,94309	0,83905	0,90490
after 10 min	1,036657	1,002749	1,00098	0,91596	0,91759
Ghost - active difference		0,13557	0,05789	0,07690	0,01269

It can be seen that Part A consistently has a lower distance travelled during active extrusion than Part B. Both for thin and reinforced tubing. The gap is lower with reinforced tubes compared to the thinner tubes.

#### Ghost extrusion

The speed of ghost extrusion was measured after active extrusion was finished.



### Conclusion

The measurements of the average speed inside the tubes show a small difference in part A and B and in the thin tubes compared to the reinforced ones. The reinforced tubes show slightly more constant speed.

Ghost extrusion for the thin tubes was more than that of the reinforced tubes. Part A (thin tubes) stopped quite a bit lower when active extrusion was finished than Part B. Meaning it had to catch up a larger distance with Part B. This explains the faster speed in the beginning.

The gap in volume (ml) extruded between active and ghost extrusion is the largest in the thin tubes with part A. Also with component B, the gap in volume is larger with the thin tubes than the reinforced tubes. This leads to the cautious conclusion that expanding of the tubes has some part in the unpredictability of the travel of the ink in the tubes.

### Discussion

Not repeated for more accurate measurements because not enough ink.

Marking of height in the tubes inaccurate: delay in time, not very visible in reinforced tubes

Tube expansion not clear cause of ghost extrusion

Extrusion through nozzle not tested

### Further research

Redo experiment, but by filming and analyzing later (e.g. kinovea)

Try with stiff tubes anyway because it might still work better with extruding through nozzle.

Other causes of unpredictability:

- Elastic deformation in system
  - o Turn until skipping
  - o Retraction value

## C.2d 3D printer try 4

Kevin van der Lans – February 21, 2022

### Introduction

The goal of this experiment is to try to extrude ink through the static mixing nozzle by using short and reinforced tubes. While we are at it, I also redo the speed measurements one tube at a time.

### Method

For this test, the ink made on February 15 was used (15/02 – Fe|0,85wt%SiO|nM).

The first few extrusions, only the distance travelled was measured. The markings to measure the speed were done once for each ink component. The extrusions to get the ink upto the static mixing nozzle were called pre-extrusions (pre-E#).

The measuring of the speed is done one tube at a time, for tube A during pre-E3 and for tube B during pre-E4.

- Mark starting point after ink is not travelling anymore, including ghost extrusion.
- Start print (G1 F1 A89 B89) and start stopwatch when extrusion starts (audio cue)
- Mark every 30 seconds the height of ink in the tube A
- Mark height of water when extrusion stopped (at 125 seconds)
- Measure distance between marks
- Divide measured distanced by 30 seconds = speed in mm/s
- Repeat step 2-6 but now measure tube B.

After each component reached the static mixing nozzle, the inks were again extruded with the same value, but only 0,2ml at the time, which corresponds to a G-code value of 18. The ink that came out of the nozzle was captured in a labeled cup and left to cure overnight. It was then checked if the inks had cured.

After active extrusion stopped, a retraction of the syringe pistons was applied with the G-codes (E# = Extrusion attempt number #):

E1) No retraction

E2) No retraction

E3) G1 F5 A-30 B-30

E4) G1 F10 A-30 B-30

E5) G1 F10 A-50 B-50

E6) G1 F20 A-50 B-50

E7) G1 F50 A-80 B-80

E8) G1 F50 A-60 B-60

After a retraction was applied, an anti-retraction was given before the actual extrusion was started, for example the g-code after E4, during E5:

G1 F10 A30 B30        *anti-retraction*

G1 F1 A18 B18 *extrude 0,2 ml*

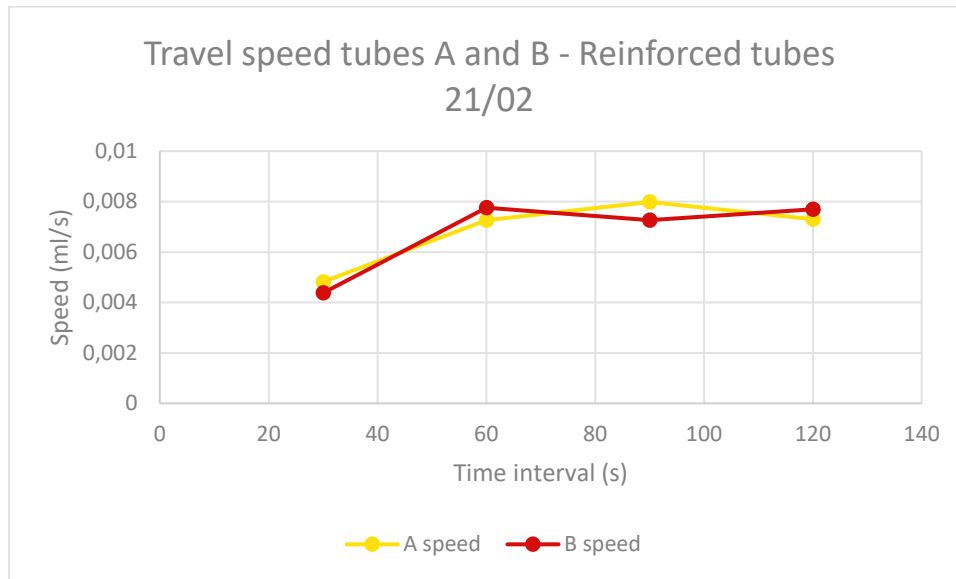
G1 F10 A-50 B-50        *retraction*

It was checked if leaking of ink out of the nozzle still occurred with the applied retraction.



## Results

In the travel speed measurements, an acceleration at the start of the extrusion can be seen again.



Time interval	A distance (mm)	A volume (ml)	A speed (ml/s)	B distance (mm)	B volume (ml)	B speed (ml/s)
30	11,5	0,14451	0,00481	10,45	0,13131	0,00437
60	17,33	0,21777	0,00725	18,52	0,23272	0,00775
90	19,06	0,23951	0,00798	17,33	0,21777	0,00725
120	17,43	0,21903	0,00730	18,37	0,23084	0,00769
Total	65,32	0,82083		64,67	0,81266	
Total after 10min	71,76	0,90176		71,91	0,90364	
Ghost extrusion	6,44	0,08092		7,24	0,09098	

The distanced the ink travelled during pre-extrusion are as follows:

pre-extrusion	A distance (mm)	B distance (mm)
pre-E1	57,76	54,87
pre-E2	70,77	70,49
pre-E3	71,76	72,02
pre-E4	72,19	71,91

## Retraction

Extrusion	Retraction G-code	Leaking occurred
E1	n/a	Yes, a lot
E2	n/a	Yes, a lot
E3	F5 A-30 B-30	Yes
E4	F10 A-30 B-30	Yes
E5	F10 A-50 B-50	Yes
E6	F20 A-50 B-50	Yes

E7	F50 A-80 B-80	No
E8	F50 A-60 B-60	Yes*
* After the retraction of -80, the next extrusion showed a large amount of air bubbles in the ink.		

### Curing

All ink samples collected during extrusion did cure:

Extrusion sample	Did it cure?
E1	Yes
E2	Yes
E3	Yes
E4	Yes
E5	Yes
E6	Yes
E7	Yes
E8	Yes

In addition, no motor skipping sound was heard during any extrusion attempt. When extrusion started however, ink did not come flowing out of the nozzle right away, although the delay was very short compared to the minutes Sanne mentioned in her test with the thin tubes (Van Vilsteren, 2021).

### Conclusion

The re-measurements of the travel speed shows again an acceleration at the beginning of extrusion, after which the speed is more-or-less constant. At this point, it is unknown what is causing this delay.

The ink was extruded through the static mixing nozzles with an equal value this time, in contrast to the attempt made with the thinner tubes in 3D printer trial 2 (February 8). All ink samples did cure, which shows a good mixing of the ink with an equal extrusion value. It can be concluded that the reinforced tubes add some stability to the extrusion system compared to the thin tubes.

To stop leaking of ink during extrusion, a large retraction of -80 was needed, which corresponds to a distance of 5,4 mm. This is quite a lot, compared to the 1,2 mm the piston travelled to extrude 0,2ml of ink. This retraction also seemed to cause air bubbles, but this was not verified with further testing.

### Discussion

The system stills shows a littlebit of delay, although it is minimal. To eliminate leaking after extrusion, a quite large retraction value was needed. There is a possibility that elastic deformation in the extrusion system is responsible for this. It is also possible that the retraction value for ink A and B are different, because of the difference in viscosity. The delay in the system is not explained by this experiment. This can again be caused by elastic deformation. Other possibilities could be the presence of airbubbles in the ink that are compressed, because the same behaviour (ghost extrusion, leaking) can be observed while only extruding the ink through the syringe.

### *Limitations*

Because the ink used in this experiment was almost 1 week old, it is possible the ink had degraded, so there is no guarantee these results will be the same with fresh ink. Also, this ink shows lower viscosity than the original (Van Vilsteren, 2021; Ink preparation trial 3 – 15/02).

The retraction values tried were not very structured, but instead more random trial and error.

### Further research

The retraction values should be examined more structured to see if there is a difference for each of the inks.

### References

Van Vilsteren, S. (2021). Designing Magnetic Soft Materials for 4D Printing [Master Thesis, Delft University of Technology]. Tu Delft Educational Repository.

<http://resolver.tudelft.nl/uuid:7e05bd4c-4720-4e1f-b13b-7b048602ce42>

## C.2e 3D printer try 5

Kevin van der Lans – February 22, 2021

### Introduction

This test is about testing retraction values in a more structured way and to see if A and B require the same retraction value to stop ghost extrusion.

### Method

To test the retraction values, the ink in tubes A and B were extruded for 0,5 ml, which corresponds with a g-code of

```
G1 F1 A45 B45
```

After a 0-measurement where no retraction as added, the retraction values of -10, -20, -40 and -60 were tried. All with a speed of F10.

The first try, A and B were extruded simultaneously. For all follow up tries, A and B were extruded separately. However, because the extrusion system does not work if a 0-value for A or B are given, the part that was not measured were given a value of 1.

After a retraction was given, in the follow-up try, an anti-retraction was given. For example, at try 3, the G-code for measuring tube A looked like this:

```
G1 F10 A1 B20      anti-retraction for A (to counter a -1) and B (to counter the previous retraction of -20)
```

```
G1 F1 A45 B1      extrude A 0,5ml and B the minimal amount because you have to  
G1 F10 A-40 B-1   retraction of A of -40 and a retraction of -1 for B
```

For the same try, but now for tube B:

```
G1 F10 A40 B1      anti-retraction for A (to counter the previous retraction of -20) and B (to counter a -1)
```

```
G1 F1 A1 B45      extrude B 0,5ml and A the minimal amount because you have to  
G1 F10 A-1 B-40   retraction of B of -40 and a retraction of -1 for A
```

At try 4, no anti-retraction was given.

For each try, the distance traveled at the end of active extrusion was measured (after 75s) and the ghost extrusion at 3 minutes and 10 minutes.

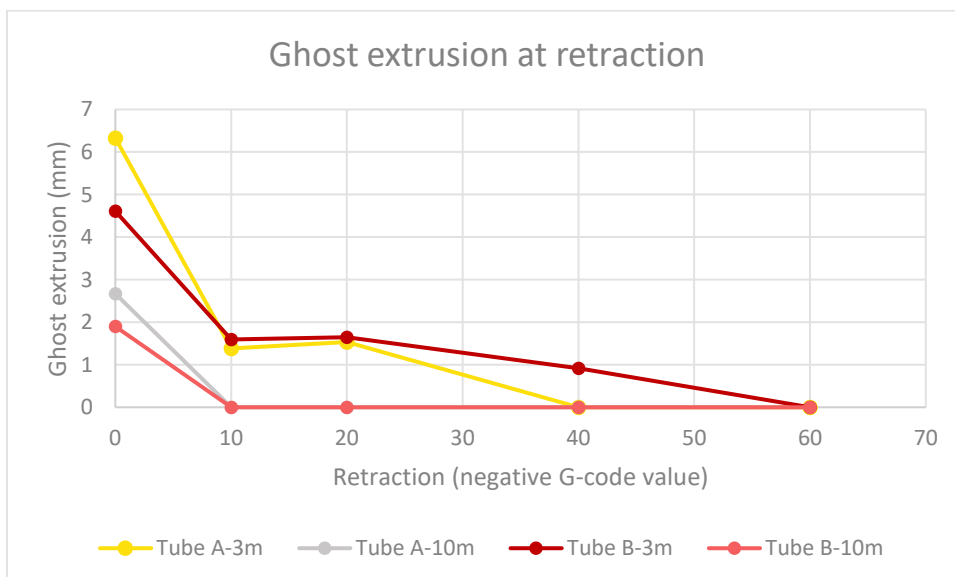
For this test, the ink made in Ink Preparation Trial 4 was used (21/02 – Fe<sub>0,85</sub>wt%SiO<sub>2</sub>InM).

After the retraction measurements, it was tried if extrusion happened after only a retraction and counter retraction:

- After try 4, the theoretical values for A and B were:  
A at -59 and B at -60
- A value of A/B40 was given to see if extrusion occurred. The theoretical value was now A at 19, B at 20
- A value of A19 and B20 was given to see if extrusion occurred. The theoretical value would now be 0 for both A and B
- With A and B both at 0, a retraction of F10 A/B-20 was given, immediately followed by F10 A/B20 to reach again to A/B0
- Lastly, a retraction and immediate anti-retraction of 40 was tried.

Results

Try 0	Tube A	Tube B
Retraction	zero (baseline)	zero (baseline)
Distance after 75 s	37,4	39,25
Distance after 3m	+6,33	+4,61
Distance after 10m	+2,67	+1,90
After anti-R	n/a	n/a
Try 1	Tube A	Tube B
Retraction	F10 A-10 B-10	F10 A-10 B-10
Distance after 75 s	36,58	38,02
Distance after 3m	+1,38	+1,59
Distance after 10m	+0	+0
After anti-R	n/a	n/a
Try 2	Tube A	Tube B
Retraction	F10 A-20 B-20	F10 A-20 B-20
Distance after 75 s	42,88	39,25
Distance after 3m	+1,53	+1,65
Distance after 10m	+0	+0
After anti-R	+17,79	+19,0
Try 3	Tube A	Tube B
Retraction	F10 A-40 B-40	F10 A-40 B-40
Distance after 75 s	38,79	37,14
Distance after 3m	+0	+0,92
Distance after 10m	+0	+0
After anti-R	+20,12	+21,27
Try 4	Tube A	Tube B
Retraction	zero (baseline)	zero (baseline)
Distance after 75 s	36,32	24,05
Distance after 3m	+0	+0
Distance after 10m	+0	+0
After anti-R	n/a	n/a



Out of the retraction tries, a retraction of -40 was enough to stop ghost extrusion for component A and a retraction of -60 was enough to stop ghost extrusion of component B. Each time, the component that was not measured did show some extrusion.

#### *After-measurement of +40*

After feeding a g-code of A/B40 to the extrusion system (with now theoretical value of A-59 and B-60), no extrusion of ink occurred in the tubes,

#### *After-measurement of A19 and B20*

After feeding the G-code A19, B20 to the system (with now theoretical value of A-19 and B-20), extrusion occurred:

A: 8,15mm

B: 2,73mm

Even though the theoretical value was now 0 for both components.

#### *Retraction with immediate anti-retraction*

For both the retraction + anti-retraction of 20 and 40, no extrusion of ink occurred in the tubes.

## Conclusion

It can be concluded that component A and B require different retraction values to eliminate ghost extrusion (-40 for A and -60 for B). However, it can not be concluded what is the cause of this. It could still be air bubbles in the ink, elastic deformation of the system or something else, for example the momentum of the ink.

The retraction values found are also different from the one used in 3D printer try 4 of -80.

Probably, the ink requires a different retraction when it has entered the static mixing nozzle. This could be because of the smaller inner diameter of the static mixing nozzles compared to the tubes.

The ink did not show extrusion when a retraction with immediate anti-retraction was given. Out of this, it can be concluded that the extrusion of the not tested tube during the retraction measurements could be the cause of the g-code value of 1 necessary to let the extrusion system operate.

## Discussion

While the cause of the delay in the system is not entirely verified with this research, it was established that ghost extrusion can be stopped with a retraction and that there is a difference in the value needed for each component. Probably, this has to do with the viscosity.

The retraction needed to stop extrusion is also quite large. Up to more distance needed to extrude ink. The value of -80 found during 3D printer try 4, was even 4,4 times more than was needed for extruding the 0,2mm.

## Further research

To see if elastic deformation is the cause of the ghost extrusion and the large needed retraction, a syringe with closed off end can be placed in the system and see at which value the motor starts skipping. A high g-code value needed before skipping occurs indicates a large elastic deformation of the system.

## C.2f 3D printer try 6

Kevin van der Lans - Februari 24, 2022

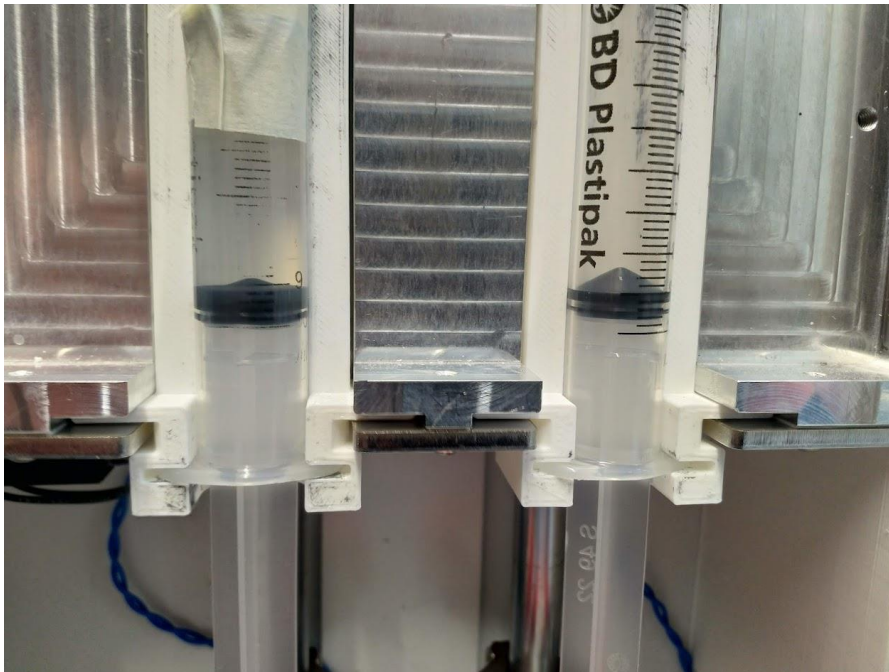
### Introduction

This experiment is to check for elastic deformation in the system, as this could be the cause for the delay in extrusion and the ghost extrusion.

### Materials

In this experiment, the modified Ultimaker 3 3D printer was used, along with the external dual syringe extrusion system.

One 10ml syringe was empty, while the other was capped off with a custom designed and 3D printed Luer cap with hot-glue inside in between the ceiling of the cap and the nozzle of the syringe to ensure a water tight sealing. Paper towels were rapped around to prevent an explosion of water and to later check if there is leakage



### Method

The capped off syringe was placed in the system, one slot at the time. In the other slot, an empty syringe was placed.

First, the G-code G1 F1 A1 B1 was fed to the system repeatedly until the motor skipping sound could be heard.

The second run, a larger g-code value was fed to the system until a motor skipping sound could be heard. These values were (in chronological order): 6, 12, 24, 36, 42, 48, 54, 60, 80, 100 and 90. These values were immediately followed by a retraction of the same value, to get back to the zero-point.

## Results

Motor A and B both needed 6 times the G1 F1 A1 B1 g-code before the motors skipped. Strangely enough, the piston would still be under tension after a retraction of -6 was applied. After 4 times a retraction of -6, the syringe was loose enough to be removed.

Try	G-Code	Theoretical total value	Motor skipping?	
			Motor A	Motor B
1	G1 F1 A1 B1	1	No	No
2	G1 F1 A1 B1	2 (+1)	No	No
3	G1 F1 A1 B1	3 (+1)	No	No
4	G1 F1 A1 B1	4 (+1)	No	No
5	G1 F1 A1 B1	5 (+1)	No	No
6	G1 F1 A1 B1	6 (+1)	Yes	Yes

The second time, a higher number of G-code was fed into the system at the time. Both motors started to skip at 90.

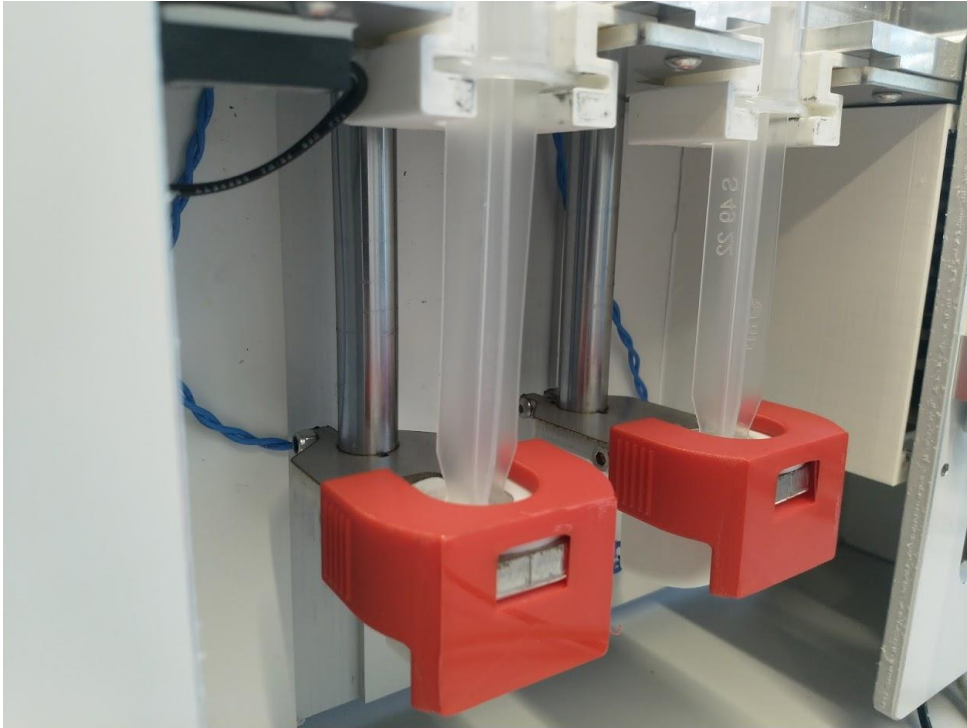
Try	G-Code	Theoretical total value	Motor skipping?	
			Motor A	Motor B
1	G1 F1 A6 B6	6	No	No
2	G1 F1 A12 B12	12	No	No
3	G1 F1 A24 B24	24	No	No
4	G1 F1 A32 B32	32	No	No
5	G1 F1 A36 B36	36	No	No
6	G1 F1 A42 B42	42	No	No
7	G1 F1 A48 B48	48	No	No
8	G1 F1 A54 B54	54	No	No
9	G1 F1 A60 B60	60	No	No
10	G1 F1 A80 B80	80	No	No
11	G1 F1 A90 B90	90	Yes	Yes
12	G1 F1 A100 B100	100	Yes	N/a

The value of 100 was not measured for B because in the run with Motor A, first 100 was tried before 90. In the run with motor B, 90 was tried first and it skipped. If the motor skipped at 90, it would also skip at 100.

During the whole experiment, the paper towels did not become wet so there was no leakage of the syringe.

After the motors stopped after executing the g-code of 90, the piston of the syringe showed a large deformation/buckling:





### Conclusion

The extrusion system does show a large deformation of about 6 mm (corresponding to a G-code of around 90). The main cause seems to be the buckling of the syringe piston. That is not surprising, given the thin construction.

Also, it seems like a g-code value of 1 does not correspond with  $1/90$ , as 6 steps of +1 were needed to achieve motor skipping, while a direct value of 90 was needed to achieve the same. This would suggest that the travel of the pistons in the extrusion system is not linear.

### Discussion

The buckling of the syringes can be easily resolved by designing stiffer pistons. However, this does not guarantee that there are not other deformations taking place in the system.

In addition, the non-linear travel of the pistons could be explained otherwise, for example a different initial pressure of the plates against the pistons or a relaxation of the piston in between feeding of g-codes.

### Further research

This research was done with water. The same experiment needs to be replicated with magnetic ink to see if the ink itself also shows compression, which would indicate the presence of air bubbles (the air inside the bubbles would be compressed, which could also be an explanation of the ghost extrusion). If the value needed to initiate motor skipping is more than 90, this would indicate the ink is compressible and might contain air bubbles.

To validate the redesigned syringe, the same experiment can be redone. Motors should start skipping sooner, as the deformation of the piston should be less.

## C.2g 3D printer try 7

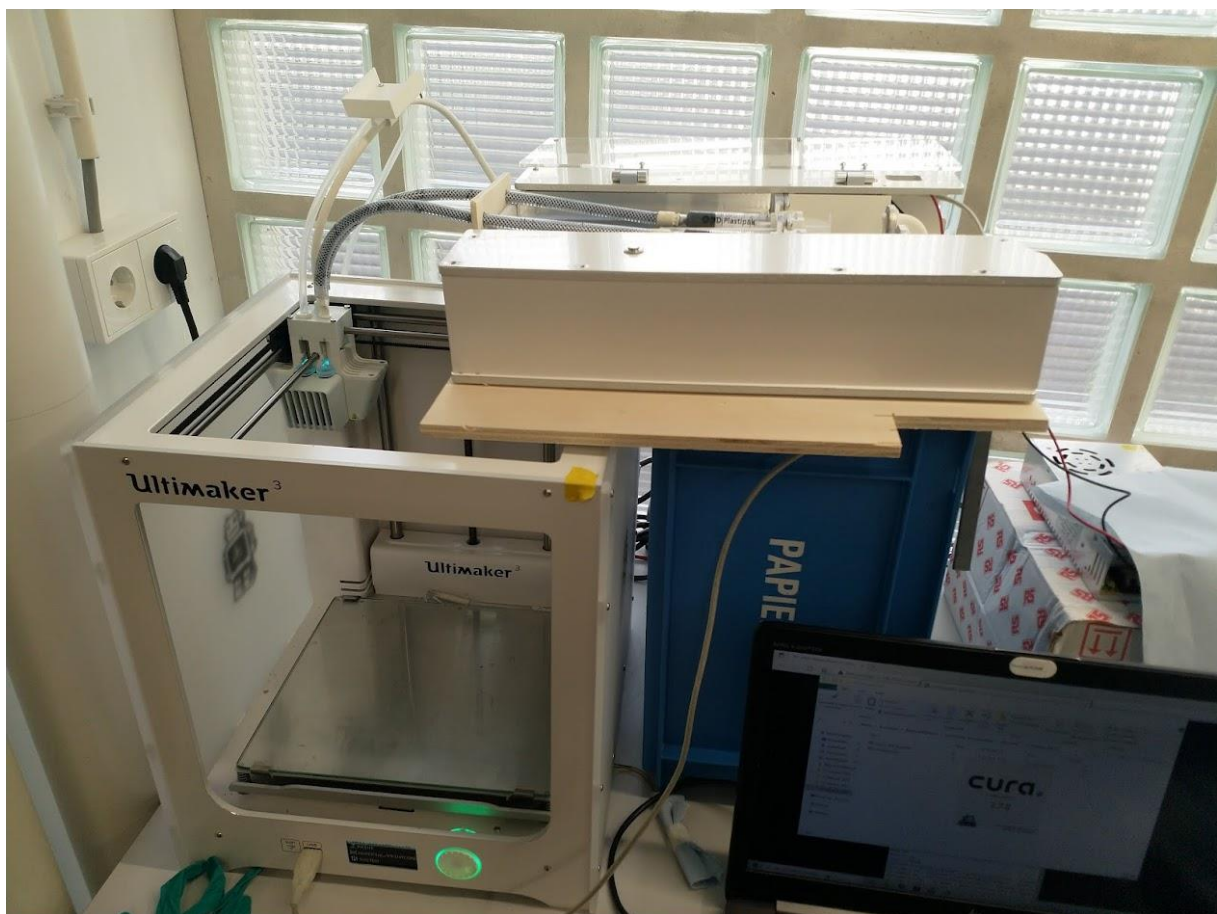
Kevin van der Lans - February 25, 2022

### Introduction

Because the last result were ink was successfully extruded through the static mixing nozzle, it is now attempted to print a geometry with it.

### Method

Place extrusion system as close to print head as possible to make tubes as short as possible. For this, a platform was improvised that could be moved manually along with the print head. Tubes were kept as short as possible, because otherwise there would not be enough ink to be extruded through the nozzle, as all ink would be inside the tubes.



First, it was made sure the ink travelled through the static mixing nozzle by extruding the ink without the nozzle in the print head. When ink started to come out, the nozzle was placed in the print head. A rectangle was attempted to print with the following G-code:

```
M107
G0 F10000 X100 Y100 Z190
M84
M400
G0 F5000 Z5
M400
G0 F200 Z0.1
M400
```

```
G1 F1 A40 B40  
G0 F200 X150 Y100  
G0 F200 Y150  
G0 F200 X50  
G0 F200 Y100  
G0 F200 X100  
M400
```

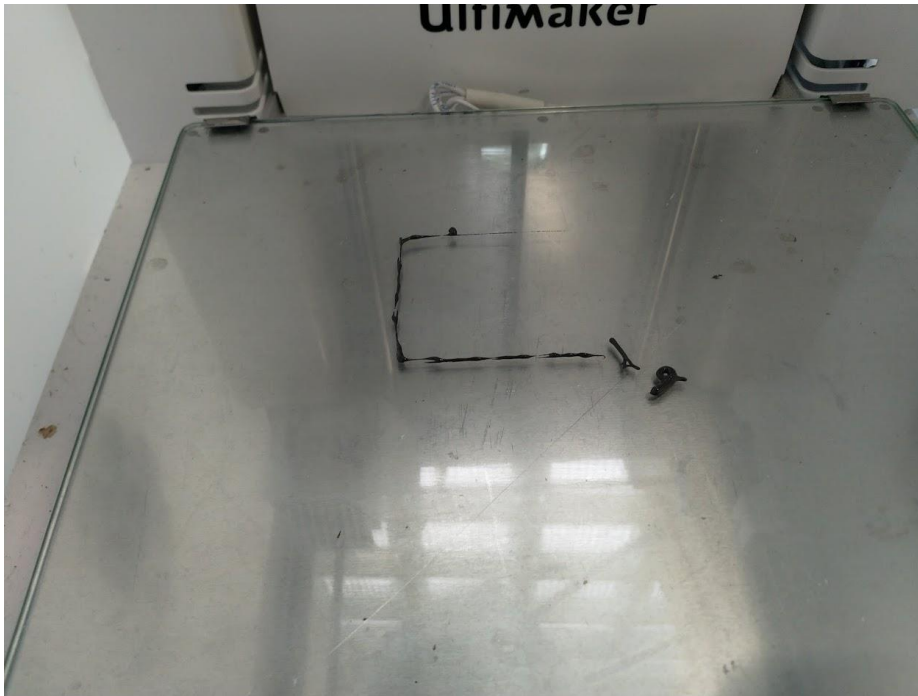
```
G4 P1000  
M400  
M106
```

```
M104 S0  
M104 T1 S0  
;End of Gcode
```

## Results



Ink got extruded through the nozzle while priming the nozzle for printing.



Part of the geometry was able to print. Although there is some under extrusion. This has to do with the flow rate of the extrusion (the speed, F-value in the g-code). This was set too low for the speed the head moved. This still needs to be calibrated. In addition, the distance between the nozzle and the printhead was too big.

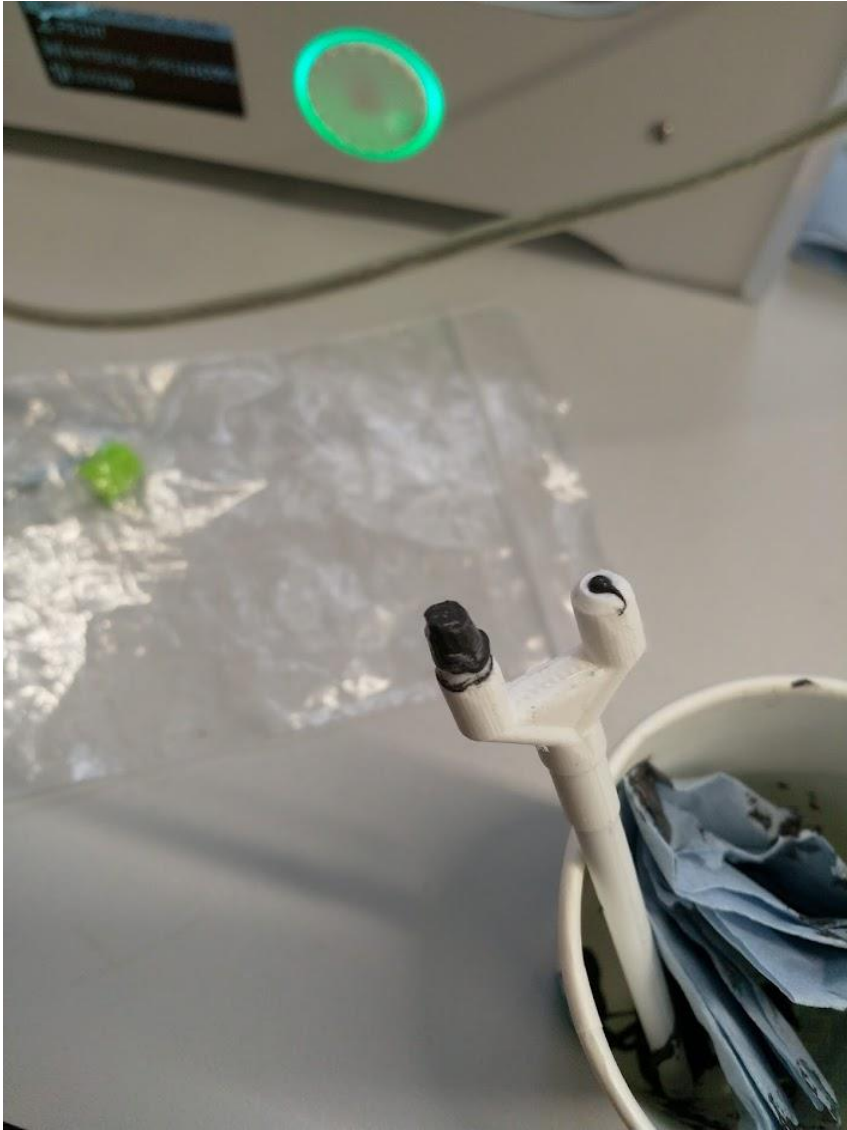
The printer needed some time before ink would actually come out of the nozzle. This was also observed during the extrusion experiment of 21/02.

### Conclusion

It is possible to print something with the magnetic ink using the current 3D printer. Some modifications still need to be made to make the process go smoother (e.g. an overhang structure of the extrusion system and stiffer syringe pistons). Also, the printer needs a bit more calibration (e.g. making sure there is enough material extruded and some additional priming at the start of printing).

### Discussion

During the experiment, a lot of static mixing nozzles broke because of the rigid tubes and sudden movements of the print head, in combination with the thin ends of the nozzle where the tubes attach to. This also needs to be redesigned to make the connection stronger.



Further research

Improvements need to be made to the printer and tested whether these improve the print result and predictability of the system.

## C.2h 3D printer try 8

Kevin van der Lans – March 3 and 4, 2022

### Introduction

The purpose of this experiment is to see when the motor starts skipping when the syringe is filled with (non-magnetized) magnetic ink. If the motors skip later (at a higher G-code distance value), this indicated that the ink is compressible and that this can be a cause of the unpredictable behaviour of the ink when extruding.

### Method

Ink was prepared according to the same recipe  $\text{Fe}|0,85\text{wt}\%|\text{SiO}|n\text{M}$  recipe from February 21.

Syringes filled with Ink A and B were sealed with a green cap and some hot glue to ensure a tight seal. First, ink A was tested in extrusion motor A. G-code values of (G1 F1) A/B70, A/B80 and A/B90 were fed to the system.

When motor A started skipping, the same procedure was repeated with ink B in motor B. For motor B, higher values were fed to the system after 90.

Afterwards, the ink was put inside a vacuum oven at room temperature with a pressure of 500 millibar for 10 minutes for two runs.



Ink B was tried again.

Ink B was but in the vacuum oven again for 10 minutes for one run and tried again in the extrusion system.

It was also tried to cause ghost extrusion without tubes, by keeping the nozzle of the syringe closed with a paper towel and push the syringe. The piston was released and after, the nozzle was made free again.



## Results

Ink A did not skip at 90, the piston was removed to check for leaking but there was none. The syringe was put back and this time made sure it was tight against the pushing plate by sending the g-code G1 F1 A5 B5 twice, moving the plate up a bit. A value of 90 was tried again and this time the motor did skip.

Ink B was tried next, with the same priming procedure but also did not skip at 90. Instead, a value of 200 was needed to make the motor skip.

After vacuuming twice at 500 millibar, ink B needed a value of 140 to make the motor skip. After vacuuming another time at 950 millibar for 10 minutes, the motor skipped at a value of 90, the same value as water needed to make the motor skip.

### *Vacuuming*

After the vacuuming procedure, some ink got out of the syringe, indicating that by drawing air out, it took a bit of ink with it. Part B showed more ink leaking than Part A (bottom corners).

### *Ghost extrusion*

Both Ink A and B showed ghost extrusion of ink out of the syringe after pressure on the piston was released, even after degassing (un-bubbling).



## Conclusion

Motor skipping showed that at least Ink B was compressible. The vacuuming did show some air inside the ink, primarily ink B. Vacuuming the ink helped in making the system more stiff, as it needed a lower g-code value to make the motor skip, which brought it to the same value of water (90). Ink B also had more air bubbles inside than ink A, presumably because ink B is less viscose and thus harder to put in the syringe and more likely to collect air bubbles during this procedure.

Degassing the ink improved motor skipping, but still ghost extrusion could be observed. Air bubbles inside the ink are thus likely to not be the only cause of this odd behaviour. Possibly, the shear thinning properties could have something to do with this or remaining friction inside the ink.

## Discussion

Glue residue made it harder for ink to come out of the nozzle of the syringe during vacuuming. Maybe hot glue is not the right way of sealing the syringes or maybe wait until the glue has cooled a bit so that it does not all flow into the nozzle.

Also important is to push the piston in the syringe a bit to make sure it is tightly against the ink in the syringe, as the vacuum oven can also pull the piston out a bit and cause a large airgap in between the piston and the ink.

## Further research

To see if degassing the ink makes the whole extrusion of the ink through the nozzle more reliable, vacuumed ink needs to be tried to print something. It can also be tried to redo the piston retraction experiment to see if the retraction to stop ghost extrusion is less with degassed ink.



## C.2i 3D printer trial 9

Kevin van der Lans – March 7 and 10, 2022

### Introduction

The goal of this test is to see if the reinforced piston, that was design as a result of the buckling of the pistons under pressure in 3D printer trial 6, would increase the stiffness in the extrusion system. For this, the 3D printer trial 6 experiment was redone with the new piston. The hypothesis is that the motor starts to skip sooner, as the piston can no longer deform to accommodate for more movement of the motors.

### Materials

In this experiment, the modified Ultimaker 3 3D printer was used, along with the external dual syringe extrusion system.

One 10ml syringe was empty, while the other was capped off with a custom designed and 3D printed Luer cap with hot-glu inside in between the ceiling of the cap and the nozzle of the syringe to ensure a water tight sealing. Paper towels were placed below the syringe to capture any leaking water.

### Method

The capped off syringe was placed in the system, slot A. Slot B was occupied by an empty syringe.

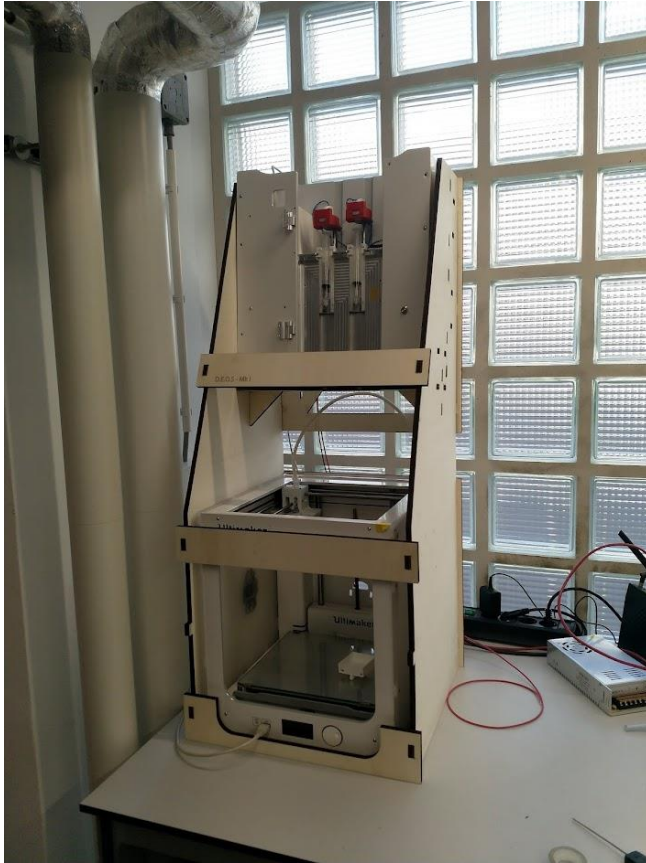
First, the G-code G1 F5 A5 B5 was fed to the system twice to make sure the pistons were tight against the pushing plates.

Next, g-code distance values of 20, 40, 70 and 50 were send to the printer to see when the motors would start to skip. After each attempt, a retraction was applied of the same value. An example g-code:

```
G1 F1 A40 B40  
G1 F10 A-40 B-40
```

Two iterations of the redesigned piston were tried. One on March 7, one on March 10 with a slightly higher diameter.

The syringes were placed upside down in the new Overhang Support system. Therefore, the "above" side of the syringes mentioned in the following section is the place where the piston enters the syringe and the "bottom" side is the nozzle of the syringe.



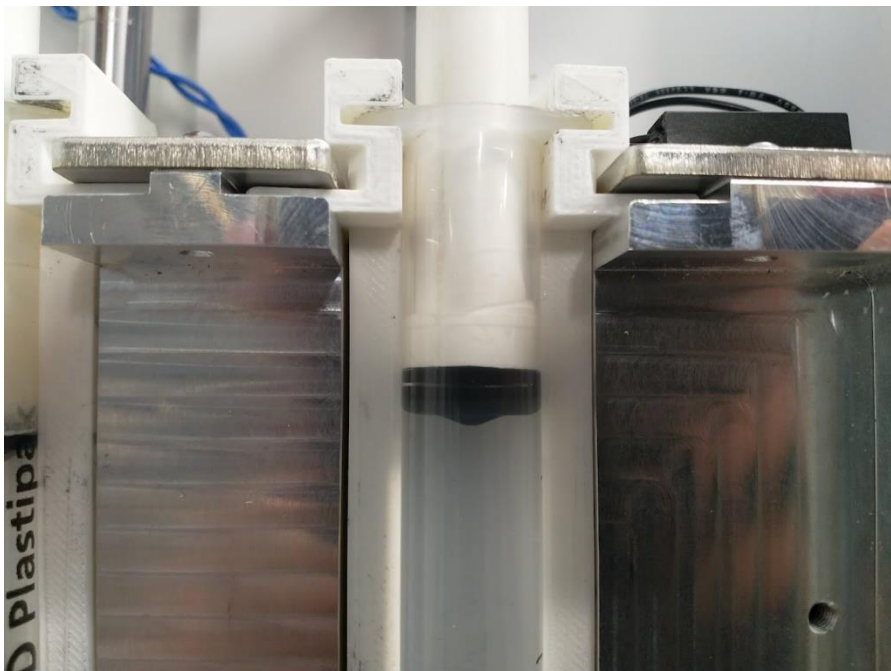
## Results

The motors never skipped during this test. This was because the syringes would constantly leak, from below or above.

Attempt	G-Code	Skipping?	Remarks
March 7			
1	G1 F1 A20 B20	No	Minor air bubbles present
2	G1 F1 A40 B40	No	
3	G1 F1 A60 B60	No	
4	G1 F1 A70 B70	No	Leaking from below
5 - refilled syringe	G1 F1 A50 B50	No	Air bubbles present, syringe was primed with g-code G1F1A50B50 in an attempt to compensate. Leaking from below
6 - refilled syringe	G1 F1 A40 B40	No	
7	G1 F1 A60 B60	No	
8	G1 F1 A70 B70	No	Leaking from above
March 10			
9	G1 F1 A20 B20	No	
10	G1 F1 A40 B40	No	Leaking from above and below
11 - grabbed new syringe	G1 F1 A40 B40	No	Leaking from above



Air bubbles got in the syringe in multiple attempts. Upon refilling the syringe, extra care was put into avoiding air bubbles.



At some point, the syringe started leaking from above in multiple attempts. The water would escape along the rubber piston cap.

### Conclusion

This test was not conclusive to determine that the newly designed stiffer pistons actually result in a stiffer and more reliable extrusion system. Water would keep leaking from the syringes before the motor got a chance to skip.

## Discussion

The fact that water starts leaking from the syringe before the motor starts to skip might not be a bad sign. It might be that, because there is no or little deformation, the water is pushed through any tiny gaps with more force, thus escaping before the motor would skip. However, that is not likely, as in Trial 6, no leaking occurred what so ever, while you would think that the pressure inside the syringe is at its maximum when the motor is skipping.

Another possibility is that the piston does not close off the syringe as well as the original piston does. The dimensions of the original and new piston do deviate slightly, as the large tolerances caused by 3D printing the syringes, makes it difficult to exactly match the dimensions of the original piston.

It is also possible that the syringe outer shell started to expand, making a gap between the black piston cap and the outer wall of the syringe.

The only two parameters that were changed in this research, however, is the placement of the extrusion system in the new Overhead Support structure and the replacement of the piston for the new and stiffer one. It is most likely the cause of the problems lie somewhere in these two parameters.

## Future research

A new piston with more accurate dimensions to that of the original can be tried to see if the procedure goes more smoothly this time. In addition, the extrusion system can be brought down again to see if this makes a difference.

The possible expanding of the syringe can be combatted with a stiff enclosure around the syringe to keep it from expanding.



## C.2j 3D printer test 10

Kevin van der Lans – March 14, 2022

### Introduction

In the previous test, water leaked out of the syringe (top or bottom), therefore it could not be established if the newly designed pistons would improve the stiffness of the extrusion system. In this test:

- ... a new method of testing piston stiffness is applied, where the water in the syringe is replaced with a piece of wood.
- ... the 3D printed pistons will be re-evaluated with the new method.
- ... the original and 3D printed pistons are compared on stiffness by means of a compression test.
- 

### Materials

For this, the modified Ultimaker 3 with external extrusion system was used. The extrusion system was placed in the Dual Extrusion Overhead Support (DEOS; the laser-cut structure). Other needed materials are: two 10ml syringes, one original piston, one redesigned 3D printed piston, a piece of wood of 9x10x55 mm.



### Method

In stead of using water in a closed off syringe, the piece of wood was used to keep the piston from travelling in the syringe, while eliminating the risk of leaking water. The wood-filled syringe was placed in slot A, while the other slot was occupied by an empty syringe.

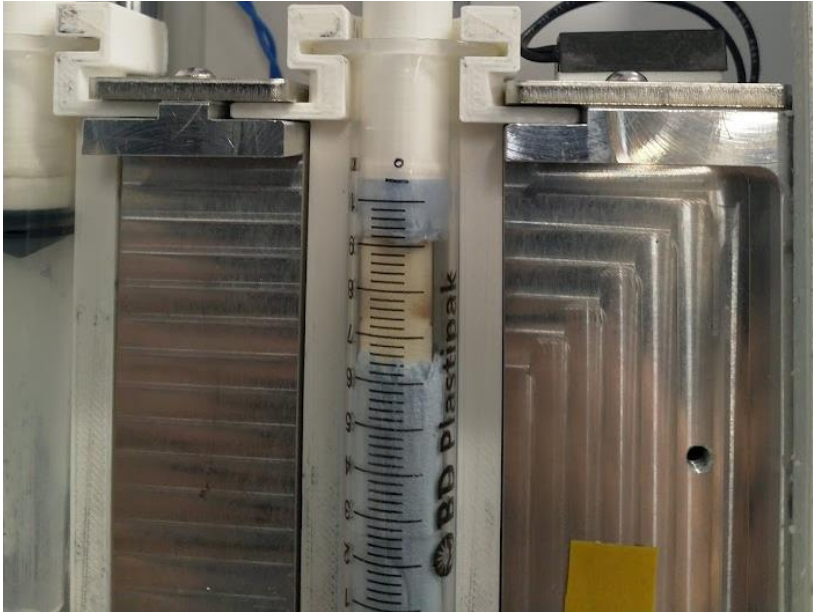
First, the original piston was tested to be able to compared the results with the previous tests and have a new bottom line to compare the new piston with.

The G-code G1 F5 A5 B5 was fed to the system to make sure the pistons were tight against the pushing plates.

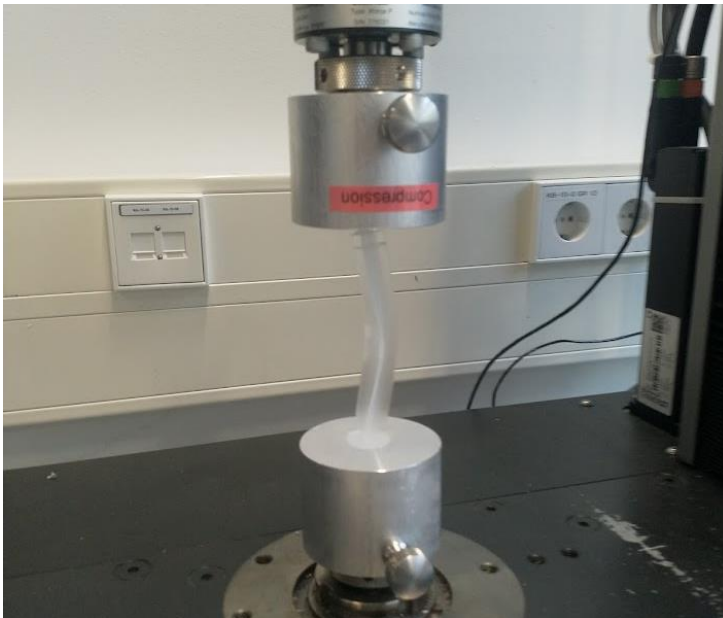
Next, g-code distance values of 20, 40, 50, 60, 70, 80 and 90 were send to the printer to see when the motors would start to skip. After each attempt, a retraction was applied of the same value. An example g-code:

G1 F1 A40 B40  
G1 F10 A-40 B-40

The same was done with the reinforced piston. In a second iteration of the experiment, the black rubber at the end of the piston was removed and the piston and wood thickened with paper towels and tape to make them fit tightly in the syringe. The experiment was repeated to see the influence/compression of the rubber bit.



The pistons were tested in the force test machine in the materials lab by means of a compression test with modules of 500N and 10kN.



## Results

The new method of the motor skipping experiment proved no difference in the moment of skipping of the water-filled syringe and the wood-filled syringe with the original piston, as they both started to make the motor skip at the G-code of 90 (see 3D printer try 6, February 24).

The 3D printed piston made the motor skip at a G-code value of 70. This is sooner than with the original piston.

G-code	Original Piston (with rubber)	3D printed piston (with rubber)
G1 F1 A20 B20	No skip	No skip
G1 F1 A40 B40	No skip	No skip
G1 F1 A50 B50	No skip	No skip
G1 F1 A60 B60	No skip	No skip
G1 F1 A70 B70	No skip	Skip
G1 F1 A80 B80	No skip	-
G1 F1 A90 B90	Skip	-

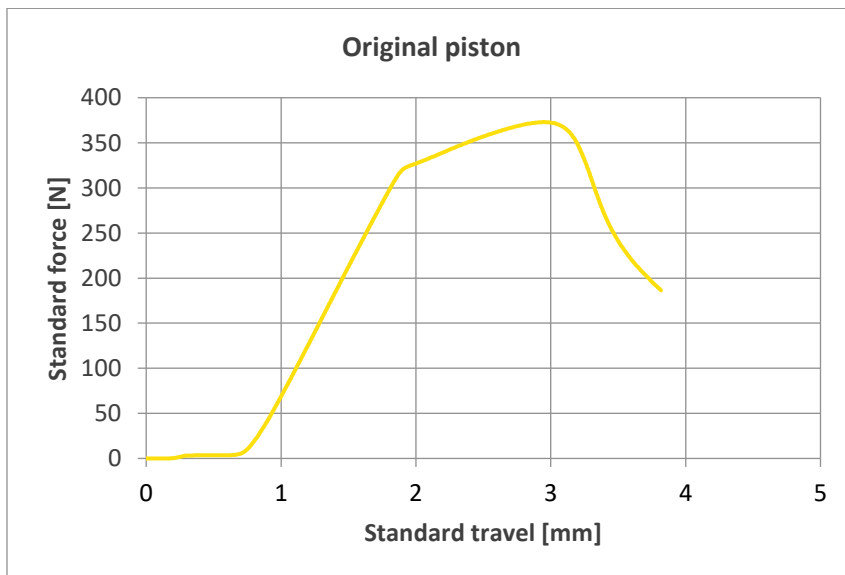
With the rubber cap removed, the original piston made the motor skipping at a value of 70, and the 3D printed piston caused skipping at a value of 50. This difference is consistent with the measurements with the rubber cap, as they both deviate a value of 20.

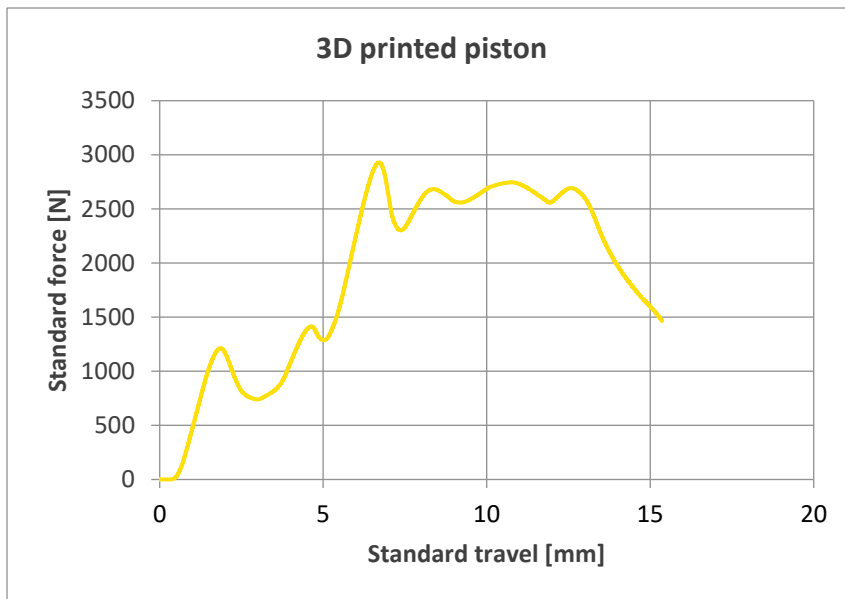
G-code	Original Piston (no rubber)	3D printed piston (no rubber)
G1 F1 A20 B20	No skip	No skip
G1 F1 A40 B40	No skip	No skip
G1 F1 A50 B50	No skip	Skip
G1 F1 A60 B60	No skip	-
G1 F1 A70 B70	Skip	-
G1 F1 A80 B80	-	-
G1 F1 A90 B90	-	-

#### Compression test

Out of the compression test done on the two pistons, it is clear that the 3D printed piston is far stiffer than the original piston.

The original piston could withstand a maximum force of 372,93N. The 3D printed piston could withstand a maximum force of 2928,48N





### Conclusion

The new piston does contribute to the stiffness of the system. It is however not the only cause of the stiffness problems. The rubber adds some elasticity as well. Combining the 3D printed piston with the lack of a rubber improved the stiffness by a g-code value of 40 over the total possible deformation of 90. This means that there is still elasticity present of a g-code value of 50 in the overall system. This can include syringe expansion, deformation of the syringe tabs or 60-to-10ml conversion piece tabs or the overall pushing assembly.

### Discussion

The results show that there is still deformation present in the system. The question is how significant these deformations are for the reliability of the extrusion of ink.

It is also questionable whether expansion of the syringe is a possible cause, as the G-code-to-skipping was 90 with the original syringe for both the wood and water filled syringes. It is possible that with the water-filled syringe, the syringe expands concentrically, while filled with wood, the syringe only expands/elongates vertically.



In this experiment, only slot A was used to test motor skipping. Maybe there is a difference with motor B.

#### Further research

To see if the extrusion is more reliable with the 3D printed piston, the system needs to be tried with (magnetic) ink. This causes a risk of leaking of ink, as the new pistons are still not optimized to avoid this leaking. It might however be that leaking will be minimal, as the ink is more viscose/thicker than plain water.

## C.2k 3D printer test 11

Kevin van der Lans - March 16, 2022

### Introduction

After troubleshooting and implementing the solutions from the previous tests, it was tried again in this test to print something with (no-magnetized) magnetic ink.

### Method

For this test, the Ultimaker 3 3D printer was used with all the improvements. Those are:

- Stiffer (3D printed) syringe pistons
- Luer connections for the static mixing nozzle (with 2x female 1/8 hose barb luer fittings)
- Overhead Support system (laser cut) which made short tubes possible. The tubes used in this test were 39 centimeters

The ink used in this test was made on March 1 with the same recipe of ink 22/02 – Fe|0,85wt%SiO|nM, but not tested on the rheological behavior.

At the start of the print, syringes were equipped with the new pistons (Part A – piston V1.8; Part B – piston V1.9) before putting them in the vacuum oven (at room temperature) and being vacuumed for 10 minutes at a pressure of 950 mbar.

The pistons were put in the dual extrusion system and tubes were attached. Next, ink was brought through the tubes towards the static mixing nozzle by feeding bits of g-code G1 F1 A89 B89 to the system until ink came out of the nozzle. During this time, the behavior of the ink in the tubes was observed.

When the ink reached the end of the static mixing nozzle, the following g-code was used to print a rectangular shape:

```
M107
```

```
G0 F10000 X100 Y100 Z190 Move head to middle of buildplate
```

```
M84
```

```
M400
```

```
G0 F10000 Z10
```

```
G0 F100 Z1
```

```
G0 F5 Z0.8 Used to determine the required offset of the buildplate to the nozzle
```

```
M400
```

```
G0 F1000 X20 Y20 Go to position (20;20) on the build plate
```

```
M400
```

```
G1 F40 A10 B10 anti-retraction of previous print
```

```
M400
```

```
G1 F1 A35 B35 print a line at the start of a print starting from (20; 20)
G0 F350 Y170 to (20; 170), so 150 mm Long
G0 F350 X18 and back from (18 ; 170)
G0 F350 Y20 to (18 ; 20)
G1 F40 A-70 B-70 retract extrusion before moving to the printed object
M400 Wait until done
```

```
G0 F1000 X100 Y100 move to start of the - in this case - rectangle
M400
```

```
G1 F40 A70 B70 anti-retraction from end of priming line
M400
```

```
G1 F1 A35 B35 start with extruding about 0.4ml for the geometry
```

```
G0 F350 X150 Y100 Movements for rectangle geometry
```

```
G0 F350 Y150
```

```
G0 F350 X50
```

```
G0 F350 Y100
```

```
G0 F350 X100
```

```
G1 F40 A-80 B-80 retraction at end of print
```

```
M400
```

```
G0 F10000 Z150 lower build plate to see the result better
```

```
M400
```

```
G4 P1000 Pause for 1 second (1000 miliseconds)
```

```
M400
```

```
M106
```

```
M104 S0 Temperature to 0
```

```
M104 T1 S0
```

```
;End of Gcode
```

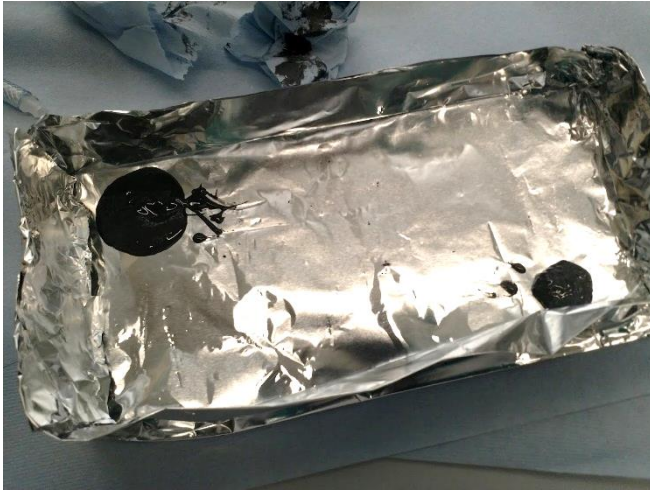
The priming line in the beginning of printing the object was there to ensure an even flow of material out of the nozzle by making sure the material was up to the exit of the nozzle when printing would start.

First, however, it was tried to print the rectangle without the priming line to be able to compare the result.

Printing the rectangle was tried several times to calibrate speeds, z-offsets and retraction values.

## Results

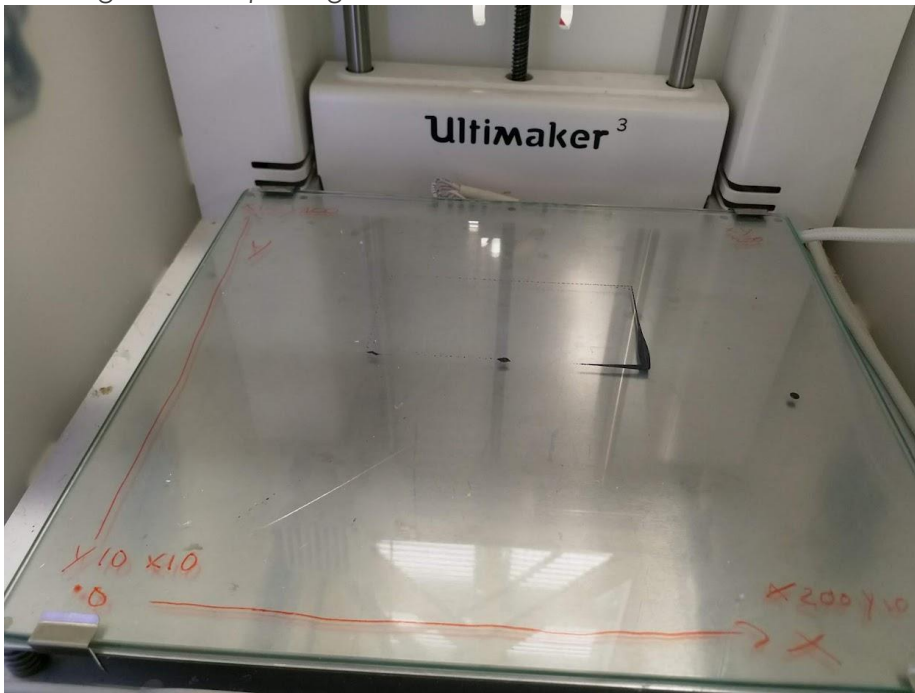
During vacuuming the syringes filled with ink, a lot of ink came out of the syringes:



When extruding ink through the tubes towards the static mixing nozzle, some delay in extrusion was still observed. Especially at the start, when the pressure inside the extrusion system is not built up yet due to its elasticity. In addition, ghost extrusion is still observed, even after 10 minutes of stopping the active extrusion.

Ink that came out of the nozzle when the ink reached the end of the nozzle was captured inside a cup and did cure, indicating a good mixture.

### *Rectangle without priming*



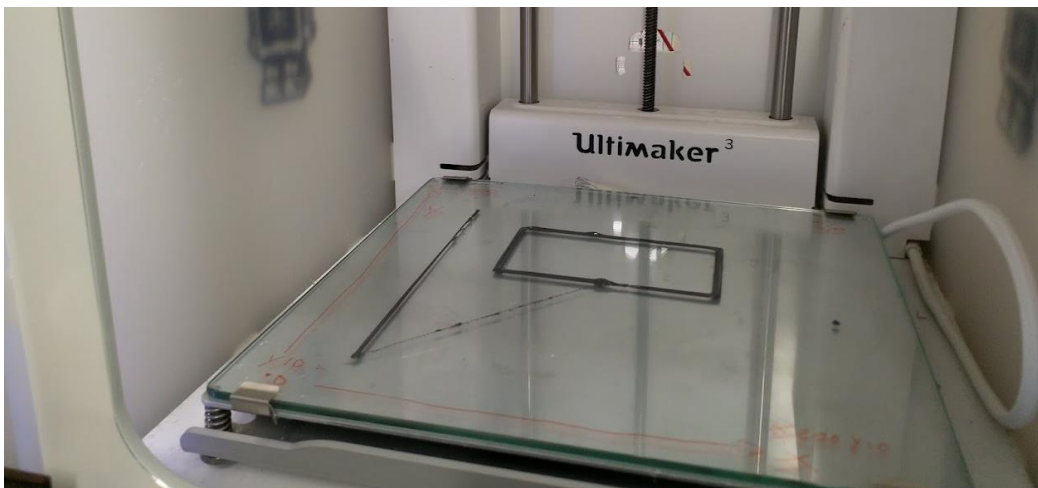
Not enough ink came out of the nozzle to be able to print a rectangle with.

### *Rectangle with priming*

When the priming line was implemented, results were much better. The rectangle shows an even flow of material. However, in the first results, too much ink was extruded.



The second attempt was better, but the buildplate was still quite close to the head.



Prior to the third attempt, the connection to the extrusion system got lost, so the system needed to be reset. This resulted in a loss of the build-up pressure in the extrusion system. The priming line showed some extrusion at the end and when printing the geometry, actual extrusion started late.



The bits that did print however, showed a nice uniform thickness. Bed adhesion was also very good.

At the end of the print, extrusion did not stop. This caused a blob at the end of the print path. This is because the extrusion was not yet completely calibrated to stop when movement of the printhead was finished. The extrusion system should have extruded a little bit less.

After letting the last printed rectangle cure for 4 days, it was observed that the final two centimeters did not cure entirely, and this that the ink was not properly mixed.



#### *Small issues*

It was found that in Part A, some ink leaked from the piston. This was a very small amount and could also have been because there was just some material at the edge of the syringe that was pulled in when the piston was inserted into the syringe.



A small leak occurred at the luer connection with the static mixing nozzle with tube B. This was however not caused by the thread connection, but with the connection with the hose barb in the tube. Likely, the tubes were just a tiny bit too short so a little gab could emerge.

### Conclusions

This test proves that, with the proper priming, this printer set up can be used to make 2D shapes with non-magnetized ink. Although some calibration between extrusion system and 3D printer is needed (e.g. matching print speed with extrusion speed).

### Discussion

Prior to this test, the used ink was not measured on rheological properties. Also, the ink was more than a week old so this could have made the ink more easy to extrude due to its degeneration.

This test also does not mean much if the result cannot be replicated with magnetized ink, which, according to Sannes report and other literature, is much more viscose (about 10x more).

Also, 3D structures are not tried in this test.

### Further research

In the next test, magnetized ink should be tried to see if it can actually be extruded through the static mixing nozzle by the motors. If not, more power can be fed to the motors to make them output more force or a dynamic mixing nozzle can be tried.

Also, more effort should be put in to calibrate the extrusion and print speeds. But only after the magnetized ink works with the 3D printer.

New longer usb cable can be tried to see if this fixes the connection loss issue or otherwise new and shorter power cables.

## C.2I 3D printer test 12

Kevin van der Lans - March 24, 2022

### Introduction

In this test, the magnetized ink is tried in the 3D printer to see if the ink is able to be extruded through the static mixing nozzle.

### Method

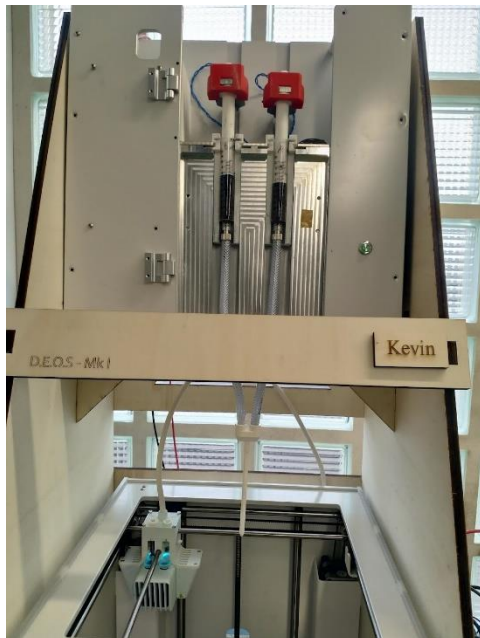
For this test, the Ultimaker 3 3D printer was used with all the improvements. Those are:

- Stiffer (3D printed) syringe pistons
- Luer connections for the static mixing nozzle (with 2x female 1/8 hose barb luer fittings)
- Overhead Support system (laser cut)
- Very short tubes of 20 cm in length, to save material wasted in the tubes, as the sole purpose of this test was to see if the ink could be extruded through the nozzle. So, it was not necessary to put the nozzle in the print head.

The ink used in this test was the magnetized Sample 2 from the ink made on March 22 (NdFeB|0,35wt%SiO|M)

At the start of the test, ink was extruded from the syringes with the cut off tabs into new syringes, equipped with the new pistons (V1.9). They were not degassed.

The pistons were put in the dual extrusion system and tubes were attached. Next, ink was brought through the tubes towards the static mixing nozzle by feeding bits of g-code G1 F1 A89 B89 to the system until ink came out of the nozzle. During this time, the behavior of the ink in the tubes and the extrusion motors was observed. Ink that did come out of the nozzle was caught in a paper cup to check on curing later.



### Results

When putting the ink in the new syringes, large air gaps arose. This happened more with Part B, therefore this syringe seems more full. This did not seem to limit the ability to extrude the ink much when enough pressure was built up. Ghost extrusion could also be observed.

Ink did come out of the nozzle. During extrusion, both motors did skip steps once in a while.





During the test, one tube got loose at the end of the syringe.

#### Conclusion

Magnetized ink is almost able to be extruded through the static mixing nozzle. The motors are a little too weak, but could be boosted a bit more. Some more improvement, like a tidier connection of the tubes with the syringes, can still be made.

#### Discussion

It does not seem to be necessary to invest time in making a dynamic mixing nozzle, but first the motors need to be boosted to see if this solves the problems. Because the ink is more viscous when magnetized, this could create more pressure in the system which causes the leaking of the tube.

#### Further research

Some time needs to be invested in making the tube connection more tight, probably with some kind of clamping mechanism of some sort. The test needs to be retried with boosted motors before a real conclusion can be drawn on the necessity of a dynamic mixing nozzle.

## **C.2m 3D Printer try 13**

Kevin van der Lans, Zjenja Doubrovski - April 6, 2022

*Boosted motors, up to 4000 mA. No effect, possibly even worse skipping. Zip ties worked well for clamping tubes.*

## C.2n 3D printer test 14

Kevin van der Lans – April 19, 2022

### Introduction

Static Mixing Nozzle (SMN) causes resistance, means more motor force needed. Less mixing spirals means more room = less resistance (probably). So, how many spirals are needed to mix the silicone to make it cure?

### Method

Four SMNs, each with less spirals:

Nozzle	# of spirals (50% left, 50% right)
default	20
1	16
2	12
3	8
4	4

Extrude plain Ecoflex 00-10 through nozzles with printer (g-code G1 F5 A89 B89) and capture in paper cups. Let cure overnight and see if it has cured the next morning.



### Results

Nozzle	Extrusion attempt	Did it cure?
1	1	Yes
	2	Yes
	3	Yes
2	1	Partly
	2	Yes
	3	Yes
3	1	Yes
	2	Yes
	3	Yes
4	1	Yes

	2	Yes
	3	Yes

### Conclusion

The ecoflex did cure in all the nozzles tested. Only 4 spirals is thus enough to mix the plain ecoflex to make it cure, which means the resistance in the nozzle can be brought down quite a bit.

### Discussion

The tested ecoflex did not have any additives in it. It could be possible that (magnetic) particles have an influence on the curing.

The ecoflex alone has a very low viscosity and formed a little puddle on the bottom of the cup rather than a small heap. It is possible that the silicone mixed a bit more once it flowed into the cup as a puddle.

### Further research

Ecoflex with Iron particles or left-over magnetized ink can be tried again with the shortest SNM to see the influence of fillers and also make the ink more like a small pile rather than a puddle in the cup.

## C.2o 3D printer trial 15

Kevin van der Lans – April 22, 2022

### Introduction

Now, we will do the same experiment as last time, but with magnetized ink.

### Method

The tubes were brought down to a length of 10 cm to spare ink. The ink was extruded through the Static Mixing Nozzle nr 4, with 4 spirals. The extrusion motors were given a default motor current of 3500mA through the firmware. A permanent magnet and magnetic shield was attached to the end of the nozzle.



Ink was captured in paper cups. A total of 6 extrusions were performed and left to cure at room temperature over the weekend.

In addition, around Extrusion 3, An attempt was made to make a figure with the extruded ink by extruding it on a small round glass plate thingy and move the plate below the static nozzle. This sample was placed inside the oven and left to cure at 120°C for about 1 hour.

### Results

The motors did not skip once during the experiment, indicating that the force needed to push the ink through the nozzle was less than what the motors could give. No leaking was detected throughout the experiment.

Out of the 6 extrusion attempts, none of the samples cure completely at room temperature. The sample placed in the oven however did cure. After placing one of the uncured samples in the oven at 120°C for about 1 hour, this sample did cure.



### *Snake like thingy*

The little figure on the glass plate cured well in the oven and shows a very responsive shape change. Although the magnetic particles should be orientated everywhere in the same direction because of the permanent magnet, the shape does seem to show different directions throughout.



Depending on the orientation of the magnet (inside the box), a different part of the snake-like shape moves up.

### Conclusions

The shorter mixing part of the SMN makes it easier for the extrusion motors to extrude magnetized ink. However, curing the silicone shows inconsistent behaviour compared to the previous test with unfilled, plain silicone. There, the silicone did cure at room temperature overnight. It seems the magnetized particles have some influence on the mixing or curing of the silicone. When placed in the oven, the silicone does cure however, so it is possible to use the short SMN to print with magnetized ink provided the printed object is cured inside an oven.

### Discussion

The magnetic particles did have an influence on the curing of the silicone. It is however not known whether this influence lies with the (chemical) curing process of the silicone or the mixing inside

the nozzle. It is possible that the silicone did not mix properly with the short mixing part and thus did not cure entirely.

It is also unknown whether the not-so-well curing of the silicone has any influence on its physical properties like tensile strength. It could be that the "forced" curing in the oven makes the material less strong (but this is just a hunch).

#### Further research

The printer needs to be tried with the full length tubes as this can add quite some resistance to the system and tube expansion could bring more problems. Also it can be tried to test samples from the full length SMN and the short SMN on tensile strength to see the influence of the mixing.

## C.2p 3D printer test 16

Kevin van der Lans - May 9, 2022

### Introduction

In the previous test, it was concluded that the magnetic ink could be extruded through the shorter static mixing nozzle (SMN). However, this test was done using very short tubes because there was not enough magnetized ink left to make it through the 39,5cm long tube and through the SMN. Equation 1 shows that the Volumetric flow rate ( $V$ ) depends on the pressure difference ( $P_1-P_2$ ) and the resistance in the tubes. The resistance in the tubes depends on the viscosity ( $\mu$ ), the inner radius of the tubes ( $r$ ) and the length of the tubes (Equation 2). It is therefore very likely that the longer tubes might cause trouble extruding the ink, as longer length results in more resistance, meaning that to keep the same flow rate, a higher pressure difference is needed, meaning more force is needed to create this pressure difference (3).

$$V = \frac{\Delta P}{R} \quad (1)$$

$$R = \frac{8 \mu L}{\pi r^4} \quad (2)$$

$$P = \frac{F}{A} \quad (3)$$

### Method

Ink was made according to the following recipe:

#### Part A

- Turn on the scale and tare it without anything on it.
- Stir the Ecoflex silicone thoroughly with a spoon.
- Place one of the cups on the scale. The measured mass was 4.4284g.
- Pour 18.9 grams of Ecoflex Part A in the cup on the scale with a spatula. The total mass was at this point 23.3302 g.
- Pour half the amount of NdFeB powder (32.55 g) in the cup with the Ecoflex Part A using a spatula. The total mass at this point was 55.8792 g
- Take the cup from the scale and mix the Iron and Ecoflex Part A together manually using a spatula for 3 minutes.
- Place the cup back on the scale. The measured mass was now 55.5998 g.
- Add half the amount of fumed silica (0.18 g) to the Ecoflex Part A/ NdFeB powder mixture. The total mass now was 55.7830 g.
- Mix again by hand for 3 minutes.

#### Part B

- Take everything off the scale and tare if necessary without anything on it.
- Place one of the cups on the scale. The measured mass was 4.2818 g.
- Pour 18.9 grams of Ecoflex Part B in the cup on the scale with a spatula. The total mass was at this point 23.1916 g.
- Pour half the amount of NdFeB powder (32.55 g) in the cup with the Ecoflex Part B using a spatula. The total mass at this point was 55.7380 g
- Take the cup from the scale and mix the Iron and Ecoflex Part B together manually using a spatula for 3 minutes.
- Place the cup back on the scale. The measured mass was now 55.4278 g.
- Add half the amount of fumed silica (0.18 g) to the Ecoflex Part B/ NdFeB powder mixture. The total mass now was 55.6077 g



- Mix again my hand for 3 minutes.

The ink put into a total of 4 syringes and tabs were cut off to be able to fit into the magnetizer. The samples were magnetized at the reactor institute after the weekend in the Versa Lab magnetized at 3 Tesla.

#### *Extrusion*

First, ink was loaded into new syringes with tabs and equipped with the stiffer 3D printed pistons. Tubes of 39,5cm length were attached via the metal luer connectors. Ink was first manually extruded into the tubes as far as it would go with manual force.

The G-code G1 F1 A89 B89 was fed to the system until ink was observed to come out of the nozzle.

Next, a line was attempted to be made with the g-code:

```
M107
G0 F10000 X100 Y100 Z190
M84
M400
```

```
G0 F10000 Z10
G0 F100 Z1
G0 F5 Z0.4
M400
```

#### *Priming Line*

```
G0 F5000 X20 Y20
M400
G1 F20 A60 B60
G0 F100 X20 Y22
M400
G1 F1 A15 B15
G0 F600 Y170 X20
G0 F600 Y170 X21
G0 F600 Y20 X21
```

```
M400
```

#### *Actual Line*

```
G0 F5000 X70 Y50

G1 F1 A20 B20
G0 F150 X120 Y50
```

```
M400
G4 P1000
M400
M106
```

It was also attempted to make a zigzag pattern with the g-code:

```
M107
G0 F10000 X100 Y100 Z190
M84
M400
```

```
G0 F10000 Z10
G0 F100 Z1
G0 F5 Z0.4
```

M400

*Priming Line*

G0 F5000 X20 Y20

M400

G1 F20 A60 B60

G0 F100 X20 Y22

M400

G1 F1 A15 B15

G0 F600 Y170 X20

G0 F600 Y170 X21

G0 F600 Y20 X21

M400

*Zigzag pattern*

G0 F5000 X70 Y50

G1 F1 A20 B20

G0 F150 X120 Y50

G0 F150 X120 Y100

G0 F150 X70 Y100

G0 F150 X70 Y150

G0 F150 X120 Y150

G1 F50 A-80 B-80

G1 F1000 X120 Y200

M400

G4 P1000

M400

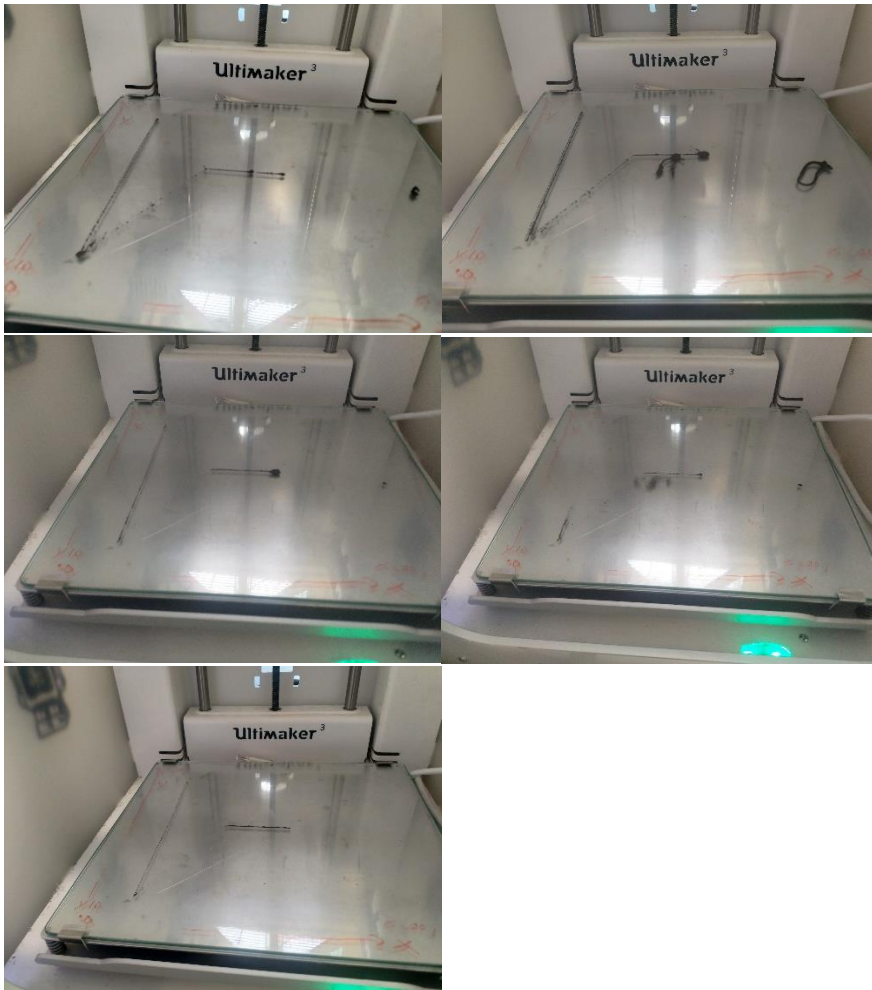
M106

## Results

When extruding the ink into the tubes manually, the increase in resistance could be felt while the ink was travelling through the tubes. At some point, manual force was no longer enough to get the ink up to the static mixing nozzle.

Ink was able to be extruded out of the nozzle. Strings of ink did come out of the nozzle in the beginning of the test during the first extrusion attempts. No motor skipping was observed.

However, when it was attempted to make the line, ink did not flow well out of the nozzle. Not a lot of ink was drawn onto the build plate.



It almost seems like less and less ink was extruded during the attempts. When making the zigzag pattern, no ink was extruded at all. The motors started skipping multiple times when the experiment progressed.

### Conclusion

Magnetic ink can be extruded out of the short SMN with the full length tubes, but for a limited time only. When extruding manually, it was observed that the length of the tubes have a significant impact on the ease of extrusion, which is in line with equation 1 and 2.

### Discussion

The cause of the progressively worse extrusion might be caused by curing of the silicone inside the nozzle. Judging on the time stamps on the taken pictures, the time between first start of extrusion and end of the experiment was about 1-1,5 hour. Normally, the silicone takes 4 hours to cure at room temperature. However, it was found that the ink extruded with the short SMN did not cure, an oven was needed. It is however possible that the ink cured to such an extent that the viscosity increased to a point where extrusion was too difficult. The heated print head next to the SMN could also accelerate this, as the display on the printer reads the head is heated to 60 degrees. It is however not verified if this is the case, as the firmware on the printer as allegedly been altered.

Another cause could be that as the motors warm up, they loose outputted force.

### Further research

New solutions need to be thought of to mitigate the extrusion problems that still exist. Now, the mixing part is in the beginning of the SMN, leaving a volume of ink that is stirred together to cure inside the nozzle, hindering the flow. This mixing part can be moved down to lessen the volume of mixed ink in the nozzle. Another thing that could be attempted is to widen the mixing area, as the radius of a tube has a very large influence on the flow resistance (eq. 2). The tubes can also be made shorter by moving the syringes down the extrusion system, but a retention solution than needs to be designed.

## C.2q 3D printer test 17

Kevin van der Lans – May 10, 2022

### Introduction

This test is a continuation of the test on May 9 (test 16). The goal is to see if the ink will extrude successfully after a minor printer modification. It was suspected that the motors would lose force when they heated up, so this is tested in this Test.

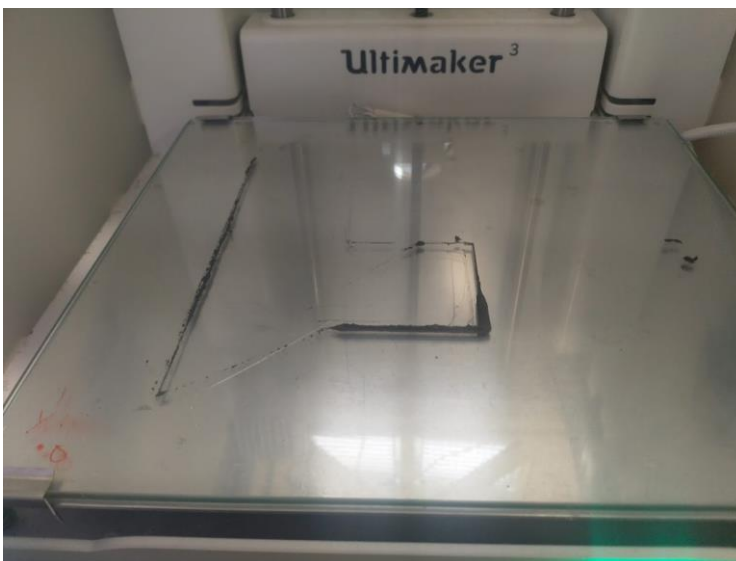
### Method

The exact same method was used as Test 16 (May 9), only this time, a 120 mm PC fan was added to cool the motors while printing.



### Results

Ink was able to be extruded out of the nozzle. It was attempted to print the zigzag pattern with it.



Extrusion showed some under-extrusion, but multiple layers were able to be printed on top of each other. However no or very limited motor skipping could be heard.

The magnetic ink did however curl up to the nozzle, so the magnetic shield still does not work properly.

#### *Curing of ink*

The printed sample was put in the oven at 120 C for about 1,5 hours to cure. However, it did not cure.



It was suspected that component B did not extrude properly and thus was not present in the mixture. Therefore, a bit of component B was added to the printed sample. After being in the oven at 120 C for 1 hour, the sample did cure.

Measuring the force exhibited by both motors with hand-held force meters from the Applied Labs revealed that both motors could deliver about 210 Newton on the pistons each.

#### Conclusion

The motors seem to have enough force to extrude the ink out of the SMN and the tubes. However, they seem to need cooling to maintain this force.

Extrusion is not always uniform, as demonstrated by the lack of component B in the sample. The reason behind this is not clear.

#### Discussion

It could be that component B had more air bubbles, resulting in compression of the trapped air rather than pushing of the ink.

#### Further research

A next attempt could be made to see if the lack of extrusion of component B was coincidental or not.

## **C.2r 3D printer test 18**

Kevin van der Lans – May 13, 2022

### Introduction

This test is a repetition of test 17 (May 10) to see if the lack of extrusion of component B was incidental or not.

### Method

The exact same method of Test 17 was used.

### Result

For some reason, both motors started skipping during the test and were unable to even extrude ink out of the nozzle.

### Conclusion

Despite the promising results from the previous tests, the system does not seem to be capable of extruding the magnetized ink always. Friday the 13<sup>th</sup>??

### Further research

It might be possible to limit the tube length a bit more. This should lower the resistance, which might be just enough for the motors to be able to push ink through without skipping.

## C.2s 3D printer test 19

Kevin van der Lans – May 20, 2022

### Introduction

Current tube length is 39,5 mm. According to equation 1, length influences the flow resistance in the tubes, which in term requires a larger pressure difference to enable a volumetric flow rate (equation 2).

$$R = \frac{8 \mu L}{\pi r^4} \quad (1)$$

$$Q = \frac{\Delta P}{R} \quad (2)$$

In term, the pressure difference is given by equation 3, where  $P_{in}$  is the pressure generated by the piston and  $P_{air}$  is the ambient pressure outside of the nozzle.  $P_{in}$  in term is given by equation 4, where  $F$  is the force applied on the piston by the motors and  $A$  is the area of the piston.

$$\Delta P = P_{in} - P_{air} \quad (3)$$

$$P_{in} = \frac{F}{A} \quad (4)$$

Table 1 shows the known variables. In reality, viscosity ( $\mu$ ) is not constant, because the ink shows shear-thinning properties. However, for comparison of the impact of the length of the tubes, a constant value is taken.

Parameter	Symbol	Value	Unit
Length	L	0.395 (old) – 0.30 (new)	Meter (m)
Viscosity	$\mu$	10000	Pascal second (Pa.s)
Tube radius	r	0.002	Meter (m)
Motor Force	F	210	Newton (N)
Piston area	A	0.00016	Square meter (m <sup>2</sup> )
Air pressure	$P_{air}$	$1.013 \times 10^5$	Pascal (Pa)

Filling in these values shows that with the old tube length, the resistance becomes  $6,29 \times 10^{14}$ . With 9,5 cm cut of from the tubes, with the newly designed syringe holder, the resistance becomes  $4,77 \times 10^{14}$ , which is a reduction of  $1,52 \times 10^{14}$ .

Piston pressure is  $1.31 \times 10^6$  Pa, or 1.31 MPa. Which means the pressure difference is  $1.21 \times 10^6$  Pa. With this, the flow rate  $V$  comes out at  $1.92 \times 10^{-9}$  m<sup>3</sup>/s (0.00000192 ml/s) with the 0,395 m long tubes and  $2.53 \times 10^{-9}$  m<sup>3</sup>/s (0.00000253 ml/s) with the 0.30 m long tubes.

Lets say we want a flow of 0.00000253 ml/s out of the long tubes, the pressure difference should be 1.6 MPa which means the motors need to provide 271,72 N. A difference of 61,72 N compared to the shorter tubes. This is equal to roughly 6 kg, which is quite a lot.

The following experiment is meant to verify the calculated result. If all goes well, the motors should have less trouble extruding ink through the nozzle, as the resistance as decreased and thus less force is needed.



## Method

In this test, the newly designed syringe holders are used. These holders lower the position of the syringe towards the print head, meaning shorter tubes can be used to transport the ink from the syringe to the head.

[picture]

## Results

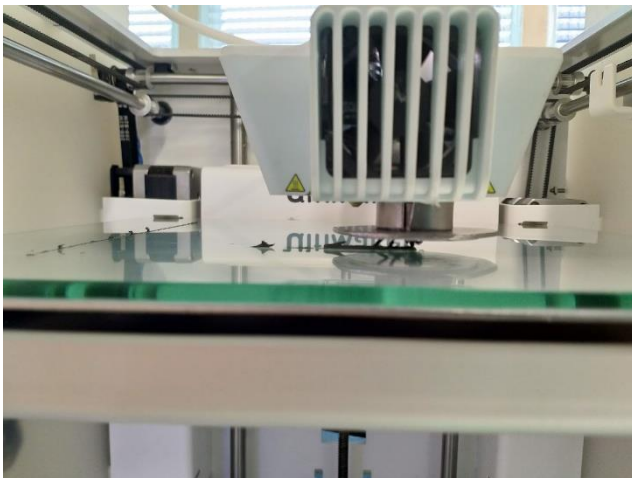
The motors were able to extrude ink, however they were skipping again from time to time, especially motor B. Also, syringe B deformed plastically (expanded) under the pressure when it was attempted to help motor B by pushing on the extrusion pushing plate thingy. This caused ink to flow passed the piston.



Ink was however extruded on the build plate, but again it did not cure, presumably again because of the lack of extruded B component.



In addition, the magnetic shield did not function as desired again, causing ink to crawl upwards to the magnet.



### Conclusion

The shortening of the tubes did not have the desired effect. It was calculated that shortening the tubed would result in much less force needed, however motor skipping still occurred. Even if the motors would be much stronger, new problems such as syringe expansion would occur.

### Further research

To further bring down resistance, the static mixing nozzle can be widened.

### **C.2f 3D printer test 20**

Kevin van der Lans – May 27, 2022

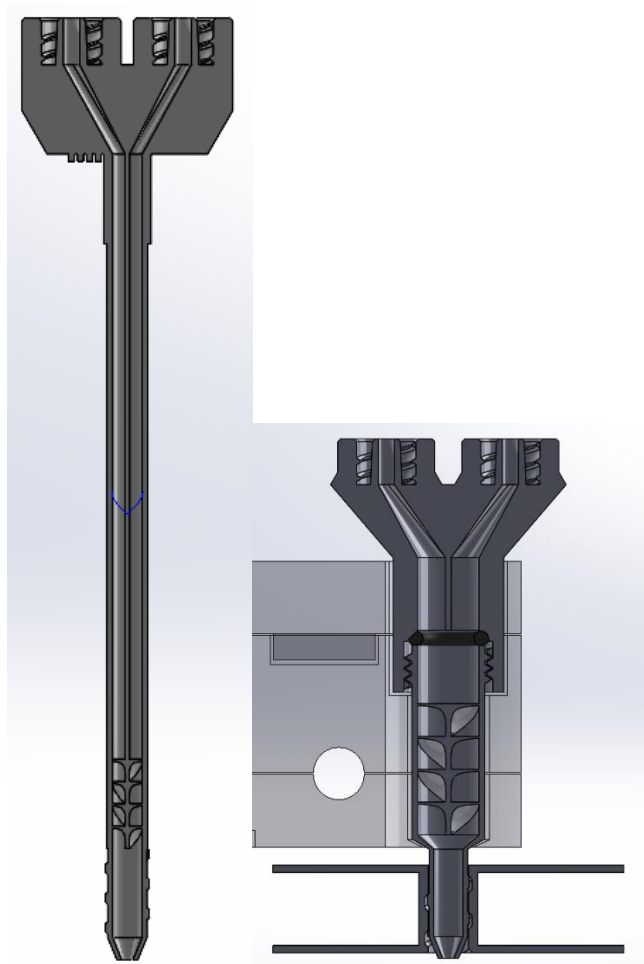
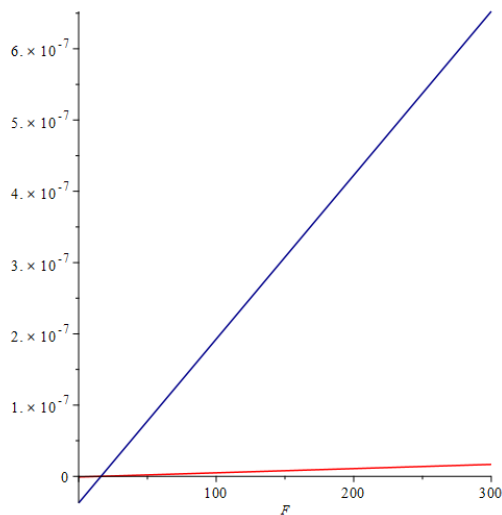
## Introduction

Looking at the equations for flow and resistance (1) and (2), it can be seen that the radius has a large impact on the flow resistance.

$$R = \frac{8 \mu L}{\pi r^4} \quad (1)$$

$$Q = \frac{\Delta P}{R} \quad (2)$$

Therefore, making the radius wider, would in theory lower force needed. With a new SMN design, the radius is more that doubled and the length was brought down as well, which would in theory lower the needed force significantly (red is old design, blue = new design).



## Method

It was attempted to extrude ink out of the new nozzle first without trying to make any shape, but with full length tubes (including the new syringe holders).

## Results

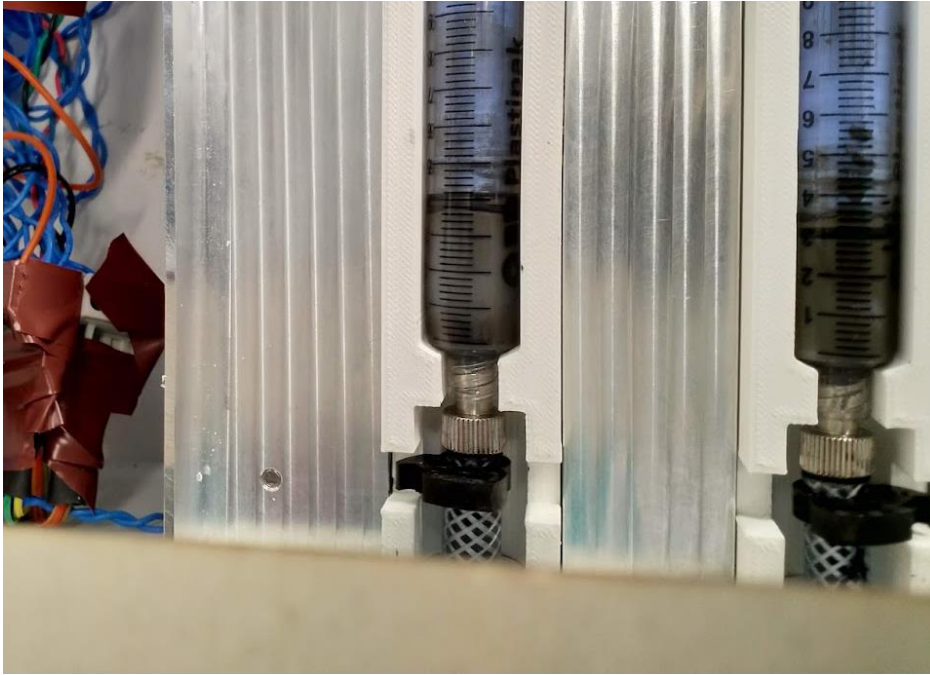
The motors were again not able to extrude anything out of the nozzle, as they skipped again (again mostly motor B). It seems that the theory does not correlate to practice.



Because the SMN is now wider, the ink moves more slowly (Bernoulli's equation). It might therefore be that the shear rate is also lower, so the viscosity of the ink is higher. To mitigate this, the speed of extrusion was increased in G-code (from G1 F1 A/B90 to G1 F10 A/B20). This resulted in extrusion of ink for a second, after which both motors started skipping intensively. The extruded ink also did not cure again.



In addition, syringes started to show signs of swelling again.



#### Conclusion

It seems that the theory does not correlate to practice. The resistance was not decreases as much as presumed. This might have been because of the lower speed the ink travels at, because the viscosity increases.

#### Further research

In the project, there is not much time left to make any further improvements. So for making some demonstrators, manual extrusion needs to be used.

# C.3 Miscellaneous experiments

Not directly involving ink preparation or the 3D printer, sorted by date

---

## C.3a 3D printer electromagnet control

Kevin van der Lans – May 24, 2022

### Introduction

The electromagnet cannot be controlled with the universal pins on the board, so maybe with reading the PWN values from the cooling fans.

### Method

A simple Arduino code was written to first see if a pwm value can be read by Arduino send by the Arduino itself.

Later, the value of the fan pins on the head of the 3D pinter was attempted to be read by connecting the signal pin to the input pin of the Arduino and the ground pin to ground on the Arduino. The head was moved up and down the bed, each turn changing the PWM value written to the fans.



### Results

```
PWM-reader | Arduino 1.8.13
Bestand Bewerken Schets Hulpmiddelen Help
Seriële monitor
PWM-reader
pinMode(4, INPUT);
//pinMode(6, OUTPUT); //to check input
Serial.begin(9600);
}

void loop() {
  // put your main code here, to run repeatedly:
  analogWrite(6, 220); //to check input

  PWM_value = digitalRead(4);
  PWM_value = pulseIn(4, HIGH);
  Serial.print("PWM value = ");
  Serial.println(PWM_value);

  delay(500);

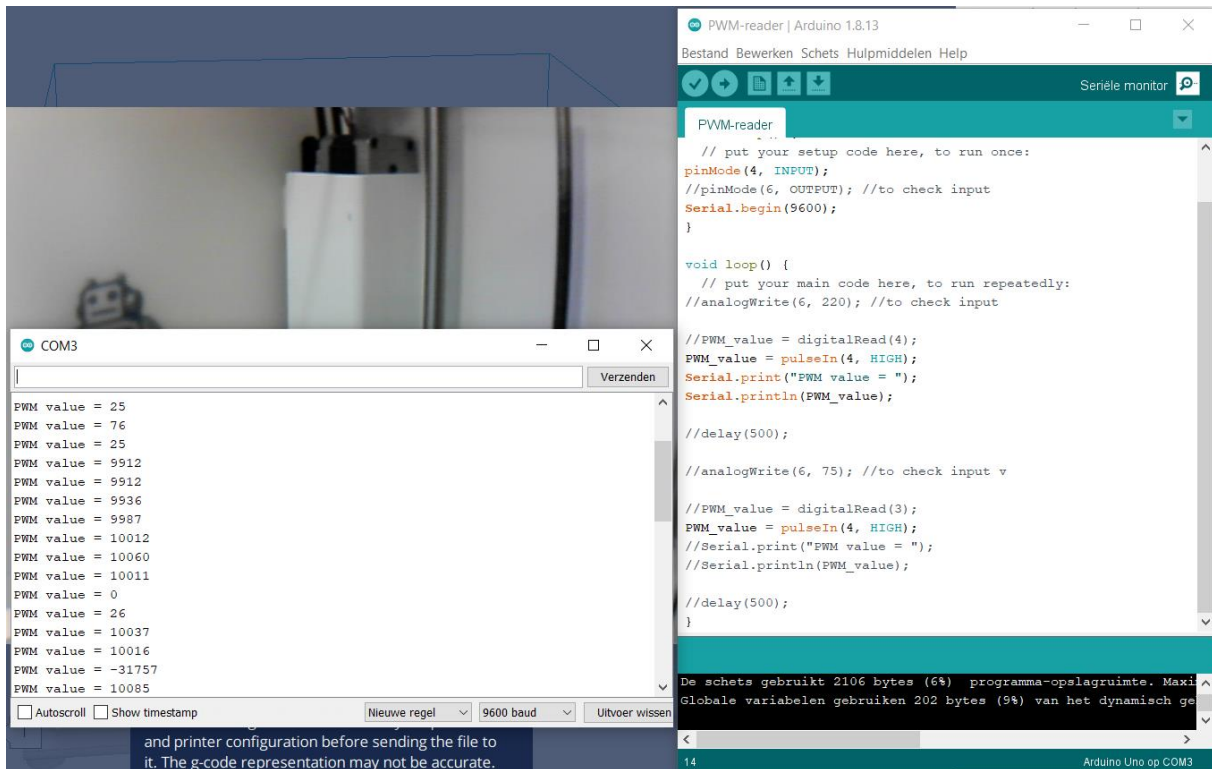
  analogWrite(6, 75); //to check input v

  //PWM_value = digitalRead(3);
  PWM_value = pulseIn(4, HIGH);
  Serial.print("PWM value = ");
  Serial.println(PWM_value);

  delay(500);
}

De schets gebruikt 2896 bytes (8% programma-opslagruimte. Maximale globale variabelen gebruiken 202 bytes (9% van het dynamisch geheugen).
COM3
Verzenden
PWM value = 879
PWM value = 298
PWM value = 878
PWM value = 298
PWM value = 878
PWM value = 299
PWM value = 878
PWM value = 299
PWM value = 878
PWM value = 299
PWM value = 878
PWM value = 298
PWM value = 878
PWM value = 298
PWM value = 878
Autoscroll Show timestamp Nieuwe regel 9600 baud Uitvoer wissen 28 Arduino Uno op COM3
```

Arduino could read the PWM value originating from the Arduino itself. However, when trying to read from the fan pins, the values were very weird, even including a minus value.



## Conclusion

The electromagnet cannot be controlled in this envisioned way. It might be that the fans are controlled differently than generic PWM. However, because the 3D printer is not working as intended and there is also no time left to make it work properly, there is no use in trying to make the electromagnet work.

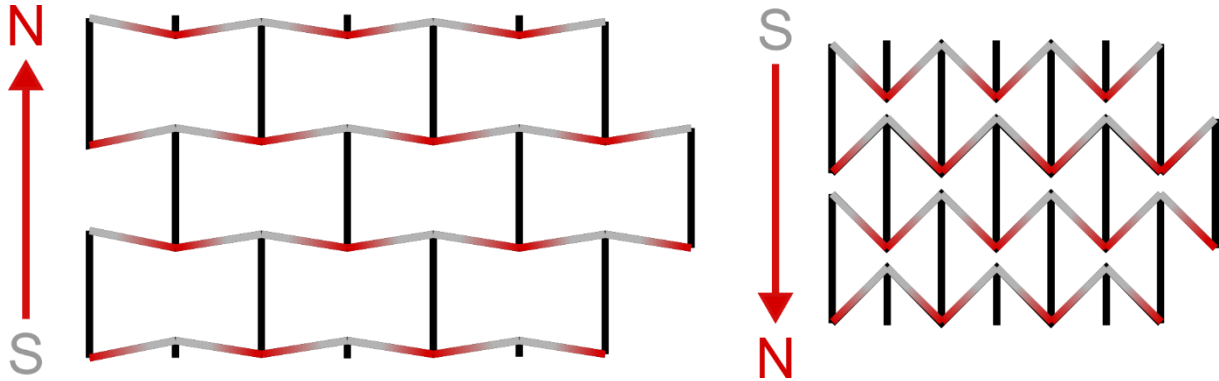


### C.3b Active auxetic metamaterial

Kevin van der Lans – June 3, 2022

#### Introduction

In this experiment, it is attempted to make an active metamaterial structure, combining active (magnetic) segments and passive segments according to the following schematic:



#### Method

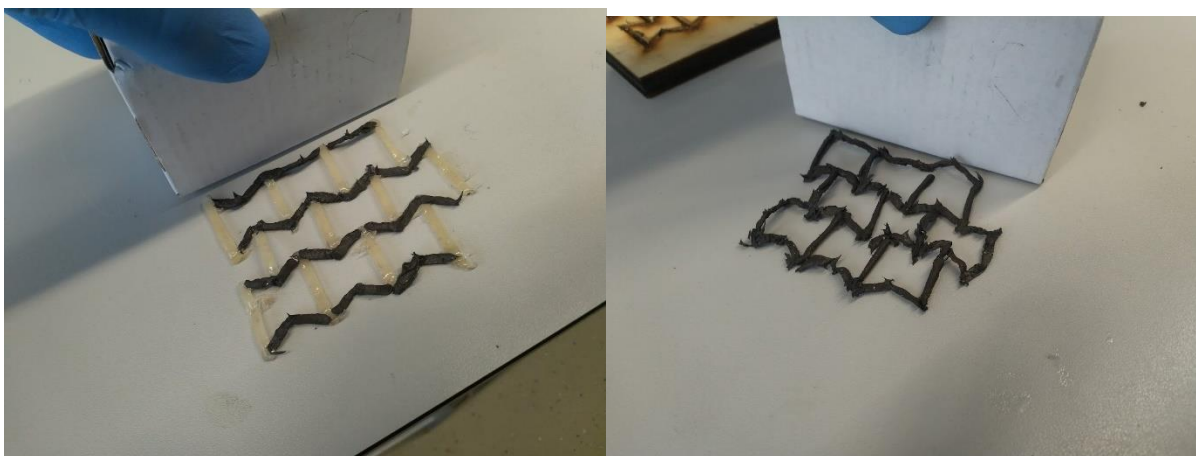
A template was laser engraved into a piece of wood, sprayed with silicone release agent. Passive segments were made with shore hardness 50 silicone with added fumed silica (0.43 grams per 16,5 grams of silicone).

Another sample was made with passive segments of magnetized magnetic ink, but without programming the magnetization direction with the use of a magnet.

For programming of the active segments, a permanent magnet was used because of issues with the electromagnet.

#### Results

The structures did not morph as desired. The active segments turned out quite big, but lacked height. Instead of moving parallel to the surface, the active segments would curl up in Z-direction. The magnetic field was not strong enough to also make the active segments further away from the magnet move.



In addition, some segments did not attach to each other because of human error.

## Conclusion

This test did not prove it is possible to make active metamaterial structures. New approaches need to be considered.

## Further research

It might be possible to make this approach work by making the structures smaller with thinner lines to make them sit in the magnetic field more uniformly and also to make movement of the active segments more easy. Another this that can be considered is to design other auxetic structures that move differently, for example contract in Z-direction, as this is more easy to control with the current magnets that are present.

### C.3c Manual electromagnet control

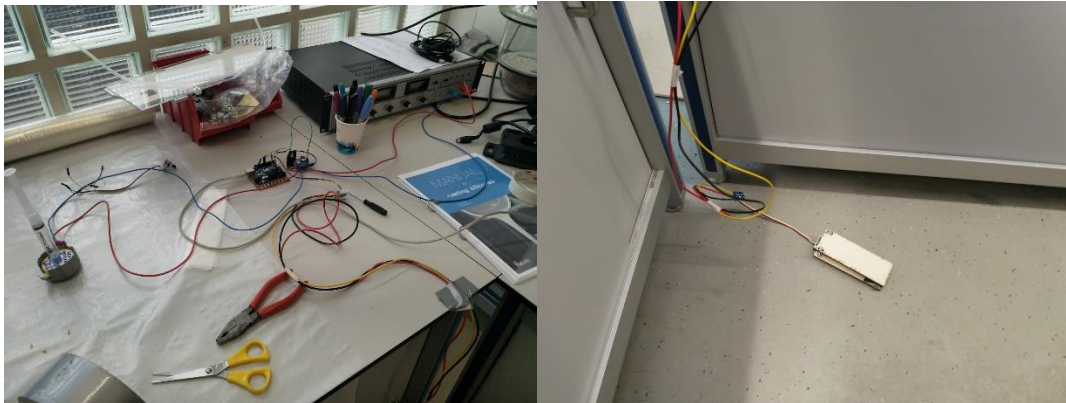
Kevin van der Lans – June 3, 2022

#### Introduction

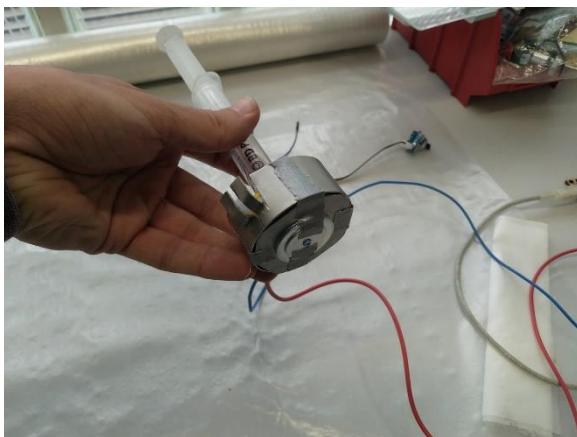
At the start of the project, it was the intention to control the electromagnet with the 3D printer via G-code. It was attempted to control the electromagnet via the PWM signal given to the cooling fans on the printhead via G-code (e.g. M106 S255 to set the fans to 100%). However, this was not achieved, as the value could not be read of the fan pin headers. To check the feasibility of using an electromagnet, the magnet was made to be able to be controlled manually via Arduino and a button hidden in a foot pedal.

#### Method

A simple script was written for Arduino to be able to switch the polarity of the electromagnet via the L298N motor driver. With a button, the polarity of the magnet is switched. The button is controlled with the foot via a foot pedal.



Attached to the magnet was a magnetic shield out of steel. However, the shield did not cover the hole magnet, as some gaps still remained because of the way the steel was cut. In short notice, it was not possible to make a new shield.

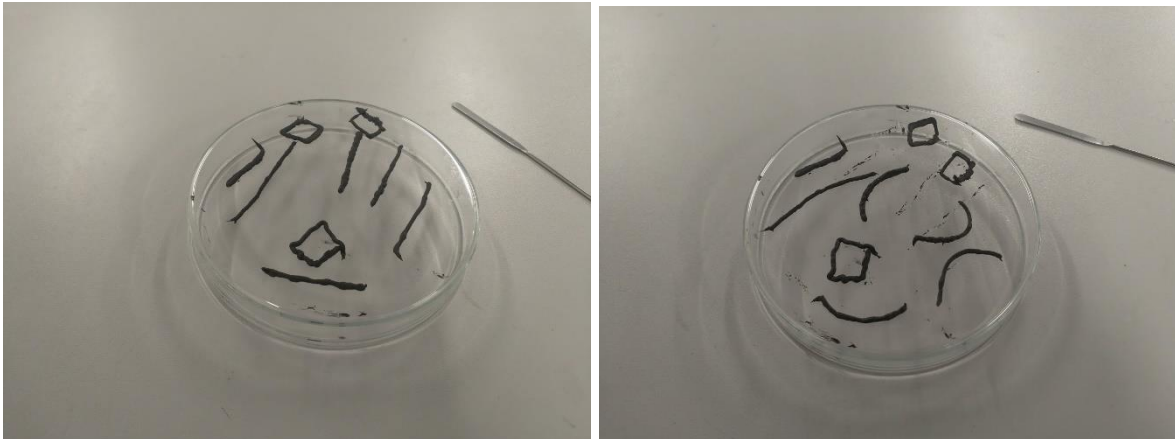


It was attempted to make some simple shapes on a glass tray manually (M-shape wires and squares).

#### Results

Although it was hard to see what was being extruded because of the big chunky magnet, it was managed to extrude some shapes.

The shapes stayed in form well when attached to the plate. But when the shapes were taken off after curing, they morphed upon themselves, curling up.



The shapes also did not actuate as desired. M-shape wires did not morph into an M, but instead just moved up one side and would rotate when the magnet used to actuate them was flipped. Squares also did not morph as desired as they would just be pulled down all together when faced with a magnetic field.



In addition to not giving the proper programming, the electromagnet would get quite warm, heating up the PLA nozzles used to attach the magnet to the syringe. Therefore, the PLA would get soft and deform, losing the grip on the magnet.



Left: new nozzle, right: used nozzle deformed by heat of electromagnet.

## Conclusion

Changing the direction of magnetic particles did not seem to work in this test. The samples did not show distinct segments with alternating magnetization direction. Unknow is why this is. It might be that the electromagnet is not strong enough to rotate the particles around or that the shield influenced the magnetization direction of the already printed samples.

## Further research

This test can be tried again with a better magnetic shield or give more power to the electromagnet. This would also heat it up more, so a better material nozzle needs to be used to stop it from melting, like ABS (although this is harder to 3D print).

### C.3d New attempt at metamaterial structures

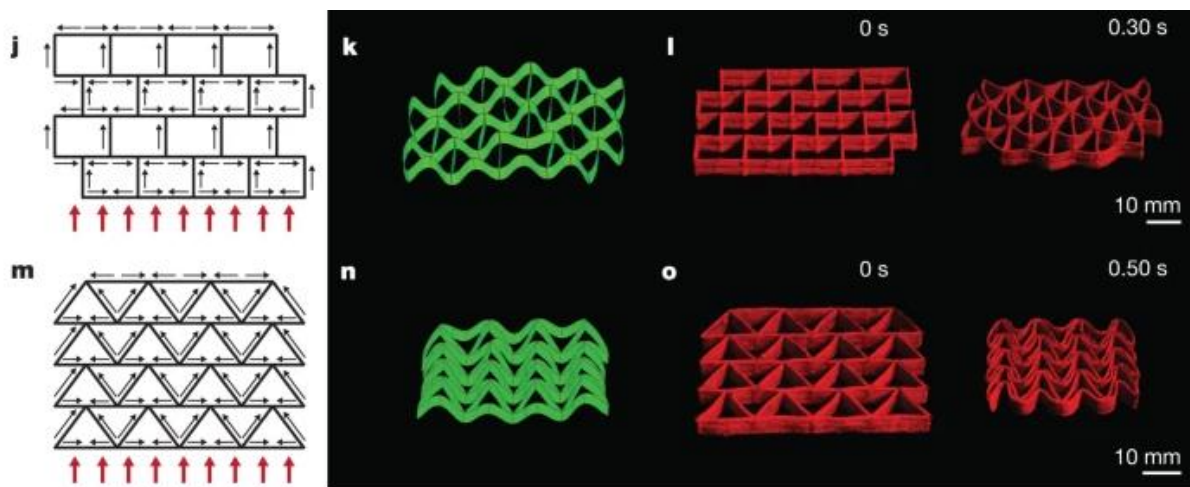
Kevin van der Lans, Sepideh Ghodrat – June 7, 2022

#### Introduction

The previous attempt at making an auxetic metamaterial structure failed. In this attempt, the lines were made thinner and structures taken from Kim et al. (2018) were used/recreated.

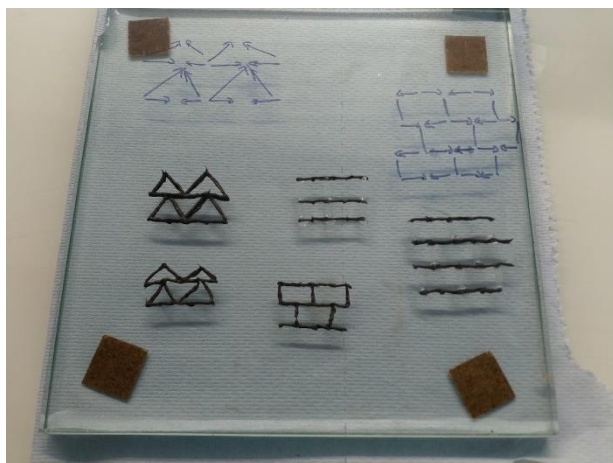
#### Method

A luer nozzle piece was used with a diameter of 1.2 mm and a permanent magnet to control the orientation of magnetic particles. The following structures were made with some vertical elements with plain silicone instead of the magnetic material, using manual extrusion.



#### Results

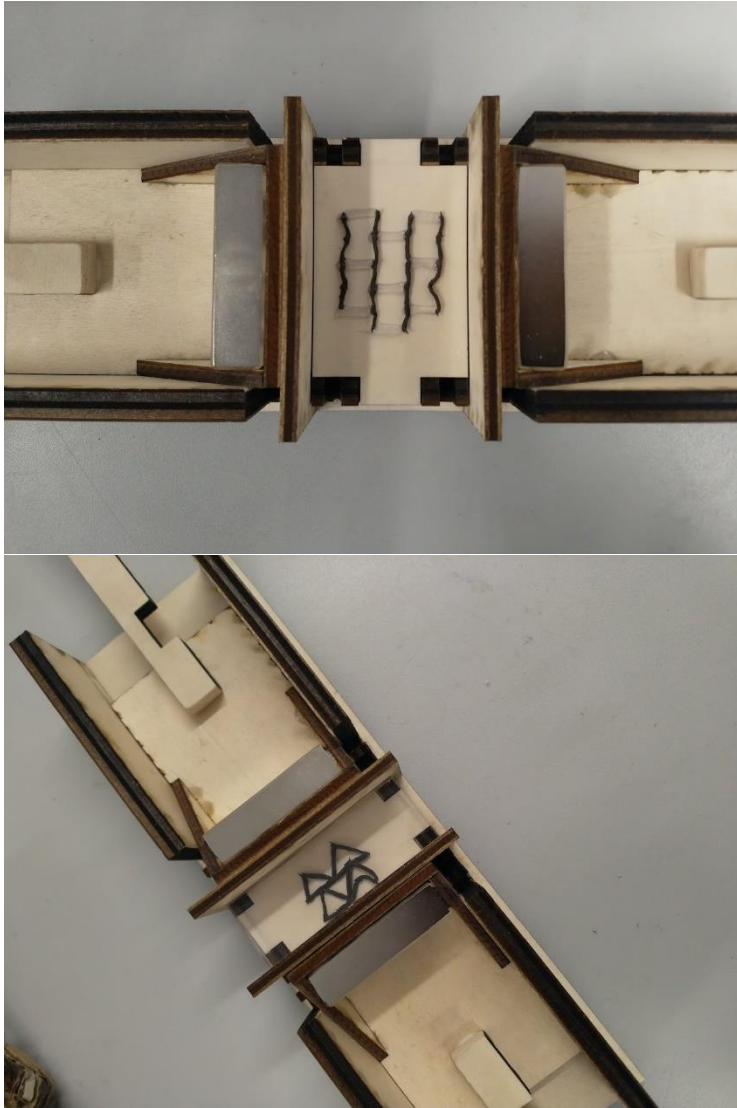
One structure was made with two layers. Those layers stayed upright pretty well. All samples also cured well in the oven.



#### Magnetic response

Out of the made structures, it seems that not all cells work. Only one cell from the triangular structure gives a good response.

Also the square had one good responding cell and some less well responding ones.



### Conclusions

Thinner and smaller structures are better, but still not as we want.

### References

Kim, Y., Yuk, H., Zhao, R., Chester, S.A. & Zhao, X. (2018). Printing ferromagnetic domains for untethered fast-transforming soft materials. *Nature*, 558, p. 274 – 279.

<https://doi.org/10.1038/s41586-018-0185-0>

### C.3e Changing texture prototypes.

Kevin van der Lans – June 16, 2022

#### Introduction

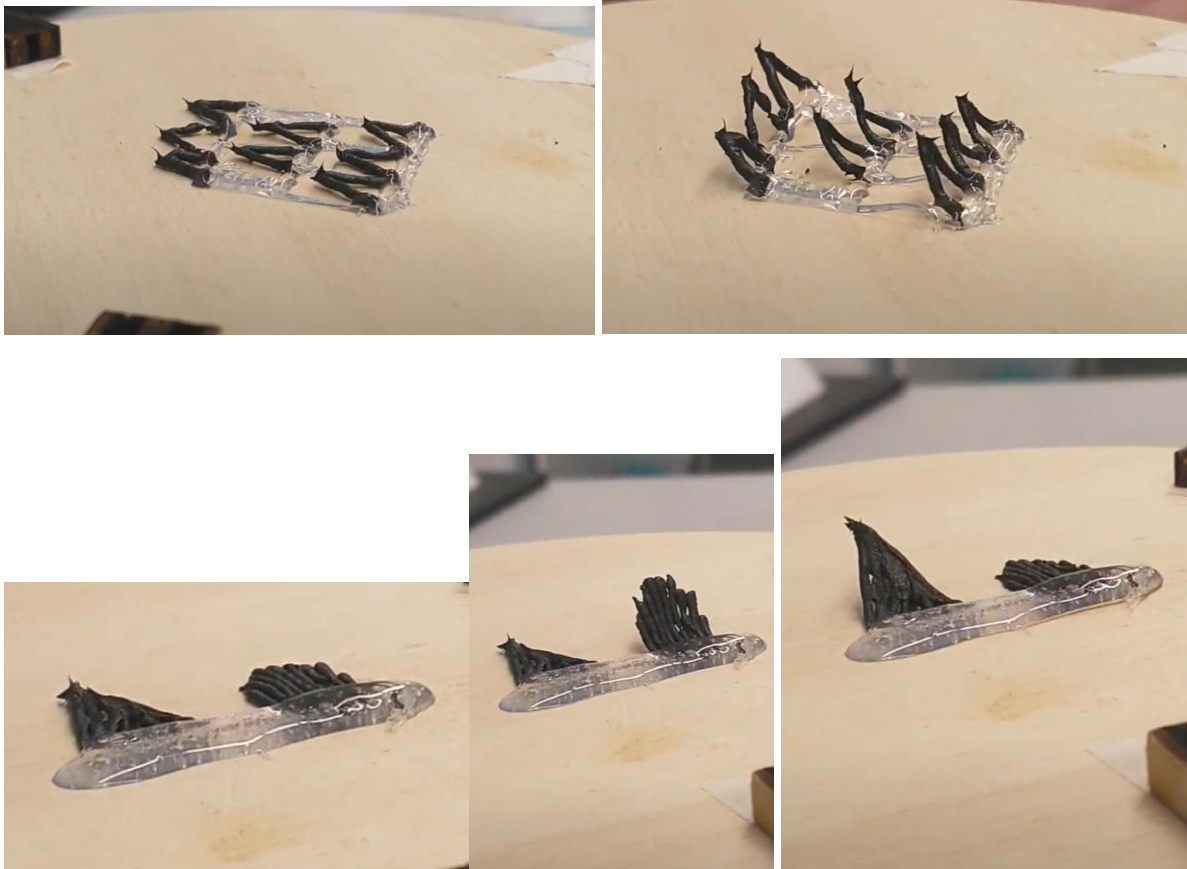
As demonstrator design I made a changing texture. Here I test some simple prototypes.

#### Method

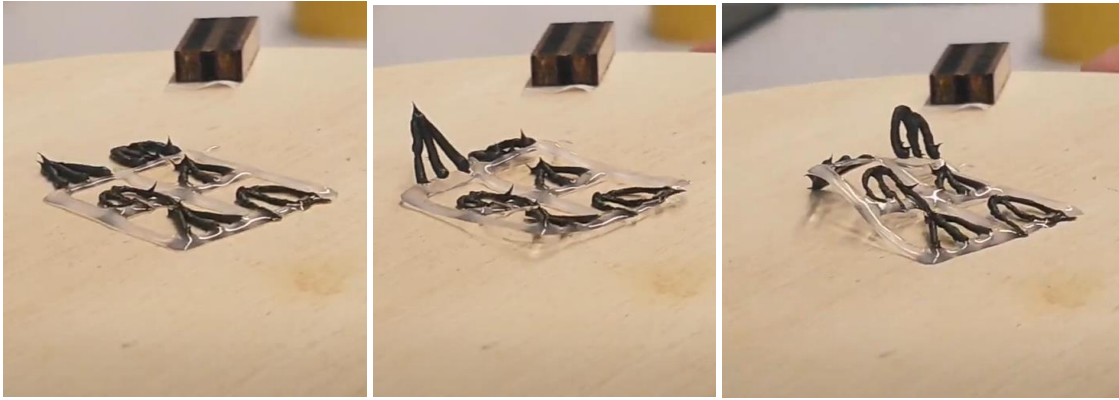
The textures were made manually with a mix of active (magnetic) ink and plain silicone. They were tested with a permanent magnet underneath the textures.

#### Results

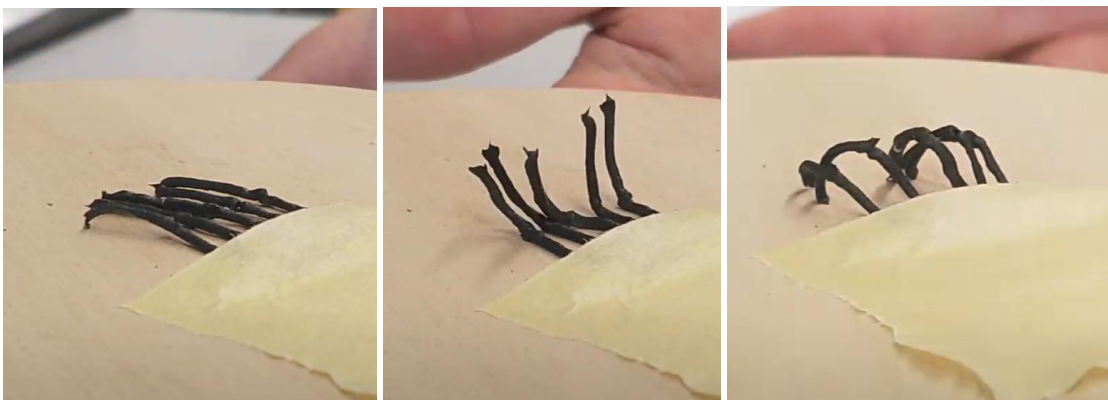
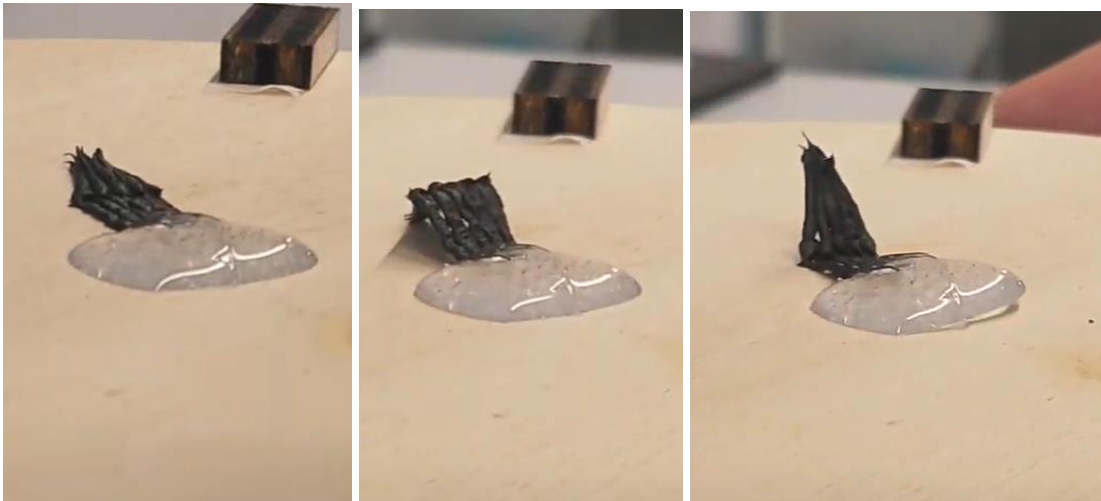
Some do good, some don't work for whatever reason.







And here the other design.



### Conclusions

The core principles of the two texture changes are proven to work. The second version has more potential for haptic feedback because the difference between the textures is felt better, while the first version fits better with the “active” experience vision of the MDD method, because it can open up doors that display different colours.

### Future research

If there is time, I can try to make a larger scale prototype of the changing texture.

### C.3f New shape recovery set-up

Kevin van der Lans – June 21/22, 2022

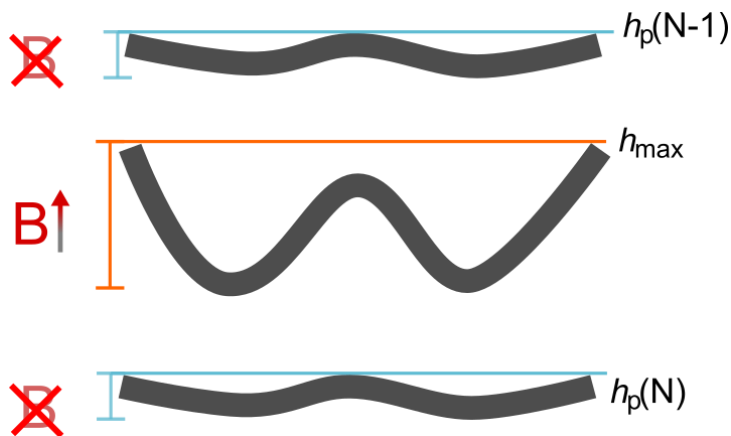
#### Introduction

In the previous shape recovery experiment, a single-magnet set-up was used. With the purchase of two, stronger block magnets, a set-up was made to allow the creation of an in-plane magnetic field to analyze shape recovery with minimal tilting of the shapes.


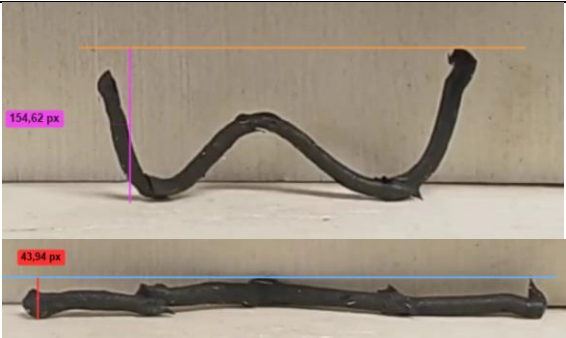
#### Method

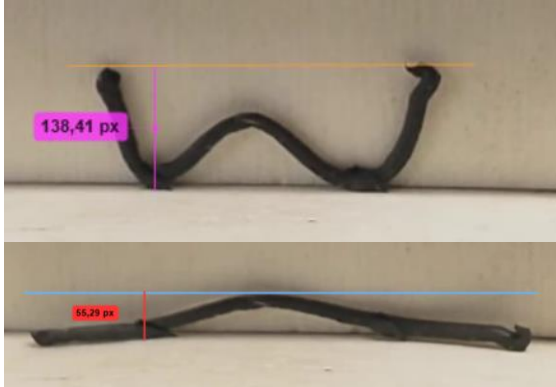
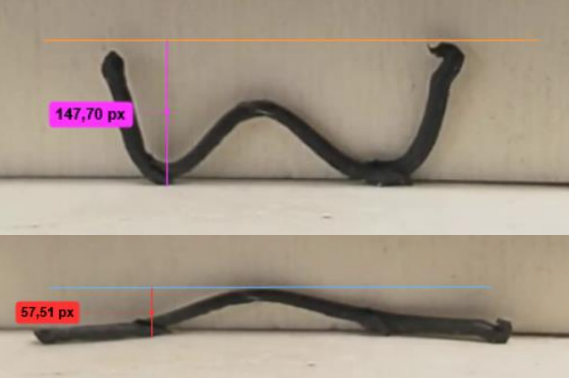
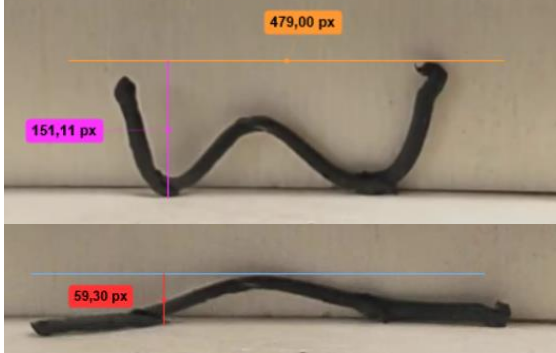
The shape change was analyzed using video and Kinovea analysis software. In stead of the angle of the shape, the height of the shape was measured. The shape recovery can then be analyzed using

$$R_r = \frac{h_{max} - h_p(N)}{h_{max} - h_p(N-1)} * 100\%$$



#### Results

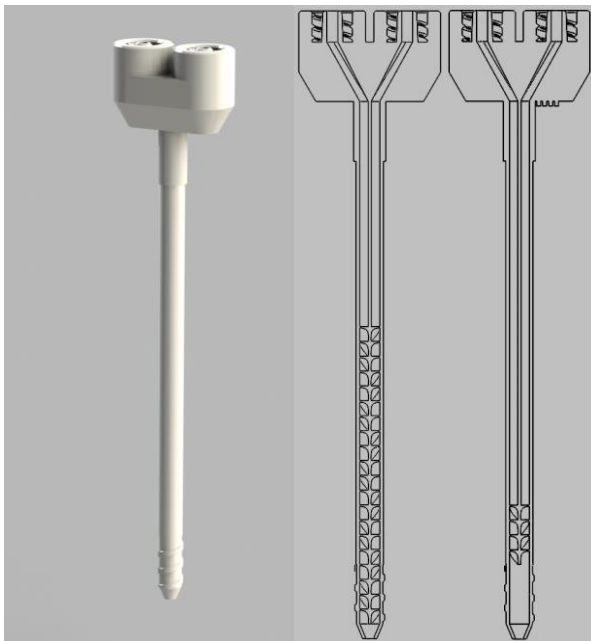
Default shape	1 <sup>st</sup> actuation
	
$R_r = \text{compared to previous cycle\% (compared to default shape\%)}$	$R_r = 88.6\% (88.6\%)$
2 <sup>nd</sup> actuation	3 <sup>rd</sup> actuation

	
Rr=88% (76.4%)	Rr = 88% (76.4%)
4 <sup>th</sup> actuation	Average shape recovery
	Rr compared to previous cycles: 90,5% Rr compared to default shape: 79.3%
Rr = 97.6% (75.6%)	

### Conclusion

The tilting of the shapes was less in this set-up. However resistance seems to still be a thing when it comes to shape recovery, as the outer feet of the W do not slide all the way outward. This may also be just a thing that contributes to shape recovery.

# Appendix D: 3D printer parts (re)designs

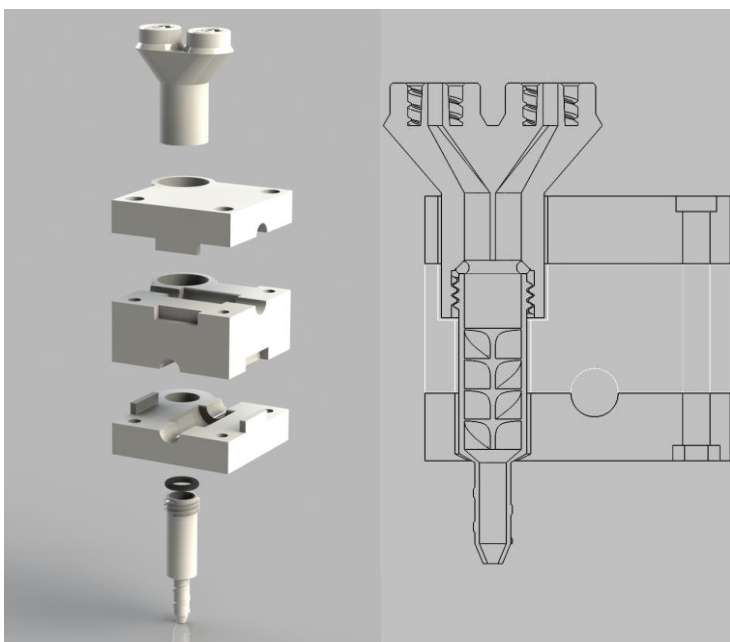
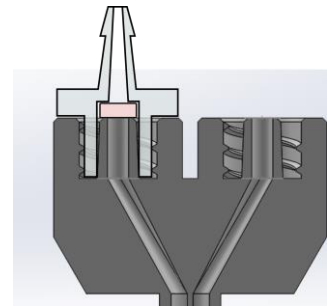


D.1: Static mixing nozzle with Luer connection for hose barb fittings

The static mixing nozzle was redesigned to be able to fit 1/8 inch female Luer hose barb fittings to attach the tubes to, as the original design kept breaking when using the thick, reinforced tubes. A little piece of silicone tubing can be placed inside the luer fitting to ensure a tight seal and avoid leaking.

The nozzle can be printed without support at 0.1mm layer height with the nozzle pointing upward. The inner stand-offs will sometimes detach during printing.

A version was made with a shorter mixing section to lower resistance. The thread at the tip of the nozzle allows it to screw into the (electro)magnet holder designed by Sanne (van Vilsteren, 2021).



D.2: New ultimaker head design

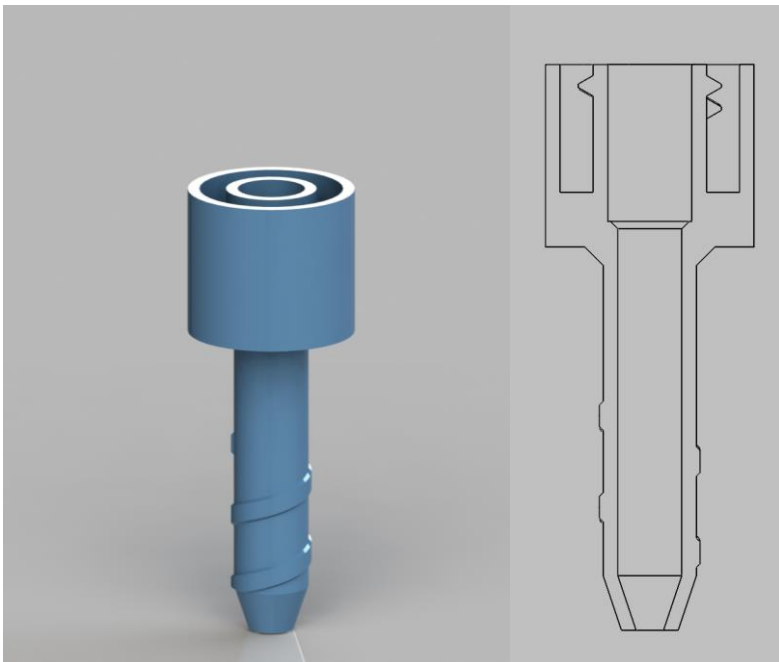
In order to fit a thicker, thinner mixing nozzle, a new print head was designed with space for linear bearings (12x19mm). The three parts are held together with long M4 bolts. The mixing nozzle was cut in half to enable printing the luer hose barb fitting connection at the top the right way up for a more reliable and consistent quality. The two sections are screwed into each other with an O-ring in between to ensure a tight seal.

### D.3: Luer fitting tightening key



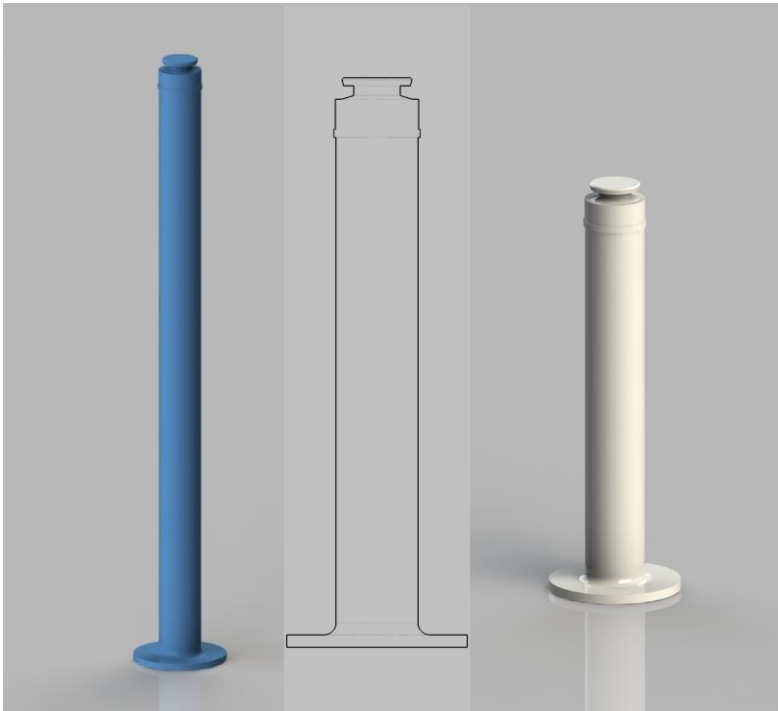
To tighten down the luer hose barb fittings into the static mixing nozzle, a little key was designed.

### D.4: Electromagnet syringe connection



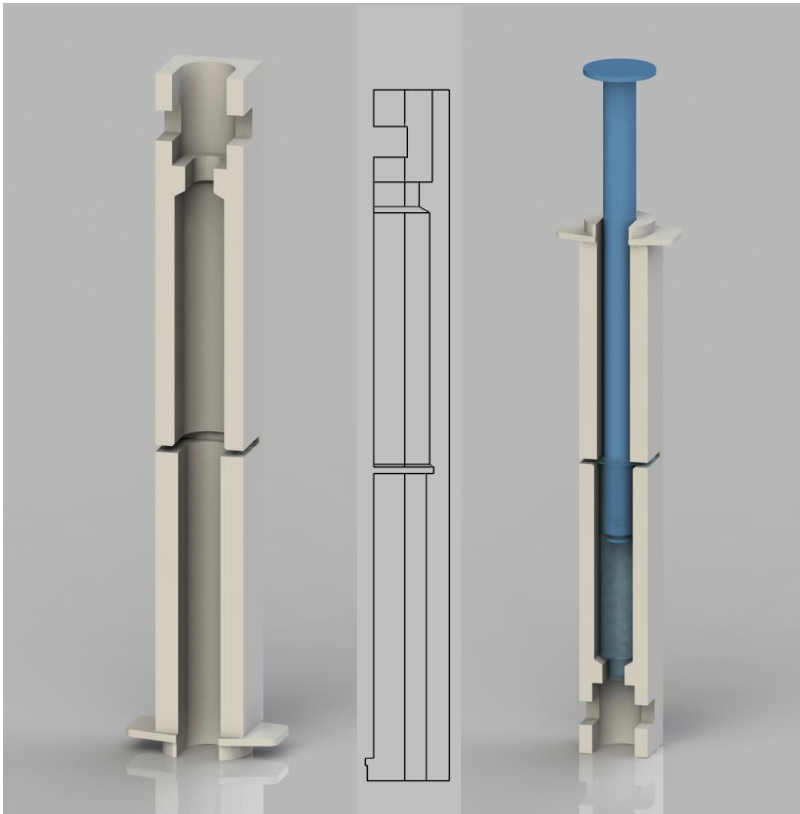
To fit the electromagnet to a 10ml syringe with Luer-lock connection, this fitting was designed. It can be FDM 3D-printed with the nozzle pointing up. No supports needed, using a brim is recommended.

### D.5: Syringe piston redesign



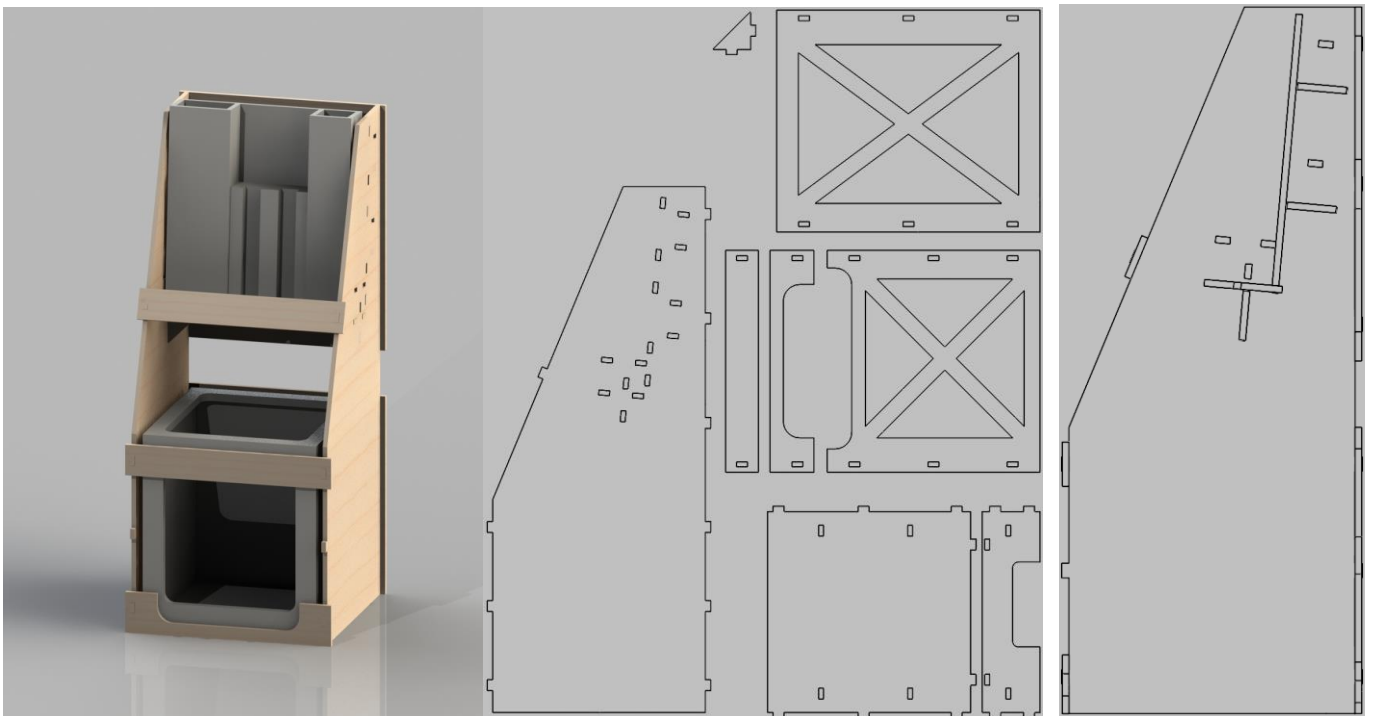
Because the default pistons would buckle under the pressure of the extrusion system, a new piston was designed for 3D printing. A grid infill of 30% was used. A longer version (blue) was made to accommodate for the extra length required when using the extended syringe conversion pieces.

When printing, support is needed in the top, where the rubber seal taken from the default syringe can be mounted.



D.6: Extended syringe holder

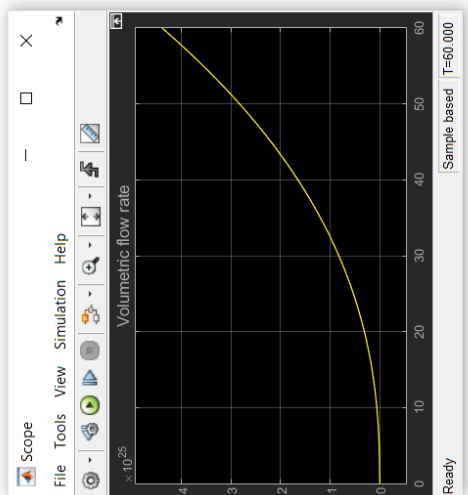
To be able to mount the syringe 10 cm lower in the extrusion system, an extended conversion piece was designed. The syringe is clamped with the tabs in the slot in the middle. Room is left at the bottom for the tube clamps and hose barb fittings.



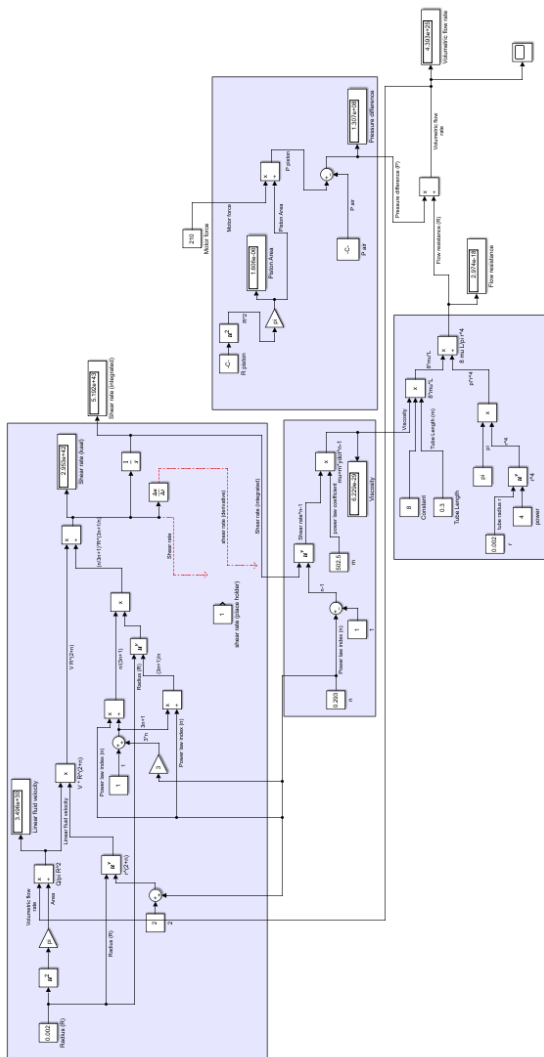
D.7: Dual Extrusion Overhead Support system.

This structure, laser cut out of 9 mm poplar wood was made to hang the extrusion system 20 cm above the print head, which allowed the use of shorter tubes. Two sets of slots for the extrusion 'chair' were made to be able to hang the system a little higher when needed.

# Appendix E: Simulink model

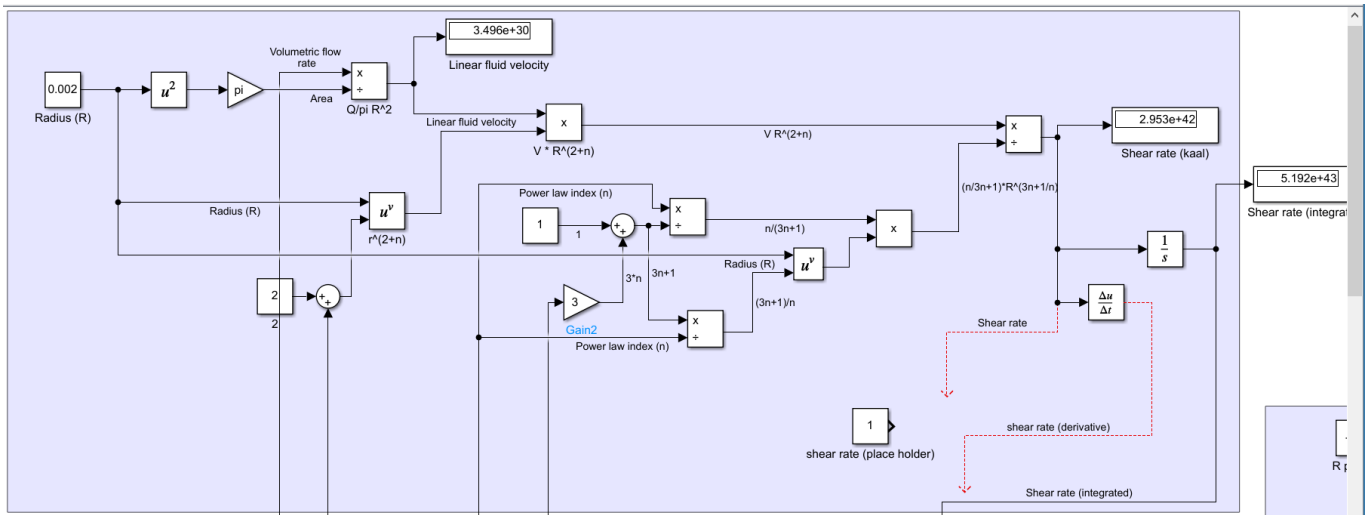


- E1: Shear rate and viscosity
- E2: Resistance and pressure
- E3: Flow rate

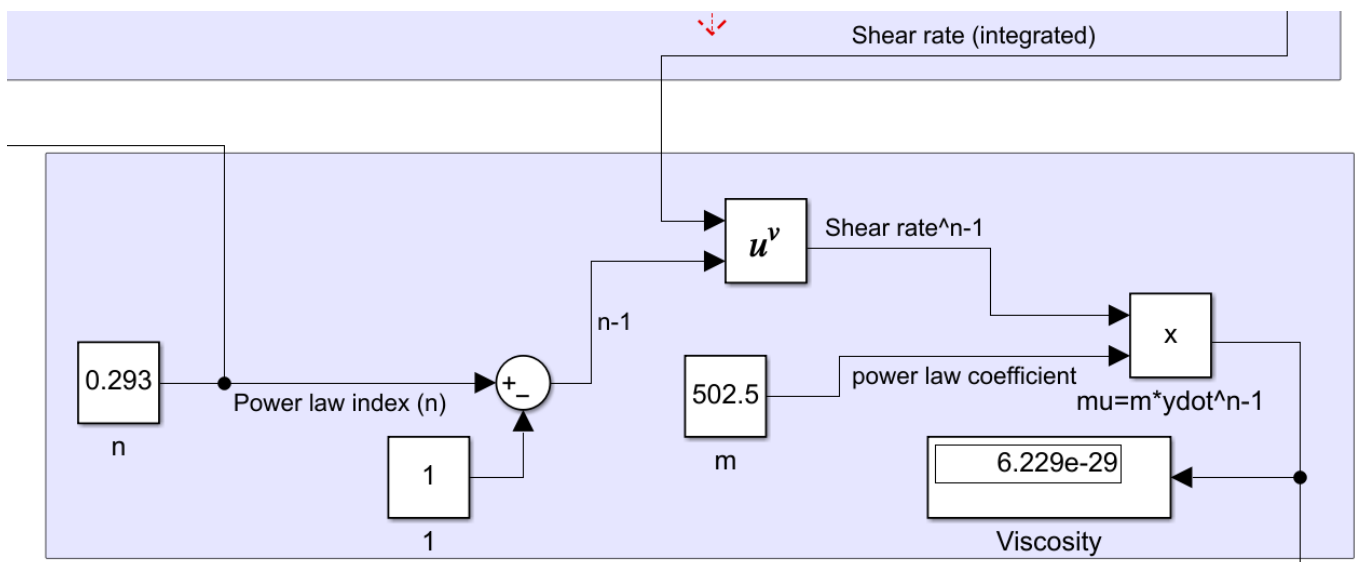


# E1: Shear rate and viscosity

$$\dot{\gamma} = \frac{V r^{(2+n)}}{\left(\frac{n}{3n+1}\right) r^{\left(\frac{3n+1}{n}\right)}}$$



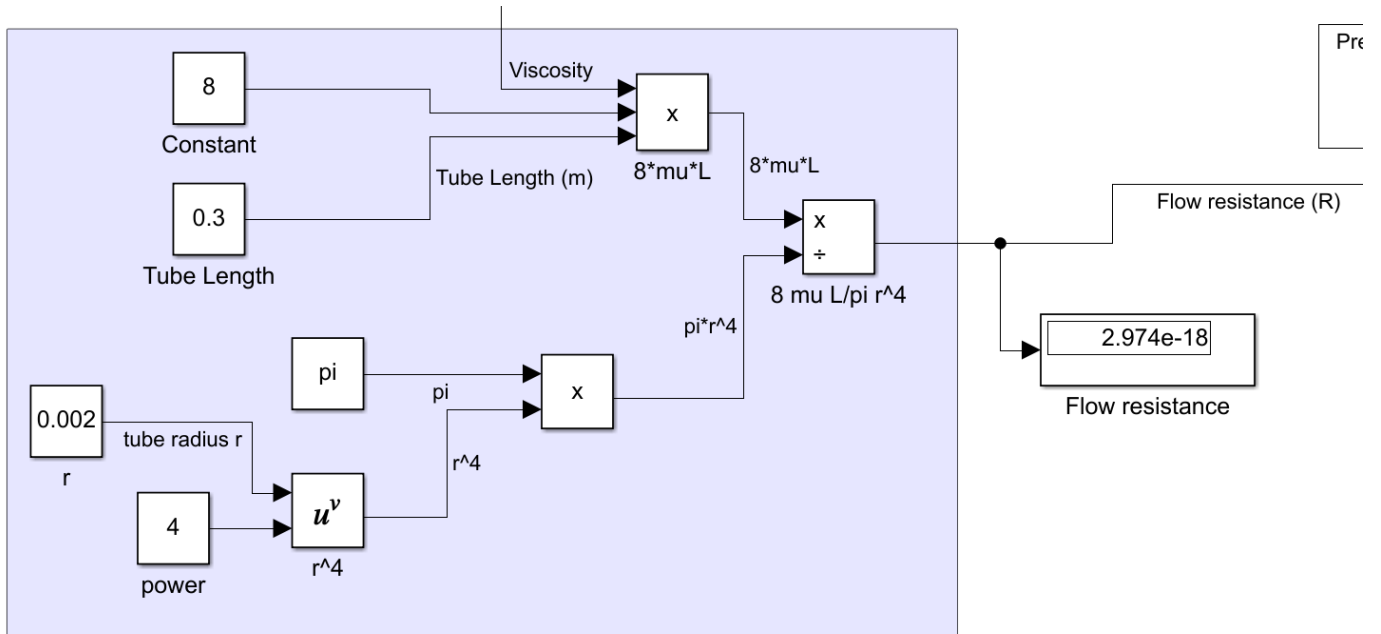
$$\mu = m \dot{\gamma}^{n-1}$$





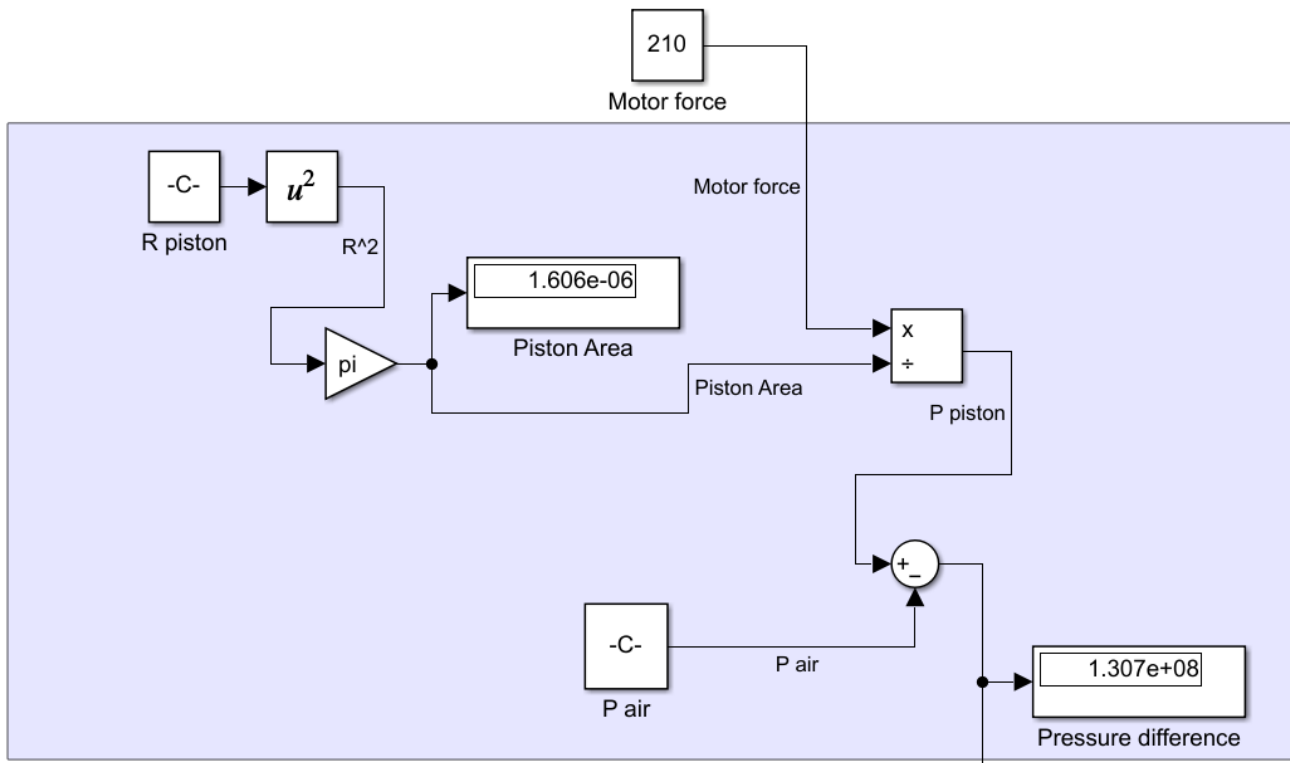
## E2: Resistance and pressure

$$R = \frac{8 \mu L}{\pi r^4}$$



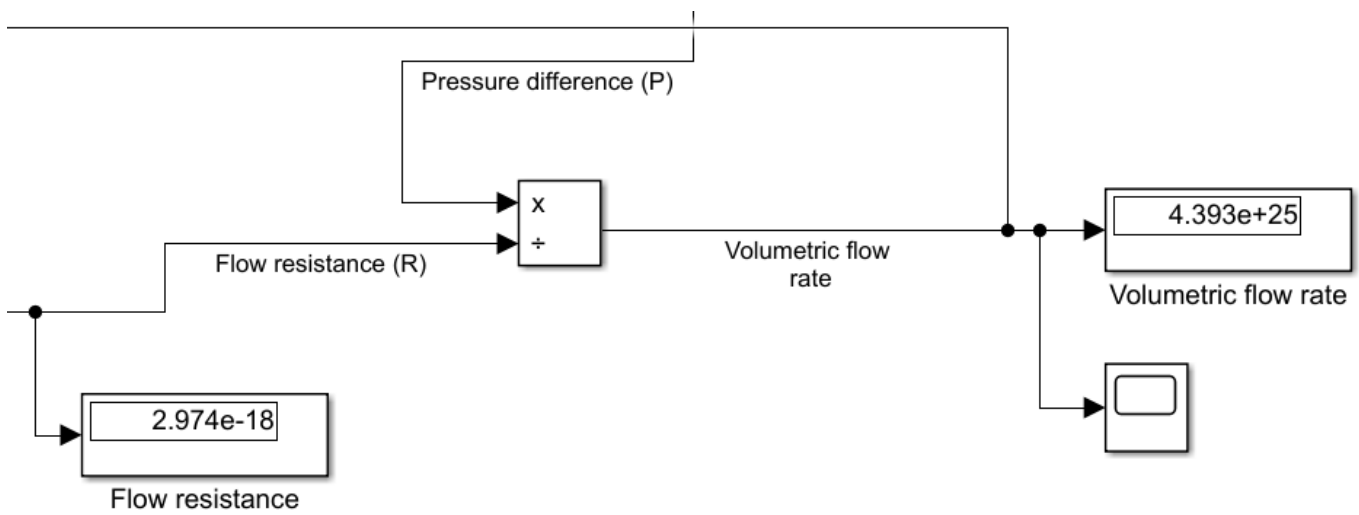
$$\Delta P = P_{piston} - P_{air}$$

$$P_{piston} = \frac{F_{motor}}{A_{piston}}$$

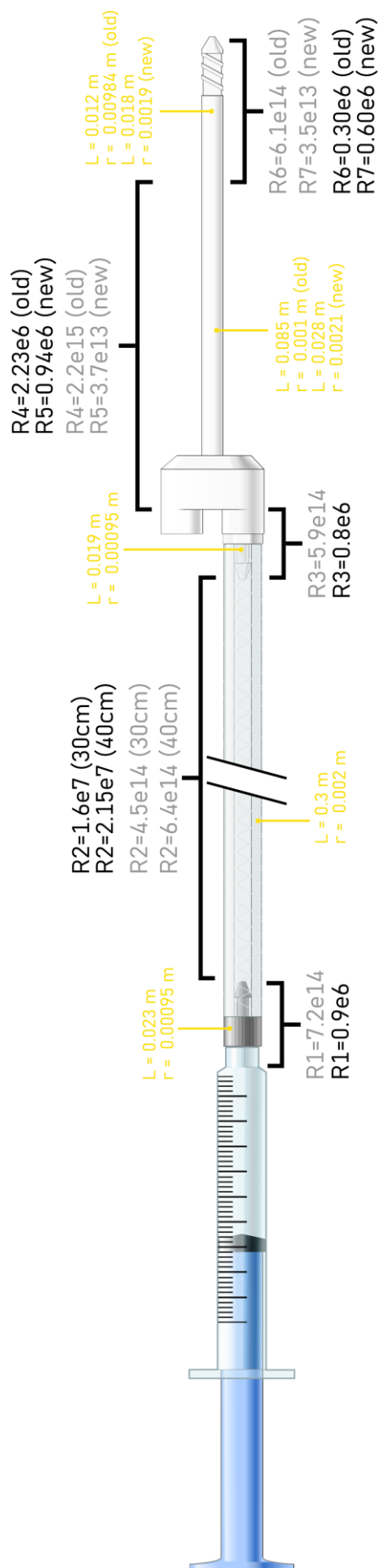


### E3: Flow rate

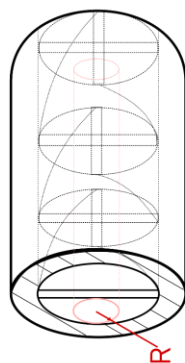
$$Q = \frac{\Delta P}{R}$$



# Appendix F: Flow resistance per section of transport system



Fixed viscosity of 10000 Pa.s  
 Dynamic viscosity with flow rate of 1 ml/125s (8e-9 m³/s) for individual parts and 2ml/125s (1.6e-8 m³/s) for the mixing part



Used radius for static mixing part

$$R = \frac{8 m \left( \frac{Q r^{2+n} (3n+1)^{n-1}}{\pi r^2 n r^n} \right) L}{\pi r^4} \quad (14)$$

# Appendix G: Material Driven Design workshop raw data

- G.1: MDD step 1; sensory qualities, emotion and meaning
- G.2: MDD step 1.5; technical characteristic association
- G.3: MDD step 4; Idea generation

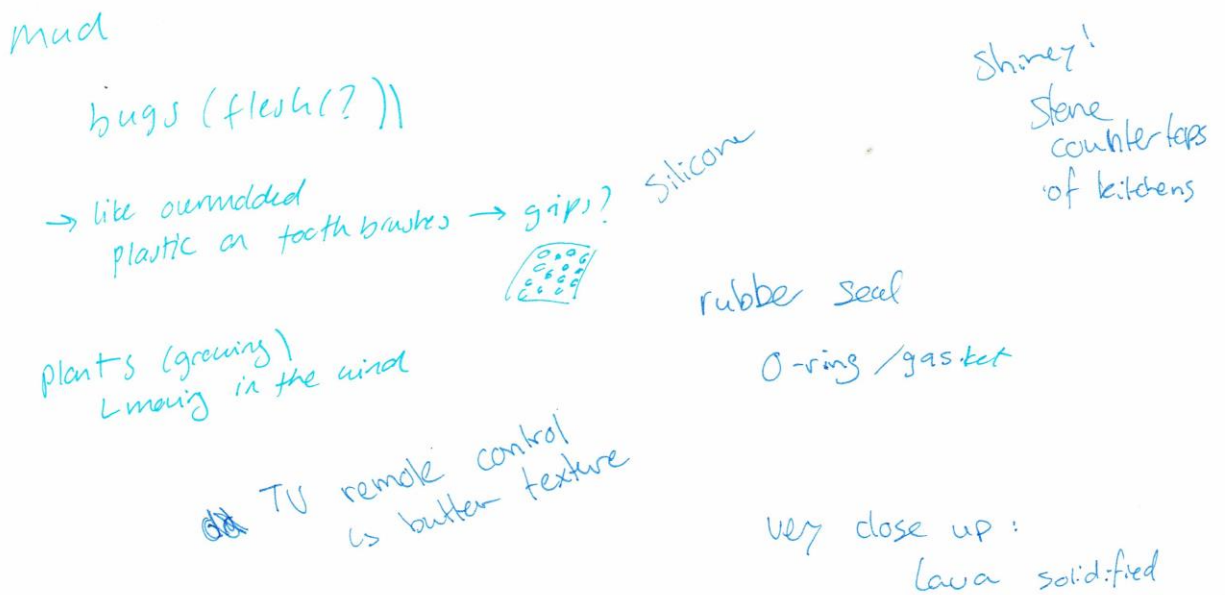
# G.1: MDD step 1; sensory qualities, emotion and meaning

## Material Driven Design – step 1

What are the sensory qualities of the material?



Associations with other (similar) materials?



What meaning(s) does this material evoke?

monsterbode  
of monsters

90's technology vibe → chunky / clumsy in use  
but does not-understandable things  
↳ wonder, randomness  
80's SF horror movie

robots for  
dangerous places

Flubber

Science museums

Primitive

Alive (bug)

Peeking head

colour gives  
lot of meaning

unfamiliar / strange

Does the material evoke certain emotions?

intreque      disgust      rich experience

care / responsibility

hesitant / cautious  
↳ when it moves

curiosity

uneasy

unexpected / alarmed  
space disease

Group → fun / cute

alone → uneasy (too alive)

How do people interact and behave with the material?

causian

don't want to touch it

observing

## G.2: MDD step 1.5; technical characteristic association

Biomedical or micro-scale use?

Weak r2

Not dangerous



tender

what if powerful magnets are used?

not permanent

chaotic

- reduced usefulness

can't hold much

close proximity needed to control it

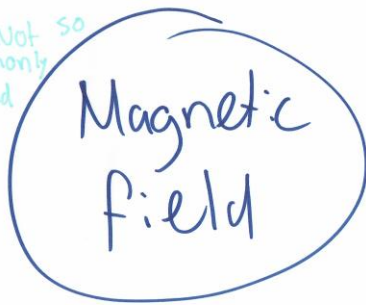
not opinionated (can change)



Wireless charging

Compass

Not so commonly found



"infinite possibilities"

unknown

RFID / NFC is magnetic field no?

high tech

teach kids about magnetism

low energy  
↓  
low force

induction cooking

opposites attract.

no backbone / unstructured  
— snail  
snake  
worm



no fixed size / volume

elastic → high speeds

rubber

problem solving

+ fit into unconventional shapes + spaces

adaptable

low E

- easy to get caught on something

Squishy

foldable  
↳ portable

- Unsettled

+ "Customizable"  
personalise

=> dynamic + living

= Surprising!

- Weak + unstable

# Shape change

shifting identity  
different modes

No motors

Optimus Prime

I can be whatever you like

liquid

Barbapapa

different profiles for different people

Sleep

teddy bear

well behaved

# Soft

Safe

understanding

comforting  
cozy

quiet

Nice to touch  
friendly

squeezy

Soft could also be freaky, like slimy

+ allows for "magic" or cool interactions

- requires external thing to control

# Remote control (small distance)

short wire

Need to stay close

inviting

not intimidating

m/works through barrier

swimming (like an RC boat)

floating -> can make it do things

distance could be extended





dangerous for very young kids → swallowing

Surgical benefits

Small

alarming  
↳ where did it go?  
(or where can it go)

little force

light weight

- easy to lose  
+ can be used in small (handheld) applications

- limited ability to do big things

s baby  
/ c

must care for it

make less blocks

more power to the user



many opportunities

Versatile  
↳ not limited to one thing

less controlled

Multi directional

Different modes

fun  
↳ unpredictable

confusing

+ Unconstrained  
+ freedom of expression  
+ Useable in 3D space

expand & contract  
↳ breathing / heartbeat

Fun  
chaotic

- short lived (reversible)

responsive

immediate

Fast

Smart (responding quickly)

unpredictable

+ enjoyable  
+ useable in scenarios w/ tight time tolerance

No waiting lines

Less irritation / stress

# G.3: MDD step 4; Idea generation

## Material Driven Design – step 4

Brainstorm ideas here!

*art music moving*  
*Visualize music*  
*Visualizing big data*  
*if alexa could move!*  
*product attachment*

*baby monitor that visualizes sound*

*Visualize music*  
*Puzzle games (like ball in box)*

*coffee table that is conversation starter*

*childrens toy*

*Shoe sole (running)*  
*sole change with polarity change*  
*↳ springs for lift*

*Wraps around you like in roller coaster*

*breathing exercises (therapy calming)*  
*sleep robot pillows*

*furniture car seat that changes to profile*

*exploring extreme environments (robotic expedition)*

*changing molds*


*barbapappa material*

*Safety / car seat (responds quickly)*  
*↳ airbag*

*Triggers something → eq. gate*  
*magnet*

*Same with mailbox*

*magnetic bag*



4D movie haptics



communication of information

change aerodynamics of vehicles

visual texture change -> eg spikey

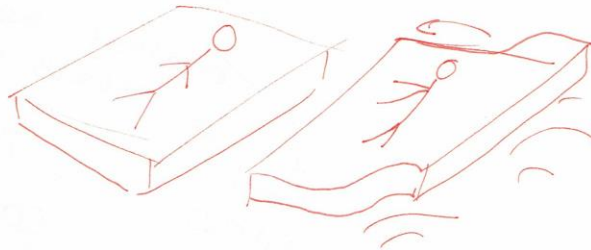
blind guiding (shoes / cane)

space exploration

↳ changing cosmic magnetic fields

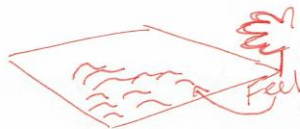
haptic traffic light

correcting mattresses



smart home applications

Screen with bumpy changing surface



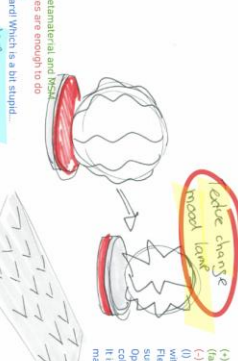
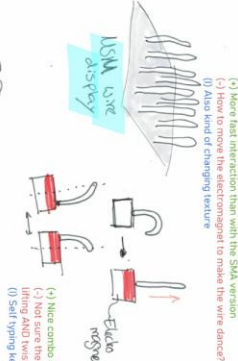
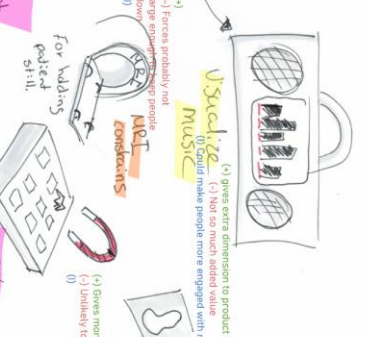
shape changing floor that transports your mail towards you

# Appendix H: Demonstrator idea selection



- H.1: PMI-method
- H.2: Harris profile

**Information**      **Ventiles**      **Electronics**  
**Haptics**      **Hebdometer**      **Miscellaneous**



## H2: Harris profile

Wishes:

1. The design shows three distinct states by means of shape change;
2. The design conveys information in a visual and haptic way;
3. The design invites users to interact with it;
4. The object shows an 'active' colour pallet (dark surface with bright accents);
5. The design fills a gap found in current applications of MSM.

Wish	Train track activation	Texture change	Bi-stable switches	Remarks
1				Bi-stable mechanisms can only show 2 states by definition
2				It is unlikely people will touch the small activated train track actions
3				People love train track miniatures, for texture it depends on the texture
4				Texture can be given colour by revealing colour underneath
5				Bi-stable fills an indirect link, which could be seen as a gap



MAGNETCALLY ACTIVATED

**SHAPE**   
**MORPHING OBJECTS**  
*MORE THAN MEETS THE EYE*

Master Thesis – Integrated Product Design

Kevin van der Lans  
July 2022

 **TU Delft** Faculty of Industrial  
Design Engineering  
Department of Sustainable Design Engineering